ABCC11 in breast cancer : Expression regulation by steroids and Structure / Function relationship study (Homology modeling and Genetic Polymorphism Influence)

Mylène Honorat Meyer

N° 246-2010 Année 2010

Thèse de l'Université de Lyon
Délivrée par l'Université Claude Bernard LYON 1

Ecole Doctorale
Biologie Moléculaire Intégrative et Cellulaire

DIPLOME DE DOCTORAT EN BIOLOGIE

Soutenue publiquement le 22 novembre 2010
par

Mme HONORAT Mylène

ABCC11 DANS LE CANCER DU SEIN:

REGULATION DE L'EXPRESSION PAR LES STEROÏDES ET

ETUDE DE LA RELATION STRUCTURE/ACTIVITE

(MODELISATION *IN SILICO* ET ROLE DU POLYMORPHISME GENETIQUE)

Direction scientifique : Dr Léa PAYEN

Jury composé de :
- Dr Michel Tod (Université Lyon 1) – *Président du jury*
- Dr Pierre Cuq (Université Montpellier 1) - *Rapporteur*
- Dr Jean-Michel Jault (Institut de Biologie Structurale, Grenoble) - *Rapporteur*
- Dr Léa Payen (Université Lyon 1) – *Directeur de thèse*
- Dr Eric Jacquet (Institut de Chimie des Substances Naturelles) – *Examinateur*
- Pr Ahcene Boumendjel (Université Joseph Fourier, Grenoble) – *Examinateur*

UNIVERSITE CLAUDE BERNARD - LYON 1

Président de l'Université	**M. le Professeur L. Collet**
Vice-président du Conseil Scientifique	M. le Professeur J-F. Mornex
Vice-président du Conseil d'Administration	M. le Professeur G. Annat
Vice-président du Conseil des Etudes et de la Vie Universitaire	M. le Professeur D. Simon
Secrétaire Général	M. G. Gay

COMPOSANTES SANTE

Faculté de Médecine Lyon Est – Claude Bernard	Directeur : M. le Professeur J. Etienne
Faculté de Médecine Lyon Sud – Charles Mérieux	Directeur : M. le Professeur F-N. Gilly
UFR d'Odontologie	Directeur : M. le Professeur D. Bourgeois
Institut des Sciences Pharmaceutiques et Biologiques	Directeur : M. le Professeur F. Locher
Institut des Sciences et Techniques de Réadaptation	Directeur : M. le Professeur Y. Matillon
Département de Biologie Humaine	Directeur : M. le Professeur P. Farge

COMPOSANTES ET DEPARTEMENTS DE SCIENCES ET TECHNOLOGIE

Faculté des Sciences et Technologies	Directeur : M. le Professeur F. Gieres
Département Biologie	Directeur : M. le Professeur C. Gautier
Département Chimie Biochimie	Directeur : Mme le Professeur H. Parrot
Département GEP	Directeur : M. N. Siauve
Département Informatique	Directeur : M. le Professeur S. Akkouche
Département Mathématiques	Directeur : M. le Professeur A. Goldman
Département Mécanique	Directeur : M. le Professeur H. Ben Hadid
Département Physique	Directeur : Mme S. Fleck
Département Sciences de la Terre	Directeur : M. le Professeur P. Hantzpergue
UFR Sciences et Techniques des Activités Physiques et Sportives	Directeur : M. C. Collignon
Observatoire de Lyon	Directeur : M. B. Guiderdoni
Ecole Polytechnique Universitaire de Lyon 1	Directeur : M. le Professeur J. Lieto
Institut Universitaire de Technologie de Lyon 1	Directeur : M. le Professeur C. Coulet
Institut de Science Financière et d'Assurance	Directeur : M. le Professeur J-C. Augros
Institut Universitaire de Formation des Maîtres	Directeur : M R. Bernard

« La sagesse, c’est d’avoir des rêves suffisamment grands pour ne pas les perdre de vue lorsqu’on les poursuit. »

Oscar Wilde

Je dédicace ce mémoire à celui qui m'a sans cesse tenu la main sur le chemin de la thèse : mon mari, Manuel Meyer.

A notre enfant à venir.

A mes parents.

A tous ceux qui se battent ou se sont battus contre le cancer pour leur vie, celle d'un proche, ou bien à travers la recherche.

REMERCIEMENTS

Je tiens tout d'abord à remercier ma famille. Je commencerai par mes parents, **Christine MERY** et **Armand HONORAT**, pour les deux remarquables exemples qu'ils sont à mes yeux, pour leur soutien et pour l'amour qui nous liera toujours. J'attends toutes les occasions que nous donnera la vie pour chaque fois vous rendre fiers et vous rappeler combien vous êtes importants aux yeux de votre enfant. Je pense aussi à ma petite sœur **Anaïs** pour qui je serai toujours là, à tout le reste de ma famille qui inclus les proches et ceux que l'on aimerait voir plus souvent, mais aussi mon parrain et ma marraine.

J'ai la chance d'avoir une seconde famille, c'est pourquoi je remercierai aussi ma belle-famille : **Paquita et Robert MEYER**, plus que des beaux-parents, des parents au cœur suffisamment grand pour me donner l'impression d'être un de leurs enfants ; mon beau-frère, mes belles-sœurs, **Roberto, Marine, Marie-France,** et mes neveux et nièces, **Lucie, Florian** et **Coline**, pour tous ces moments où les liens du sang ne veulent finalement plus rien dire et que seul l'amour qui nous unit compte.

Je continuerai et finirai de remercier ma famille par la personne la plus importante à mes yeux. Il représente à lui seul bien plus que ce que je pouvais attendre de cette vie : mon âme sœur, mon meilleur ami et mon mari, **Manuel MEYER**. Il y a tellement de choses pour lesquelles je voudrais le remercier mais il me faudrait ajouter un tome à ce mémoire ! Alors je vais essayer d'être succincte en le remerciant tout d'abord de ne pas être parti en courant quand je lui ai fait part de mes perspectives de « longues » études qui mettaient certains de nos projets personnels entre parenthèse. Mais plus sérieusement, merci de toujours avoir été là pour moi, de croire en moi de façon inconditionnelle et de toujours me donner l'impression d'être quelqu'un d'important quand je vois mon reflet dans tes yeux. Sans ton soutien et ta présence, je n'aurai jamais pu accomplir tout ce que j'ai fait au cours de ces 8 dernières années. Grâce à toi, j'ai pu m'épanouir dans la joie et la peine, dans la complicité et la différence, dans la musique et les silences qui suffisent à se comprendre, dans nos projets réalisés et à venir. J'aimerais pouvoir te rendre autant ! Et j'espère que te donner ton premier fils te remplira suffisamment le cœur pour que tu imagines, ne serait-ce qu'une seconde, jusqu'à quel point il est possible d'aimer quelqu'un. JTM mon bouille.

Je tiens aussi à remercier tout particulièrement mes amis pour tous ces moments de joies, de doutes, de rires et de larmes, ces moments d'évasion, ces moments qui vous permettent de comprendre, qu'être heureux, c'est être entouré des gens qu'on aime.

A présent, j'aimerai remercier le Professeur **Charles Dumontet** pour m'avoir accueillit au sein de son équipe riche de par la qualité des interactions entre ses différents membres. Je suis consciente de la chance d'avoir eu accès à un laboratoire « sur-équipé », où il a été facile de mettre en œuvre toutes les idées qui traversent nos têtes de scientifiques.

Je continuerai en remerciant le Dr **Léa Payen**, mon super directeur de thèse, qui a su tirer le meilleur de moi et qui m'a permit de réaliser une thèse dans des conditions plus que favorables. Grâce à sa prévoyance et à sa perspicacité, nous avons pu mener de nombreux travaux et ainsi assurer le déroulement plus que convenable de ma thèse. Son soutien et son implication dans ma formation m'ont permis de m'approcher au plus près du métier d'enseignant-chercheur, aussi bien par la mise en place de projets scientifiques ou de collaborations que par la prise en charge d'enseignements au sein de l'Université. Je suis très reconnaissante pour tout ce qu'elle m'a transmis et heureuse que nous ayons pu être aussi complémentaires l'une pour l'autre.

Je tiens également à remercier les personnes qui ont plus ou moins travaillé avec moi. Pour commencer, je pense à **Aurélia MESNIER** qui aussi passé beaucoup de temps sur ABCC11 avant que je ne vienne y poser ma patte.

Je pense aussi à tous ceux avec qui j'ai pu collaborer :

- le Pr **Jérôme GUITTON** que j'ai submergé d'échantillons à doser par HPLC MS-MS ;
- le Dr **Attilio DI PIETRO**, le Dr **Pierre FALSON**, le Dr **Hélène CORTAY**, **Ophélie ARNAUD** et **Doriane LORENDEAU** avec qui j'ai eu la chance de vivre de fructueuses collaborations et d'enrichissantes discussions autour de nos protéines ABC fétiches ;
- le Dr **Raphaël TERREUX** qui m'a initié aux perspectives du monde bio-informatique.

Je remercie également les membres de mon comité de thèse : le Pr **Olivier FARDEL** et le Dr **Caroline MOYRET LALLE**. Merci de m'avoir accompagnée, d'avoir eu un regard critique sur mon travail et de m'avoir donné vos conseils pour que tout se déroule bien pendant et après ma thèse.

J'ai une pensée toute particulière pour la ligue nationale contre le cancer et ses donateurs anonymes grâce à qui mon travail a été soutenu financièrement pendant 3 ans.

Un immense merci pour les charly's angels : **Eva-Laure MATERA**, **Emeline PERRIAL** et **Stéphanie HERVEAU** dont l'importance n'est plus à démontrer au sein du laboratoire. Même si nous ne travaillions pas sur les mêmes projets, leur expérience technique infaillible, leur disponibilité à toute épreuve et leur organisation du tonnerre m'ont souvent aidée. Maintenant, je dois m'excuser car après mon départ, il va falloir trouver :

- une autre secrétaire pour répondre au téléphone et vous sortir des manips pour prendre les appels, peu importe la pièce que vous ayez choisie pour manipuler en paix;
- un autre utilisateur des TCL pour apporter les journaux chaque matin ;
- une autre maniaque pour nettoyer, re-nettoyer les paillasses, les hottes, les bains-marie ou bien ranger et trier les tiroirs, les boîtes d'enzymes ou d'anticorps… ;
- une autre experte pour dépanner l'imprimante super méga pratique… quand elle fonctionne ;
- une autre volontaire pour déménager le laboratoire tous les 2 mois, pour monter des meubles en kit (surtout ceux avec des panneaux coulissants) ou pour éponger la pièce noire après chaque orage (sur ce coup là, je fais confiance à Saïd);
- une autre âme persévérante pour travailler dans un bureau qui prend l'eau pendant les travaux de la façade;
- une autre cuisinière pour alimenter le labo en patisserie, tout du moins en crumble ;

Je remercie aussi mes compatriotes thésards (anciens et actuels) qui m'ont fait part de leur expérience ou qui ont simplement partagé leurs années de thèse avec moi : **Lars JORDHEIM**, **Anne BEGHIN**, **Sandra GHAYAD**, **Stéphane DALLE**, **Jennifer AIM** et surtout **Rouba SLEIMAN, Lina RESLAN et Ines TAGGOUG** (avec lesquelles j'ai aimé partager les « joies » de la thèse et les richesses de nos cultures respectives) et pour finir **Minh NGOC DUONG** (héritier du flambeau des thésards pour les années à venir).

Je tiens à remercier tout spécialement **Saïd BENNIA**, notre homme à TOUT faire, qui a su se rendre indispensable de par ses dons multiples, son dynamisme et sa bienveillance.

Je pense aussi à tous ceux qui ont un jour foulé le sol du labo de cyto (technicien(ne)s, stagiaires) dont la liste serait trop longue mais dont le passage ne sera pas oublié.

Et pour finir, je remercie le **chocolat**, sans qui le labo du cyto ne survivrait pas…

RESUME EN FRANÇAIS

Première cause de décès par cancer chez la femme, le cancer du sein développe souvent une résistance à la chimiothérapie pouvant impliquer des transporteurs ABC (ATP Binding Cassette). Ils transportent les médicaments hors de la cellule et diminuent leur efficacité thérapeutique. Nous nous sommes intéressés à la protéine **ABCC11 ou MRP8 (Multidrug Resistance Protein 8)**, exprimée dans le sein et responsable de l'efflux de certains anticancéreux (5FdUMP et méthotrexate).

Nous avons démontré que l'expression d'ABCC11 était **dépendante des voies de signalisation impliquant ER (Récepteur aux œstrogènes) ou PR (Récepteurs à la Progestérone)**. De plus, le tamoxifène (antagoniste d'ER) et la dexaméthasone (activateur de PR), utilisés en association avec la chimiothérapie, induisent l'expression d'ABCC11 et influenceraient négativement la réponse aux traitements anticancéreux à base de substrats d'ABCC11. L'expression d'ABCC11 a été positivement corrélée à celles d'ER et PR dans des cancers du sein.

En parallèle, nous avons généré **2 modèles *in silico*** en conformation ouverte vers l'intracellulaire ou vers l'extracellulaire et identifier des acides aminés potentiellement critiques dans l'architecture de la protéine ainsi que dans la liaison avec certains substrats (5FdUMP et GMPc).

Nous avons également généré les outils moléculaires permettant l'étude de l'**impact de 13 SNP (Single Nucleotide Polymorphism)** non synonymes d'ABCC11. En raison d'une instabilité des lignées cellulaires, l'étude n'a pu être menée à son terme.

Notre travail a ainsi contribué à une meilleure caractérisation d'ABCC11 et souligne sa potentielle valeur pronostic et prédictive dans le traitement du cancer du sein.

TITRE EN ANGLAIS

ABCC11 in breast cancer: Expression regulation by steroids and Structure/Function relationship study (Homology modeling and Genetic Polymorphism Influence).

RÉSUMÉ EN ANGLAIS

Leading cause of woman death by cancer, breast cancer can unfortunately develops chemotherapy resistance involving ABC (*ATP Binding Cassette*) transporters. They transport drugs out of cells and decrease their therapeutic efficiency. We studied one ABCC sub-family member: **ABCC11 or MRP8 (*Multidrug Resistance Protein 8*)**, expressed in breast and responsible for anticancer agent efflux (5FdUMP and methotrexate).

We have demonstrated that ABCC11 expression was **associated with ER (*Estrogen Receptor*) and PR (*Progesterone Receptor*) signaling pathways**. Furthermore, tamoxifen (ER antagonist) and dexamethasone (PR activator), used in association with chemotherapy, increased ABCC11 expression and would negatively influence the response of ABCC11 substrate based anticancer treatments. Moreover, ABCC11 expression was positively correlated to ER and PR expression in breast cancer.

In parallel, we have generated **two *in silico* models obtained by homology.** They represent two different spatial conformations: intracellular-facing (ready to bind substrate) or extracellular-facing (ready to release substrate). This has allowed us to identify amino acid residues potentially essential for the protein architecture and for substrate binding (5FdUMP and cGMP).

In order to analyze **SNP (*Single Nucleotide Polymorphism*) impact** on ABCC11 expression and function, we generated vectors coding a wild-type or a mutated ABCC11 with 13 non-synonymous SNPs. But, we did not succeed to create stable expressing cell lines to make a complete study of those SNPs.

In conclusion, our work led to ABCC11 better characterization and underlined its putative prognostic and predictive value in breast cancer treatment.

MOTS CLES EN FRANÇAIS

Cancer du sein, Transporteurs ABC, ABCC11, MRP8, Récepteur aux œstrogènes, Récepteurs à la progestérone, Modélisation par homologie, SNP.

MOTS CLÉS EN ANGLAIS

Breast cancer, ABC transporters, ABCC11, MRP8, Estrogen receptor, Progesterone receptor, Homology modeling, SNP.

INTITULE ET ADRESSE DU LABORATOIRE

Unité Inserm 590

Laboratoire de cytologie analytique

Faculté de Pharmacie
8 Avenue Rockefeller
69373 LYON Cedex 08

SOMMAIRE

LISTE DES ABREVIATIONS

5FdUMP	5-FluoroDésoxy-Uracile MonoPhosphate
5FdURD	5-Fluoro-2'-Deoxyuridine
5FU	5-FluoroUracil
ABC	ATP-Binding Cassette
Amp	Ampicilline
Ara	Aracytine
BCRP	Breast Cancer Resistance Protein
BET	Bromure d'Ethidium
BHE	Barrière Hémato-Encéphalique
BHM	Barrière Hémato-Méningée
BHT	Barrière hémato-testiculaire
CFTR	Cystic Fibrosis Transmembrane Regulator
CS	Cellules souches
CT	Crossing Threshold
Dauno	Daunorubicine
DBD	DNA Binding Domain
DDT	Dichlorodiphenyltrichloroethane
DEPC	Diethyl Pyrocarbonate
DEX	Déxaméthasone
DHEAS	Dehydroepiandrosterone Sulfate
DHFR	Dihydrofolate-réductase
DMEM	Dulbecco's Modified Eagle Medium
E1S	Estrone-3-sulfate
E2	Oestrogènes
E217βG	17beta-oestradiol-17beta-D-glucuronide
ECL	Enhanced ChemoLuminescence
EGF	Epidermial Growth Factor
ER	Récepteurs aux œstrogènes
ERCC1	Excision Repair Cross-Complementing protein
ERE	Estrogen Response Element
ERKO	Estrogen Receptor Knock Out
Fluda	Fludarabine
FSH	Follicle Stimulating Hormone
FT	Facteurs de Transcription
Gemci	Gemcitabine
GR	Récepteur aux glucocorticoïdes
GSH	Gluthation
HER2	Human Epidermal growth factor Receptor 2
HSP	Heat Shock Protein
IGF-I	Insulin-like Growth Factor I
LBD	Ligand Binding Domain
LC-MS/MS	Liquid Chromatography-Tandem Mass Spectrometry

LCR	Liquide céphalorachidien
LH	Luteinising Hormone
LHRH	Luteinising Hormone Releasing Hormone
LTC4	Leucotriène C4
MAPK	Mitogen-Activated Protein Kinase
MDR	MultiDrug Resistance
M-MLV-RT	Moloney Murine Leukemia Virus Reverse Transcriptase
MRP	MultiDrug Resistance Protein
MSD	Membrane Spanning Domain
MTT	Bromure de 3-(4,5-dimethylthiazol-2-yl)-2,5-diphenyl tetrazolium
MTX	Méthotrexate
NBD	Nucleotide Binding Domain
NFκB	Nuclear Factor Kappa B
NK	Natural Killer
OMS	Organisation Mondiale de la Santé
PAH	Acide P-aminohippurique
PCN	Pregnenolone-16α-carbonitrile
PCR	Polymerase Chain Reaction
Perme	Permetrexed
Pgp	P-glycoprotéine
PKA	Protéine kinase A
PKC	Protéine kinase C
PRE	Progesterone Response Element
PROG	Progestérone
PVDF	Polyfluorure de vinylidène
PXR	Récepteur au pregnane X
RFC	Reduced Folate Carrier
RT	Rétro-Transcription
SCID	Severe Combined Immunodeficiency
SERM	Selective Estrogen Receptor Modulator
SNP	Single Nucleotide Polymorphism
STAT	Signal Transducers and Activators of Transcription
TGF-β	Transforming Growth Factor β
TGI	Tractus gastro-intestinale
TK1	Thymidine Kinase 1
TK2	Thymidine Kinase 2
TM	Traversées Membranaires
UMPK	UMP kinase

LISTE DES FIGURES

LISTE DES TABLEAUX

LISTE DES PUBLICATIONS

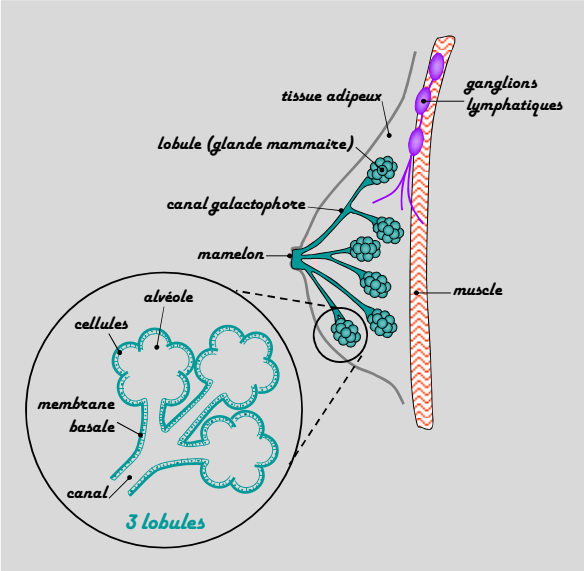

Figure 1. Organisation histologique du tissu mammaire normal.

Carcinome non infiltrant ou *in situ*

- **Carcinome intracanalaire ou canalaire *in situ* (CCIS)**
- **Carcinome lobulaire *in situ***

Carcinome infiltrant ou invasif

- **Carcinome infiltrant de type non spécifique (canalaire TNS)**
  - Carcinome de type mixte
  - Carcinome pléomorphe
  - Carcinome avec cellules géantes ostéoclastiques
  - Carcinome avec aspects choriocarcinomateux
  - Carcinome avec aspects mélanocytaires
- **Carcinome lobulaire infiltrant**
- **Carcinome tubuleux**
- **Carcinome cribriforme infiltrant**
- **Carcinome médullaire Carcinome produisant de la mucine**
  - Carcinome mucineux
  - Cystadénocarcinome et carcinome à cellules cylindriques sécrétantes
  - Carcinome à cellules en bague à chaton
- **Tumeurs neuroendocrines du sein**
  - Carcinome neuroendocrine de type solide
  - Carcinoïde atypique
  - Carcinome à petites cellules
  - Carcinome neuroendocrine à grandes cellules
- **Carcinome papillaire infiltrant**
- **Carcinome micropapillaire infiltrant**
- **Carcinome apocrine**
- **Carcinome métaplasique**
  - Carcinome métaplasique de type épithélial pur
    - *Carcinome épidermoïde*
    - *Adénocarcinome avec métaplasie à cellules fusiformes*
    - *Carcinome adénosquameux*
    - *Carcinome mucoépidermoïde*
  - Carcinome métaplasique mixte à composante épithéliale et conjonctive
- **Carcinome à cellules riches en lipides**
- **Carcinome sécrétant**
- **Carcinome oncocytique**
- **Carcinome adénoïde kystique**
- **Carcinome à cellules acineuses**
- **Carcinome à cellules claires (riches en glycogène)**
- **Carcinome sébacé**
- **Carcinome inflammatoire**

Maladie de Paget du mamelon

Figure 2. Classification des cancers du sein (OMS 2003 [1]).

A. INTRODUCTION

I. LE CANCER DU SEIN

Avec 519 000 décès par an, le cancer du sein est la cinquième cause mondiale de décès par cancer et représente environ 1 % de la mortalité mondiale (OMS février 2009). Chez la femme, le cancer du sein se place en première position. En France, il se classe en huitième position des causes de décès (3 % des décès français – OMS 2002). Il représente donc un problème majeur de santé publique.

1. Classification des cancers du sein

Le tissu mammaire est un tissu complexe formé par des glandes mammaires ou lobules reliés au mamelon par des canaux galactophores et entourés de tissue adipeux (**Figure 1**). Un lobule est constitué par plusieurs alvéoles formées par une couche de cellules qui reposent sur une membrane basale.

Les cancers du sein sont très hétérogènes. L'OMS a établit une classification officielle des cancers du sein en 1981 uniquement basée sur des critères morphologiques. Elle a été modifiée en 2002 et prend en compte des paramètres immuno-histochimiques (**Figure 2**). La plupart des noms donnés dépendent de la région mammaire où les cellules cancéreuses ont débuté leur prolifération. Le carcinome canalaire est le type le plus fréquent et provient de cellules canalaires. Le carcinome lobulaire est un autre type qui a débuté dans les lobules. Si le cancer reste dans la zone canalaire ou lobulaire, il est dit carcinome non-invasif ou *in situ*. A l'inverse, si la tumeur s'étend au tissu conjonctif en traversant la membrane basale, le carcinome est dit invasif ou infiltrant.

Parmi tous les types invasifs, certains sont dits de bon pronostic : les carcinomes tubuleux, mucineux, adénoïde kystiques et cribriformes infiltrants. Les types les plus fréquents sont les carcinomes infiltrants de type non spécifique (70 à 80%) et les carcinomes lobulaires infiltrants (5 à 15%). Les carcinomes médullaire, micropapillaire infiltrant, sécrétant juvénile et apocrine infiltrant sont rares. Les types les plus rares sont les carcinomes à cellules claires riches en glycogène, les carcinomes à cellules riches en lipides, les carcinomes à cellules en bague à chaton, les tumeurs neuroendocrines, les carcinomes à cellules géantes ostéoclastiques et les carcinomes à cellules acineuses, à cellules oncocytaires, sébacé, avec aspects choriocarcinomateux ou mélanocytaires.

Molécules naturelles		Produit Chimiques	
Ligands Physiologiques	**Phyto-œstrogènes**	**Environnementaux**	**Antagonistes (SERM ou purs)**
17β-estradiol estriol estrone	apigénine coumestrol génistéine kaempférol naringénine	alkylphenol bisphenol A chlordecone dichlorodiphenyltrichloroethane (DDT) methoxychlore hydroxybiphenyl polychloriné	afimoxifène arzoxifène bazedoxifène clomifène femarelle fulvestrant lasofoxifène ormeloxifène raloxifène tamoxifène toremifène

Tableau 1. Les différents ligands d'ER.

2. Quelques marqueurs essentiels

Les cancers du sein sont considérés selon leur type histologique mais aussi selon différents autres critères comme l'expression de marqueurs spécifiques (développés dans les paragraphes suivants), l'envahissement des ganglions axillaires ou la présence de métastase. L'envahissement des ganglions axillaires correspond à l'observation de cellules cancéreuses dans un ou plusieurs ganglions sentinelles situés sous les aisselles (premiers ganglions recevant le drainage lymphatique de la région tumorale). Plus le nombre de ganglions envahis est important, plus le risque de métastases est élevé [2]. La présence de ces métastases locales n'est pas dangereuse en elle-même mais leur présence/absence est un des facteurs pronostiques les plus efficaces dans le cancer du sein [3, 4]. En parallèle à l'envahissement ganglionnaire, le développement de métastases est aussi un facteur pronostique important. Les cellules de la tumeur primitive peuvent passer par la voie sanguine et/ou lymphatique et envahir l'espace pleural ou péritonéale provoquant la formation d'épanchement. Ces cellules au pouvoir de migration important peuvent aller s'installer dans d'autres organes pour former des métastases. Les organes préférentiellement touchés sont les poumons, le foie et les os. Les femmes développent fréquemment des métastases osseuses [5-8].

2.1 Récepteurs aux œstrogènes

Le tissu mammaire est un tissu sous forte imprégnation hormonale. Il exprime plusieurs récepteurs aux hormones tels que les récepteurs aux œstrogènes (ER) et les récepteurs à la progestérone. Ils font tous deux partie de la superfamille des récepteurs nucléaires qui régulent l'expression de gènes. Bien que les ligands physiologiques d'ER soient les œstrogènes, ces récepteurs sont capables de lier de nombreuses autres molécules naturelles ou synthétiques (**Tableau 1**).

2.1.1. Structure

ER existe sous deux isoformes ERα (alpha, NR3A1) et ERβ (béta, NR3A2). Ils sont respectivement composés de 595 et 530 acides aminés et sont codés par des gènes différents (respectivement 6q et 14q) [9-11]. ERα a été identifié par Jensen et Jacobsen en 1962 au cours d'une étude de l'effet des œstrogènes (E2) sur l'utérus [12]. L'isoforme n'a été cloné que 23 ans plus tard [13]. Jusqu'en 1996, découverte d'ERβ, ERα étais le seul récepteur des œstrogènes connu [14]. La découverte d'ERβ ouvrit de nouveaux horizons sur la compréhension des effets multiples des œstrogènes même sur des tissus n'exprimant pas ERα.

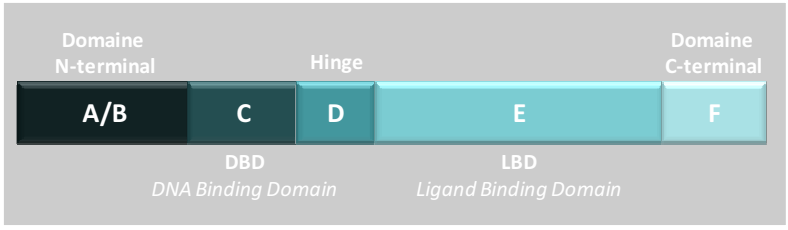

Figure 3. Structure générale des récepteurs aux œstrogènes.

De nombreux tissus dits « hormono-dépendants » expriment ces récepteurs. Ils peuvent être classés en deux groupes : les tissus cibles classiques des œstrogènes (utérus, sein, placenta, foie, système nerveux central, système cardio-vasculaire et os) et les tissus cibles non classiques des œstrogènes (prostate, testicule, ovaire, épiphyse, thyroïde, parathyroïde, glande surrénale, pancréas, vésicule biliaire, peau, système urinaire, tissus lymphoïde et érythrocytes) [15]. Les tissus cibles classiques expriment fortement ERα et répondent aux œstrogènes par une augmentation de la transcription des gènes. Les tissus cibles non classiques expriment faiblement ou pas ERα. Certains expriment fortement ERβ (prostate, épithélium, système uro-génital, follicules ovariens).

Les deux ER, bien que différenciés, présentent une structure biochimique commune et une homologie de séquence. Ces protéines sont composées par six domaines [16] (**Figure 3**) :

- le domaine N-terminal (domaines A et B) est impliqué dans les interactions inter- et intramoléculaires et dans l'activation de la transcription de gènes. Il contient un domaine de transactivation constitutivement actif (AF-1) qui s'associe avec des co-répresseurs ou co-activateurs. Ce domaine peut être sujet à la phosphorylation [16, 17].
- le domaine de liaison à l'ADN (DBD pour *DNA Binding Domain* ou domaine C) présente une structure en deux doigts de zinc qui permet la dimérisation du récepteur et sa liaison aux éléments de réponse aux œstrogènes (ERE pour *Estrogen Response Element* ou ER3) de séquence AGGTCANNNTGACCT.
- le domaine « hinge » (domaine D) intervient dans la dimérisation du récepteur et dans sa liaison aux protéines de chocs thermiques (Hsp pour *Heat Shock Protein*). Ce domaine subi des modifications post-transcriptionnelles de type acétylation [17] ou sumoylation [18].
- le domaine C-terminal (domaines E et F) contient le domaine de liaison à E2 (LBD pour *Ligand Binding Domain* ou domaine E) qui travaille en synergie avec les domaines A et B dans la régulation de la transcription, ainsi que le domaine F qui module l'activité transcriptionnelle d'ER [16]. Le LBD est également capable d'interagir avec les protéines chaperonnes de type Hsp 90 [19].

La plus grande homologie entre ERα et ERβ est retrouvée au niveau des domaines C (97 % d'identité) et E (59.1 %) [20]. Les domaines A, B, D et F sont moins conservés.

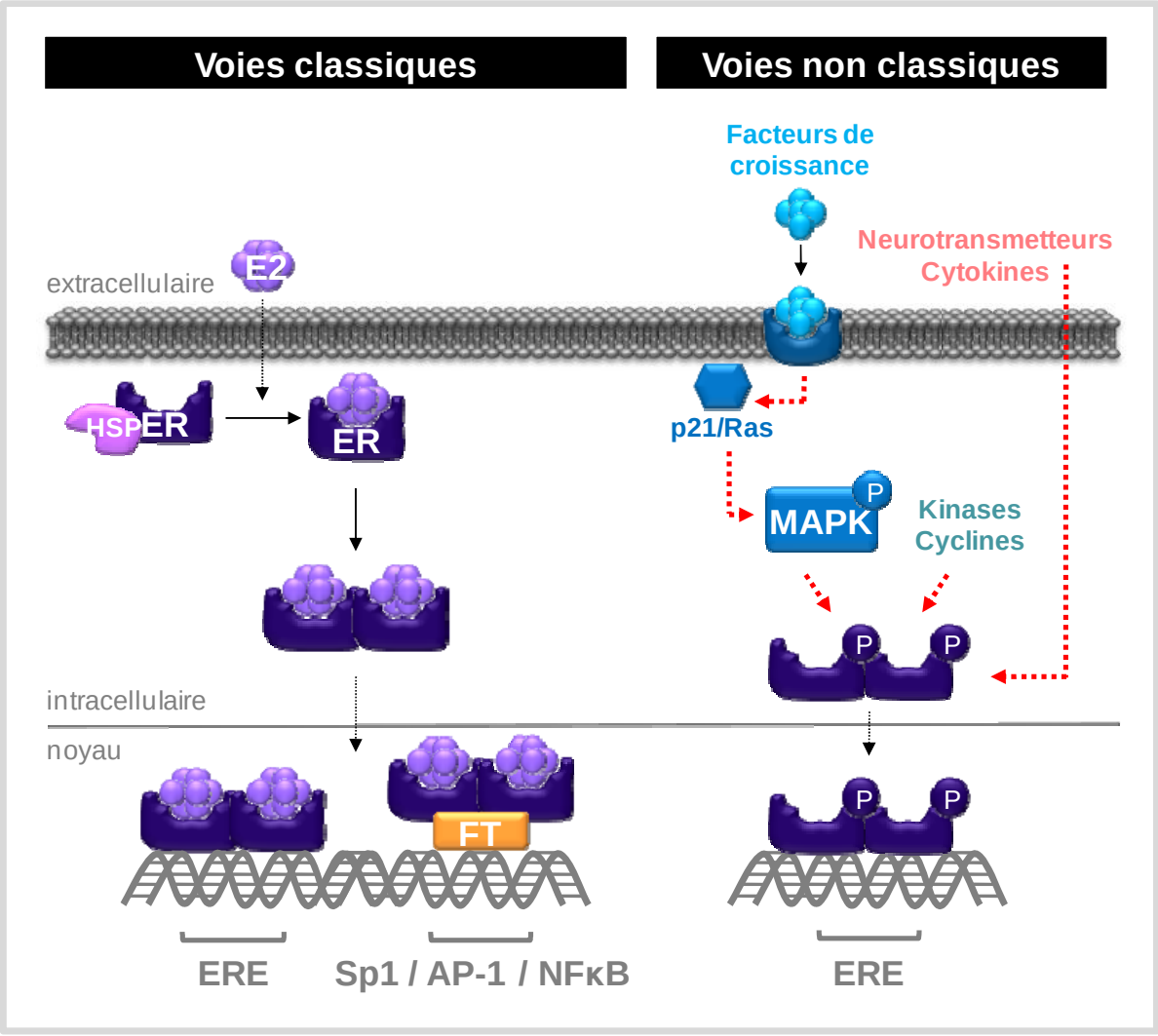

Figure 4. Mécanismes génomiques d'action des récepteurs aux œstrogènes.
E2 : œstrogènes ; ER : récepteurs aux œstrogènes ; HSP : protéine de choc thermique ; ERE : élément de réponse aux œstrogènes ; FT: facteurs de transcription; MAPK; mitogen activated protein kinase.

Malgré ces similarités, ERα et ERβ jouent des rôles différents. ERα est impliqué dans la prolifération induite via E2 alors qu'ERβ serait plutôt un gène suppresseur de tumeur [20-22]. ER présentent deux domaines à fonction d'activation de la transcription (AF). La région AF-1 située dans la portion N-terminale est impliquée dans la fonction activatrice du récepteur indépendamment de la fixation du ligand, et ce, via une altération de la phosphorylation du récepteur [23]. A l'inverse, le domaine AF-2 localisé en C-terminal permet une activation transcriptionnelle dépendant d'E2 [15, 24]. Les régions AF-1 et AF-2 interagissent avec différents co-activateurs ou corépresseurs et peuvent ainsi agir séparément ou de manière synergique. La contribution de ces deux domaines est dépendante du phénotype cellulaire. En effet, la fonction d'AF-1 est majoritaire dans les cellules bien différenciées, tandis que les cellules indifférenciés montrent une augmentation de l'activité transcriptionnelle d'ER grâce à la fonction d'AF-2 [25].

2.1.2. Mécanisme d'action

Le mécanisme moléculaire des ER est strictement dépendant de leur localisation cellulaire. Ils sont majoritairement localisés dans le cytoplasme et dans le noyau des cellules [26], bien qu'une fraction soit présente à la membrane plasmique [27, 28]. Le modèle mécanistique classique (mécanisme génomique) considère qu'en absence de ligand, ER est cytoplasmique et associé à des protéines Hsp (Hsp90, 70 et 56) qui le maintiennent dans un état inactif [16, 29] (**Figure 4**). La fixation du ligand à ER induit la dissociation du récepteur des protéines Hsp, la dimérisation et la translocation au noyau où ER se fixe directement à la séquence ERE sur le promoteur des gènes [30]. L'activation de la transcription de ces gènes dépend ensuite du recrutement de cofacteurs spécifiques (co-activateurs ou co-répresseurs) et de la machinerie transcriptionnelle basale [31]. En plus de l'interaction directe avec ERE, ER peut réguler la transcription sans se fixer directement à l'ADN (mécanisme non classique). Pour cela, ER s'associe avec des facteurs de transcription spécifiques tels que Sp-1 et AP-1 qui vont eux-mêmes se fixer sur le promoteur des gènes. ER peut également interagir avec NFKB (*Nuclear Factor Kappa B*) et induire une inhibition de la transcription via E2 [16].

En parallèle de la voie génomique classique, les ER peuvent être activés par une phosphorylation indépendante de la présence des œstrogènes [16] (**Figure 4**). Différentes molécules sont capables d'induire cette voie: 1) des kinases cellulaires telles que la PKA (Protéine kinase A) et la PKC (Protéine Kinase C), 2) des signaux extracellulaires (facteurs de croissance, neurotransmetteurs, cytokines) et 3) des régulateurs du cycle cellulaire (cycline A et D1).

Les facteurs de croissance représentent un groupe important d'activateurs d'ER, les autres signaux extracellulaires pouvant moduler l'activité d'ER étant représentés par l'héréguline, l'interleukine 2 et la dopamine. Les facteurs de croissance comptent parmi eux l'EGF (*Epidermial Growth Factor*) [32], l'insuline, l'IGF-I (*Insulin-like Growth Factor I*) et le TGF-β (*Transforming Growth Factor β*). Ils activent leurs récepteurs membranaires qui, par l'intermédiaire de p21Ras, vont alors déclencher une cascade de phosphorylation de MAPK (*Mitogen-Activated Protein Kinase*) [33]. Ces MAPK sont responsables de l'activation d'ERα en phosphorylant le site AF-1. Dans certains cas, la cible est le site AF-2 suggérant que différents médiateurs peuvent être impliqués. D'autre part, certaines activations d'ER peuvent être indépendantes des MAPK.

2.1.3. ER et cancer du sein

Les œstrogènes et les récepteurs aux œstrogènes jouent un rôle dans le contrôle du développement, le comportement sexuel et les fonctions reproductives. En effet, les souris femelles n'exprimant par ER (Knock out pour ER ou ERKO) sont stériles et présentent des anomalies anatomiques de l'utérus, des ovaires et des glandes mammaires [34, 35]. Les souris males ERKO sont moins fertiles bien que leur appareil génital paraissent normal du point de vue anatomique [34-36]. De plus, les deux genres présentent un tissu osseux moins dense [34]. Les souris femelles ERKO montrent un comportement caractéristiques des males (moins maternelles et plus agressives) [37] alors que les males semblent moins agressifs [38].

Le rôle critique du récepteur ERα dans la régulation de la croissance des cancers du sein est bien établi même si les mécanismes de cancérogénèse via E2 sont encore sujet au débat [39]. Les cancers du sein sont en effet classés selon l'expression d'ERα. La majorité des cancers sont ER positifs (70 %) et sont associés à un bon pronostic. Les cancers ER+ sont soumis à une thérapie ciblée (hormonothérapie), même si une proportion significative de patients présente ou développe une résistance au traitement. A l'inverse, les cancers ER négatif montre un phénotype plus agressif, métastatique et malin, entrainant un mauvais pronostic. Actuellement, l'expression d'ER est communément analysée par immuno-histochimie, à l'aide d'anticorps monoclonaux spécifiques. Au niveau du diagnostic, seul le marquage nucléaire est considéré comme positif (le marquage doit être supérieur à 10 % des cellules). L'expression d'ERβ, quant à elle, serait aussi un bon marqueur pronostic même s'il semblerait qu'il vaille mieux considérer le rapport entre ERα et ERβ que la seule expression d'ERβ [40].

2.2 Récepteurs à la progestérone

Tout comme ER, les récepteurs à la progestérone (PR) font partis de la superfamille des récepteurs nucléaires et sont exprimés au niveau du tissu mammaire. Ils sont capables de réguler l'expression de gènes en réponse à leur ligand physiologique, la progestérone, ou à d'autres modulateurs tels que la mifépristone ou le RU486 (antagoniste de PR) [41]. La progestérone est en particulier impliquée dans les fonctions reproductrices. Les souris femelles KO pour PR montrent d'ailleurs des anomalies importantes au niveau des organes reproducteurs. Elles sont incapables d'ovuler et montrent un développement anormal de l'utérus et des glandes mammaires [42].

2.2.1. Structure

PR existe sous deux isoformes dénommées PRA et PRB et codés par un seul gène sous le contrôle de deux promoteurs séparés [43]. PRA est une forme tronquée de PRB. En effet, PRA ne comporte pas les 164 acides aminés N-terminaux de PRB. La structure des PR est similaire à celle de ER et se composent de 6 domaines différemment conservés [44]:

- le domaine N-terminal (domaines A et B) peut être phosphorylé et est impliqué dans l'activation de la transcription. Il contient le seul site de sumoylation de PR [17];
- le domaine de liaison à l'ADN (DBD ou domaine C) présente une structure en deux doigts de zinc qui permet la dimérisation du récepteur et sa liaison aux éléments de réponses à la progestérone (PRE pour *Progesterone Response Element*) ;
- le domaine de liaison au ligand (LBD ou domaine E) qui reconnait les ligands et permet la dimérisation du récepteur ;
- les domaines D et F.

Les domaines C et E sont très conservés alors que les domaines A, B, D et F sont plus variables. Les deux PR présentent deux domaines d'activation de la transcription. Le premier AF-1 est localisé dans la région N-terminale et, comme pour ER, est activé indépendamment de la fixation du ligand. Le deuxième AF-2 est dépendant de la fixation du ligand et contenu dans le LBD en C-terminal. De plus, PRB présente en amont un troisième domaine (AF-3) absent chez PRA [45].

2.2.2. Mécanisme d'action

Bien que les deux formes de PR présentent des structures similaires et qu'ils soient identiques dans la fixation de l'ADN et du ligand, des études ont démontré qu'ils n'étaient pas fonctionnellement identiques. Dans la plupart des cas, PRB agit comme un activateur de la transcription de gènes alors que PRA agit comme un répresseur dominant de la transcription de PRB et d'autres récepteurs nucléaires [46]. Le domaine AF-3 de PRB est partiellement responsable de son activité transcriptionnelle plus élevée. Un domaine d'inhibition de la fonction a été décrit en N-terminal [47]. Il n'agit que sur AF-1 et 2 mais pas sur AF-3 ce qui expliquerait le potentiel activateur de PRB.

La voie d'activation de PR implique que PR soit inactif en absence de son ligand et associé à des protéines chaperonnes de type Hsp (Hsp 90, 70 et 40) ou non [48, 49]. La fixation du ligand engendre la libération du récepteur, sa dimérisation et sa translocation au noyau où il se fixe sur l'élément de réponse à la progestérone (PRE pour *Progesterone Response Element*). Le recrutement de co-régulateurs permet d'assurer une modulation efficace de la transcription des gènes [45, 50]. De la même manière qu'ER, PR peut agir indirectement sur la transcription des gènes via les protéines Sp1, AP-1 ou STAT (*Signal Transducers and Activators of Transcription*) [49]. En parallèle, PR peut aussi être activé en étant phosphorylé par certaines MAPK [17].

2.2.3. PR et cancer du sein

Le niveau d'expression de PRA et de PRB est spécifique à chaque tissu ou type cellulaire. Le rapport entre les niveaux d'expression de PRA et PRB définit la réponse physiologique et pharmacologique à la progestérone. Dans le tissu mammaire, ce rapport est constant de la puberté à la grossesse mais diffèrent selon les espèces [51]. Des études utilisant des souris génétiquement déficiente en l'expression de PRA (PRA-/-) ont démontré que PRB est surtout impliqué dans la réponse à la progestérone au cours des processus normaux de prolifération et de différenciation de la glande mammaire [52]. La surexpression de PRA face à PRB ou l'inverse est associée à un développement anormal de la glande mammaire des souris [53, 54]. La régulation de l'expression de PRA et PRB et le rapport entre les deux isoformes sont donc nécessaires pour une réponse appropriée de la glande mammaire à la progestérone. Une proportion significative de faibles niveaux de PRB (et donc de rapports PRA/B élevés) a été observée dans des échantillons de cancer du sein [55]. Ces données soulignent la probable implication du déséquilibre PRA/PRB dans le développement et la progression du cancer du sein.

L'expression du récepteur à la progestérone est analysée par marquage immuno-histochimique dans le but d'améliorer la valeur pronostic d'ER [56]. En effet, les cancers du sein ER+ et PR+ présentent un meilleur pronostic que les cancers ER+ et PR-.

2.3 Le récepteur HER2

Le récepteur aux facteurs de croissance épidermaux humain 2 (HER2 pour *Human Epidermal growth factor Receptor 2*) est amplifié dans 25 à 30 % des cancers du sein. Dans ce cas, la protéine (aussi appelée ERBB2) est exprimée d'une manière anormalement élevée à la surface des cellules cancéreuses [57, 58]. Les cancers du sein surexprimant HER2 sont agressifs et de mauvais pronostic [57-61]. Le rôle direct de l'amplification d'HER2 a été démontré dans la tumorigenèse [62-65], en faisant une cible thérapeutique de choix.

Plusieurs anticorps monoclonaux furent développés chez la souris et dirigés contre le domaine extracellulaire de la protéine HER2. Ils sont capables d'inhiber, *in vitro* et *in vivo*, la prolifération de cellules cancéreuses humaines qui surexpriment HER2 [66, 67]. Afin de minimiser l'immunogénicité chez l'homme, l'anticorps le plus efficace a été modifié en alliant une partie de l'anticorps murin (région fixant la protéine) avec une immunoglobuline G humaine (région structurale) [68]. Cet anticorps (Trastuzumab ou Herceptin™) a été testé *in vitro* et *in vivo* sur des cellules de carcinomes mammaires qui surexprimaient HER2 [68, 69]. L'Herceptin™ inhibe la croissance des tumeurs [70]. Ces effets sont synergiques en association avec certains anticancéreux comme le cisplatine [71], le carboplatine [72], la doxorubicine, le cyclophosphamide, le méthotrexate ou le paclitaxel [69, 72-74]. Les essais cliniques ont démontré que l'anticorps n'était pas toxique et efficace sur des tumeurs métastatiques HER2 positive ne répondant pas à la chimiothérapie [75, 76]. En accord avec les résultats précliniques, son efficacité est supérieure lorsqu'il est utilisé en parallèle d'une chimiothérapie [76, 77] et améliore le traitement de cancers du sein métastatiques HER2 positif [78].

HER2 est détectée au niveau protéique par un marquage immuno-histochimique ou au niveau génétique par marquage de l'amplification (hybridation *in situ*).

3. Les traitements du cancer du sein

3.1 Les différents traitements

- ☑ La chirurgie reste le principal traitement. Pendant l'opération, la tumeur est prélevée (tumorectomie) et une analyse anatomopathologique est réalisée pour définir le type et les marqueurs principaux. Cette étape préalable est indispensable à l'établissement d'un traitement chimiothérapeutique personnalisé. Si la tumeur est petite (inférieure à 2 ou 3 cm), le sein peut être conservé. Dans le cas contraire, le médecin procède à une mastectomie (ablation totale du sein).

- ☑ Le curage axillaire (ablation des ganglions axillaires) permet de limiter la diffusion et l'établissement des métastases. Il est indispensable sauf pour les petites tumeurs pour lesquelles seule une partie des ganglions est prélevée pour analyse anatomo-pathologique du ganglion sentinelle. Il s'agit du premier ganglion recevant le drainage lymphatique de la tumeur. Dans le cas où il révèle un envahissement, le curage ganglionnaire est réalisé.

- ☑ La radiothérapie utilise des radiations pour détruire les cellules cancéreuses. Elle peut être néo-adjuvante (avant la chirurgie) en cas d'inflammation ou de cancer évolué. Après une chirurgie conservatrice, une radiothérapie adjuvante doit toujours être réalisée car elle diminue significativement le risque de récidive locale. La radiothérapie sera d'autant plus importante que la femme est jeune. En cas d'ablation totale, la radiothérapie est indiquée, dans certains cas, pour diminuer le risque de récidive locale. En fonction de la localisation de la tumeur et de son type, les chaînes ganglionnaires peuvent aussi être irradiées.

- ☑ La chimiothérapie fait intervenir de nombreux agents anticancéreux qui ciblent les cellules qui prolifèrent rapidement. Elle peut être néo-adjuvante (en cas d'inflammation ou de cancer évolué) ou adjuvante (post-chirurgie). Elle n'est pas systématique mais dépend du type de tumeur. Dans le cas de rechute, un traitement général par chimiothérapie peut être appliqué.

- ☑ L'hormonothérapie est employée dans les cancers du sein dits « hormono-dépendants » (exprimant les récepteurs aux œstrogènes). Cette thérapie cible ER (utilisation d'anti-œstrogènes) ou repose sur la suppression de ligand disponible pour ER (inhibition de leur sécrétion ou de leur synthèse). Elle peut être utilisée de manière adjuvante en parallèle de la chimiothérapie. Dans le cas de rechute, l'hormonothérapie peut être prescrite comme traitement général.

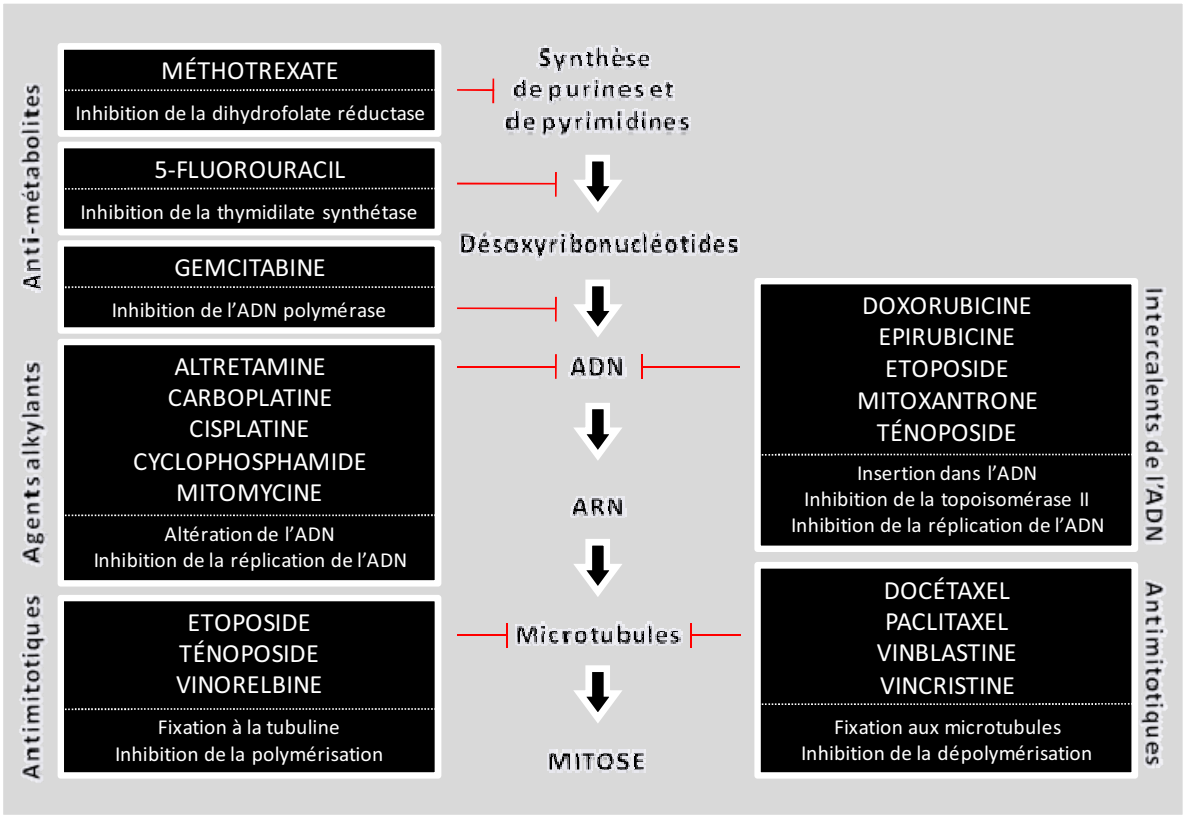

Figure 5. Différents types d'agents anticancéreux utilisés dans le traitement du cancer du sein.

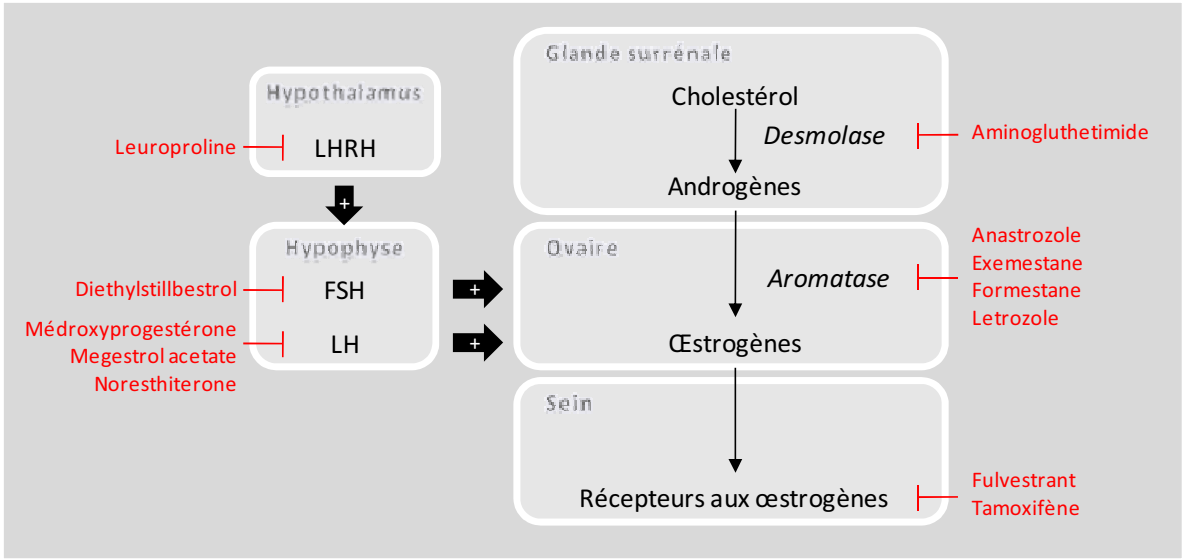

Figure 6. Médicaments utilisés dans l'hormonothérapie du cancer du sein.
FSH Follicule Stimulating Hormone; LHRH Luteinising Hormone Releasing Hormone; LH Luteinising Hormone

☑ Les thérapies ciblées reposent sur l'action de molécules ciblant un acteur cellulaire en particulier. Elles peuvent, par exemple, faire intervenir des anticorps monoclonaux dirigés contre un antigène surexprimé par les cellules cancéreuses (ex : Heceptine® et HER2).

3.2 La chimiothérapie

Dans le cadre du cancer du sein, différentes sortes d'anticancéreux sont utilisés (**Figure 5**) :

- Les anti-métabolites sont similaires aux métabolites normaux et se positionnent à leur place pour affecter le métabolisme de la cellule (5-FluoroUracil, gemcitabine, méthotrexate).
- Les agents alkylants provoquent des lésions de l'ADN empêchant sa duplication et donc la prolifération cellulaire (altrétamine, carboplatine, cisplatine, cyclophosphamide, mitomycine).
- Les intercalants de l'ADN s'insèrent au sein de l'hélice double brin de l'ADN et bloque la réplication de l'ADN et de ce fait la prolifération cellulaire (doxorubicine, épirubucine, étoposide, mitoxantrone, ténoposide).
- Les antimitotiques inhibent la polymérisation ou la dépolymérisation des microtubules formant le fuseau nécessaire à la phase de mitose (docétaxel, étoposide, paclitaxel, ténoposide, vinblastine, vincristine, vinorelbine).

Du fait de leur intervention sur différents acteurs du cycle cellulaire, les agents anticancéreux vont différemment être actifs selon les phases de ce cycle. Par exemple, les intercalants de l'ADN agissent au cours de la réplication de l'ADN et donc au cours de la phase S. Les antimitotiques, comme l'indiquent leur nom, vont eux agir pendant la phase M.

3.3 L'hormonothérapie

L'hormonothérapie fait intervenir différentes molécules (**Figure 6**) et consiste soit à:

- supprimer la sécrétion d'œstrogènes par le biais d'une ovariectomie ou par l'administration d'inhibiteurs de l'ovulation (diethylstilbestrol), de progestatifs (médroxyprogestérone, megestrol acetate, noresthiterone) ou d'analogues de la LH-RH ou *Luteinising Hormone Releasing Hormone* (leuprororeline);

- inhiber la liaison aux récepteurs aux œstrogènes de manière compétitive grâce à des anti-œstrogènes. Parmi ces agents se distingue le tamoxifène qui est un SERM (*Selective Estrogen Receptor Modulator*) dont l'effet peut être antagoniste ou agoniste selon le tissu exprimant ER. Le fulvestrant, quant à lui, est un anti-œstrogène pur.

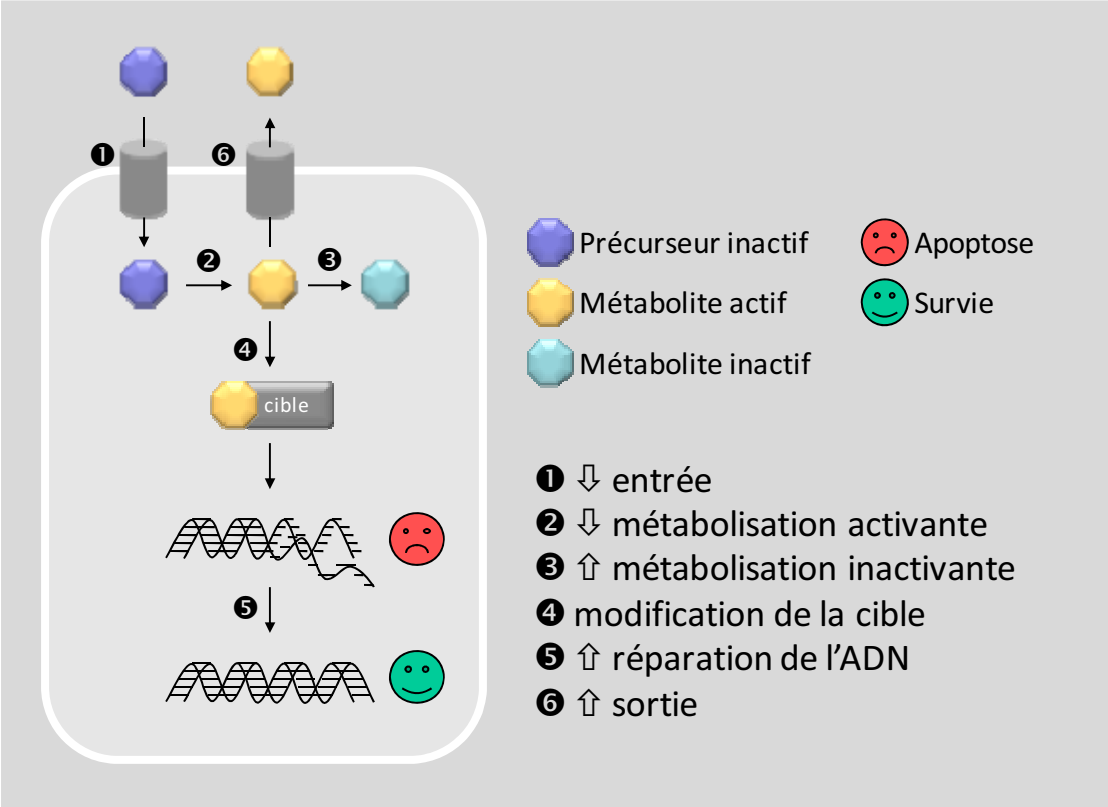

Figure 7. Principaux mécanismes de résistance à la chimiothérapie.

▪ inhiber la synthèse des stéroïdes surrénaliens (principale source d'œstrogènes) chez la femme ménopausée par l'administration d'inhibiteurs enzymatiques des hydroxylases (aminogluthéthimide, formestane) ou d'inhibiteurs de l'aromatase qui convertit les androgènes en œstrogènes (anastrozole, exemestane, formestane, létrozole).

4. Résistance à la chimiothérapie

Différents mécanismes cellulaires conduisant à un échec thérapeutique ont été décrits. La résistance peut être innée ou acquise au cours du traitement. La résistance intrinsèque survient dès le début de la chimiothérapie, sans phase de sensibilité. La chimiorésistance acquise se traduit par une première phase de sensibilité au traitement suivi par une phase de progression de la maladie. C'est le cas de nombreuses tumeurs solides comme le cancer du sein. Les mécanismes de résistance sont nombreux (**Figure 7**) et interviennent à différents niveaux :

- diminution de l'entrée du médicament. Certains anticancéreux nécessitent l'intervention d'un transporteur pour entrer dans la cellule et agir. Si l'expression du transporteur en question est diminuée alors la concentration intracellulaire en anticancéreux sera inefficace. Le méthotrexate, par exemple, est un folate pris en charge par le transporteur RFC (*Reduced Folate Carrier*). Une diminution de l'expression des RFC peut induire une résistance aux méthotrexate [79].
- diminution de la métabolisation en métabolite actif. De nombreuses molécules sont administrées sous forme de précurseurs et nécessitent une métabolisation pour devenir active. Si le mécanisme d'activation est diminué, la quantité de métabolite actif diminue et l'efficacité thérapeutique s'amoindrie. Le 5-FluoroUracil (5FU) est transformé en métabolite actif par l'UMPK (UMP kinase). Lorsque cette kinase est moins exprimée, la quantité de métabolite cytotoxique est diminuée et les cellules sont résistantes [80].
- augmentation de la métabolisation en métabolite inactif. Les métabolites actifs des anticancéreux peuvent à leur tour être métabolisés et perdre leur activité. Dans certains cas de résistance, cette métabolisation inactivante est accrue et induit logiquement une diminution de l'efficacité du traitement. Le méthotrexate, par exemple, est métabolisé en 7-hydroxy-méthotrexate qui présente moins d'affinité pour la cible et est donc moins efficace [81].

- altération de la cible du médicament. La cible peut être modifiée au niveau qualitatif (mutation) pour ne plus être reconnue par le médicament. La cible peut également être modifiée au niveau quantitatif (amplification du gène codant la cible). Dans ce cas, la quantité de médicament devient insuffisante pour avoir un effet toxique. Ceci est observé dans le cadre de traitement par les vinca-alcaloïdes dont la cible, la tubuline, n'est plus reconnue en raison d'une mutation sur son site de liaison. Les cibles contre lesquelles sont dirigés les anti-métabolites, comme la thymidylate synthétase pour le 5FU et la DHFR (dihydrofolate-réductase) pour le méthotrexate peuvent subir des modifications qualitatives et/ou quantitatives [82].
- échappement à l'apoptose. Les mécanismes de réparation de l'ADN sont accélérés suite à l'amplification des gènes codant pour les protéines impliquées dans la réparation. De cette façon, les dommages à l'ADN induits par le médicament n'induisent plus l'apoptose. La surexpression d'ERCC1 (*Excision Repair Cross-Complementing protein*) rend les cellules résistantes aux dommages causés par le cisplatine [83] en augmentant le processus de réparation de l'ADN.
- augmentation de l'efflux du médicament. Certains transporteurs tels que les transporteurs ABC (*ATP-Binding Cassette*) font sortir les anticancéreux de la cellule. La surexpression de telles protéines diminuent la concentration intracellulaire des médicaments et donc leur efficacité thérapeutique. La diversité des substrats pris en charge par ces protéines permet aux cellules qui les sur-expriment de développer un phénotype de résistance multiple aux médicaments ou phénotype MDR (*MultiDrug Resistance*). Ce point fera l'objet du paragraphe suivant.

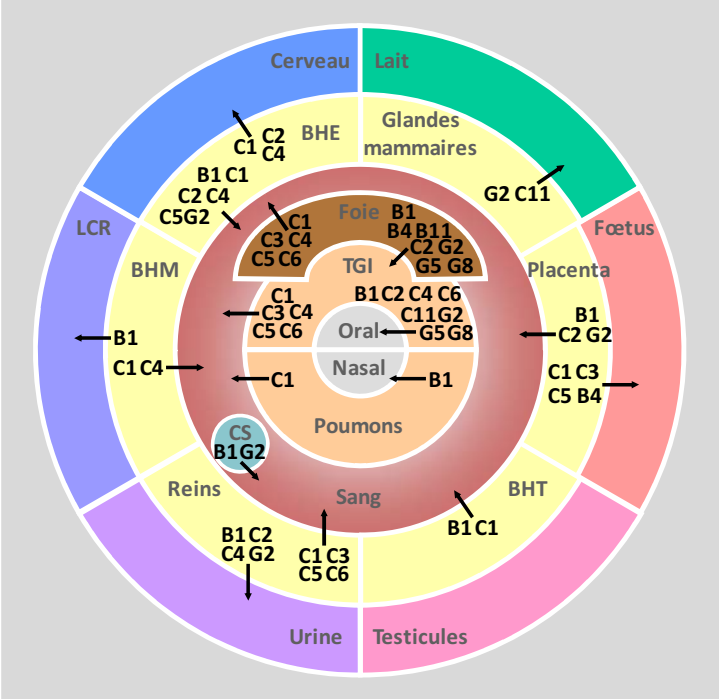

Figure 8. Expression des transporteurs ABC au niveau des barrières de l'organisme.
BHE = Barrière hémato-encéphalique ; BHM = Barrière hémato-méningée ; BHT = Barrière hémato-testiculaire ; CS = Cellules souches ; LCR = Liquide céphalorachidien ; TGI = Tractus gastro-intestinale. Inspirée par Szakács *et al. 2006 [84]*.

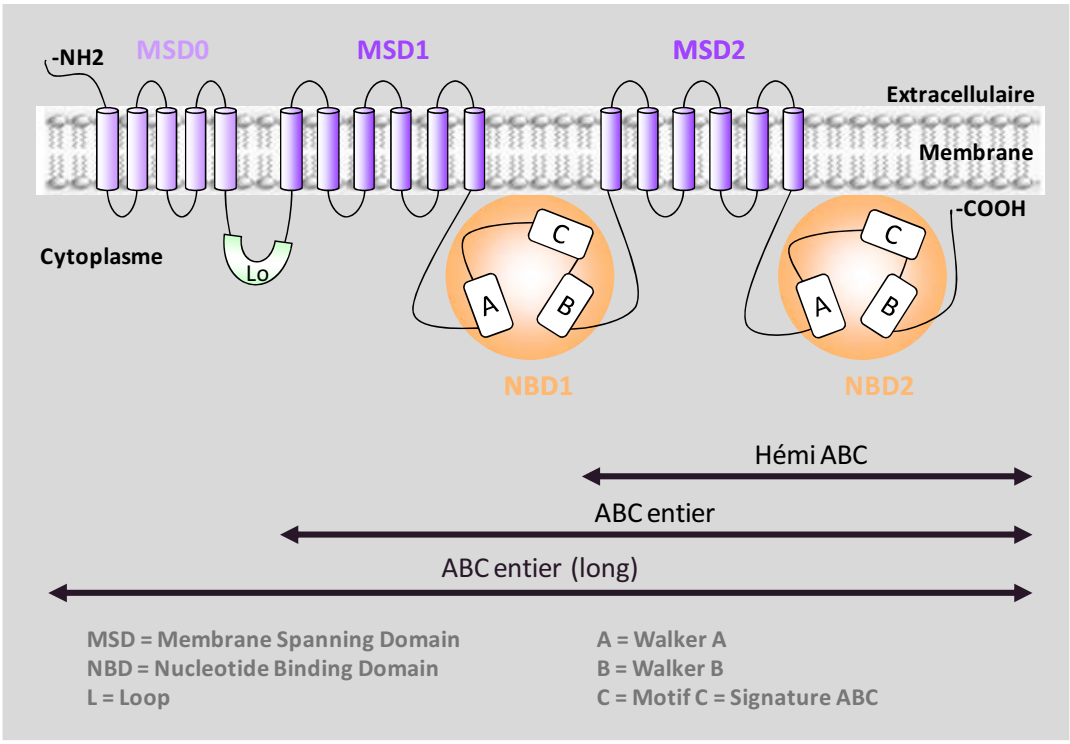

Figure 9. Structure des transporteurs ABC.
Les différents domaines constituants les transporteurs ABC sont schématisés et certaines séquences consensus sont représentées (A, B et C).

II. LES TRANSPORTEURS ABC

Avec 48 membres, les transporteurs ABC (*ATP Binding Cassette*) humains représentent l'une des plus grandes familles de protéines. Ces protéines sont classées en 7 sous-familles d'ABCA à ABCG, en fonction de leur homologie de séquence en acide aminés. Elles sont exprimées de manière ubiquitaire et souvent retrouvées au niveau des barrières de l'organisme telles que la barrière hémato-encéphalique (BHE) [85], le foie [86] ou les intestins [87]. Ces protéines sont capables d'effluer de nombreuses molécules endogènes et exogènes de structures et de fonctions variées : anions organiques, conjugués au glutathion, analogues de nucléosides, peptides [88]… Du fait de leur localisation, elles sont impliquées dans des processus physiologiques cruciaux en régulant l'élimination de molécules endogènes et exogènes (**Figure 8**). Lorsqu'elles sont exprimées sur la membrane apicale, elles sont responsables de l'élimination des xénobiotiques du foie, des reins et du tractus gastro-intestinale. Elles jouent également un rôle protecteur des testicules et du cerveau au niveau de la BHE.

1. Structure des transporteurs ABC

Les transporteurs ABC partagent la même topologie structurale avec la présence de MSD (*Membrane Spanning Domain*) et de NBD (*Nucleotide Binding Domain*). Les domaines MSD correspondent à plusieurs traversées membranaires (TM) sous la forme d'hélices α. Ils constituent un passage pour le substrat, vers le milieu extracellulaire. La fixation et l'hydrolyse de l'ATP, nécessaire à l'activité de transport, a lieu au niveau des NBD cytoplasmiques. Différents arrangements se distinguent sous la forme de transporteurs entiers ou d'hémi-transporteurs (**Figure 9**). Les transporteurs entiers contiennent au moins 2 MSD et 2 NBD alors que les hémi-transporteurs ne comportent qu'un seul MSD et un seul NBD. Le fonctionnement de ces transporteurs est détaillé ultérieurement dans la partie « Etude structure/activité d'ABCC11 ».

2. Les différentes sous-familles

La sous-famille **ABCA** comporte 13 membres et est constituée de transporteurs entiers suivant le schéma MSD1-NBD1-MSD2-NBD2 (**Tableau 2**) [88]. Elle est exprimée de manière ubiquitaire. Bien que les fonctions de tous ses membres ne soient pas encore décrites, certains sont impliqués dans l'homéostasie du cholestérol et des phospholipides (ABCA1) ou dans la vision (ABCA4).

Symbole	Alias	Gène	Expression	Orientation	Fonction
ABCA1	ABC1	9q31.1	Nombreux tissus		Efflux des phospholipides et du cholestérol
ABCA2	ABC2	9q34.3	Cerveau, Rein, Poumon, Cœur		Résistance aux médicaments
ABCA3	ABC3, ABCC	16p13.3	Poumons et autres tissus		Sécrétion de surfactant?
ABCA4	ABCR	1p21.3	Rétine, Cellules photoréceptrices		Efflux de N-Retinylidiene-PE
ABCA5		17q24.3	Muscle, Cœur, Testicules		NR
ABCA6		17q24.3	Foie		NR
ABCA7		19p13.3	Leucocytes, Thymus, Rate, Moelle osseuse		NR
ABCA8		17q24.3	Ovaire		NR
ABCA9		17q24.3	Cœur		NR
ABCA10		17q24.3	Muscle, Cœur, Monocytes		NR
ABCA12		2q34	Estomac		NR
ABCA13		7p12.3	Trachée, Testicules, Moelle osseuse		NR
ABCB1	PGP, MDR	7q21.12	Nombreux tissus	A	MDR
ABCB2	TAP1	6p21.3	Nombreux tissus		Transport de peptides
ABCB3	TAP2	6p21.3	Nombreux tissus		Transport de peptides
ABCB4	PGY3	7q21.12	Hépatocytes	A	Transport de phosphatidylcholine biliaire
ABCB5		7p21.1	Nombreux tissus		NR
ABCB6	MTABC3	2q35	Mitochondries		Transport de fer
ABCB7	ABC7	Xq21-q22	Mitochondries		Transport des précurseurs Fe/S (hème)
ABCB8	MABC1	7q36.1	Mitochondries		NR
ABCB9		12q24.31	Cœur, Cerveau, Lysosome		NR
ABCB10	MTABC2	1q42.13	Mitochondries		NR
ABCB11	SPGP	2q24.3	Hépatocytes		Transport de sels biliaires
ABCC1	MRP1	16p13.12	Nombreux tissus	B	MDR
ABCC2	MRP2	10q24.2	Foie, Intestin, Rein	A	Efflux d'anions organiques + MDR
ABCC3	MRP3	17q21.33	Intestin, Rein	B	Efflux d'anions organiques + MDR
ABCC4	MRP4	13q32.1	Nombreux tissus	A / B	Transport de nucléosides (MDR)
ABCC5	MRP5	3q27.1	Nombreux tissus	B	Transport de nucléosides (MDR)
ABCC6	MRP6	16p13.12	Rein, Hépatocytes	B	Transport de peptides et conjugués anioniques
ABCC7	CFTR	7q31.31	Poumon, Intestin	A	Canal aux ions chlorures
ABCC8	SUR	11p15.1	Pancréas		Régulation de canaux potassiques ATP dépendants
ABCC9	SUR2	12p12.1	Tous tissus		Régulation de canaux potassiques ATP dépendants
ABCC10	MRP7	6p21.1	Tous tissus (faibles)		Transport d'oestradiol et leucotriène C4
ABCC11	MRP8	16q12.1	Tous tissus	A	Transport de nucléotides cycliques + MDR
ABCC12		16q12.1	Tous tissus (faibles)		NR
ABCC13		21q11.2	Foie fœtal, Moelle osseuse, Leucocytes		NR
ABCD1	ALD	Xq28	Peroxysome		Transport d'acides gras à longue chaine
ABCD2	ALDL1, ALDR	12q11	Peroxysome		Transport d'acides gras
ABCD3	PXMP1, PMP70	1p22.1	Peroxysome		Transport d'acides gras
ABCD4	PMP69, P70R	14q24.3	Peroxysome		Transport d'acides gras
ABCE1	OABP, RNS4I	4q31.31	Ovaires, Testicules, Rate		Inhibiteur de la ribonucléase L
ABCF1	ABC50	6p21.1	Tous tissus		NR
ABCF2		7q36.1	Tous tissus		NR
ABCF3		3q27.1	Tous tissus		NR
ABCG1	ABC8, White	21q22.3	Cerveau, Rate, Poumon		Transport du cholestérol
ABCG2	MXR, BCRP	4q22	Placenta, Sein, Foie, Intestins	A	MDR
ABCG4	White2	11q23	Macrophages, Cerveau, Œil, Rate		NR
ABCG5	White3	2p21	Foie, Petit intestin	A	Transport du stérol
ABCG8		2p21	Foie, Petit intestin	A	Transport du stérol

Tableau 2. Les membres de la famille des transporteurs ABC.

A = Apical; B = Basolatéral; BHE= Barrière hémato-encéphalique; MDR (Multidrug Resistance) = Résistance multiple aux médicaments; NR = non renseigné.

Avec ses 11 membres, la sous-famille **ABCB** est la seule à comporter à la fois des transporteurs entiers et des hémi-transporteurs (**Tableau 2**) [88]. Ils peuvent être retrouvés dans divers tissus bien que certains (ABCB7, 8 et 10) soient exclusivement retrouvés au niveau des mitochondries. Ces derniers sont impliqués dans le métabolisme du fer. Les autres sont impliqués dans diverses fonctions allant de la présentation de l'antigène (ABCB2 et 3) à la sécrétion de la bile (ABCB4 et 11). La protéine ABCB1 également appelé P-glycoprotéine (Pgp) est le transporteur ABC humain le plus décrit. Son expression apicale au niveau de la BHE en fait un élément clé de la protection du cerveau contre les xénobiotiques (ex : ivermectine). Elle est également très largement impliquée dans le développement du phénotype MDR. De ce fait, son expression constitue un facteur prédictif chez les patients atteint de leucémies myéloïdes aigues et traités par un de ses substrats, la daunorubicine [89].

La sous-famille **ABCC** est constituée de 12 transporteurs entiers plus ou moins ubiquitaires et exprimés pour certains en apical ou bien en basolatéral (**Tableau 2**) [88]. Un 13ème membre a été rattaché à cette sous-famille mais son gène serait un pseudo-gène. Certains de ces membres (ABCC1, 2, 3, 6, 7, 8, 9 et 10) se distinguent par la présence d'un domaine MSD N-terminal supplémentaire (MSD0). Un des membres les plus décrits de cette sous-famille est ABCC7 ou CFTR (*Cystic Fibrosis Transmembrane Regulator*) dont la mutation est responsable du développement de la mucoviscidose. Les autres membres peuvent être impliqués dans la sécrétion de la bilirubine (ABCC2) ou de l'insuline (ABCC8 et 9) mais la plupart sont impliqués dans le phénotype MDR et regroupés sous le nom de MRP (*MultiDrug Resistance Protein*). Ces protéines MRP font l'objet d'une revue (suivant ce paragraphe) « *Multidrug Resistance-Associated Protein (MRP/ABCC Proteins*) » par M. Honorat et col.

Les 4 hémi-transporteurs de la sous-famille **ABCD** sont quant à eux exclusivement exprimés dans le peroxysome (**Tableau 2**) [88]. Ils participent à la régulation du transport des acides gras. Exprimés de façon ubiquitaire, les protéines des sous-familles **ABCE** (1 membre) et **ABCF** (3 membres) sont particulières puisqu'elles ne présentent qu'un domaine NBD. Ni MSD, ni fonction de transport n'ont été rapportés à ce jour (**Tableau 2**) [88]. Les 5 protéines **ABCG** sont des hémi-transporteurs inversés (structure NBD-MSD) impliqués dans le transport du cholestérol et des stérols (comme le sitostérol d'origine végétale) (**Tableau 2**) [88]. ABCG2 ou BCRP (*Breast Cancer Resistance Protein*) est particulièrement décrite dans les phénotypes MDR. Tout comme ABCB1, elle constitue un facteur prédictif dans la leucémie myéloïde aigue traités par un de ses substrats, la mitoxantrone [89] ainsi que dans d'autres cancers [90].

3. Les protéines MRP de la sous-famille ABCC

→ Publication 1. « **Multidrug Resistance-Associated Protein (MRP/ABCC Proteins)** » par M. Honorat et coll.

Chapitre publié dans Wiley series in Drug Deiscovery end Development (2009)

2

MULTIDRUG RESISTANCE-ASSOCIATED PROTEIN (MRP/ABCC PROTEINS)

MYLÈNE HONORAT,[1] CHARLES DUMONTET,[1] AND LEA PAYEN[1,2]

[1]*Université de Lyon, Lyon, France; Inserm, Lyon, France; Centre Léon Bérard Lyon, France; Université de Lyon, Lyon1, France*

[2]*Université de Lyon, Lyon, France; Université Lyon 1, Laboratoire de Toxicologie, Lyon, France*

CONTENTS

ABC Transporters and Multidrug Resistance, by Ahcène Boumendjel, Jean Boutonnat and Jacques Robert

2.1. INTRODUCTION

Subsequent to the discovery of P-glycoprotein (P-gp), investigations of cancer cells displaying the multidrug resistance (MDR) phenotype not associated with MDR1 expression led to the discovery of ABCC1, the founding member of the ABCC subfamily (1). At present, this subfamily C includes a total of 13 ABCC proteins, including the gene defective in cystic fibrosis (ABCC7) and the two sulfonylurea receptor genes (SUR1, SUR2). Most of these proteins (ABCC1–6 and ABCC10–12) have been identified as active ATP-dependent membrane transporters for organic anions or therapeutic compounds. In contrast to these active transporters, ABCC7, the cystic fibrosis transmembrane conductance regulator (CFTR), is a regulated chloride channel, while ABCC8 (SUR1) and ABCC9 (SUR2) are sulfonylurea receptors and best described as intracellular adenosine triphosphate (ATP) sensors, regulating the permeability of specific K+ channels.

Genetic variation in these genes is the cause of or contributes to a wide variety of human disorders with Mendelian and complex inheritance, including Pseudoxanthoma elasticum (PXE) (ABCC6), cystic fibrosis (CFTR/ABCC7), persistent hyperinsulinemic hypoglycemia of infancy (SUR1/ABCC8), and MDR phenotypes (ABCC1). Hereditary deficiency of ABCC2, known as Dubin–Johnson syndrome (DJS) in humans, causes an increased concentration of bilirubin glucuronosides in blood.

Several members of different ATP-binding cassette (ABC) transporter subfamilies are capable of transporting an extraordinarily structurally diverse array of endo- and xenobiotics and their metabolites across cell membranes. Together, these transporters play an important role in the absorption, distribution, and elimination of exogenous (aflatoxin B1 metabolites, pesticides) and endogenous molecules (leukotriene C4 [LTC4], E217bG) in the body.

In this chapter, current knowledge of the biochemical, physiological, and pharmacological properties of nine members of the multidrug resistance protein (MRP)-related ABCC subfamily (ABCC1, ABCC2, ABCC3, ABCC4, ABCC5, ABCC6, ABCC10, ABCC11, and ABCC12) are summarized.

2.2. STRUCTURAL SIMILARITIES AMONG ABCC PROTEINS

The identification of the complete set of human ABCC genes allows a comprehensive phylogenetic analysis of this subfamily. The proposed nomenclature and topology of “short” and “long” ABCC proteins is in excellent agreement with the phylogenetic tree obtained (Fig. 2.1).

At present, there are no high-resolution structural data available on any eukaryotic ABCC transporter, in part due to the difficulty of obtaining crystals with these proteins. Therefore, biochemical experiments (mutagenesis analyses, photolabeling studies) are important to elucidate their membrane topology, their transport and catalytic functions, their positions, and the orientations of membrane-spanning segments within the polypeptide chain (2–5). The members of the ABCC subfamily fall into two different subclasses (“short” and “long”) on the basis of the phylogenetic tree, their domain arrangement, and the membrane topology (Fig. 2.2).

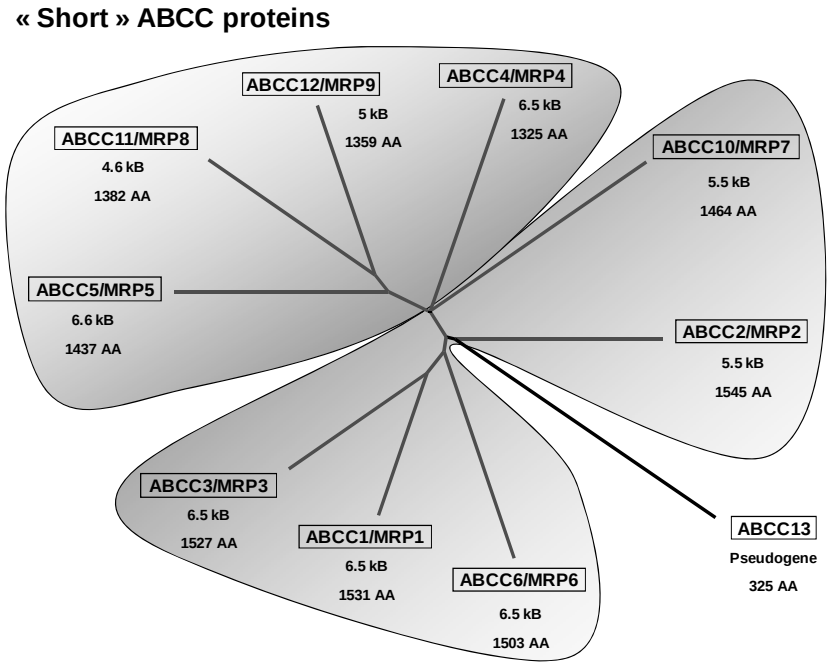

Figure 2.1. Dendrograms based on entire sequences (structural similarities) of the full-length ABCC proteins. Dendrograms are based on ClustalW alignments and were generated using Tree View. Topologies of short and long ABCC proteins were reported respectively in red and blue writing. The transcript and protein size were also indicated for each ABCC proteins.

The membrane topology model for human ABCC1 was described when the hydrophobicity analysis of the aligned sequences yielded a close matching of the transmembrane segments, thus suggesting a 6 + 6 transmembrane α-helix topology for the reference transporter ABCB1 as well. However, ABCC1 contains an N-terminal extension of about 250 amino acids. This highly hydrophobic amino-terminal segment of ABCC1 was suggested to be membrane embedded with five transmembrane helices transmembrane domain (TMD0) and an extracellular N-terminal amino acid (Fig. 2.2) (2, 6, 7).

ABCC1, 2, 3, ABCC6, and ABCC10 proteins form a subcluster within which each member possesses the N-terminal TMD0 (approximately 250 additional amino acids). The N-terminal TMD0 is absent from ABCC4, 5, 11, and 12. The presence of a TMD0-like domain in the long ABCC transporter is unique. The TMD0 of ABCC1 does not play a crucial role in transport activity of the protein, while the presence of the L0 is necessary for ABCC1-like transport activity and for the proper intracellular routing of the protein (5, 8). TMD0 has been described as important for ABCC1 retention in, or recycling to, the plasma membrane. TMD0 becomes essential for trafficking of ABCC1 when the COOH-terminal region of the protein is mutated. This means that the TMD0 of ABCC1 plays a role in the internalization of ABCC1 (5). In the case of ABCC1, the extracellular position of the NH2 terminus is supported by a large amount of experimental data (2, 9). Very recently, Yang et al. demonstrated a new function of the TMD0-L0 region in the dimerization ability of ABCC1. These recent findings suggest that ABCC1 may exist and function as a dimer and that TMD0-L0 likely plays a role in some structural and regulatory functions (10).

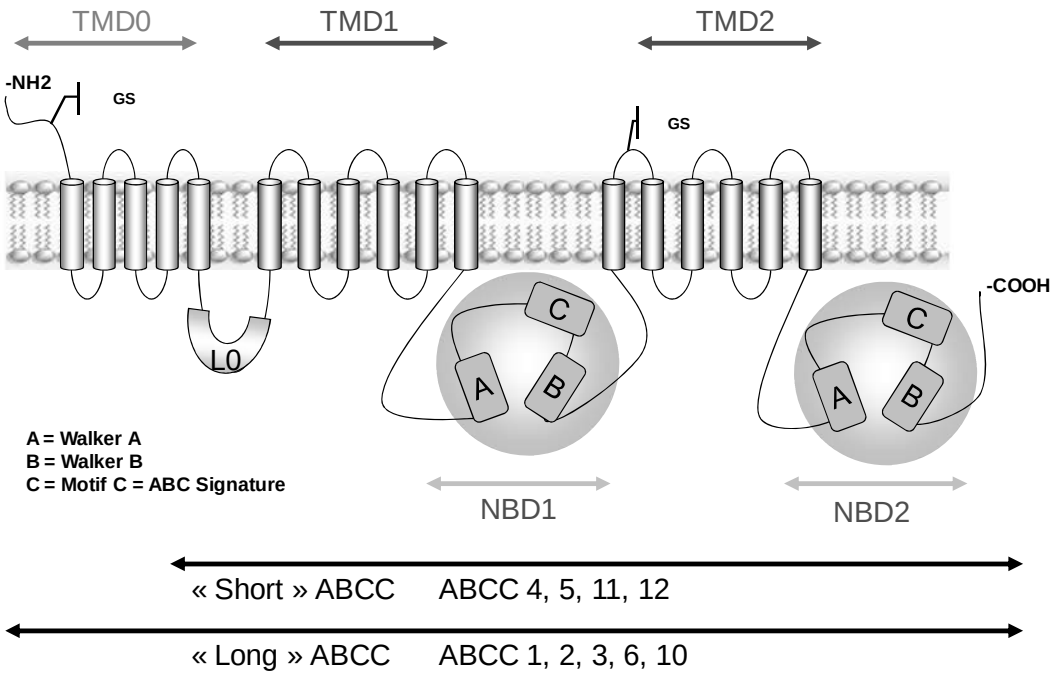

Figure 2.2. Topology of "short" and "long" ABCC proteins. The figure illustrates a simple probable topology of the "long" and "short" multidrug resistance proteins (ABCC). GS represents the glycosylation sites.

2.2.1. Transport Cycle

To achieve export, ABCC transporters require a minimum of two TMDs that form the ligand-binding sites and provide specificity for the transported substrate and two nucleotide-binding domains (NBDs) that bind and hydrolyze ATP to drive the translocation of the bound substrate (Fig. 2.3). Substrate binding is thought to occur through interactions within these transmembrane helices, as suggested by photolabeling experiments and site-directed mutagenesis analyses (11–25). The TMDs are not homologous between proteins of the ABCC subfamilies, explaining how different ABCC transporters can handle extremely diverse substrates, including glucuronide metabolites or reduced gluthatione (GSH) conjugates (see PART IV).

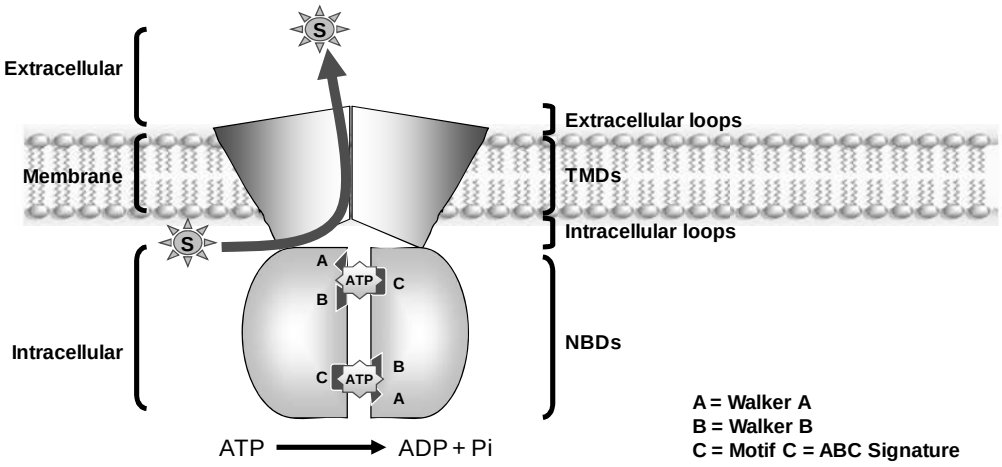

Figure 2.3. The minimal ABC transporter has four domains. Two transmembrane domains (TMDs) bind the ligand, while transport is driven by ATP binding and hydrolysis by the two nucleotide-binding domains (NBDs).

In contrast to the TMDs, the structural similarities between NBDs imply that they share a common evolutionary origin. NBDs have several characteristic motifs, including the Walker A and B motifs common to many nucleotidebinding proteins and other motifs like the ABC signature (motif C), stacking aromatic D-, H-, and Q-loops, which are unique and highly conserved in the ABCC subfamily. Thus, it is appropriate to consider an ABC transporter (at least in the closed dimer form, Fig. 2.3) as having two ATP-binding pockets with both NBDs contributing to each pocket, rather than each NBD having a separate ATP-binding site. Structural data show that the two ATP-binding pockets are not independent but are located at the interface of an NBD dimer "sandwich" (26–28). This implicates that the two NBDs act in concert as a single step rather than influencing distinct steps in the transport cycle (Fig. 2.4). The minimal ABC transporter has four domains. Two TMDs bind the ligand, while transport is driven by ATP binding and hydrolysis by the two NBDs. The Walker A motif appears to wrap around the phosphate chain of ATP, with the nitrogens of the residues within this motif extensively hydrogen bonding with the γ-phosphate of the bound nucleotide. The Walker B motif contributes an aspartate residue that coordinates and stabilizes a magnesium ion, which is required for ATP hydrolysis (29–31). Similarly, Asp and His in the D- and H-loop, respectively, make contact with water that stabilizes the binding of the nucleotide, while the conserved Gln residue in the Q-loop interacts with the catalytic Mg2+ and hydrolyzes a water molecule. The Q-loop glutamine also interacts with the γ-phosphate of ATP via a water molecule. In addition, the position of the Q-loop is important because it is in a position to couple the ligand-binding sites within the TMDs to the ATP-binding sites of the NBDs. These structural data are fully reviewed by Deeley et al. (4), Linton and Higgins (32), and Sauna and Ambudkar (33).

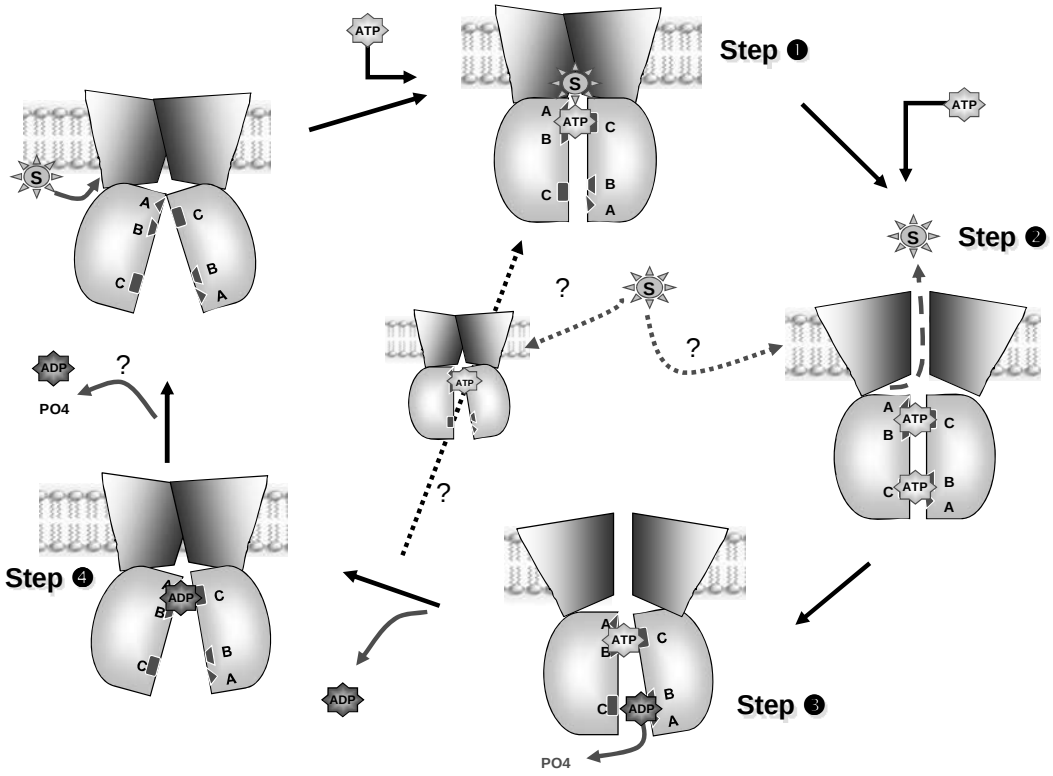

Figure 2.4. Schematic of the "ATP switch" model for the transport cycle of an ABCC transporter. The TMDs are spanning the membrane; the NBDs at the cytoplasmic face of the membrane. The transporter in its basal state (top left) has the NBDs in "open dimer" configuration with low affinity for ATP and a high-affinity, substrate binding site in the TMDs exposed to the inner leaflet of the membrane.

The “ATP-switch” model is the product of recent advances in structure determination and of biochemical data from a number of ABC transporters (4, 33, 34). Transport activity is a multistep process involving communication via conformational changes between NBDs and TMDs. The driver for transport is an on–off “switch” between two principal conformations of the NBDs: a “closed dimmer” formed by binding two ATP molecules at the dimer interface (step 3) and an “open dimmer” resulting from the dissociation of the “closed dimmer,” facilitated by ATP hydrolysis and PO4/ADP release. The “switch” from the “open” to the “closed” conformation of the NBD dimer induces conformational changes necessary for transport in the TMDs. The reverse of this switch, from the “closed” dimer to the “open” dimer after ATP hydrolysis (steps 3–4), resets the transporter to be ready for the next transport cycle (Figs. 2.3 and 2.4). In Fig. 2.4, we describe a model of the hypothetical transport cycle of ABCC1, based on the schematic for export of vinblastine by ABCB1/P-gp adapted from Linton and Higgins and fully described in the review, “Structure and Function of ABC Transporters” (4, 32).

Step 1. The cycle is initiated by binding of substrate (such as LTC4, GSH) to its high-affinity site(s), thereby strongly increasing affinity of NBD1 for ATP.

Step 2. This initial binding of ATP by NBD1 facilitates the binding of a second molecule of ATP at NBD2. Consequently, a “closed dimmer” formed by binding two ATP molecules at the dimer interface is performed. The conformational changes resulting from ATP binding are transmitted to the TMDs such that the substrate-binding site is exposed extracellularly and its affinity for substrate is reduced. Substrate is released extracellularly.

Steps 3–4. To restore the basal conformation, hydrolysis of ATP may occur sequentially at the NBDs. Sequential release of PO4, then ADP, restores the transporter to its basal configuration. The protein maintains a lowaffinity state following hydrolysis of ATP at NBD2, as long as NBD1 is occupied by ATP and ADP has not been released by NBD2. These data are strongly supported by experimental data (34). Nevertheless, how the protein resets for another cycle remains to be elucidated and hinges on whether or not NBD1 is catalytically active (Fig. 2.4) (4).

Interestingly, in the ABCC proteins, this catalytic cycle deviates in some cases from the scheme commonly described for other ABC proteins. In ABCC1, the NBDs behave very differently with respect to both ATP binding and hydrolysis. High-affinity binding of azido-ATP to NBD1 is readily demonstrable, while under hydrolytic conditions in the presence of vanadate, ADP is trapped predominantly by NBD2. Furthermore, binding of azido-ATP and the trapping of ADP by NBD2 requires that NBD1 be able to bind and possibly to hydrolyze ATP. In contrast, binding of ATP by NBD1 remains readily detectable when NBD2 is inactivated by mutations that eliminate ATP binding or ATPase activity. Mutation of the Walker A motifs in each NBDs also has different effects on transport activity (35, 36). Mutation of the conserved Walker A Lys residue in NBD1 only partially inactivates the protein while the comparable mutation in NBD2 essentially eliminates transport activity by a significant alteration of the tertiary structure of the protein (35–37). In addition, structural analysis of NBD1 revealed that the Walker A Ser-685 forms a hydrogen bond with the Walker B Asp792 and interacts with magnesium and the betaphosphate of the bound ATP. The interaction between the hydroxyl group of 685 residue and the carboxyl group of Asp792 plays a crucial role for the protein folding, and the interactions of the hydroxyl group at 685 with magnesium and the beta-phosphate of the bound ATP play an important role for ATP-binding and ATP-dependent solute transport (38). Recently, the acid glutamate following the Walker B motif in most NBDs of ABC proteins has been described to be critical for cleavage of the β-γ phosphodiester bond of ATP. Nevertheless, in NBD1 of ABCC1 (and other ABCC,

Fig. 2.4), this residue is Asp. The lack of glutamate has a profound effect on the ATP binding and hydrolysis characteristics of the NBD and, as a consequence, on the catalytic cycle of ABCC1 (39). Interconversion of these two residues profoundly affects the ability of the mutated NBDs to bind, hydrolyze, and release nucleotides (39). Therefore, regardless of whether the bound ATP at NBD1 is hydrolyzed or not, the release of the bound nucleotide from NBD1 may bring the protein back to its original conformation and facilitate the protein's starting of a new cycle of ATP-dependent solute transport (40). Similarly, substitution of H827 of H-loop in NBD1 with residues that prevented formation of these hydrogen bonds had no effect on the ATP-dependent solute transport, whereas corresponding mutations in NBD2 almost abolished the ATP-dependent solute transport completely (41). In contrast, substitutions of H1486 in H-loop of NBD2 with residues that might potentially form these hydrogen bonds exerted either full function or partial function, implying that hydrogen-bond formation between the residue at 1486 and the gamma-phosphate of the bound ATP and/or other residues, such as putative catalytic base E1455, together with S769, G771, T1329, and K1333, etc., holds firmly all the components necessary for ATP binding/hydrolysis so that the activated water molecule can efficiently hydrolyze the bound ATP at NBD2.

In recent years, due to crystallographic studies, much progress has been made in the elucidation of the three-dimensional structures of ABC transporters, including novel models for nucleotide hydrolysis and translocation catalysis. However, site-directed mutagenesis as well as the identification of natural mutations is still a major tool to evaluate effects of individual amino acids on the overall function of ABC transporters. These data were fully reported in the review specially dedicated to Frelet's mutation analysis (3).

2.2.2. Genomic Organization

Adjacent to the ABCC6 gene, the ABCC1 gene maps to chromosome 16p13.1 and was identified in the small-cell lung carcinoma cell line NCI-H69 (Fig. 2.5) (1). Nine alternative splicings were later described (nine isoforms: P33527-1, P33527-2, P33527-3, P33527-4, P33527-5, P33527-6, P33527-7, P33527-8, P33527- 9). The ABCC2 (MRP2/canalicular multispecific organic anion transporter [cMOAT]), ABCC3 (MRP3), ABCC4 (MRP4, MOATB), and ABCC5 (MRP5/ MOATC) genes map respectively to chromosomes 10q24, 17q21.3, 13q32, and 3q27 (Fig. 2.1). The genomic organization of ABCC1, 2, 3, 4, 5, and 6 is fully and clearly described on the following website (http://nutrigene.4t.com/ humanabc.htm). The human ABCC10 gene, consisting of 22 exons and 21 introns, greatly differs from other members of the human ABCC subfamily. It is localized on chromosome 6 (6p21). The ABCC10 cDNA sequence encodes a 1492 amino acid ABC transporter whose structural architecture resembles that of ABCC1 in that its transmembrane helices are arranged in three TMDs (see Fig. 2.1).

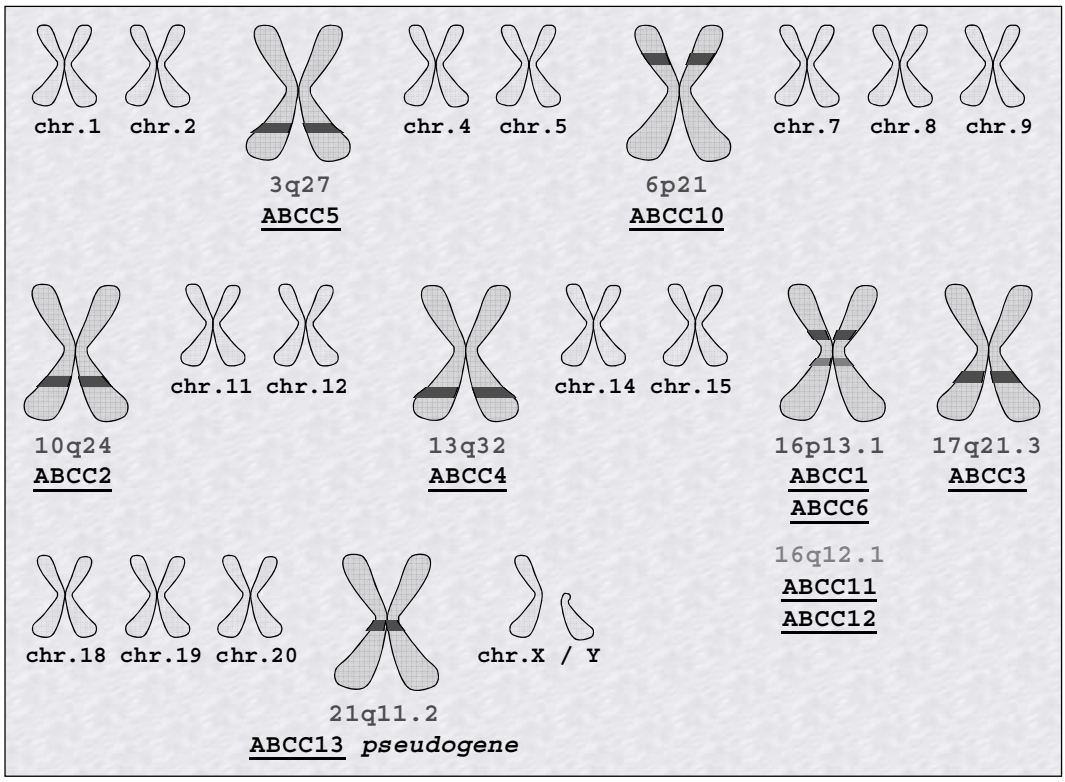

Figure 2.5. Localization of human ABCC genes on chromosome. chr. = chromosome.

However, in contrast to the latter transporters, a conserved N-linked glycosylation site is not found at the N-terminus of ABCC10 (42).

Phylogenetic analysis determined that ABCC11 and ABCC2 are derived by duplication and are most closely related to the ABCC gene. They are tandemly located on human chromosome 16q12.1 (Fig. 2.5) (43, 44). The ABCC11 gene produces two major transcripts of 4.5 kb (abundant in breast) and 4.1 kb (abundant in testis). The 4.5-kb transcript has an open reading frame of 1382 amino acids. The 4.5-kb ABCC11 transcript consists of 31 exons and is located in a genomic region of over 80.4 kb on chromosome 16q12.1 (43, 45). Similarly the ABCC12 gene also has two major transcripts of 4.5 kb and 1.3 kb. In hormonally regulated tissue such as breast cancer, normal breast, and testis, the ABCC2 gene transcript is 4.5 kb in size and encodes a 100-kDa protein. When compared with closely related ABC family members, it lacks transmembrane domains 3, 4, 11, and 12, and the second NBD. In other tissues including brain, skeletal, muscle, and ovary, the transcript size is 1.3 kb. Because of the unusual topology of the two variants of ABCC12, the authors speculated that they may have a different function from other family members. The cloned murine Abcc12 cDNA was 4511 bp long, comprising a 4101 bp open reading frame. The deduced peptide consists of 1367 amino acids and exhibits high sequence identity (84.5%) with human ABCC12. In addition to the Abcc12 transcript, two splicing variants encoding short peptides (775 and 687 amino acid residues) were detected. In spite of the genes coding for both ABCC11 and ABCC12 being tandemly located on human chromosome 16q12.1, no putative mouse orthologous gene corresponding to the human ABCC11 was detected at the mouse chromosome 8D3 locus (Fig. 2.5).

The ABCC13 gene appears to have undergone a process of gradual pseudogenization in mammals. On chromosome 21q11.2, spanning 90 kb is an ABCC13 gene-like sequence with the highest similarity to ABCC2. The open reading frame of this transcript is capable of encoding a polypeptide of only 325 amino acids, compared to the 1500 amino acids of the

most-related ABC transporter. The Abcc13 gene is highly expressed in the fetal liver, bone marrow, and colon. Its expression in peripheral blood leukocytes of adult humans was much lower and no detectable levels were observed in differentiated hematopoietic cells (46). The human locus is now thought to be a pseudogene incapable of encoding a functional ABC protein (47).

2.3. ENDOGENOUS EXPRESSION LEVELS AND PHYSIOLOGICAL FUNCTIONS OF ABCC PROTEINS

ABCC transporters play an important role in mediating the cytoplasmic concentration of endogenous and exogenous substances. They therefore influence the pharmacokinetic profile of a variety of drugs. Numerous ABCC members are associated with a broad spectrum of physiological functions, including detoxification, defense against xenobiotics, and oxidative stress. By virtue of their localization in the plasma membranes in the intestine, liver, blood–brain, and other vital biological barriers, a majority of ABCC drug transporters limit xenobiotic absorption from the gut and xenobiotic entry into the central nervous system and cause drug–drug interactions, decreased drug efficacy, and MDR for chemotherapeutic agents (Figs 2.6 and 2.7). They are also present in liver and kidney, organs important for the excretion of potentially toxic xenobiotics, metabolites, and endogenous waste products. Thus, elucidating which drug entities are substrates for ABCC drug transporters is a crucial step both in drug development and for adequate use of therapeutic compounds. Tissue distribution and ontogeny data are important components of understanding and extrapolating pharmacokinetic data from mice to humans and are crucial to elaborating various knockout models to explore specific physiological functions of ABCCs.

Another interesting observation is that an altered level of ABCC expression due to exposure to hormones or xenobiotics (environmental toxins or drugs) may change the kinetic parameters of ABCC substrates (such as vincristine or methotrexate) and may therefore have clinical implications. These specific regulation mechanisms are briefly summarized in this Part. Regulation of ABCC expression by xenobiotics are fully described in the referenced reviews (48–52).

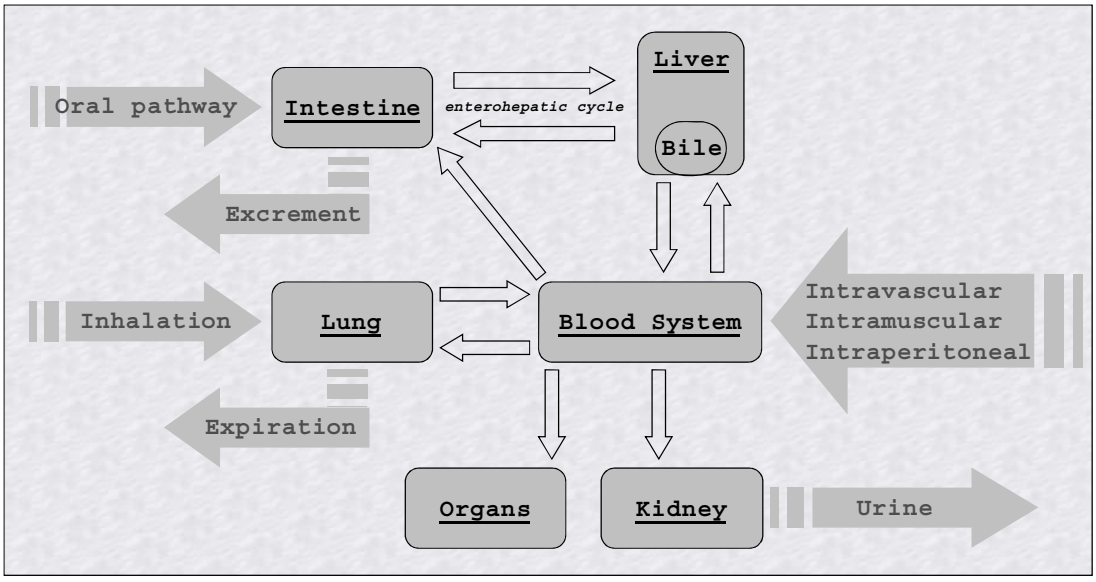

Figure 2.6. Molecule transit in the human body. This scheme illustrates absorption and excretion phenomena of substances with the principal pathways by which endo and exogenous molecules travel within the human body thanks to ABCC transport.

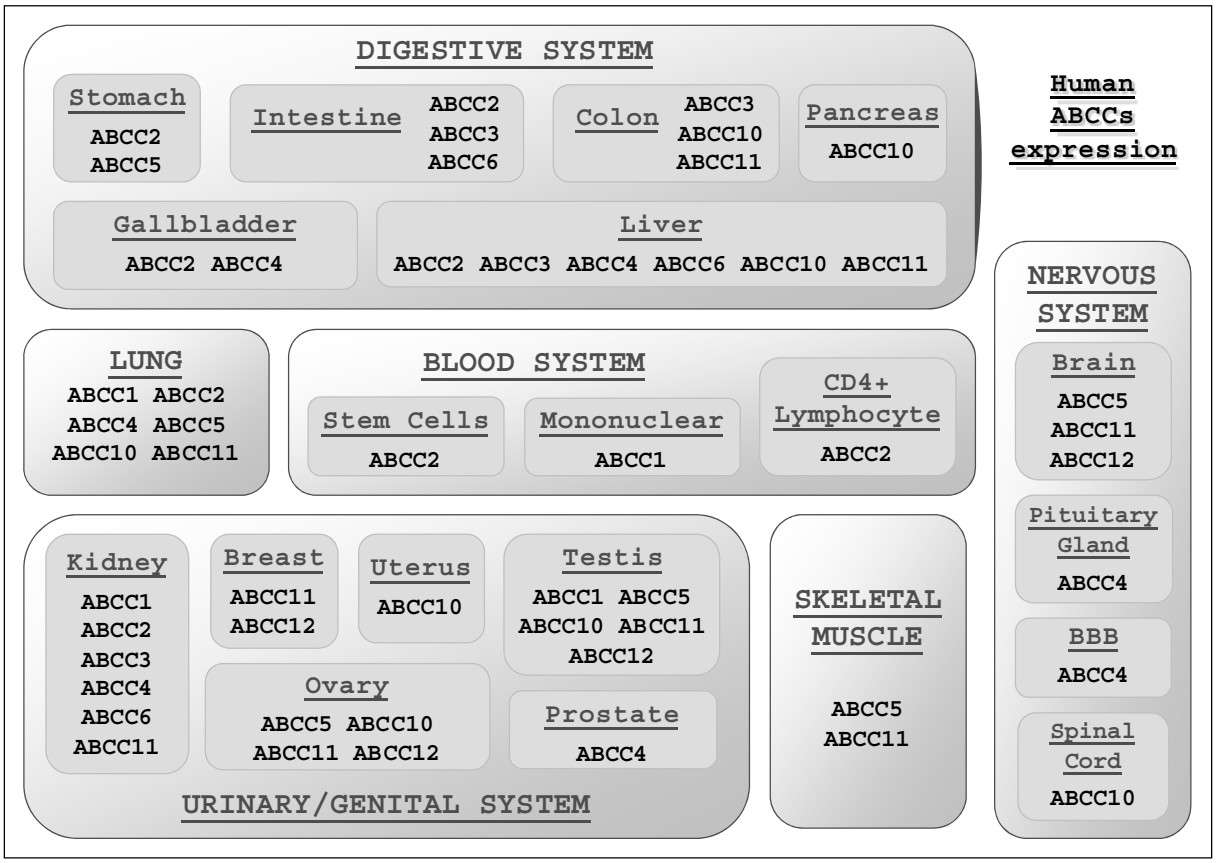

Figure 2.7. ABCC protein expression in human tissues. This scheme illustrates the principal tissues where ABCC protein and transcript expression have been described.

2.3.1. ABCC1

Described in 1992 (1), ABCC1 is found ubiquitously expressed in normal tissues, with highest levels in the lung, testis, kidney, and peripheral blood mononuclear cells (15). In polarized cells, ABCC1 is localized to basolateral plasma membranes (53–56). ABCC1 was found to be localized to the luminal side of brain capillary endothelial cells (Figs. 2.7 and 2.8) (57).

ABCC1 functions as a multispecific organic anion transporter, with (oxidized) glutathione (GSSG), cysteinyl leukotrienes, glucuronides, sulfate conjugates of steroid hormones, bile salts, and activated aflatoxin B1 as substrates. It also transports drugs (such as vincristine) and other hydrophobic compounds in the presence of glutathione. Furthermore, the ability of ABCC1 to transport both GSH and GSSG raises the possibility that the protein contributes to maintenance of the cell redox state. The levels of free GSH are decreased in cells overexpressing the protein and are increased in tissues from Abcc1-/- mice that normally express high levels of the protein (58–60). The GSH and GSH-conjugate transport by ABCC1 is fully described in the review by Cole and Deeley (61). Furthermore GSH is released by cells undergoing apoptosis. Several studies strongly supported that ABCC1 is responsible for this GSH release (62, 63). Furthermore, verapamil (the S-isomer but not the R-isomer) triggers apoptosis through stimulation of GSH extrusion mediated by ABCC1. Induction of apoptosis of ABCC1 cells may represent a novel approach in anticancer treatment (64, 65).

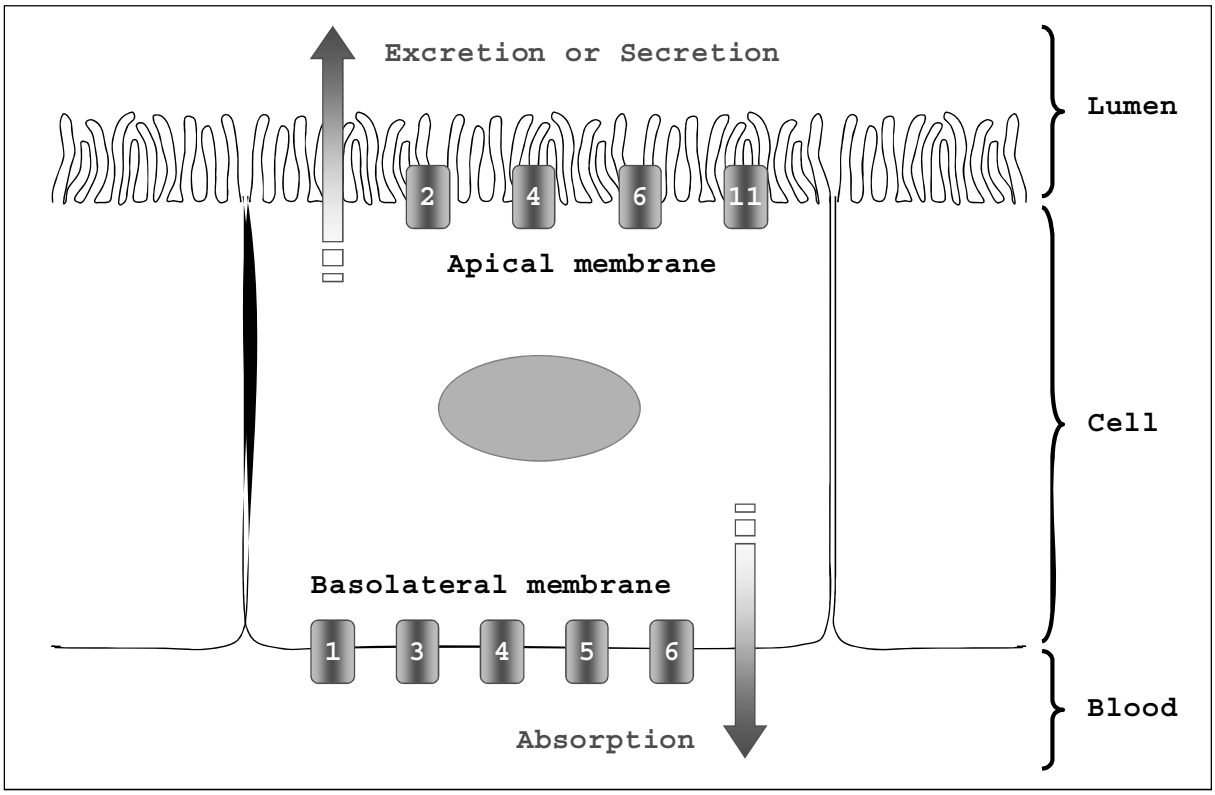

Figure 2.8. ABCC protein expression in polarized cells. Proteins are symbolized by their number (1 = ABCC1, 2 = ABCC2, and so on…).

Like Mdr1a−/−/1b−/− and Bcrp1/Abcg2−/− knockout mice, ABCC1−/− knockout mice were found to be viable, healthy, and fertile (58, 66). These models allowed the characterization of the crucial functions of ABCC1. Particular data of Abcc1−/− knockout mice strongly supported a role for ABCC1 in xenobiotic defense by transporting various substrates, including toxic molecules present in tobacco smoke, which is the principal risk factor for chronic obstructive pulmonary disease. Very recently, van der Deen et al. (67) demonstrated that using mice lacking both Abcc1 and Mdr1a/1b genes (called triple knockout [TKO] mice), Abcc1−/− mice display elevated glutathione levels in tissues that normally have a high Abcc1 expression, for example, in the lungs possibly as a compensation mechanism for the elevated pulmonary oxidative stress (58, 67). A decrease of the inflammatory response to cigarette smoke exposure in the lungs of Abcc1/Mdr1a/1b TKO mice was observed compared to wild-type mice. A possible explanation of the lower inflammatory response in TKO mice is an impaired transport of the proinflammatory mediator LTC4 (66), an important physiological high-affinity substrate for ABCC1. Nevertheless, during inflammation, other cytokines can be produced such as interleukin-6 (IL-6). The first evidence for a putative role of IL-6 in the regulation of Abcc1 expression in HepG2 cells and in liver was described (68, 69). Recently, a positive regulation of Abcc1, 3, 4 expression levels has been reported (70) in normal human epidermal keratinocytes and in primary human dermal fibroblasts exposed to IL-6 in combination with its soluble α-receptor or oncostatin. Since ABCC1 and ABCC4 have been shown to function as a prostaglandin derivate efflux transporter (71–73) and IL-6-type cytokines are known to induce the expression of COX-2 in certain cell types (74, 75), it is tempting to speculate that increased prostaglandin efflux might be one additional means by which IL-6 can contribute to inflammation. Mice lacking Abcc4 exhibited a decrease in plasma prostaglandin metabolites and an increase in inflammatory pain threshold compared to wild-type mice, which confirms ABCC4 involvement in inflammatory situations (73).

Other interesting observations have shown the crucial importance of ABCC1 expression in the migration of dendritic cells from peripheral tissues to the lymph nodes. Dendritic cells are antigen-presenting cells involved in T-cell activation. They acquire antigens in peripheral tissues and migrate to lymph nodes where they localize to the T-cell-rich paracortex (76). Migration of dendritic cells was reduced in Abcc1-/- mice and restored to the levels found in wild-type animals when exogenous cysteinyl leukotrienes (LTC4 and LTD4) were administered. Thus, LTC4 efflux from these cells by ABCC1 is critical for migration.

To study the age influence on ABCC-related activity in cells from the immune system, ABCC-related activity was studied in murine bone marrow cells and thymocytes of young (3–4 weeks old), adult (2–3 months old), and old (18 months old) mice. Although all thymocytes expressed the ABCC1 molecule in an active form and aging did not affect this pattern, the authors observed a modification of ABCC-related activity in the bone marrow according to age. This alteration of ABCC transport activity may be related to other protein isoforms of this subfamily (77).

After severe injury, the liver can undergo partial regeneration. This process depends in part on proliferation and differentiation of hepatic progenitor cells. After treatment of rats with 2-acetylaminofluorene (2-AAF) followed by partial hepatectomy, treated animals showed increased hepatic mRNA levels of the genes encoding MRPs Mdr1b, Abbc1, and Abcc3 in periportal progenitor cells and of the Mdr1b protein in periportal hepatocytes. These functional upregulations of Abcc1 and Abcc3 proteins may have a cytoprotective role in conditions of severe hepatotoxicity (78). By contrast, Abcc2 protein levels did not change during liver regeneration following partial hepatectomy in rats, suggesting that ABCC2-mediated secretion is well-preserved in the growing liver (79). But a switch in expression from the apical Abbc2 to the basolateral Abcc1 protein has also been reported in cultured rat hepatocytes entering the cell cycle (80). Consequently, as in human proliferating hepatocytes and in periportal progenitor cells Abcc1 levels are strongly increased, this upregulation of Abcc1 may be associated with cell proliferation. Furthermore, in mouse hematopoietic cells, Abcc1 is expressed, and 50% of precursor cells showed Abcc activity (Fluo-3 transport activity) (77). Taken altogether, this indicates that Abcc1 plays a physiological function in immature cells.

2.3.2. ABCC2

ABCC2 has been cloned from various species, including humans, dogs, mice, rats, and rabbits and is physiologically expressed predominantly at the hepatocyte canalicular membrane (81–86). It is also present at the brush-border membrane of renal proximal tubule cells (87, 88), at the absorptive enterocytes (89, 90), and at the apical membrane of gallbladder epithelial cells (Figs. 2.7 and 2.8) (91). Its location in the brain is a matter of debate. Most previous studies failed to determine Abcc2 mRNA or protein in the brain or cell preparations from the brain of different species, including humans (92). Taipalensuu et al. focused on the human jejunum and found a transporter expression with the following ranking: ABCC2 > MDR1 β ABCC3 > ABCC5 and ABCC1 > ABCC4 (93). In addition, Abcc2 mRNA transcripts have been detected in low levels in other tissues in the rat, including the lung and the stomach (94), and in peripheral blood cells, especially in CD4+ lymphocytes (95). ABCC2 colocalizes with ABCB1 and ABCG2 (96). Expression of ABCC2 in nuclear membranes in human tissues is specific for poorly differentiated cells, including stem cells (97).

During development in the rat, ABCC2 levels are low in the fetal liver, and they increase neonatally after birth to reach adult levels at 4 weeks (98). Rat liver progenitor cells also minimally express ABCC2 (99). During pregnancy, ABCC2 levels decreased in the liver but remained preserved in the small intestine (100, 101). In human placenta, ABCC2 has been

detected on apical syncytiotrophoblast membranes (102). The placenta serves, in part, as a barrier to exclude noxious substances from the fetus. In humans, a single-layered syncytium of polarized trophoblast cells and the fetal capillary endothelium separate the maternal and fetal circulations. Immunofluorescence and immunoblotting studies demonstrated that ABCC2 was localized in the apical syncytiotrophoblast membrane while ABCC1 and ABCC3 were predominantly expressed in blood vessel endothelia. Given the cellular distribution of these transporters, ABCC isoforms were suggested to serve to protect fetal blood from entry of organic anions and to promote the excretion of glutathione/ glucuronide metabolites in the maternal circulation.

Genetic variation in the ABCC2 gene results in the DJS, a disease characterized by conjugated hyperbilirubinemia. Mutations leading to DJS are either associated with complete absence of immunohistochemically detectable ABCC2 in affected patients or impaired protein maturation and sorting (103– 113). Acquired or hereditary deficiency of ABCC2 causes an increased concentration of bilirubin glucuronides in blood because of their efflux from hepatocytes via the basolateral ABCC3, which compensates for the deficiency in ABCC2-mediated apical efflux (114). The natural Abcc2 mutant TR- 90 and Eisai hyperbilirubinemic (EHBR) rats have significantly contributed to the understanding of human ABCC2 transport characteristics. Mutant rats lacking the cMOAT, designated further as ABCC2, have a hyperbilirubinemic phenotype and impaired secretion of bilirubin glucuronides, sulphated bile salts, GS S-conjugates, and GSH into the bile (115). Abcc2−/− mice are healthy and exhibit biochemical abnormalities (116–118). These rats and mice serve as models for Dubin–Johnson disease as this disorder is caused by mutations in the ABCC2 gene.

Abcc2 expression is reported as markedly altered in various rat models of cholestasis such as bile duct ligation and endotoxin- or phalloidin-induced cholestasis (119–122). All three cholestatic models resulted in a marked decrease in Abcc2 protein and its tissue localization at the canalicular membrane, except in ethinylestradiol-treated rats. After endotoxin treatment, the normally sharply delineated canalicular staining of Abcc2 had changed to a fuzzy pattern, suggesting an abnormal localization in a subapical compartment. Simultaneously, an upregulation of Abcc1 and mdr1b is observed and may confer resistance to hepatocytes against cytokine-induced metabolic stress and also compensate the canalicular excretion deficiency of Abcc2 (122).

ABCC2 likely plays a major role in the pharmacokinetics of many drugs through the regulation of their intestinal absorption and their biliary or renal elimination. Consequently, an alteration of its expression by exposure to hormones or xenobiotics and also of its activity may change the kinetic parameters of drugs. Indeed, biliary secretion of endogenous substrates such as bilirubin conjugates may be impaired. Recently, it has been shown that ABCC2 expression levels are regulated by hormones. For example, ethynylestradiol strongly reduces Abcc2 expression in rats (123). Similarly, sexual steroids decrease Abcc2 expression at a posttranscriptional level in pregnancy (124). In contrast, dexamethasone (DEX) has been described to increase ABCC2 protein expression in various tissues (125) and liver (126, 127). RU486 and the antiglucocorticoid PCN were also found to increase Abcc2 transcipts in primary hepatocytes. Using Pregnane X receptor (PXR) −/− mice, Kast et al. (128) fully demonstrated that DEX and PCN regulated Abcc2 expression by activation of PXR signalling pathway. This was supported by the fact that PXR has been shown to bind with the ER-8 motif found in ABCC2 promoter as a heterodimer with the 9-cis retinoic acid receptor (94, 128). Other PXR agonists such as the peptide mimetic HIV protease inhibitor ritonavir also induced ABCC2 mRNA levels in primary human hepatocytes (129). Furthermore, *in vivo* administration of rifampicin to humans also increased ABCC2 mRNA and protein in the duodenum (130). Interestingly, induction of ABCC2 by PXR ligands is associated with

upregulation of other PXR-controlled detoxifying proteins such as cytochrome P450 3A4 and P-gp (129), thus outlining their coordinated expression in response to certain xenobiotics. Complementary data about regulation of ABCC2 expression by xenobiotics are reported in the following reviews (48–50).

2.3.3. ABCC3

Cloned in human, rat, and mouse (94, 131–135) and detected in liver, intestine, and adrenal gland, ABCC3 is found on basolateral membranes of intrahepatic bile-duct epithelial cells (cholangiocytes), hepatocytes surrounding the portal tracts, intestinal epithelial cells (90, 136, 137), and polarized Madin–Darby canine kidney (MDCK) cells transfected with an ABCC3 construct (Figs. 2.7 and 2.8) (114, 138, 139). ABCC3 expression is higher in the colon than in the ileum (140). Furthermore, ABCC3 appeared to be the most abundantly expressed transporter in investigated parts of the human intestine, except for the terminal ileum, where MDR1 showed the highest expression. All transporters showed alterations in their expression levels from the duodenum to the sigmoid colon. The ranking of transporter gene expression in the duodenum was ABCC3 >> ABCB1 > ABCC2 > ABCC5 > ABCC4 > ABCC1. In the terminal ileum, the ranking order was as follows: ABCB1 > ABCC3 >> ABCC1 ~ ABCC5 ~ ABCC4 > ABCC2. In all segments of the colon (ascending, transverse, descending, and sigmoid), the transporter gene expression showed the following order: ABCC3 >> ABCB1 > ABCC4 ~ ABCC5 > ABCC1 >> ABCC2 (141).

Under normal conditions, only low levels of ABCC3 are found in the liver; however, strong ABCC3 staining was observed in hepatocytes from ABCC2- deficient Dubin–Johnson patients (114). This has been demonstrated in rodent models of DJS (e.g., the EHBR rat), in which ABCC3 mRNA and protein expression in the liver and the kidney are increased significantly (142).

Furthermore, induction of Abcc3 also occurs in cholestatic rat (143) and human livers (114, 138), which further supports upregulation of Abcc3 as a protective mechanism (i.e., bilirubin and metabolite removal) when ABCC2 is either absent or nonfunctional. In fact, ABCC2 and ABCC3 expression was inversely correlated under conditions of reduced ABCC2 expression. ABCC3 is a highly inducible retrograde transporter that can efflux organic anions from hepatocytes into blood for eventual excretion into urine (144, 145). Furthermore, its localization on basolateral membranes of cholangiocytes and enterocytes suggests that ABCC3 may also be involved in the recirculation of bile salts from these cells into the blood (enterohepatic circulation). Nevertheless, two recent reports have presented controversial data, showing that bile acid homeostasis is not perturbed in Abcc3−/− mice (146, 147).

2.3.4. ABCC4

ABCC4 is expressed at low levels in a variety of human tissues with high levels occurring in pituitary cells (148), lung, prostate, and proximal tubules in the kidney (149–157). ABCC4 was clearly localized by confocal laser scanning microscopy to the luminal side of brain capillary endothelial cells. The ABCC4 protein was also detected in astrocytes of the subcortical white matter (57). ABCC4 can also release prostaglandins from cells, thus suggesting its involvement in inflammatory processes (72).

The accumulation of adefovir and tenofovir in kidney was significantly greater in Abcc4 knockout mice, suggesting that ABCC4 is involved in the luminal efflux of both adefovir and tenofovir (158). ABCC4 is relatively highly expressed at the blood–brain barrier (BBB), suggesting that ABCC4 may play a role in nucleotide penetration or retention in the brain (159, 160). ABCC4, 5, and 11 are efflux transporters of cGMP and cAMP. Thus, these transporters may play roles in the regulation of intracellular levels of cyclic nucleotides,

which are important as “second messengers” of intracellular signalling. The membrane localization of ABCC4 in polarized cells remains unresolved. Although ABCC4 was found in the basolateral membrane of tubuloacinar cells of the prostate (161) and in the sinusoidal membrane of human, rat, and mouse hepatocytes (162, 163), ABCC4 was localized in the apical membranein kidney proximal tubule epithelia (159, 160). It has also been reported at low expression in the liver, suggesting that the role of ABCC4 in hepatic transport is minor under basal conditions.

Furthermore, using Abcc4–/– mice as a model system, and the nucleotide analogue (PMEA) as a probe, Kruh et al. (164) demonstrated the ability of ABCC4 to function *in vivo* as an endogenous resistance factor. Abcc4-null mice treated with PMEA exhibit increased lethality associated with marked toxicity in bone marrow, spleen, thymus, and gastrointestinal tract. An increase of PMEA penetration into the brain was also observed in Abcc4–/– mice, suggesting that the pump may be a component of the BBB for nucleoside-based analogues (164).

2.3.5. ABCC5

ABCC5 is expressed in almost every tissue of the human body, with highest expression in skeletal muscle followed by the brain (Figs. 2.7 and 2.8) (149, 165). ABCC5 in mice is predominantly expressed in the brain with significant expression in gonads, placenta, lung, and stomach. ABCC5 is preferentially localized in the basal membrane of syncytiotrophoblasts and in and around fetal vessels. Transcripts of ABCC5 decrease with gestational age (166). ABCC5 was clearly located at the luminal side of brain capillary endothelial cells and was also detected in astrocytes of the subcortical white matter and in pyramidal neurons (57).

The tissue expression of mouse ABCC5 is reported to be similar to that in humans and rats (135, 167, 168). ABCC5 knockout mice are healthy and fertile and do not show any observable physiological dysfunctions. Even if the substrate pattern of ABCC5 is much narrower than that of ABCC4, ABCC5 serves as a transporter for organic anions and drugs, including vincristine, LTC4, etoposide, PMEA, or daunorubicin (156, 157, 169–171). ABCC5 is routed to the basolateral membrane in polarized cells, including ABCC5- transfected MDCKII cells.

2.3.6. ABCC6

Although expression levels of ABCC6 are consistently and constitutively high in the liver of humans, mice, and rats, the functional significance of this expression still remains poorly understood. In the liver, ABCC6 is localized to both the basolateral (high level) and canalicular (low level) plasma membranes of hepatocytes (172–175).

ABCC6 was initially cloned from rat liver (143) and has been subsequently cloned in humans and mice (172, 174, 176). The mouse and rat ABCC6 orthologs show greater than 78% amino-acid identity with human ABCC6. Mutations in the ABCC6 gene have been implicated in the etiology of PXE, a hereditary connective tissue disorder characterized by loss of tissue elasticity (affecting skin, retina, and blood vessels) (177–180). The phenotype of the Abcc6-/- mouse shares calcification of elastic fibers with the human PXE disease, which makes this model a useful tool to further investigate the etiology of PXE (181). Abcc6/1(-/-) and Abcc6/3(-/-) double knockout mice exhibited connective tissue mineralization similar to that observed in Abcc6(-/-) mice (182), suggesting that Abcc1 and Abcc3 do not modulate the effects of Abcc6 in this mouse model.

The physiological importance of ABCC6 expression in the liver remains to be further elucidated. The only ABCC6 substrate identified thus far is BQ123, a cyclopentapeptide antagonist of the endothelin receptor (179). Because of its constitutive expression in the liver and its capacity to transport BQ123, ABCC6 was suggested to function as a transporter for small peptides involved in cellular signaling and/or autocrine or paracrine regulation of hepatocellular functions (172, 179). Chinese hamster ovary cells transfected with ABCC6 cDNA show increased resistance to a variety of anticancer agents, including etoposide, doxorubicin, daunorubicin, and cisplatin, but not to vincristine or vinblastine (179).

2.3.7. ABCC10

Information on the ABCC10 protein expression pattern in tissues has not yet been reported. Using reverse transcriptase polymerase chain reaction, ABCC10 transcripts were detected in most tissues with relatively higher levels reported in the pancreas, testis, colon, spinal cord, tonsils, lung, trachea, and skin (42), with significant intestinal expression and moderate expression in the liver, ovary, uterus, and placenta (42, 183). Two Abcc10 genes have also been identified in mice (Mrp7A and Mrp7B). They show more than 80% aminoacid similarity with their human counterparts (184). Murine Abcc10 is 84% identical to ABCC10. Its transcript is expressed in many tissues with highest levels in the testis, ovary, gut, kidney, and lung (42, 135, 185). Rat Abcc10 transcripts were reported to have been expressed in the liver, kidney, and ileum (186).

ABCC10 transports anticancer compounds, estrogen-glucuronides, and leukotrienes (42, 183, 187). Fluorescence *in situ* hybridization indicated that ABCC10 gene maps to chromosome 6p12–21 in proximity to several genes associated with glutathione conjugation and synthesis, suggesting its involvement in phase III (cellular extrusion) of detoxification. ABCC10 transports estradiol-17β-glucuronide that was susceptible to competitive inhibition by LTC4, glycolithocholate 3-sulfate, MK571, and lipophilic agents (cyclosporine A). Of the inhibitors tested, LTC4 was the most potent, in agreement with the possibility that it is a substrate of the pump (183). Drug resistance to docetaxel and, to a lesser degree, paclitaxel, vincristine, and vinblastine was reported (188). ABCC10 does not transport methotrexate, DNP-SG, monovalent bile salts (glycocholic acid and taurocholate), or cyclic nucleotides (cAMP and cGMP) (183). Further studies examining substrate specificity, subcellular localization, and physiological function are needed to clarify the role, if any, that ABCC10 may play in the development of the MDR phenotype in salivary gland adenocarcinoma cell lines (189).

2.3.8. ABCC11

In spite of contradictory data about ABCC11 transcript expression in tissues (Figs. 2.7 and 2.8), ABCC11 levels are expressed in a variety of human tissues, including normal breast, ovary, lung, testis, kidney, liver, colon, and brain (43– 45). In transfected MDCKII and HepG2 cells, ABCC11 is localized at the apical pole (190). Despite extensive searches within the mouse genome, a murine ABCC11 ortholog was not found (191).

ABCC11 mediates transport of estradiol-17β-glucuronide, dehydroepiandrosterone 3-sulfate, as well as LTC4 and the monoanionic bile acids taurocholate and glycocholate, but not prostaglandin E1 or E2 (190, 192). Because ABCC11-transfected cells show no resistance to vincristine, doxorubicin, etoposide, or taxol, it is unlikely these compounds are its substrates. Taken altogether, the resistance profiles of ABCC4, ABCC5, and ABCC11 are similar but not completely identical. In ABCC11-transfected LLC-PK1 cells, ABCC11 is responsible for resistance to the pyrimidine analogs 5′-fluoro-5′-deoxyuridine, 5′-fluorouracil, and 5′-fluoro-2′-deoxyuridine. As 5-fluorouracil is an essential component in the treatment of breast, colon, and head-and-neck tumors, expression of ABCC11 in those types of cancers would be of particular interest. It is worth mentioning that breast cancer is a hormonally responsive tumor

and ABCC11 is able to transport steroid sulphates. Recently, the notion that expression of ABCC11 in estrogen receptor α-positive breast cancers may contribute to decreased sensitivity to chemotherapy combinations that include 5-fluorouracil was reported (193). Consequently, ABCC11 may be a potential predictive tool in the choice of anticancer therapies in estrogen receptor positive breast cancers. Additional studies, including protein expression studies in tumors, should be carried out to characterize the potential contribution of ABCC11 to the chemosensitivity of these cancers.

In the study of eight families, the chromosomal localization of the paroxysmal kinesigenic choreoathetosis (PKC) critical region is 16p11.2-q12, a section where the ABCC11 gene is localized. PKC, the most frequently described type of paroxysmal dyskinesia, is characterized by recurrent, brief attacks of involuntary movements induced by sudden voluntary movements. This disease was linked to ABCC11 mutations. Consequently, several studies suggested that specific mutations of ABCC11 could be related to this hereditary disorder. However, recently, it has been demonstrated that mutations of ABCC11 can be ruled out as the cause of PKC (194).

A surprising physiological function of ABCC11 has been found by two interesting genetic analyses. For the first time, genetic evidence was observed for an association between the degree of apocrine colostrum secretion and human earwax type. Earwax (cerumen) is secreted by ceruminous apocrine glands. Human earwax consists of wet and dry types. Dry earwax, which lacks cerumen, is frequent in East Asians, whereas wet earwax is common in other populations. Earwax type is a Mendelian trait, with wet earwax dominant to the dry type. Yoshiura et al. determined that a single nucleotide polymorphism at nucleotide 538 (538G→A; 180Gly→Arg) of the ABCC11 gene (rs17822931) is responsible for determination of earwax type (195). The AA genotype corresponds to dry earwax, and GA and GG to the wet type. In membrane vesicle assays from transfected cells with ABCC11 180Gly (wild-type) or ABCC11 180 Arg (variant), cells with allele Arg show a lower excretory activity for cGMP than those with allele Gly. Furthermore, frequency of women without colostrum among dry-type women was significantly higher than that among wet-type women ($p < 0.0002$) (196). Consequently, ABCC11 may be crucial in the lactation process. Furthermore, similarly to ABCC3 and ABCC5 transporters, ABCC11 expression can be downregulated *in vitro* by estrogen in mammary cells (193, 197). This specific ABCC11 regulation likely involved estrogen receptor α (193). These ABCC regulations by estrogen in estrogen receptors α-positive cells may suggest that the hormonal environment may have an impact on mammary gland function.

2.3.9. ABCC12

Little is known about the ABCC12 protein. The gene has two major transcripts of 4.5 and 1.3 kb. In breast cancer, normal breast, and testis, the ABCC12 gene transcript is 4.5 kb in size and encodes a 100-kDa protein. In other tissues including the brain, skeletal muscle, and ovary, the transcript size is 1.3 kb. This smaller transcript encodes a nucleotide-binding protein of approximately 25 kDa in size (44, 45, 198). Because the 4.5-kb RNA is highly expressed in breast cancer and not expressed at detectable levels in essential normal tissues, ABCC12 could be a useful target for the immunotherapy of breast cancer. The unusual topology of the two variants of ABCC12 suggests that they may have a different function from other family members. In testis, the transcript has been localized to Sertoli cells of the seminiferous tubules, with lower levels in Leydig cells. ABCC12 mRNA is also widely expressed in fetal tissues such as liver, spleen, kidney, and lung (44). The mouse abcc12 gene was expressed at high levels exclusively in the seminiferous tubules in the testis (191).

Transport activity of ABCC12 as well as localization in polarized cells remain to be examined. With the recent identification of the murine ortholog, the generation of a knockout mouse would be useful regarding the physiological significance of ABCC12 (191).

REFERENCES

1. Cole SP, Bhardwaj G, Gerlach JH, Mackie JE, Grant CE, Almquist KC et al. 1992. Overexpression of a transporter gene in a multidrug-resistant human lung cancer cell line. *Science* 258: 1650–1654.

2. Bakos E, Hegedus T, Hollo Z, Welker E, Tusnady GE, Zaman GJ et al. 1996. Membrane topology and glycosylation of the human multidrug resistanceassociated protein. *J Biol Chem* 271: 12322–12326.

3. Frelet A and Klein M. 2006. Insight in eukaryotic ABC transporter function by mutation analysis. *FEBS Lett* 580: 1064–1084.

4. Deeley RG, Westlake C, and Cole SP. 2006. Transmembrane transport of endoand xenobiotics by mammalian ATP-binding cassette multidrug resistance proteins. *Physiol Rev* 86: 849–899.

5. Westlake CJ, Cole SP, and Deeley RG. 2005. Role of the NH2-terminal membrane spanning domain of multidrug resistance protein 1/ P-glycoprotein 1 in protein processing and trafficking. *Mol Biol Cell* 16: 2483–2492.

6. Kast C and Gros P. 1997. Topology mapping of the amino-terminal half of multidrug resistance-associated protein by epitope insertion and immunofluorescence. *J Biol Chem* 272: 26479–26487.

7. Kast C and Gros P. 1998. Epitope insertion favors a six transmembrane domain model for the carboxy-terminal portion of the multidrug resistance-associated protein. *Biochemistry* 37: 2305–2313.

8. Bakos E, Evers R, Szakacs G, Tusnady GE, Welker E, Szabo K et al. 1998. Functional multidrug resistance protein (MRP1) lacking the N-terminal transmembrane domain. *J Biol Chem* 273: 32167–32175.

9. Hipfner DR, Almquist KC, Leslie EM, Gerlach JH, Grant CE, Deeley RG et al. 1997. Membrane topology of the multidrug resistance protein (MRP). A study of glycosylation-site mutants reveals an extracytosolic NH2 terminus. *J Biol Chem* 272: 23623–23630.

10. Yang Y, Liu Y, Dong Z, Xu J, Peng H, Liu Z et al. 2007. Regulation of function by dimerization through the amino-terminal membrane-spanning domain of human ABCC1/MRP1. *J Biol Chem* 282: 8821–8830.

11. Daoud R, Desneves J, Deady LW, Tilley L, Scheper RJ, Gros P et al. 2000. The multidrug resistance protein is photoaffinity labeled by a quinoline-based drug at multiple sites. *Biochemistry* 39: 6094–6102.

12. Daoud R, Julien M, Gros P, and Georges E. 2001. Major photoaffinity drug binding sites in multidrug resistance protein 1 (MRP1) are within transmembrane domains 10-11 and 16-17. *J Biol Chem* 276: 12324–12330.

13. Daoud R, Kast C, Gros P, and Georges E. 2000. Rhodamine 123 binds to multiple sites in the multidrug resistance protein (MRP1). *Biochemistry* 39: 15344–15352.

14. Haimeur A, Conseil G, Deeley RG, and Cole SP. 2004. Mutations of charged amino acids in or near the transmembrane helices of the second membrane spanning domain differentially affect the substrate specificity and transport activity of the multidrug resistance protein MRP1 (ABCC1). *Mol Pharmacol* 65: 1375–1385.

15. Haimeur A, Deeley RG, and Cole SP. 2002. Charged amino acids in the sixth transmembrane helix of multidrug resistance protein 1 (MRP1/ABCC1) are critical determinants of transport activity. *J Biol Chem* 277: 41326–41333.

16. Mao Q, Qiu W, Weigl KE, Lander PA, Tabas LB, Shepard RL et al. 2002. GSHdependent photolabeling of multidrug resistance protein MRP1 (ABCC1) by [125I]LY475776. Evidence of a major binding site in the COOH-proximal membrane spanning domain. *J Biol Chem* 277: 28690–28699.

17. Zhang DW, Cole SP, and Deeley RG. 2001. Identification of an amino acid residue in multidrug resistance protein 1 critical for conferring resistance to anthracyclines. *J Biol Chem* 276: 13231–13239.

18. Zhang DW, Cole SP, and Deeley RG. 2001. Identification of a nonconserved amino acid residue in multidrug resistance protein 1 important for determining substrate specificity: Evidence for functional interaction between transmembrane helices 14 and 17. *J Biol Chem* 276: 34966–34974.

19. Zhang DW, Cole SP, and Deeley RG. 2002. Determinants of the substrate specificity of multidrug resistance protein 1: Role of amino acid residues with hydrogen bonding potential in predicted transmembrane helix 17. *J Biol Chem* 277: 20934–20941.

20. Zhang DW, Gu HM, Vasa M, Muredda M, Cole SP, and Deeley RG. 2003. Characterization of the role of polar amino acid residues within predicted transmembrane helix 17 in determining the substrate specificity of multidrug resistance protein 3. *Biochemistry* 42: 9989–10000.

21. Zhang DW, Gu HM, Situ D, Haimeur A, Cole SP, and Deeley RG. 2003. Functional importance of polar and charged amino acid residues in transmembrane helix 14 of multidrug resistance protein 1 (MRP1/ABCC1): Identification of an aspartate residue critical for conversion from a high to low affinity substrate binding state. *J Biol Chem* 278: 46052–46063.

22. Qian YM, Grant CE, Westlake CJ, Zhang DW, Lander PA, Shepard RL et al. 2002. Photolabeling of human and murine multidrug resistance protein 1 with the high affinity inhibitor [125I]LY475776 and azidophenacyl-[35S]glutathione. *J Biol Chem* 277: 35225–35231.

23. Situ D, Haimeur A, Conseil G, Sparks KE, Zhang D, Deeley RG et al. 2004. Mutational analysis of ionizable residues proximal to the cytoplasmic interface of membrane spanning domain 3 of the multidrug resistance protein, MRP1 (ABCC1): Glutamate 1204 is important for both the expression and catalytic activity of the transporter. *J Biol Chem* 279: 38871–38880.

24. Zhang DW, Nunoya K, Vasa M, Gu HM, Theis A, Cole SP et al. 2004. Transmembrane helix 11 of multidrug resistance protein 1 (MRP1/ABCC1): Identification of polar amino acids important for substrate specificity and binding of ATP at nucleotide binding domain 1. *Biochemistry* 43: 9413–9425.

25. Zhang DW, Nunoya K, Vasa M, Gu HM, Cole SP, and Deeley RG. 2006. Mutational analysis of polar amino acid residues within predicted transmembrane helices 10 and 16 of multidrug resistance protein 1 (ABCC1): Effect on substrate specificity. *Drug Metab Dispos* 34: 539–546.

26. Smith PC, Karpowich N, Millen L, Moody JE, Rosen J, Thomas PJ et al. 2002. ATP binding to the motor domain from an ABC transporter drives formation of a nucleotide sandwich dimer. *Mol Cell* 10: 139–149.

27. Locher KP, Lee AT, and Rees DC. 2002. The *E. coli* BtuCD structure: A framework for ABC transporter architecture and mechanism. *Science* 296: 1091–1098.

28. Chen J, Lu G, Lin J, Davidson AL, and Quiocho FA. 2003. A tweezers-like motion of the ATP-binding cassette dimer in an ABC transport cycle. *Mol Cell* 12: 651–661.

29. Diederichs K, Diez J, Greller G, Müller C, Breed J, Schnell C et al. 2000. Crystal structure of MalK, the ATPase subunit of the trehalose/maltose ABC transporter of the archaeon Thermococcus litoralis. *EMBO J* 19: 5951–5961.

30. Gaudet R and Wiley DC. 2001. Structure of the ABC ATPase domain of human TAP1, the transporter associated with antigen processing. *EMBO J* 20: 4964– 4972.

31. Hung LW, Wang IX, Nikaido K, Liu PQ, Ames GF, and Kim SH. 1998. Crystal structure of the ATP-binding subunit of an ABC transporter. *Nature* 396: 703–707.

32. Linton KJ and Higgins CF. 2007. Structure and function of ABC transporters: The ATP switch provides flexible control. *Pflugers Arch* 453: 555–567.

33. Sauna ZE and Ambudkar SV. 2007. About a switch: How P-glycoprotein (ABCB1) harnesses the energy of ATP binding and hydrolysis to do mechanical work. *Mol Cancer Ther* 6: 13–23.

34. Higgins CF and Linton KJ. 2004. The ATP switch model for ABC transporters. *Nat Struct Mol Biol* 11: 918–926.

35. Gao M, Cui HR, Loe DW, Grant CE, Almquist KC, Cole SP et al. 2000. Comparison of the functional characteristics of the nucleotide binding domains of multidrug resistance protein 1. *J Biol Chem* 275: 13098–13108.

36. Hou Y, Cui L, Riordan JR, and Chang X. 2000. Allosteric interactions between the two non-equivalent nucleotide binding domains of multidrug resistance protein MRP1. *J Biol Chem* 275: 20280–20287.

37. Buyse F, Hou YX, Vigano C, Zhao Q, Ruysschaert JM, and Chang XB. 2006. Replacement of the positively charged Walker A lysine residue with a hydrophobic leucine residue and conformational alterations caused by this mutation in MRP1 impair ATP binding and hydrolysis. *Biochem J* 397: 121–130.

38. Yang R, Scavetta R, and Chang XB. 2008. The hydroxyl group of S685 in Walker A motif and the carboxyl group of D792 in Walker B motif of NBD1 play a crucial role for multidrug resistance protein folding and function. *Biochim Biophys Acta* 1778: 454–465.

39. Payen LF, Gao M, Westlake CJ, Cole SP, and Deeley RG. 2003. Role of carboxylate residues adjacent to the conserved core Walker B motifs in the catalytic cycle of multidrug resistance protein 1 (ABCC1). *J Biol Chem* 278: 38537–38547.

40. Yang R, McBride A, Hou YX, Goldberg A, and Chang XB. 2005. Nucleotide dissociation from NBD1 promotes solute transport by MRP1. *Biochim Biophys Acta* 1668: 248–261.

41. Yang R and Chang XB. 2007. Hydrogen-bond formation of the residue in H-loop of the nucleotide binding domain 2 with the ATP in this site and/or other residues of multidrug resistance protein MRP1 plays a crucial role during ATP-dependent solute transport. *Biochim Biophys Acta* 1768: 324–335.

42. Hopper E, Belinsky MG, Zeng H, Tosolini A, Testa JR, and Kruh GD. 2001. Analysis of the structure and expression pattern of MRP7 (ABCC10), a new member of the MRP subfamily. *Cancer Lett* 162: 181–191.

43. Bera TK, Lee S, Salvatore G, Lee B, and Pastan I. 2001. MRP8, a new member of ABC transporter superfamily, identified by EST database mining and gene prediction program, is highly expressed in breast cancer. *Mol Med* 7: 509–516.

44. Yabuuchi H, Shimizu H, Takayanagi S, and Ishikawa T. 2001. Multiple splicing variants of two new human ATP-binding cassette transporters, ABCC11 and ABCC12. *Biochem Biophys Res Commun* 288: 933–939.

45. Tammur J, Prades C, Arnould I, Rzhetsky A, Hutchinson A, Adachi M et al. 2001. Two new genes from the human ATP-binding cassette transporter superfamily, ABCC11 and ABCC12, tandemly duplicated on chromosome 16q12. *Gene* 273: 89–96.

46. Yabuuchi H, Takayanagi S, Yoshinaga K, Taniguchi N, Aburatani H, and Ishikawa T. 2002. ABCC13, an unusual truncated ABC transporter, is highly expressed in fetal human liver. *Biochem Biophys Res Commun* 299: 410–417.

47. Annilo T and Dean M. 2004. Degeneration of an ATP-binding cassette transporter gene, ABCC13, in different mammalian lineages. *Genomics* 84: 34–46.

48. Haimeur A, Conseil G, Deeley RG, and Cole SP. 2004. The MRP-related and BCRP/ABCG2 multidrug resistance proteins: Biology, substrate specificity and regulation. *Curr Drug Metab* 5: 21–53.

49. Payen L, Sparfel L, Courtois A, Vernhet L, Guillouzo A, and Fardel O. 2002. The drug efflux pump MRP2: Regulation of expression in physiopathological situations and by endogenous and exogenous compounds. *Cell Biol Toxicol* 18: 221–233.

50. Catania VA, Sánchez Pozzi EJ, Luquita MG, Ruiz ML, Villanueva SS, Jones B et al. 2004. Co-regulation of expression of phase II metabolizing enzymes and multidrug resistance-associated protein 2. *Ann Hepatol* 00: 311–317.

51. Fromm MF. 2002. The influence of MDR1 polymorphisms on P-glycoprotein expression and function in humans. *Adv Drug Deliv Rev* 54: 1295–1310.

52. van de Water FM, Masereeuw R, and Russel FG. 2005. Function and regulation of multidrug resistance proteins (MRPs) in the renal elimination of organic anions. *Drug Metab Rev* 37: 443–471.

53. Mayer R, Kartenbeck J, Büchler M, Jedlitschky G, Leier I, and Keppler D. 1995. Expression of the MRP gene-encoded conjugate export pump in liver and its selective absence from the canalicular membrane in transport-deficient mutant hepatocytes. *J Cell Biol* 131: 137–150.

54. Peng KC, Cluzeaud F, Bens M, Van Huyen JP, Wioland MA, Lacave R et al. 1999. Tissue and cell distribution of the multidrug resistance-associated protein (MRP) in mouse intestine and kidney. *J Histochem Cytochem* 47: 757–768.

55. Pei QL, Kobayashi Y, Tanaka Y, Taguchi Y, Higuchi K, Kaito M et al. 2002. Increased expression of multidrug resistance-associated protein 1 (mrp1) in hepatocyte basolateral membrane and renal tubular epithelia after bile duct ligation in rats. *Hepatol Res* 22: 58–64.

56. Scheffer GL, Kool M, de Haas M, de Vree JM, Pijnenborg AC, Bosman DK et al. 2002. Tissue distribution and induction of human multidrug resistant protein 3. *Lab Invest* 82: 193–201.

57. Nies AT, Jedlitschky G, Konig J, Herold-Mende C, Steiner HH, Schmitt HP et al. 2004. Expression and immunolocalization of the multidrug resistance proteins, MRP1-MRP6 (ABCC1-ABCC6), in human brain. *Neuroscience* 129: 349–360.

58. Lorico A, Rappa G, Finch RA, Yang D, Flavell RA, and Sartorelli AC. 1997. Disruption of the murine MRP (multidrug resistance protein) gene leads to increased sensitivity to etoposide (VP-16) and increased levels of glutathione. *Cancer Res* 57: 5238–5242.

59. Versantvoort CH, Broxterman HJ, Bagrij T, Scheper RJ, and Twentyman PR. 1995. Regulation by glutathione of drug transport in multidrug-resistant human lung tumour cell lines overexpressing multidrug resistance-associated protein. *Br J Cancer* 72: 82–89.

60. Versantvoort CH, Bagrij T, Wright KA, and Twentyman PR. 1995. On the relationship between the probenecid-sensitive transport of daunorubicin or calcein and the glutathione status of cells overexpressing the multidrug resistance-associated protein (MRP). *Int J Cancer* 63: 855–862.

61. Cole SP and Deeley RG. 2006. Transport of glutathione and glutathione conjugates by MRP1. *Trends Pharmacol Sci* 27: 438–446.

62. Franco R and Cidlowski JA. 2006. SLCO/OATP-like transport of glutathione in FasL-induced apoptosis: Glutathione efflux is coupled to an organic anion exchange and is necessary for the progression of the execution phase of apoptosis. *J Biol Chem* 281: 29542–29557.

63. Hammond CL, Marchan R, Krance SM, and Ballatori N. 2007. Glutathione export during apoptosis requires functional multidrug resistance-associated proteins. *J Biol Chem* 282: 14337–14347.

64. Trompier D, Chang XB, Barattin R, du Moulinet D'Hardemare A, Di Pietro A, and Baubichon-Cortay H. 2004. Verapamil and its derivative trigger apoptosis through glutathione extrusion by multidrug resistance protein MRP1. *Cancer Res* 64: 4950–4956.

65. Perrotton T, Trompier D, Chang XB, Di Pietro A, and Baubichon-Cortay H. 2007. (*R*)- and (*S*)-verapamil differentially modulate the multidrug-resistant protein MRP1. *J Biol Chem* 282: 31542–31548.

66. Wijnholds J, Evers R, van Leusden MR, Mol CA, Zaman GJ, and Mayer U et al. 1997. Increased sensitivity to anticancer drugs and decreased inflammatory response in mice lacking the multidrug resistance-associated protein. *Nat Med* 3: 1275–1279.

67. van der Deen M, Timens W, Timmer-Bosscha H, van der Strate BW, Scheper RJ, Postma DS et al. 2007. Reduced inflammatory response in cigarette smoke exposed Mrp1/Mdr1a/1b deficient mice. *Respir Res* 8: 49–65.

68. Lee G and Piquette-Miller M. 2001. Influence of IL-6 on MDR and MRP-mediated multidrug resistance in human hepatoma cells. *Can J Physiol Pharmacol* 79: 876–884.

69. Lickteig AJ, Slitt AL, Arkan MC, Karin M, and Cherrington NJ. 2007. Differential regulation of hepatic transporters in the absence of tumor necrosis factor-alpha, interleukin-1beta, interleukin-6, and nuclear factor-kappaB in two models of cholestasis. *Drug Metab Dispos* 35: 402–409.

70. Dreuw A, Hermanns HM, Heise R, Joussen S, Rodriguez F, Marquardt Y et al. 2005. Interleukin-6-type cytokines upregulate expression of multidrug resistanceassociated proteins in NHEK and dermal fibroblasts. *J Invest Dermatol* 124: 28–37.

71. Evers R, Cnubben NH, Wijnholds J, van Deemter L, van Bladeren PJ, and Borst P. 1997. Transport of glutathione prostaglandin A conjugates by the multidrug resistance protein 1. *FEBS Lett* 419: 112–116.

72. Reid G, Wielinga P, Zelcer N, van der Heijden I, Kuil A, de Haas M et al. 2003. The human multidrug resistance protein MRP4 functions as a prostaglandin efflux transporter and is inhibited by nonsteroidal anti-inflammatory drugs. *Proc Natl Acad Sci U S A* 100: 9244–9249.

73. Lin ZP, Zhu YL, Johnson DR, Rice KP, Nottoli T, Hains BC et al. 2008. Disruption of cAMP and PGE2 transport by Mrp4 deficiency alters cAMP-mediated signaling and nociceptive response. *Mol Pharmacol* 73: 243–251.

74. Bernard C, Merval R, Lebret M, Delerive P, Dusanter-Fourt I, Lehoux S et al. 1999. Oncostatin M induces interleukin-6 and cyclooxygenase-2 expression in human vascular smooth muscle cells: Synergy with interleukin-1beta. *Circ Res* 85: 1124–1131.

75. Repovic P, Mi K, and Benveniste EN. 2003. Oncostatin M enhances the expression of prostaglandin E2 and cyclooxygenase-2 in astrocytes: Synergy with interleukin- 1beta, tumor necrosis factor-alpha, and bacterial lipopolysaccharide. *Glia* 42: 433–446.

76. Robbiani DF, Finch RA, Jager D, Muller WA, Sartorelli AC, and Randolph GJ. 2000. The leukotriene C(4) transporter MRP1 regulates CCL19 (MIP-3beta, ELC)-dependent mobilization of dendritic cells to lymph nodes. *Cell* 103: 757–768.

77. Kyle-Cezar F, Echevarria-Lima J, and Rumjanek VM. 2007. Independent regulation of ABCB1 and ABCC activities in thymocytes and bone marrow mononuclear cells during aging. *Scand J Immunol* 66: 238–248.

78. Ros JE, Libbrecht L, Geuken M, Jansen PL, and Roskams TA. 2003. High expression of MDR1, MRP1, and MRP3 in the hepatic progenitor cell compartment and hepatocytes in severe human liver disease. *J Pathol* 200: 553–560.

79. Vos TA, Ros JE, Havinga R, Moshage H, Kuipers F, Jansen PL et al. 1999. Regulation of hepatic transport systems involved in bile secretion during liver regeneration in rats. *Hepatology* 29: 1833–1839.

80. Roelofsen H, Hooiveld GJ, Koning H, Havinga R, Jansen PL, and Muller M. 1999. Glutathione S-conjugate transport in hepatocytes entering the cell cycle is preserved by a switch in expression from the apical MRP2 to the basolateral MRP1 transporting protein. *J Cell Sci* 112 (Pt 9): 1395–1404.

81. Buchler M, Konig J, Brom M, Kartenbeck J, Spring H, Horie T et al. 1996. cDNA cloning of the hepatocyte canalicular isoform of the multidrug resistance protein, cMrp, reveals a novel conjugate export pump deficient in hyperbilirubinemic mutant rats. *J Biol Chem* 271: 15091–15098.

82. Taniguchi K, Wada M, Kohno K, Nakamura T, Kawabe T, Kawakami M et al. 1996. A human canalicular multispecific organic anion transporter (cMOAT) gene is overexpressed in cisplatin-resistant human cancer cell lines with decreased drug accumulation. *Cancer Res* 56: 4124–4129.

83. van Kuijck MA, van Aubel RA, Busch AE, Lang F, Russel FG, Bindels RJ et al. 1996. Molecular cloning and expression of a cyclic AMP-activated chloride conductance regulator: A novel ATP-binding cassette transporter. *Proc Natl Acad Sci U S A* 93: 5401–5406.

84. Fritz F, Chen J, Hayes P, and Sirotnak FM. 2000. Molecular cloning of the murine cMOAT ATPase. *Biochim Biophys Acta* 1492: 531–536.

85. Conrad S, Viertelhaus A, Orzechowski A, Hoogstraate J, Gjellan K, Schrenk D et al. 2001. Sequencing and tissue distribution of the canine MRP2 gene compared with MRP1 and MDR1. *Toxicology* 156: 81–91.

86. Keppler D and Konig J. 1997. Hepatic canalicular membrane 5: Expression and localization of the conjugate export pump encoded by the MRP2 (cMRP/cMOAT) gene in liver. *FASEB J* 11: 509–516.

87. Schaub TP, Kartenbeck J, Konig J, Vogel O, Witzgall R, Kriz W et al. 1997. Expression of the conjugate export pump encoded by the mrp2 gene in the apical membrane of kidney proximal tubules. *J Am Soc Nephrol* 8: 1213–1221.

88. Schaub TP, Kartenbeck J, Konig J, Spring H, Dorsam J, Staehler G et al. 1999. Expression of the MRP2 gene-encoded conjugate export pump in human kidney proximal tubules and in renal cell carcinoma. *J Am Soc Nephrol* 10: 1159–1169.

89. Mottino AD, Hoffman T, Jennes L, and Vore M. 2000. Expression and localization of multidrug resistant protein mrp2 in rat small intestine. *J Pharmacol Exp Ther* 293: 717–723.

90. Rost D, Mahner S, Sugiyama Y, and Stremmel W. 2002. Expression and localization of the multidrug resistance-associated protein 3 in rat small and large intestine. *Am J Physiol Gastrointest Liver Physiol* 282: 720–726.

91. Rost D, Konig J, Weiss G, Klar E, Stremmel W, and Keppler D. 2001. Expression and localization of the multidrug resistance proteins MRP2 and MRP3 in human gallbladder epithelia. *Gastroenterology* 121: 1203–1208.

92. Hoffmann K, Gastens AM, Volk HA, and Loscher W. 2006. Expression of the multidrug transporter MRP2 in the blood-brain barrier after pilocarpine-induced seizures in rats. *Epilepsy Res* 69: 1–14.

93. Taipalensuu J, Tornblom H, Lindberg G, Einarsson C, Sjoqvist F, Melhus H et al. 2001. Correlation of gene expression of ten drug efflux proteins of the ATPbinding cassette transporter family in normal human jejunum and in human intestinal epithelial Caco-2 cell monolayers. *J Pharmacol Exp Ther* 299: 164–170.

94. Cherrington NJ, Hartley DP, Li N, Johnson DR, and Klaassen CD. 2002. Organ distribution of multidrug resistance proteins 1, 2, and 3 (Mrp1, 2, and 3) mRNA and hepatic induction of Mrp3 by constitutive androstane receptor activators in rats. *J Pharmacol Exp Ther* 300: 97–104.

95. Oselin K, Mrozikiewicz PM, Pahkla R, and Roots I. 2003. Quantitative determination of the human MRP1 and MRP2 mRNA expression in FACS-sorted peripheral blood CD4+, CD8+, CD19+, and CD56+ cells. *Eur J Haematol* 71: 119–123.

96. Schinkel AH and Jonker JW. 2003. Mammalian drug efflux transporters of the ATP binding cassette (ABC) family: An overview. *Adv Drug Deliv Rev* 55: 3–29.

97. Surowiak P, Materna V, Kaplenko I, Spaczynski M, Dolinska-Krajewska B, Gebarowska E et al. 2006. ABCC2 (MRP2, cMOAT) can be localized in the nuclear membrane of ovarian carcinomas and correlates with resistance to cisplatin and clinical outcome. *Clin Cancer Res* 12: 7149–7158.

98. Tomer G, Ananthanarayanan M, Weymann A, Balasubramanian N, and Suchy FJ. 2003. Differential developmental regulation of rat liver canalicular membrane transporters Bsep and Mrp2. *Pediatr Res* 53: 288–294.

99. Ros JE, Roskams TA, Geuken M, Havinga R, Splinter PL, and Petersen BE. 2003. ATP binding cassette transporter gene expression in rat liver progenitor cells. *Gut* 52: 1060–1067.

100. Cao J, Stieger B, Meier PJ, and Vore M. 2002. Expression of rat hepatic multidrug resistance-associated proteins and organic anion transporters in pregnancy. *Am J Physiol Gastrointest Liver Physiol* 283: 757–766.

101. Mottino AD, Hoffman T, Jennes L, Cao J, and Vore M. 2001. Expression of multidrug resistance-associated protein 2 in small intestine from pregnant and postpartum rats. *Am J Physiol Gastrointest Liver Physiol* 280: G1261–G1273.

102. St-Pierre MV, Serrano MA, Macias RI, Dubs U, Hoechli M, Lauper U et al. 2000. Expression of members of the multidrug resistance protein family in human term placenta. *Am J Physiol Regul Integr Comp Physiol* 279: R1495–R1503.

103. Hashimoto K, Uchiumi T, Konno T, Ebihara T, Nakamura T, Wada M et al. 2002. Trafficking and functional defects by mutations of the ATP-binding domains in MRP2 in patients with Dubin-Johnson syndrome. *Hepatology* 36: 1236–1245.

104. Kajihara S, Hisatomi A, Mizuta T, Hara T, Ozaki I, Wada I et al. 1998. A splice mutation in the human canalicular multispecific organic anion transporter gene causes Dubin-Johnson syndrome. *Biochem Biophys Res Commun* 253: 454–457.

105. Keitel V, Kartenbeck J, Nies AT, Spring H, Brom M, and Keppler D. 2000. Impaired protein maturation of the conjugate export pump multidrug resistance protein 2 as a consequence of a deletion mutation in Dubin-Johnson syndrome. *Hepatology* 32: 1317–13728.

106. Mor-Cohen R, Zivelin A, Rosenberg N, Shani M, Muallem S, and Seligsohn U. 2001. Identification and functional analysis of two novel mutations in the multidrug resistance protein 2 gene in Israeli patients with Dubin-Johnson syndrome. *J Biol Chem* 276: 36923–36930.

107. Paulusma CC, Kool M, Bosma PJ, Scheffer GL, ter Borg F, Scheper RJ et al. 1997. A mutation in the human canalicular multispecific organic anion transporter gene causes the Dubin-Johnson syndrome. *Hepatology* 25: 1539–1542.

108. Shoda J, Suzuki H, Suzuki H, Sugiyama Y, Hirouchi M, Utsunomiya H et al. 2003. Novel mutations identified in the human multidrug resistance-associated protein 2 (MRP2/ABCC2) gene in a Japanese patient with Dubin-Johnson syndrome. *Hepatol Res* 27: 323–326.

109. Tate G, Li M, Suzuki T, and Mitsuya T. 2002. A new mutation of the ATP-binding cassette, sub-family C, member 2 (ABCC2) gene in a Japanese patient with Dubin- Johnson syndrome. *Genes Genet Syst* 77: 117–121.

110. Toh S, Wada M, Uchiumi T, Inokuchi A, Makino Y, Horie Y et al. 1999. Genomic structure of the canalicular multispecific organic anion-transporter gene (MRP2/ cMOAT) and mutations in the ATP-binding-cassette region in Dubin-Johnson syndrome. *Am J Hum Genet* 64: 739–746.

111. Tsujii H, König J, Rost D, Stöckel B, Leuschner U, and Keppler D. 1999. Exonintron organization of the human multidrug-resistance protein 2 (MRP2) gene mutated in Dubin-Johnson syndrome. *Gastroenterology* 117: 653–660.

112. Wada M, Toh S, Taniguchi K, Nakamura T, Uchiumi T, Kohno K et al. 1998. Mutations in the canilicular multispecific organic anion transporter (cMOAT) gene, a novel ABC transporter, in patients with hyperbilirubinemia II/Dubin- Johnson syndrome. *Hum Mol Genet* 7: 203–207.

113. Wakusawa S, Machida I, Suzuki S, Hayashi H, Yano M, and Yoshioka K. 2003. Identification of a novel 2026G→C mutation of the MRP2 gene in a Japanese patient with Dubin-Johnson syndrome. *J Hum Genet* 48: 425–429.

114. König J, Rost D, Cui Y, and Keppler D. 1999. Characterization of the human multidrug resistance protein isoform MRP3 localized to the basolateral hepatocyte membrane. *Hepatology* 29: 1156–1163.

115. Muller M and Jansen PL. 1997. Molecular aspects of hepatobiliary transport. *Am J Physiol* 272: G1285–G1303.

116. Chu XY, Strauss JR, Mariano MA, Li J, Newton DJ, Cai X et al. 2006. Characterization of mice lacking the multidrug resistance protein MRP2 (ABCC2). *J Pharmacol Exp Ther* 317: 579–589.

117. Vlaming ML, Mohrmann K, Wagenaar E, de Waart DR, Elferink RP, Lagas JS et al. 2006. Carcinogen and anticancer drug transport by Mrp2 in vivo: Studies using Mrp2 (Abcc2) knockout mice. *J Pharmacol Exp Ther* 318: 319–327.

118. Nezasa K, Tian X, Zamek-Gliszczynski MJ, Patel NJ, Raub TJ et al. 2006. Altered hepatobiliary disposition of 5 (and 6)-carboxy-2′,7′-dichlorofluorescein in Abcg2 (Bcrp1) and Abcc2 (Mrp2) knockout mice. *Drug Metab Dispos* 34: 718–723.

119. Huang L, Smit JW, Meijer DK, and Vore M. 2000. Mrp2 is essential for estradiol- 17-beta(D-glucuronide)-induced cholestasis in rats. *Hepatology* 32: 66–72.

120. Rost D, Kartenbeck J, and Keppler D. 1999. Changes in the localization of the rat canalicular conjugate export pump Mrp2 in phalloidin-induced cholestasis. *Hepatology* 29: 814–821.

121. Trauner M, Arrese M, Soroka CJ, Ananthanarayanan M, Koeppel TA, Schlosser SF et al. 1997. The rat canalicular conjugate export pump (Mrp2) is down-regulated in intrahepatic and obstructive cholestasis. *Gastroenterology* 113: 255–264.

122. Vos TA, Hooiveld GJ, Koning H, Childs S, Meijer DK, Moshage H et al. 1998. Up-regulation of the multidrug resistance genes, Mrp1 and Mdr1b, and downregulation of the organic anion transporter, Mrp2, and the bile salt transporter, Spgp, in endotoxemic rat liver. *Hepatology* 28: 1637–1644.

123. Ruiz ML, Villanueva SS, Luquita MG, Vore M, Mottino AD, and Catania VA. 2006. Ethynylestradiol increases expression and activity of rat liver MRP3. *Drug Metab Dispos* 34: 1030–1034.

124. Cao J, Huang L, Liu Y, Hoffman T, Stieger B, Meier PJ et al. 2001. Differential regulation of hepatic bile salt and organic anion transporters in pregnant and postpartum rats and the role of prolactin. *Hepatology* 33: 140–147.

125. Demeule M, Jodoin J, Beaulieu E, Brossard M, and Beliveau R. 1999. Dexamethasone modulation of multidrug transporters in normal tissues. *FEBS Lett* 442: 208–214.

126. Courtois A, Payen L, Guillouzo A, and Fardel O. 1999. Up-regulation of multidrug resistance-associated protein 2 (MRP2) expression in rat hepatocytes by dexamethasone. *FEBS Lett* 459: 381–385.

127. Turncliff RZ, Meier PJ, and Brouwer KL. 2004. Effect of dexamethasone treatment on the expression and function of transport proteins in sandwich-cultured rat hepatocytes. *Drug Metab Dispos* 32: 834–839.

128. Kast HR, Goodwin B, Tarr PT, Jones SA, Anisfeld AM, Stoltz CM et al. 2002. Regulation of multidrug resistance-associated protein 2 (ABCC2) by the nuclear receptors pregnane X receptor, farnesoid X-activated receptor, and constitutive androstane receptor. *J Biol Chem* 277: 2908–2915.

129. Dussault I, Lin M, Hollister K, Wang EH, Synold TW, and Forman BM. 2001. Peptide mimetic HIV protease inhibitors are ligands for the orphan receptor SXR. *J Biol Chem* 276: 33309–33312.

130. Fromm MF, Kauffmann HM, Fritz P, Burk O, Kroemer HK, Warzok RW et al. 2000. The effect of rifampin treatment on intestinal expression of human MRP transporters. *Am J Pathol* 157: 1575–1580.

131. Hirohashi T, Suzuki H, and Sugiyama Y. 1999. Characterization of the transport properties of cloned rat multidrug resistance-associated protein 3 (MRP3). *J Biol Chem* 274: 15181–15185.

132. Kiuchi Y, Suzuki H, Hirohashi T, Tyson CA, and Sugiyama Y. 1998. cDNA cloning and inducible expression of human multidrug resistance associated protein 3 (MRP3). *FEBS Lett* 433: 149–152.

133. Kiuchi Y, Dawson PA, and Sugiyama Y. 2005. Analysis of the in vivo functions of Mrp3. *FEBS Lett* 68: 160–168.

134. Uchiumi T, Hinoshita E, Haga S, Nakamura T, Tanaka T, Toh S et al. 1998. Isolation of a novel human canalicular multispecific organic anion transporter, cMOAT2/ MRP3, and its expression in cisplatin-resistant cancer cells with decreased ATPdependent drug transport. *Biochem Biophys Res Commun* 252: 103–110.

135. Maher JM, Slitt AL, Cherrington NJ, Cheng X, and Klaassen CD. 2005. Tissue distribution and hepatic and renal ontogeny of the multidrug resistance-associated protein (Mrp) family in mice. *Drug Metab Dispos* 33: 947–955.

136. Shoji T, Suzuki H, Kusuhara H, Watanabe Y, Sakamoto S, and Sugiyama Y. 2004. ATP-dependent transport of organic anions into isolated basolateral membrane vesicles from rat intestine. *Am J Physiol Gastrointest Liver Physiol* 287: 749–756.

137. Hirohashi T, Suzuki H, Takikawa H, and Sugiyama Y. 2000. ATP-dependent transport of bile salts by rat multidrug resistance-associated protein 3 (Mrp3). *J Biol Chem* 275: 2905–2910.

138. Kool M, van der Linden M, de Haas M, Scheffer GL, de Vree JM, Smith AJ et al. 1999. MRP3, an organic anion transporter able to transport anti-cancer drugs. *Proc Natl Acad Sci U S A* 96: 6914–6919.

139. Soroka CJ, Lee JM, Azzaroli F, and Boyer JL. 2001. Cellular localization and upregulation of multidrug resistance-associated protein 3 in hepatocytes and cholangiocytes during obstructive cholestasis in rat liver. *Hepatology* 33: 783–791.

140. Ballestero MR, Monte MJ, Briz O, Jimenez F, Gonzalez-San Martin F, and Marin JJ. 2006. Expression of transporters potentially involved in the targeting of cytostatic bile acid derivatives to colon cancer and polyps. *Biochem Pharmacol* 72: 729–738.

141. Zimmermann C, Gutmann H, Hruz P, Gutzwiller JP, Beglinger C, and Drewe J. 2005. Mapping of multidrug resistance gene 1 and multidrug resistance-associated protein isoform 1 to 5 mRNA expression along the human intestinal tract. *Drug Metab Dispos* 33: 219–224.

142. Kuroda M, Kobayashi Y, Tanaka Y, Itani T, Mifuji R, Araki J et al. 2004. Increased hepatic and renal expressions of multidrug resistance-associated protein 3 in Eisai hyperbilirubinuria rats. *J Gastroenterol Hepatol* 19: 146–153.

143. Hirohashi T, Suzuki H, Ito K, Ogawa K, Kume K, Shimizu T et al. 1998. Hepatic expression of multidrug resistance-associated protein-like proteins maintained in Eisai hyperbilirubinemic rats. *Mol Pharmacol* 53: 1068–1075.

144. Slitt AL, Cherrington NJ, Maher JM, and Klaassen CD. 2003. Induction of multidrug resistance protein 3 in rat liver is associated with altered vectorial excretion of acetaminophen metabolites. *Drug Metab Dispos* 31: 1176–1186. 32

145. Trauner M and Boyer JL. 2003. Bile salt transporters: Molecular characterization, function, and regulation. *Physiol Rev* 83: 633–671.

146. Belinsky MG, Dawson PA, Shchaveleva I, Bain LJ, Wang R, Ling V et al. 2005. Analysis of the in vivo functions of Mrp3. *Mol Pharmacol* 68: 160–168.

147. Zelcer N, van de Wetering K, de Waart R, Scheffer GL, Marschall HU, Wielinga PR et al. 2006. Mice lacking Mrp3 (Abcc3) have normal bile salt transport, but altered hepatic transport of endogenous glucuronides. *J Hepatol* 44: 768–775.

148. Andric SA, Kostic TS, and Stojilkovic SS. 2006. Contribution of multidrug resistance protein MRP5 in control of cyclic guanosine 5′-monophosphate intracellular signaling in anterior pituitary cells. *Endocrinology* 147: 3435–3445.

149. Kool M, de Haas M, Scheffer GL, Scheper RJ, van Eijk MJ, Juijn JA et al. 1997. Analysis of expression of cMOAT (MRP2), MRP3, MRP4, and MRP5, homologues of the multidrug resistance-associated protein gene (MRP1), in human cancer cell lines. *Cancer Res* 57: 3537–3547.

150. Lee K, Belinsky MG, Bell DW, Testa JR, and Kruh GD. 1998. Isolation of MOAT-B, a widely expressed multidrug resistance-associated protein/canalicular multispecific organic anion transporter-related transporter. *Cancer Res* 58: 2741–2747.

151. Chen C and Klaassen CD. 2004. Rat multidrug resistance protein 4 (Mrp4, Abcc4): Molecular cloning, organ distribution, postnatal renal expression, and chemical inducibility. *Biochem Biophys Res Commun* 317: 46–53.

152. Schuetz JD, Connelly MC, Sun D, Paibir SG, Flynn PM, Srinivas RV et al. 1999. MRP4: A previously unidentified factor in resistance to nucleoside-based antiviral drugs. *Nat Med* 5: 1048–1051.

153. Chen ZS, Lee K, and Kruh GD. 2001. Transport of cyclic nucleotides and estradiol 17-beta-D-glucuronide by multidrug resistance protein 4. Resistance to 6- mercaptopurine and 6-thioguanine. *J Biol Chem* 276: 33747–33754.

154. Lai L and Tan TM. 2002. Role of glutathione in the multidrug resistance protein 4 (MRP4/ABCC4)-mediated efflux of cAMP and resistance to purine analogues. *Biochem J* 361: 497–503.

155. Wielinga PR, Reid G, Challa EE, van der Heijden I, van Deemter L, de Haas M et al. 2002. Thiopurine metabolism and identification of the thiopurine metabolites transported by MRP4 and MRP5 overexpressed in human embryonic kidney cells. *Mol Pharmacol* 62: 1321–1331.

156. Wielinga PR, van der Heijden I, Reid G, Beijnen JH, Wijnholds J, and Borst P. 2003. Characterization of the MRP4- and MRP5-mediated transport of cyclic nucleotides from intact cells. *J Biol Chem* 278: 17664–17671.

157. Reid G, Wielinga P, Zelcer N, De Haas M, Van Deemter L, Wijnholds J et al. 2003. Characterization of the transport of nucleoside analog drugs by the human multidrug resistance proteins MRP4 and MRP5. *Mol Pharmacol* 63: 1094–1103.

158. Imaoka T, Kusuhara H, Adachi M, Schuetz JD, Takeuchi K, and Sugiyama Y. 2007. Functional involvement of multidrug resistance-associated protein 4 (MRP4/ ABCC4) in the renal elimination of the antiviral drugs adefovir and tenofovir. *Mol Pharmacol* 71: 619–627.

159. van Aubel RA, Smeets PH, Peters JG, Bindels RJ, and Russel FG. 2002. The MRP4/ABCC4 gene encodes a novel apical organic anion transporter in human kidney proximal tubules: Putative efflux pump for urinary cAMP and cGMP. *J Am Soc Nephrol* 13: 595–603.

160. Leggas M, Adachi M, Scheffer GL, Sun D, Wielinga P, Du G et al. 2004. Mrp4 confers resistance to topotecan and protects the brain from chemotherapy. *Mol Cell Biol* 24: 7612–7621.

161. Lee K, Klein-Szanto AJ, and Kruh GD. 2000. Analysis of the MRP4 drug resistance profile in transfected NIH3T3 cells. *J Natl Cancer Inst* 92: 1934–1940.

162. Rius M, Nies AT, Hummel-Eisenbeiss J, Jedlitschky G, and Keppler D. 2003. Cotransport of reduced glutathione with bile salts by MRP4 (ABCC4) localized

to the basolateral hepatocyte membrane. *Hepatology* 38: 374–384.

163. Zelcer N, Reid G, Wielinga P, Kuil A, van der Heijden I, Schuetz JD, and Borst P. 2003. Steroid and bile acid conjugates are substrates of human multidrug-resistance protein (MRP) 4 (ATP-binding cassette C4). *Biochem J* 371: 361–367.

164. Belinsky MG, Guo P, Lee K, Zhou F, Kotova E, Grinberg A et al. 2007. Multidrug resistance protein 4 protects bone marrow, thymus, spleen, and intestine from nucleotide analogue-induced damage. *Cancer Res* 67: 262–268.

165. Belinsky MG, Bain LJ, Balsara BB, Testa JR, and Kruh GD. 1998. Characterization of MOAT-C and MOAT-D, new members of the MRP/cMOAT subfamily of transporter proteins. *J Natl Cancer Inst* 90: 1735–1741.

166. Meyer Zu Schwabedissen HE, Grube M, Heydrich B, Linnemann K, Fusch C, Kroemer HK et al. 2005. Expression, localization, and function of MRP5 (ABCC5), a transporter for cyclic nucleotides, in human placenta and cultured human trophoblasts: Effects of gestational age and cellular differentiation. *Am J Pathol* 166: 39–48.

167. Suzuki T, Sasaki H, Kuh HJ, Agui M, Tatsumi Y, Tanabe S et al. 2000. Detailed structural analysis on both human MRP5 and mouse mrp5 transcripts. *Gene* 242: 167–173.

168. Maher JM, Cherrington NJ, Slitt AL, and Klaassen CD. 2006. Tissue distribution and induction of the rat multidrug resistance-associated proteins 5 and 6. *Life Sci* 78: 2219–2225.

169. McAleer MA, Breen MA, White NL, and Matthews N. 1999. pABC11 (also known as MOAT-C and MRP5), a member of the ABC family of proteins, has anion transporter activity but does not confer multidrug resistance when overexpressed in human embryonic kidney 293 cells. *J Biol Chem* 274: 23541–23548.

170. Jedlitschky G, Burchell B, and Keppler D. 2000. The multidrug resistance protein 5 functions as an ATP-dependent export pump for cyclic nucleotides. *J Biol Chem* 275: 30069–30074.

171. Wijnholds J, Mol CA, van Deemter L, de Haas M, Scheffer GL, Baas F et al. 2000. Multidrug-resistance protein 5 is a multispecific organic anion transporter able to transport nucleotide analogs. *Proc Natl Acad Sci U S A* 97: 7476–7481.

172. Madon J, Hagenbuch B, Landmann L, Meier PJ, and Stieger B. 2000. Transport function and hepatocellular localization of mrp6 in rat liver. *Mol Pharmacol* 57: 634–641.

173. Scheffer GL, Hu X, Pijnenborg AC, Wijnholds J, Bergen AA, and Scheper RJ. 2002. MRP6 (ABCC6) detection in normal human tissues and tumors. *Lab Invest* 82: 515–518.

174. Beck K, Hayashi K, Nishiguchi B, Le Saux O, Hayashi M, and Boyd CD. 2003. The distribution of Abcc6 in normal mouse tissues suggests multiple functions for this ABC transporter. *J Histochem Cytochem* 51: 887–902.

175. Sinko E, Ilias A, Ujhelly O, Homolya L, Scheffer GL, Bergen AA et al. 2003. Subcellular localization and N-glycosylation of human ABCC6, expressed in MDCKII cells. *Biochem Biophys Res Commun* 308: 263–269.

176. Belinsky MG and Kruh GD. 1999. MOAT-E (ARA) is a full-length MRP/cMOAT subfamily transporter expressed in kidney and liver. *Br J Cancer* 80: 1342–1349.

177. Hu X, et al. 2003. Analysis of the frequent R1141X mutation in the ABCC6 gene in pseudoxanthoma elasticum. *Invest Ophthalmol Vis Sci* 44 (5): 1824–1829.

178. Hu X, Plomp A, Wijnholds J, Ten Brink J, van Soest S, van den Born LI et al. 2003. ABCC6/MRP6 mutations: Further insight into the molecular pathology of pseudoxanthoma elasticum. *Eur J Hum Genet* 11: 215–224.

179. Belinsky MG, Chen ZS, Shchaveleva I, Zeng H, and Kruh GD. 2002. Characterization of the drug resistance and transport properties of multidrug resistance protein 6 (MRP6, ABCC6). *Cancer Res* 62: 6172–6177.

180. Bergen AA, Plomp AS, Hu X, de Jong PT, and Gorgels TG. 2007. ABCC6 and pseudoxanthoma elasticum. *Pflugers Arch* 453: 685–691.

181. Gorgels TG, Hu X, Scheffer GL, van der Wal AC, Toonstra J, de Jong PT et al. 2005. Disruption of Abcc6 in the mouse: Novel insight in the pathogenesis of pseudoxanthoma elasticum. *Hum Mol Genet* 14: 1763–1773.

182. Li Q, Jiang Q, and Uitto J. 2008. Pseudoxanthoma elasticum: Oxidative stress and antioxidant diet in a mouse model (Abcc6(−/−). *J Invest Dermatol* 128: 1160–1164.

183. Chen ZS, et al. 2003. Characterization of the transport properties of human multidrug resistance protein 7 (MRP7, ABCC10). *Mol Pharmacol* 63 (2): 351–358.

184. Kao HH, Chang MS, Cheng JF, and Huang JD. 2003. Genomic structure, gene expression, and promoter analysis of human multidrug resistance-associated protein 7. *J Biomed Sci* 10: 98–110.

185. Takayanagi S, Kataoka T, Ohara O, Oishi M, Kuo MT, and Ishikawa T. 2004. Human ATP-binding cassette transporter ABCC10: Expression profile and p53- dependent upregulation. *J Exp Ther Oncol* 4: 239–246.

186. Augustine LM, Markelewicz RJ, Jr., Boekelheide K, and Cherrington NJ. 2005. Xenobiotic and endobiotic transporter mRNA expression in the blood-testis barrier. *Drug Metab Dispos* 33: 182–189.

187. Kruh GD, Guo Y, Hopper-Borge E, Belinsky MG, and Chen ZS. 2007. ABCC10, ABCC11, and ABCC12. *Pflugers Arch* 453: 675–684.

188. Hopper-Borge E, Chen ZS, Shchaveleva I, Belinsky MG, and Kruh GD. 2004. Analysis of the drug resistance profile of multidrug resistance protein 7 (ABCC10): Resistance to docetaxel. *Cancer Res* 64: 4927–4930.

189. Naramoto H, Uematsu T, Uchihashi T, Doto R, Matsuura T, Usui Y et al. 2007. Multidrug resistance-associated protein 7 expression is involved in crossresistance to docetaxel in salivary gland adenocarcinoma cell lines. *Int J Oncol* 30: 393–401.

190. Bortfeld M, Rius M, Konig J, Herold-Mende C, Nies AT, and Keppler D. 2006. Human multidrug resistance protein 8 (MRP8/ABCC11), an apical efflux pump for steroid sulfates, is an axonal protein of the CNS and peripheral nervous system. *Neuroscience* 137: 1247–1257.

191. Shimizu H, Taniguchi H, Hippo Y, Hayashizaki Y, Aburatani H, and Ishikawa T. 2003. Characterization of the mouse Abcc12 gene and its transcript encoding an ATP-binding cassette transporter, an orthologue of human ABCC12. *Gene* 310: 17–28.

192. Chen ZS, Guo Y, Belinsky MG, Kotova E, and Kruh GD. 2005. Transport of bile acids, sulfated steroids, estradiol 17-beta-D-glucuronide, and leukotriene C4 by human multidrug resistance protein 8 (ABCC11). *Mol Pharmacol* 67: 545–557.

193. Honorat M, Mesnier A, Vendrell J, Guitton J, Bieche I, Lidereau R et al. 2008. ABCC11 expression is regulated by estrogen in MCF7 cells, correlated with estrogen receptor alpha expression in postmenopausal breast tumors and overexpressed in Tamoxifen-resistant breast cancer cells. *Endocr Relat Cancer* 15: 125–138.

194. Du T, Feng B, Wang X, Mao W, Zhu X, and Li L et al. 2008. Localization and mutation detection for paroxysmal kinesigenic choreoathetosis. *J Mol Neurosci* 34: 101–107.

195. Yoshiura K, Kinoshita A, Ishida T, Ninokata A, Ishikawa T, Kaname T et al. 2006. A SNP in the ABCC11 gene is the determinant of human earwax type. *Nat Genet* 38: 324–330.

196. Miura K, Yoshiura K, Miura S, Shimada T, Yamasaki K, Yoshida A et al. 2007. A strong association between human earwax-type and apocrine colostrum secretion from the mammary gland. *Hum Genet* 121: 631–633.

197. Vendrell JA, Magnino F, Danis E, Duchesne MJ, Pinloche S, Pons M et al. 2004. Estrogen regulation in human breast cancer cells of new downstream gene targets involved in estrogen metabolism, cell proliferation and cell transformation. *J Mol Endocrinol* 32: 397–414.

198. Bera TK, Iavarone C, Kumar V, Lee S, Lee B, and Pastan I. 2002. MRP9, an unusual truncated member of the ABC transporter superfamily, is highly expressed in breast cancer. *Proc Natl Acad Sci U S A* 99: 6997–7002.

B. REGULATION DE L'EXPRESSION D'ABCC11 PAR LES STEROÏDES

I. HORMONO-REGULATION DES TRANSPORTEURS ABC

Tout comme le tissu mammaire normal, le tissu mammaire cancéreux est sujet à une forte imprégnation hormonale. Cette caractéristique a permis de mettre en œuvre des thérapies ciblées pour cette dépendance hormonale (hormonothérapie). Les transporteurs ABC étant exprimés dans ce tissu ainsi que dans d'autres tissus hormono-dépendants, de nombreuses études ont été réalisées concernant la régulation de leur expression par les hormones stéroïdes telles que les œstrogènes ou la progestérone. De plus, pour certains d'entre eux, leur expression peut être corrélée à l'expression des récepteurs hormonaux.

→ Publication 2. « **Expression level and hormonal regulation of ABC transporters in breast cancer.** » par M. Honorat et coll.

Revue acceptée dans Current Cancer Therapy Review

Expression Level and Hormonal Regulation of ABC Transporters in Breast Cancer

Honorat M[2,3], Guitton J[1,4,5], Dumontet C[2,3] and Payen L[1,2,3,4,*]

[1]*Université de Lyon, Lyon1, ISPB, Lyon, F-69008, France*

[2]*Inserm, U590, Lyon, F-69008, France*

[3]*Centre Léon Bérard, FNCLCC, Lyon, F-69008, France*

[4]*Université de Lyon, Faculté de pharmacie, Laboratoire de Toxicologie, Lyon, F-69008, France*

[5]*Hospices Civils de Lyon, Centre Hospitalier Lyon-Sud, Laboratoire de ciblage thérapeutique en cancérologie, Pierre Bénite, F-69495, France*

Abstract: Breast cancer remains the most common malignancy amongst women and its incidence continues to increase worldwide. Breast cancer is a heterogeneous disease with distinct molecular subtypes characterized by differential response to targeted (tamoxifen) and chemotherapeutic agents (5-FluoroUracil, methotrexate). Epidemiological observations emphasize the hormone dependency of breast cancer and the importance of endocrine therapies to treat the hormonally dependent cancers. ATP Binding Cassette (ABC) transporters form one of the largest of all protein families and are central to many important biomedical phenomena, including resistance mechanism of cancers. They are able to transport a variety of compounds through membranes against steep concentration gradients at the cost of ATP hydrolysis. After providing an overview of their tissue distribution, and various procedures to experimentally quantify their transport activity, we summarized the current literature regarding the putative regulation of ABC transporter expression levels by hormonal therapies including estrogens and tamoxifen, as well as the potential impact on the overall health of patients with breast cancer. Elucidation of the resistance mechanisms in cancers is essential for the rational choice of anticancer and adjuvant therapies given to the patients.

Keywords: Breast cancer, ABC transporters, MDR phenotype, endocrine regulation.

1. INTRODUCTION

With 548 000 deaths/year, breast cancer is the worldwide leading cause of death by cancer (WHO July 2008) and constitutes one of the major public health issues. Breast cancer is the most frequent cancer in women (1/10 in the Western World). Given the continuing growth and aging of the world's population, the impact on the global burden of cancer incidence on mortality will be substantial. For a better understanding of the complexity of breast cancer, the histological normal breast tissue, described in Fig. (**1**), shows that several compartments as ducts, lobules, or fatty tissue compose it.

Because of its large heterogeneity, breast cancer is classified into various categories according to various criteria as histological forms, histological grade of tumour and markers including ER (estrogen receptors) and ERBB2 (human epidermal growth factor receptor 2). Various types of breast cancer exist, usually subdivided into non-invasive (*in situ*) and invasive cancer. *In situ* carcinoma is characterized by cancer cell growth within the ducts without penetration of the basement membrane. These non-invasive cancers can affect ducts and lobules (*in situ* intraductal and *in situ* lobular carcinoma). Invasive carcinoma is characterised by basement membrane penetration of a duct with ductal carcinoma *in situ* and aggregation of neoplastic cells into mammary stroma. The most frequent invasive carcinoma is the ductal type with a 50 to 80 % rate. Tubular and mucinous carcinomas seem to have the best survival rate with figures from 80 to 100 % over 10 years. Medullary carcinomas have a survival rate superior to 50 %. Recently, basal carcinoma subgroup of breast cancer was fully defined by Korsching *et al* (2008) [1]. Some histological types of breast cancer without being exhaustive are summarized in Table **1**.

Globally, breast cancer still has a poor prognosis. At five year, survival rate is only 25 % for patients with node involvement (cancer cells found in breast proximal node). ERBB2 expression leads to herceptin® based therapy. This antibody therapy leads to improve anti-cancer therapy efficiency of ERBB2 positive tumours. ER and PR are important diagnostic markers and their co-expression is associated with good prognosis. ER positive breast cancer patients (60-70 %) benefit for endocrine therapies including tamoxifen (TAM) or fulvestrant. Nevertheless almost all responding patients acquire overtime resistance to the action of TAM with disease progress. Classical chemotherapies prescribed for breast

*Address correspondence to this author at the INSERM U590, Laboratoire de Cytologie Analytique, Institut des sciences biologiques et pharmaceutiques (ISPB) 8, Avenue Rockefeller, 69008 Lyon, France; Tel: +33-4-78777236; Fax: +33-4-78777088;
E-mail: Lea.payen@recherche.univ-lyon1.fr

1573-3947/10 $55.00+.00

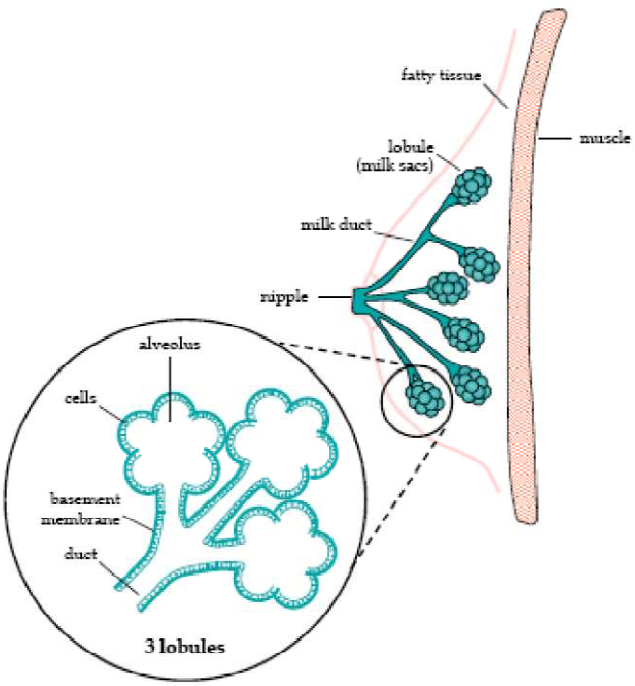

Fig. (1). The histological organization of normal mammary tissue.

cancer also combine anticancer drugs including cyclophosphamide, 5-FluoroUracil (5-FU), adriamycine, or methotrexate (MTX). There is another important category, with worse prognosis: the triple-negative (ER-negative, PR-negative, ERBB2 not overexpressed) breast cancer. This category has distinct clinical and pathologic features. It is a clinical problem because of its aggressive behaviour and lack of targeted therapies, leaving chemotherapy as the mainstay of treatment. Most triple-negative tumours fall into the basal-like molecular subtype of breast cancer, but the terms are not completely synonymous [4]. Furthermore, ER-negative, PR-negative and ERBB2-negative basal-like and ERBB2 positive and ER-negative subtypes are more sensitive to anthracycline-based neoadjuvant chemotherapy than ER-positive and PR-positive luminal breast cancers [5]. The poorer prognosis of basal-like and ERBB2 positive and ER-negative breast cancers could be explained by a higher likelihood of relapse in patients in whom pathologic complete response was not achieved (Table **1**) [5]. Taken altogether, resistance mechanisms often occurred in breast cancer relapses. They are due to multi-factorial events such as an alteration of apoptosis pathways, metabolism actors or efflux transporters. In this review, we focused on multi-drug resistance (MDR) phenotype involving ABC transporters.

ABC transporter family contains 49 members, classified into seven sub-families named ABCA to ABCG. ABC transporters are composed by 1, 2 or 3 membrane spanning domains (MSDs) alternating with nucleotide binding domains (NBDs). Typically, MSDs include six membrane crossings while cytoplasmic NBDs are especially involved in ATP binding and hydrolysis that is necessary for transport activity of substrates across the plasma membrane. NBDs contain several ABC consensus sequences including walker A, walker B and signature sequences. The classical and most common organisation, represented by ABCB1 (P-glycoprotein/P-gp), ABCC4, 5, 11 and 12, follows a MSD1-NBD1-MSD2-NBD2 structure. However, ABCC1, 2, 3, 6 and 10 contain an additional N-terminal "extension". This highly hydrophobic amino-terminal segment of ABCC1, named MSD0 was suggested to be membrane embedded with five transmembrane helices and to have an extracellular amino-terminus [6-9]. The presence of a MSD0-like domain in the "long" ABCC transporters is unique. The MSD0 of ABCC1 does not play a crucial role in the protein transport activity, while the intracellular loop L0 present between MSD0 and MSD1 is necessary for ABCC1 protein in its transport activity and for proper intracellular routing [10, 11]. MSD0 has been described to be important for ABCC1 retention in, or recycling to the plasma membrane [11]. Recent findings suggested that ABCC1 may exist and function as a dimer and that MSD0-L0 likely plays a role in some structural and regulatory functions [12].

ABCG2 (Breast Cancer Resistance Protein/BCRP) is a 72-kDa protein composed of 665 amino acids distributed in one N-terminal NBD followed by one C-terminal MSD. Therefore, its structure is half the most common size and is in reverse configuration to most other ABC proteins comprising two NBDs and two MSDs. Thus the half-transporter ABCG2 is believed to homodimerize, or possibly oligomerize in order to function [13]. Recently a specific function for ABCG2 has been discovered, showing its interaction with heme and other porphyrins, to protect cells and/or tissues from protoporphyrin accumulation under hypoxic conditions. Therefore, individuals who carry deficient ABCG2 alleles may be more susceptible to porphyrin-induced toxicity [14, 15].

The most characterized ABC transporters are ABCB1, ABCG2 and ABCCs. In cancerous tissues, their overexpression plays a major role in conferring the MDR phenotype by significantly reducing intracellular anticancer drug accumulation. In many healthy tissues, particularly those involved in secretory (e.g. gastrointestinal tract) or barrier (e.g. blood-brain barrier) roles, multidrug efflux pumps provide an inherent or inducible host cell defence mechanism against damage by endo- and xenobiotics. They can influence absorption, distribution, metabolism and excretion (ADME) of their substrates including anticancer drugs, toxins and cellular metabolites... Indeed, ABC transporters are able to transport functionally and structurally-unrelated anticancer molecules, explaining their large substrate spectrum. ABCB1 transports hydrophobic compounds while ABCC1, ABCC2 and ABCG2 are organic anion carriers. ABCC4, 5 and 11 can particularly transport nucleoside analogs in addition to organic conjugates. Taken altogether, high expression of these ABC proteins in breast cancer may contribute to decreased sensitivity to chemotherapy combinations containing anticancer drugs. These data also suggest that ABC protein expression levels may be a potential predictive tool in the choice of anticancer drugs in breast cancer. For example, doxorubicine (DXR), epirubicin (EPI), paclitaxel or methotrexate (MTX) are transported by at least four ABC

Table 1. Non Exhaustive Classification of Breast Cancer Histological Types

Histological Types of Breast Cancer			
Type	**Characteristics**	**Frequency**	**10 Year Survival Rate**
Non-invasive			
Intraductal	- cancer ductal cells		
Lobular carcinoma *in situ*	- cancer ductal and lobular cells		
Invasive			
Invasive ductal carcinoma	- ductal cancer cell origin	50-80 %	35-50 %
Invasive lobular carcinoma	- lobular cancer cell origin	5-15 %	35-50 %
Mucinous carcinoma	- abundant extracellular mucin surrounding nests of cancer cells	< 5 %	80-100 %
Medullary carcinoma	- ductal cancer cell origin, syncitial arrangement - lymphocytic or plasmacellular infiltrate	1-7 %	50-90 %
Tubular carcinoma	- well differentiated cancer - uniform angulated small ducts invading mammary stroma	1-6 %	90-100 %
Apocrine carcinoma	- apocrine epithelium resembling cancer cells - androgen receptor expression		
Luminal carcinoma	- luminal cytokeratins expression, ER and estrogen regulated genes - often histological grade I tumours		
Basal carcinoma	- mainly grade 3 invasive ductal carcinomas. - usually ER, PR and ERBB2 negative - similar protein expression pattern with stem/progenitor cells		
Basal like carcinoma	- association with high grade, poor prognosis, and younger patient age - ER, PR and ERBB2 triple-negative phenotype		poor prognosis
Non basal like carcinoma	- carcinoma opposed to basal like carcinoma		
Frequencies and survival rates from Weigelt et al. (2005) [2]			
Breast Cancer markers			
Name	**Characteristics**	**Frequency**	**Prognosis**
ER positive cancer	- ER expressing cancers which therapy includes endocrine drugs	60-70 %	excellent
PR positive cancer	- PR expressing cancers which therapy includes endocrine drugs when it is ER positive	≈ 53 %	excellent
ERBB2 positive cancer	- ERBB2 expressing cancers which therapy includes herceptin® antibody		
ER, PR, ERBB2 triple-negative cancer	- ER, PR and ERBB2 non expressing cancers		poor
Primary carcinoma	- cancer developing in its originate tissue		
Metastatic carcinoma	- cancer with metastases resulting from cancer cell migration		poor
ER = Estrogen Receptor; PR = Progesterone Receptor; ERBB2 = Human Epidermal growth factor Receptor 2			
Frequencies from Yu et al. (2008) [3]			

proteins (Table **2**). 5-FU, vinorelbine, gemcitabine and cisplatine (CisPt) seem to be transported by less and specific ABC proteins. No finding is yet available concerning ABC transport of newly used drugs such as exemestane, anastrazole, letrozole, fulvestrant, megestrol, caelys or epophilone.

Table 2. Anticancer Drugs Used in Breast Cancer Therapy. Classical Anticancer Agent Used in Breast Cancer Therapies are Cited in this Table. Symbols Indicate if Transport (☑) or Chemo-Resistance (☒) has been Described for Each Molecule. Filled Square (■) Signify no Transport Ability or no Chemo-Resistance has been Observed for this Substrate

Drug	ABCB1	ABCG2	ABCC1	ABCC2	ABCC3	ABCC4	ABCC5	ABCC10	ABCC11
Doxorubicin	☑	☒	☒	☒			☒	■	■
Epirubicin	☑	☑	☒	☒					
Docetaxel	☑			☑				☒	
Paclitaxel	☑	■	☑	☑	☒	■		☑	■
Cyclophosphamide	■		☑	☑		☒			
Capecitabine - 5-FU		☑				■	☑	■	☑
Vinorelbine	☒							☒	
Gemcitabine							☒	☒	
Methotrexate	☒	☒	☑	☑	☑	☑	☑		☑
Cisplatine		■	■	☒			☒	■	
Carboplatine						■			
Tamoxifen	■								
References	[16] [17] [18] [19] [20] [21] [22] [23] [24] [25]	[26] [27] [28] [29]	[30] [31] [32]	[33] [31] [34] [35]	[36] [37]	[38] [39]	[40] [41] [42]	[43] [44]	[45, 46]

Since it is well known that gene expression is highly dependent of feminine sexual hormones in reproductive organs such as mammary tissue, we focused our review on findings about the sexual steroid regulation of ABC transporter expression levels in breast and placenta cell lines. To clarify known data about this subject, we provided an overview of their tissue distribution and various procedures to experimentally quantify transport activity for anticancer drug used in breast cancer therapy. For the first time, an overview of the current literature is summarized regarding the *in vivo* expression of ABCB1, ABCCs and ABCG2 in breast tumours according to histological types, prognostic, and markers, as well as the potential impact on the overall health of patients.

2. INTRACELLULAR DOSAGE OF DRUGS FREQUENTLY USED IN BREAST CANCER THERAPY

2.1. Introduction

Drug efflux by ABC transporters are currently studied by various *in vitro* methods based on fluorescent (DXR, calcein, rhodamine …) or [3H] labelled molecules. Several approaches can be set up as (1) the determination of ATPase activity in cell membrane enriched with the ABC transporter in the presence or not of substrates or tested compounds. This assay is based on the measure of inorganic phosphate produced from ATP hydrolysis [47, 48]. (2) In case of polarized cells, the transcellular transport assay may be useful to characterize the transport properties (apical to basal or basal to apical) of ABC substrates. This test consists to follow a drug across cells, seeded on a porous membrane filter, which express the efflux pumps [49, 50]. (3) The most common way is to study the intracellular or extracellular accumulation and efflux of drugs. For accumulation assay, the intracellular concentration of a substrate is measured after an uptake phase in the presence or absence of inhibitors [51, 52]. For efflux assays, cells are loaded (uptake period) with a substrate. After removing extracellular substrate, cells are then re-incubated at 37°C in free medium. The ABC representative transport function is shown in aliquots of intracellular compartment and/or efflux medium. Substrates are quantified either in cells and/or in extracellular compartment. Rhodamine-123, calcein-AM and daunorubicin are commonly used as fluorescent ABC probes [53]. The substrate transport is studied in absence or in presence of modulators with a potential affinity for ABC protein, thus susceptible to modify the concentration of the fluorescent probe. This assay allows automation and a high throughput screening (flow cytometry, spectrofluometry). However, due to the presence of multiple substrate and modulatory binding sites, fluorescent probes may be only partially representative of ABC transporter activity [54-58]. Indeed, fluorescent and anticancer drugs might bind on different sites, and then the transport properties might be different. The use of a specific anticancer drug as ABC substrate is likely highly relevant approach for evaluating ABC pumps impact on anticancer drug resistance. Nevertheless, it requires disposing to a validated analytical method for the quantification of this anticancer sub-

strate. The use of radio-labelled probe allows getting around this analytical drawback. However, the radio-labelled probe must be available. Currently, it must also be taken into account the safety requirements associated with radioactive substance handling.

2.2. Technical Methods

In this first section, we described the basic knowledge of principle of analytical tools used for the ABC substrate quantification in biological matrix. This is required for a better understanding of advantages, limits and interests of available analytical approaches. We briefly reported the principle of liquid chromatography (LC) coupled with mass spectrometry (MS) a powerful technique for the quantification of drugs, the absorption atomic spectroscopy (AAS) and the inductively coupled plasma-mass spectrometry (ICP-MS) both used for the quantification of platinum derivatives. Among these analytical techniques, we only focused our report on the most described configurations allowing the drug quantification.

Methods specifically dedicated to transport properties of ABC substrates in *in vitro* cellular matrix are scarce, while numerous assays have been described for the quantification of these compounds in plasma, serum or tissues. However, most of these techniques constitute a good basis and should be adaptable for the quantification in cells. The relevance of the transfer of the method from clinical samples to cellular matrix must be evaluated in term of limit of quantification (LOQ) and interference according to the analytical device used.

a) LC-MS/MS Method

LC is a common separation technique suitable for numerous organic drugs. Usually, LC separation method is coupled with a UV (ultraviolet) or fluorescent detectors, for appropriated chemical structure molecules. Nevertheless, recently, the hyphenated technique including the MS (Mass Spectrometer) as detector with LC has made a considerable progress to become the gold standard in numerous quantitative applications. The MS is a detector designed to separate gas phase ions according to their mass to charge ratio (m/z) value. For most drugs, currently MS detection is the most sensitive and specific tool. In this section, we only presented the main configuration of the MS detector used for the quantification of small molecules [59].

MS detector is composed by two main components: the ion source and the mass analyzer [60, 61]. The ion source, based on the atmospheric pressure ionization (API) technique, generates ions from the analyte molecules and separates these ions from the mobile phase [62, 63]. Consequently, this interface between LC and MS is a crucial element. Mobile phases used in LC-MS usually consist of a mixture of a volatile buffer such as ammonium acetate or formate and an organic solvent such as acetonitrile or methanol. The two main ionization techniques are the electrospray ionization (ESI) and the atmospheric pressure chemical ionization (APCI) [64, 65]. Both are considered to be soft ionization method. ESI is useful for the determination of ionic or very polar compounds and constitutes the main technique used for analyzing drugs. Although ESI is very sensitive, the sensitivity deteriorates with the presence of non-volatile buffers and other additives. APCI is applicable for weak-polar molecules [66]. Numerous drugs are reported to be only ionized in ESI mode. Exception exists like 5-FU that can be analyzed in both modes (see below). For each molecule, the relevant approach to select most suitable positive or negative ionization mode is to test these different conditions. If the compound has a functional group that readily accept a proton, then positive ion detection is frequently used and the protoned molecular ion $[M+H]^+$ is usually the dominant species depend the molecule, the composition of mobile phase, cation and/or solvent adducts can be observed such as $[M+Na]^+$, $[M+K]^+$, $[M+CH3CN]^+$. Inversely, if the molecule has functional group that readily lose a proton, the negative ion detection is selected and the deprotoned molecular ion [M-H]- is probably the most abundant species. In negative mode, adducts can also be measured such as [M+HCOO]-.

A quadrupole mass filter is composed by two pairs of rods (four parallel rods arranged in square), one set is at positive electrical potential, and the other is at negative potential. Direct current and radiofrequency voltages are applied to opposite pairs of rods and are rapidly switched. The result is that an electrostatic filter is established that only allows ions of a single m/z ratio pass through the rods to the detector at a given instant in time. Quadrupole analyzer can operate in scanning mode and in selected ion monitoring (SIM) mode. In this last mode, the mass spectrometer monitors only few m/z ratios i.e. few compounds. SIM mode is used for the quantification. An instrument may be constituted by one mass analyzer ("simple quad") and the name of the hyphenated technique is LC-MS. In a tandem mass spectrometer ("triple quad" or LC-MS/MS), two analyzers are separated by a collision cell. The first quadrupole selected a first ion (precursor or parent) in SIM mode which is fragmented. The second quadrupole analyze a specific fragment (daughter ion) also in SIM mode. Such mode is named multiple reaction monitoring (MRM) or selected reaction monitoring (SRM). In this case, the selectivity is increased since the signal to noise ratio is enhanced by a clear decrease of the chemical noise. It is a high specific and highly sensitive mode [60].

Although LC-MS (and LC-MS/MS) constitutes a high sensitive and selective analytical tool, matrix effects modify the MS response of an analyte [67, 68]. This phenomenon can lead to either a reduced signal (ion suppression) or an increased signal (ion enhancement). Ionization suppression is mostly observed and is the consequence of the presence of nonvolatile endogenous compounds from sample into the source [69, 70]. These interferences may alter the precision, the accuracy and the limit of quantification. Thus, the presence of a potential matrix effect should be always studied through the validation procedure of the assay. An appropriate pre-treatment (extraction procedure) of the sample generally avoids this effect. Liquid/liquid extraction (LLE) and solid phase extraction (SPE) are the two most frequently used techniques for sample preparation. Another approach consists to modify the chromatographic separation in order to select a portion of the chromatogram without matrix effect. APCI source is commonly considered to be less exposed to matrix effect than ESI source [68].

LC-MS and LC-MS/MS are powerful flexible analytical tools for the quantification of drug in complex matrix and will continue to be a major technique for this application.

b) Atomic Absorption Spectroscopy (AAS)

Atomic absorption spectroscopy (AAS) is an appropriated and specific technique for quantification of metals and metalloïds. The principle is that ground state metal absorbs light at specific wavelengths [71]. The characteristic wavelength is specific element. The liquid sample is aerosolized, mixed with combustible gases and ignited in a flame (≈2 300°K); this method converts the sample from metal ion into atomic state. A cathode lamp, made of the element being quantified, emits the characteristic spectrum of it. The light beam from the lamp passes through the flame and the decrease amount of the light intensity due to absorption by the compound is quantified. AAS, as other analytical assays, requires calibration. Various elements can affect the ground state population of the element such as spectral interferences (e.g. background radiation from matrix), broadening of the spectral line.

c) Inductively Coupled Plasma-Mass Spectrometry (ICP-MS)

Inductively coupled plasma-mass spectrometry (ICP-MS) can quantify the same elements as AAS but with a clear advantage to couple the accurate and the low detection limit of a mass spectrometer. ICP-MS is capable of trace analysis in the range of ng/L level. The principle of ICP technology is the same as previously described for AAS. Samples are decomposed to neutral elements in high temperature plasma. The plasma is produced by the interaction of an intense magnetic field on a tangential flow of argon. Ions produced are mostly atomic and singly charged, corresponding to an ideal situation for MS detector. The very high temperature (≈ 6,000-8,000°K) removes solvent residues and allows the atomization and the ionization of the samples. The ions produced passes through the interface region and are directed into the mass spectrometer where analyte ions are quantified on their particular m/z ratio. There are several types of mass analyzers which can be coupled to ICP, but the most common for the quantification is the quadrupole type [72-74].

2.3. Taxanes

a) Paclitaxel

Various transport assays had been developed to explore the transport of taxanes by ABC transporters. The optimal uptake phase was in the range of 60 to 180 min exposure since maximum taxane cell concentration was observed over this period. Currently various assays using 3H-paclitaxel were described. Paclitaxel accumulation was measured for drug concentration range from 25 nM to 6 µM [75-77]. The radioactivity was determined by liquid scintillation counting in a beta counter. More precisely, Strobel *et al.* assessed the non specific binding of the 3H-paclitaxel in the presence of 100-fold excess of cold drug in uptake assay and Jang *et al.* took into account the intracellular presence of 7-epitaxol, an epimerization product of paclitaxel, and the total radioactivity was expressed in paclitaxel equivalents [23, 76].

Two other studies are based on the intracellular quantification of paclitaxel by LC coupled with UV detector [75, 78]. Few details were furnished concerning the analytical techniques. Discrepancy was observed between Oguri's and Crowe's studies; indeed paclitaxel concentrations used were respectively 0.1 µM and 10 µM [75, 78].

Recently, a selective and sensitive assay was described for the quantification of paclitaxel in cultured cells exposed to low drug concentrations [79]. The technique is based on micro-LC-MS/MS and a selective solid phase extraction (SPE) was optimized and validated to concentrate paclitaxel from cellular samples. Both approaches allow obtaining an ultra low quantification limit of 20 pg/mL which is considerably lower than limit of quantification (LOQ) published with conventional LC-MS/MS assays [80-82]. Selective SPE reduced the complexity of the cell samples and, because ESI source is concentration dependent, low flow capillary LC was preferred to enhance peak concentration in the source and thus the analytical sensitivity. Gaspar *et al.* do not mentioned the potential adduct formation and especially with Na+ and K+ cations when positive ion mode is selected. Others and we have observed that the formation of [M+Na]+ and [M+K]+ particularly in the case of paclitaxel, should be evaluated. Indeed, paclitaxel and docetaxel are molecules prone to this phenomenon. The adduct formation depends on several parameters such as the molecule structure, the composition of the mobile phase used for the chromatographic separation, or the type of matrix. It is necessary to ascertain that the adduct process is reproducible according to analytical conditions. On the contrary case, the selection of the most abundant transition in MRM mode will be unsure and the accuracy of the method will be decreased. The use of a labeled stable isotope internal standard may be relevant; however the availability of such compounds may compromise this approach. Convenient "chemical" solutions have been proposed to solve this problem such as the addition of alkali metal complexation products, or the addition of primary amines or sodium acetate to replace all adducts by one desired [83-85].

b) Docetaxel

At our knowledge, no sensitive method has been proposed for the quantification of docetaxel in cells except with radiolabelled compounds. For example, intracellular accumulation of docetaxel was performed with 14C-docetaxel [22]. However, numerous assays have been published on its quantification in human plasma by LC-MS/MS [81, 86, 87]. The transfert of such assays should be relatively easy to carry out. Currently, paclitaxel is usually used as internal standard for the docetaxel quantification and inversely. Thus, the thorough description of Gaspar *et al.* for the quantification of paclitaxel by micro-LC-MS/MS could be transferred for docetaxel [79].

2.4. Derivatives of Platinum (Pt)

a) Cisplatin (CisPt)

Numerous discrepancies are described on CisPt uptake according CisPt exposure length, concentration, cell lines, and finally method of quantification. Moreover, in studies, it is not always clearly indicated whether concentrations are calculated using the platin (Pt) atom or using the drug containing the Pt as reference. Consequently, the comparison of

the assays, from an analytical point of view, seems to be difficult.

Usually, following an incubation period with CisPt, cells were washed and digested. The mineralization may involve heating associated with concentrated acid (such as nitric acid or perchloric acid) overnight treatment [88-90]. Other procedures are more complex involving concentrated acid, hydrogen peroxide and microwave treatment [91]. Furthermore, digestion with sodium hydroxide that is responsible for important signal suppression, is not adequate [92].

Several works were based on the determination of CisPt by AAS [93-95]. The operating mode was roughly the same: the cellular exposure period is short since uptake was linear within to the 60-120 min time range, the cells were treated with high concentration around 100 µM CisPt. Kröning *et al.* reported a limit of detection at 0.2 µM Pt in sample with AAS [95].

The high sensitivity of ICP-MS to measure trace of Pt allowed the study of CisPt transport properties using lower concentration of CisPt. Cells were incubated for a long period (24 h) with sub-acute drug concentration from 0.1 to 2 µM [88, 90]. With ICP-MS technique spectral and non spectral interferences may be occurred. For Pt determination, the spectral interferences comprise isobaric and molecular interferences. Main abundant Pt isotopes are 194Pt+ (33.0 %), 195Pt+ (33.8 %), and 196Pt+ (25.2 %). Only the last isotope presents an isobaric interference with 196Hg [92]. However this interference can be avoided by choosing an interference free isotope. Since Pt is an element with high mass, the molecular interferences are less observed than with element with lower mass. Although the signals from hafnium oxides may interfere with whose of 194Pt+ and 195Pt+, the risk of interference is not significant for application for which Pt is added to the biological sample [89]. The non spectral interferences may be due to matrix components, such as solid or organic compounds leading to signal suppression. Another origin may be the extensive loading of the sample by an element, such as sodium, which will be ionized to the detriment of element with higher ionization energy [89]. Nevertheless, ICP-MS provides excellent performance and sensitivity which makes the technique suitable to study uptake, efflux and accumulation with low concentration substrate [96].

Beside methods for the determination of total Pt concentrations such as AAS and ICP-MS, other assays have been described. Several assays were proposed based on high-performance liquid chromatography (HPLC) with a pre- or post-column derivatization. Although these methods can be considered as an alternative to AAS, they are time-consuming and are less sensitive [97, 98]. An interesting technique was recently proposed using electrospray ionization (ESI) mass spectrometry [99]. CisPt was quantified after a rapid derivatization with diethyldithiocarbamate (DDC) followed by an extraction with isoamylalcohol (IAA) and oxalic acid. Then 1 µL of IAA was directly injected into the ESI-MS device and Pt(DDC)3+ and Ag(DDC)2+ were measured at m/z 639 and 405, respectively.

b) Carboplatin

The methods available for the quantification of carboplatin are, as for CisPt, methods determining the element platinum, such as AAS or ICP, and selective methods analyzing the compound itself. A selective method presents the advantage to separate the carboplatin to other compounds containing Pt such as degradation or metabolism species, which could interfere. Numerous assays based on high-performance liquid chromatography (HPLC) have also been described for the carboplatin quantification in plasma. Various detections have been proposed such as UV [100, 101] or electrochemical [102, 103]. However, the LOQ is approximatly 500 ng/mL due to the lack of UV absorbance by carboplatin and the non-specific detection. Recently, extremely sensitive assays using LC-ICP-MS have been described for the quantification of Cis-Pt and carboplatin [104, 105]. These assays combine the high specificity of the chromatographic separation and the high sensitivity of the ICP-MS detector. Other analytical assays are available including a technique based on LC-MS for the quantification of carboplatin in tumor homogenates with a LOQ equal to 30 ng/mL [106] and an LC-MS/MS method with high sensitivity detection level (2 ng/mL) in plasma sample [107]. Nevertheless, the use of LC-MS/MS for the quantification of platinum drugs is still challenging due to the three isotopes of platinum and two of chlorine (^{35}Cl, ^{37}Cl) in case of CisPt. Currently, molecular species are complex and sensitivity can be limited by the distribution of the MS signal between the different isotopes.

2.5. Nucleoside Derivatives

a) 5-Fluorouracil (5-FU)

5-FU is a well-known substrate of cellular transporters [108]. This substrate transport properties had been demonstrated in cells using tritium radio-labelled 5-FU ([3H-5FU]) for ABCC5, ABCG2 and ABCC11 [40, 109, 110]. Nevertheless, numerous methods based on chromatography have been proposed for the quantification of 5-FU in biological samples, especially in plasma. The liquid chromatography coupled with UV or MS (and MS/MS) detection is usually used [111-113]. Coupled with UV detection, classically the pretreatment consists to a protein precipitation followed by a liquid/liquid extraction and the LOQ is approximately 25 ng/mL [114, 115]. The MS/MS detection is more powerful and decreases the LOQ to 1 - 5 ng/mL [116, 117]. According to the complexity of the biological matrix, a simple and rapid protein precipitation is performed [117]. 5-FU is a drug analyzed in negative mode, either with ESI or with APCI source [116-118]. Although ESI is more frequently used than APCI, the performances of both modes are comparable and the choice must be adjusted according to interferences and/or a potential biological matrix effect. The quantification of 5-FU can also be carried out with gas-chromatography (GC) coupled with mass spectrometry (GC-MS). Methods for 5-FU involving GC require a derivatization prior to gas chromatographic analysis [119-121]. This stage is performed to modify an analyte functionality in order to decrease its polarity and enhance its volatility. However, the choice of the derivatizing agents is important since in some cases interferences and compound instability were described [119]. The

LOQ for 5-FU analyzed with GC-MS is in the same range than those described with LC-MS.

5-fluoro-2'-deoxyuridine-5'-monophosphate (5-FdUMP) is the pharmacological active metabolite of 5-FU. 5-FdUMP inhibits thymidylate synthase and is a substrate of the efflux ABCC5 and ABCC11 pumps which have recently been associated with 5-FU resistance mechanisms [45, 109]. Few methods described the quantification of 5-FdUMP. One is based on liquid chromatography with counter ion and using [3H-5FU]. It was successfully developed in cell lines for the quantification of 5-FU and its metabolites [122, 123]. 5-FdUMP quantification was also performed using [3H-5FU] in L1210 cells. This assay was time-consuming due to a pretreatment by periodate and methylamine in order to eliminate ribonucleotides [124]. Other assays used LC-UV with counter ion or based on strong cation exchanger were published for the separation of 5-FU and 5-FdUMP in plasma. However, poor sensitivity was obtained and interfering peaks from endogenous compounds were observed, especially for 5-FdUMP [125, 126]. The last method based on capillary electrophoresis coupled with UV detection cannot detect 5-FdUMP in cell samples due to a poor sensitivity [127].

b) Gemcitabine

Gemcitabine quantification can be based on LC-UV technique with anion exchange chromatography [128, 129]. Accumulation of gemcitabine and determination of the ribonucleotides triphosphate were carried out in cell lines exposed at 1 and 10 µM of gemcitabine for 4 h or 24 h [128, 130]. Sample pre-treatment consists to an acidic precipitation followed by neutralization. Following VanHaperen's analytical approach, the LOQ is around 25 ng of gemcitabine injected. LC-UV methods have also been described for the quantification of gemcitabine in plasma [131-133]. After an acidic protein precipitation, the LOQ reached was approximately 2 ng of gemcitabine injected [133]. Additional techniques based on LC-MS/MS were also described for the quantification of gemcitabine in plasma or urine [134, 135]. The LOQ from plasma data is 25 pg injected [134]. In most assays, the sample pre-treatment corresponds to a simple precipitation with either acid or acetonitrile. This is due to an elevated hydrophily of the molecule unfavourable to LLE or SPE.

2.6. Cyclophosphamide (CPM)

Since the molecule is highly polar and reactive, quantification of CPM in biological sample is a challenge. Moreover, its extraction from biological matrix is difficult due to its high solubility. Numerous methods have been described for CPM quantification. GC classical analysis involves a derivatization procedure (often with trifluoroacetic anhydre) prior to the injection into the device. Although some authors proposed methods without derivatization, it has been demonstrated a thermal decomposition of underivatized CPM [136, 137]. Most of the GC methods were based on nitrogen-phosphorus detector (ECD) since CPM structure contains both atoms and confers a high selectivity and sensitivity to this detector [138-140]. GC-MS assays were also described after derivatization procedure [141, 142]. The LOQ with GC-ECD or GC-MS was in the range 10 to 30 pg injected when samples were extracted with LLE. Before the last decade development of LC-MS/MS, LC was not a suitable analytical method for the quantification of CPM. Due to a lack of chromophore in the structure, UV detection is not selective and sensitive enough for the determination of low concentrations [143, 144]. Recently assays based on LC-MS/MS were described for the CPM quantification in urine or plasma [145, 146]. These methodologies involve the ESI source and detection in positive mode. With a rapid and simple sample preparation such as protein precipitation by acetonitrile, an assay was described with a LOQ of 375 pg injected [147]. Thus, LC-MS/MS allows the determination of CPM with low LOQ and requires no derivatization unlike with GS analysis. Finally, numerous publications based on LC-MS/MS are concerned both with CPM and/or ifosfamide (IFM) [148, 149]. Since both structures are very close, assays described for IFM are also suitable for CPM determination.

2.7. Methotrexate (MTX)

Several authors used radio-labelled [3H-MTX] as substrate for the study of various ABC transporter [31, 36]. Separative techniques are exclusively based on liquid chromatography. Numerous assays have been published for the quantification of MTX in biological fluids, mostly in blood but also in tissues. A wide range of chromatographic conditions (reverse phase separation, ion-pairing and ion exchange chromatography) have been proposed coupled with detection techniques such as UV, fluorimetry, electrochemistry and MS. A complete review has been published on separation method for MTX [150]. This work summarizes the instrumental conditions and the performance over than methods published from 1975 to 2000. In the present review, we only focused on the most sensitive techniques previously described and the methods published from 2001. Actually, several assays are useful for the quantification of high concentration of MTX such as observed in blood for cancer treatment [151-153]. However for the study concerning uptake and efflux mechanisms, sensitive assay is requires such as obtained when fluorimetry or MS (and especially MS/MS) detection are used. In this case, the maximum detection sensitivity is 50-100 fold higher than that achieved by UV detection [150].

At present, MTX is not a fluorescent molecule and several assays proposed pre-chromatographic or, mostly, post-chromatographic oxidation [154, 155]. The oxidative degradation of MTX produces a fluorescent pterine-carboxylic acid. Post-chromatographic photo-oxidation is based on the action of H_2O_2 (present in mobile phase from 0.1 to 0.5 %) and UV irradiation at 254 nm [152, 156, 157]. This approach requires in one hand an online photo-reactor and in second hand restricts chromatographic conditions (neutral pH and isocratic elution were used) which are aggressive for chromatographic column [158]. Recently, an assay based on online post-column coulometric electrochemical oxidation and fluorescence detection have been proposed [159]. Sample preparation for plasma consists to a methanol precipitation followed by LLE. The LOQ from plasma samples using fluorescence detection are in the range from 0.6 to 2.5 ng injected [158, 159].

Sensitive methods using LC-MS/MS have been published in recent years for the quantification of MTX. Stein-

borner *et al.* proposed a fully automated techniques including semi-robotic LLE in 96-well plate [160]. The apparatus was configured with a trapping column prior to analytical column in order to enhance the volume of sample injected. Actually, small analytical column (1 mm internal diameter) was used to achieve improved ESI sensitivity. An other study described a 384-well SPE for LC-MS/MS determination of MTX [161]. Determination of MTX based on the use of small sample volume (10 µL) has also been performed from mouse plasma and brain tissue [162]. The sample plasma preparation consists to a simple protein precipitation procedure. In these three specific assays, the time of analysis were particularly rapid since run-time was between 1.5 to 4 min [160-162]. Uchida *et al.* used MTX as internal reference to evaluate the inhibitory effect of more than 50 compounds on ABCC4 transport activity from vesicle-uptake [163]. This study used LC-MS/MS device, however the assay has not been only developed for MTX and the analytical conditions have not been optimized for MTX quantification. LC-MS/MS assay based on SPE sample procedure and micro-HPLC analysis have been described for the simultaneous determination of low levels of MTX and CPM in human urine [164]. The LOQ from urine or plasma samples using MS/MS detection are about 4 pg injected, clearly inferior to a fluorescence detection [162, 164].

2.8. Vinorelbine (VNB)

Efflux and uptake phases of VNB have been studied with radio labelled [3H-VNB] [165, 166]. For example, the substrate was incubated for 5, 10, 20, 30 and 60 min for the uptake phase. During efflux study, aliquots were removed every minute for radioactivity counting for 15 min [166].

HPLC has been widely used in the quantification of VNB. Two assays report its quantification into cells, one with UV detection, and another one with fluorescent detection [167, 168]. VNB shows sufficient intrinsic fluorescence (without derivatization or chemical reaction) to choose this handle detection mode. As previously described with other substrates, UV detection shows a lower selectivity and sensitivity than fluorescent detection [169, 170]. Using this last mode, the LOQ from cellular samples was about 6 ng injected [167]. An assay based on HPLC coupled with coulometric detection has been proposed for the quantification in rabbit plasma [171]. This electrochemical detection is very sensitive (LOQ 500 pg injected) but stays difficult to handle. A method have also been proposed using capillary electrophoresis coupled with UV detection [172]. However, no data from biological matrix has been furnished. Ragot *et al.* described a method based on LC-MS for the quantification of VNB in human serum with a LOQ equal to 20 pg injected [173]. However, the LLE proposed was time-consuming. Two assays using LC-MS/MS have also been recently published [174] [175]. The LOQ was 16 fg of VNB injected after a SPE extraction [174]. The interest of this method, besides the sensitivity, was the short time for LC analysis allowing to high-throughput analysis.

2.9. Antracyclines

a) Doxorubicine (DXR)

Antracyclines present the advantage of their inherent fluorescence due to the conjugated aglycone ring system. Numerous studies are based on this detection mode for intracellular quantification of DXR since LOQ in the fmol range can be reached. Most described assays involved either direct detection of fluorescence without separation or chromatographic separation (LC or capillary electrophoresis (CE)) prior to detection.

Riganti *et al.* used a simple spectrofluorimeter in order to calculate the kinetics of the drug accumulation and efflux [24]. For uptake phase, 4 µM of DXR have been incubated for different periods. For the drug efflux, cells were incubated with 1 to 250 µM DXR for 10 min, then cells were washed, resuspended, and the intracellular drug content was analysed. The transport measurement was also studied by continuous monitoring of DXR fluorescence [176]. This method allows to assess the transport assuming that fluorescence characteristic of the probe changes when it moves between intra- and extracellular medium. Extracellular DXR fluorescence is about 6.5-fold higher than intracellular [176]. Thus following the time dependant change in DXR fluorescence intensity can monitor transport. Fluorescent flow cytometry analyses were carried out for DXR uptake and efflux on MCF7 and MCF7/adr (ABCB1 positive) resistant cell lines [177, 178]. Drug accumulation and drug efflux studies were performed with 1.7 or 5 µM of DXR as substrate concentration [177, 178].

Two reviews published in 2001 concerning the separation and the quantification of anthracyclines in biological matrices allowing an overview on main techniques [179, 180]. Capillary electrophoresis (CE) coupled with laser induced fluorescence was successfully used for the quantification of DXR in cells [181, 182]. This assay involved a specific device but allows to reach an exceptional LOQ, about 3-order of magnitude lower than those expected with conventional LC-fluorescence assays [182]. Numerous methods based on LC separation with fluorescence detection have been described in plasma tissues and cells [183-185]. In the Grosse *et al.* study, DXR was incubated at 0.1 µM for 10^6 cells [185]. LLE was performed prior to chromatographic analysis. A high sensitive method, with LC separation and fluorescence detection, from small sample volume (20 µL) coupled to a simple protein precipitation procedure was recently described [186]. Assays based on LC-MS and LC-MS/MS apparatus have also been described for DXR quantification [187, 188]. ESI source was used and sample preparation procedure involves SPE, LLE or simple protein precipitation with acetonitrile.

b) Epirubicin (EPI)

EPI differs from DXR in the inversion of stereochemistry at C-4' (darnosamine ring). From an analytical point of view, both drugs are comparables and techniques usable for DXR are also being for EPI. Thus numerous assays based on LC coupled with fluorescence detection and MS or MS/MS detection have been described for EPI [189][190]. Anyway, some of them describe the simultaneous quantification of both drugs EPI and DXR [191-194].

2.10. Conclusion

ABC substrate breast anticancer agent can be quantified by various technic summurized in Table **3**. Taken altogether, due to high sensitivity and selectivity, LC-MS/MS becomes

Table 3. Most Suitable Techniques for Cellular Quantification of ABC Substrates Used in Breast Anticancer Therapy. MS : Mass Spectrometry (or Tandem Mass Spectrometry), NPD : Nitrogen-Phosphor Detector, UV : Ultra-Violet, Fluo. : Fluorescence, ETC : Electrochemical, LIF : Laser Induced Fluorescence, (1) : Without Liquid Chromatographic Separation, Quantification has only been Made with the Detector; (2) : Derivatization Required; (3) : Poorly Sensitive; (4) : Drug Naturally not Fluorescent

Chromatographic separation Mode	Gas		Liquid				Capillary Electrophoresis				
Detection mode	**NPD**	**MS**	**UV**	**Fluo.**	**MS**	**ETC**	**Fluo.**	**LIF**	**UV**	**AAS**	**ICP-MS**
Paclitaxel			x		x				x		
Docetaxel			x		x				x		
Cisplatine					x (1)					x	x
Carboplatine			x		x	x				x	x
5-FluoroUracil	x (2)		x		x						
5-FdUMP			x (3)		x						
Gemcitabine			x		x						
Cyclophosphamide	x (2)	x (2)	x (3)		x						
Methotrexate			x	x (4)	x	x					
Vinorelbine			x	x	x	x			x		
Doxorubicine			x	x	x	x	x	x	x		
Epirubicine			x	x	x	x	x	x	x		

the first choice for the analysis of drugs in biological matrices from small sample volumes. This technique is particularly suitable when low LOQ and accurate data are required such as whose necessary for *in vitro* uptake and efflux studies.

3. DISTRIBUTION OF ABC TRANSPORTERS IN NON-REPRODUCTIVE AND REPRODUCTIVE TISSUES

We summarized in Table **4** the ABC mRNA and/or protein levels in normal tissues. Tissues were classified in 2 sub-classes: reproductive and non-reproductive tissues (Table **4**). Some of ABC proteins (ABCB1, ABCC1, ABCG2 and ABCC5) are ubiquitously expressed in the body while others are tissue specific (ABCC2, ABCC3, ABCC4). Furthermore, all mentioned transporters did not show identical expression levels along the gastrointestinal tract (from the duodenum to colon). Indeed, the ranking of expression levels in the duodenum was ABCC3 >> ABCB1 > ABCC2 > ABCC5 > ABCC4 > ABCC1 [195]. In the terminal ileum, the ranking order was as follows: ABCB1 > ABCC3 >> ABCC1 ~ ABCC5 ~ ABCC4 > ABCC2. In all segments of the colon (ascending, transverse, descending and sigmoidal colon), their expression levels showed the following order: ABCC3 >> ABCB1 > ABCC4 ~ ABCC5 > ABCC1 >> ABCC2 [195]. Finally, in polarized cells such as hepatocytes or enterocytes, ABCB1, ABCC2, ABCG2 and ABCC11 are localized at the apical surface, while ABCC1, ABCC3, ABCC5 are present at the basal surface [196, 197]. To simplify the understanding of this section, we described expression tissue patterns according the ABC transporter classification.

3.1. ABCB1 and ABCG2

ABCB1 and ABCG2 are strongly involved in cellular protection by elimination of drugs, explaining their high expression at numerous physiological barriers (Table **4**) [26, 197-199, 200]. ABCB1 protein expression is found at the canalicular pole of hepatocytes, epithelial cells in biliary ducts of liver [196, 197], epithelial ducts of pancreas [197] and epithelial proximal tubules of kidney [197]. ABCG2 protein expression is detected in placental syncytiotrophoblasts, small intestine, colon, liver canalicular membrane and in ducts and lobules of mammary tissue [201]. In male or female reproductive tissues, ABCB1 is expressed with the highest level in placenta trophoblasts and an intermediate level in mammary gland, endometrium glandular epithelial cells and prostate [196].

ABCG2 protein is also located at the blood brain barrier, with main location at the luminal surface of microvessel endothelium [202] and in veinous and capillary endothelium [201] and likely participates to the drug distribution in brain. In addition, ABCB1 protein is also strongly found in endothelial cells of capillary blood vessels at blood-brain barrier [196, 203] (Table **4**). It is well illustrated in multidrug resistant (*mdr/abcb1*) knockout mice. Though *abcb1* knockout mice were healthy, fertile, lived a normal life span and had neither abnormalities in anatomy, nor abnormalities in any physiologic parameters, *abcb1* knockout mice have altered central nervous system (CNS) penetration, enhanced oral absorption, and altered excretion (both urinary and biliary) of some ABCB1 substrate drugs when it was compared with wild-type mice.

Table 4. ABC Transporter Expression in Non Reproductive or Reproductive Tissues

Non Reproductive Tissues										
Tissue		**ABCB1**	**ABCG2**	**ABCC1**	**ABCC2**	**ABCC3**	**ABCC4**	**ABCC5**	**ABCC10**	**ABCC11**
Nervous system	Brain	[198]	[26]	[205; 206]				[206]	[208]	[226; 227]
	Blood brain barrier	[203]	[202]							
Cardiovascular system	Heart	[197]		[204; 206]				[206]	[208]	[227; 228]
	Capillary blood vessels	[196]	[201]		[212]					
Lung		[198]	[199]	[204; 205; 206]	[205]	[206]	[199; 206]	[206]		[227; 228]
Skeletal muscle				[199; 204; 206]				[199; 206]		[227; 228]
Gastro-intestinal tract	Stomach			[206]	[205]	[199; 206]		[206]	[208]	
	Small intestine	[199]	[26; 208; 199]	[204]	[199]	[199; 205]				
	Jejunum	[198; 197]								
	Colon	[198; 197]	[26; [201]	[206]		[199; 206]		[206]	[208; 209]	[228]
	Rectum	[198]								
	Liver	[196; 198; 197]	[26; 201]	[206]	[199; 205; 206; 213]	[199; 205; 206]	[219]	[206]		[226; 227; 228]
	Gall Bladder			[206]	[214]	[214]	[206]	[206]		
Pancreas		[197]		[204; 206]		[199; 206]		[206]	[210]	[227; 228]
Spleen				[206]		[206]		[206]	[208]	[228]
Urinary tract	Kidney	[196; 198; 197]		[204; 205; 206]	[199; 206; 215]	[206]	[199; 206]	[206]	[208]	[228]
	Bladder			[200]		[206]	[206]	[206]		
Reproductive tissues										
Tissue		**ABCB1**	**ABCG2**	**ABCC1**	**ABCC2**	**ABCC3**	**ABCC4**	**ABCC5**	**ABCC10**	**ABCC11**
Female	Breast	[196]	[201]	[207]	[207]			[207]		[226]
	Ovary		[26]	[206]				[206]		[227; 228]
	Uterus	[196]	[199]	[204]						
	Placenta	[196]	[201]	[204; 206]	[216]			[206]	[199]	[227; 228]
Male	Prostate	[196]	[26]	[204]			[199]			[227; 228]
	Testis		[26]	[199; 204; 206]				[206]	[208; 209; 211]	[199; 227; 228]
					RNA		**protein**		**RNA + protein**	

3.2. ABCC1, ABCC2, ABCC3 and ABCC10

ABCC1 is ubiquitously expressed in the body and especially present in reproductive tissues including breast, ovary, uterus, prostate and testis [204]. ABCC1 transcripts are highly expressed in tissues including lung, stomach, colon, or testis and at lower level in brain, heart, skeletal muscle,

pancreas, ovary, placenta and mammary epithelium cells (Table 4) [199, 204-207]. Though little is known about ABCC10 (an other ABCC transporter), its RNA are detected in brain, heart, stomach, colon, pancreas spleen and kidney [208-210] in placenta [199] and sertoli cells of testis [211].

In contrast to ABCC1, ABCC2 and ABCC3 mRNA are tissue specific. ABCC2 RNA were highly detected in liver and found in lung, stomach, small intestine, and kidney [199, 205, 206]. ABCC2 proteins are localized at the apical surface of polarized cells such as capillary endothelium [212], hepatocytes [213], gall bladder epithelia [214] and kidney proximal cells [215]. In reproductive tissues, ABCC2 transcripts are also detected in lactating mammary epithelium cells [207] and at apical surface of syncytiotrophoblasts [216]. A deficiency in ABCC2 expression is found in acquired or hereditary syndrome, the latter known as Dubin-Johnson syndrome in humans. It is associated with conjugated hyperbilirubinaemia [217]. In Dubin-Johson patient cells, basolateral ABCC3 transport activity is increased and causes an increased concentration of bilirubin glucuronosides in blood [217]. This basolateral ABCC3 expression is reported in Table **4**. In placenta, ABCC3 proteins are predominantly expressed in the apical syncytiotrophoblast [216].

3.3. ABCC4, ABCC5 and ABCC11

ABCC4 and ABCC5 mRNA are expressed in various tissues reported in Table **4**. ABCC4 and ABCC5 were clearly localized at the luminal side of brain capillary endothelial cells and in astrocytes of the subcortical white matter [218]. Furthermore, ABCC4 distinguishes itself from the other ABC family members by its dual membrane localisation in polarized cell types. In prostate tubuloacinar cells, hepatocytes and choroid plexus epithelium, ABCC4 is localized to the basolateral membrane, whereas it is expressed at the apical membrane of renal proximal tubule cells and the luminal side of brain capillary endothelium (Table **4**) [219]. In a colonic epithelial cell line, the protein was found to be localised to both the apical and basolateral membrane, with a higher apical abundancy [220]. Finally, ABCC4 mRNA are detected in prostate and ovary [199, 221], while ABCC5 mRNA is found in ovary, placenta and testis [206] as well as breast in lactating mammary epithelium cells [207]. ABCC5 is preferentially localized in the basal membrane of syncytiotrophoblasts and in and around foetal vessels, with transcripts decreasing with gestational age [222]. Multiple mRNA species for the *abcc5* locus has been described [223-225]. The various *abcc5* splicing transcripts are abundantly expressed in the human retina and in many other tissues at varying levels [224].

In spite of contradictory data about ABCC11 expression pattern, ABCC11 expression was detected at mRNA level in various tissues (Table **4**). All reproductive tissues expressed ABCC11 mRNA with high level in prostate and testis, moderate level in breast and ovary and low level in placenta [199, 226-228]. The *abcc11* gene produces two major transcripts of 4.5 kb (abundant in breast) and 4.1 kb (abundant in testis) [226, 227].

4. IN VITRO REGULATION OF ABC TRANSPORTERS BY OESTROGEN AND PROGESTERONE DERIVATIVES

The actions of estrogens and progesterone, well known female hormones, are largely and respectively mediated by their cognate intracellular receptors, estrogen receptors (ER) and progesterone receptors (PR). These receptors are members of the nuclear receptor superfamily, which function as transcription factors that regulate their target gene expression. Proper functioning of ER and PR maintain the normal responsiveness of reproductive tissues to steroid stimulations allowing the normal development and function of reproductive tissues. Since many factors can alter ER and PR expression or function, these situations may induce pathological conditions.

The ER family has two different subtypes: ER alpha (ER alpha) and beta (ER beta). Recently, Bay et. Al fully described the relationship of breast cancer, estrogen receptor and ligands, especially the centrality of the estrogen receptor, which mediates on one hand the hormone-induced gene transcription and on the other hand the anti-estrogen (tamoxifen/TAM, fluvestrant) action against breast cancer [229].

The progesterone (PROG) plays a key function by acting through PR isoforms, PRA and PRB. Upon hormone binding, receptors become activated, resulting in dissociation from the oligomeric complex, dimerization, and binding to specific hormone response elements (HREs) of genes. Binding of PR to progesterone response elements (PRE) promotes the formation of a stable initiation complex, resulting in gene transcription. As with ER receptors, co-regulators are recruited by liganded or unliganded PR, either to enhance or to suppress transcription activity and to modulate PR function [230]. These two isoforms have different cellular regulatory effects [231]. Various antagonists effectively compete for PROG binding to PR and render the receptor transcriptionally inactive or substantially reduce its activation. Mifepristone (RU486) inhibits PROG mediated regulation of expression by interacting with PR. RU486 antagonist effect is more based upon its ability to induce different conformational changes in PR instead of promoting efficient binding of PR to target DNA sequences [232].

As both ER and PR status are crucial for breast cancer treatment and ABC transporters are expressed in breast, we focused, in this review section, findings about *in vitro* regulation of ABC transporters by female steroid hormones.

4.1. ABCB1 and ABCG2

Controversial data were reported in independent studies about estrogen regulatory effect on ABCG2 and ABCB1 expressions (Table **5**). For example, though E2 did not alter ABCB1 transcript in either ER alpha positive breast-cancer MCF-7/MDR and T47D/MDR cells, estrone, diethylstilbestrol and E2 down-regulated ABCB1 protein expression in these model cells, decreasing ABCB1 efflux activity and cell resistance to vincristine [233] while it had no effect on ER negative cells. In addition, the E2-mediated down-regulation of ABCB1 was reversed by TAM in MCF7/MDR cells. Taken altogether, the ABCB1 regulation by ER alpha might be through a post-transcriptional mechanism [233]. In con-

Table 5. ABC Transporter Expression Regulation by Hormones in Breast, Ovary or Placenta Cells. ⇩ and ⇧ Respectively Symbolize a Down and an Up regulation. ⇧ or ⇩Signifies Controversial Data or Data Depending on Cell Lines or Models. Ø Signifies no Expression Modulation was Reported. Abbreviations: E2 (Estrogen), ER (Estrogen Receptor), PROG (Progesterone), PR (Progesterone Receptor)

Breast cells		
Protein	Pathways	
	E2/ER	PROG/PR
ABCB1	⇧ or ⇩	Ø
ABCG2	⇧ or ⇩	⇧ or ⇩
ABCC1	Ø	
ABCC3	⇩	
ABCC5	⇩	
ABCC11	⇩	
Ovary cells		
Protein	Pathways	
	E2/ER	PROG/PR
ABCB1	Ø	
ABCG2	⇧	
Placenta cells		
Protein	Pathways	
	E2/ER	PROG/PR
ABCB1	⇧	⇧
ABCG2	⇧ or ⇩	⇧
ABCC1	Ø	Ø
ABCC2		

trast and likely due to the tissue specificity of ER signalling pathways, in trophoblast cells, mRNA and protein were significantly up-regulated following E2 treatment [234]. Surprisingly, as E2, TAM also increased ABCB1 RNA transcript levels in MCF7 cells through SXR activation and not ER signalling pathway [235]. Nevertheless, ADR-resistant MCF7 cells (clonal selection of MCF7 cells resistant to adriamicin) lost the regulation of ABCB1 expression by TAM [236]. In addition, in an unique ER alpha negative fulvestrant-resistant cell line (MCF7/F), derived from ER alpha positive MCF7 cells, ABCB1 expression levels were not modified [237]. TAM did not regulate ABCB1 expression in hamster ovary [238] while in placental cells, E2 stimulated ABCB1 expression that was associated with an increase of digoxin transport activity [234].

Similarly, contradictory effect of E2 was observed on ABCG2 regulation in breast cells. Fe *et al.* (107) first identified a functional ERE motif in the 5' flanking region -190/-161 of *abcg2* promoter. E2 enhanced ABCG2 transcript levels in the ER-positive T47D:A18 [239] and MCF7 cells [237, 240]. In agreement with transcript levels, Zhang *et al.* [237, 240] described an ABCG2 protein up-regulation by E2, in MCF7 cells transfected with ABCG2 gene under its own promoter control, while surprisingly, Liu *et al.* reported that ABCG2 protein levels were decreased by E2 exposure [237]. In addition, we and others observed that at physiologic levels, E2 markedly decreased endogenous ABCG2 expression levels in ER alpha-positive MCF7 cells [241] and T47D cells [242] while no regulation of ABCG2 expression was found in ER alpha positive T47D cells by Yasuda et al [243]. Since both TAM and ER alpha small interfering RNA exposures partially reversed E2-mediated ABCG2 down-regulation, Imai *et al.* concluded that interaction of E2 and ER alpha was required for ABCG2 expression regulation in MCF7/BCRP cells [242]. Nevertheless, since ABCG2 RNA levels were not altered in the presence of E2 and pulse-chase labeling experiments from MCF7/BCRP cells suggested that E2 treatment decreased protein production (synthesis and maturation), ABCG2 regulation by E2 had to be through

post-transcriptional mechanisms [242]. These discrepancies may also be partially explained by the fact that E2 regulation of gene expression is strongly dependent of "cellular context" [244, 245]. Similarly, numerous contradictory data were reported about E2 regulatory effect on ABCG2 expression levels in placental BeWo cell line. Theses discrepancies should be attributed to the experimental conditions and cellular or tissue context. In contrast to Ee's study [246], E2 exposure decreased ABCG2 protein expression [247, 248] although E2 had no effect on ABCG2 promoter response [243]. To complete findings on E2 ABCG2 expression regulation, ABCG2 mRNA expression was induced by estrogen in ovarian-cancer cells (PA-1) over-expressing ER alpha [239] and in human trophoblasts [234].

Furthermore, the gene promoters of ABCB1 and ABCG2 were studied. Studies of molecular mechanism regulating ABCG2 expression lead to identification of a TATA-less promoter, with several Sp1, AP1, and AP2 sites, hypoxia response elements, a CCAAT box downstream from a putative CpG island and a peroxisome proliferator activated receptor response element [239, 249-252]. In parallel way, Zampieri and *et al.* observed that ER alpha positive MCF7 cells were more resistant to doxorubicin (a well known ABCB1 substrate) than ER beta positive T47D cells. This resistance was likely linked to an increase of ABCB1 expression by E2 in MCF7 cells through activation of AP1 and Sp1 transcription factors. In contrast E2 did not regulate ABCB1 expression in T47D cells [253]. These findings were supported by the fact that neither ERE, nor PRE were yet described in *abcb1* promoter, and that ER and PR signalling pathways may be activated though stimulation of AP-1 and Sp1 sites of *abcb1* promoter [253].

As observed for ABCG2 expression regulation by E2, PROG strongly regulated ABCG2 expression levels (Table 5.). In breast cells, PROG increased ABCG2 promoter response, which was inhibited by RU486 or mithramycin A addition in T47D cells [243], while PROG decreased ABCG2 expression in MCF7 cells [254]. Similarly, dexamethasone (DEX) was able to strongly decrease ABCG2 expression in PR-positive MCF7 and in PR-negative MDA-MB-231 breast cells. Nevertheless, in PR-negative MDA-MB-231 cells stably transfected with PRA and PRB, ABCG2 expression was strongly up-regulated by DEX and PROG [254]. In addition, two other Pregnane X Receptor (PXR) and/or Glucocorticoid Receptor (GR) ligands were also able to down-regulate ABCG2 expression in PXR- and GR-positive MCF7 cells [254]. Consequently, ABCG2 expression might be the resultant of multiple signalling pathway activation including PXR, PR, GR or/and ER pathways. In placental cell (BeWo), ABCG2 protein expression was up-regulated by PROG [248, 255]. This up-regulation was increased by PRB transfection but not by PRA transfection. PRB role was confirmed at molecular level with specific *abcg2* promoter activation. Indeed, a novel PRE was found in *abcg2* promoter region between -187 and -173. PRA and PRB can both bind to this PRE. PRE-mediated activation of *abcg2* promoter was reduced with a mutated or deleted-PRE promoter. This PRE corresponds to the ERE discovered by Ee *et al.* [239]. In T47D cell, PROG also activates ABCG2 promoter [243]. In contrast to ABCG2 regulation by PROG, little is known about ABCB1 regulation by progestins. ABCB1 expression was not altered by PROG in MCF7/MDR cells [233], while ABCB1 expression was slightly increased in trophoblast cells treated by PROG [234].

4.2. ABCC1, ABCC2, ABCC3, ABCC4, ABCC5 and ABCC10

The promoters were cloned and specific, functional motifs were described.

❑ *ABCC1*

Abcc1 promoter region was initially cloned by Zhu *et al.* [256] who described a TATA-less promoter in a GC-rich region (nucleotides -91 to +103) and discovered a SP1 site essential for optimal ABCC1 transcriptional activity [257]. Promoter region potentially contains a NFKB site (http://www.humanabc.bio.titech.ac.jp/). The human endogenous RNA 5'-UTR contains a GC-rich region of approximately 160 nucleotides, including a GCC triplet repeat and a 57-bp direct repeat. Given the lack of identifiable TATA, CAAT, or Inr elements within the *abcc1* gene 5'-UTR, these findings were consistent with a role for the conserved GC-boxes in specifying the transcription initiation sites of each gene [258]. Thirteen protein binding sites were identified of which six were sequence specific. Differences in levels of protein binding occurred with a putative antioxidant response element (ARE)/AP-1 binding site at -511 to -477 [259]. Since a putative AP-1 had been found in *abcc1* promoter, ER signalling pathways may stimulate this last one. Although no ABCC1 regulation by E2 had been described in breast tissue, a regulatory mechanism could be possible. Nevertheless, no ABCC1 mRNA expression regulation by E2 was found in cytotrophoblast from human placenta [234] and in fulvestrant-resistant ER alpha negative MCF7 cells [237]. In contrast to the default of ABCC1 regulation by E2, ABCC1 mRNA were increased by PROG in trophoblast [234] without any repercussion at protein level. Thus, currently no ABCC1 protein modulation was ever observed for any other female steroid hormone.

❑ *ABCC2*

The coordinated transcriptional regulation of ABCC2 is shown to be modulated by the activities of nuclear factors such as Y-box protein1, FXR, SHP, PXR, CAR, and HNF4α [260-264]. Furthermore, to target more precisely ER signalling pathways, two putative AP-1 and one Sp1 sites were located on *abcc2* promoter [265], while no direct ERE or PRE putative sites had been found on its promoter sequence. Recently, a functional ABCC2 protein was found to be over-expressed in TAM resistant MCF7 cells. Furthermore, this regulation might be directly related to PXR and PI3 kinase pathways [266]. In contrast, in other anti-estrogen resistant cell lines, fulvestrant-resistant ER alpha negative MCF7/F cells, no alteration of ABCC2 protein level was observed [237].

There is no current finding about PROG regulation in breast cancer cells. PXR, CAR (the constitutive androstane receptor) or GR are largely involved in ABCC2 regulation by xenobiotics. Then we logically reported numerous data about ABCC2 expression regulation by DEX, RU486 and oltipraz in human and rodent hepatocytes [267-270] and in

liver and kidney plasma membrane cells of DEX treated rat [271].

❑ *ABCC3*

Since genomatix software analysis led to the identification of ERE, Sp1, AP-1 and NFKB sequences in *abcc3* promoter [272], it had been hypothesized a possible regulation of ABCC3 by female steroids. Indeed, ABCC3 mRNA and protein levels were found decreased by E2 in ER alpha positive MVLN cells derived from MCF7 breast cancer cells [272]. Abolishment of this regulation by cycloheximide indicated that a *de novo* synthesis was required. Furthermore, ABCC3 mRNA tended to be up-regulated by the anti-estrogens: TAM or fulvestrant [272]. In renal cells of gonadectomized or hypophysectomized mice, E2 increased ABCC3 expression, strongly suggesting an E2 specific response depending on cell tissue origin [273].

❑ *ABCC4*

Little is described about ABCC4 expression regulation by female steroid hormones. While *abcc4* promoter contains two Sp1 sites (http://www.humanabc.bio.titech.ac.jp/) which may be involved in ER signalling pathways, E2 treated gonadectomized mice showed no modulation of renal ABCC4 mRNA levels [273]. Likely tissue specific, other regulation pathways may regulate ABCC4 expression. Indeed, the peroxisome proliferator-activated receptor (PPAR) alpha agonist clofibrate was also able to regulate ABCC4 expression [274]. In contrast, DEX (GR and PXR activator) failed to modulate Abcc4 in rat kidney or brain capillary membranes [271], while no data about ABCC4 regulation is currently available in breast cells.

❑ *ABCC5*

ABCC5 expression levels were down-regulated by E2 [272] in ER positive MVLN breast cancer cells and an ERE motif has also been identified in the promoter of *abcc5* [275]. Consequently, these findings strongly support the idea of an endocrine regulation of ABCC5 in breast tissue. Furthermore, genomatix software analysis led to the identification of Sp1 binding sites in the promoter region of *abcc5* [272] and promoter also seems to contain one AP-1 sequence (http://www.humanabc.bio.titech.ac.jp/). Those Sp1 and AP-1 sites could also be involved in ER alpha signalling pathways and might led to ABCC5 down-regulation by E2. In contrast, the anti-estrogen TAM did not have any effect on ABCC5 mRNA level while fulvestrant may slightly down-regulate ABCC5 mRNA in ER alpha positive MVLN cells [272].

❑ *ABCC10*

The nucleotide sequence of human *abcc10* gene 5′ flanking region had been reported [276]. 5' RACE carried out with CWR22Rv1 and HepG2 cell lines identified two new ABCC10 transcripts with very short 5' UTR sequences. The predicted binding sites for transcription factors marked on the sequence were identified by Genomatix MatInspector software. A single transcription start site was identified for CWR22Rv1 (−428) and HepG2 (−418) cell lines. They found one putative ARE, one cAMP-responsive element binding protein (CREB), one ERE, two hepatic nuclear factor 2/4 (HNF 2/4), two PRE, one sterol regulatory element binding protein (SRE), four E2F sequences and at least 3 SP1 sites [276]. The presence of these ERE, SP1 and PRE strongly suggested that ABCC10 expression is possibly regulated by female steroid in breast tissue but no data are yet available.

❑ *ABCC11*

Recently ABCC11 transporter was reported to be regulated in ER alpha positive MCF7 breast cells by E2, while its expression was not modified in ER alpha negative MDA-MB-231 cells [241]. The involvement of ER alpha was supported by the fact that two antiestrogens (fulvestrant and TAM) abrogated E2-mediated down-regulation. Furthermore ABCC11 expression was up-regulated in MCF7 cells exposed to TAM for 72 h, and was over-expressed in TAM resistant cell lines. This over-expression was associated with an enhancement of drug resistance to 5-FU, consistent with the reported ability of ABCC11 to confer resistance to this agent. *In silico* analysis of *abcc11* promoter region (-5000 kb) using Genomatix MatInspector software revealed at least 2 ERE, 2 Sp1, 5 AP-1 and 4 NF-kB putative binding sequences [241]. ERE binding site presence was confirmed in the reported genome wide analysis of promoter occupancy by the estrogen receptor [275].

5. ABC TRANSPORTER EXPRESSION LEVELS IN BREAST CANCER

Many patients suffering from breast cancer receive chemotherapy for treatment. However, a number of these patients do not well respond to chemotherapy and only a moderate percentage (usually less than 30 %) obtains a complete or optimal response. Extensive studies have been conducted on mechanisms believed to be responsible for this chemoresistance, including the involvement of ABC transporters. The role of ABC transporters in clinical treatment and tumour recurrence is still opened to discussion. In acute myeloid leukemia, the link is well illustrated between MDR phenotype and ABC transporters [277-280]. For example, *abcb1* and/or *abcg2* gene over-expression association with tumour drug resistance and poor patient outcome is widely accepted [277, 279]. In contrast findings for adult acute lymphoblastic leukemia are still conflicting [279, 281, 282]. Furthermore, the contribution of other ABC proteins including ABCC1-5, ABCC10, ABCC11 and ABCG2 transporters is still underway in cancer chemoresistance [208, 241, 278, 283-286]. In addition, it should be bear in mind that a number of ABC transporters have not yet been linked to drug resistance (ABCC6, ABCC7/CFTR), but they also might have prognostic relevance.

Breast cancer is a complex disease caused by the progressive accumulation of multiple gene mutations combined with epigenetic dis-regulation of critical genes and protein pathways. There is a substantial inter-individual variability between the patient age and the cancer phenotype. Consequently, a lot of efforts should be focused at both population and individual levels to develop new treatment strategies. The BRCA1 (breast cancer 1, early onset) and BRCA2 mutations increase the risk of breast cancers. This discovery had radically transformed our understanding of breast cancer

genetic basis, leading to improve management of high-risk women. A better understanding of tumour host biology has led to improvements in multidisciplinary management of breast cancer. Traditional pathologic evaluation is being complemented by more sophisticated genomic approaches. From genomic profiling studies, a number of genomic biomarkers have been developed for clinical use, and increasingly, pharmacogenetic end points are being incorporated into clinical trial design. The present challenge is to learn how to use and link molecular signatures of an individual with his tumour to improve patient outcome.

Though, a large number of molecular prognostic markers have already been reported in the literature, little is known about the relationship between ABC transporters and patient outcome. Previously, a formal meta-analysis of published data had been carried out on ABCB1 and ABCC1 expression and functional significance in breast cancer [287]. Here, we provide an updated review of ABCB1, ABCG2, ABCC1-5, ABCC10 and ABCC11 expression in various histological types, histological grades, steroid status and their potential clinical role and potential predictive value in breast cancer.

To carry out this updated review, we used the Platform web site (http://www.oncomine.org/) which is a powerful tool to collect genomic expression profiling studies. This Oncomine Web Platform facilitates therapeutic target discovery and validation. Genomic profiling data are biotechnological processes, which are being used to establish relationship between gene expression levels and certain standard criteria (histological forms, markers…). There were mostly univariate analyses (methods for analyzing data on a single variable at a time) while multivariate analyses (methods for analyzing data from more than one variable) would be a powerful tool for determining the relationship between ABC transporters and various breast cancer criteria. This may partially explain the discrepancy between study findings. Furthermore, though large heterogeneity of breast cancers is largely documented, the findings should be validated by an independent group of researchers, and ideally, a prospective study should confirm the prognostic and predictive significance of tested markers.

In this review section, we summarized ABC transporter transcript expression levels in breast cancers according to histological and prognostic criteria. We must keep in mind that additional multivariate analysis needs to be carried out in junction with established markers (ER alpha, ERBB2….) to assess its independent value. We have not carried out a formal meta-analysis of published Oncomine data. We have completed our findings through literature searches in databases including PubMed Medline (http://www.ncbi.nlm.nih.gov/). Studies often report different levels of positivity for protein and RNA expression which introduce heterogeneity in findings. For each study, we have used data corresponding to the minimum definition of positivity provided by the authors. To obtain a more synthetic and encompassing view of findings, whenever feasible, we have pooled the data from comparable studies in tables. Despite these limits, we can observe trend associations between various breast cancer criteria and ABC transporter transcript expression levels.

5.1. Comparison of ABC Transporter Expression in Normal Mammary Tissues Versus Breast Cancer Tissues

We compared transcript expression levels of ABC transporters in normal mammary tissues and various histological breast tumours. Since the cohort size of normal mammary tissues was usually limited (N<10), we observed discrepancy data between various studies. Nevertheless, we noticed that ABCG2 (Richardson_Breast_2 study - Normal Breast (N=7) versus Breast Carcinoma (N=40) and Finak_Breast study - Breast Stroma - Normal Breast (N=6) versus Breast Carcinoma (N=53)) and ABCB1 (Richardson_Breast_2 study and Radvanyi_Breast study Normal Breast (N=9) versus Breast Carcinoma (N=47)) expression levels were globally and significantly decreased in total breast carcinomas compared to normal breast. ABCG2 decreased expression in tumours was confirmed at protein level in Faneyte's study [288]. With immunohistochemistry approach used in Faneyte's study, ABCG2 was detected in vessels and normal breast epithelium but not in tumour cells [288]. This low expression was independently confirmed by Kanzaki *et al.* [289].

Globally, ABCB1 low expression in breast carcinomas was reported in Oncomine findings and was also confirmed by Vaclavikova *et al.* [290]. The percentage of the tumour cell population expressing ABCB1, distributed focally, varied from less than 5 % to greater than 30 % in locally advanced breast cancer. ABCB1 expression was observed significantly more often in tumours that showed less than partial response to the preoperative chemotherapy [291]. Although ABCB1 (protein and RNA) was expressed and detected in most tumours and normal breast samples [287], its expression was down-regulated in 79.5 % of tumours compared with the normal samples [290]. Taken altogether, we could conclude that Oncomine data and literature findings about ABCG2 and ABCB1 were in agreements. Furthermore, the presence and effect of single nucleotide polymorphisms (SNPs) on ABCB1 expression levels had been studied and related to cancer. High frequencies of the variant alleles in *abcb1* exon 12 (1236C>T, 38.3%) and exon 26 (3435C>T, 54.0%) were observed. and individuals with these variant alleles had significantly lower ABCB1 expression levels in their tumours. Subsequently, ABCB1 SNPs may influence its expression level in tumours to modify breast cancer resistance phenotype [290]. This strongly suggested that an heterogeneity expression levels of transporter may be directly related to polymorphisms and completely independent to the normal or cancerous status of the tissue.

Transcript ABCC1 expression was moderately detected in normal and cancer breast tissues [292]. In addition, Finak_Breast study (Stroma - Normal Breast (N=6) versus Breast Carcinoma (N=53)) reported a decreased expression in breast stroma carcinomas compared to normal tissues. Nevertheless, Ito *et al.* reported that ABCC1 mRNA levels were significantly higher in breast cancers than in normal breast tissues [293]. This discrepancy may be directly linked to histological breast cancer studies in these independent cohorts of patients. Furthermore, ABCC1 expression was not related to patient's age, menopausal status or tumour size [294].

Little findings were available on that point for other ABCC transporters. ABCC3 (Richardson_Breast_2 study -

Normal Breast (N=7) versus Breast Carcinoma (N=40)) and ABCC10 (Radvanyi_Breast study - Normal Breast (N=9) versus Breast Carcinoma (N=47)) transcript expression levels were decreased in breast carcinoma compared to normal breast. ABCC4 (Richardson_Breast_2 study) and ABCC5 (Finak_Breast study - Breast Stroma - Normal Breast (N=6) versus Breast Carcinoma (N=53)) expression levels in breast carcinoma were increased compared to normal tissue. No significant difference was observed for ABCC11.

Since gene expression levels may be completely dependent on histological origin and other criteria developed later in this review (including histological grade and specific markers such as ER, PR and ERBB2), we compared transporter expression levels from normal breast tissue and from ductal carcinoma, the most frequent invasive tumours. In contrast to observations made in total breast carcinomas, we observed discrepancies in ABCG2, ABCC2 and ABCC10 expression levels. For example, ABCG2 was strongly down-expressed in Richardson_Breast_2's study (comparing Normal Breast (N=7) versus Breast Carcinoma (N=40)), while no difference was clearly found in Folgueira_Breast_2 (comparing Normal Breast (N=18) versus Invasive Ductal Carcinoma (N=100)). This may suggest that histological form is an important variation factor. Nevertheless, it may also be directly linked to the cohort size or sample heterogeneity as we noticed an important heterogeneity in ABCG2 expression in patients. Furthermore in ductal carcinoma, Karnoub_Breast study (comparing Normal Breast (N=15) versus Invasive Ductal Breast Carcinoma (N=7)) showed that ABCC3, ABCC4, ABCC5 and ABCC10 were over-expressed in comparison with normal breast tissue. Nevertheless these data were not confirmed in Folgueira_Breast_2 study. One of the rational explanations is the cohort size, which is very tiny in Karnoub_Breast study in comparison to Folgueira_Breast_2 study.

We also noticed that ABCB1 and ABCC4 were respectively down- and over-expressed in lobular carcinoma compared to normal breast tissue (Turashvili_Breast study; comparing Adjacent Normal Lobular (N=5) versus Invasive Lobular Carcinoma (N=5)). Sorlie_Breast study (comparing Benign Breast (N=7) versus Breast Carcinoma (N=78)) reported that ABCB1 and ABCC1 transcript expression levels were decreased while ABCC5 was increased in breast carcinoma compared to benign tissues.

In conclusion, we observed too many discrepancies. Consequently, additional multivariate analysis needs to be carried out in junction with histological types to assess independent value of transporter expression levels in normal compared to cancerous tissues.

5.2. Comparison of ABC Transporter Expression According to Breast Cancer Histological Types

Breast cancer classification was developed as a tool for oncologists to organize different types of cancers according to certain standard criteria. It is based on tumour extent, spread extent to axillary lymph nodes and metastasis presence. In this review, we reported ABC transporters expression levels according histological forms, axillary lymph nodes spread (Table **6**), histological grade classification (Table **7**) and metastasis development.

a) Histological Form

Breast cancer is a heterogeneous disease that encompasses a wide range of histopathological types including invasive ductal carcinoma, lobular carcinoma, medullary carcinoma, mucinous carcinoma, tubular carcinoma, and apocrine carcinoma among others. This was fully described in the introduction (cf Table **1**).

Firstly, in agreement with higher incidence of ABCB1 expression in lobular than in ductal breast carcinoma reported in Leonessa's review [287], Bittner_breast study (Class 1 (Ductal Breast Carcinoma (N=264) and Mucinous Breast Carcinoma (N=8)) versus Class 2 (Lobular Breast Carcinoma (N=38))) reported that ABCB1 and ABCG2 expression levels were increased in lobular carcinomas while ABCC10 and ABCC1 expression levels were decreased. No difference was observed for other transporters.

Secondly, in Genestier_Breast study (Class 1 (Ductal (N=45)) versus Class 2 (Medullary (N=5))), ABCC5 and ABCC11 levels were decreased in medullary tumours, while ABCC1, ABCC4 and ABCC10 expression levels were increased in medullary cancers in comparison to ductal cancers.

Thirdly, though the tumour cohort size is highly different in Bittner_breast study (Class 1 (Ductal Breast Carcinoma (N=264), Lobular Breast Carcinoma (N=38)) versus Class 2 (Mucinous Breast Carcinoma (N=8)), ABCC1 expression was only decreased in mucinous carcinoma compared to ductal and lobular carcinoma. Additional findings were reported for ABC transporter expressions and histological forms of breast tumours. Especially in Richardson_Breast_2 study (Class 1 (Non Basal-like Carcinoma (N=20)) versus Class 2 (Basal-like Carcinoma (N=18)), they found a decrease of ABCC3 and ABCC11 but an increase of ABCC4 in basal like carcinoma compared to non-basal-like carcinoma. Basal-like breast cancer is associated with high grade, poor prognosis, and younger patient age. Clinically, a triple-negative phenotype definition (ER, PR and ERBB2) is commonly used to identify the basal-like tumours. For a better understanding of these findings about very variable phenotypes of tumours, it would be worth to compare directly but not to mix various types in compared groups (mucinous, lobular and ductal…). A meta-analysis should be recommended for this analysis to be confident with these findings.

b) Axillary Lymph Nodes

Detection of tumour cells in lymph nodes is an indication of tumour spread and is clinically used as a prognostic tool and a guide to therapy [295]. In breast cancer, the axillary lymph nodes are often the first site to harbour metastases. The metastasis risk is majored with the increasing number of lymph-node presence [2]. These regional metastases are not life threatening per se. Yet their presence or absence is the most powerful prognostic factor currently available for breast cancer disease course [295, 296]. Nevertheless, approximately one-third of women with negative lymph nodes develop distant metastases, whereas about one-third of patients with positive lymph nodes remain free of distant metastases 10 years after local therapy [297, 298].

Table 6. Relationships between ABC expression levels and nodal involvement of breast tumours. The study line indicates the study name, the compared classes and inside brackets the number of tumour samples. The list of reported studies is without being exhaustive and white cases indicated either no significant P-value or the P-value was not found. P < 0.05 was considered significant (T- test)

Lymph Node Status									
	ABCB1	**ABCG2**	**ABCC1**	**ABCC2**	**ABCC3**	**ABCC4**	**ABCC5**	**ABCC10**	**ABCC11**
	↓↓↓	↓↓↓			↑↑↑				
Study	*Ivshina_Breast*				*Pollack_breast*				
	Negative (159) vs Positive (81)				**Negative (11) versus Positive (32)**				
P-value	2,90E-02	3,50E-02			3,00E-03				
T-test	2,21	2,123			-3,185				
Study	*Miller_Breast*				*VandeVijver_Breast*				
	Negative (158) vs Positive (84)				**Negative (151) versus Positive (144)**				
P-value	2,90E-02	3,30E-02			3,60E-02				2,40E-02
T-test	2,204	2,15			-2,106				-2,268
Study	*Zhao_Breast (Ductal carcinoma)*				*Chin_Breast*				
	Negative (16) vs Positive (18)				**Negative (51) versus Positive (67)**				
P-value		8,20E-02	3,70E-02		5,00E-02				
T-test		1,8	-2,194		-1,979				
Study					*Huang_Breast*				
					Negative (19) versus Positive (69)				
P-value						4,90E-02	9,00E-03		
T-test						-2,042	-2,776		

As auxiliary lymph node status is still one of the most powerful prognostic factors for breast cancer patients, we evaluated the variation of ABC transporter levels according to lymph node invasion. Although the number of studies was small (N<5), ABCB1 and ABCG2 expression levels seemed to be decreased in the presence of lymph node invasion in two independent studies (Table **6**), while in one study (Table **6**), ABCC1, ABCC3, ABCC4, ABCC5 and ABCC11 seemed to be increased in the presence of lymph node invasion (Table **6**). In addition, ABCC1 expression showed a higher level in lymph nodes than in their corresponding primary tumours [299]. In contrast to Zhao_Breast report, ABCC1 protein expression was reported to be independent of tumour size and lymph node involvement [300]. Furthermore, ABCC1 expression was not related to differentiation grade or lymph node involvement [294].

In contrast, ABCB1 mRNA expression was associated with axillary lymph node invasion at surgery in 81 % cases, compared with 54.2 % in the group with undetectable ABCB1 expression [301]. He *et al.* findings confirmed that 61 % positive ABCB1 and 40 % ABCB1 negative breast cancers have more than four axillary lymph nodes involved [302]. Persistence of ABCB1-positivity after treatment was significantly associated with axillary lymph node metastasis ($P < 0.05$). Furthermore, in a logistic regression multivariate model, histologic types other than ductal, and the combination of ABCB1 with lung resistant protein (LRP) positivity emerged as independent predictors of axillary lymph node invasion at the time of rescue mastectomy [301].

c) Histological Grades

Once previous criteria are determined, they are combined in order to be assigned to an overall "Grade" of I, II and III. The lower the number, the less the cancer has spread. Grade I cancers are the least advanced and often have a better prognosis, or outlook for survival. Higher grade cancers are often more advanced and have a higher risk of metastasis. In several reports, we noticed that there were discrepancy in relationship between expression levels of transporters and histological grade. One of the rational explanations is the heterogeneity of tumour samples, expression of markers (ER alpha, ERBB2) and cohort sizes.

Globally, although Leonessa's analysis strongly suggested that there was no consistent or convincing evidence for a significant correlation between ABCB1 and grade [287], using Oncomine data base, ABCB1, ABCG2 and ABCC11 expression levels were lower with the histological high grade. In contrast ABCC1-4 and ABCC10 expression levels were increased with the histological high grade. These

data suggested that ABCC1-4 and ABCC10 may be involved in chemoresistance of histological high grade tumours to methotrexate, epirubicin and so on. Surprisingly, we observed contradictory data for the relationship between ABCC5 expression level and the histological grade (Table **7**). Leonessa *et al.* (2003) showed a certain inverse correlation between ABCB1 expression and N stage. N0 stage corresponds to cancer that has not spread to nearby lymph nodes. N1 stage is employed for cancer that has spread to 1 to 3 axillary (underarm) lymph node(s) and/or for the case where tiny amounts of cancer are found in internal mammary lymph nodes (those near the breast bone) on sentinel lymph node biopsy. N2 stage mentions cancer that has spread to 4 to 9 axillary lymph nodes under the arm, or cancer that has enlarged the internal mammary lymph nodes. ABCB1 expression was observed in 17/21 (81 %) N0 cases, 13/19 (68.4 %) N1 cases, and 6/15 (40 %) N2 cases [287, 303, 304].

d) Metastasis

Primary breast cancer cells metastasize through vessels to various distant organs, preferentially to lung, liver and bones. Patients frequently develop metastases at multiple sites. In women with metastatic breast cancer, skeletal involvement is very frequent, with reported incidences between 47 and 85 % in autopsy series and 69–80 % when defined radiographically [305-308]. In patients with metastatic spinal tumours, the primary cancer histopathology has frequently been shown to have significant prognostic value [309-315].

Currently, few data are available concerning expression levels of ABC transporters in metastasis. Nevertheless, as ABC transporters are largely involved in MDR phenotype, it appeared important to analyse whether their expression levels are altered in metastasis process. Six Oncomine studies are reported in this review. As type, markers of breast cancers were not taken in account in this specific analysis and discrepancy observations were made.

ABCB1 expression levels were down in metastasis developing breast cancers in VandeVijver study (breast carcinoma - metastasis negative (N=194) versus positive (N=101)) and in Radvanyi study (metastasis negative (N=47)) versus positive (N=7)), while no difference were reported in Desmedt study (negative (N=154)) versus positive (N=35) at 5 Years). Globally, in VandeVijver study, they analysed a large and similar number of tumours (negative (N=194) versus positive (N=101)), which strengthened their findings. In VandeVijver cohort, ABCB1 expression was decreased while ABCC5 and ABCC10 expression levels were increased in the presence of metastasis. In contrast with reported Oncomine data, no difference in ABCB1 expression was observed between metastatic and non-metastatic cases in four independent studies [287, 303, 304, 316, 317].

Furthermore in Minn_Breast's study, they analysed expression levels according to bone or lung metastasis events. Interestingly, according to the metastasis localisation, ABCB1, ABCC1 and ABCC10 were differentially expressed. For example, ABCB1 expression was decreased when there is lung metastasis development (no metastasis (N=51)) versus lung metastasis (N=14) at 5 years) while it was increased in bone metastasis case (no metastasis (49) versus bone metastasis (N=11) at 5 years). Nevertheless, additional studies must be carried out to statute on that point.

In conclusion, since axillary lymph nodes are often the first site to harbour metastases and histological grade 3 has a higher metastasis risk, we compared the possible association between these three criteria. We observed trend of positive association between high histological grade and lymph node positive status, while this association is partially lost when we compared them with metastasis presence. Recently, we independently confirmed the inverse association between ABCC11 expression and positive lymph node status and high histological grade III [241]. Additionally, in 213 breast carcinomas, ABCB1 quantitative immunocytochemistry strongly correlated ($r = 0.865$; two-sided, $P < 0.0001$) with the quantitative analysis of mRNA levels. Therefore it strengthened Oncomine findings. Nevertheless, the ABCB1 expression was found to be independent from patient age, tumour size, histologic types, grades and nodal status [318]. Consequently, additional independent studies have to be carried out to statute on these aspects.

5.3. Steroid- Receptor Expression

a) Estrogen Receptor Expression

Histopathological evidences suggest that approximately two-thirds of breast cancers express ER marker. Of particular interest is their ER status because endocrine adjuvant therapy (tamoxifen, fulvestrant) remains a cornerstone of breast cancer treatment. With the discovery of a second ER, ER beta and its variant isoforms, the definition of ER status is potentially more complex. In breast tumours, there are two ER beta expression cohorts. One cohort where ER beta is co-expressed with ER alpha and the other cohort expressing ER beta alone. In the latter subgroup of currently defined ER negative patients, ER beta has the potential to be a therapeutic target. Evidence so far supports the idea that the role of ER beta is different in ER alpha negative than in ER alpha positive breast cancers [319].

In this review, the ER status is mostly defined by the ER alpha status. In our analysis (transporter expression level versus steroid receptor status), we did not take in account the histological tumour origins (ductal, lobular…) nor the ER beta expression, which may be a limit and the explanation of discrepancy findings between studies.

Nevertheless, ABCC1, ABCC2, ABCC4 and ABCC10 expression levels appeared clearly decreased in ER positive tumours, while ABCG2, ABCC5 and ABCC11 expression levels were strongly increased (Table **8**). We confirmed the high expression of ABCC11 in cohort of postmenopausal patients [241, 320]. In complete agreement with Oncomine findings, ABCC1 protein expression was positive in 80 % of breast carcinomas and more frequent in ER-negative carcinomas [300]. However, in contrast to Oncomine findings, ABCC1 expression was not related to ER status [294]. Surprisingly, contradictory data were observed for ABCB1 and ABCC3. In agreement with the last observation, Leonessa's review reported a not clear correlation between ABCB1 and ER [287]. Furthermore, recently ABCB1 SNPs presence in exons 12 (1236C>T, 38.3 % frequency) and 26 (3435C>T, 54.0 % frequency) were significantly correlated to lower

Table 7. Relationships between ABC expression levels and histological grades. The study line indicates the study name, the compared classes and inside brackets the number of tumour samples. The list of reported studies is without being exhaustive and white cases indicated either no significant P-value or the P-value was not found. P < 0.05 was considered significant (Correlation)

Histological Grade Correlation between 3 groups: Grade 1 ; Grade 2 ; Grade 3 Ex: ABCG2 expression were observed Grade 3 < Grade 2 < Grade 1									
	ABCB1	**ABCG2**	**ABCC1**	**ABCC2**	**ABCC3**	**ABCC4**	**ABCC5**	**ABCC10**	**ABCC11**
	↓↓↓	↓↓↓	↑↑↑	↑↑↑	↑↑↑	↑↑↑		↑↑↑	↓↓↓
Study	*Miller_Breast*		**3 groups: Elston Grade 1 (67); Elston Grade 2 (128); Elston Grade 3 (54)**						
P-value	6,90E-06	9,80E-06	8,50E-05		5,00E-03	1,20E-02		2,70E-04	
Correlation	-0,281	-0,276	0,247		0,176	0,159		0,229	
Study	*Ivshina_Breast (2006)*		**3 groups: Elston Grade 1 (68), Elston Grade 2 (126), Elston Grade 3 (55)**						
P-value	9,50E-06	9,30E-06	7,80E-05		2,00E-03	5,00E-03		1,00E-04	
Correlation	-0,276	-0,277	0,248		0,198	0,179		0,244	
Study	*Ginestier_Breast*		**3 groups: Grade 1 (4) and 2 (12) Grade 3 (39)**						
P-value	1,00E-03	7,00E-03	2,00E-03	3,44E-01			1,30E-02		
Correlation	-0,418	-0,36	0,406	0,01			-0,333		
Study	*Sotiriou_Breast_3*		**3 groups: Grade 1 (67) and 2 (46) Grade 3 (59)**						
P-value	3,70E-02	2,20E-05		1,00E-03				2,00E-03	
Correlation	-0,159	-0,317		0,248				0,236	
Study	*Bittner_Breast*		**3 groups: Grade 1 (30), Grade 2 (107) Grade 3 (141)**						
P-value		1,10E-07	2,00E-03			3,70E-02		4,30E-07	1,10E-02
Correlation		-0,312	0,187			0,125		0,298	-0,151
Study	*Hess_Breast*		**3 groups: Grade 1 (2), Grade 2 (54) Grade 3 (77)**						
P-value								1,70E-06	
Correlation								0,401	
Study	*vantVeer_Breast*		**3 groups: Grade 1 (12), Grade 2 (27 Grade 3 (78)**						
P-value	4,70E-02		3,30E-02			2,20E-02		5,00E-03	
Correlation	-0,185		0,198			0,213		0,257	
Study	*Zhao_Breast*		**3 groups: Grade 1 (5), Grade 2 (20) Grade 3 (13)**						
P-value	3,50E-02	3,60E-04							
Correlation	-0,368	-0,592							
Study	*Chin_Breast_2*		**Invasive Breast Carcinoma - 3 groups: Grade 1 (41) and 2 (57 Grade 3 (72)**						
P-value							3,70E-02	5,00E-03	
Correlation							0,16	0,214	
Study	*Farmer_Breast*		**Apocrine 3 groups: Grade 1 (22) and 2 (16) Apocrine grade 3 (8)**						
P-value		2,00E-03	4,80E-02	1,20E-05			3,00E-03		
Correlation		-0,448	0,294	0,596			-0,434		
Study	*Ma-Breast*		**Ductal breast carcinoma *in situ* 3 groups: Grade I and grade 2 Grade 3**						
P-value	3,00E-03								
Correlation	0,528								
Study	*Finak_Breast*		**Breast carcinoma stroma - 3 groups: Grade 1 (3), Grade 2 (23) Grade 3 (27)**						
P-value						2,50E-02			1,30E-02
Correlation						0,308			-0,339
Study	*Ma_Breast_3*		**3 groups: Grade 1 (3), Grade 2 (39) Grade 3 (18)**						
P-value			2,40E-02					9,00E-03	
Correlation			0,291					0,333	
Study	*Ma_Breast*		**Ductal breast carcinoma -3 groups: Grade 1 (5) and 2 (9) Grade 3 (9)**						
P-value	2,90E-02								
Correlation	0,454								

Table 8. Relationships between ABC expression levels and ER status of breast tumours. The study line indicates the study name, the compared classes and inside brackets the number of tumour samples. The list of reported studies is without being exhaustive and white cases indicated either no significant P-value or the P-value was not found. $P < 0.05$ was considered significant (T-test)

Estrogen Receptor Status									
	ABCB1	**ABCG2**	**ABCC1**	**ABCC2**	**ABCC3**	**ABCC4**	**ABCC5**	**ABCC10**	**ABCC11**
	↕↕↕	↑↑↑	↓↓↓	↓↓↓	↕↕↕	↓↓↓	↑↑↑	↓↓↓	↑↑↑
Study	***Desmedt_Breast***		**Negative (64) versus Positive (134)**						
P-value	4,60E-02	2,80E-05	6,00E-05		4,00E-03	6,40E-08	5,00E-03	2,60E-09	
T-test	-2,017	-4,345	4,132		-2,96	5,681	-2,85	6,472	
Study	***Bittner_Breast***		**Negative (78) versus Positive (154)**						
P-value			2,00E-03	2,00E-03		1,00E-06	1,10E-04	3,80E-10	8,00E-03
T-test			3,222	3,239		5,051	-3,93	6,763	-2,686
Study	***Saal_Breast***		**Negative (60) versus Positive (45)**						
P-value	1,20E-02			5,50E-04	3,00E-02	4,00E-03	2,40E-02	9,50E-04	
T-test	2,549			3,579	2,198	2,926	-2,294	3,405	
Study	***Chin_Breast***		**Negative (43) versus Positive (75)**						
P-value		6,50E-06	2,00E-03			8,00E-03	4,20E-02	8,10E-04	
T-test		-4,726	3,161			2,707	-2,058	3,47	
Study	***Wang_Breast***		**Negative (77) versus Positive (209)**						
P-value		3,60E-05	***1,40E-05***	3,10E-04		2,60E-04	3,10E-11	***2,30E-05***	
T-test		-4,274	4,47E+00	3,738		3,726	-6,983	4,39E+00	
Study	***Ginestier_Breast***		**Negative (28) versus Positive (27)**						
P-value		4,90E-02	7,00E-03	7,00E-03		2,00E-05	1,70E-04		5,00E-02
T-test		-2,013	2,806	2,798		4,74E+00	-4,085		-2,006
Study	***Minn_Breast_2***		**Negative (42) versus Positive (57)**						
P-value			4,40E-02		2,40E-02	6,00E-03	6,00E-03	6,70E-05	
T-test			2,044		-2,297	2,847	-2,829	4,197	
Study	***Miller_Breast***		**Negative (34) versus Positive (213)**						
P-value			3,60E-02			2,80E-02	1,70E-02	1,90E-04	
T-test			2,173			2,267	-2,468	4,071	
Study	***Richardson_Breast_2***		**Negative (24) versus Positive (15)**						
P-value					4,00E-03	1,80E-05	5,00E-02		5,40E-04
T-test					-3,134	5,016	-2,074		-3,878
Study	***Ivshina_Breast***		**Negative (34) versus Positive (211)**						
P-value			***0,038***			3,70E-02	0,014	1,70E-04	
T-test			2,15			2,151	-2,56	4,12E+00	
Study	***vandeVijver_Breast***		**Negative (69) versus Positive (226)**						
P-value	4,10E-02			6,00E-03		4,20E-07	5,50E-06	6,40E-06	7,00E-03
T-test	-2,062			2,799		5,522	-4,707	4,712	-2,77

Table 8. contd…

Estrogen Receptor Status									
	ABCB1	**ABCG2**	**ABCC1**	**ABCC2**	**ABCC3**	**ABCC4**	**ABCC5**	**ABCC10**	**ABCC11**
Study	***Boersma_Breast***		**Negative (52) versus Positive(41)**						
P-value						1,50E-05		5,90E-04	
T-test						4,595		3,565	
Study	***Hess_Breast***		**Negative (51) versus Positive (82)**						
P-value						7,20E-04	1,50E-04	2,00E-03	
T-test						3,502	-3,914	3,235	
Study	***Bild_Breast***		**Negative (48) versus Positive (110)**						
P-value	4,50E-02		5,00E-02	5,00E-02			1,70E-04		
T-test	2,034		1,986	1,986			-3,882		
Study	***Zhao_Breast***		**Ductal breast carcinoma- Negative (11) versus Positive (24)**						
P-value	4,40E-02						1,60E-02	2,30E-02	
T-test	-2,611						-2,65	2,504	
Study	***Sotiriou_Breast_3***		**Negative (34) versus Positive (85)**						
P-value		1,60E-04		1,60E-04	6,90E-04			1,90E-04	
T-test		-3,997		4,075	-3,547			3,978	
Study	***Finak_Breast***		**Negative (10) versus Positive (43)**						
P-value				4,60E-02			2,10E-02		
T-test				-2,173			-2,546		
Study	***Sorlie_Breast***		**Negative (18) versus Positive (56)**						
P-value				2,80E-02			2,30E-02		
T-test				2,307			-2,367		
Study	***Perou_Breast***		**Ductal breast carcinoma – Negative (9) versus Positive (26)**						
P-value					3,10E-02				
T-test					2,477				

ABCB1 expression levels in breast tumours. These SNPs also correlated with ER status of patients [290]. Of the studied clinical and pathological characteristics, patients carrying variant alleles, which conferred lower ABCB1 expression had significantly more frequent ER-negative status in comparison with wild-type carriers [290].

b) Progesterone Receptor Expression

Recently, a retrospective analysis of early breast cancer treated with tamoxifen, found that hormonal therapy was more efficient on ER-positive/PR-positive tumours than on ER-positive/PR-negative tumours. Furthermore, in a multivariate analysis including lymph node involvement, tumour size, and age, PR status was shown as an independent predictive factor for benefit from adjuvant endocrine therapy [321, 322].

Nevertheless, we must bear in mind that there is two isoforms of PR: PRA and PRB. There is a single human PR gene encoding these two isoforms with two distinct promoter regions in exon 1. These two isoforms have different cellular regulatory effects [231]. PRs are ligand-activated transcription factors. They act in concert with intracellular signaling pathways as "sensors" of multiple growth factor inputs to hormonally regulated tissues, such as breast. Though PRA and PRB are similarly expressed in normal breast luminal epithelial cells, PRA/PRB expression is early disrupted in breast carcinogenesis, resulting in frequent predominance of one isoform [231]. Studies have shown that in poor prognostic tumours, the ratio between PRA and PRB is altered, with a predominance of PRA and loss of PRB [245, 323]. PRA and PRB regulate different subsets of genes involved in particular functional pathways [231]. Consequently, we focused our attention on ABC transporter expression levels and PR status. Though Leonessa's report found seven studies reporting no correlation between ABCB1 and ER or PR, we noticed using Oncomine data that ABCB1, ABCC1, ABCC2,

Table 9. Relationships between ABC expression levels and PR status of breast tumours. The study line indicates the study name, the compared classes and inside brackets the number of tumour samples. The list of reported studies is without being exhaustive and white cases indicated either no significant P-value or the P-value was not found. $P < 0.05$ was considered significant (T- test)

Progesterone Receptor Status									
	ABCB1	**ABCG2**	**ABCC1**	**ABCC2**	**ABCC3**	**ABCC4**	**ABCC5**	**ABCC10**	**ABCC11**
	↓↓↓	↔↔	↓↓↓	↓↓↓	↔↔	↓↓↓	↑↑↑	↓↓↓	↑↑↑
Study	***Chin_Breast***		**Negative (51) versus Positive (66)**						
P-value	1,20E-02					5,20E-02		8,40E-05	
T-test	2,55					1,972		4,086	
Study	***Bild_Breast***		**Negative (57) versus Positive (101)**						
P-value	4,60E-02			6,90E-02		1,30E-02	1,00E-03	5,70E-02	
T-test	2,034			1,837		2,535	-3,238	1,928	
Study	***Bittner_Breast***		**Negative (108) versus Positive (122)**						
P-value			1,50E-02	4,10E-02		1,00E-03	3,10E-02	7,30E-08	3,60E-02
T-test			2,448	2,057		3,334	-2,217	5,59	-2,115
Study	***Ginestier_Breast***		**Negative (34) versus Positive (21)**						
P-value			2,10E-02	2,30E-02		7,00E-05		9,00E-04	
T-test			2,386	2,35E+00		4,317		3,547	
Study	***Minn_Breast_2***		**Negative (55) versus Positive (43)**						
P-value						4,00E-03		3,00E-03	
T-test						2,941		3,00E+00	
Study	***Ma_Breast_2***		**Negative (6) versus Positive (34)**						
P-value									3,00E-03
T-test									3,395

ABCC4 and ABCC10 were down-expressed in PR positive tumours, while ABCC5 and ABCC11 levels were increased (Table **9**). Although we and others demonstrated that ABCG2 was regulated by progesterone, the physiological ligand for PR [243, 254], ABCG2 expression levels were not associated with PR status in breast cancers (Table **9**). In complete agreement with Oncomine findings, ABCC1 protein expression was positive in 80 % of breast carcinomas and more frequent in PR-negative carcinomas [300]. ABCC1 expression was not related to PR levels [294].

On one hand, though ER and PR are members of different steroid hormone receptor sub-families, there are considerable biological evidences for cross-talk between their signalling pathways. On the other hand, among all 1,836 cases reported in Yu's study, approximately 42.8 % of patients had ER-positive / PR-positive tumours, 20. 2% ER-positive / PR-negative, 25.9 % ER-negative /PR-negative, and 11.0 % ER-negative/ PR-positive tumours [3]. As attended, in most cases we observed similar associations between ABC transporter expression levels and ER or PR status. This might be likely related to the presence of 60-70 % ER positive tumours in patient cohorts and the cross-talk between signalling pathways of ER and PR. Nevertheless, for ABCB1 and ABCG2, contradictory effects were reported. No clear relationship was made between ABCB1 expression levels and ER status, while two independent studies indicated that ABCB1 expression levels were decreased in progesterone positive cohort. This discrepancy may be directly linked to the variability (tissue origin, histological grade…) of tumour cohorts.

5.4. ERBB2- Status

Despite the discrepancies observed between various studies, several associations between ERBB2-positive status and the classical clinicopathological parameters were noted. There are clear relationships between ERBB2 positivity and the lack of steroid receptors, the histological subtypes, histological grade... In univariate analyses, ERBB2 is strongly associated with poor prognosis. ERBB2 is a marker of aggressiveness of the tumour. However, ERBB2 does not retain a clinical prognostic significance in multivariate analyses, since it is associated with several strong prognostic parameters. When considering the prognostic value of ERBB2 in relation to treatment, a significantly worse survival of the

Table 10. Relationships between ABC expression levels and breast tumours disease free survival. The study line indicates the study name, the compared classes and in brackets the number of tumour samples. The list of reported studies is without being exhaustive and white cases indicated either no significant P-value or the P-value was not found. $P < 0.05$ was considered significant (T- test)

Disease Free Survival over 5 Years									
	ABCB1	**ABCG2**	**ABCC1**	**ABCC2**	**ABCC3**	**ABCC4**	**ABCC5**	**ABCC10**	**ABCC11**
	↓↓↓	↓↓↓	↑↑↑		↑↑↑		↑↑↑	↑↑↑	↑↑↑
Study	***VandeVijver_Breast***		**No Recurrence (196) versus Recurrence (79)**						
P-value	1,00E-03						9,00E-03	6,60E-04	
T-test	3,289						-2,636	-3,476	
Study	***Huang_Breast***		**No Recurrence (18) versus Recurrence (34)**						
P-value		1,20E-02			4,00E-03				
T-test		2,635			-3,126				
Study	***Wang_Breast***		**No Recurrence (180) versus Recurrence (93)**						
P-value			5,00E-03				1,00E-03	6,40E-04	
T-test			-2,857				-3,235	-3,474	
Study	***Sotiriou_Breast_3***		**No Recurrence (85) versus Recurrence (28)**						
P-value	1,90E-02		5,00E-03						
T-test	2,412		-2,914						
Study	***Ma_Breast_3***		**No Recurrence (42) versus Recurrence (18)**						
P-value									1,00E-02
T-test									-2,704
Study	***Sorlie_Breast_2***		**No Recurrence (10) versus Recurrence (34)**						
P-value					2,20E-02				
T-test					-2,476				
Study	***Ma_Breast_2***		**No Recurrence (26) versus Recurrence (14)**						
P-value									2,60E-02
T-test									-2,319

treated patients is noted in ERBB2-positive patients. This suggested that ERBB2 could be a marker of reduced response to anticancer chemotherapies.

We only observed a positive association between ERBB2 and respectively ABCC3 (Bittner_Breast study - negative (N=152) versus positive (N=60); Hess_Breast study - negative (N=51) versus positive (N=82); Boersma_Breast study - negative (N=75) versus positive (N=10); Saal_Breast study - negative (N=78) versus positive (N=24)), ABCC4 (Bittner_Breast study), ABCC10 (Bittner_Breast study; Hess_Breast study; Saal_Breast study) and ABCC11 (Richardson_Breast_2 study - negative (N=29) versus positive (N=8)). In most cases, we noticed a positive association except for ABCG2 (Bittner_Breast's study). This data may suggest that ABCC3, ABCC10 and ABCC11 expression levels are associated with a significantly worse outcome. Although, inverse association for ABCC10 was reported in Boersma_Breast study, this result might be directly linked to the low number of ERBB2-positive tumours (N=10) included in this study compared to the number of ERBB2-negative tumours (N=75). We did not found any association for ABCB1, ABCC1, ABCC2, ABCC5 transporters. Recently, we observed similar findings about ABCC11 expression levels and ERBB2 status [241]. In agreement with Oncomine data, the amplification of ABCC3 is present in primary breast tumours and occurs predominantly in ERBB2-amplified and luminal tumours [37]. This ABCC3 drug transporter overexpression is responsible for conferring *in vitro* resistance to paclitaxel and monomethyl-auristatin-E [37]. Charpin *et al.* observed that the ABCB1 expression was independent to ERBB2 expression [318].

5.5. Breast Carcinoma – Survival

a) Recurrence

The disease free survival is defined as the time length after treatment during which no disease is found. Since ABC transporters, especially ABCB1 and ABCG2, are wildly involved in MDR phenotype, we summarized in the following Table **10**, findings from Oncomine reports, about the expression levels of ABC transporters and disease free survival with the presence or absence of recurrences. Though only

trends could be made, in various studies, we observed that ABCB1 and ABCG2 could be linked to a decrease of expression levels in positive recurrences, while an increase of ABCC1, ABCC3, ABCC5, ABCC10 and ABCC11 expression levels was clearly associated to positive recurrences (Table **10**).

VandeVijver_Breast and Wang_Breast carried out two complementary analyses. They differentiated positive- and negative-ER cohorts. We clearly observed that the ER status is a critical element in the analysis of ABC expression levels and recurrences. Evidently, ABCC4 expression levels were respectively decreased and increased in ER-positive (VandeVijver_Breast study - no recurrence (N=164) versus recurrence (N=51)) and ER-negative (vandeVijver_Breast study - no recurrence (N=32) versus recurrence (N=28)) recurrent breast tumour cohorts, while no association was detected in total cohort (ER-positive and negative tumours; VandeVijver_Breast study - no recurrence (N=196) versus recurrence (N=79)). In contrast, no association was reported in the similar approach of Wang_Breast. Furthermore, in agreement with VandeVijver_Breast studies, ABCC5 and ABCC10 levels were increased in the same way in global cohort (Wang_Breast study - no recurrence (N=180) versus recurrence (N=93)) and in the ER-positive cohort (Wang_Breast study - no recurrence (N=135) versus recurrence (N=66)) while no modification of ABCC5 and ABCC10 expression levels was reported in the ER-negative cohort (Wang_Breast study - no recurrence (N=47) versus recurrence (N=27). This may be directly linked to the fact that 60-70 % of tumours are in fact ER positive tumours. In addition, although no difference was found in VandeVijver_Breast study, Wang_Breast report showed that ABCC2 expression levels were increased in recurrent ER-negative breast carcinoma (Wang_Breast study - no recurrence (N=45) versus relapse (N=27)) while no difference was noticed in ER-positive breast carcinoma (Wang_Breast study - no recurrence (N=135) versus recurrence (N=66)) and in global cohort (Wang_Breast study - no recurrence (N=180) versus recurrence (N=93)).

b) Survival and Death

We reported the relationships between ABC transporter expression level and patient survival. Though discrepancies appeared, we observed that ABCB1 and ABCG2 were down-expressed in worse outcome while ABCC3, ABCC4, ABCC5 and ABCC10 appeared increased with mortality. No association was made with ABCC1, ABCC2 and ABCC11 (Table **11**), while numerous studies reported a decrease of ABCG2 expression levels in "dead" group and no correlation was reported in Kanzaki's study [289]. Furthermore in Burger's study, high expression of ABCB1 was found to be significantly associated with a poor progression-free survival while expression levels of ABCG2, ABCC1, or ABCC2 were not related with the length of progression-free survival [324]. Patients with ABCC1-negative carcinomas had longer overall and disease-free survival as compared to those with ABCC1-positive carcinomas [300]. Frequently, the evolution of cancerous disease is by the outcome of recurrences; we tried to evaluate the possible association of free survival (with or without recurrences) and global survival (alive/dead). As attended, we observed a trend association between these two criteria. Nevertheless, additional clinical and meta-analysis studies must be conducted.

Breast Carcinoma – Therapy Response

Resistance to chemotherapy is a significant obstacle to appropriate cancer treatment. Since resistance mechanism involved multiple actors including ABC transporters, we reported the possible relationships between expression levels of ABC transporters and various therapy responses. Extensive studies have demonstrated that ABCB1, ABCC1, and ABCG2 are particularly well known as mediators leading to resistance to various anticancer drugs including anthracyclines. We have already fully described the anti-cancer drugs used in breast cancer therapies in the introduction section.

a) Therapies Including Substrates of ABC Transporters

Leonessa *et al.* fully described the expression of ABCB1 following either recent or remote anticancer treatment [287]. An adequate evaluation of chemotherapy efficiency may be obtained in studies where these cancers are evaluated for ABC protein expression before and after chemotherapy. Leonessa *et al.* compiled findings from independent studies and concluded that ABCB1 was detected in 43 % before and in 64 % after systemic treatment [291, 317, 325-327]. Consequently 37 % of negative tumours before treatment were positive following chemotherapy [287]. Comparing pooled data, the presence of ABCB1 before chemotherapy appeared to correlate with complete remission rate, while no association was detected for the overall remission [287]. In agreement with previous findings, sequential tumour samples from patients receiving primary chemotherapy were analysed for ABCB1 expression before and after treatment in advanced breast cancer. After treatment, ABCB1 expression levels were significantly enhanced in tumour samples ($p = 0.0033$) [328]. In agreement, at mRNA level, ABCB1 expression was found to be significantly induced by chemotherapy (n=40) [329].

More precisely, Tolcher *et al.* observed that 18 % of paclitaxel treated metastatic disease were ABCB1 positive before paclitaxel therapy while 76 % were positive after therapy [330]. This strongly suggested that 58 % of tumours became ABCB1 positive after paclitaxel exposition. More recently, Park *et al.* studied the relationship between ABC transporter gene expression and chemotherapy responsiveness in early breast cancer patients who underwent sequential weekly paclitaxel/FEC (5-FU, epirubicin and CPM) neoadjuvant therapy [331]. Several ABC transporters including ABCC5 and ABCC11 showed significant increased expression in the residual disease. To complete Park's study, Hess_Breast report (Residual disease (N= 99) versus Complete chemotherapy response (N= 34)) showed that chemotherapy response is related to ABC transporter expression levels. In this study, a partial response to paclitaxel and 5-FU, DXR, CPM (T/FAC) chemotherapy was associated to a low expression levels of ABCC4 and ABCC10 and to a high expression level of ABCC2 and ABCC5. In Burger's study, they studied ABC transporter expression in the subgroup of patients treated with anthracycline-based chemotherapy (5-FU, ADR/epirubicin and CPM). They found a correlation between response and expression of ABCG2 and ABCC1, whereas such an association was not present in the CPM,

Table 11. Relationships between ABC expression levels and survival (alive/dead) of breast tumours. The study line indicates the study name, the compared classes and inside brackets the number of tumours samples. The list of reported studies is without being exhaustive and white cases indicated either no significant P-value or the P-value was not found. $P < 0.05$ was considered significant (T- test)

Survival over 5 years									
	ABCB1	**ABCG2**	**ABCC1**	**ABCC2**	**ABCC3**	**ABCC4**	**ABCC5**	**ABCC10**	**ABCC11**
	↓↓↓	↓↓↓			↑↑↑			↑↑↑	
Study	***VandeVijver_Breast***		**Alive (232) versus Dead (48)**						
P-value	1,00E-03					1,50E-02		3,00E-03	
T-test	3,395					-2,501		-3,03	
Study	***Ivshina_Breast***		**Alive (158) versus Dead (69)**						
P-value	5,00E-03	4,00E-03			1,40E-02				
T-test	2,878	2,913			-2,482				
Study	***Pawitan_Breast***		**Alive (121) versus Dead (38)**						
P-value	2,00E-02	6,00E-04			2,50E-02			2,10E-04	
T-test	2,402	3,65			-2,308			-3,873	
Study	***Boersma_Breast***		**Inflammatory breast carcinoma - Alive (6) versus Dead (18)**						
P-value		1,10E-02							
T-test		3,469							
Study	***Bild_Breast***		**Alive (60) versus Dead (42)**						
P-value		1,60E-02			1,50E-02				
T-test		2,478			-2,483				
Study	***Boersma_Breast***		**Non-inflammatory breast carcinoma - Alive (31) versus Dead (38)**						
P-value					3,00E-03				
T-test					-3,098				
Study	***Desmedt_Breast***		**Alive (135) versus Dead (56)**						
P-value							1,50E-02		
T-test							-2,484		

MTX, and 5-FU-treated group of patients. ABCB1 expression levels might have some predictive value for clinical outcome [324]. ABCC1 expression independently predicted shorter relapse-free survival (RFS) and overall survival (OS) in patients treated with CPM, MTX, and 5-FU [332].

Furthermore, Chang_breast study (docetaxel resistant (14) versus docetaxel sensitive (10)) found significant higher levels of ABCG2 and ABCC3 for docetaxel resistant tumours compared to sensitive tumours while lower levels of ABCC5 were found in docetaxel resistant tumours.

Recently few studies reported the effect of SNPs on ABC transporter expression and possible association with prognosis and response to chemotherapies. Obata *et al.* observed no association between several SNPs within *abcb1* gene [promoter 1T/C, promoter 2(-41)A>G, exon 12 1236C>T, exon 26 3435C>T and exon 28 4036A>G] and chemotherapy response or prognosis in advanced ovarian cancer. In contrast, they observed, a significant relevance (p=0.01) between chemotherapy response and ABCC1 exon-17 SNP (G2168A) involving amino acid substitution. But no significant relationship was observed between protein expression and chemotherapy response or disease-free survival time. In Asian breast cancer patients receiving adjuvant chemotherapy, the influence on doxorubicin disposition of three high frequency ABCB1 polymorphisms (1236C>T, 2677G>A/T, and 3435C>T) and the ABCG2 421C>A polymorphism was also investigated. The allelic frequency of the ABCB1 1236T, 2677T, 2677A, and 3435T variants were respectively 60 %, 38 %, 7 %, and 22 %, and the frequency of the ABCG2 421A allele was 23 %. No significant influence on doxorubicin pharmacokinetic parameters was observed in relation to the ABCG2 421C>A polymorphism [333]. The linked ABCB1 1236-2677-3435 genotypes were found to signifi-

cantly influence the disposition of doxorubicin, in Asian breast cancer patients. Patients who were homozygous for the variant allele at the three loci showed significantly increased exposure levels, peak plasma concentrations and reduced clearance [333].

b) Therapy Response According to Steroid Status

It is well known that ER presence is correlated with a better prognosis both in terms of increased disease-free survival and overall survival. TAM as an adjuvant therapy is effective in both pre- and postmenopausal patients with ER positive tumours. However, 25–35 % of all ER positive tumours do not respond to TAM (*de novo* resistance), and even those that did initially respond ultimately develop resistance (acquired resistance) [334]. Approximatly 30 % of the initially TAM-responsive metastatic tumours that subsequently developped resistance to TAM have lost ER expression. Low steroid receptor levels are often associated with metastasis. Furthermore, we observed that ABC transporter expression levels were strongly dependent on ER status (cf table **8**). Though cohort was limited (N=7), ABCC2 expression was lower in T/FAC complete response group compared to residual disease group (Hess_Breast study - ER positive breast carcinomas - residual disease (N=75) versus complete chemotherapy response (N=7)). Similar approach was performed on ER-negative cohort (Hess_Breast study ER negative breast carcinomas - residual disease (N=24) versus complete chemotherapy response (N=27)). Interestingly, ABCC2 and ABCC1 expression levels were higher in resistant group while ABCB1 and ABCC10 expression levels were decreased in resistant cohort. These proteins transport various anticancer drugs that may be the link with a modification of the classical chemotherapy.

c) Endocrine Therapy

Keen *et al.* evaluated the correlation between ABCB1 protein levels, before and after a 3-month treatment with TAM, and observed the response rates in 43 patients. The response rates to TAM were 85 % in ABCB1 negative versus 35 % in ABCB1 positive cases [335]. Nevertheless this correlation was not confirmed in the following reported Ma's study [336]. Indeed, to better characterize actors involved in TAM resistance, Ma *et al.* [336] identified gene expression patterns in hormone receptor-positive, early-stage invasive breast cancers. They performed a microarray gene expression analysis of tumours from women uniformly treated with adjuvant TAM alone. Within this cohort, 46 % of women developed distant metastasis with a median time to recurrence of 4 years and 54 % of women remained disease-free with median follow-up of 10 years. Very interestingly, among the identification of differentially expressed genes, an approximately 3-fold increase of ABCC11 expression was found in non responding patients [336]. This data strongly suggested that ABCC11 might be highly expressed in TAM resistance cells. This was supported by our *in vitro* data: we found an ABCC11 expression increase in TAM-resistant cell lines [241]. More recently, Miller_Breast_2 study (status pre-letrozole treatment (N=58) versus post-letrozole treatment (N=58)) found a positive effect of letrozole (nonsteroidal aromatase inhibitor; inhibitor of estrogen synthesis) on ABCG2 and ABCC4 expression levels in 58 patients.

6. OVERALL CONCLUSION

Heterogeneity of findings is a common feature of studies evaluating the expression and prognostic role of ABC proteins, due to both methodological and biological factors. Since in most cases, reproducibility has not been assessed in other populations or inconsistent results have also sometimes emerged, more clinical studies are needed to be conducted to clarify the relationship between the ABC transporter expression levels and tumour recurrence, patient free survival and therapy efficiency. Therefore, multicenter large-scale clinical studies or statistical meta-analyses that integrate all the published results should be required. Some different reasons of the low expression level associated with ABC transporter could have been proposed. One of the rational explanations is that transcript expression levels of ABC transporter are not always proportional to protein expression levels, which directly cause the decreased function. The linkage analysis revealed that ER status and PR status are often tightly linked to gene regulation mechanisms. This report suggested that the expression levels of ABC transporters in human breast cancer cells may be affected by the presence of female reproductive steroids and likely have an impact on the clinical response to neoadjuvant chemotherapy and outcome of patients. Consequently, transcriptional profiling of these genes may be useful to help the therapy choice by clinician and predict the pathologic response to chemotherapy in breast cancer patients.

ACKNOWLEDGEMENTS

This work was supported by grants from the Association de Recherche contre le Cancer (ARC 4007), with funds from INSERM and the Ligue Contre le Cancer fellowship (to M. Honorat).

ABBREVIATIONS

5-FU	=	5-FluoroUracil
AAS	=	atomic absorption spectroscopy
ABC	=	ATP binding cassette
ADME	=	absorption, distribution, metabolism and excretion
APCI	=	atmospheric pressure chemical ionization
API	=	atmospheric pressure ionization
ARE	=	antioxidant response element
BCRP	=	breast cancer resistance protein
CAR	=	constitutive androstane receptor
CE	=	capillary electrophoresis
CisPt	=	Cisplatin
CNS	=	central nervous system
CPM	=	cyclophosphamide
CREB	=	cAMP-responsive element binding protein
DDC	=	diethyldithiocarbamate
DXR	=	doxorubicine
ECD	=	nitrogen-phosphorus detector

EPI	=	epirubicin
ER	=	estrogen receptors
ERAP	=	estrogen receptor associated protein
ERBB2	=	human epidermal growth factor receptor 2
ERE	=	estrogen response element
ESI	=	electrospray ionization
GC	=	gas-chromatography
GR	=	glucocorticoid receptor
HNF	=	hepatic nuclear factor
HPLC phy	=	high-performance liquid chromatogra-
HRE	=	hormone response element
IAA	=	isoamylalcohol
ICP-MS	=	inductively coupled plasma-mass spectrometry
LC	=	liquid chromatography
LOQ	=	limit of quantification
LLE	=	liquid/liquid extraction
LRP	=	lung resistant protein
MRM	=	multiple reaction monitoring
MS	=	mass spectrometry
MSD	=	membrane spanning domain
NBD	=	nucleotide binding domain
NMR	=	nuclear magnetic resonance
OS	=	overall survival
P-gp	=	P-glycoprotein
PPAR	=	peroxisome proliferator-activated receptor
PR	=	progesterone receptor
PRE	=	progesterone response element
Pt	=	platin
PXR	=	pregnane X receptor
RFS	=	relapse-free survival
SIM	=	selected ion monitoring
SPE	=	solid phase extraction
SRE	=	steroid regulatory element
SRM	=	selected reaction monitoring
TAM	=	tamoxifen
T/FAC	=	paclitaxel and 5-FU, doxorubicin, cyclophosphamide
VNB	=	vinorelbine

REFERENCES

[1] Korsching E, Jeffrey SS, Meinerz W, *et al.* Basal carcinoma of the breast revisited: an old entity with new interpretations. J Clin Pathol 2008; 61: 553-60.

[2] Weigelt B, Peterse JL, van 't Veer LJ. Breast cancer metastasis: markers and models. Nat Rev Cancer 2005; 5: 591-602.

[3] Yu KD, Di GH, Wu J, *et al.* Breast cancer patients with estrogen receptor-negative/progesterone receptor-positive tumors: being younger and getting less benefit from adjuvant tamoxifen treatment. J Cancer Res Clin Oncol 2008; 134: 1347-54.

[4] Irvin WJ, Jr.Carey LA. What is triple-negative breast cancer? Eur J Cancer 2008; 44: 2799-805.

[5] Carey LA, Dees EC, Sawyer L, *et al.* The triple negative paradox: primary tumor chemosensitivity of breast cancer subtypes. Clin Cancer Res 2007; 13:2329-34.

[6] Bakos E, Hegedus T, Hollo Z, *et al.* Membrane topology and glycosylation of the human multidrug resistance-associated protein. J Biol Chem 1996; 271:12322-326.

[7] Kast CGros P. Topology mapping of the amino-terminal half of multidrug resistance-associated protein by epitope insertion and immunofluorescence. J Biol Chem 1997; 272: 26479-87.

[8] Kast C,Gros P. Epitope insertion favors a six transmembrane domain model for the carboxy-terminal portion of the multidrug resistance-associated protein. Biochemistry 1998; 37:2305-13.

[9] Hipfner DR, Almquist KC, Leslie EM, *et al.* Membrane topology of the multidrug resistance protein (MRP). A study of glycosylation-site mutants reveals an extracytosolic NH2 terminus. J Biol Chem 1997; 272:23623-30.

[10] Bakos E, Evers R, Szakacs G, *et al.* Functional multidrug resistance protein (MRP1) lacking the N-terminal transmembrane domain. J Biol Chem 1998; 273:32167-75.

[11] Westlake CJ, Cole SPDeeley RG. Role of the NH2-terminal membrane spanning domain of multidrug resistance protein 1/ABCC1 in protein processing and trafficking. Mol Biol Cell 2005; 16: 2483-92.

[12] Yang Y, Liu Y, Dong Z, *et al.* Regulation of function by dimerization through the amino-terminal membrane-spanning domain of human ABCC1/MRP1. J Biol Chem 2007; 282: 8821-30.

[13] Robey RW, To KK, Polgar O, *et al.* ABCG2: A perspective. Adv Drug Deliv Rev 2008.

[14] Krishnamurthy PS, Chuetz JD. The ABC transporter Abcg2/Bcrp: role in hypoxia mediated survival. Biometals 2005; 18:349-58.

[15] Krishnamurthy P, Schuetz JD. Role of ABCG2/BCRP in biology and medicine. Annu Rev Pharmacol Toxicol 2006; 46: 381-410.

[16] Ueda K, Cardarelli C, Gottesman MMPastan I. Expression of a full-length cDNA for the human "MDR1" gene confers resistance to colchicine, doxorubicin, and vinblastine. Proc Natl Acad Sci U S A 1987; 84: 3004-8.

[17] Clarke R, Currier S, Kaplan O, *et al.* Effect of P-glycoprotein expression on sensitivity to hormones in MCF-7 human breast cancer cells. J Natl Cancer Inst 1992; 84: 1506-12.

[18] Adams DJ, Knick VC. P-glycoprotein mediated resistance to 5'-nor-anhydro-vinblastine (Navelbine). Invest New Drugs 1995; 13; 13-21.

[19] Callaghan R, Higgins CF. Interaction of tamoxifen with the multidrug resistance P-glycoprotein. Br J Cancer 1995; 71: 294-299.

[20] de Graaf D, Sharma RC, Mechetner EB, Schimke RT, Roninson IB. P-glycoprotein confers methotrexate resistance in 3T6 cells with deficient carrier-mediated methotrexate uptake. Proc Natl Acad Sci U S A 1996; 93: 1238-142.

[21] Sparreboom A, van Asperen J, Mayer U, *et al.* Limited oral bioavailability and active epithelial excretion of paclitaxel (Taxol) caused by P-glycoprotein in the intestine. Proc Natl Acad Sci USA 1997; 94: 2031-5.

[22] Shirakawa K, Takara K, Tanigawara Y, *et al.* Interaction of docetaxel ("Taxotere") with human P-glycoprotein. Jpn J Cancer Res 1999; 90; 1380-6.

[23] Jang SH, Wientjes MG, Au JL. Kinetics of P-glycoprotein-mediated efflux of paclitaxel. J Pharmacol Exp Ther 2001; 298: 1236-42.

[24] Riganti C, Miraglia E, Viarisio D, *et al.* Nitric oxide reverts the resistance to doxorubicin in human colon cancer cells by inhibiting the drug efflux. Cancer Res 2005; 65: 516-525.

[25] Choi CH. ABC transporters as multidrug resistance mechanisms and the development of chemosensitizers for their reversal. Cancer Cell Int 2005; 5:30.

[26] Doyle LA, Yang W, Abruzzo LV, *et al.* A multidrug resistance transporter from human MCF-7 breast cancer cells. Proc Natl Acad Sci USA 1998; 95: 15665-70.

[27] Han B, Zhang JT. Multidrug resistance in cancer chemotherapy and xenobiotic protection mediated by the half ATP-binding cassette

transporter ABCG2. Curr Med Chem Anticancer Agents 2004; 4: 31-42.

[28] Kamiyama N, Takagi S, Yamamoto C, *et al*. Expression of ABC transporters in human hepatocyte carcinoma cells with cross-resistance to epirubicin and mitoxantrone. Anticancer Res 2006; 26:885-888.

[29] Yuan J, Lv H, Peng B, *et al*. Role of BCRP as a biomarker for predicting resistance to 5-fluorouracil in breast cancer. Cancer Chemother Pharmacol 2008;

[30] Cole SP, Sparks KE, Fraser K, *et al*. Pharmacological characterization of multidrug resistant MRP-transfected human tumor cells. Cancer Res 1994; 54: 5902-10.

[31] Hooijberg JH, Broxterman HJ, Kool M, *et al*. Antifolate resistance mediated by the multidrug resistance proteins MRP1 and MRP2. Cancer Res 1999; 59: 2532-5.

[32] Deeley RG, Cole SP. Substrate recognition and transport by multidrug resistance protein 1 (ABCC1). FEBS Lett 2006; 580: 1103-11.

[33] Cui Y, Konig J, Buchholz JK, *et al*. Drug resistance and ATP-dependent conjugate transport mediated by the apical multidrug resistance protein, MRP2, permanently expressed in human and canine cells. Mol Pharmacol 1999; 55: 929-37.

[34] Qiu R, Kalhorn TF, Slattery JT. ABCC2-mediated biliary transport of 4-glutathionylcyclophosphamide and its contribution to elimination of 4-hydroxycyclophosphamide in rat. J Pharmacol Exp Ther 2004; 308:1204-12.

[35] Huisman MT, Chhatta AA, van Tellingen O, Beijnen JHSchinkel AH. MRP2 (ABCC2) transports taxanes and confers paclitaxel resistance and both processes are stimulated by probenecid. Int J Cancer 2005;116: 824-9.

[36] Hirohashi T, Suzuki HSugiyama Y. Characterization of the transport properties of cloned rat multidrug resistance-associated protein 3 (MRP3). J Biol Chem 1999; 274:15181-5.

[37] O'Brien C, Cavet G, Pandita A, *et al*. Functional genomics identifies ABCC3 as a mediator of taxane resistance in HER2-amplified breast cancer. Cancer Res 2008; 68: 5380-9.

[38] Chen ZS, Lee K, Walther S, *et al*. Analysis of methotrexate and folate transport by multidrug resistance protein 4 (ABCC4): MRP4 is a component of the methotrexate efflux system. Cancer Res 2002; 62: 3144-50.

[39] Tian Q, Zhang J, Tan TM, *et al*. Human multidrug resistance associated protein 4 confers resistance to camptothecins. Pharm Res 2005; 22:1837-53.

[40] Pratt S, Shepard RL, Kandasamy RA, *et al*. The multidrug resistance protein 5 (ABCC5) confers resistance to 5-fluorouracil and transports its monophosphorylated metabolites. Mol Cancer Ther 2005; 4: 855-63.

[41] Wielinga P, Hooijberg JH, Gunnarsdottir S, *et al*. The human multidrug resistance protein MRP5 transports folates and can mediate cellular resistance against antifolates. Cancer Res 2005; 65: 4425-30.

[42] Oguri T, Achiwa H, Sato S, *et al*. The determinants of sensitivity and acquired resistance to gemcitabine differ in non-small cell lung cancer: a role of ABCC5 in gemcitabine sensitivity. Mol Cancer Ther 2006; 5: 1800-6.

[43] Hopper-Borge E, Chen ZS, Shchaveleva I, Belinsky MG, Kruh GD. Analysis of the drug resistance profile of multidrug resistance protein 7 (ABCC10): resistance to docetaxel. Cancer Res 2004; 64: 4927-30.

[44] Hopper-Borge E, Xu X, Shen T, *et al*. Human multidrug resistance protein 7 (ABCC10) is a resistance factor for nucleoside analogues and epothilone B. Cancer Res 2009; 69: 178-84.

[45] Guo Y, Kotova E, Chen ZS, *et al*. MRP8, ATP-binding cassette C11 (ABCC11), is a cyclic nucleotide efflux pump and a resistance factor for fluoropyrimidines 2',3'-dideoxycytidine and 9'-(2'-phosphonylmethoxyethyl)adenine. J Biol Chem 2003; 278: 29509-14.

[46] Chen ZS, Guo Y, Belinsky MG, Kotova E, Kruh GD. Transport of bile acids, sulfated steroids, estradiol 17-beta-D-glucuronide, and leukotriene C4 by human multidrug resistance protein 8 (ABCC11). Mol Pharmacol 2005; 67: 545-57.

[47] Sarkadi B, Price EM, Boucher RC, Germann UA, Scarborough GA. Expression of the human multidrug resistance cDNA in insect cells generates a high activity drug-stimulated membrane ATPase. J Biol Chem 1992; 267: 4854-8.

[48] Urbatsch IL, al-Shawi MK, Senior AE. Characterization of the ATPase activity of purified Chinese hamster P-glycoprotein. Biochemistry 1994; 33: 7069-76.

[49] Evers R, Zaman GJ, van Deemter L, *et al*. Basolateral localization and export activity of the human multidrug resistance-associated protein in polarized pig kidney cells. J Clin Invest 1996; 97; 1211-8.

[50] Yamazaki M, Neway WE, Ohe T, *et al*. In vitro substrate identification studies for p-glycoprotein-mediated transport: species difference and predictability of *in vivo* results. J Pharmacol Exp Ther 2001; 296: 723-35.

[51] Sugiyama Y, Kusuhara H, Suzuki H. Kinetic and biochemical analysis of carrier-mediated efflux of drugs through the blood-brain and blood-cerebrospinal fluid barriers: importance in the drug delivery to the brain. J Control Release 1999; 62; 179-86.

[52] Alvarez M, Robey R, Sandor V, *et al*. Using the national cancer institute anticancer drug screen to assess the effect of MRP expression on drug sensitivity profiles. Mol Pharmacol 1998; 54; 802-14.

[53] Schwab D, Fischer H, Tabatabaei A, Poli S, Huwyler J. Comparison of *in vitro* P-glycoprotein screening assays: recommendations for their use in drug discovery. J Med Chem 2003; 46: 1716-25.

[54] Aller SG, Yu J, Ward A, *et al*. Structure of P-glycoprotein reveals a molecular basis for poly-specific drug binding. Science 2009; 323: 1718-22.

[55] Rothnie A, Conseil G, Lau AY, Deeley RG, Cole SP. Mechanistic differences between GSH transport by multidrug resistance protein 1 (MRP1/ABCC1) and GSH modulation of MRP1-mediated transport. Mol Pharmacol 2008; 74: 1630-40.

[56] Zelcer N, Huisman MT, Reid G, *et al*. Evidence for two interacting ligand binding sites in human multidrug resistance protein 2 (ATP binding cassette C2). J Biol Chem 2003; 278: 23538-44.

[57] Karwatsky JMGeorges E. Drug binding domains of MRP1 (ABCC1) as revealed by photoaffinity labeling. Curr Med Chem Anticancer Agents 2004; 4:19-30

[58] Nicolle E, Boumendjel A, Macalou S, *et al*. QSAR analysis and molecular modeling of ABCG2-specific inhibitors. Adv Drug Deliv Rev 2008.

[59] Janiszewski JS, Rogers KJ, Whalen KM, *et al*. A high-capacity LC/MS system for the bioanalysis of samples generated from plate-based metabolic screening. Anal Chem 2001; 73:1495-501

[60] Oliveira EJWatson DG. Liquid chromatography-mass spectrometry in the study of the metabolism of drugs and other xenobiotics. Biomed Chromatogr 2000;14: 351-72.

[61] Clarke NJ, Rindgen D, Korfmacher WA, Cox KA. Systematic LC/MS metabolite identification in drug discovery. Anal Chem 2001; 73: 430A-9A.

[62] Niessen WM. Progress in liquid chromatography-mass spectrometry instrumentation and its impact on high-throughput screening. J Chromatogr A 2003; 1000: 413-36.

[63] Rosenberg E. The potential of organic (electrospray- and atmospheric pressure chemical ionisation) mass spectrometric techniques coupled to liquid-phase separation for speciation analysis. J Chromatogr A 2003; 1000: 841-89.

[64] Bruins AP. Liquid chromatography-mass spectrometry with ion-spray and electrospray interfaces in pharmaceutical and biomedical research. J Chromatogr 1991; 554: 39-46.

[65] Fenn JB, Mann M, Meng CK, Wong SF, Whitehouse CM. Electrospray ionization for mass spectrometry of large biomolecules. Science 1989; 246: 64-71.

[66] Taylor PJ. High-performance liquid chromatography-mass spectrometry in the clinical laboratory. Ther Drug Monit 2005; 27: 689-93.

[67] Little JL, Wempe MF, Buchanan CM. Liquid chromatography-mass spectrometry/mass spectrometry method development for drug metabolism studies: Examining lipid matrix ionization effects in plasma. J Chromatogr B Analyt Technol Biomed Life Sci 2006; 833: 219-230.

[68] King R, Bonfiglio R, Fernandez-Metzler C, Miller-Stein C, Olah T. Mechanistic investigation of ionization suppression in electrospray ionization. J Am Soc Mass Spectrom 2000; 11: 942-50.

[69] Bonfiglio R, King RC, Olah TV, Merkle K. The effects of sample preparation methods on the variability of the electrospray ionization response for model drug compounds. Rapid Commun Mass Spectrom 1999; 13: 1175-85.

[70] Dams R, Huestis MA, Lambert WE, Murphy CM. Matrix effect in bio-analysis of illicit drugs with LC-MS/MS: influence of ioniza-

tion type, sample preparation, and biofluid. J Am Soc Mass Spectrom 2003; 14: 1290-4.
[71] Howe MM. Atomic absorption spectrometry theory, instrumentation and application. Am J Med Technol 1967; 33; 105-19.
[72] Ray SJ, Andrade F, Gamez G, *et al*. Plasma-source mass spectrometry for speciation analysis: state-of-the-art. J Chromatogr A 2004; 1050: 3-34.
[73] Beauchemin D. Inductively coupled plasma mass spectrometry. Anal Chem 2006; 78: 4111-36
[74] Ammann AA. Inductively coupled plasma mass spectrometry (ICP MS): a versatile tool. J Mass Spectrom 2007; 42: 419-27.
[75] Oguri T, Ozasa H, Uemura T, *et al*. MRP7/ABCC10 expression is a predictive biomarker for the resistance to paclitaxel in non-small cell lung cancer. Mol Cancer Ther 2008; 7; 1150-5.
[76] Strobel T, Kraeft SK, Chen LB, Cannistra SA. BAX expression is associated with enhanced intracellular accumulation of paclitaxel: a novel role for BAX during chemotherapy-induced cell death. Cancer Res 1998; 58: 4776-81.
[77] Bleicher RJ, Xia H, Zaren HA, Singh SV. Biochemical mechanism of cross-resistance to paclitaxel in a mitomycin c-resistant human bladder cancer cell line. Cancer Lett 2000; 150: 129-35.
[78] Crowe A. The influence of P-glycoprotein on morphine transport in Caco-2 cells. Comparison with paclitaxel. Eur J Pharmacol 2002; 440: 7-16.
[79] Gaspar JR, Qu J, Straubinger NL, Straubinger RM. Highly selective and sensitive assay for paclitaxel accumulation by tumor cells based on selective solid phase extraction and micro-flow liquid chromatography coupled to mass spectrometry. Analyst 2008; 133: 1742-8.
[80] Basileo G, Breda M, Fonte G, Pisano R, James CA. Quantitative determination of paclitaxel in human plasma using semi-automated liquid-liquid extraction in conjunction with liquid chromatography/tandem mass spectrometry. J Pharm Biomed Anal 2003; 32: 591-600.
[81] Mortier KA, Renard V, Verstraete AG, *et al*. Development and validation of a liquid chromatography-tandem mass spectrometry assay for the quantification of docetaxel and paclitaxel in human plasma and oral fluid. Anal Chem 2005; 77: 4677-83.
[82] Vainchtein LD, Thijssen B, Stokvis E, *et al*. A simple and sensitive assay for the quantitative analysis of paclitaxel and metabolites in human plasma using liquid chromatography/tandem mass spectrometry. Biomed Chromatogr 2006; 20: 139-48.
[83] Iyer SS, Gao S, Zhang ZP, Kellogg GE, Karnes HT. A molecular model to explain paclitaxel and docetaxel sensitivity changes through adduct formation with primary amines in electrospray ionization mass spectrometry. Rapid Commun Mass Spectrom 2005; 19: 1221-6.
[84] Mortier KA, Zhang GF, van Peteghem CH, Lambert WE. Adduct formation in quantitative bioanalysis: effect of ionization conditions on paclitaxel. J Am Soc Mass Spectrom 2004; 15: 585-92.
[85] Jemal M, Almond RB, Teitz DS. Quantitative bioanalysis utilizing high-performance liquid chromatography/electrospray mass spectrometry via selected-ion monitoring of the sodium ion adduct [M+Na]+. Rapid Commun Mass Spectrom 1997; 11:1083-8.
[86] Guitton J, Cohen S, Tranchand B, *et al*. Quantification of docetaxel and its main metabolites in human plasma by liquid chromatography/tandem mass spectrometry. Rapid Commun Mass Spectrom 2005; 19: 2419-26.
[87] Huang Q, Wang GJ, Sun JG, *et al*. Simultaneous determination of docetaxel and ketoconazole in rat plasma by liquid chromatography/electrospray ionization tandem mass spectrometry. Rapid Commun Mass Spectrom 2007; 21: 1009-18.
[88] Samimi G, Kishimoto S, Manorek G, Breaux JK, Howell SB. Novel mechanisms of platinum drug resistance identified in cells selected for resistance to JM118 the active metabolite of satraplatin. Cancer Chemother Pharmacol 2007; 59; 301-12.
[89] Bjorn E, Nygren Y, Nguyen TT, *et al*. Determination of platinum in human subcellular microsamples by inductively coupled plasma mass spectrometry. Anal Biochem 2007; 363: 135-42.
[90] Ghezzi A, Aceto M, Cassino C, Gabano E, Osella D. Uptake of antitumor platinum(II)-complexes by cancer cells, assayed by inductively coupled plasma mass spectrometry (ICP-MS). J Inorg Biochem 2004; 98: 73-8.
[91] Breda M, Maffini M, Mangia A, Mucchino C, Musci M. Development and validation of an inductively coupled plasma mass spectrometry method with optimized microwave-assisted sample digestion for the determination of platinum at ultratrace levels in plasma and ultrafiltrate plasma. J Pharm Biomed Anal 2008; 48; 435-9.
[92] Brouwers EE, Tibben M, Rosing H, Schellens JH, Beijnen JH. The application of inductively coupled plasma mass spectrometry in clinical pharmacological oncology research. Mass Spectrom Rev 2008; 27: 67-100.
[93] Salerno M, Yahia D, Dzamitika S, *et al*. Impact of intracellular chloride concentration on cisplatin accumulation in sensitive and resistant GLC4 cells. J Biol Inorg Chem 2009; 14: 123-32.
[94] Zisowsky J, Koegel S, Leyers S, *et al*. Relevance of drug uptake and efflux for cisplatin sensitivity of tumor cells. Biochem Pharmacol 2007; 73: 298-307.
[95] Kroning R, Lichtenstein AK, Nagami GT. Sulfur-containing amino acids decrease cisplatin cytotoxicity and uptake in renal tubule epithelial cell lines. Cancer Chemother Pharmacol 2000; 45; 43-9.
[96] Brouwers EE, Tibben MM, Rosing H, *et al*. Sensitive inductively coupled plasma mass spectrometry assay for the determination of platinum originating from cisplatin, carboplatin, and oxaliplatin in human plasma ultrafiltrate. J Mass Spectrom 2006; 41: 1186-94.
[97] Hanada K, Nagai N, Ogata H. Quantitative determination of unchanged cisplatin in rat kidney and liver by high-performance liquid chromatography. J Chromatogr B Biomed Appl 1995; 663: 181-6.
[98] Lopez-Flores A, Jurado R, Garcia-Lopez P. A high-performance liquid chromatographic assay for determination of cisplatin in plasma, cancer cell, and tumor samples. J Pharmacol Toxicol Methods 2005; 52: 366-72.
[99] Minakata K, Nozawa H, Okamoto N, Suzuki O. Determination of platinum derived from cisplatin in human tissues using electrospray ionization mass spectrometry. J Chromatogr B Analyt Technol Biomed Life Sci 2006; 832: 286-91.
[100] Duncan GF, Faulkner HC, 3rd, Farmen RH, Pittman KA. Liquid chromatographic procedure for the quantitative analysis of carboplatin in beagle dog plasma ultrafiltrate. J Pharm Sci 1988; 77: 273-6.
[101] Tyczkowska K, Page RL, Riviere JE. Determination of carboplatin in canine plasma by liquid chromatography with ultraviolet-visible detection and confirmation by atomic absorption spectroscopy. J Chromatogr 1990; 527: 447-53.
[102] Parsons PJ, LeRoy AF. Determination of cis-diamminedichloroplatinum(II) in human plasma using ion-pair chromatography with electrochemical detection. J Chromatogr 1986; 378: 395-408.
[103] Parsons PJ, Morrison PF, LeRoy AF. Determination of platinum-containing drugs in human plasma by liquid chromatography with reductive electrochemical detection. J Chromatogr 1987; 385: 323-35.
[104] Hann S, Stefanka Z, Lenz K, Stingeder G. Novel separation method for highly sensitive speciation of cancerostatic platinum compounds by HPLC-ICP-MS. Anal Bioanal Chem 2005; 381: 405-12.
[105] Bell DN, Liu JJ, Tingle MD, McKeage MJ. Specific determination of intact cisplatin and monohydrated cisplatin in human plasma and culture medium ultrafiltrates using HPLC on-line with inductively coupled plasma mass spectrometry. J Chromatogr B Analyt Technol Biomed Life Sci 2006; 837: 29-34.
[106] Guo P, Li S, Gallo JM. Determination of carboplatin in plasma and tumor by high-performance liquid chromatography-mass spectrometry. J Chromatogr B Analyt Technol Biomed Life Sci 2003; 783: 43-52.
[107] Desjardins C, Saxton P, Lu SX, *et al*. A high-performance liquid chromatography-tandem mass spectrometry method for the clinical combination study of carboplatin and anti-tumor agent eribulin mesylate (E7389) in human plasma. J Chromatogr B Analyt Technol Biomed Life Sci 2008; 875: 373-82.
[108] Yuan JH, Cheng JQ, Jiang LY, *et al*. Breast cancer resistance protein expression and 5-fluorouracil resistance. Biomed Environ Sci 2008; 21: 290-5.
[109] Oguri T, Bessho Y, Achiwa H, *et al*. MRP8/ABCC11 directly confers resistance to 5-fluorouracil. Mol Cancer Ther 2007; 6: 122-7.
[110] Washtien WL, Santi DV. Assay of intracellular free and macromolecular-bound metabolites of 5-fluorodeoxyuridine and 5-fluorouracil. Cancer Res 1979; 39: 3397-404.
[111] Kosovec JE, Egorin MJ, Gjurich S, Beumer JH. Quantitation of 5-fluorouracil (5-FU) in human plasma by liquid chromatogra-

phy/electrospray ionization tandem mass spectrometry. Rapid Commun Mass Spectrom 2008; 22: 224-30.

[112] Del Nozal MJ, Bernal JL, Pampliega A, Marinero P, Pozuelo M. Determination of the concentrations of 5-fluorouracil and its metabolites in rabbit plasma and tissues by high-performance liquid chromatography. J Chromatogr B Biomed Appl 1994; 656: 397-405.

[113] Casale F, Canaparo R, Serpe L, *et al*. Plasma concentrations of 5-fluorouracil and its metabolites in colon cancer patients. Pharmacol Res 2004; 50: 173-9.

[114] Escoriaza J, Aldaz A, Calvo E, Giraldez J. Simple and sensitive determination of 5-fluorouracil in plasma by high-performance liquid chromatography. Application to clinical pharmacokinetic studies. J Chromatogr B Biomed Sci Appl 1999; 736: 97-102.

[115] Loos WJ, de Bruijn P, van Zuylen L, *et al*. Determination of 5-fluorouracil in microvolumes of human plasma by solvent extraction and high-performance liquid chromatography. J Chromatogr B Biomed Sci Appl 1999; 735: 293-7.

[116] Siethoff C, Orth M, Ortling A, Brendel E, Wagner-Redeker W. Simultaneous determination of capecitabine and its metabolite 5-fluorouracil by column switching and liquid chromatographic/tandem mass spectrometry. J Mass Spectrom 2004; 39: 884-9.

[117] Woo YA, Kim GH, Jeong EJ, Kim CY. Simultaneous determination of doxifluridine and 5-fluorouracil in monkey serum by high performance liquid chromatography with tandem mass spectrometry. J Chromatogr B Analyt Technol Biomed Life Sci 2008; 875: 487-92.

[118] Pisano R, Breda M, Grassi S, James CA. Hydrophilic interaction liquid chromatography-APCI-mass spectrometry determination of 5-fluorouracil in plasma and tissues. J Pharm Biomed Anal 2005; 38: 738-45.

[119] Kubo M, Sasabe H, Shimizu T. Highly sensitive method for the determination of 5-fluorouracil in biological samples in the presence of 2'-deoxy-5-fluorouridine by gas chromatography-mass spectrometry. J Chromatogr 1991; 564:137-45.

[120] Bates CD, Watson DG, Willmott N, Logan H, Goldberg J. The analysis of 5-fluorouracil in human plasma by gas chromatography-negative ion chemical ionization mass spectrometry (GC-NICIMS) with stable isotope dilution. J Pharm Biomed Anal 1991; 9:19-21.

[121] Anderson LW, Parker RJ, Collins JM, *et al*. Gas chromatographic-mass spectrometric method for routine monitoring of 5-fluorouracil in plasma of patients receiving low-level protracted infusions. J Chromatogr 1992; 581: 195-201.

[122] Fanciullino R, Giacometti S, Mercier C, *et al*. In vitro and in vivo reversal of resistance to 5-fluorouracil in colorectal cancer cells with a novel stealth double-liposomal formulation. Br J Cancer 2007; 97: 919-26.

[123] Ciccolini J, Peillard L, Evrard A, *et al*. Enhanced antitumor activity of 5-fluorouracil in combination with 2'-deoxyinosine in human colorectal cell lines and human colon tumor xenografts. Clin Cancer Res 2000; 6: 1529-35.

[124] Dreyer R, Cadman E. Use of periodate and methylamine for the quantitation of intracellular 5-fluoro-2'-deoxyuridine-5'-monophosphate by high-performance liquid chromatography. J Chromatogr 1981; 219: 273-84.

[125] Barberi-Heyob M, Merlin JL, Weber B. Analysis of 5-fluorouracil in plasma and urine by high-performance liquid chromatography. J Chromatogr 1992; 581: 281-6.

[126] Guerrieri A, Palmisano F, Zambonin PG, De Lena M, Lorusso V. Solid-phase extraction of fluoropyrimidine derivatives on a copper-modified strong cation exchanger: determination of doxifluridine, 5-fluorouracil and its main metabolites in serum by high-performance liquid chromatography with ultraviolet detection. J Chromatogr 1993; 617: 71-7.

[127] Prochazkova A, Liu S, Friess H, Aebi S, Thormann W. Determination of 5-fluorouracil and 5-fluoro-2'-deoxyuridine-5'-monophosphate in pancreatic cancer cell line and other biological materials using capillary electrophoresis. J Chromatogr A 2001; 916: 215-24.

[128] Ruiz van Haperen VW, Veerman G, Boven E, *et al*. Schedule dependence of sensitivity to 2',2'-difluorodeoxycytidine (Gemcitabine) in relation to accumulation and retention of its triphosphate in solid tumour cell lines and solid tumours. Biochem Pharmacol 1994; 48; 1327-39.

[129] van Moorsel CJ, Pinedo HM, Veerman G, *et al*. Mechanisms of synergism between cisplatin and gemcitabine in ovarian and non-small-cell lung cancer cell lines. Br J Cancer 1999; 80;981-990

[130] Ruiz van Haperen VW, Veerman G, Eriksson S, *et al*. Development and molecular characterization of a 2',2'-difluorodeoxycytidine-resistant variant of the human ovarian carcinoma cell line A2780. Cancer Res 1994; 54: 4138-43.

[131] Freeman KB, Anliker S, Hamilton M, *et al*. Validated assays for the determination of gemcitabine in human plasma and urine using high-performance liquid chromatography with ultraviolet detection. J Chromatogr B Biomed Appl 1995; 665: 171-81.

[132] Venook AP, Egorin MJ, Rosner GL, *et al*. Phase I and pharmacokinetic trial of gemcitabine in patients with hepatic or renal dysfunction: Cancer and Leukemia Group B 9565. J Clin Oncol 2000; 18: 2780-7.

[133] Wang LZ, Goh BC, Lee HS, Noordhuis P, Peters GJ. An expedient assay for determination of gemcitabine and its metabolite in human plasma using isocratic ion-pair reversed-phase high-performance liquid chromatography. Ther Drug Monit 2003; 25: 552-7.

[134] Sottani C, Zucchetti M, Zaffaroni M, Bettinelli M, Minoia C. Validated procedure for simultaneous trace level determination of the anti-cancer agent gemcitabine and its metabolite in human urine by high-performance liquid chromatography with tandem mass spectrometry. Rapid Commun Mass Spectrom 2004; 18: 1017-23.

[135] Marangon E, Sala F, Caffo O, *et al*. Simultaneous determination of gemcitabine and its main metabolite, dFdU, in plasma of patients with advanced non-small-cell lung cancer by high-performance liquid chromatography-tandem mass spectrometry. J Mass Spectrom 2008; 43: 216-23.

[136] de Bruijn EA, van Oosterom AT, Leclercq PA, *et al*. Monitoring the behaviour of 4-ketocyclophosphamide versus cyclophosphamide during capillary gas chromatography by mass spectrometry. Biomed Environ Mass Spectrom 1987; 14: 643-7.

[137] de Bruin EA, Tjaden UR, van Oosterom AT, Leeflang P, Leclercq PA. Determination of the underivatized antineoplastic drugs cyclophosphamide and 5-fluorouracil and some of their metabolites by capillary gas chromatography combined with electron-capture and nitrogen-phosphorus selective detection. J Chromatogr 1983; 279: 603-8.

[138] Kalhorn TF, Ren S, Howald WN, Lawrence RF, Slattery JT. Analysis of cyclophosphamide and five metabolites from human plasma using liquid chromatography-mass spectrometry and gas chromatography-nitrogen-phosphorus detection. J Chromatogr B Biomed Sci Appl 1999; 732: 287-98.

[139] Huitema AD, Tibben MM, Kerbusch T, *et al*. Simultaneous determination of N,N',N''-triethylenethiophosphoramide, cyclophosphamide and some of their metabolites in plasma using capillary gas chromatography. J Chromatogr B Biomed Sci Appl 1998; 716: 177-86.

[140] Huitema AD, Reinders C, Tibben MM, Rodenhuis S, Beijnen JH. Sensitive gas chromatographic determination of the cyclophosphamide metabolite 2-dechloroethylcyclophosphamide in human plasma. J Chromatogr B Biomed Sci Appl 2001; 757: 349-57.

[141] Jardine I, Fenselau C, Appler M, *et al*. Quantitation by gas chromatography-chemical ionization mass spectrometry of cyclophosphamide, phosphoramide mustard, and nornitrogen mustard in the plasma and urine of patients receiving cyclophosphamide therapy. Cancer Res 1978; 38: 408-15.

[142] Momerency G, Van Cauwenberghe K, Slee PH, Van Oosterom AT, De Bruijn EA. The determination of cyclophosphamide and its metabolites in blood plasma as stable trifluoroacetyl derivatives by electron capture chemical ionization gas chromatography/mass spectrometry. Biol Mass Spectrom 1994; 23: 149-58.

[143] Burton LC, James CA. Rapid method for the determination of ifosfamide and cyclophosphamide in plasma by high-performance liquid chromatography with solid-phase extraction. J Chromatogr 1988; 431: 450-4.

[144] Rustum AM, Hoffman NE. Determination of cyclophosphamide in whole blood and plasma by reversed-phase high-performance liquid chromatography. J Chromatogr 1987; 422: 125-34.

[145] Kasel D, Jetter A, Harlfinger S, Gebhardt W, Fuhr U. Quantification of cyclophosphamide and its metabolites in urine using liquid chromatography/tandem mass spectrometry. Rapid Commun Mass Spectrom 2004; 18: 1472-8.

[146] de Jonge ME, van Dam SM, Hillebrand MJ, *et al*. Simultaneous quantification of cyclophosphamide, 4-hydroxycyclophosphamide,

N,N',N''-triethylenethiophosphoramide (thiotepa) and N,N',N''-triethylenephosphoramide (tepa) in human plasma by high-performance liquid chromatography coupled with electrospray ionization tandem mass spectrometry. J Mass Spectrom 2004; 39: 262-71

[147] Sadagopan N, Cohen L, Roberts B, Collard W, Omer C. Liquid chromatography-tandem mass spectrometric quantitation of cyclophosphamide and its hydroxy metabolite in plasma and tissue for determination of tissue distribution. J Chromatogr B Biomed Sci Appl 2001; 759: 277-84.

[148] Liu Z, Chan KKWang JJ. Tandem mass spectrometric analysis of cyclophosphamide, ifosfamide and their metabolites. Rapid Commun Mass Spectrom 2005; 19: 2581-90.

[149] Storme T, Mercier L, Deroussent A, *et al*. Liquid chromatography-mass spectrometry assay for quantitation of ifosfamide and its N-deschloroethylated metabolites in rat microsomal medium. J Chromatogr B Analyt Technol Biomed Life Sci 2005; 820; 251-9.

[150] Rubino FM. Separation methods for methotrexate, its structural analogues and metabolites. J Chromatogr B Biomed Sci Appl 2001; 764: 217-54.

[151] Albertioni F, Pettersson B, Beck O, *et al*. Simultaneous quantitation of methotrexate and its two main metabolites in biological fluids by a novel solid-phase extraction procedure using high-performance liquid chromatography. J Chromatogr B Biomed Appl 1995; 665: 163-70.

[152] Albertioni F, Rask C, Eksborg S, *et al*. Evaluation of clinical assays for measuring high-dose methotrexate in plasma. Clin Chem 1996; 42:39-44.

[153] Cociglio M, Hillaire-Buys DAlric C. Determination of methotrexate and 7-hydroxymethotrexate by liquid chromatography for routine monitoring of plasma levels. J Chromatogr B Biomed Appl 1995; 674: 101-10.

[154] Duran Meras I, Espinosa Mansilla ARodriguez Gomez MJ. Determination of methotrexate, several pteridines, and creatinine in human urine, previous oxidation with potassium permanganate, using HPLC with photometric and fluorimetric serial detection. Anal Biochem 2005; 346: 201-9.

[155] Emara S, Razee S, Khedr AMasujima T. On-line precolumn derivatization for HPLC determination of methotrexate using a column packed oxidant. Biomed Chromatogr 1997; 11: 42-6.

[156] Beck O, Seideman P, Wennberg MPeterson C. Trace analysis of methotrexate and 7-hydroxymethotrexate in human plasma and urine by a novel high-performance liquid chromatographic method. Ther Drug Monit 1991; 13: 528-32.

[157] Yu Z, Westerlund DBoos KS. Determination of methotrexate and its metabolite 7-hydroxymethotrexate by direct injection of human plasma into a column-switching liquid chromatographic system using post-column photochemical reaction with fluorimetric detection. J Chromatogr B Biomed Sci Appl 1997; 689: 379-86.

[158] McCrudden EATett SE. Improved high-performance liquid chromatography determination of methotrexate and its major metabolite in plasma using a poly(styrene-divinylbenzene) column. J Chromatogr B Biomed Sci Appl 1999; 721: 87-92

[159] Li H, Luo W, Zeng Q, *et al*. Method for the determination of blood methotrexate by high performance liquid chromatography with on-line post-column electrochemical oxidation and fluorescence detection. J Chromatogr B Analyt Technol Biomed Life Sci 2007; 845:164-8.

[160] Steinborner SHenion J. Liquid-liquid extraction in the 96-well plate format with SRM LC/MS quantitative determination of methotrexate and its major metabolite in human plasma. Anal Chem 1999; 71: 2340-5.

[161] Rule G, Chapple MHenion J. A 384-well solid-phase extraction for LC/MS/MS determination of methotrexate and its 7-hydroxy metabolite in human urine and plasma. Anal Chem 2001; 73: 439-43.

[162] Guo P, Wang X, Liu L, *et al*. Determination of methotrexate and its major metabolite 7-hydroxymethotrexate in mouse plasma and brain tissue by liquid chromatography-tandem mass spectrometry. J Pharm Biomed Anal 2007; 43:1789-95.

[163] Uchida Y, Kamiie J, Ohtsuki STerasaki T. Multichannel liquid chromatography-tandem mass spectrometry cocktail method for comprehensive substrate characterization of multidrug resistance-associated protein 4 transporter. Pharm Res 2007; 24: 2281-96.

[164] Barbieri A, Sabatini L, Indiveri P, *et al*. Simultaneous determination of low levels of methotrexate and cyclophosphamide in human urine by micro liquid chromatography/electrospray ionization tandem mass spectrometry. Rapid Commun Mass Spectrom 2006; 20: 1889-93.

[165] Rahmani-Jourdheuil D, Coloma F, Placidi M, Rahmani R. Human hepatic uptake of two vinca alkaloids: navelbine and vincristine. J Pharm Sci 1994; 83:468-71.

[166] Stuckler D, Singhal J, Singhal SS, *et al*. RLIP76 transports vinorelbine and mediates drug resistance in non-small cell lung cancer. Cancer Res 2005; 65: 991-8.

[167] Debal V, Morjani H, Millot JM, *et al*. Determination of vinorelbine (Navelbine) in tumour cells by high-performance liquid chromatography. J Chromatogr 1992; 581: 93-9.

[168] Van Belle SJ, De Smet M, Monsaert C, *et al*. High-performance liquid chromatographic determination of navelbine in MO4 mouse fibrosarcoma cells and biological fluids. J Chromatogr 1992; 576: 351-7.

[169] Gauvin A, Pinguet F, Poujol S, Astre C, Bressolle F. High-performance liquid chromatographic determination of vinorelbine in human plasma and blood: application to a pharmacokinetic study. J Chromatogr B Biomed Sci Appl 2000; 748: 389-99.

[170] Robieux I, Vitali V, Aita P, *et al*. Sensitive high-performance liquid chromatographic method with fluorescence detection for measurement of vinorelbine plasma concentrations. J Chromatogr B Biomed Appl 1996; 675: 183-7.

[171] Mouchard-Delmas C, Gourdier B, Vistelle R. Determination of vinorelbine in rabbit plasma by high-performance liquid chromatography with coulometric detection. J Chromatogr B Biomed Appl 1995; 663: 390-4.

[172] Barthe L, Ribet JP, Pelissou M, *et al*. Optimization of the separation of Vinca alkaloids by nonaqueous capillary electrophoresis. J Chromatogr A 2002; 968:241-50.

[173] Ragot S, Sauvage FL, Rousseau A, *et al*. Sensitive determination of vinorelbine and its metabolites in human serum using liquid chromatography-electrospray mass spectrometry. J Chromatogr B Biomed Sci Appl 2001; 753:167-78.

[174] Damen CW, Rosing H, Tibben MM, *et al*. A sensitive assay for the quantitative analysis of vinorelbine in mouse and human EDTA plasma by high-performance liquid chromatography coupled with electrospray tandem mass spectrometry. J Chromatogr B Analyt Technol Biomed Life Sci 2008; 868: 102-9.

[175] Van Heugen JC, De Graeve J, Zorza GPuozzo C. New sensitive liquid chromatography method coupled with tandem mass spectrometric detection for the clinical analysis of vinorelbine and its metabolites in blood, plasma, urine and faeces. J Chromatogr A 2001; 926: 11-20.

[176] Roepe PD. Analysis of the steady-state and initial rate of doxorubicin efflux from a series of multidrug-resistant cells expressing different levels of P-glycoprotein. Biochemistry 1992; 31: 12555-64.

[177] Mealey KL, Barhoumi R, Burghardt RC, Safe S, Kochevar DT. Doxycycline induces expression of P glycoprotein in MCF-7 breast carcinoma cells. Antimicrob Agents Chemother 2002; 46: 755-61.

[178] Arancia G, Calcabrini A, Meschini S, Molinari A. Intracellular distribution of anthracyclines in drug resistant cells. Cytotechnology 1998; 27: 95-111.

[179] Chen CL, Thoen KK, Uckun FM. High-performance liquid chromatographic methods for the determination of topoisomerase II inhibitors. J Chromatogr B Biomed Sci Appl 2001; 764: 81-119.

[180] Zagotto G, Gatto B, Moro S, Sissi C, Palumbo M. Anthracyclines: recent developments in their separation and quantitation. J Chromatogr B Biomed Sci Appl 2001; 764: 161-71.

[181] Eder AR, Arriaga EA. Micellar electrokinetic capillary chromatography reveals differences in intracellular metabolism between liposomal and free doxorubicin treatment of human leukemia cells. J Chromatogr B Analyt Technol Biomed Life Sci 2005; 829: 115-22.

[182] Anderson AB, Gergen J, Arriaga EA. Detection of doxorubicin and metabolites in cell extracts and in single cells by capillary electrophoresis with laser-induced fluorescence detection. J Chromatogr B Analyt Technol Biomed Life Sci 2002; 769: 97-106.

[183] Zhou Q, Chowbay B. Determination of doxorubicin and its metabolites in rat serum and bile by LC: application to preclinical pharmacokinetic studies. J Pharm Biomed Anal 2002; 30: 1063-74.

[184] Alvarez-Cedron L, Sayalero ML, Lanao JM. High-performance liquid chromatographic validated assay of doxorubicin in rat plasma and tissues. J Chromatogr B Biomed Sci Appl 1999; 721: 271-8.

[185] Grosse PY, Bressolle F, Pinguet F. *In vitro* modulation of doxorubicin and docetaxel antitumoral activity by methyl-beta-cyclodextrin. Eur J Cancer 1998; 34: 168-74.

[186] Urva SR, Shin BS, Yang VC, Balthasar JP. Sensitive high performance liquid chromatographic assay for assessment of doxorubicin pharmacokinetics in mouse plasma and tissues. J Chromatogr B Analyt Technol Biomed Life Sci 2009; 877: 837-41.

[187] Mazuel C, Grove J, Gerin G, Keenan KP. HPLC-MS/MS determination of a peptide conjugate prodrug of doxorubicin, and its active metabolites, leucine-doxorubicin and doxorubicin, in dog and rat plasma. J Pharm Biomed Anal 2003; 33: 1093-102.

[188] Arnold RD, Slack JE, Straubinger RM. Quantification of Doxorubicin and metabolites in rat plasma and small volume tissue samples by liquid chromatography/electrospray tandem mass spectroscopy. J Chromatogr B Analyt Technol Biomed Life Sci 2004; 808: 141-52.

[189] Barker IK, Crawford SM, Fell AF. Determination of plasma concentrations of epirubicin and its metabolites by high-performance liquid chromatography during a 96-h infusion in cancer chemotherapy. J Chromatogr B Biomed Appl 1996; 681; 323-9.

[190] Dodde WI, Maring JG, Hendriks G, *et al*. Determination of epirubicin and its metabolite epirubicinol in saliva and plasma by HPLC. Ther Drug Monit 2003; 25; 433-40.

[191] Nicholls G, Clark BJ, Brown JE. Solid-phase extraction and optimized separation of doxorubicin, epirubicin and their metabolites using reversed-phase high-performance liquid chromatography. J Pharm Biomed Anal 1992; 10; 949-57.

[192] Ricciarello R, Pichini S, Pacifici R, *et al*. Simultaneous determination of epirubicin, doxorubicin and their principal metabolites in human plasma by high-performance liquid chromatography and electrochemical detection. J Chromatogr B Biomed Sci Appl 1998; 707: 219-25

[193] Lachatre F, Marquet P, Ragot S, *et al*. Simultaneous determination of four anthracyclines and three metabolites in human serum by liquid chromatography-electrospray mass spectrometry. J Chromatogr B Biomed Sci Appl 2000; 738: 281-91.

[194] Sottani C, Tranfo G, Bettinelli M, *et al*. Trace determination of anthracyclines in urine: a new high-performance liquid chromatography/tandem mass spectrometry method for assessing exposure of hospital personnel. Rapid Commun Mass Spectrom 2004; 18: 2426-36.

[195] Zimmermann C, Gutmann H, Hruz P, *et al*. Mapping of multidrug resistance gene 1 and multidrug resistance-associated protein isoform 1 to 5 mRNA expression along the human intestinal tract. Drug Metab Dispos 2005; 33: 219-24.

[196] Cordon-Cardo C, O'Brien JP, Boccia J, *et al*. Expression of the multidrug resistance gene product (P-glycoprotein) in human normal and tumor tissues. J Histochem Cytochem 1990; 38: 1277-87.

[197] Thiebaut F, Tsuruo T, Hamada H, *et al*. Cellular localization of the multidrug-resistance gene product P-glycoprotein in normal human tissues. Proc Natl Acad Sci U S A 1987; 84: 7735-8.

[198] Fojo AT, Ueda K, Slamon DJ, *et al*. Expression of a multidrug-resistance gene in human tumors and tissues. Proc Natl Acad Sci U S A 1987; 84: 265-9.

[199] Nishimura M, Naito S. Tissue-specific mRNA expression profiles of human ATP-binding cassette and solute carrier transporter superfamilies. Drug Metab Pharmacokinet 2005; 20: 452-77.

[200] Gutmann H, Hruz P, Zimmermann C, Beglinger C, Drewe J. Distribution of breast cancer resistance protein (BCRP/ABCG2) mRNA expression along the human GI tract. Biochem Pharmacol 2005; 70: 695-9.

[201] Maliepaard M, Scheffer GL, Faneyte IF, *et al*. Subcellular localization and distribution of the breast cancer resistance protein transporter in normal human tissues. Cancer Res 2001; 61: 3458-64.

[202] Cooray HC, Blackmore CG, Maskell L, Barrand MA. Localisation of breast cancer resistance protein in microvessel endothelium of human brain. Neuroreport 2002; 13: 2059-63.

[203] Cordon-Cardo C, O'Brien JP, Casals D, *et al*. Multidrug-resistance gene (P-glycoprotein) is expressed by endothelial cells at blood-brain barrier sites. Proc Natl Acad Sci U S A 1989; 86: 695-8.

[204] Flens MJ, Zaman GJ, van der Valk P, *et al*. Tissue distribution of the multidrug resistance protein. Am J Pathol 1996; 148:1237-47.

[205] Cherrington NJ, Hartley DP, Li N, Johnson DR, Klaassen CD. Organ distribution of multidrug resistance proteins 1, 2, and 3 (Mrp1, 2, and 3) mRNA and hepatic induction of Mrp3 by constitutive androstane receptor activators in rats. J Pharmacol Exp Ther 2002; 300:97-104.

[206] Kool M, de Haas M, Scheffer GL, *et al*. Analysis of expression of cMOAT (MRP2), MRP3, MRP4, and MRP5, homologues of the multidrug resistance-associated protein gene (MRP1), in human cancer cell lines. Cancer Res 1997; 57: 3537-47.

[207] Alcorn J, Lu X, Moscow JA, McNamara PJ. Transporter gene expression in lactating and nonlactating human mammary epithelial cells using real-time reverse transcription-polymerase chain reaction. J Pharmacol Exp Ther 2002; 303: 487-96.

[208] Kruh GD, Guo Y, Hopper-Borge E, Belinsky MG, Chen ZS. ABCC10, ABCC11, and ABCC12. Pflugers Arch 2007; 453:675-84.

[209] Hopper E, Belinsky MG, Zeng H, *et al*. Analysis of the structure and expression pattern of MRP7 (ABCC10), a new member of the MRP subfamily. Cancer Lett 2001; 162: 181-91.

[210] Takayanagi S, Kataoka T, Ohara O, *et al*. Human ATP-binding cassette transporter ABCC10: expression profile and p53-dependent upregulation. J Exp Ther Oncol 2004; 4: 239-46.

[211] Augustine LM, Markelewicz RJ, Jr., Boekelheide K, Cherrington NJ. Xenobiotic and endobiotic transporter mRNA expression in the blood-testis barrier. Drug Metab Dispos 2005; 33:182-9.

[212] Miller DS, Nobmann SN, Gutmann H, *et al*. Xenobiotic transport across isolated brain microvessels studied by confocal microscopy. Mol Pharmacol 2000; 58: 1357-67.

[213] Mayer R, Kartenbeck J, Buchler M, *et al*. Expression of the MRP gene-encoded conjugate export pump in liver and its selective absence from the canalicular membrane in transport-deficient mutant hepatocytes. J Cell Biol 1995; 131: 137-50.

[214] Rost D, Konig J, Weiss G, *et al*. Expression and localization of the multidrug resistance proteins MRP2 and MRP3 in human gallbladder epithelia. Gastroenterology 2001; 121: 1203-8.

[215] Schaub TP, Kartenbeck J, Konig J, *et al*. Expression of the MRP2 gene-encoded conjugate export pump in human kidney proximal tubules and in renal cell carcinoma. J Am Soc Nephrol 1999;10: 1159-69.

[216] St-Pierre MV, Serrano MA, Macias RI, *et al*. Expression of members of the multidrug resistance protein family in human term placenta. Am J Physiol Regul Integr Comp Physiol 2000; 279: R1495-503

[217] Jedlitschky G, Hoffmann U, Kroemer HK. Structure and function of the MRP2 (ABCC2) protein and its role in drug disposition. Expert Opin Drug Metab Toxicol 2006; 2: 351-66.

[218] Nies AT, Jedlitschky G, Konig J, *et al*. Expression and immunolocalization of the multidrug resistance proteins, MRP1-MRP6 (ABCC1-ABCC6), in human brain. Neuroscience 2004; 129: 349-60.

[219] Rius M, Nies AT, Hummel-Eisenbeiss J, Jedlitschky G, Keppler D. Cotransport of reduced glutathione with bile salts by MRP4 (ABCC4) localized to the basolateral hepatocyte membrane. Hepatology 2003; 38: 374-84.

[220] Li C, Krishnamurthy PC, Penmatsa H, *et al*. Spatiotemporal coupling of cAMP transporter to CFTR chloride channel function in the gut epithelia. Cell 2007; 131: 940-51.

[221] Ritter CA, Jedlitschky G, Meyer zu Schwabedissen H, *et al*. Cellular export of drugs and signaling molecules by the ATP-binding cassette transporters MRP4 (ABCC4) and MRP5 (ABCC5). Drug Metab Rev 2005; 37:253-78.

[222] Meyer Zu, Schwabedissen HE, Grube M, Heydrich B, *et al*. Expression, localization, and function of MRP5 (ABCC5), a transporter for cyclic nucleotides, in human placenta and cultured human trophoblasts: effects of gestational age and cellular differentiation. Am J Pathol 2005; 166: 39-48.

[223] McAleer MA, Breen MA, White NL, Matthews N. pABC11 (also known as MOAT-C and MRP5), a member of the ABC family of proteins, has anion transporter activity but does not confer multidrug resistance when overexpressed in human embryonic kidney 293 cells. J Biol Chem 1999; 274: 23541-8.

[224] Stojic J, Stohr H, Weber BH. Three novel ABCC5 splice variants in human retina and their role as regulators of ABCC5 gene expression. BMC Mol Biol 2007; 8: 42.

[225] Suzuki T, Nishio K, Sasaki H, *et al*. cDNA cloning of a short type of multidrug resistance protein homologue, SMRP, from a human lung cancer cell line. Biochem Biophys Res Commun 1997; 238: 790-4.

[226] Bera TK, Lee S, Salvatore G, Lee B, Pastan I. MRP8, a new member of ABC transporter superfamily, identified by EST database mining and gene prediction program, is highly expressed in breast cancer. Mol Med 2001; 7: 509-16.

[227] Tammur J, Prades C, Arnould I, *et al*. Two new genes from the human ATP-binding cassette transporter superfamily, ABCC11 and ABCC12, tandemly duplicated on chromosome 16q12. Gene 2001; 273: 89-96.

[228] Yabuuchi H, Shimizu H, Takayanagi S, Ishikawa T. Multiple splicing variants of two new human ATP-binding cassette transporters, ABCC11 and ABCC12. Biochem Biophys Res Commun 2001; 288: 933-9.

[229] Bai ZGust R. Breast cancer, estrogen receptor and ligands. Arch Pharm (Weinheim) 2009; 342: 133-49.

[230] Gao X, Nawaz Z. Progesterone receptors - animal models and cell signaling in breast cancer: Role of steroid receptor coactivators and corepressors of progesterone receptors in breast cancer. Breast Cancer Res 2002; 4: 182-6.

[231] Mote PA, Graham JD, Clarke CL. Progesterone receptor isoforms in normal and malignant breast. Ernst Schering Found Symp Proc 2007; 77-107.

[232] Gass EK, Leonhardt SA, Nordeen SK, Edwards DP. The antagonists RU486 and ZK98299 stimulate progesterone receptor binding to deoxyribonucleic acid *in vitro* and *in vivo*, but have distinct effects on receptor conformation. Endocrinology 1998; 139: 1905-19.

[233] Mutoh K, Tsukahara S, Mitsuhashi J, Katayama K, Sugimoto Y. Estrogen-mediated post transcriptional down-regulation of P-glycoprotein in MDR1-transduced human breast cancer cells. Cancer Sci 2006; 97: 1198-204.

[234] Evseenko DA, Paxton JW, Keelan JA. Independent regulation of apical and basolateral drug transporter expression and function in placental trophoblasts by cytokines, steroids, and growth factors. Drug Metab Dispos 2007; 35: 595-601.

[235] Nagaoka R, Iwasaki T, Rokutanda N, *et al*. Tamoxifen activates CYP3A4 and MDR1 genes through steroid and xenobiotic receptor in breast cancer cells. Endocrine 2006; 30: 261-8.

[236] De Vincenzo R, Scambia G, Panici BP, *et al*. Modulatory effect of tamoxifen and ICI 182,780 on adriamycin resistance in MCF-7 human breast-cancer cells. Int J Cancer 1996; 68: 340-8.

[237] Liu H, Cheng D, Weichel AK, *et al*. Cooperative effect of gefitinib and fumitremorgin c on cell growth and chemosensitivity in estrogen receptor alpha negative fulvestrant-resistant MCF-7 cells. Int J Oncol 2006; 29:1237-46.

[238] Kang Y, Perry RR. Modulatory effects of tamoxifen and recombinant human alpha-interferon on doxorubicin resistance. Cancer Res 1993; 53: 3040-5.

[239] Ee PL, Kamalakaran S, Tonetti D, *et al*. Identification of a novel estrogen response element in the breast cancer resistance protein (ABCG2) gene. Cancer Res 2004; 64:1247-51.

[240] Zhang Y, Zhou G, Wang H, *et al*. Transcriptional upregulation of breast cancer resistance protein by 17beta-estradiol in ERalpha-positive MCF-7 breast cancer cells. Oncology 2006; 71: 446-55.

[241] Honorat M, Mesnier A, Vendrell J, *et al*. ABCC11 expression is regulated by estrogen in MCF7 cells, correlated with estrogen receptor {alpha} expression in postmenopausal breast tumors and overexpressed in tamoxifen-resistant breast cancer cells. Endocr Relat Cancer 2008; 15: 125-38.

[242] Imai Y, Ishikawa E, Asada S, Sugimoto Y. Estrogen-mediated post transcriptional down-regulation of breast cancer resistance protein/ABCG2. Cancer Res 2005; 65: 596-604.

[243] Yasuda S, Kobayashi M, Itagaki S, Hirano T, Iseki K. Response of the ABCG2 promoter in T47D cells and BeWo cells to sex hormone treatment. Mol Biol Rep 2008.

[244] Acconcia F, Kumar R. Signaling regulation of genomic and nongenomic functions of estrogen receptors. Cancer Lett 2006; 238:1-4.

[245] McKenna NJ, O'Malley BW. Combinatorial control of gene expression by nuclear receptors and coregulators. Cell 2002; 108: 465-74.

[246] Ee PL, He X, Ross DDBeck WT. Modulation of breast cancer resistance protein (BCRP/ABCG2) gene expression using RNA interference. Mol Cancer Ther 2004; 3: 1577-83.

[247] Yasuda S, Itagaki S, Hirano T, Iseki K. Effects of sex hormones on regulation of ABCG2 expression in the placental cell line BeWo. J Pharm Pharm Sci 2006; 9:133-9.

[248] Wang H, Zhou L, Gupta A, *et al*. Regulation of BCRP/ABCG2 expression by progesterone and 17beta-estradiol in human placental BeWo cells. Am J Physiol Endocrinol Metab 2006; 290: E798-807.

[249] Bailey-Dell KJ, Hassel B, Doyle LA, Ross DD. Promoter characterization and genomic organization of the human breast cancer resistance protein (ATP-binding cassette transporter G2) gene. Biochim Biophys Acta 2001; 1520: 234-41.

[250] Krishnamurthy P, Ross DD, Nakanishi T, *et al*. The stem cell marker Bcrp/ABCG2 enhances hypoxic cell survival through interactions with heme. J Biol Chem 2004; 279: 24218-25.

[251] To KK, Polgar O, Huff LM, Morisaki K, Bates SE. Histone modifications at the ABCG2 promoter following treatment with histone deacetylase inhibitor mirror those in multidrug-resistant cells. Mol Cancer Res 2008; 6:151-64.

[252] Szatmari I, Vamosi G, Brazda P, *et al*. Peroxisome proliferator-activated receptor gamma-regulated ABCG2 expression confers cytoprotection to human dendritic cells. J Biol Chem 2006; 281: 23812-23.

[253] Zampieri L, Bianchi P, Ruff P, Arbuthnot P. Differential modulation by estradiol of P-glycoprotein drug resistance protein expression in cultured MCF7 and T47D breast cancer cells. Anticancer Res 2002; 22: 2253-9.

[254] Honorat M, Mesnier A, Di Pietro A, *et al*. Dexamethasone down-regulates ABCG2 expression levels in breast cancer cells. Biochem Biophys Res Commun 2008; 375: 308-14.

[255] Wang H, Lee EW, Zhou L, *et al*. Progesterone receptor (PR) isoforms PRA and PRB differentially regulate expression of the breast cancer resistance protein in human placental choriocarcinoma BeWo cells. Mol Pharmacol 2008; 73: 845-54.

[256] Zhu Q, Center MS. Cloning and sequence analysis of the promoter region of the MRP gene of HL60 cells isolated for resistance to adriamycin. Cancer Res 1994; 54:4488-92.

[257] Zhu Q, Center MS. Evidence that SP1 modulates transcriptional activity of the multidrug resistance-associated protein gene. DNA Cell Biol 1996; 15: 105-11.

[258] Muredda M, Nunoya K, Burtch-Wright RA, *et al*. Cloning and Characterization of the Murine and Rat mrp1 Promoter Regions. Mol Pharmacol 2003; 64: 1259-69.

[259] Kurz EU, Cole SP, Deeley RG. Identification of DNA-protein interactions in the 5' flanking and 5' untranslated regions of the human multidrug resistance protein (MRP1) gene: evaluation of a putative antioxidant response element/AP-1 binding site. Biochem Biophys Res Commun 2001; 285; 981-90.

[260] Geier A, Mertens PR, Gerloff T, *et al*. Constitutive rat multidrug-resistance protein 2 gene transcription is down-regulated by Y-box protein 1. Biochem Biophys Res Commun 2003; 309: 612-8.

[261] Kast HR, Goodwin B, Tarr PT, *et al*. Regulation of multidrug resistance-associated protein 2 (ABCC2) by the nuclear receptors pregnane X receptor, farnesoid X-activated receptor, and constitutive androstane receptor. J Biol Chem 2002; 277: 2908-15.

[262] Eloranta JJ, Meier PJ, Kullak-Ublick GA. Coordinate transcriptional regulation of transport and metabolism. Methods Enzymol 2005; 400: 511-30.

[263] Qadri I, Hu LJ, Iwahashi M, *et al*. Interaction of hepatocyte nuclear factors in transcriptional regulation of tissue specific hormonal expression of human multidrug resistance-associated protein 2 (abcc2). Toxicol Appl Pharmacol 2009; 234: 281-92.

[264] Vollrath V, Wielandt AM, Iruretagoyena MChianale J. Role of Nrf2 in the regulation of the Mrp2 (ABCC2) gene. Biochem J 2006; 395: 599-609.

[265] Tanaka T, Uchiumi T, Hinoshita E, *et al*. The human multidrug resistance protein 2 gene: functional characterization of the 5'-flanking region and expression in hepatic cells. Hepatology 1999; 30:1507-12.

[266] Choi HK, Yang JW, Roh SH, Han CY, Kang KW. Induction of multidrug resistance associated protein 2 in tamoxifen-resistant breast cancer cells. Endocr Relat Cancer 2007; 14: 293-303.

[267] Fardel O, Payen L, Courtois A, Vernhet L, Lecureur V. Regulation of biliary drug efflux pump expression by hormones and xenobiotics. Toxicology 2001; 167: 37-46.

[268] Courtois A, Payen L, Guillouzo A, Fardel O. Up-regulation of multidrug resistance-associated protein 2 (MRP2) expression in rat hepatocytes by dexamethasone. FEBS Lett 1999; 459: 381-5.

[269] Courtois A, Payen L, Vernhet L, *et al*. Differential regulation of canalicular multispecific organic anion transporter (cMOAT) expression by the chemopreventive agent oltipraz in primary rat hepatocytes and in rat liver. Carcinogenesis 1999; 20: 2327-30.

[270] Micuda S, Fuksa L, Brcakova E, *et al*. Zonation of multidrug resistance-associated protein 2 in rat liver after induction with dexamethasone. J Gastroenterol Hepatol 2008; 23: e225-30.
[271] Bauer B, Hartz AM, Lucking JR, *et al*. Coordinated nuclear receptor regulation of the efflux transporter, Mrp2, and the phase-II metabolizing enzyme, GSTpi, at the blood-brain barrier. J Cereb Blood Flow Metab 2008; 28: 1222-34.
[272] Vendrell JA, Magnino F, Danis E, *et al*. Estrogen regulation in human breast cancer cells of new downstream gene targets involved in estrogen metabolism, cell proliferation and cell transformation. J Mol Endocrinol 2004; 32: 397-414.
[273] Maher JM, Cheng X, Tanaka Y, Scheffer GL, Klaassen CD. Hormonal regulation of renal multidrug resistance-associated proteins 3 and 4 (Mrp3 and Mrp4) in mice. Biochem Pharmacol 2006; 71: 1470-8.
[274] Moffit JS, Aleksunes LM, Maher JM, *et al*. Induction of hepatic transporters multidrug resistance-associated proteins (Mrp) 3 and 4 by clofibrate is regulated by peroxisome proliferator-activated receptor alpha. J Pharmacol Exp Ther 2006; 317: 537-45.
[275] Laganiere J, Deblois G, Lefebvre C, *et al*. From the Cover: Location analysis of estrogen receptor alpha target promoters reveals that FOXA1 defines a domain of the estrogen response. Proc Natl Acad Sci USA 2005; 102; 11651-6.
[276] Dabrowska M, Sirotnak FM. Regulation of transcription of the human MRP7 gene. Characteristics of the basal promoter and identification of tumor-derived transcripts encoding additional 5' end heterogeneity. Gene 2004; 341; 129-39.
[277] Benderra Z, Faussat AM, Sayada L, *et al*. MRP3, BCRP, and P-glycoprotein activities are prognostic factors in adult acute myeloid leukemia. Clin Cancer Res 2005; 11: 7764-72.
[278] Benderra Z, Faussat AM, Sayada L, *et al*. Breast cancer resistance protein and P-glycoprotein in 149 adult acute myeloid leukemias. Clin Cancer Res 2004; 10:7896-902.
[279] Wuchter C, Leonid K, Ruppert V, *et al*. Clinical significance of P-glycoprotein expression and function for response to induction chemotherapy, relapse rate and overall survival in acute leukemia. Haematologica 2000; 85: 711-21.
[280] Laupeze B, Amiot L, Drenou B, *et al*. High multidrug resistance protein activity in acute myeloid leukaemias is associated with poor response to chemotherapy and reduced patient survival. Br J Haematol 2002; 116: 834-8.
[281] Tafuri A, Gregorj C, Petrucci MT, *et al*. MDR1 protein expression is an independent predictor of complete remission in newly diagnosed adult acute lymphoblastic leukemia. Blood 2002; 100:974-81.
[282] Wattel E, Lepelley P, Merlat A, *et al*. Expression of the multidrug resistance P glycoprotein in newly diagnosed adult acute lymphoblastic leukemia: absence of correlation with response to treatment. Leukemia 1995; 9: 1870-4.
[283] Steinbach D, Wittig S, Cario G, *et al*. The multidrug resistance-associated protein 3 (MRP3) is associated with a poor outcome in childhood ALL and may account for the worse prognosis in male patients and T-cell immunophenotype. Blood 2003; 102: 4493-8.
[284] Suvannasankha A, Minderman H, O'Loughlin KL, *et al*. Breast cancer resistance protein (BCRP/MXR/ABCG2) in adult acute lymphoblastic leukaemia: frequent expression and possible correlation with shorter disease-free survival. Br J Haematol 2004; 127: 392-8.
[285] Park S, Shimizu C, Shimoyama T, *et al*. Gene expression profiling of ATP-binding cassette (ABC) transporters as a predictor of the pathologic response to neoadjuvant chemotherapy in breast cancer patients. Breast Cancer Res Treat 2006; 99: 9-17.
[286] Plasschaert SL, de Bont ES, Boezen M, *et al*. Expression of multidrug resistance-associated proteins predicts prognosis in childhood and adult acute lymphoblastic leukemia. Clin Cancer Res 2005; 11: 8661-8.
[287] Leonessa F, Clarke R. ATP binding cassette transporters and drug resistance in breast cancer. Endocr Relat Cancer 2003; 10:43-73.
[288] Faneyte IF, Kristel PM, Maliepaard M, *et al*. Expression of the breast cancer resistance protein in breast cancer. Clin Cancer Res 2002; 8: 1068-74.
[289] Kanzaki A, Toi M, Nakayama K, *et al*. Expression of multidrug resistance-related transporters in human breast carcinoma. Jpn J Cancer Res 2001; 92: 452-8.
[290] Vaclavikova R, Nordgard SH, Alnaes GI, *et al*. Single nucleotide polymorphisms in the multidrug resistance gene 1 (ABCB1): effects on its expression and clinicopathological characteristics in breast cancer patients. Pharmacogenet Genomics 2008; 18: 263-73.
[291] Ro J, Sahin A, Ro JY, *et al*. Immunohistochemical analysis of P-glycoprotein expression correlated with chemotherapy resistance in locally advanced breast cancer. Hum Pathol 1990; 21: 787-91.
[292] Dexter DW, Reddy RK, Geles KG, *et al*. Quantitative reverse transcriptase-polymerase chain reaction measured expression of MDR1 and MRP in primary breast carcinoma. Clin Cancer Res 1998; 4: 1533-42.
[293] Ito K, Fujimori M, Nakata S, *et al*. Clinical significance of the increased multidrug resistance-associated protein (MRP) gene expression in patients with primary breast cancer. Oncol Res 1998; 10: 99-109.
[294] Nooter K, Brutel de la Riviere G, Look MP, *et al*. The prognostic significance of expression of the multidrug resistance-associated protein (MRP) in primary breast cancer. Br J Cancer 1997; 76: 486-93.
[295] Stacker SA, Achen MG, Jussila L, Baldwin ME, Alitalo K. Lymphangiogenesis and cancer metastasis. Nat Rev Cancer 2002; 2: 573-83.
[296] McGuire WL. Prognostic factors for recurrence and survival in human breast cancer. Breast Cancer Res Treat 1987; 10: 5-9.
[297] Rosen PR, Groshen S, Saigo PE, Kinne DW, Hellman S. A long-term follow-up study of survival in stage I (T1N0M0) and stage II (T1N1M0) breast carcinoma. J Clin Oncol 1989; 7: 355-66.
[298] Hellman S. Karnofsky Memorial Lecture. Natural history of small breast cancers. J Clin Oncol 1994; 12;2229-2234
[299] Zochbauer-Muller S, Filipits M, Rudas M, *et al*. P-glycoprotein and MRP1 expression in axillary lymph node metastases of breast cancer patients. Anticancer Res 2001; 21: 119-24.
[300] Filipits M, Malayeri R, Suchomel RW, *et al*. Expression of the multidrug resistance protein (MRP1) in breast cancer. Anticancer Res 1999; 19: 5043-9.
[301] Schneider J, Gonzalez-Roces S, Pollan M, *et al*. Expression of LRP and MDR1 in locally advanced breast cancer predicts axillary node invasion at the time of rescue mastectomy after induction chemotherapy. Breast Cancer Res 2001; 3: 183-91.
[302] He L, Hao C, Lin B, Wang Y, Gao F. P-glycoprotein expression in primary breast cancer. Chin Med Sci J 1995; 10:12-15.
[303] Sun SS, Hsieh JF, Tsai SC, *et al*. Expression of mediated P-glycoprotein multidrug resistance related to Tc-99m MIBI scintimammography results. Cancer Lett 2000; 153: 95-100.
[304] Schneider J, Romero H. Correlation of P-glycoprotein overexpression and cellular prognostic factors in formalin-fixed, paraffin-embedded tumor samples from breast cancer patients. Anticancer Res 1995; 15:1117-21.
[305] Coleman RE, Rubens RD. The clinical course of bone metastases from breast cancer. Br J Cancer 1987; 55: 61-66.
[306] Esteva FJ, Valero V, Pusztai L, *et al*. Chemotherapy of metastatic breast cancer: what to expect in 2001 and beyond. Oncologist 2001; 6: 133-46.
[307] Harrison KM, Muss HB, Ball MR, Mc. Whorter M, Case D. Spinal cord compression in breast cancer. Cancer 1985; 55: 2839-44.
[308] LoRusso P. Analysis of skeletal-related events in breast cancer and response to therapy. Semin Oncol 2001; 28: 22-7.
[309] Barcena A, Lobato RD, Rivas JJ, *et al*. Spinal metastatic disease: analysis of factors determining functional prognosis and the choice of treatment. Neurosurgery 1984; 15: 820-7.
[310] Bilsky MH, Lis E, Raizer J, Lee H, Boland P. The diagnosis and treatment of metastatic spinal tumor. Oncologist 1999; 4: 459-69.
[311] Jonsson B, Sjostrom L, Olerud C, *et al*. Outcome after limited posterior surgery for thoracic and lumbar spine metastases. Eur Spine J 1996; 5: 36-44.
[312] Jonsson B, Petren-Mallmin M, Jonsson H, Jr., Andreasson I, Rauschning W. Pathoanatomical and radiographic findings in spinal breast cancer metastases. J Spinal Disord 1995; 8: 26-38.
[313] Klekamp J, Samii H. Surgical results for spinal metastases. Acta Neurochir (Wien) 1998; 140: 957-967.
[314] Mercadante S. Malignant bone pain: pathophysiology and treatment. Pain 1997; 69:1-18.
[315] Onimus M, Papin P, Gangloff S. Results of surgical treatment of spinal thoracic and lumbar metastases. Eur Spine J 1996; 5: 407-11.
[316] Verrelle P, Meissonnier F, Fonck Y, *et al*. Clinical relevance of immunohistochemical detection of multidrug resistance P-glycoprotein in breast carcinoma. J Natl Cancer Inst 1991; 83:111-6.

[317] Decker DA, Morris LW, Levine AJ, *et al*. Immunohistochemical analysis of P-glycoprotein expression in breast cancer: clinical correlations. Ann Clin Lab Sci 1995; 25: 52-9.

[318] Charpin C, Vielh P, Duffaud F, *et al*. Quantitative immunocytochemical assays of P-glycoprotein in breast carcinomas: correlation to messenger RNA expression and to immunohistochemical prognostic indicators. J Natl Cancer Inst 1994; 86: 1539-45.

[319] Skliris GP, Leygue E, Watson PH, Murphy LC. Estrogen receptor alpha negative breast cancer patients: estrogen receptor beta as a therapeutic target. J Steroid Biochem Mol Biol 2008; 109: 1-10.

[320] Bieche I, Girault I, Urbain E, Tozlu S, Lidereau R. Relationship between intratumoral expression of genes coding for xenobiotic-metabolizing enzymes and benefit from adjuvant tamoxifen in estrogen receptor alpha-positive postmenopausal breast carcinoma. Breast Cancer Res 2004; 6: R252-63.

[321] Bardou VJ, Arpino G, Elledge RM, Osborne CK, Clark GM. Progesterone receptor status significantly improves outcome prediction over estrogen receptor status alone for adjuvant endocrine therapy in two large breast cancer databases. J Clin Oncol 2003; 21: 1973-9.

[322] Yu KD, Liu GY, Di GH, *et al*. Progesterone receptor status provides predictive value for adjuvant endocrine therapy in older estrogen receptor-positive breast cancer patients. Breast 2007; 16: 307-15.

[323] McKenna NJ, O'Malley BW. Nuclear receptors, coregulators, ligands, and selective receptor modulators: making sense of the patchwork quilt. Ann N Y Acad Sci 2001; 949: 3-5.

[324] Burger H, Foekens JA, Look MP, *et al*. RNA expression of breast cancer resistance protein, lung resistance-related protein, multidrug resistance-associated proteins 1 and 2, and multidrug resistance gene 1 in breast cancer: correlation with chemotherapeutic response. Clin Cancer Res 2003; 9: 827-36.

[325] Koh EH, Chung HC, Lee KB, *et al*. The value of immunohistochemical detection of P-glycoprotein in breast cancer before and after induction chemotherapy. Yonsei Med J 1992; 33:137-42.

[326] Chevillard S, Pouillart P, Beldjord C, *et al*. Sequential assessment of multidrug resistance phenotype and measurement of S-phase fraction as predictive markers of breast cancer response to neoadjuvant chemotherapy. Cancer 1996; 77: 292-300.

[327] Chung HC, Gong SJ, Yoo NC, *et al*. P-glycoprotein as an intermediate end point of drug resistance to neoadjuvant chemotherapy in locally advanced gastric cancer. Yonsei Med J 1996; 37:397-404.

[328] Lizard-Nacol S, Genne P, Coudert B, *et al*. MDR1 and thymidylate synthase (TS) gene expressions in advanced breast cancer: relationships to drug exposure, p53 mutations, and clinical outcome of the patients. Anticancer Res 1999; 19: 3575-81.

[329] Arnal M, Franco N, Fargeot P, *et al*. Enhancement of mdr1 gene expression in normal tissue adjacent to advanced breast cancer. Breast Cancer Res Treat 2000; 61:13-20.

[330] Tolcher AW, Cowan KH, Solomon D, *et al*. Phase I crossover study of paclitaxel with r-verapamil in patients with metastatic breast cancer. J Clin Oncol 1996; 14: 1173-84.

[331] Park S, Shimizu C, Shimoyama T, *et al*. Gene expression profiling of ATP-binding cassette (ABC) transporters as a predictor of the pathologic response to neoadjuvant chemotherapy in breast cancer patients. Breast Cancer Res Treat 2006.

[332] Filipits M, Pohl G, Rudas M, *et al*. Clinical role of multidrug resistance protein 1 expression in chemotherapy resistance in early-stage breast cancer: the Austrian Breast and Colorectal Cancer Study Group. J Clin Oncol 2005; 23: 1161-8.

[333] Lal S, Wong ZW, Sandanaraj E, *et al*. Influence of ABCB1 and ABCG2 polymorphisms on doxorubicin disposition in Asian breast cancer patients. Cancer Sci 2008; 99: 816-23.

[334] Johnston SR. Acquired tamoxifen resistance in human breast cancer--potential mechanisms and clinical implications. Anticancer Drugs 1997; 8: 911-30.

[335] Keen JC, Miller EP, Bellamy C, Dixon JM, Miller WR. P-glycoprotein and resistance to tamoxifen. Lancet 1994; 343: 1047-8.

[336] Ma XJ, Wang Z, Ryan PD, *et al*. A two-gene expression ratio predicts clinical outcome in breast cancer patients treated with tamoxifen. Cancer Cell 2004; 5: 607-16.

II. REGULATION DE L'EXPRESSION D'ABCC11 PAR LES ŒSTROGENES

L'expression d'ABCC11 dans le tissu mammaire et le fait qu'elle transporte certains médicaments utilisés dans les cancers du sein (métabolites du 5FU et méthotrexate) nous ont conduits à étudier la régulation d'ABCC11 par les œstrogènes. Aucune donnée n'existant à ce sujet, nous avons décidé d'analyser l'influence de ces antagonistes sur l'expression d'ABCC11 et l'expression d'ABCC11 basale dans les tumeurs du sein ER positives et négatives.

→ Publication 3. « **ABCC11 expression is regulated by estrogen in MCF7 cells, correlated with estrogen receptor α expression in postmenopausal breast tumors and overexpressed in tamoxifen-resistant breast cancer cells** » par M. Honorat et coll.

Article publié dans Endocrine Related Cancer (2008)

Nous avons ainsi démontré que les œstradiols (E2) régulent de manière négative l'expression en ARN ABCC11, dans des cellules MCF7 (carcinome mammaire) exprimant le récepteur aux œstrogènes (ER). Cette régulation est inhibée par des antagonistes d'E2 : l'ICI 182 780 et le tamoxifène. De plus, au sein de tumeurs de patientes post-ménopausées, l'expression d'ABCC11 a été corrélée de manière positive avec l'expression d'ERα.

En parallèle, l'expression d'ABCC11 s'est montrée positivement régulée par l'exposition des MCF7 au tamoxifène. Dans des lignées cellulaires résistantes au tamoxifène, une surexpression d'ABCC11 a même été observée. Ces mêmes cellules montrent une résistance au 5-FluoroUracil dont le métabolite actif (5FdUMP) est transporté par ABCC11.

Ainsi, la surexpression d'ABCC11, au sein de cancers du sein ER positif, pourrait contribuer à une diminution de la sensibilité aux chimiothérapies à base de substrats d'ABCC11. De même, le traitement de ces tumeurs par le tamoxifène diminuerait cette sensibilité en augmentant l'expression d'ABCC11 et donc l'efflux de ses substrats anticancéreux.

Endocrine-Related Cancer (2008) **15** 125–138

ABCC11 expression is regulated by estrogen in MCF7 cells, correlated with estrogen receptor α expression in postmenopausal breast tumors and overexpressed in tamoxifen-resistant breast cancer cells

Mylène Honorat[1,2,3], Aurelia Mesnier[1,2,3], Julie Vendrell[1,2,3], Jérôme Guitton[1,4,5], Ivan Bieche[6,7], Rosette Lidereau[6,7], Gary D Kruh[8], Charles Dumontet[1,2,3], Pascale Cohen[1,2,3] and Lea Payen[1,2,3,4]

[1]Université de Lyon, Lyon1, ISPB, Lyon F-69008, France
[2]Inserm, U590, Lyon F-69008, France
[3]Centre Léon Bérard, FNCLCC, Lyon F-69008, France
[4]Laboratoire de Toxicologie, Faculté de Pharmacie, Université de Lyon, Lyon F-69008, France
[5]Laboratoire de Ciblage Thérapeutique en Cancérologie, Hospices Civils de Lyon, Centre Hospitalier Lyon-Sud, Pierre Bénite F-69495, France
[6]Centre René Huguenin, FNCLCC, St-Cloud F-92210, France
[7]Inserm, U735, St-Cloud F-92210, France
[8]University of Illinois at Chicago Cancer Center, 239 Medical Center Administration Building (MC700), 914 South Wood Street, Chicago, Illinois 60612, USA

(Correspondence should be addressed to L Payen, INSERM U590, Laboratoire de Cytologie Analytique, Institut des Sciences Biologiques et Pharmaceutiques (ISPB) 8, Avenue Rockefeller, 69008 Lyon, France;
Email: lea.payen@recherche.univ-lyon1.fr)

M Honorat and A Mesnier contributed equally to this work

Abstract

ABCC11 (Multidrug resistance protein 8; MRP8), a plasma membrane ATP-binding cassette transporter, has been implicated in drug resistance of breast cancer by virtue of its ability to confer resistance to fluoropyrimidines and to efflux methotrexate, and by its expression in this tumor. Expression of ABCC11 in breast, a hormonally regulated tissue, as well as the pump's ability to transport estrogen conjugates, suggest the possibility that expression of ABCC11 may be susceptible to regulation by estrogen. However, nothing is currently known about regulation of this gene. In this study, estradiol (E_2) treatment reduced expression of ABCC11 mRNA in estrogen receptor (ER)-α-positive MCF7 cells, and E_2 antagonists such as ICI 182 780 and tamoxifen (TAM) abrogated E_2-mediated downregulation. ABCC11 expression was positively correlated with ER-α expression in both breast cell lines, and two independent series of tumors from postmenopausal patients. In addition, expression of ABCC11 was upregulated in MCF7 cells exposed to TAM for 72 h, and was overexpressed in TAM-resistant cell lines. Drug sensitivity analysis of the TAM-resistant cells indicated that they were also resistant to 5-fluorouracil (5-FU), consistent with the reported ability of ABCC11 to confer resistance to this agent. These studies indicate that ABCC11 expression is negatively regulated by E_2, but that ABCC11 expression is high in high-expressing ER-α breast cancers. Our findings support the notion that expression of ABCC11 in ER-α-positive breast cancers may contribute to decreased sensitivity to chemotherapy combinations that include 5-FU. ABCC11 may be a potential predictive tool in the choice of anticancer therapies in ER-positive breast cancers resistant to TAM.

Endocrine-Related Cancer (2008) **15** 125–138

Endocrine-Related Cancer (2008) **15** 125–138
1351–0088/08/015–125 © 2008 Society for Endocrinology *Printed in Great Britain*
DOI: 10.1677/ERC-07-0189
Online version via http://www.endocrinology-journals.org

Introduction

Breast cancer is a complex and heterogeneous disease, with a range of overlapping clinical phenotypes with significant variations in prognosis and outcome. Histological type, grade, lymph node involvement, and estrogen receptor (ER) status influence prognosis and the probability of response to therapies. ER-positive breast cancers are responsive to endocrine therapies, such as the selective ER modulator (SERM), OH-tamoxifen (TAM), and the pure antagonist ICI 182 720 (fulvestrant; Howell 2006). However, almost all responding patients acquire resistance to TAM. Several mechanisms for this phenomenon have been suggested, including alteration of the availability or metabolism of TAM, alterations in the function of the ER-α and in the ER-α signaling cascade, and alterations in growth factor signaling pathways (MAPK, AKT; Dorssers *et al.* 2001, Acconcia & Kumar 2006, Girault *et al.* 2006, Milano *et al.* 2006). Treatment with cytotoxic chemotherapy is employed for patients with ER-negative and ER-positive hormone-refractory breast cancers. Standard agents include cyclophosphamide, methotrexate, vinca alkaloids anthracyclines, taxanes, and 5-fluorouracil (5-FU), with the latter agent recently assuming a larger role as a result of the availability of congeners that can be orally administered.

One of the mechanisms of drug resistance in cancer cells is increased efflux mediated by members of the ATP-binding cassette (ABC) family. Numerous studies have been conducted on expression of ABCB1 (multidrug resistance, MDR1/P-glycoprotein (P-gp)), ABCC1 (Multidrug resistance associated protein 1 MRP1), and ABCG2 (breast cancer resistance protein; BCRP) in breast cancers (Burger *et al.* 2003, Larkin *et al.* 2004). Recently, another ABC transporter, ABCC11 (Multidrug resistance protein 8; MRP8) has been implicated as a resistance factor in breast cancer (Park *et al.* 2006, Kruh *et al.* 2007). ABCC11 transcript has been reported to be expressed in normal mammary tissue, in breast cancer cell lines and in breast tumors, as well as in liver and brain (Bera *et al.* 2001, Annereau *et al.* 2004, Bieche *et al.* 2004, Bortfeld *et al.* 2006). In addition, ectopic expression of ABCC11 is *in vitro* able to confer resistance to fluoropyrimidines, a class of agents that is widely employed in treating breast cancer (Guo *et al.* 2003, Oguri *et al.* 2007). This capability is attributable to ABCC11-mediated efflux of 5-FdUMP, the toxic intracellular metabolite of fluoropyrimidines. ABCC11 is also able to transport methotrexate (Chen *et al.* 2005), another agent that is employed in the treatment of breast cancer. The involvement of ABCC11 may also extend to physiological compounds that effluxed by this transporter in that notable physiological substrates of the pump include glucuronate and sulfate steroid conjugates, such as estradiol-17-β-D-glucoronide ($E_2$17βG), desulfate estrone 1-sulfate (E1S), and dehydroepiandrosterone sulfate (DHEAS) (Chen *et al.* 2005). These resistance and transport activities, in combination with expression of ABCC11 in breast, a hormonally regulated tissue, suggest the possibility that expression of ABCC11 may be susceptible to regulation by estrogen. Were this the case, it could have important implications for treating breast cancer. However, nothing is currently known about regulation of expression of this gene. Here, we analyzed *in vitro* the effect of estrogen on ABCC11 expression and evaluated the relationship between ABCC11 expression levels and ER-α expression in breast cancer cell lines and tumor samples from postmenopausal patients.

Our results show that ABCC11 is negatively regulated by estradiol (E_2) and that ABCC11 mRNA levels are increased in high-expressing ER-α breast cancers from independent series of tumors. In a first step, we used series A of tumors ('training set') including 60 primary tumors collected from postmenopausal women at the Pathology Department of Val d'Aurelle Cancer Center (Montpellier, France). Our independent collaborator (Dr I Bieche, Paris) validated our observations, in two independent series B and C ('validation sets') obtained from women at a second institution (Centre René Huguenin, St-Cloud, France).

In addition, ABCC11 is overexpressed in a cell line made resistant to TAM, and this overexpression is associated with increased resistance to 5-FU. These findings suggest that, in ER-positive breast cancers, ABCC11 may contribute to decreased sensitivity to chemotherapy combinations containing 5-FU and that its expression may be a predictive tool in the choice of anticancer therapies.

Materials and methods

Materials and chemicals

5-FU, 5-FdURD, E_2, MK571, and TAM were purchased from Sigma. 7a,17b-[9-[(4,4,5,5,5-pentafluoropentyl)-sulfinyl]-nonyl]-estra-1,3,5(10)-triene-3,17-diol (ICI 182 780) from Tocris Cookson Inc. (Ellisville, MO, USA) was kindly provided by Pr P Cohen (UMR 590 Lyon). HCl was purchased from Merck. TRIZol RNA extraction kit, murine Moloney leukemia virus reverse transcriptase (MMLV), Taq DNA polymerase and complete high-glucose Dulbecco's modified Eagle's medium (DMEM), L-glutamine, and

penicillin–streptomycin were manufactured by Gibco, and fetal bovine sera (FBS) from PAN Biotech GmbH (Aidenbach, Germany).

Cell culture

The six ER-α-positive (MCF7, ZR 7530, UACC 818, ZR 751, T47D, and BT474) and the six ER-negative (MDA MB 453, BT20, SK BR3, MDA MB 435, MDA MB 175, and MDA MB 231) breast cell lines were grown according to the ATCC's (Type Culture Collection) recommendations.

To avoid interferences by steroids present in classical media, cell lines were first purged for 4 days in DMEM without phenol red and supplemented with 3% steroid-depleted, dextran-coated charcoal-treated fetal calf serum (DCC medium). Then to study the response of MCF7 cells to E_2, TAM, and ICI 182 780, the cells were supplemented with specific steroids under the following pharmacological conditions: steroid-depleted medium (vehicle), 10^{-9} M E_2, 2×10^{-7} M TAM, or 10^{-7} M ICI 182 780. No effects of the vehicle on cell viability and ABCC11 mRNA expression were observed at these concentration.

MVLN cells are an ER-α-positive cells derived from MCF7 cells (Demirpence *et al.* 1993). Isolation of clones from TAM-treated MVLN cells was done after treatment with 10^{-7} M TAM in DCC medium (Badia *et al.* 2000). Using a cell growth assay, the DNA content of 10^{-7} M TAM- and 10^{-9} M E_2-treated-resistant clones was two and fourfold higher (Badia *et al.* 2000) respectively than that of cells grown in DCC medium. Conversely, in parental MVLN cells, TAM inhibited cell proliferation by half (Badia *et al.* 2000). Furthermore, Vendrell *et al.* (2005) carried out TAM dose–response experiments to measure the concentration giving rise to a 50% reduction in cellular viability (IC50 values). These data have been demonstrated on several TAM-resistant cellular clones selected from MVLN. These TAM-resistant cells are kindly provided by Prof P Cohen (Inserm, U590, Lyon F-69008, France).

Breast samples

All experimental procedures complied with French laws and regulations and were approved by the National Ethics Committee. Sixty primary tumors from patients with no therapy prior to surgery were collected from postmenopausal women at the Pathology Department of Val d'Aurelle Cancer Center (Montpellier, France; series A). The malignancy of infiltrating carcinomas was scored according to the histopronostic system of Scarff–Bloom–Richardson (Bloom & Richardson 1957). The high expression of ER-α was determined by a real-time quantitative PCR (QRT-PCR) assay and confirmed in most of the case at the protein level by a radioligand-binding assay (with a cut-off level for positively set at 10 fmoles/mg protein according to the WHO typing system). For RNA extraction, breast tumors were disrupted with a tissue grinder under liquid nitrogen.

To confirm the inter-relationship between mRNA level of ABCC11 and ER-α expression levels, we also analyzed an independent set of tumors from an independent series of 42 primary breast tumors (series B; 21 ER-negative and 21 ER-positive tumors) excised from women at a second institution (Centre René Huguenin, St-Cloud, France).

Finally, to investigate the relationship between mRNA levels of ABCC11 during breast cancer progression, we analyzed tumor RNA of 10 normal breast tissues, 12 benign breast tumors, 11 invasive ductal grade I breast tumors, 30 invasive ductal grade II breast tumors, 32 invasive ductal grade III breast tumors, and 14 distant metastasis (series C).

Quantitative real-time (QRT)-PCR

Total mRNA was extracted using TRIZol method (Jordheim *et al.* 2004) and QRT-PCR was performed in a Lightcycler (Roche) in combination with the Light-Cycler Faststart DNA Master Sybr Green I (Roche). cDNA reverse transcription was performed on 1 μg total RNA with MMLV reverse transcriptase and 0.5 μg hexamer according to the manufacturer's instructions. The primer pairs for ABCC11 were 5′-GTCTGGGTTCTCATCCACACATCC-3′ (forward), 5′-CCAGAGCTTTGCTGGGGTCTTGTA-3′ (reverse). The thermal cycling conditions comprised an initial denaturation step at 95 °C for 8 min, and 50 cycles at 95 °C for 15 s and 63 °C for 7 s and 72 °C for 15 s. A specific set of gene primers including PNR2/PS2 (estrogen inducible protein) and ESR1/ER-α (estrogen receptor alpha) primers was described in Vendrell *et al.* (2005). For each set of primers, a standard curve was made with serial dilutions from a control cDNA sample in order to evaluate the efficiency of the primers and to relatively quantify the expression level of each sample. All measurements were normalized to the expression of the 18S or 28S ribosomal genes, considered as stable housekeeping genes (Applied Biosystems).

For the independent series B and C, ABCC11 expression was quantified using a validated and independent method developed by Dr I Bieche (Tozlu *et al.* 2006). The increase in fluorescent signal associated with exponential growth of PCR products is detected by the laser detector of the ABI Prism 7900

Sequence Detection System (Perkin–Elmer Applied Biosystems, Foster City, CA, USA), using PE Biosystems analysis software according to the manufacturer's manuals. All PCRs were performed using an ABI Prism 7900 Sequence Detection System, the SYBR Green PCR Core Reagents kit (Perkin–Elmer Applied Biosystems; Bieche *et al.* 2004). The thermal cycling conditions comprised an initial denaturation step at 95 °C for 10 min, and 50 cycles at 95 °C for 15 s, and 65 °C for 1 min. Results, expressed as n-fold differences in target gene expression relative to the TATA box-binding protein (*TBP*) gene (termed 'N_{target}'), were determined by the formula:

$$N_{target} = 2^{\Delta C_{t\ sample}},$$

where the ΔC_t value of the sample was determined by subtracting the average C_t value of the target gene from the average C_t value of the *TBP* gene. The N_{target} values of the samples were subsequently normalized such that the mean of the N_{target} values of the normal breast samples would equal a value of 1.

Immunoblotting

SDS-PAGE of crude membrane proteins was carried out using 8% acrylamide gels. Proteins (150 µg) were transferred to poly vinylidine difloride (PDVF) membranes (Millipore, Bedford, MA, USA) using 25 mM Tris-base, 192 mM glycine, and 20% methanol buffer. ABCC11 polypeptides were detected using an enhanced chemiluminescence kit (Amersham) and the ABCC11 polyclonal antibody (Santa Cruz Biotechnology, Heidelburg, Germany). Various polypeptide amounts were estimated by comparison with cell-expressed positive and negative control cell lines (pCDNA3 HEK293T and ABCC11 HEK293T cells) loaded using the same conditions. Equal protein loading was confirmed by α-tubulin immunoblotting of the PDVF membrane. Densitometry of the film images was performed using ImageJ software (National Institutes of Health, http://rsb.info.nih.gov/ij/). The relative protein expression levels were calculated by dividing the integrated densitometry values obtained for 150 µg total membrane protein from E_2-treated cells by the integrated densitometry value obtained for the comparable amounts of total membrane proteins from vehicle-treated cells. Each comparison was performed three times in independent experiments.

Cytotoxicity assays

MCF7 cells were plated at 5000 cells per well in 96-well plates (Becton Dickinson, San Jose, CA, USA) in a volume of 100 µl and incubated for 24 h at 37 °C before 100 µl medium containing different drug concentrations was added. The cytotoxicity assay was carried out as described in Jordheim *et al.* (2004).

5-FdUMP efflux assays

Based on specific ABCC11 capability to transport 5-FdUMP and endogenous nucleosides (AMPc and GMPc), we developed an assay for the quantification of 5-FdUMP using high-performance liquid chromatography coupled to mass spectrometry (HPLC-MS/MS). This approach has two great advantages: 1) it quantified specifically and sensitively various metabolites of 5-FU and 2) in contrast to several fluorescent substrates which are substrate of various ABCC proteins, 5-FdUMP is restricted substrate to ABCC5 and ABCC11 (Guo *et al.* 2003, Pratt *et al.* 2005). Analysis of 5-FdUMP efflux has, however, been shown to permit evaluation of ABCC11 activity in transfected cells with ABCC11 cDNA that do not overexpress other MDR transporter in comparison with parental cell line (Guo *et al.* 2003, Oguri *et al.* 2007).

Cells were first loaded with 100 µM 5-FdURD in the DMEM (without FBS) for 15 min at 37 °C. During this uptake period, 5-FdURD, a metabolite of 5-FU, is metabolized into 5-FdUMP by thymidylate kinase into cells (Parker & Cheng 1990). After washing three times with ice-cold PBS, conditions which inhibit all active transport, intracellular 5-FdUMP accumulation was quantified by HPLC MS/MS in an aliquot of cells.

To quantify 5-FdUMP efflux, cells were then re-incubated at 37 °C in 5-FdURD-free medium for 15 min. The representative transport function of ABCC11 is shown in aliquots of efflux medium, thus making it possible to directly investigate secretion of 5-FdUMP in the medium in the presence or absence of specific and well-known inhibitor of ABCC11 transport activity (MK571). To carry out HPLC analysis, these cells were lysed in 500 µl of pure methanol, then the samples were centrifuged at 20000 ***g*** (14 000 rpm). for 2 min. The supernatants were evaporated under a stream of nitrogen and residues were resuspended in water solution before injection in HPLC device. 5-chlorouracil was used as internal standard. Results were normalized to cellular protein content (Bradford assay) determined in parallel using Bio-Rad assay.

Statistical analysis

Data were analyzed for statistical significance using Mann–Whitney's test, Spearman's test, or Student's

t-test. Differences with P values of <0.05 were considered statistically significant.

Results

ABCC11 expression is regulated by estrogen

The effect of estrogen on ABCC11 expression in ER-α-positive MCF7 cells was analyzed by exposing cells to 1 nM E_2 and measuring ABCC11 transcript by QRT-PCR. As a positive control for these experiments, *PNR2/PS2*, a gene whose expression is known to be upregulated by E_2, was used (Berry *et al.* 1989). PNR2/PS2 mRNA levels were increased approximately fourfold, with maximal induction observed as early as 6 h (Fig. 1). By contrast with PNR2/PS2, ABCC11 expression levels decreased as a result of treatment with E_2. ABCC11 expression was not altered after 6 h exposure to E_2 (Fig. 1), whereas maximal repression was achieved after 24 h of exposure. In contrast to the effect of E_2 on ABCC11 expression in MCF7 cells, estrogen treatment did not affect expression of ABCC11 in ER-α-negative MDA MB 231 cells (Fig. 1).

In breast tissue, TAM and ICI 182 780 antagonize E_2-mediated gene regulation by binding to ER-α. As expected, PNR2/PS2 upregulation by E_2 was abrogated by 100 nM ICI 182 780 and 200 nM TAM (Fig. 2).

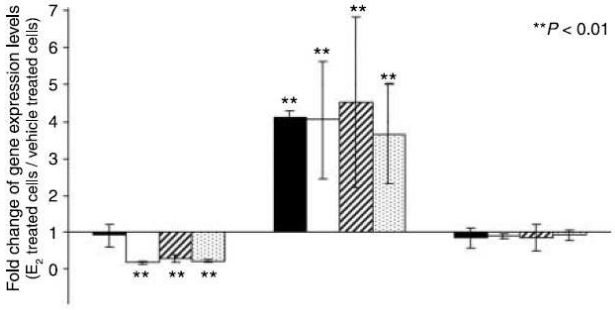

	ABCC11	PNR2/PS2	ABCC11
■ 6 h	0.92	4.13	0.84
□ 26 h	0.18	4.05	0.89
▨ 46 h	0.29	4.52	0.85
▨ 72 h	0.22	3.67	0.92
	MCF7 cells (ER alpha positive)		MDA MB 231 cells (ER alpha negative)

Figure 1 Effect of E_2 on expression of ABCC11 transcript in MCF7 (ER-α-positive) and MDA MB 231 (ER-α-negative) cell lines. Cells were exposed to 1 nM E_2 for 6–72 h, and ABCC11 transcript levels were measured by QRT-PCR at various time points. As a positive control for E_2 effect, PNR2/PS2 transcript levels were also measured. Fold change (mean values were indicated below the figure) of mRNA levels was quantitated as described in Materials and methods. The QRT-PCR values indicated below are means ± S.E.M. of at least three independent experiments. $^{**}P<0.01$; Student's *t*-test.

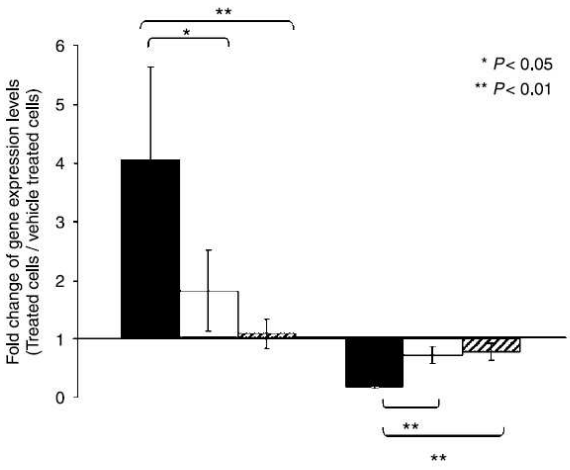

	PNR2/PS2	ABCC11
■ E_2	4.05	0.18
□ OH-TAM / E_2	1.84	0.74
▨ ICI 182 780 / E_2	1.10	0.79

Figure 2 Effect of estrogen receptor antagonists on E_2-mediated repression of ABCC11 transcript. MCF7 cells were exposed to 1 nM E_2 for 24 h, and ABCC11 transcript levels were measured by QRT-PCR. As a positive control for antagonist effect, PNR2/PS2 transcript levels were also measured. Fold change (mean values were indicated below the figure) of mRNA levels was quantitated as described in Materials and methods. The QRT-PCR values indicated below are means ± S.E.M. of at least three independent experiments. $^{*}P<0.05$; $^{**}P<0.01$; Student's *t*-test.

Under the same conditions, these agents abrogated E_2-mediated downregulation of ABCC11 expression (Fig. 2).

Crude membrane fractions were further carried out from MCF7 cells exposed to 1 nM E_2 for 72 h (Fig. 3). The expression of the ABCC11 protein was analyzed by immunoblotting. The affinity-purified ABCC11 antibody, which is directed against amino acids 929–1144 of the human ABCC11 protein, detected a glycoprotein of ~150 kDa in both samples (Fig. 3). Under our experimental conditions, additional bands below 150 kDa, probably due to proteolytic degradation of ABCC11, were also detected in HEK293T cells transfected with pCDNA3 ABCC11 vector (Fig. 3A). Similar observations had been described by Bortfeld *et al.* (2006). Analysis of the immunoblots revealed that in MCF7 cells, E_2 slightly decreased ABCC11 protein expression compared with the vehicle control (Fig. 3B).

Expression of ABCC11 mRNA is correlated with expression of ER-α and ERBB2

Based upon the observation that ABCC11 expression is repressed *in vitro* by E_2, we next evaluated whether there was a correlation between ABCC11 and ER-α

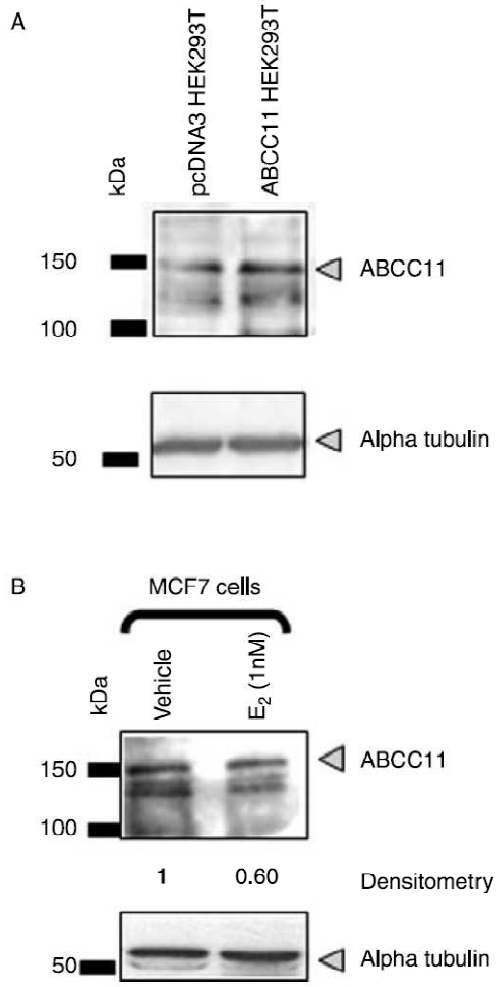

Figure 3 (A) Basal expression of ABCC11 in HEK293T-transfected cells with ABCC11 expression vector. Crude membranes (150 μg) of HEK293T-transfected cells with ABCC11 or empty vector pCDNA3 were transferred onto PDVF sheet. After incubation with ABCC11 antibody, the blot was developed as described in Materials and methods. Equal protein loading was confirmed by α-tubulin immunoblotting of the PDVF membrane and is shown below the blot. (B) ABCC11 western blot analysis of crude membrane proteins treated by E_2. Crude membrane fractions were prepared from MCF7-treated cells exposed to vehicle or 1 nM E_2 for 72 h. Crude membranes (150 μg) were transferred onto PDVF sheet after electrophoresis. After incubation with ABCC11 antibody, the blot was developed as described in Materials and methods. Equal protein loading was confirmed by α-tubulin immunoblotting of the PDVF membrane and is shown below the blot.

expression in breast cancer cell lines. ABCC11 expression was analyzed in six ER-α-positive (MCF7, ZR 7530, UACC 818, ZR 751, T47D, and BT474) and six ER-α-negative (MDA MB 453, BT20, SK BR3, MDA MB 435, MDA MB 175, and MDA MB 231) cancer cells. We applied the non-parametric Mann–Whitney's test, the raw data from ER-α-negative cell lines and ER-α-positive cell lines, were first be combined into a set of N cell lines, which were then ranked from ER-α expression status. ABCC11 mRNA expression was significantly higher ($P=0.0021$; Mann–Whitney's test) in ER-α-positive cells than in ER-α-negative cells (Fig. 4).

We next sought to determine whether there was a correlation between ABCC11 and ER-α in breast cancer samples. To accomplish this, ABCC11 expression was analyzed in primary breast tumors excised from 60 postmenopausal women. The samples were classified into subgroups according to gene expression levels (ER-α, ERBB2, PNR2/PS2, and ER-β), age, tumor size, and histological grade. ER-α expression was measured by QRT-PCR, and the cut off was the median of the total population. Significantly higher levels of ABCC11 mRNA in ER-α high-expressing tumors compared with those in ER-α low-expressing cancer samples were observed ($P=0.003$; Mann–Whitney's test; Table 1). The expression levels of *ABCC11* in the ER high-expressing group were approximately sevenfold higher than in ER low-expressing group. We observed a significant positive correlation between the mRNA levels of ABCC11 and ER-α levels (Spearman's rank correlation coefficient $=0.341$; $P=0.007$; Table 1). ABCC11 expression also correlated with high PNR2/PS2 and ERBB2 expression levels while it did not correlate with expression of ER-β (Table 1).

Furthermore, in tumors with low ERBB2 expression ($n=47$, the chosen cut off was 2.5-fold the median value, this group represented 73% total tumors), ABCC11 expression levels correlated with ER-α expression levels (Spearman's rank correlation coefficient $=0.46$; $P=0.0011$). In ERBB2 low-expressing group, the correlation between ABCC11 and ER-α was likely independent of ERBB2 expression. A high correlation between ERBB2 and ABCC11 expression was also found in the low ER-α expressing group ($n=30$, Spearman's rank correlation coefficient $=0.676$; $P=0.00004$). We observed no correlation between ER-α and ERBB2 expression in the small size of our set of tumors A ($n=60$; data not shown).

In an independent set of 42 patients (tumor series B), included ER-α-positive and -negative tumors, we found a significant positive correlation between ABCC11 and ER-α status (median $=2.3$; $P=0.0077$ with Mann–Whitney's test, Spearman's rank correlation coefficient $=0.32$; $P=0.03$). Furthermore, the correlation between ABCC11 and ER-α expression in patient with low-expressing ERBB2 was confirmed ($n=32$, $P<10^{-5}$ with Mann–Whitney's test, Spearman's rank correlation coefficient $=0.57$; $P=0.0005$) and ABCC11 and ERBB2 correlation was also confirmed in patient

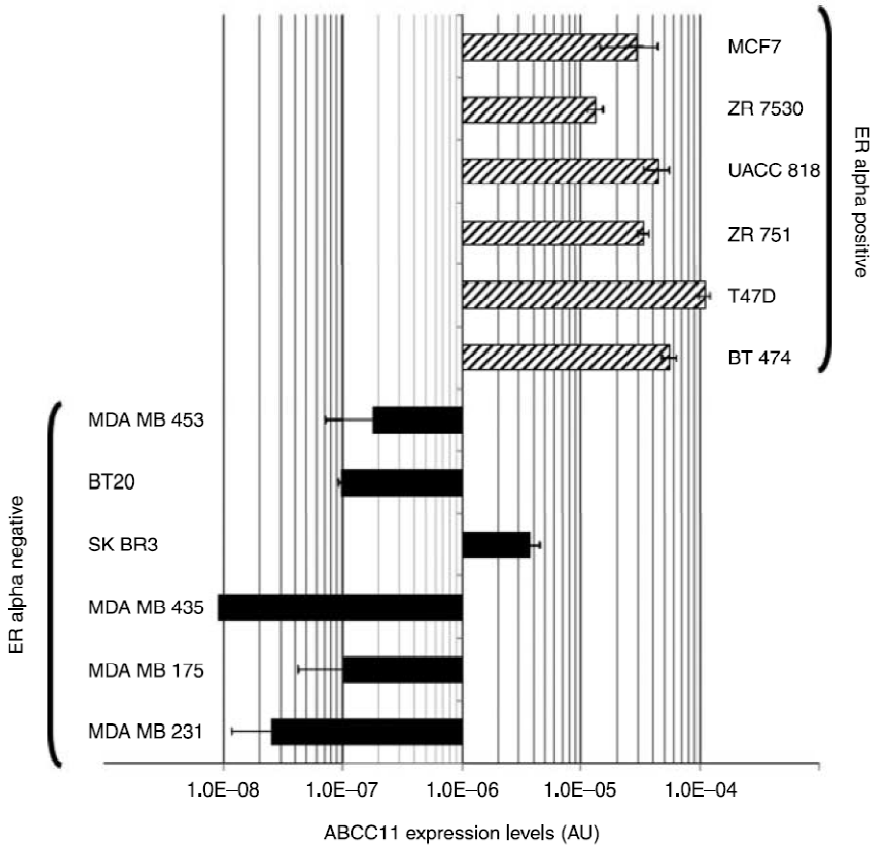

Figure 4 Expression of ABCC11 in breast cancer cell lines. ABCC11 transcript levels were measured by QRT-PCR in various ER-α-positive or -negative breast cancer cell lines. mRNA levels are expressed as arbitrary PCR units (AU) as described in Materials and methods. The QRT-PCR values indicated below are means ± S.E.M. of at least three experiments; *y* is a logarithmic scale.

with low-expressing ER-α ($n=21$, Spearman's rank correlation coefficient = 0.66; $P=0.0009$).

In tumor series B, we compared ABCC11 levels between various tumors with normal tissues. The median of ABCC11 expression was 1.0 (range 0.14–10.87), 0.06 (range 0.01–186.33), and 3.55 (range 0.05–42.42) respectively in 6 normal breast tissues, 21 ER-negative tumors, and 21 ER-positive tumors. There was a trend towards respectively lower and higher ABCC11 levels in ER-α-negative and α-positive breast tumors, in comparison with normal breast samples.

Furthermore, in tumor series A, we also observed that ABCC11 expression levels were significantly lower in tumors with histological grade III compared with grade II ($P=0.003$ with Mann–Whitney's test; Table 2) and large tumor size ($P=0.005$ with Mann–Whitney's test; Table 2). We suggest that the correlation was directly related to the high proportion of tumors with ER-α high-expressing tumors in grade II subgroup compared the weak proportion of ER-α high-expressing tumors in grade III subgroup. A positive correlation was also found for tumor size (Spearman's rank correlation coefficient = 0.507; $P=0.013$; Table 1). However, tumor size information was only available for 23 patients, essentially with high expression levels of ER-α. No correlation was found with age or the presence or absence of nodal involvement (Table 2).

To further evaluate the role of ABCC11 during the breast cancer progression, the expression of ABCC11 was analyzed in normal breast tissues, benign breast tumors, invasive ductal grade I breast tumors, invasive ductal grade II breast tumors, invasive ductal grade III breast tumors, and distant metastasis (series C). ABCC11 expression increased gradually from normal breast tissue to benign tumors, grade I and II invasive ductal tumors; then decreased in the grade III tumors (twofold in comparison with histological grade II tumors) and in metastatic tumors (30-fold decrease; Table 2). The expression level of ABCC11 was respectively increased (by ~14-fold) and slightly decreased in grade III tumors and metastatic tumors compared with normal tissue (Table 2). In this independent series C, a trend towards increased ABCC11 expression in grade II tumors compared with

Table 1 (A) Relationships between ABCC11 mRNA expression with expression of estrogen receptor (ER)-α, ER-β, ERBB2, and PNR2/PS2 in breast tumors from postmenopausal patients. Expressions of ABCC11, ER-α, ER-β, ERBB2, and PNR2/PS2 were measured by QRT-PCR in a collection of primary breast cancer samples from postmenopausal patients. (B) Correlation between ABCC11 expression with ER-α, PNR2/PS2, ER-β, and ERBB2 expression levels, or tumor size in breast tumors from postmenopausal patients

		ABCC11 mRNA expression[a]	
	Number of patients (n=)	Median	*P* value[b]
(A)			
ER-α expression[a,c]			
>4.1	30	15.59 range (0.59–289.69)	0.003
<4.1	30	2.22 range (0.12–354.45)	
ER-β expression[a,c]			
>0.66	30	3.43 range (0.13–289.69)	0.17 (NS)
<0.66	30	9.16 range (0.12–354.45)	
PNR2/PS2 expression[a,c]			
>0.59	29	15.15 range (0.66–289.69)	0.002
<0.59	31	2.22 range (0.12–354.45)	
ERBB2 expression[a,d]			
>2.5	13	89.82 range (4.44–354.45)	0.001
<2.5	47	5.58 range (0.12–289.69)	

		ABCC11 mRNA expression		
	Number of patients (n=)	Spearman	*t*(*N*-2)	*P* value[b]
(B)				
ER-α expression[a]	60	0.341	2.767	0.007
PNR2/PS2 expression[a]	60	0.427	3.596	0.0006
ER-β expression[a]	60	−0.043	−0.326	0.74 (NS)
ERBB2 expression[a]	60	0.552	5.047	<0.0001
Age (56–86)[e]	25	−0.207	−1.017	0.31 (NS)
Tumor size[f]	23	0.507	2.697	0.013

$P<0.05$ was considered significant (Spearman's test).
[a]QRT-PCR expression levels.
[b]*P* values were considered statistically significant if $P<0.05$.
[c]The median value was chosen as the cut off.
[d]2.5-*X* median value was selected as the cut off.
[e]Information only available for 25 patients.
[f]Information only available for 23 patients.

grade III was confirmed. The strong decrease of ABCC11 expression in metastatic tissue may be partially due to the weaker proportion of ER-α-positive tumors compared with ER-α-negative tumors (data not shown).

ABCC11 upregulation by TAM in MCF7 cells and ABCC11 overexpression in TAM-resistant breast cancer cells

As patients with ER-α-positive breast tumors are typically treated with ER antagonists such as TAM, we studied the effect of this agent on ABCC11 expression levels in MCF7 cells. Interestingly, treatment with 200 nM TAM for 72 h increased ABCC11 mRNA levels by twofold (no effect was observed after 24 h; Fig. 5A).

To explore the possible correlation between TAM resistance and expression of ABCC11 in ER-α-positive cells, we analyzed ABCC11 levels in CL6.7 ER-α-positive TAM-resistant cell line derived by growth of MVLN cells for 6 months (Badia *et al*. 2000, Vendrell *et al*. 2005) and described in Materials and methods. Significant increase in ABCC11 expression was observed in CL6.7 cells compared with MVLN parental cells. In contrast, the expression of ABCC5, another MRP family member that is able to confer resistance to 5-FU was not increased (Fig. 5B).

During the 72 h incubation, 5-FdURD, a metabolite of 5-FU, is metabolized into 5-FdUMP by thymidylate kinase into cells. This metabolite inhibits the thymidylate synthase (anticancer properties). According to the literature, 5-FdUMP is secreted by ABCC11 in the

Table 2 (A) Relationships between ABCC11 expression with patient age, grade, size, and nodal involvement of breast tumors from postmenopausal patients. (B) Relationships between ABCC11 expression with the grade in series C

		ABCC11 mRNA expression	
Clinical status	**Number of patients** ($n=$)	**Median**	***P* value**[a]
(A)			
Histological grade			
II	31	15.16	0.003
III	26	2.22	
Age (56–86)[b]			
>68	11	7.23	0.31 (NS)
<68	14	13.76	
Tumor size[c]			
>20	13	20.61	0.005
<20	10	6.41	
Nodes[d]			
A-NbggEnv >1	9	10.84	0.48 (NS)
A-NbggEnv=00	15	20.23	

		ABCC11 mRNA expression	
Clinical status	**Number of patients** ($n=$)	**Median**	***P* value**[a] **(Histological class/-grade II)**
(B)			
Normal	10	1.00 range (0.70–22.34)	0.0089
Benign breast tumors	12	6.20 range (0.23–395.79)	0.43 (NS)
Grade I	11	13.70 range (0.63–98.28)	0.4 (NS)
Grade II	30	25.96 range (0.1–966.51)	–
Grade III	32	14.80 range (0.04–897.14)	0.34 (NS)
Metastatic	14	0.83 range (0.05–61.12)	0.0019

$P<0.05$ was considered significant (Mann–Whitney's test).
[a]*P* values (Mann–Whitney's test) were considered statistically significant if $P<0.05$.
[b]Information only available for 25 patients.
[c]Information only available for 23 patients.
[d]Information only available for 24 patients.

extracellular medium and is responsible for resistance to 5-FU (Guo *et al*. 2003, Oguri *et al*. 2007). We evaluated whether the overexpression of ABCC11 in CL6.7 cells was correlated to decreased sensitivity to 5-FU and 5-FdURD pro-drugs. Then, 5-FdURD or 5-FU dose–response experiments (MTT cytotoxicity assay) were performed to measure the concentration giving rise to a 50% reduction in cellular viability (IC50 values). The 5-FU IC50 values (means±s.d.) from four independent experiments were 84.50±13.70 and 225.00±127.67 nmol/ml in the MVLN and CL6.7 cell lines respectively. The 5-FdURD IC50 values (means±s.d.) from four independent experiments were 88.20±67.96 and 321.25±237.08 nmol/ml in the MVLN and CL6.7 cell lines respectively. The CL6.7 cell line displayed a 2.6- and 3.6-fold relative resistance to 5-FU and 5-FdURD respectively compared with MVLN (Mann–Whitney's test; $P<0.05$; Table 3).

The difference in extracellular 5-FdUMP concentrations in the presence and absence of MK571 was used as a measure of MK571 inhibitable 5-FdUMP efflux activity of the CL6.7 and MVLN cells. At the end of the uptake period, similar intracellular amounts of 5-FdUMP were observed in the two cell lines (CL6.7 and MVLN) and were estimated by HPLC MS/MS at 6.5 ng/μg total protein. At the end of efflux period, extracellular concentrations of 5-FdUMP were quantified in aliquots of efflux medium, thus making it possible to directly investigate efflux of 5-FdUMP in the medium. 5-FdUMP concentrations were estimated at 0.862 and 0.954 ng/μg total protein for CL6.7 and MVLN cells respectively (Table 3). We observed that 15 μM MK571 markedly blocked by approximately twofold the efflux of 5-FdUMP in CL6.7 cells while it had a very weak inhibitory effect on MVLN cells (Table 3).

Discussion

The aim of this work was to explore molecular mechanisms of ABCC11 regulation. In MCF7 cells,

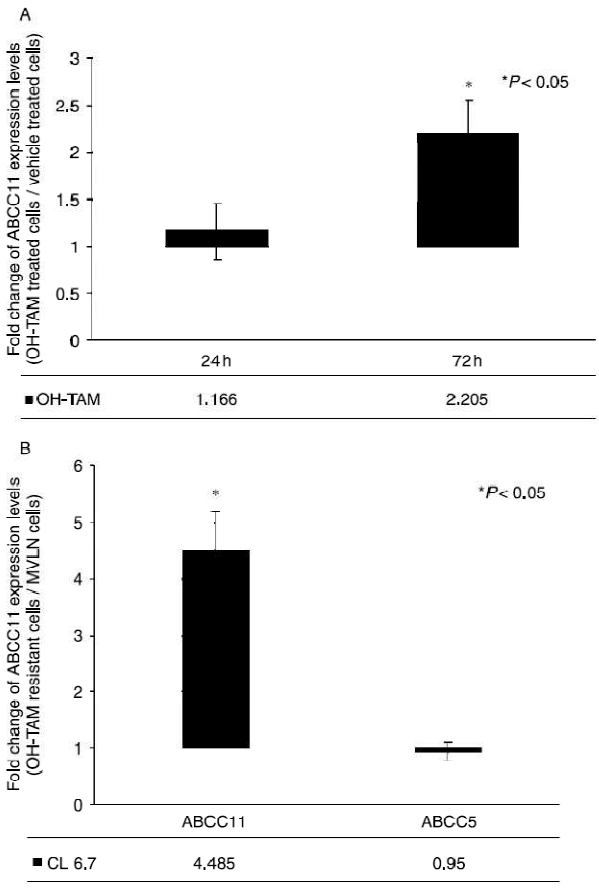

Figure 5 (A) Effect of TAM on ABCC11 expression in MCF7 cells. Cells were exposed to 200 nM TAM for 24 or 72 h and ABCC11 transcript levels were measured by QRT-PCR at various time points. Fold change (mean values were indicated below the figure) of mRNA levels was quantitated as described in Materials and methods. The QRT-PCR values indicated below are means ± S.E.M. of at least three independent experiments. *$P<0.05$; Student's *t*-test. B) Basal expression of ABCC11 and ABCC5 in TAM-resistant cell lines. Basal expression levels were measured by QRT-PCR in TAM cell line CL6.7 and MVLN cells. Fold change (mean values were indicated below the figure) of mRNA levels was quantitated as described in Materials and methods. The QRT-PCR values indicated below are means ± S.E.M. of at least three independent experiments. *$P<0.05$; Student's *t*-test.

estrogen downregulation was blocked by coexposure to TAM or ICI 182 780. In contrast, no effect was observed in MDA MB 231 ER-negative cells. These data indicate the involvement of ER-dependant pathways in the regulation of ABCC11 expression. Several studies have demonstrated that coactivators and corepressors form complexes with ERs which are involved in various regulating estrogen pathways (Smith & O'Malley 2004, Acconcia & Kumar 2006, Girault *et al.* 2006, Howell 2006). At the molecular level, ER activation appears to result in altered transcriptional activity and expression profiles of various target genes (Vendrell *et al.* 2004). Besides classical interaction with the ERE motifs, ligand-activated ER also regulates gene expression by interacting directly with the AP-1 protein complex, the Sp1 protein, and the NF-κB protein (Paech *et al.* 1997, Biswas *et al.* 2005). To support our findings, we carried out an *in silico* analysis of the human ABCC11 promoter region (−5000 pb chr 16: 38685979) using Genomatix software (GEMS Launcher software, München, Germany). This analysis revealed at least five ERE-, two Sp1-, five AP-1-, and four NF-κB-binding sites. The presence of these ERE-binding sites in the ABCC11 promoter is supported by a recently reported genome wide analysis of promoter occupancy by the ER (Laganiere *et al.* 2005). ERE responsive elements have also been identified in the promoters of other ABC transporters, such as ABCC3, ABCC5, and ABCG2, and expression of these transporters are downregulated by E_2 exposure (Ee *et al.* 2004*a*, Vendrell *et al.* 2004, Imai *et al.* 2005, Wang *et al.* 2005).

In Szakacs *et al.* (2004) study, ABCC11 level was shown to be differently expressed in breast cancer cell lines. For the first time, we demonstrated that endogenous expression levels of ABCC11 in breast cell lines were directly correlated with ER-α status (Fig. 4). Since ER status influences prognosis in breast cancer and probability response to systemic therapies, we evaluated the potential relationship between ABCC11 expression and clinical status in series A and an independent series B of tumors. We found that ABCC11 expression was positively correlated with ER-α and ERBB2. We found similar observations in macro-array database of Richardson Breast 2 (Oncomine web site; http://www.oncomine.org/main/index.jsp). Breast cancers with high expression level of ER-α respond better to endocrine therapies and consequently ER-α predicts better outcome (predictive value; Kathleen 2002) while the evidence that ERBB2 abnormalities predict resistance to TAM therapy and relative sensitivity to chemotherapy regimens including adriamycin is presented in Ross & Fletcher (1998). We also noticed that in ERBB2 low-expressing group, the correlation between ABCC11 and ER-α was independent of ERBB2 expression.

In tumor series A, the relatively high level of expression of ABCC11 in grade II group compared with grade III group, might be related to the high expression of ER-α (70% of grade II tumors were ER-α high-expressing tumors while only 23% grade III tumors were ER-α high-expressing tumors). In Bieche's independent series C, ABCC11 expression was strongly decreased in metastatic tumors in comparison with histological grade II tumors likely due to the weaker proportion of ER-α-positive tumors in this subgroup. Metastatic cells are typically more undifferentiated and

Table 3 (A) Sensitivity of MVLN parental and tamoxifen (TAM)-resistant CL6.7 cells to 5-fluorouracil (5-FU) and 5-FdURD. IC50 values were determined by the MTT assay, and resistance ratios were calculated as described in Materials and methods ($n=4$). (B) Modulation of 5-FdUMP efflux by MK571 in CL6.7 and MVLN cells. Concentrations of 5-FdUMP (ng/ml) were normalized to cellular protein content

Drugs	Cell lines	IC50 (nmol/ml)	S.D.	Resistance ratio	*P* value[a]
(A)					
5-FU	CL6.7	225.00	±127.67	2.61	0.0286
	MVLN	84.50	±13.70		
5-FdURD	CL6.7	321.25	±237.08	3.47	0.0317
	MVLN	88.20	±67.96		

	(5-FdUMP) ng/μg total protein			
Cell lines	(5-FdUMP)	S.D.	Efflux factor	*P* value[b]
(B)				
CL6.7				
MK571	0.453	±0.148	1.9	0.0347
–	0.862	±0.351		
MVLN				
MK571	0.816	±0.169	1.2	0.2479 (NS)
–	0.954	±0.335		

[a]$P<0.05$ with Mann–Whitney's *t*-test. The values are the mean±S.D. of at least four independent experiments. [b]$P<0.05$ with Student's *t*-test by bilateral and by pairs.

aggressive cells, whereas ER-positive tumors are more differentiated and have lower metastatic potential than ER-negative tumors (McGuire 1986, Garcia *et al.* 1992). We also noticed a trend towards increased ABCC11 expression in grade III compared with metastatic (Table 2). However, the set of tumors was small and these results should be confirmed on a larger cohort.

Surprisingly, while ABCC11 expression positively correlated with ER expression levels in breast tumors, we are the first to find that ABCC11 expression is reduced *in vitro* by estrogen exposure. In the literature, it has been reported that ABCG2, another ABC transporter, highly involved in MDR mechanisms (MDR phenotype) of various cancers, was also down-regulated *in vitro* by estrogens at physiological levels in the estrogen responsive MCF7 cells, but not in estrogen non-responsive human cancer cells (post-transcriptional mechanism; Imai *et al.* 2005). In addition, in another ER-positive cell line (T47D:A18), it had been described that ERE functional motif in ABCG2 promoter lead to an upregulation of ABCG2 mRNA (Ee *et al.* 2004*b*). In the human choriocarcinoma placental BeWo cells, E_2 by itself likely downregulated ABCG2 expression through an ER pathway (Wang *et al.* 2005). In this same cell line (BeWo cells), controversial data were reported by Ee *et al.* (2004*a*), since these authors reported an upregulation of ABCG2 expression. Furthermore using the Oncomine web site, various meta-analyses reported correlations of biological parameters in breast cancer samples. For example, in the Chin Breast analysis and the Wang Breast analysis, we found a positive correlation between ABCG2 and ER-α expression. In complementary, in another meta-analysis (Lin *et al.* 2004), they compared the expression profiles of genes in response with E_2 and plotted the average relative expression ratios of each gene (ER-positive/ER-negative) across all samples from the breast cancer studies. There was strong concordance between the estrogen responsive genes identified in T47D cells and genes differentially expressed in breast tumors. Nevertheless, they noted a subset (29.5%; 13/44) of genes that exhibited opposite responses following estrogen treatment *in vitro* as compared with the ER-status-associated expression in tumors (Lin *et al.* 2004). Taken altogether, these data about ABCG2 expression regulation, strongly suggested that various regulatory pathways can lead to regulation of *ABC* genes. Even if *in vitro* E_2 reduced strongly ABCC11 expression in MCF7 cells, *in vivo* it had been associated with ER expression. However, it is well known that regulation of gene expression by estrogen is strongly dependent of 'cellular context' (McKenna & O'Malley 2002, Acconcia & Kumar 2006). Indeed, the discovery of regulator molecules has been the key to understanding of estrogen regulation of gene expression in spatial and temporal contexts (McKenna & O'Malley 2002). The transcriptional activities of the ER are regulated by a vast array of cellular proteins. The observation that these transcriptional activities are manifested in a tissue-selective

manner suggests that the receptor does not function in isolation, but rather, requires specific cellular factors for maximal responses. The complex network of coactivators and corepressors provides for balanced, sensitive control of ER target gene expression (Hall & McDonnell 2005). In addition to genomic regulatory pathway, other mechanisms including phosphorylation, acetylation, and ubiquitination modifications had been described to influence ER action (McKenna & O'Malley 2002, Smith & O'Malley 2004). Overall, post-translational modification of cofactors appears to provide a mechanism to integrate extracellular signaling pathways, regulate assembly and dissociation of coregulators, and enhance or decrease the transcriptional efficacy of ER cofactor complexes. Taken altogether, these *in vitro* validated estrogen responsive genes were also differentially expressed in ER-positive primary tumors, and may therefore have direct biological and clinical significance.

ER-positive breast cancer patients benefit from endocrine therapy, including the SERM TAM and the pure antagonist ICI 182 780 (Howell 2006). Nevertheless, almost all responding patients acquire resistance to the action of TAM over time and the disease progresses. Recently, Ma *et al.* (2004) identified gene expression patterns in hormone receptor positive, early stage invasive breast cancers that might predict response to therapy. They performed microarray gene expression analysis of tumors from 60 women uniformly treated with adjuvant TAM alone. Within this cohort, 46% women developed distant metastasis with a median time to recurrence of 4 years ('TAM recurrences') and 54% women remained disease-free with median follow-up of 10 years ('TAM non-recurrences'). Very interestingly, among the identification of 19 differentially expressed genes, we found an approximately threefold increase of ABCC11 expression in non-responder patients. These data strongly suggested that ABCC11 might be highly expressed in TAM resistance cells. But no data were available to determine whether ABCC11 overexpression was associated with increased resistance levels to ABCC11 substrates. Consequently, we explored the possible association between ABCC11 expression and 5-FU resistance phenotype in various TAM-resistant models. As observed for basal expression of ABCG2 in ICI 182 780-resistant cells (Liu *et al.* 2006), we found for the first time an increase of ABCC11 levels by 4.485-fold (Fig. 5B) and 7.5-fold (data not shown) in CL6.7 and CL6.32 cells respectively compared with that observed in parental MVLN cells. Liu *et al.* (2006) related ABCG2 overexpression to down-expression of ER-α. Although, a decrease of ER-α expression by approximately threefold was observed in CL6.7 cells compared with parental MVLN cells (Badia *et al.* 2000), molecular mechanisms involved in ABCC11 overexpression in TAM-resistant cells remain to be clarified. To confirm these data, a 2.7-fold increase of ABCC11 mRNA levels was found in another cell line (VP267) derived from a patient suffering from breast cancer resistant to TAM compared with VP229 (data not shown). VP229 is a TAM-sensitive cell line established from a primary breast tumor removed before any pharmacological treatment, whereas VP267 was derived from the same patient after a local recurrence following TAM treatment (McCallum & Lowther 1996).

As reported in Ma's study concerning increase of ABCC11 expression levels in TAM-resistant tumors from breast cancer patients, we found *in vitro* models (sensitive MVLN, and CL6.7 and CL6.32 TAM-resistant cells and sensitive VP267 and TAM-resistant VP229 cells) which are able to potentially reproduce ABCC11 overexpression in TAM-resistant cells. As it is difficult to evaluate directly drug efficiency of 5-FU therapy in isolated primary breast cancer cells, we decided to evaluate *in vitro* the drug sensibility to 5-FU of CL6.7 TAM-resistant cell model in comparison with MVLN-sensitive parental cell line. This *in vitro* tool allows the exploration of overexpression ABCC11 consequences on 5-FU resistance levels in TAM-resistant cells. Since chemotherapy combinations including 5-FU are the treatment of choice for patients with hormone-refractory breast cancer and 5-FdUMP, the active metabolite of 5-FU, is a substrate of ABCC11 and ABCC5 (Guo *et al.* 2003, Pratt *et al.* 2005), we studied the effect of prolonged 5-FU exposure on cell proliferation. Since ABCC5 levels were similar in CL6.7 and MVLN cells, we suggest that the variation of resistance levels to 5-FU was likely related to ABCC11 in CL6.7 cells (Table 3). Previously, an increase of resistance level to 5-FU was specifically demonstrated in LLC-PK1 cells stably expressing ABCC11 (Guo *et al.* 2003). In addition, the MK571 inhibitable 5-FdUMP efflux activity, observed in CL6.7 cells, could also be attributed to ABCC11. Taken altogether, these data strongly suggested that ABCC11 is functional in CL6.7 cells and related to the increase of 5-FU resistance level in CL6.7 cells. These data strongly strengthen the hypothesis that prolonged exposure of breast cancer cells to TAM is involved in an upregulation of ABCC11 and may have deleterious consequences on 5-FU therapies of these breast cancers.

In conclusion, ABCC11 expression is regulated by estrogen and ABCC11 endogenous levels is increased in ER-positive breast cancers. The latter finding strengthens the hypothesis that high expression levels of ABCC11 in the ER-positive breast cancers may contribute to decreased sensitivity to chemotherapy

combinations containing 5-FU and possibly methotrexate. These data also suggest that ABCC11 may be a potential predictive tool in the choice of 5-FU containing treatments in ER-positive breast cancers resistant to TAM.

Acknowledgements

This work was supported by grants from the Association de Recherche contre le Cancer (ARC), the Ligue Contre le Cancer (Comité de la Saône et Loire) with funds from INSERM and a Master II fellowship (to M Honorat) from CROUS Lyon1 (*université Lyon 1*), and by NIH grant CA073728 (to G Kruh). The HPLC MS/MS approach was supported by grants from Ligue contre le Cancer Comité du Rhône and APICIL's groupement. JA Vendrell was supported by a fellowship from the Ligue Nationale Contre le Cancer (France). We are grateful to the Val d'Aurelle Hospital for providing tumor breast samples. We thank Dr Badia (INSERM, Montpellier) for providing the MVLN, CL6.7, and CL6.32 cells. The authors declare that there is no conflict of interest that would prejudice the impartiality of this scientific work.

References

Acconcia F & Kumar R 2006 Signaling regulation of genomic and nongenomic functions of estrogen receptors. *Cancer Letters* **238** 1–14.

Annereau JP, Szakacs G, Tucker CJ, Arciello A, Cardarelli C, Collins J, Grissom S, Zeeberg BR, Reinhold W, Weinstein JN *et al.* 2004 Analysis of ATP-binding cassette transporter expression in drug-selected cell lines by a microarray dedicated to multidrug resistance. *Molecular Pharmacology* **66** 1397–1405.

Badia E, Duchesne MJ, Semlali A, Fuentes M, Giamarchi C, Richard-Foy H, Nicolas JC & Pons M 2000 Long-term hydroxytamoxifen treatment of an MCF-7-derived breast cancer cell line irreversibly inhibits the expression of estrogenic genes through chromatin remodeling. *Cancer Research* **60** 4130–4138.

Bera TK, Lee S, Salvatore G, Lee B & Pastan I 2001 MRP8, a new member of ABC transporter superfamily, identified by EST database mining and gene prediction program, is highly expressed in breast cancer. *Molecular Medicine* **7** 509–516.

Berry M, Nunez AM & Chambon P 1989 Estrogen-responsive element of the human pS2 gene is an imperfectly palindromic sequence. *PNAS* **86** 1218–1222.

Bieche I, Girault I, Urbain E, Tozlu S & Lidereau R 2004 Relationship between intratumoral expression of genes coding for xenobiotic-metabolizing enzymes and benefit from adjuvant tamoxifen in estrogen receptor alpha-positive postmenopausal breast carcinoma. *Breast Cancer Research* **6** R252–R263.

Biswas DK, Singh S, Shi Q, Pardee AB & Iglehart JD 2005 Crossroads of estrogen receptor and NF-κB signaling. *Science's STKE* **2005** pe27.

Bloom HJ & Richardson WW 1957 Histological grading and prognosis in breast cancer; a study of 1409 cases of which 359 have been followed for 15 years. *British Journal of Cancer* **11** 359–377.

Bortfeld M, Rius M, Konig J, Herold-Mende C, Nies AT & Keppler D 2006 Human multidrug resistance protein 8 (MRP8/ABCC11), an apical efflux pump for steroid sulfates, is an axonal protein of the CNS and peripheral nervous system. *Neuroscience* **137** 1247–1257.

Burger H, Foekens JA, Look MP, Meijer-van Gelder ME, Klijn JG, Wiemer EA, Stoter G & Nooter K 2003 RNA expression of breast cancer resistance protein, lung resistance-related protein, multidrug resistance-associated proteins 1 and 2, and multidrug resistance gene 1 in breast cancer: correlation with chemotherapeutic response. *Clinical Cancer Research* **9** 827–836.

Chen ZS, Guo Y, Belinsky MG, Kotova E & Kruh GD 2005 Transport of bile acids, sulfated steroids, estradiol 17-beta-D-glucuronide, and leukotriene C4 by human multidrug resistance protein 8 (ABCC11). *Molecular Pharmacology* **67** 545–557.

Demirpence E, Duchesne MJ, Badia E, Gagne D & Pons M 1993 MVLN cells: a bioluminescent MCE-7-derived cell line to study the modulation of estrogenic activity. *Journal of Steroid Biochemistry and Molecular Biology* **46** 355–364.

Dorssers LC, Van der Flier S, Brinkman A, van Agthoven T, Veldscholte J, Berns EM, Klijn JG, Beex LV & Foekens JA 2001 Tamoxifen resistance in breast cancer: elucidating mechanisms. *Drugs* **61** 1721–1733.

Ee PL, He X, Ross DD & Beck WT 2004*a* Modulation of breast cancer resistance protein (BCRP/ABCG2) gene expression using RNA interference. *Molecular Cancer Therapeutics* **3** 1577–1583.

Ee PL, Kamalakaran S, Tonetti D, He X, Ross DD & Beck WT 2004*b* Identification of a novel estrogen response element in the breast cancer resistance protein (ABCG2) gene. *Cancer Research* **64** 1247–1251.

Garcia M, Derocq D, Freiss G & Rochefort H 1992 Activation of estrogen receptor transfected into a receptor-negative breast cancer cell line decreases the metastatic and invasive potential of the cells. *PNAS* **89** 11538–11542.

Girault I, Bieche I & Lidereau R 2006 Role of estrogen receptor alpha transcriptional coregulators in tamoxifen resistance in breast cancer. *Maturitas* **54** 342–351.

Guo Y, Kotova E, Chen ZS, Lee K, Hopper-Borge E, Belinsky MG & Kruh GD 2003 MRP8, ATP-binding cassette C11 (ABCC11), is a cyclic nucleotide efflux pump and a resistance factor for fluoropyrimidines 2′,3′-dideoxycytidine and 9′-(2′-phosphonylmethoxy-ethyl)adenine. *Journal of Biological Chemistry* **278** 29509–29514.

Hall JM & McDonnell DP 2005 Coregulators in nuclear estrogen receptor action: from concept to therapeutic targeting. *Molecular Interventions* **5** 343–357.

Howell A 2006 Pure oestrogen antagonists for the treatment of advanced breast cancer. *Endocrine-Related Cancer* **13** 689–706.

Imai Y, Ishikawa E, Asada S & Sugimoto Y 2005 Estrogen-mediated post transcriptional down-regulation of breast cancer resistance protein/ABCG2. *Cancer Research* **65** 596–604.

Jordheim LP, Cros E, Gouy MH, Galmarini CM, Peyrottes S, Mackey J, Perigaud C & Dumontet C 2004 Characterization of a gemcitabine-resistant murine leukemic cell line: reversion of *in vitro* resistance by a mononucleotide prodrug. *Clinical Cancer Research* **10** 5614–5621.

Kathleen IP 2002 Prognostic and predictive factors for individualized therapy. *3rd International BCIRG Conference*.

Kruh GD, Guo Y, Hopper-Borge E, Belinsky MG & Chen ZS 2007 ABCC10, ABCC11, and ABCC12. *Pflugers Archiv* **453** 675–684.

Laganiere J, Deblois G, Lefebvre C, Bataille AR, Robert F & Giguere V 2005 From the cover: location analysis of estrogen receptor alpha target promoters reveals that FOXA1 defines a domain of the estrogen response. *PNAS* **102** 11651–11656.

Larkin A, O'Driscoll L, Kennedy S, Purcell R, Moran E, Crown J, Parkinson M & Clynes M 2004 Investigation of MRP-1 protein and MDR-1 P-glycoprotein expression in invasive breast cancer: a prognostic study. *International Journal of Cancer* **112** 286–294.

Lin CY, Strom A, Vega VB, Kong SL, Yeo AL, Thomsen JS, Chan WC, Doray B, Bangarusamy DK, Ramasamy A *et al.* 2004 Discovery of estrogen receptor alpha target genes and response elements in breast tumor cells. *Genome Biology* **5** R66.

Liu H, Cheng D, Weichel AK, Osipo C, Wing LK, Chen B, Louis TE & Jordan VC 2006 Cooperative effect of gefitinib and fumitremorgin c on cell growth and chemosensitivity in estrogen receptor alpha negative fulvestrant-resistant MCF-7 cells. *International Journal of Oncology* **29** 1237–1246.

Ma XJ, Wang Z, Ryan PD, Isakoff SJ, Barmettler A, Fuller A, Muir B, Mohapatra G, Salunga R, Tuggle JT *et al.* 2004 A two-gene expression ratio predicts clinical outcome in breast cancer patients treated with tamoxifen. *Cancer Cell* **5** 607–616.

McCallum HM & Lowther GW 1996 Long-term culture of primary breast cancer in defined medium. *Breast Cancer Research and Treatment* **39** 247–259.

McGuire WL 1986 In *Hormone Receptors in Breast Cancer, Cancer Surveys*, vol 5, pp. 527 536. Ed RD Bulbrook. Oxford University Press: Oxford, UK.

McKenna NJ & O'Malley BW 2002 Combinatorial control of gene expression by nuclear receptors and coregulators. *Cell* **108** 465–474.

Milano A, Dal Lago L, Sotiriou C, Piccart M & Cardoso F 2006 What clinicians need to know about antioestrogen resistance in breast cancer therapy. *European Journal of Cancer* **42** 2692–2705.

Oguri T, Bessho Y, Achiwa H, Ozasa H, Maeno K, Maeda H, Sato S & Ueda R 2007 MRP8/ABCC11 directly confers resistance to 5-fluorouracil. *Molecular Cancer Therapeutics* **6** 122–127.

Paech K, Webb P, Kuiper GG, Nilsson S, Gustafsson J, Kushner PJ & Scanlan TS 1997 Differential ligand activation of estrogen receptors ERalpha and ERbeta at AP1 sites. *Science* **277** 1508–1510.

Park S, Shimizu C, Shimoyama T, Takeda M, Ando M, Kohno T, Katsumata N, Kang YK, Nishio K & Fujiwara Y 2006 Gene expression profiling of ATP-binding cassette (ABC) transporters as a predictor of the pathologic response to neoadjuvant chemotherapy in breast cancer patients. *Breast Cancer Research* **1** 9–17.

Parker WB & Cheng YC 1990 Metabolism and mechanism of action of 5-fluorouracil. *Pharmacology and Therapeutics* **48** 381–395.

Pratt S, Shepard RL, Kandasamy RA, Johnston PA, Perry W III & Dantzig AH 2005 The multidrug resistance protein 5 (ABCC5) confers resistance to 5-fluorouracil and transports its monophosphorylated metabolites. *Molecular Cancer Therapeutics* **4** 855–863.

Ross JS & Fletcher JA 1998 The HER-2/neu oncogene in breast cancer: prognostic factor, predictive factor, and target for therapy. *Oncologist* **3** 237–252.

Smith CL & O'Malley BW 2004 Coregulator function: a key to understanding tissue specificity of selective receptor modulators. *Endocrine Reviews* **25** 45–71.

Szakacs G, Annereau JP, Lababidi S, Shankavaram U, Arciello A, Bussey KJ, Reinhold W, Guo Y, Kruh GD, Reimers M *et al.* 2004 Predicting drug sensitivity and resistance: profiling ABC transporter genes in cancer cells. *Cancer Cell* **6** 129–137.

Tozlu S, Girault I, Vacher S, Vendrell J, Andrieu C, Spyratos F, Cohen P, Lidereau R & Bieche I 2006 Identification of novel genes that co-cluster with estrogen receptor alpha in breast tumor biopsy specimens, using a large-scale real-time reverse transcription-PCR approach. *Endocrine-Related Cancer* **13** 1109–1120.

Vendrell JA, Magnino F, Danis E, Duchesne MJ, Pinloche S, Pons M, Birnbaum D, Nguyen C, Theillet C & Cohen PA 2004 Estrogen regulation in human breast cancer cells of new downstream gene targets involved in estrogen metabolism, cell proliferation and cell transformation. *Journal of Molecular Endocrinology* **32** 397–414.

Vendrell JA, Bieche I, Desmetz C, Badia E, Tozlu S, Nguyen C, Nicolas JC, Lidereau R & Cohen PA 2005 Molecular changes associated with the agonist activity of hydroxytamoxifen and the hyper-response to estradiol in hydroxytamoxifen-resistant breast cancer cell lines. *Endocrine-Related Cancer* **12** 75–92.

Wang H, Zhou L, Gupta A, Vethanayagam RR, Zhang Y, Unadkat JD & Mao Q 2005 Regulation of BCRP/ABCG2 expression by progesterone and 17β-estradiol in human placental BeWo cells. *American Journal of Physiology. Endocrinology and Metabolism* **290** E798–E807.

Afin de pouvoir analyser l'activité de transport des cellules exprimant ABCC11, et dans le cadre d'une collaboration avec l'équipe du Pr. J. Guitton, nous avons également participé à la mise au point d'une méthode de dosage des métabolites du 5FU et de deux nucléotides monophosphates par LC-MS/MS (*Liquid Chromatography-Tandem Mass Spectrometry*). Cette méthode a permit de déterminer la production intracellulaire de 5FdURD et de 5FdUMP à partir du 5FU ainsi que la sécrétion de 5FdUMP et de 5FU par des cellules en culture qui expriment des transporteurs ABC.

→ Publication 4. « **Simultaneous quantification of 5-FU, 5-FUrd, 5-FdUrd, 5-FdUMP, dUMP and TMP in cultured cell models by LC-MS/MS** » par D. Carli, M. Honorat, S. Cohen, M. Megherbi, B. Vignal, C. Dumontet, L. Payen et J. Guitton

Article publié dans Journal of Chromatography B (2009)

Journal of Chromatography B, 877 (2009) 2937–2944

Contents lists available at ScienceDirect

Journal of Chromatography B

journal homepage: www.elsevier.com/locate/chromb

Simultaneous quantification of 5-FU, 5-FUrd, 5-FdUrd, 5-FdUMP, dUMP and TMP in cultured cell models by LC-MS/MS

Delphine Carli[a,b,e], Mylène Honorat[c,d,g], Sabine Cohen[a,b,f], Mehdi Megherbi[a,b,e], Bruno Vignal[a,b,f], Charles Dumontet[c,d,g], Léa Payen[c,d,g,h], Jérôme Guitton[a,b,c,d,e,h,*]

[a] Hospices Civils de Lyon, F-69495, Pierre Bénite, France
[b] Centre Hospitalier Lyon-Sud, France
[c] Université de Lyon, F-69373, Lyon, France
[d] Université de Lyon 1, France
[e] Laboratoire de ciblage thérapeutique en cancérologie, France
[f] Laboratoire de biochimie-toxicologieFrance
[g] Inserm U590 Oncogenèse et Progression Tumorale, Centre Léon Bérard, France
[h] ISPBL, Faculté de pharmacie, Laboratoire de Toxicologie, France

ARTICLE INFO

Article history:
Received 6 February 2009
Accepted 1 July 2009
Available online 18 July 2009

Keywords:
5-FU
Mass spectrometry
Intracellular
5-FdUMP
Metabolite

ABSTRACT

To specifically quantify several metabolites of 5-fluorouracil (5-FU) and two endogenous monophosphate nucleotides, we developed an original method based on a liquid chromatography–tandem mass spectrometry (LC-MS/MS). This assay allowed the determination of: (i) the intracellular production of 5-fluoro-2′-deoxyuridine-5′-monophosphate (5-FdUMP) from 5-FU or 5-fluoro-2′-deoxyuridine (5-FdUrd), (ii) the impact of 5-FdUMP concentration on the intracellular 2′-deoxyuridine-5′-monophosphate (dUMP)/thymidine-5′-monophosphate (TMP) ratio, and (iii) the secretion extent of 5-FdUMP and 5-FU from human cultured cells by ABC transporters. Under our experimental conditions, cells were incubated with 5-FU or 5-FUrd. Then, cellular proteins were precipitated by methanol. This procedure provided high extraction recovery. In addition, to measure 5-FU and 5-FdUMP secretion from cells, we carried out quantification of these molecules in culture medium. Media were either directly injected (5-FU) or underwent a solid phase extraction using Oasis Wax extraction cartridge (5-FdUMP). Separation of analytes was performed on a dC18 Atlantis 3.5 μm, (100 mm × 2.1 mm i.d) column with isocratic mode using ammonium formate buffer/methanol/water (5/5/90, v/v) as mobile phase. The run time did not exceed 6.2 min. The analytes were ionized in an electrospray interface under negative ion mode. We validated the method over a range of 2.5–150 ng mL^{-1} according to the compounds. Intra- and inter-assay variability was lower than 10% over seven days. All compounds were stable in cells or in culture medium when samples were stored at −20 °C for at least two weeks, and after three freeze-thaw cycles. No matrix effect was observed in both media.

1. Introduction

The 5-Fluorouracil (5-FU) anticancer drug has been widely used for fifty years in the treatment of several human solid tumors including colorectal and breast cancers [1,2]. The pyrimidine 5-FU undergoes a complex metabolic pathway leading to the production of cytotoxic metabolites such as fluorouridine triphosphate and deoxyfluorouridine triphosphate that are respectively incorporated into RNA and DNA (Fig. 1) [3]. Among the metabolites, 5-fluoro-2′-deoxyuridine-5′-monophosphate (5-FdUMP) plays a key role. Indeed, 5-FdUMP inhibits thymidylate synthase (TS), the enzyme that transforms 2′-deoxyuridine-5′-monophosphate (dUMP) to thymidine-5′-monophosphate (TMP) that leads to intracellular depletion of thymidine [4]. Conversely, 5-FdUMP is a substrate of the efflux pumps such as ABCC5 and ABCC11 that have recently been associated with 5-FU resistance mechanisms [5,6].

Several assays described the quantification of 5-FU and its metabolites 5-fluorouridine (5-FUrd) and 5-fluoro-2′-deoxyuridine (5-FdUrd) [7–12]. However, few of them included the quantification of the pharmacologically active 5-FdUMP metabolite. Among these methods, the first one used tritium radiolabeled 5-FU ([^{3}H-5FU]) and a chromatographic separation with counter ion. The quantification of 5-FU and its phosphate metabolites was successfully developed in cell lines [13,14]. The second method for the quantification of 5-FdUMP was performed in L1210 cells using

* Corresponding author at: Laboratoire de ciblage thérapeutique en cancérologie, Hospices Civils de Lyon, Centre Hospitalier Lyon-Sud, Pierre Bénite, F-69495, France.
E-mail address: jerome.guitton@recherche.univ-lyon1.fr (J. Guitton).

1570-0232/$ – see front matter © 2009 Elsevier B.V. All rights reserved.
doi:10.1016/j.jchromb.2009.07.004

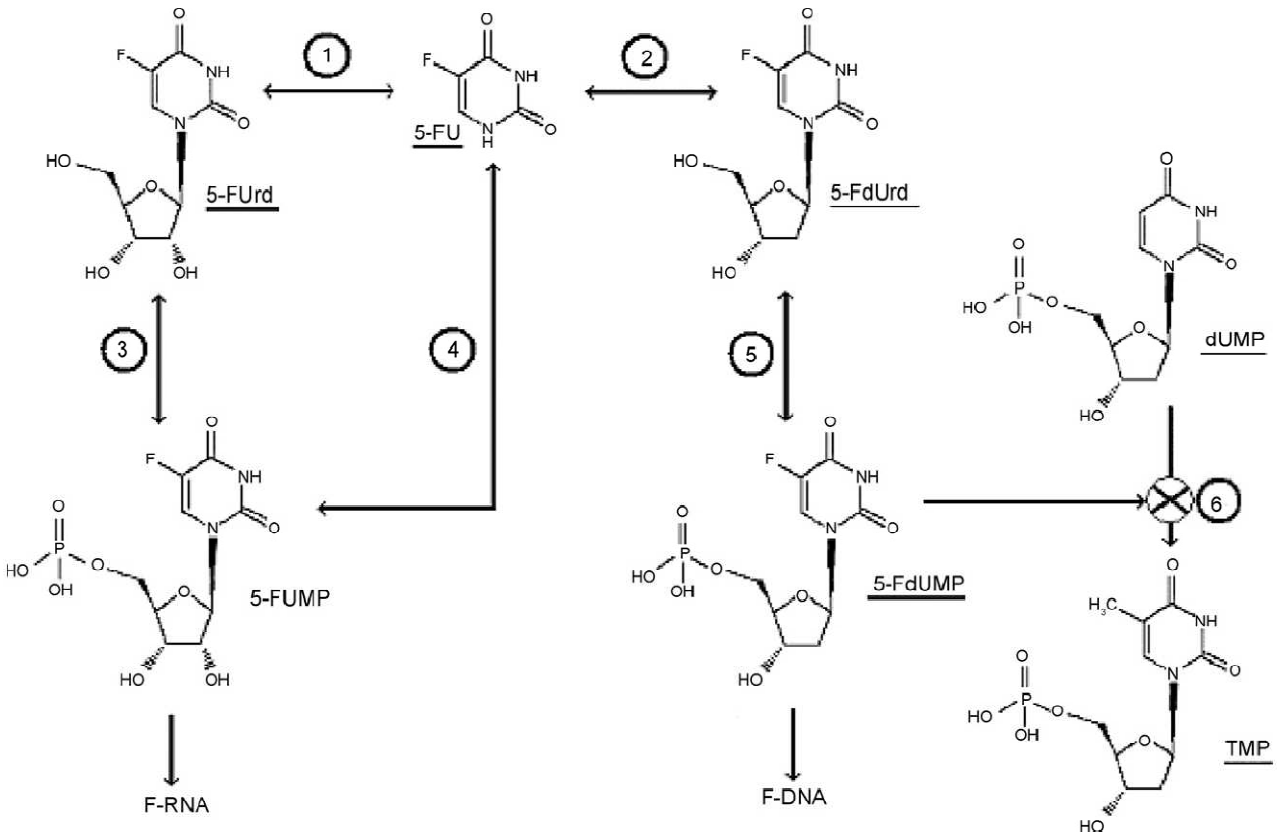

Fig. 1. Partial intracellular anabolism pathways of 5-fluorouracil (5-FU). The compounds underlined were quantified in the present study. 5-fluorouracil (5-FU), 5-fluorouridine (5-FUrd), 5-fluoro-2′-deoxyuridine (5-FdUrd), 5-fluorouridine-5′-monophosphate (5-FUMP), 5-fluoro-2′-deoxyuridine-5′-monophosphate (5-FdUMP), 2′-deoxyuridine-5′-monophosphate (dUMP), thymidine-5′-monophosphate (TMP). 1: uridine phosphorylase, 2: thymidine phosphorylase, 3: uridine kinase, 4: thymidine kinase, 5: pyrimidine phosphoribosyl transferase, 6: thymidylate synthase.

also [^{3}H-5FU], but it was time-consuming due to a pre-treatment with periodate and methylamine to eliminate ribonucleotides [15]. Other assays using LC-UV with counter ion or based on strong cation exchangers have been published for the separation of 5-FU, 5-FUrd, 5-FdUrd and 5-FdUMP in plasma. However, poor sensitivity was obtained and interfering peaks from endogenous compounds were observed, especially for 5-FdUMP [16,17]. The latest method was based on capillary electrophoresis coupled with UV detection but it could not detect 5-FdUMP in cells due to poor sensitivity [18].

In the present study we have developed an assay in cultured cell models to simultaneously quantify 5-FU derivatives (5-FUrd, 5-FdUrd, 5-FdUMP) and endogenous molecules (dUMP and TMP). We assessed that the dUMP and TMP concentrations were modified via TS inhibition by 5-FdUMP. 5-FU and 5-FdUMP molecules were also quantified in extracellular compartment (culture medium). Here we describe a rapid, sensitive and specific method based on LC-MS/MS technology to quantify various 5-FU derivatives present in cells and effluxed culture media.

2. Experimental

2.1. Reagents and chemicals

5-Fluorouracil (5-FU), 5-Chlorouracil (5-CU), 5-fluorouridine (5-FUrd), 5-fluoro-2′-deoxyuridine (5-FdUrd), 5-fluoro-2′-deoxyuridine-5′-monophosphate (5-FdUMP), 2′-deoxyuridine-5′-monophosphate (dUMP), thymidine-5′-monophosphate (TMP), as pure standards, were purchased from Sigma (Saint-Quentin Fallavier, France). All products were stored at +4 °C in the dark, except for 5-FdUMP that was stored at −20 °C. HPLC-grade acetonitrile was obtained from Merck (Darmstadt, Germany). Acetic acid (Ultra, >99.5% pure) was supplied by Fluka (Steinhein, Germany). Methanol was from Carlo Erba (Milano, Italy). Milli-Q deionized water was used throughout the study.

2.2. Standard solutions, calibration standards and quality controls

Stock solutions (1 mg mL^{-1}) of 5-FU, 5-FUrd, 5-FdUrd, 5-FdUMP, dUMP, TMP and 5-CU were prepared in methanol and stored at −20 °C. Standard solutions were made daily by further dilution of stock solutions with methanol. For calibration curves, methanol (total volume 500 μL) was spiked with 25 μL of the appropriately diluted standard solutions. Final concentrations were 2.5, 5, 7.5, 25, 50 ng mL^{-1} for TMP (7.8–388 nM), 7.5, 15, 22.5, 75, 150 ng mL^{-1} for 5-FU (57.7–1154 nM) and 5, 10, 15, 50, 100 ng mL^{-1} for 5-FUrd (19.1–382 nM), 5-FdUrd (20.3–407 nM), 5-FdUMP (15.3–307 nM), dUMP (16.2–325 nM). Quality controls (C1 and C2, respectively) were prepared at the following concentrations: 11.25 and 112.5 ng mL^{-1} for 5-FU (86.5 and 865 nM), 7.5 and 75 ng mL^{-1} for 5-FUrd (28.6 and 286 nM), 5-FdUrd (30.5 and 305 nM), 5-FdUMP (23 and 230 nM), dUMP (24.4 and 244 nM), 3.75 and 37.5 ng mL^{-1} for TMP (11.7 and 117 nM). Blank cell samples without 5-FU derivatives were also carried out (dUMP and TMP are endogenous compounds). All samples were subjected to the sample procedure as described below.

2.3. Sample preparation

2.3.1. Cellular quantification of 5-FU, 5-FUrd, 5-FdUrd, 5-FdUMP, dUMP and TMP.

Samples diluted in 500 μL of methanol were used for calibration curves, quality control or cell incubation. 5-CU was used as

internal standard and added at 200 ng mL^{-1}. Then samples were centrifuged at 12,000 × *g* for 5 min at +10 °C. The supernatant was removed and evaporated to dryness under a stream of nitrogen. The residues were resuspended in 300 μL of water and 10 μL was injected in the HPLC device.

2.3.2. Quantification of 5-FU in culture medium.

Quantification of 5-FU was performed by directly injecting 10 μL of the cell culture medium into the LC-MS/MS device. 5-CU was used as internal standard and added at 500 ng mL^{-1}.

2.3.3. Quantification of 5-FdUMP in cell culture medium.

In this case, dUMP was used as internal standard. We carried out a solid phase extraction (SPE) according to the following procedure: an Oasis Wax (60 mg), extraction cartridges (Waters, Milford, USA) was conditioned under vacuum with 2 mL of methanol and 2 mL of acetic acid (1%). dUMP (500 ng mL^{-1}) was added to 300 μL Dulbecco's Modified Eagle's Medium (DMEM), then the mixture was applied to an adsorbent SPE column. After a slow percolation, the cartridge was successively washed with 1 mL of acetic acid (1%), 2 mL of water and 1 mL of methanol/ammonium hydroxide 0.1% (30/70, v/v). The elution was performed with 1 mL of methanol/ammonium hydroxide 3% (90/10, v/v). This eluted solution was evaporated at +30 °C under a gentle stream of nitrogen. The residue was reconstituted in 300 μL of water. After vortexing, the sample was centrifuged 5 min at 4000 × *g*, and the clear supernatant was transferred to a glass vial kept at +10 °C into the autosampler and 10 μL was injected.

2.4. HPLC conditions

The high-performance liquid chromatographic system consisted of a ThermoElectron Surveyor MS pump equipped with and Surveyor autosampler injector (ThermoElectron, San Jose, USA). Samples were separated on a dC18 column Atlantis, 3.5 μm, (100 mm × 2.1 mm i.d) (Waters, Milford, USA). The separation was performed with isocratic mode using a mixture of ammonium formate buffer (5 mM, pH 4)/methanol/water (5/5/90, v/v). The mobile phase was delivered through the column (temperature maintained at +30 °C) at a flow rate of 200 μL min^{-1}.

2.5. Mass spectrometry conditions

LC-MS/MS analyses were acquired using a Quantum-Ultra (ThermoElectron, San Jose, USA) triple quadrupole mass spectrometer equipped with an Ion Max API source. The instrument was operated in negative ion mode with electrospray (ESI) source. The position (*x*, *y*, *z*) of the ESI probe was optimized with 5-FdUMP. Argon was used as collision gas at 1.5 mTorr. Spray voltage and capillary temperature were set respectively at 3.5 kV and 350 °C. Pressures for the nitrogen sheath gas, auxiliary gas and sweep gas were respectively maintained at 40, 15 and 5 units (units refer to an arbitrary value set by the X-calibur software). The $[M-H]^-$ ions of different compounds were passed through the first quadrupole (Q1), then after fragmentation, daughter ions were passed through the third quadrupole (Q3) with full-width at half maximum height of 0.7 *m*/*z* for both quadrupoles. Compounds were quantified in selected reaction monitoring (SRM) mode with 100 ms dwell time per channel. The transitions and collision energies are summarized in Table 1.

2.6. Calibration curves and validation procedure

Calibration curves were constructed by plotting the ion abundance peak area ratio (analyte/internal standard) as a function of cell culture analyte concentrations. The significance of the slope and the validity of the linear calibration curves were tested using Fisher–Snedecor's *F*-test ($p < 0.05$). Homocedasticity was statistically determined using Cochran's test ($p < 0.05$).

Table 1
Transitions monitored and collision energies used.

	Transitions (*m*/*z*)	Collision energy (eV)
5-FU	129 → 42	25
5-FUrd	261 → 129	20
5-FdUrd	245 → 155	15
5-FdUMP	325 → 195	15
TMP	321 → 195	20
dUMP	307 → 195	18
5-CU (I.S.)	145 → 42	28

For intracellular quantification, seventeen independent calibration curves were prepared. Seven runs included a calibration curve and quality control samples (QC) at two different concentrations (see above) in six replicates. For the quantification in DMEM, five runs including a calibration curve and quality control samples were performed. For each analyte, the lower limit of quantification (LLOQ) was chosen as the concentration of the lowest calibration standard. The upper limit of quantification was chosen as the concentration of the upper calibration standard.

The accuracy and precision of the assay were respectively assessed by the mean relative percentage deviation from the nominal concentrations and the within-run precision (WRP) and between-run precision (BRP). The within-run precision was determined as $WRP = 100 \times (\sqrt{MS_{wit}}/GM)$. The between-run precision was estimated as $BRP = 100 \times (\sqrt{(MS_{bet} - MS_{wit})/n}/GM)$. MS_{wit}, MS_{bet}, n, GM, represented the within-groups mean square, the between-groups mean square, the number of replicate observations within each run and the grand mean, respectively. These parameters were calculated using the software Statview for windows version 5.0 (SAS institute, Cary, USA).

The extraction efficiency of analytes was calculated from the QC samples. The determination was made by comparing the mean peak areas from samples obtained through the extraction procedure with those obtained from direct injection of the same amount dissolved in the mobile phase.

2.7. Stability

The stability study was carried out in duplicate and was performed from cellular samples for all the compounds using QC1 and QC2 and from DMEM for 5-FU and 5-FdUMP using two concentrations (50 and 400 ng mL^{-1}). The freeze-thaw stability was tested following three cycles at −20 °C. The auto-sampler stability at +10 °C was tested by analyzing the compounds every 2 h during 8 h. The long-term freezing stability at −20 °C was tested by re-analyzing the samples two weeks after the first analysis.

2.8. Matrix effect

To investigate the effects of the matrix components on the suppression of the ESI signal, a post-column infusion system with syringe pump (flow rate 5 μL min^{-1}) was used to deliver the different compounds (1 μg mL^{-1}). Effluent from the HPLC column combined with the infused analytes entered into the detector. Extract samples from cells or DMEM and from no extract DMEM were successively injected.

2.9. In vitro cell models

Human breast MCF7 and human kidney HEK 293T cell lines were cultured in DMEM supplemented with 10% fetal bovine serum (FBS) under 5% CO_2 at +37 °C. All experiments were performed in

exponentially growing cells. At approximately 80% confluence, the medium was removed and replaced with FBS-free DMEM. Following incubation period with 5-FU derivates, DMEM was removed and stored at −20 °C for the quantification of 5-FU and 5-FdUMP. Cells were washed three times with ice-cold PBS and then 500 μL of methanol supplemented with internal standard was added. The MCF7 cell line was used for the development of the method in the presence of 100 μM 5-FdUrd. Experiments were performed using MCF7 or HEK 293T cell lines, respectively incubated with 5-FdUrd or 5-FU at various concentrations (0, 5, 10, 20, 50, 100 μM) and various incubation times (0, 5, 10, 15, 30, 45 min). Total protein content was determined using the Bradford Protein Assay method (Bio-Rad laboratories, CA, USA).

3. Results and discussion

3.1. Liquid chromatography

5-FU, 5-FUrd, and 5-FdUrd are hydrophilic compounds. For 5-FdUMP, dUMP and TMP, the phosphate group increases the polarity compared to their nucleoside analogues. This makes the chromatographic retention of these molecules a challenge by LC-MS since a limited number of mobile phases are suitable for both LC separation and MS detection. One way to overcome this problem is the use of a volatile ion-pair reagent as previously described for monophosphate nucleotides [13,16]. Another possibility is to perform the chromatographic separation based on hydrophilic interaction chromatography (Hilic). This method presents the advantage of requiring a high percentage of organic solvent favourable for MS detection. However, the concentration of buffer which must be present to obtain reproducible retention times and good peak shapes leads to a strong decrease in the MS response for 5-FU derivatives and endogenous molecules. This observation comes from our own experience but had also previously been reported by Siethoff et al. for the quantification of 5-FU by LC–MS/MS [19]. Finally, we chose a highly aqueous mobile phase with a dC18 Atlantis column specifically developed for this analytical condition. The buffer concentration was a critical parameter for the sensitivity of our present method (Fig. 2). Indeed, the response for all analytes decreased inversely with the buffer concentration. However, a final concentration of buffer in mobile phase at 0.25 mM allowed obtaining a good peak shape and an acceptable sensitivity. The best compromise between runtime, sensitivity and peak shape was observed with the present conditions rather than those tested

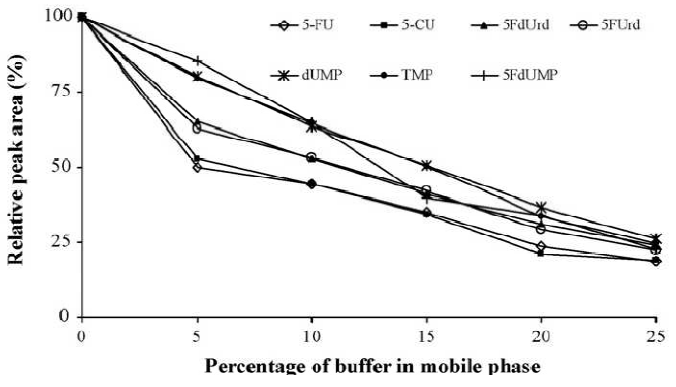

Fig. 2. Response of the mass spectrometry detector according to the composition of the mobile phase.
The first condition was methanol/water (5/95, v/v). Then for other conditions, methanol was maintained at 5% and ammonium formate buffer (5 mM, pH 4) was introduced from 5 to 25% (final concentration through the analytical column from 0.25 to 1.25 mM). The data represents the peak area ratio between experimental conditions and the basal condition (without buffer).

with Hilic column. The chromatography was performed with isocratic condition and the run time did not exceed 6.2 min. The mobile phase was initially discarded, and then automatically switched to the detector at 2.3 min and the compounds were detected from 3 to 5.2 min. Following this procedure, using LC-MS/MS analysis, no interfering endogenous peaks were observed from cells (Fig. 3).

Direct injection of DMEM into the LC-MS/MS device allowed monitoring 5-FU, 5-FdUrd, 5-FUrd and 5-CU. However, under this condition, monophosphate compounds show very broad peaks. DMEM includes numerous constituents (amino acids, minerals, vitamins, . . .) and some of them are at a high concentration such as glucose, phosphate buffer, NaCl. We suggested that DMEM contents altered the chromatographic behaviour and the mass response (see matrix effect) of highly hydrophilic monophosphate derivatives while other non-monophosphate compounds were not affected. Consequently, we performed a SPE prior to the chromatographic analysis for the quantification of 5-FdUMP in DMEM.

3.2. Mass spectrometry

The optimal mass spectrometry conditions for the detection of all compounds were achieved in negative ion mode. All compounds predominantly formed deprotonated ions ($[M-H]^-$). The fragmentation of 5-FU ($[M-H]^-$ ion at m/z 129) consists in a cleavage of the ring leading to a daughter ion at m/z 42 as previously described [20]. For the monophosphate compounds the major ion produced by fragmentation was the deoxyribose monophosphate ion (m/z 195) obtained by cleavage of the glycosidic bond. The SRM transitions were 307 → 195, 321 → 195 and 325 → 195 for dUMP, TMP and 5-FdUMP, respectively (data not shown). The fragmentation also yields the expected [M-195] fragment ion corresponding to the ion of the uracile base for dUMP (m/z 111), the thymidine base for TMP (m/z 125) and to 5-FU for 5-FdUMP (m/z 129). This fragmentation pathway was the same as the one described for stavudine-monophosphate [21]. The fragmentation of 5-FUrd and 5-FdUrd corresponded to the cleavage of the glycosidic bond yielding an ion at m/z 129 or the cleavage of the sugar ring leading to respectively an ion at m/z 155 and 171 for 5-FdUrd and 5-FUrd. Although the fragmentation pathway was the same for both compounds, the intensities of the daughter ions reported in Fig. 4 were very different.

3.3. Method validation

For analysis of endogenous compounds, the choice of the sample matrix for the preparation of calibration standards and QC samples is challenging. During the method development numerous, cell samples were spiked at various concentrations with exogenous compounds 5-FU, 5-FUrd, 5-FdUrd, 5-FdUMP and 5-CU (I.S.). Then the results were compared with those obtained when methanol was spiked at the same concentrations. In both cases, the sample preparation was carried out under the same procedure. No significant difference was observed between the two matrices. Consequently, calibration curves and QC samples for all the analytes, including endogenous compounds dUMP and TMP, were performed from the methanol matrix.

The calibration curves were constructed by analyzing data as plots of peak area ratio of analyte/internal standard versus the analyte concentration. Results showed that a weighting factor had to be applied. The weighting factor 1/[concentration] was found to provide the best fit. Then, raw data points were fitted to a linear or quadratic least-squares regression curve. The determination coefficient (r^2) of the linear regression was at least equal to 0.992 for all compounds. Calibration curves for analytes on seventeen individual days are presented in Table 2. For all concentrations the inter-day precision (CV) was lower than 10% and the accuracy was in the

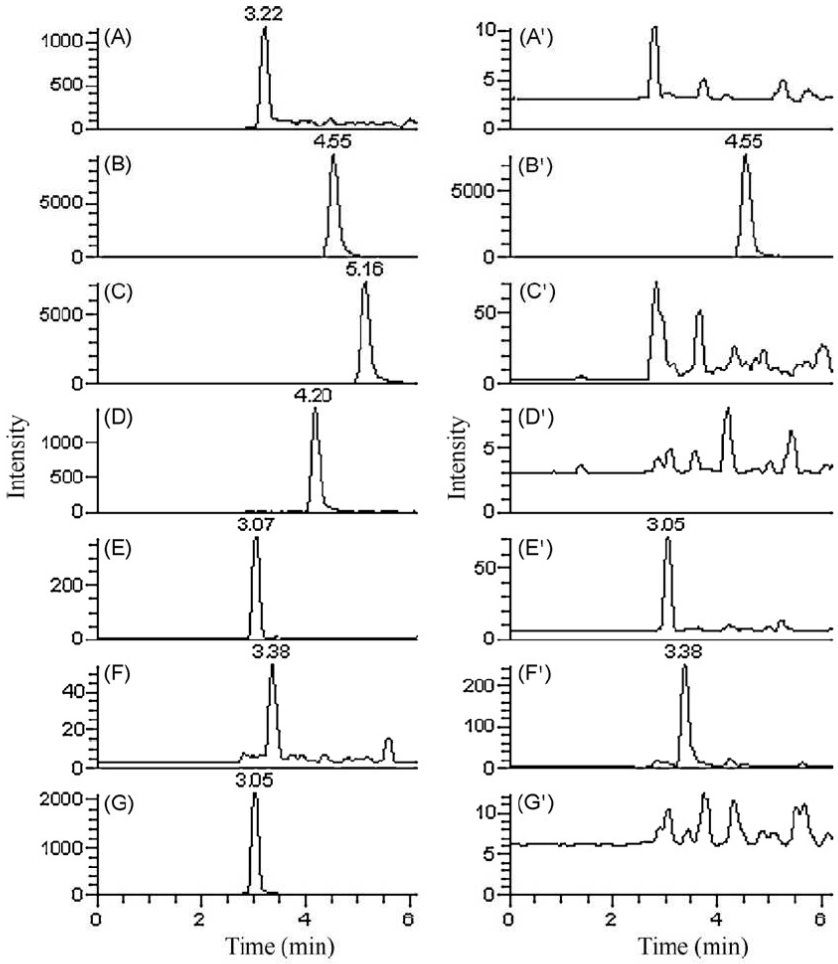

Fig. 3. Chromatograms obtained after incubation for 15 min of MCF7 cells with (left) 5-FdUrd and without (blank) (right) 5-FdUrd.
(A and A′) 5-fluorouracil (5-FU); (B and B′) 5-Chlorouracil (5-CU) (I.S.); (C and C′) 5-fluoro-2′-deoxyuridine (5-FdUrd); (D and D′) 5-fluorouridine(5-FUrd); (E and E′) 2′-deoxyuridine-5′-monophosphate (dUMP); (F and F′) thymidine-5′-monophosphate (TMP); (G and G′) 5-fluoro-2′-deoxyuridine-5′-monophosphate (5-FdUMP).

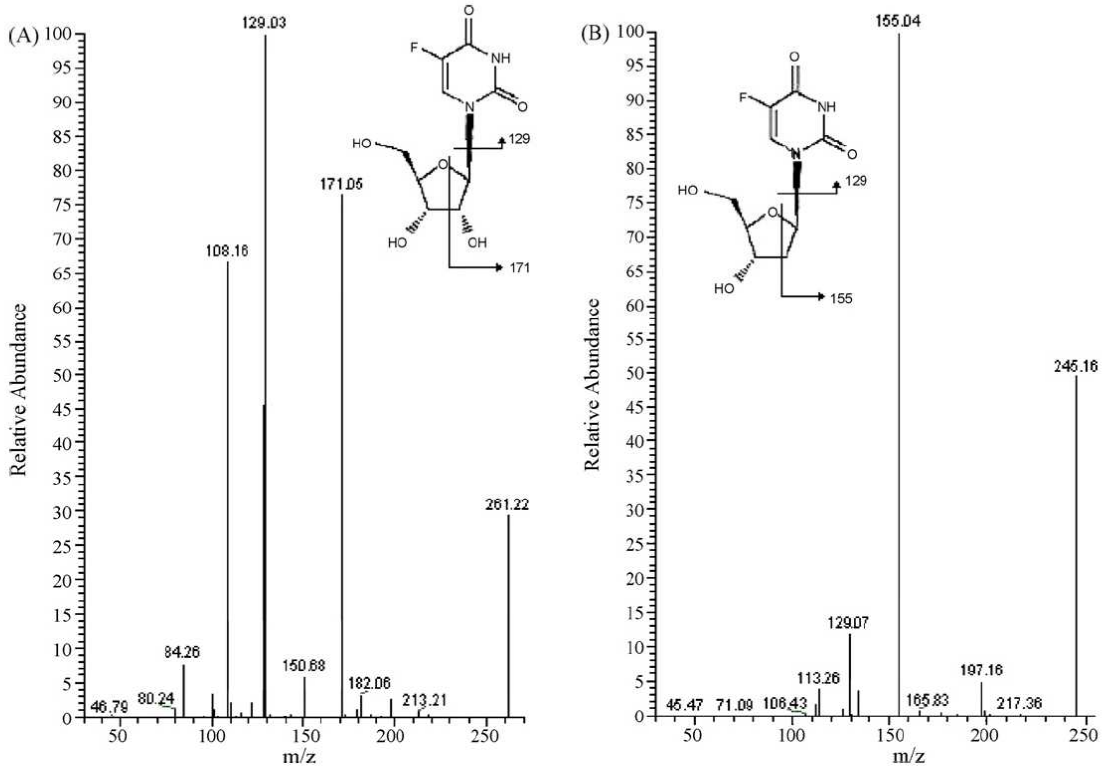

Fig. 4. Product ion mass spectrum (partial fragmentation) of 5-fluorouridine (5-FUrd–[M–H]$^-$: 261.22) (A) and 5-fluoro-2′-deoxyuridine (5-FdUrd–[M–H]$^-$: 245.16) (B).

Table 2
Inter-day validation of the intracellular determination of 5-FU, several metabolites of 5-FU and dUMP and TMP. Data from seventeen calibration curves prepared as a single replicate and analyzed on seventeen different days.

Concentration (ng mL^{-1})		Precision (%) (between-run)	Accuracy (%)
Spiked	Found (mean ± SD, 17 days)		
5-FU			
7.5	7.2 ± 0.7	9.2	96.1
15	15.9 ± 1.2	7.7	105.8
22.5	22.8 ± 1.6	6.9	101.2
75	71.8 ± 4.5	6.3	95.7
150	152.5 ± 4.4	2.9	101.7
5-FUrd			
5	4.9 ± 0.4	8.6	97.4
10	10.3 ± 0.8	7.6	103.3
15	15.3 ± 1.3	8.2	102.0
50	49.7 ± 1.7	3.4	99.5
100	100.0 ± 0.6	0.6	100.0
5-FdUrd			
5	5.1 ± 0.4	7.1	101.2
10	10.1 ± 0.6	6.0	100.8
15	14.9 ± 1.3	8.5	99.7
50	48.2 ± 2.3	4.9	96.5
100	101.9 ± 2.4	2.4	101.9
5-FdUMP			
5	5.8 ± 0.4	6.0	116.4
10	9.7 ± 0.7	7.4	96.8
15	14.0 ± 1.1	7.5	93.4
50	47.4 ± 3.7	7.7	94.7
100	103.8 ± 3.9	3.8	103.8
TMP			
2.5	2.5 ± 0.2	9.4	98.1
5	5.2 ± 0.5	8.7	104.3
7.5	7.5 ± 0.6	8.0	99.6
25	25.0 ± 0.6	2.5	100.1
50	50.0 ± 0.2	0.4	100.0
dUMP			
5	5.0 ± 0.4	7.2	99.4
10	10.5 ± 0.7	6.6	105.2
15	14.3 ± 1.3	9.2	95.5
50	50.5 ± 1.1	2.3	100.9
100	99.8 ± 0.4	0.4	99.8

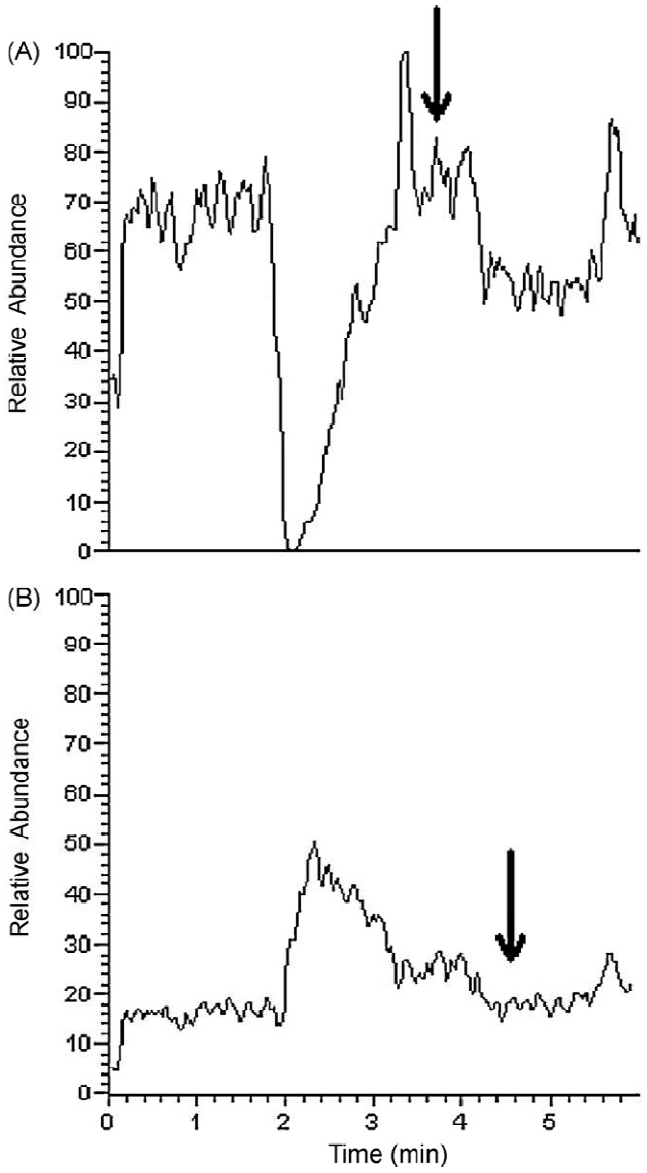

Fig. 5. Ionization suppression study of 5-FU (A) and 5-CU (B) from no extract DMEM sample. Arrow indicates the retention time of compounds.

Table 3
Assessment of accuracy and precision. Data from six replicates for each concentration and analyzed on seven different days.

Concentration (ng mL^{-1})		Precision (%)		Accuracy (%)
Spiked	Found (mean ± SD)	Within-run	Between-run	
5-FU				
11.25 (C1)	11.5 ± 1.1	8.4	5.0	101.9
112.5 (C2)	114.2 ± 6.8	4.9	3.5	101.5
5-FUrd				
7.5 (C1)	7.5 ± 0.7	7.8	6.1	100.7
75 (C2)	73.5 ± 4.2	5.3	2.1	98.0
5-FdUrd				
7.5 (C1)	7.2 ± 0.6	5.8	5.7	96.9
75 (C2)	73.5 ± 3.9	4.2	3.5	98.0
5-FdUMP				
7.5 (C1)	7.5 ± 0.7	7.0	5.4	99.6
75 (C2)	70.0 ± 6.0	8.0	3.7	93.4
TMP				
3.75 (C1)	3.8 ± 0.3	7.0	2.9	101.5
37.5 (C2)	36.5 ± 1.7	4.5	1.4	93.3
dUMP				
7.5 (C1)	7.2 ± 0.7	8.1	5.8	95.6
75 (C2)	74.9 ± 5.5	6.5	3.4	100.0

range of 93.4–105.8% except for 5-FdUMP at 5 ng mL^{-1}. The resulting assay precision and accuracy data are presented in Table 3. The within-run precision of the assay was less than 8.5% for each concentration on two QC samples. The between-run precision of the assay was less than 6.5% for all the QC samples. Assay accuracy was in the range of 93.3–101.9%. For all compounds, the lower limit of quantification was set at the lowest calibration standard. At this concentration, precision was within 20% and accuracy between 80 and 120%.

The extraction recovery was studied from cellular matrix. 5-FU, 5-FUrd, 5-FdUrd, 5-FdUMP concentrations were measured in cells or in mobile phase spiked at the concentration of QC1 and QC2 ($n = 6$). For both concentrations tested and for all compounds, the recovery was greater than or equal to 90% except 5-FU and 5-FdUrd at QC2. This latter compound gave a slightly lower recovery rate at 85%.

The quantification of 5-FU and 5-FdUMP was studied between 25 and 500 ng mL^{-1} in DMEM. For both compounds the within- and the between-run precisions were less than 6.0% and accuracy was less than 5.0%.

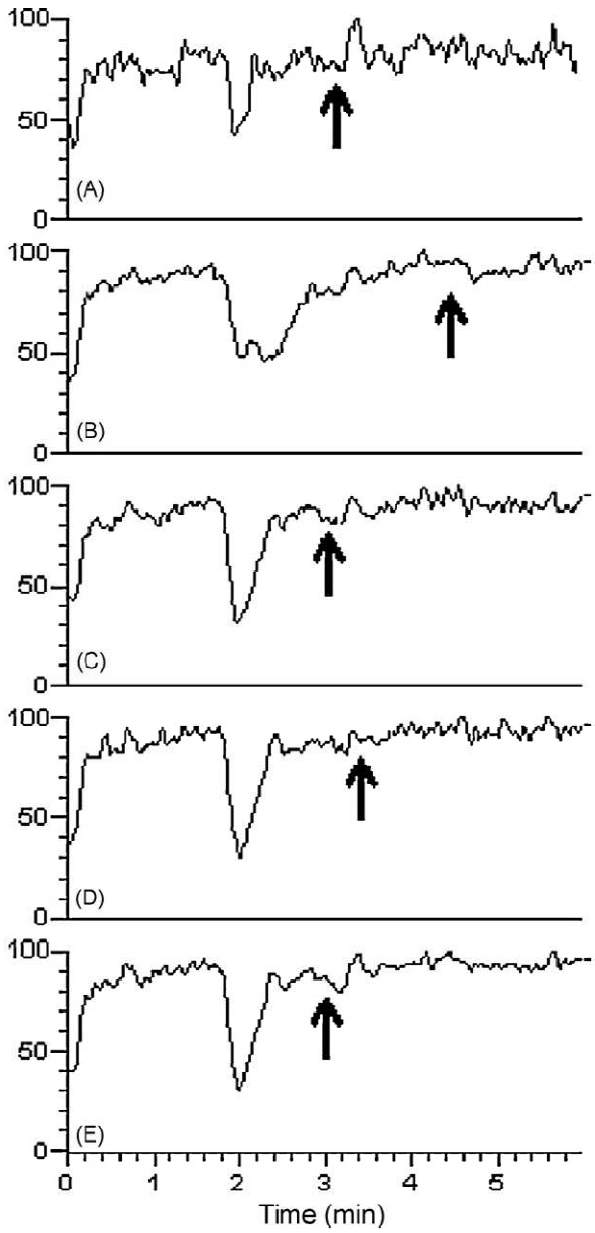

Fig. 6. Ionization suppression study of 5-FU (A), 5-FdUrd (B), dUMP (C), TMP (D) and 5-FdUMP (E) from cellular sample. Arrow indicates the retention time of compounds.

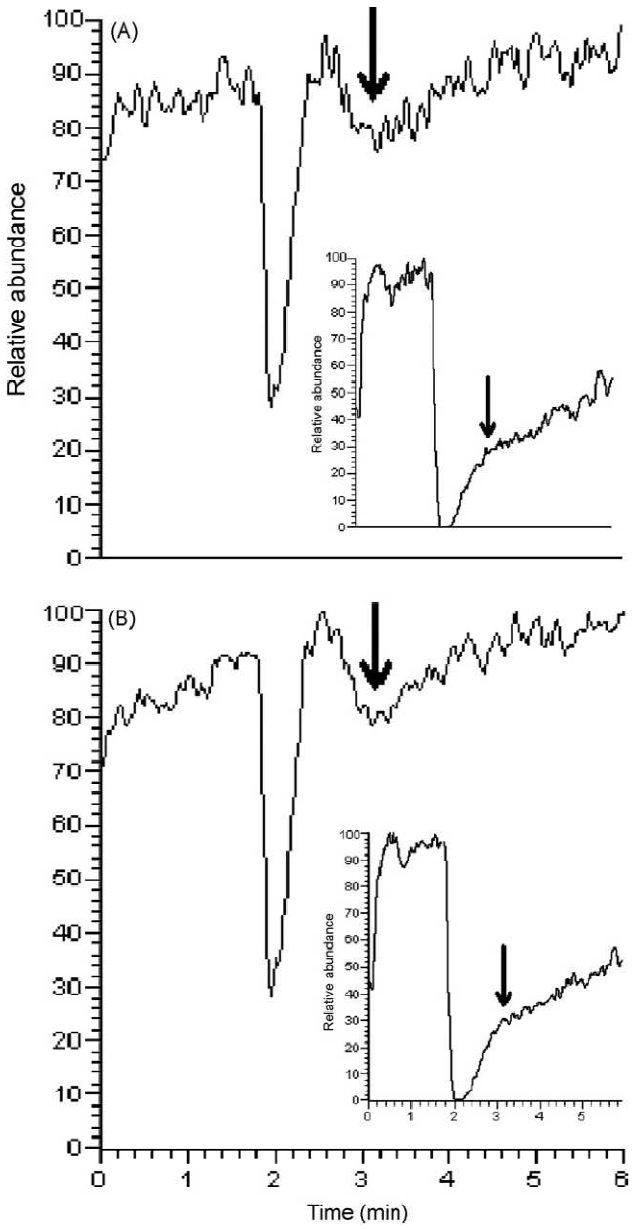

Fig. 7. Ionization suppression study of dUMP (A), and 5-FdUMP (B) from extract DMEM sample. Inset shows the ionization suppression from no extract DMEM sample.
Arrow indicates the retention time of compounds.

3.4. Assessment of stability

No significant degradation (<10%) was observed after three freeze–thaw cycles for concentrations tested from cellular samples as well as from cell culture medium (5-FU and 5-FdUMP). After extraction, when glass vials were maintained in the autosampler at +10 °C, all compounds from both matrices did not show degradation for at least 8 h. This allowed analyzing over 65 samples within a single run. Finally, no significant degradation (<10%) was observed when cellular or DMEM samples were kept at −20 °C for at least two weeks.

3.5. Matrix effect

No matrix effect was observed from no extract DMEM sample for 5-FU and 5-CU analysis (Fig. 5) or from cellular sample (Fig. 6). A broad region of ionization suppression was observed for monophosphate compounds when DMEM sample was analyzed without extraction, while SPE procedure allowed clearing this phenomenon (Fig. 7).

3.6. Application

As shown in Fig. 8, the present methodology allows following the evolution of intracellular concentration of the compounds of interest (see Fig. 1 for the metabolic pathway). The amount of 5-FdUMP increased with time linearly during 30 min (Fig. 5A) and with the concentration of substrate 5-FdUrd (Fig. 5B). Furthermore, the yield of 5-FdUrd and 5-FUrd increased with time when 5-FU is used as substrate (Fig. 5C). Interestingly, the inhibition of TS by 5-FdUMP was observed by monitoring an accumulation of dUMP and a slight decrease in TMP (Fig. 5D). This assay was also used to study the efflux transport of 5-FU and 5-FdUMP by quantification of both compounds in the cells and in DMEM incubation medium (data not shown) [22].

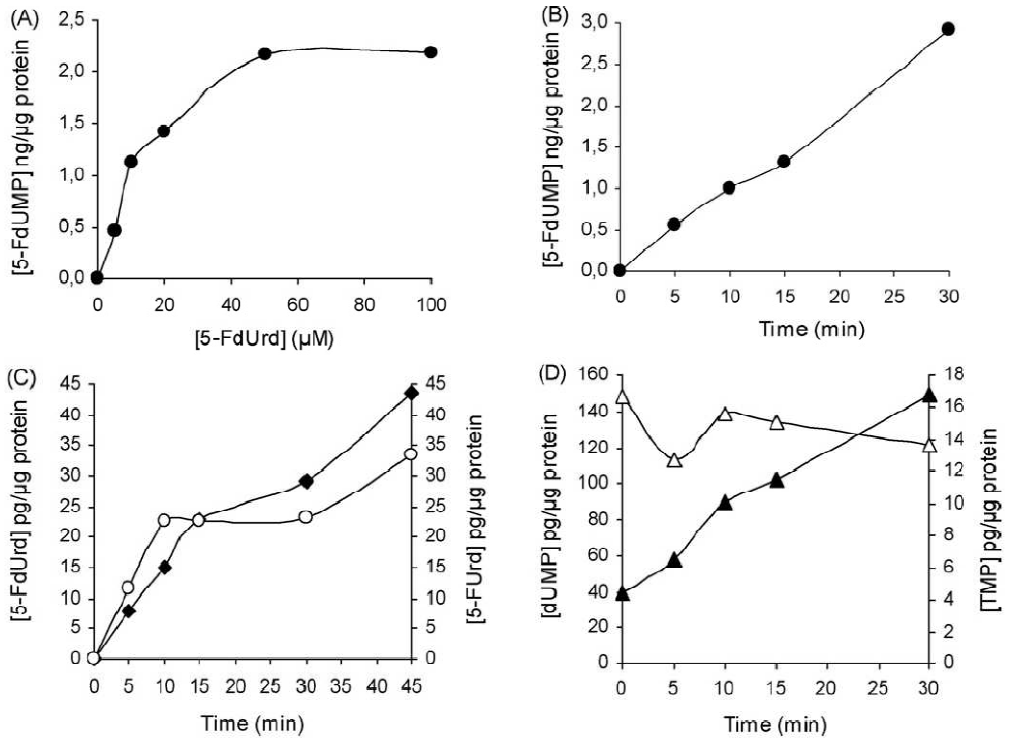

Fig. 8. Evolution of intracellular concentration of several compounds according to time and substrate concentration in MCF7 and HEK 293T cells.
(A and B) Intracellular concentration of 5-FdUMP (closed circle) in MCF7 cells according to variable 5-FdUrd concentrations at a fixed 15 min incubation time (A), according to time with a fixed 5-FdUrd concentration to 20 µM (B). (C) Intracellular concentration of 5-FdUrd (open circle) and 5-FUrd (closed square) in HEK 293T cells depending on time with 20 µM 5-FU. (D) Intracellular concentration of dUMP (closed triangle–left scale) and TMP (open triangle–right scale) in MCF7 cells depending on time with 20 µM 5-FdUrd.

4. Conclusion

A LC-MS/MS methodology was developed for the quantitative determination of 5-FU, 5-FUrd, 5-FdUrd, 5-FdUMP, dUMP, TMP in cell culture systems. This method provides accuracy, specificity, sensitivity for the analytes studied, without the safety requirements associated with radioactive substance handling. The technique described includes simple sample preparation steps and better selectivity in detection compared to conventional LC–UV assays. The current methodology also has the potential to be used for the determination of compounds in other fluid such as cell culture medium. In this case, an additional step with a solid phase extraction is needed for the determination of monophosphate compounds.

Acknowledgements

This work was supported by the INSERM and Université Lyon 1 (UMR 590) and by grants from the Association poure la Recherche contre le Cancer (ARC 4007). M.H. is a recipient of doctoral fellowships from the French National Ligue contre le Cancer.

References

[1] P. Comella, Ther. Clin. Risk Manag. 3 (2007) 421.
[2] V.G. Kaklamani, W.J. Gradishar, Expert Rev. Anticancer Ther. 2 (2003) 137.
[3] R. Martino, V. Gilard, F. Desmoulin, M. Malet-Martino, J. Pharm. Biomed. Anal. 38 (2005) 871.
[4] R. Matuo, F.G. Sousa, A.E. Escargueil, I. Grivicich, D. Garcia-Santos, J.A. Chies, J. Saffi, A.K. Larsen, J.A. Henriques, J. Appl. Toxicol. 4 (2008) 308.
[5] T. Oguri, Y. Bessho, H. Achiwa, H. Ozasa, K. Maeno, H. Maeda, S. Sato, R. Ueda, Mol. Cancer Ther. 1 (2007) 122.
[6] Y. Guo, E. Kotova, Z.S. Chen, K. Lee, K.E. Hopper-Borge, M.G. Belinsky, G.D. Kruh, J. Biol. Chem. 278 (2003) 29509.
[7] M.J. Del Nozal, J.L. Bernal, A. Pamliega, P. Marrinero, M. Pozuelo, J. Chromatogr. B: Biomed. Appl. 656 (1994) 397.
[8] F. Casale, R. Canaparo, L. Serpe, E. Muntoni, C.D. Pepa, M. Costa, L. Mairone, G.P. Zara, G. Fornari, M. Eandi, Pharmacol. Res. 50 (2004) 173.
[9] Y. Xu, J.L. Grem, J. Chromatogr. B: Anal. Technol. Biomed. Life Sci. 783 (2003) 273.
[10] F. Casale, R. Canaparo, E. Muntoni, L. Serpe, G.P. Zara, C. Della Pepa, E. Berno, M. Costa, M. Eandi, Biomed. Chromatogr. 16 (2002) 446.
[11] M. Jung, G. Berger, U. Pohlen, S. Päuser, R. Reszka, H.J. Buhr, J. Chromatogr. B: Biomed. Sci. Appl. 702 (1997) 193.
[12] J.M. Joulia, F. Pinguet, P.Y. Grosse, C. Astre, F. Bressolle, J. Chromatogr. B: Biomed. Sci. Appl. 692 (1997) 427.
[13] J. Ciccolini, L. Peillard, A. Evrard, P. Cuq, C. Aubert, A. Pelegrin, P. Formento, G. Milano, J. Catalin, Clin. Cancer Res 6 (2000) 1529.
[14] J. Ciccolini, L. Peillard, C. Aubert, P. Formento, G. Milano, J. Catalin, Fundam. Clin. Pharmacol. 14 (2000) 147.
[15] R. Dreyer, E. Cadman, J. Chromatogr. 219 (1981) 273.
[16] M. Barberi-Heyob, J.L. Merlin, B. Webér, J. Chromatogr. 573 (1992) 247.
[17] A. Guerrieri, F. Palmisano, P.G. Zambonin, M. De Lena, V. Lorusso, J. Chromatogr. 617 (1993) 71.
[18] A. Procházková, S. Liu, H. Friess, S. Aebi, W. Thormann, J. Chromatogr. A 916 (2001) 215.
[19] C. Siethoff, M. Orth, A. Ortling, E. Brendel, W. Wagner-Redeker, J. Mass Spectrom. 39 (2004) 884.
[20] A. Salvador, L. Millerioux, A. Renou, Chromatographia 63 (2006) 609.
[21] A. Pruvost, E. Negredo, H. Benech, F. Theodoro, J. Puig, E. Grau, E. García, J. Moltó, J. Grassi, B. Clotet, Antimicrob. Agents Chemother. 49 (2005) 1907.
[22] M. Honorat, A. Mesnier, J. Vendrell, J. Guitton, I. Bieche, R. Lidereau, G.D. Kruh, C. Dumontet, P. Cohen, L. Payen, Endocr. Relat. Cancer 15 (2008) 125.

III. REGULATION DE L'EXPRESSION D'ABCC11 PAR LA PROGESTERONE

L'expression d'ABCC11 étant dépendante de la présence des ER et de ses ligands, nous nous sommes demandés si d'autres hormones telles que la progestérone (PROG) pouvait avoir une influence. De plus, nous nous sommes intéressés à la déxaméthasone (DEX) qui est capable d'activer les voies intracellulaires impliquant le récepteur à la progestérone (PR) ou d'autres récepteurs comme le récepteur aux glucocorticoïdes (GR) ou le récepteur au pregnane X (PXR). En effet, ce médicament est prescrit dans le cadre de traitement antiémétique compatible avec une chimiothérapie ou en thérapie adjuvante.

→ Publication 5. Article « **ABCC11 (Multidrug Resistance Protein 8) expression is regulated by dexamethasone in breast cancer cells and is associated to progesterone receptor status in breast tumors** » par M. Honorat et coll.

Article en révision dans International Journal of Breast Cancer

Nous avons ainsi démontré que le niveau d'expression en ARN et en protéine d'ABCC11 est augmenté par un traitement à la PROG ou à la DEX, dans des cellules MCF7 (PR positive). A l'inverse, dans des cellules PR négatives (MDA-MB-231), aucune modification significative n'est observée. Ceci suggère une implication des voies de signalisation dépendante de PR.

En parallèle, dans les cellules MCF7, nous avons observé que l'expression d'ABCC11 était fortement diminuée par l'action du pregnenolone-16α-carbonitrile (PCN) et de manière modérée par le clotrimazole. Les cellules MCF7 sont GR et PXR positives. L'effet modéré du clotrimazole (activateur de PXR) laisse penser que PXR n'est probablement pas impliqué. Le PCN, quant à lui, active à la fois PXR et GR et montre un effet avéré. Par élimination d'une régulation via PXR, il semblerait donc que ce soit GR qui soit recruté pour la régulation de l'expression d'ABCC11. Pourtant, aucune régulation n'a été observée dans les cellules MDA-MB-231, également GR et PXR positives. Ceci suggère une régulation fortement dépendante du type et du contexte cellulaire (différent recrutement de co-activateurs ou corépresseurs).

De plus, le niveau d'ABCC11 a été positivement corrélé à l'expression de PR dans des tumeurs de patientes post-ménopausées. Cette corrélation est d'autant plus forte que l'on considère la sous-classe des tumeurs ER négative et PR positive (affranchissement du biais lié à la corrélation entre ABCC11 et ER). Ainsi dans ce type de cancers du sein, la surexpression d'ABCC11 pourrait induire une diminution de la sensibilité aux chimiothérapies incluant des substrats d'ABCC11. Ce phénomène pourrait s'avérer d'autant plus vrai chez les patientes traitées en parallèle par la DEX.

ABCC11 (MULTIDRUG RESISTANCE PROTEIN 8) EXPRESSION IS REGULATED BY DEXAMETHASONE IN BREAST CANCER CELLS AND IS ASSOCIATED TO PROGESTERONE RECEPTOR STATUS IN BREAST TUMORS.

Mylène Honorat [a,b,c], *Aurélia Mesnier* [a,b,c], *Julie Vendrell* [a,b,c], *Attilio Di Pietro* [e], *Valérie Lin* [f], *Charles Dumontet* [a,b,c], *Pascale Cohen* [a,b,c] *and Léa Payen* [a,b,c,d, §]

a Université de Lyon, Lyon1, Lyon, F-69008, France ;
b Inserm, U590, Lyon, F-69008, France ;
c Centre Léon Bérard, FNCLCC, Lyon, F-69008, France ;
d Université de Lyon, Faculté de Pharmacie, ISPB, Laboratoire de Toxicologie, Lyon, F-69008, France ;
e Equipe labellisée Ligue 2009, Institut de Biologie et Chimie des Protéines, UMR 5086 CNRS/Université Lyon 1, IFR128 BioSciences Gerland-Lyon Sud, F-69367 Lyon Cedex 07, France ;
f School of Biological Sciences, Nanyang Technological University, Singapore

§ Corresponding author: Dr. PAYEN Lea, INSERM U590, Université Lyon 1, 8 Avenue Rockefeller, 69008 Lyon, France / E-mail: Lea.Payen@recherche.univ-lyon1.fr / Tel.: +33-4-78777236 / Fax: +33-4-78777088.

ABSTRACT

The ATP-binding cassette multidrug resistance protein 8 (MRP8/ABCC11) mediates the excretion of anticancer drugs. ABCC11 mRNA and protein levels were enhanced by DEX (dexamethasone) and by PROG (progesterone) in MCF7 (progesterone receptor (PR)-positive) but not in MDA-MB-231 (PR-negative) breast cancer cells. This suggested a PR-signalling pathway involvement in ABCC11 regulation. Nevertheless, pregnenolone-16α-carbonitrile (GR antagonist) and clotrimazole strongly and moderately decreased ABCC11 expression levels in Glucocortocoid Receptor (GR)- and Pregnane X Receptor (PXR)-positive MCF7 cells but not in MDA-MB-231 cells (GR- and PXR-positive). Thus, GR-signalling pathway involvement could not be excluded in ABCC11 regulation in MCF7 cells. Furthermore, ABCC11 levels were positively correlated with the PR status of postmenopausal patient breast tumours from two independent cohorts. Thus, in the sub-class of breast tumors (Estrogen Receptor (ER)-negative / PR-positive), the elevated expression level of ABCC11 may alter the sensitivity to ABCC11 anticancer substrates, especially under treatment combinations with DEX.

INTRODUCTION

Among the members of the ATP-binding cassette (ABC) transporter superfamily, MRP8/ABCC11 (MultiDrug Resistance Protein 8) is a full-length ABC transporter associated with resistance to methotrexate and fluoropyrimidines, two classes of agents widely used for breast cancer treatments [1, 2]. ABCC11 transcripts were overexpressed in estrogen receptor (ER)-positive breast cancers [3]. As apically expressed, ABCC11 proteins are likely to play a significant role in absorption, distribution and elimination of its substrates [4]. ABCC11-mediated transport of anticancer drugs, combined with its expression levels in a hormonally-regulated breast tissue, suggest that the pump expression may be regulated by xenobiotics. Dexamethasone (DEX), a potent anti-inflammatory factor, has already found very broad clinical applications for treatment of diverse conditions, ranging from associated diseases and asthma to cancer therapy [5]. DEX is a well-known activator of numerous signal transduction and molecular gene-regulation pathways. It frequently involves nuclear receptors, including pregnane X receptor (PXR), glucocorticoid receptor (GR) and progesterone receptor (PR) [6]. The aim of this work was to determine whether a DEX treatment may lead to any change in the expression level of ABCC11 protein in MCF7 breast cancer cells, an endocrine-related cell model.

MATERIALS AND METHODS

Chemicals and Cell Lines - DEX, PROG, clotrimazole and pregnenolone 16α-carbonitrile (PCN) were purchased from Sigma Aldrich (France). TRIZol RNA extraction kit, murine moloney leukemia virus reverse transcriptase (MMLV-RT), Taq DNA polymerase, complete high-glucose Dulbecco's modified Eagle's medium (DMEM), L-glutamine and penicillin-streptomycin were manufactured by Gibco (France), and fetal bovine sera by PAN Biotech GmbH (Aidenbach, Germany). To avoid interference by steroids present in classical media, cell lines were first purged for 4 days in DMEM without phenol red, supplemented with 3% steroid-depleted, dextran-coated and charcoal-treated, fetal calf serum (DCC medium). The culture media were then used in either presence or absence of various molecules as described in Honorat *et al* (2008) [3]. We used (PR-positive, ER-positive, GR-positive and PXR-positive) MCF7 and (PR-negative, ER-negative, GR-positive and PXR-positive) MDA-MB231 cells stably transfected with both empty pBK-CMV and pSG5-plasmids (called pSG5-MDA-MB231). The last cell line is derived from MDA-MB-231 cells and displays a similar phenotype about PR and ER status.

Breast tumor samples - All experimental procedures were performed in compliance with french laws and regulations and were approved by the Ethics Committee. Sixty primary tumors from patients, with no therapy prior to surgery, were collected from postmenopausal women at the Pathology Department of Val d'Aurelle Cancer Center (Montpellier, France) [7]. The malignancy of infiltrating carcinomas was scored according to the histological prognostic system of Scarff–Bloom–Richardson [8]. The ER positive status was determined at the protein level by a radio-ligand binding assay (with a cut-off level for positivity set at 10 fmol/mg of protein according to the WHO typing system) and confirmed by an ER quantitative RT–PCR assay. The PR status was measured at the protein level by a binding assay as previously described [9].

In parallel, normalized data from an independent cohort of 245 breast tumors (Bittner_breast's study) were extracted from the GEO web site. ABCC11 expression levels were analyzed in breast tumors whose PR and ER clinical status were indicated (mostly defined by immunohistochemistry (IHC)).

Quantitative real-time RT-PCR (QRT-PCR) - Total mRNA extraction and QRT-PCR were performed as described in Honorat *et al.* (2008) [3].

Immunoblotting and quantification - Protein expression was analysed by immunoblotting analysis as previously described [3]. Densitometry was performed using the ImageJ® software.

Statistical analysis - Data were analyzed for statistical significance using either Mann Whitney's test or Student's t test. Differences with P-values < 0.05 were considered as statistically significant.

RESULTS AND DISCUSSION

The expression levels of ABC transporters are highly regulated by xenobiotics, including estrogens, PROG and DEX [2]. These regulations may control the availability of many substrates, including anticancer drugs, by either increasing or decreasing their elimination from cells. They can influence the cell sensitivity to their substrates. Consequently, we characterized DEX regulation pathways of ABCC11 in PR-positive MCF7 cells. For the first time, ABCC11 expression levels were shown to be increased in a time-dependent manner by 5 µM DEX, with a trend towards higher ABCC11 levels after a 24-h exposure, and a maximal and significant induction after 48-72 h (Figure 1A) in DEX-treated cells compared to vehicle-treated cells. Furthermore, DEX strongly enhanced ABCC11 mRNA levels in a dose-

dependent manner (Figure 1B). ABCC11 mRNA amounts were slightly up-regulated after 48-h exposure to a very low DEX concentration (0.001 µM, Figure 1B); higher concentrations (0.05 µM) were however required to reach a maximal and significant induction. The molecular mechanisms of *ABCC11* regulation were further explored by demonstrating that, in MCF7 cells, the physiological PR ligand PROG regulated ABCC11 expression in the same way as DEX, while DEX and PROG did not modify ABCC11 expression in PR-negative pSG5-MDA-MB-231 breast cells. PROG at 15 µM induced ABCC11 gene expression in MCF7 cells, whereas no regulation was observed in PR-negative pSG5-MDA-MB-231 cells (Figure 2A). In agreement, by immunoblotting, both DEX and PROG increased ABCC11 protein expression, by at least 2-fold, in comparison to the vehicle control (Figure 2B). Additional bands, observed below 116 kDa, were probably due to proteolytic degradation of ABCC11 as described by Bortfeld and al [4]. DEX can activate PR-signalling pathways [6, 10]. Since ABCC11 regulation by DEX and PROG only occurred in PR-positive MCF7 cells and not in PR-negative pSG5-MDA-MB-231 cells, we hypothesized that the effects of DEX and PROG on ABCC11 expression could be partially related to PR-signalling pathways. Interestingly, by in silico analysis of the human ABCC11 promoter region (- 5000, chr16: 38685979-), we found two progesterone-response elements (PRE).

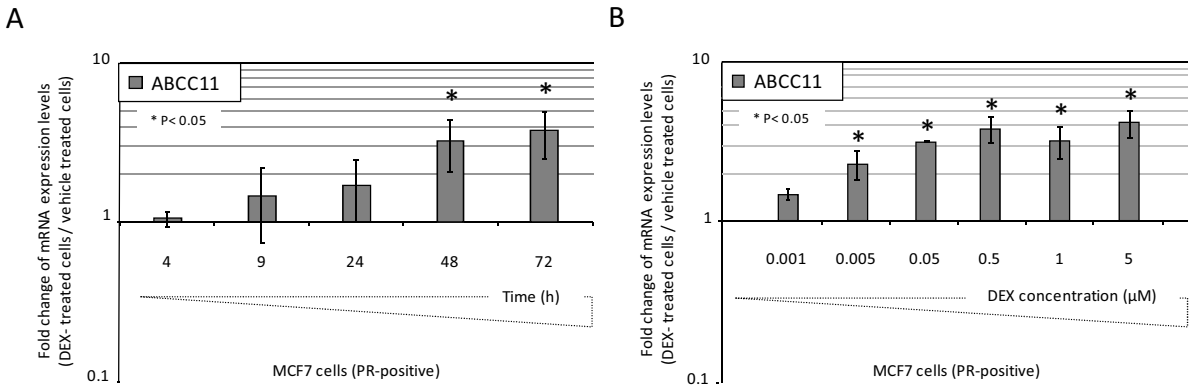

Figure 1 - DEX time-course and dose-dependent effects on ABCC11 mRNA expression. MCF7 cells were exposed to 5 µM DEX for 4 to 72 h (A) or to DEX concentrations ranging from 0.001 to 5 µM (B). Fold change of mRNA levels of ABCC11 was determined by QRT-PCR. The QRT-PCR values indicated below are means +/- S.D. of at least 4 independent experiments; y is a logarithmic scale. * P <0.05; Student's t test.

Based upon the observation that ABCC11 expression levels were up-regulated by DEX, we next evaluated whether ABCC11 expression was also regulated by other ligands of GR and PXR. PCN is known as a weak hPXR activator and as a potential GR antagonist [11-13]. PCN at 5 µM and 10 µM strongly decreased ABCC11 expression in MCF7 cells and had no effect in MDA-MB-231 cells (Figure 3). Though MDA-MB-231 cells strongly expressed GR, no effects of either DEX or PROG were observed on ABCC11 expression (Figure 2A). The default of PCN, DEX and PROG effects via GR in MDA-MB-231 cells may be directly related to the "cellular context". Indeed, GR may regulate gene transcription by various mechanisms: synergistic activity where transcription factors bound at other DNA sites cooperate with ligand-activated GR bound to a consensus glucocorticoid-response element (GRE); interference with the actions of other transcription factors (e.g., AP-1 and NF-κB) through protein-protein interactions, which does not require GR binding to DNA; and either repression or stimulation via requisite interactions of GR with other transcription factors all bound at so-called composite GREs [14-16]. DEX had been demonstrated to increase c-fms transcript and protein levels in breast cells (SKBR3 and BT20), but not in others (MCF7)

[17]. Consequently, in MCF7 cells, the involvement of GR-signalling pathways could not be completely excluded and is somehow suggested by the GRE motif revealed in the in silico analysis of the human ABCC11 promoter region (- 5000) using the Genomatix software.

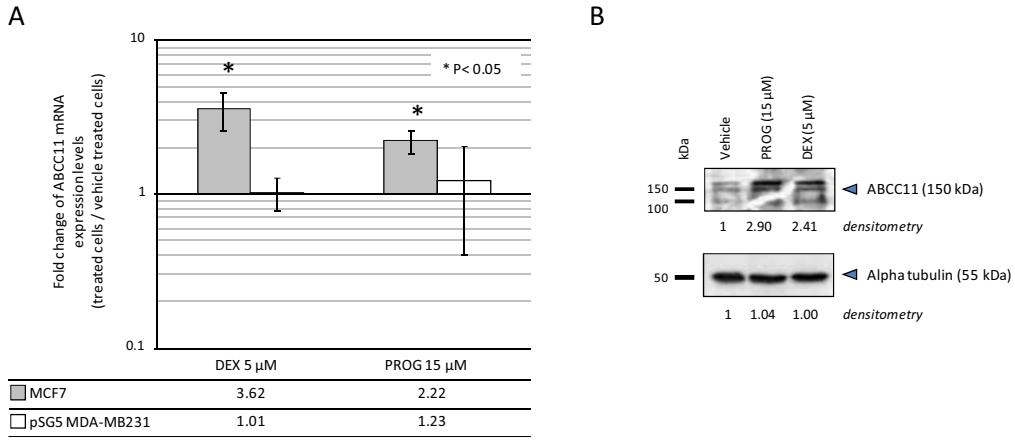

Figure 2 - Alterations of ABCC11 mRNA and protein level by DEX and PROG. A) Cells were exposed to either 5 µM DEX or 15 µM PROG for 72 h. Fold change of mRNA levels of ABCC11 was determined by QRT-PCR. The QRT-PCR values indicated below are means +/- S.E. of 4 independent experiments; y is a logarithmic scale. * P <0.05; Student's t test. **B)** Crude membrane fractions (150 µg) were prepared from cells exposed to either vehicle, 5 µM DEX or 15 µM PROG for 72 h.

Finally, we used clotrimazole, a powerful human PXR ligand to explore PXR signalling pathways. Clotrimazole at 5-10 µM did not produce a major effect on ABCC11 expression in MCF7 cells and had no effect on ABCC11 expression in MDA-MB231 cells (Figure 3). In addition, little is known about PROG direct interaction with PXR-signalling pathway, and PCN and DEX were relatively weak activators of human PXR as compared to clotrimazole. Although PCN weakly decreased ABCC11 expression in PXR-positive MCF7 cells, no regulatory effect was observed in PXR-positive MDA-MB-231 cells. We may then suggest that PXR-signalling pathway was likely not directly involved in ABCC11 regulation by DEX and PROG. The overall results suggest that regulation of ABCC11 expression by PROG and DEX is at least partially linked to PR signalling pathways.

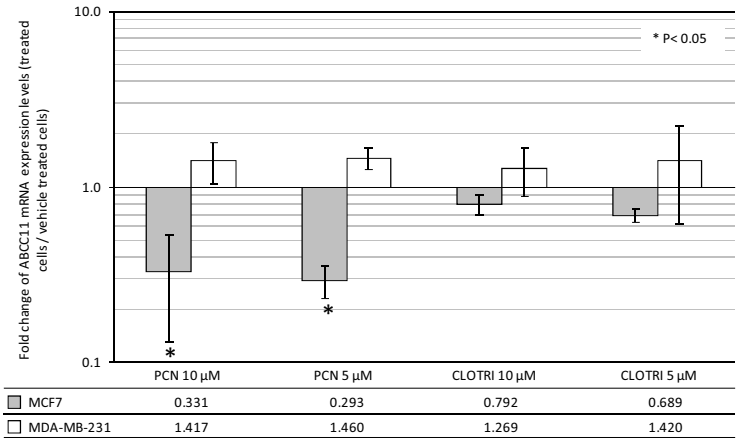

Figure 3 - Alteration of ABCC11 mRNA level by clotrimazole and PCN. MCF7 cells were treated for 72 h with 15 µM PROG, 5 - 10 µM clotrimazole or 5 - 10 µM PCN. Fold change of mRNA levels of ABCC11 was determined by QRT-PCR. The QRT-PCR values indicated below are means ± SE. at least three independent experiments. *P < 0.05; Student's t test.

Currently, the PR-positive status of breast tumors is recognized as an important indicator of the likelihood of response to endocrine agents [18]. Approximately two-thirds of breast cancers express the estrogen receptor alpha (ERα), some of them being PR-negative. PR absence significantly correlated with a less differentiated phenotype of breast tumors [18]. Based upon our in vitro observation, we evaluated whether there was any correlation between ABCC11 expression and PR status in 60 breast cancers from postmenopausal women (fully described [3, 7]). In this local cohort of patient, the PR and ER status were evaluated at the protein level by binding assays [7]. Significantly higher ABCC11 mRNA levels were observed in PR positive tumors than in PR-negative samples (ABCC11 levels were approximately 6-fold higher in the PR-positive groups than in the PR-negative groups; p = 0.014 Mann Withney's test (Table 1)). To confirm those observations, we extracted and analysed the normalized data of ABCC11 expression level of 245 breast tumors from an independent cohort (Bittner_breast's study from the GEO web site). We only retained breast tumors whose PR and ER clinical status, mostly defined by immunohistochemistry (IHC), were indicated. We validated a positive association between PR status and ABCC11 expression levels in this larger cohort of breast tumors (Table 1; p = 0.003).

We previously observed a high significant ABCC11 mRNA levels in breast cancer tumors possessing high levels of ERα compared to those having low levels [3]. We validated a positive association between ABCC11 expression level and ER status in Bittner's breast cohort (n = 159; ER-negative tumors; n = 86 ; ER-positive tumors; p = 0.0004 Mann Whitney's test). We decided to carry out sub-classes of tumors according their ER status. In our tumor cohort, the ABCC11 mRNA level difference between breast tumors according to PR-status was only found significant in patients with ER-negative status. ABCC11 expression levels were approximately 11-fold higher in the ER-/PR+ sub-group than in ER-/PR- patient (p=0.009 ; Mann Whitney's test). While not reaching significant difference (p = 0.076), a tendency had been found in the ER-negative sub-group of Bittner's Breast cohort. The median ratio between PR-/PR+ was approximately 9-fold (Table 1). This might be directly related to the tiny number of ER-/PR+ tumors (n=3). Since this repartition is representative of clinical situation (ER-positive status is frequently associated with PR-positive status), this observation fully justify the limited number of ER-/PR+ tumors in studied clinical cohorts.

By contrast, in both cohorts, tumors with ER-positive status did not show any correlation between ABCC11 expression levels and PR status (Table 1). This suggests that in ER-positive breast tumors, the ER status is mainly associated in ABCC11 mRNA levels, while in ER-negative breast tumors ABCC11 expression levels are associated with PR-status.

Table 1	Sub-group	n	Median	Range (min-max)	Ratio (sub-group 2 median/ sub-group 1 median)	p ‡
Present study†§	PR-	26	**2,22**	(0,1-289)	5,79	**0,014**
	PR+	34	**12,86**	(0,6-354)		
	ER-/PR-	23	**1,50**	(0,1-177)	11,21	**0,009**
	ER-/PR+	12	**16,82**	(0,8-354)		
	ER+/PR-	3	**33,37**	(8,9-289)	0,36	0,181
	ER+/PR+	22	**11,99**	(0,6-286)		
Bittner's study	PR-	116	**86,50**	(2,4-12494)	2,47	**0,003**
	PR+	129	**213,50**	(1,7-11933)		
	ER-/PR-	83	**53,80**	(2,4-12494)	9,80	0,075
	ER-/PR+	3	**527,10**	(199,8-1866)		
	ER+/PR-	33	**225,10**	(4,6-4950)	0,87	0,871
	ER+/PR+	125	**196,00**	(1,7-11933)		

Present study: n = 60 tumors
Bittner's study: n = 245; From normalized data published on GEO web site GSE2109 - ABCC11 (224146_s_at).
† ABCC11 QRT-PCR expression levels
§ PR and ER status were measured at the protein level by binding assay.
‡ P-values were considered to be statistically significant if P < 0,05 (Mann Whitney's test).

Table 1 - Relationships between ABCC11 mRNA expression, PR-status and ER-status in breast tumors from postmenopausal patients.

CONCLUSION

Currently, breast chemotherapies frequently include 5-FU (metabolized in cells to 5FdUMP, which is an ABCC11 substrate). Interestingly, Park et al. studied the relationship between ABC transporter gene expression and chemotherapy responsiveness in early breast cancer patients who underwent sequential weekly paclitaxel/FEC (5-FU, epirubicin and cyclophosphamide) neoadjuvant therapy. Several ABC transporters including ABCC5 and ABCC11 showed significant increased expression in the residual disease [19]. Taken altogether, the association between PR and ABCC11, in a sub-group of breast tumors with low expression of ER, highlighted how ABCC11 might constitute a putative marker of 5-FU anticancer resistance.

Furthermore, by altering ABCC11 expression levels, DEX, an adjuvant anticancer drug, may significantly contribute to chemo-resistance mechanisms to ABCC11 substrates. High expression levels of ABCC11 in PR-positive breast tumors with low expression of ER alpha may contribute to a decreased sensitivity to chemotherapeutic combinations containing 5-FU. Future work is needed to investigate this point.

ACKNOWLEDGEMENTS

This work was supported by the INSERM (UMR 590) and Université Lyon 1, and by grants from the Association de la Recherche contre le Cancer (ARC 4007) and the Ligue Nationale contre le Cancer (Equipe labellisée Ligue 2009 and 2010 funding from the Comité de la Drôme). M.H. is recipient of a doctoral fellowship from the French Ligue National contre le Cancer.

We are grateful to the Val d'Aurelle Hospital for providing tumor breast samples. We thank our colleagues Drs Catherine Grenot, Anne Nies and Dietrich Keppler (Heidelberg, Germany) for helpful collaboration.

REFERENCE LIST

1. Guo Y, Kotova E, Chen ZS, Lee K, Hopper-Borge E, Belinsky MG, Kruh GD: MRP8, ATP-binding cassette C11 (ABCC11), is a cyclic nucleotide efflux pump and a resistance factor for fluoropyrimidines 2',3'-dideoxycytidine and 9'-(2'-phosphonylmethoxyethyl)adenine. J Biol Chem 2003, 278(32):29509-29514.
2. Honorat M, Guitton J, Dumontet C, Payen L: Expression level and hormonal regulation of ABC transporters in breast cancer. Current cancer therapy review 2010:in press.
3. Honorat M, Mesnier A, Vendrell J, Guitton J, Bieche I, Lidereau R, Kruh GD, Dumontet C, Cohen P, Payen L: ABCC11 expression is regulated by estrogen in MCF7 cells, correlated with estrogen receptor {alpha} expression in postmenopausal breast tumors and overexpressed in tamoxifen-resistant breast cancer cells. Endocr Relat Cancer 2008, 15(1):125-138.
4. Bortfeld M, Rius M, Konig J, Herold-Mende C, Nies AT, Keppler D: Human multidrug resistance protein 8 (MRP8/ABCC11), an apical efflux pump for steroid sulfates, is an axonal protein of the CNS and peripheral nervous system. Neuroscience 2006, 137(4):1247-1257.
5. McNamara S, Kilbride L: Treating primary brain tumours with dexamethasone. Nurs Times 1999, 95(47):54-57.
6. Leo JC, Guo C, Woon CT, Aw SE, Lin VC: Glucocorticoid and mineralocorticoid cross-talk with progesterone receptor to induce focal adhesion and growth inhibition in breast cancer cells. Endocrinology 2004, 145(3):1314-1321.
7. Vendrell JA, Ghayad S, Ben-Larbi S, Dumontet C, Mechti N, Cohen PA: A20/TNFAIP3, a new estrogen-regulated gene that confers tamoxifen resistance in breast cancer cells. Oncogene 2007, 26(32):4656-4667.
8. Bloom HJ, Richardson WW: Histological grading and prognosis in breast cancer; a study of 1409 cases of which 359 have been followed for 15 years. Br J Cancer 1957, 11(3):359-377.

9. De Goeij AF, Scheres HM, Rousch MJ, Hondius GG, Bosman FT: Progesterone receptor quantification with radiolabeled promegestone (R 5020) in frozen sections of endometrium and breast cancer tissue. J Steroid Biochem 1988, 29(5):465-474.

10. Honorat M, Mesnier A, Di Pietro A, Lin V, Cohen P, Dumontet C, Payen L: Dexamethasone down-regulates ABCG2 expression levels in breast cancer cells. Biochem Biophys Res Commun 2008, 375(3):308-314.

11. Tsurufuji S, Sugio K, Takemasa F: The role of glucocorticoid receptor and gene expression in the anti-inflammatory action of dexamethasone. Nature 1979, 280(5721):408-410.

12. Marek CJ, Tucker SJ, Konstantinou DK, Elrick LJ, Haefner D, Sigalas C, Murray GI, Goodwin B, Wright MC: Pregnenolone-16alpha-carbonitrile inhibits rodent liver fibrogenesis via PXR (pregnane X receptor)-dependent and PXR-independent mechanisms. Biochem J 2005, 387(Pt 3):601-608.

13. Schuetz EG, Guzelian PS: Induction of cytochrome P-450 by glucocorticoids in rat liver. II. Evidence that glucocorticoids regulate induction of cytochrome P-450 by a nonclassical receptor mechanism. J Biol Chem 1984, 259(3):2007-2012.

14. Pearce D, Matsui W, Miner JN, Yamamoto KR: Glucocorticoid receptor transcriptional activity determined by spacing of receptor and nonreceptor DNA sites. J Biol Chem 1998, 273(46):30081-30085.

15. Pearce D, Yamamoto KR: Mineralocorticoid and glucocorticoid receptor activities distinguished by nonreceptor factors at a composite response element. Science 1993, 259(5098):1161-1165.

16. Diamond MI, Miner JN, Yoshinaga SK, Yamamoto KR: Transcription factor interactions: selectors of positive or negative regulation from a single DNA element. Science 1990, 249(4974):1266-1272.

17. Sapi E, Flick MB, Gilmore-Hebert M, Rodov S, Kacinski BM: Transcriptional regulation of the c-fms (CSF-1R) proto-oncogene in human breast carcinoma cells by glucocorticoids. Oncogene 1995, 10(3):529-542.

18. Osborne CK, Schiff R, Arpino G, Lee AS, Hilsenbeck VG: Endocrine responsiveness: understanding how progesterone receptor can be used to select endocrine therapy. Breast 2005, 14(6):458-465.

19. Park S, Shimizu C, Shimoyama T, Takeda M, Ando M, Kohno T, Katsumata N, Kang YK, Nishio K, Fujiwara Y: Gene expression profiling of ATP-binding cassette (ABC) transporters as a predictor of the pathologic response to neoadjuvant chemotherapy in breast cancer patients. Breast Cancer Res Treat 2006.

REVISION

Editor's comment

Since one of the main points of discussion in the paper is the relationship to progesterone receptor, and as estrogen receptor is also mentioned throughout, I feel that it would be appropriate to add into the methodology some further information regarding the technique and the cut-off for determination of these important features (rather than simply a reference to another of your papers, in which the methodology is mentioned some way down the text). It would seem from the reference, that this was by ligand-binding assay - was this really the case? Was immunohistochemistry not used?

Reviewer's comment

The authors present data suggesting that expression of the ABCC11 gene is upregulated at both RNA and protein levels. The manuscript is generally well written and the conclusions drawn are logical and sound based on the data presented. However, there are some inconsistencies within the manuscript that need to be addressed.

Methods Page 3: It is unclear why the MDA-MB-231 cells that have been used have been transfected with empty vectors. Why not use the parental cell line?

Results Pages 4 and 7: Significant and maximal induction of gene expression was achieved with 0.05uM DEX (Figure 1B). In the experiments presented in Figure 2, 5uM DEX was used. Why was this concentration used when 100 fold less would have been enough for maximal induction?

The ponceau stained gel in Figure 2B is off poor quality and not really required with alpha-tubulin being used as a loading control.

Page 9: The whole section describing the patient sample is very confusing. Tumours have been sub-grouped according to ER status (line 8). It is not at all clear where the sub groups of tumours come from. Are these a sub-group of the Bittner's study or a separate group? It is also very unclear whether the previous observations (lines4/5) are based on the Bittner's tumours or a different cohort. This section needs re-writing so that it is clearer and makes more sense.

IV. REGULATION DE L'EXPRESSION D'ABCG2 PAR LA PROGESTERONE

Un autre acteur important dans la résistance aux chimiothérapies et exprimé dans le cancer du sein est ABCG2 ou BCRP (*Breast Cancer Resistance Protein*). Tout comme ABCC11, ABCG2 est exprimée dans le tissu mammaire et soumise à une régulation dépendante des ER comme nous l'avons rapporté dans la revue : "*Expression level and hormonal regulation of ABC transporters in breast cancer*.". Afin de savoir si les récepteurs à la progestérone intervenaient aussi dans la régulation de l'expression de cette protéine, nous nous sommes intéressés à l'impact de la déxaméthasone.

→ Publication 6. « **Dexamethasone down-regulates ABCG2 expression levels in breast cancer cells** » par M. Honorat et coll.

Article publié dans Biochemical and Biophysical Research Communications (2008)

Nous avons démontré que la déxaméthasone (DEX) et la progestérone (PROG) régulaient négativement l'expression d'ABCG2 dans les cellules MCF7 (PR positives) et dans les cellules MDA-MB-231 (PR négatives). A l'inverse, dans des cellules exprimant PRA et PRB de manière stable, ABCG2 a été régulée positivement par la DEX et la PROG. Ces observations suggèrent que l'expression d'ABCG2 est régulée par des voies faisant intervenir PR. De plus, l'effet de la DEX a été abolit par la présence de cycloheximide (inhibiteur de la synthèse protéique) ce qui indique que la régulation d'ABCG2 fait intervenir une étape de synthèse protéique.

La présence d'une régulation dans les cellules MDA-MB-231 n'exprimant pas PR pourrait s'expliquer par l'implication d'autres récepteurs tels que PXR ou GR retrouvés sur ces cellules. La DEX est en effet capable d'activer ces récepteurs. Dans les cellules MCF7 (PXR et GR positives), nous avons d'ailleurs observé que le PCN (faible activateur de PXR humain et activateur de GR) et le clotrimazole (activateur puissant de PXR) avaient un effet régulateur sur l'expression d'ABCG2. Ceci suggère que la régulation de l'expression d'ABCG2 par la DEX pourrait également faire intervenir GR et PXR.

Pour finir, le traitement à la DEX a été associé à une augmentation de la sensibilité à la mitoxantrone, expliquée par la diminution de l'expression d'ABCG2 qui transporte cet agent anticancéreux. Ainsi, la DEX, dans le contexte d'une thérapie à base de substrats d'ABCG2, pourrait avoir des effets bénéfiques sur l'efficacité thérapeutique.

Biochemical and Biophysical Research Communications 375 (2008) 308–314

Contents lists available at ScienceDirect

Biochemical and Biophysical Research Communications

journal homepage: www.elsevier.com/locate/ybbrc

Dexamethasone down-regulates ABCG2 expression levels in breast cancer cells ☆

Mylène Honorat [a,b,c], Aurélia Mesnier [a,b,c], Attilio Di Pietro [d], Valérie Lin [e], Pascale Cohen [a,b,c], Charles Dumontet [a,b,c], Léa Payen [a,b,c,d,*]

[a] Université de Lyon, Lyon1, Lyon, F-69008, France
[b] INSERM U590, Université Lyon 1, Laboratoire de cytologie analytique, Rockefeller, 8, Avenue Rockefeller, Lyon F-69008, France
[c] Centre Léon Bérard, FNCLCC, Lyon, F-69008, France
[d] IBCP, UMR 5086 CNRS, Université de Lyon, Lyon, F-69007, France
[e] School of Biological Sciences, Nanyang Technological University, Singapore

ARTICLE INFO

Article history:
Received 24 July 2008
Available online 8 August 2008

Keywords:
ABCG2
Progesterone receptors
Expression regulation
ABC transporters
Breast cancer
Multidrug resistance
Dexamethasone
Progesterone

ABSTRACT

The breast cancer resistance protein ABCG2 effluxes a variety of drugs and is believed to play an important role in multidrug resistance to chemotherapy. We show here for the first time that dexamethasone (DEX) and progesterone (PROG) are able to strongly inhibit ABCG2 expression in progesterone receptor (PR)-positive MCF7 and PR-negative MDA-MB-231 breast cells. In contrast, in the latter cells stably-transfected with progesterone receptor isoforms A and B, ABCG2 expression was strongly up-regulated by DEX and PROG. In addition, two other ligands of Pregnane X Receptor (PXR) and/or Glucocorticoid Receptor (GR) were also able to down-regulate ABCG2 expression in PXR- and GR-positive MCF7 cells. ABCG2 expression regulation by DEX likely resulted from the activation of PR-, PXR-, and/or GR-signaling pathways. ABCG2 expression inhibition by DEX was associated with increased sensitivity to mitoxantrone, a known ABCG2 substrate. The findings suggest that DEX may be useful in improving drug efficacy under certain conditions.

The emergence of multidrug resistance is often characterized by reduced intracellular levels of cytotoxic drugs, and is frequently associated with over-expression of members of the ATP-Binding Cassette (ABC) family including breast cancer resistance protein (BCRP/ABCG2). ABCG2 over-expression is associated to resistance against anticancer agents including mitoxantrone (MIT) [1]. ABCG2-mediated drug secretion may be influenced by any factors susceptible to affect ABCG2 expression. Such ABCG2 transport activity of anticancer drugs, in a hormonally-regulated breast tissue suggests that ABCG2 expression may be altered by potent synthetic glucocorticoid molecules such as dexamethasone (DEX). The presence of steroid-response elements (ERE, PRE) has already been reported in the ABCG2 promoter [2,3]. To date, nothing is known about the molecular mechanism by which DEX regulates ABCG2 expression in breast cancer cells.

Key players in hormone regulation events are nuclear receptors which may affect ABCG2 expression [2,3]. Various glucocorticoids, including DEX, efficiently interact with progesterone receptors (PR) [4]. The two forms of PR, namely PRA and PRB, are transcribed from a single gene under the control of separate promoters. The main structural difference between PRA and PRB is that the former lacks the first 164 N-terminal amino acids present in the latter [5]. To date, there is increasing evidence that PRA and PRB are functionally different, and that the balance between these two forms is involved in PROG differential effects on diverse physiological targets [6]. DEX also influences gene transcription, through activation of Glucorticoid Receptor (GR) and Pregnane X Receptor (PXR) [7].

Previously, it has been shown that hormones such as 17 β-estradiol (E2) and progesterone (PROG) can regulate ABCG2 expression in human placental BeWo cells [3,8,9]. Consequently, in order to better characterize steroid regulation in the hormonally-regulated mammary tissue, we investigated the molecular mechanism by which ABCG2 expression is regulated by DEX in MCF7 cells.

Abbreviations: ABC, ATP-Binding Cassette; BCRP/ABCG2, breast cancer resistance protein; CHX, cycloheximide; DEX, dexamethasone; E2, estrogen; GRE, glucocorticoid-response element; MIT, mitoxantrone; PCN, pregnenolone 16$_\alpha$-carbonitrile; PROG, progesterone; PR, progesterone receptor; PRA or PRB, progesterone receptor A or B; PRE, progesterone-response element; ERE, estrogen-response element; PXR, Pregnane X Receptor; QRT-PCR, quantitative real-time polymerase chain reaction.

☆ This work was supported by grants from the Association pour la Recherche sur le Cancer (ARC), funds from the INSERM, and a fellowship to M.H. from the "Ligue Nationale Contre le Cancer".

* Corresponding author. Address: INSERM U590, Université Lyon 1, Laboratoire de cytologie analytique, Rockefeller, 8, Avenue Rockefeller, Lyon F-69008, France. Fax: +33 478777088.
E-mail address: lea.payen@rechercheb.univ-lyon1.fr (L. Payen).

0006-291X/$ - see front matter © 2008 Elsevier Inc. All rights reserved.
doi:10.1016/j.bbrc.2008.07.149

Materials and methods

Chemicals and cell lines: E2, DEX, PROG, RU486, clotrimazole, pregnenolone 16$_\alpha$-carbonitrile (PCN), and trypan blue were purchased from Sigma Aldrich (France). TRIZol RNA extraction kit, murine moloney leukemia virus reverse transcriptase (MMLV-RT), Taq DNA polymerase, complete high-glucose Dulbecco's modified Eagle's medium (DMEM), L-glutamine and penicillin–streptomycin were manufactured by Gibco (France), and fetal bovine sera by PAN Biotech GmbH (Aidenbach, Germany).

ABC28 (PRA and PRB double positive) and CTC15 (vector-transfected) breast cell lines were described in Leo et al. [10]. They are MDA-MB-231 derived cell lines, generated respectively by co-transfection with hPR1 and hPR2 expression vectors (cDNAs respectively encoding PRB and PRA in pSG5 plasmid, ABC28 cells) and pSG5 empty vector (CTC15 cells).

To avoid interference by steroids present in classical media, cell lines were cultured in DMEM medium without phenol red, and supplemented with 6% steroid-depleted, dextran-coated charcoal-treated, fetal calf serum in presence or not of various pharmacological molecules as described in Honorat et al. [11].

Quantitative real-time RT-PCR (QRT-PCR): Total mRNA was extracted using TRIZol® method and QRT-PCR was performed in a Lightcycler® (Roche, France) in combination with the LightCycler Faststart DNA Master Sybr Green I (Roche, France) as described in Honorat et al. [11]. The specific ABCG2 primers were ABCG2-5′-TGTACTGGCGAAGAAGAATATTTGGT-3′ (forward), and ABCG2-5′-GCCACGTGATTCTTCCACAA-3′ (reverse). All measurements were normalized to expression of the 18-S ribosomal genes, considered as stable housekeeping genes (Applied Biosystems).

Immunoblotting: As described in Honorat et al. [11], protein expression was analyzed by immunoblotting analysis. The progesterone receptor Ab-8 (Lab vision Biotechnology), ABCG2 BXP21 or alpha-tubulin (Santa-Cruz biotechnology) mouse monoclonal antibodies were used. Ponceau is a reversible protein dye which allows checking transfer and gel loading. Densitometry was performed using the ImageJ® software.

Trypan blue assay: 20,000 MCF7 cells per well were plated in 24-well plates (Becton Dickinson, San Jose, CA, USA) in a volume of 900 µl of DCC medium. Cells were incubated for 24 h at 37 °C before adding 100 µl of DCC medium either containing or not 5 µM DEX. After a 24-h incubation at 37 °C in either presence or absence of DEX, 100 µl of DCC medium containing 0.25 or 0.5 µM MIT were added. In brief, cell mortality was evaluated 72 h after MIT addition. Trypan blue assays of anticancer drug-challenged cells were performed as previously described by Graidist [12]. Both floating and attached cells were assayed. At least 150 cells per treatment were counted after being stained with trypan blue (0.2%). Assays were performed in six-plicate in five independent experiments.

Statistical analysis: Data were analyzed for statistical significance using Student's *t* test. Differences with *P*-values <0.05 were considered as statistically significant.

Results

ABCG2 levels are regulated by DEX, PROG, and RU486 in MCF7 cells

By QRT-PCR, ABCG2 expression levels were shown to be strongly decreased, in a time-dependent manner, by 5 µM DEX (Fig. 1A). The ABCG2 mRNA amount was slightly down-regulated after a 4-h exposure to DEX, and the ABCG2 level decrease was already maximal after 9 h and remained stable up to 72 h. The ABCG2 levels were decreased in a concentration-dependent manner (Fig. 1B): after 48 h, ABCG2 mRNA amounts were slightly down-regulated at 0.005 µM DEX, with a maximal effect reached at 0.5 µM.

We also analyzed the mRNA levels in MCF7 cells after DEX treatment in either presence or absence of the protein synthesis inhibitor cycloheximide (CHX). MCF7 cells grown in the presence of CHX alone were used as a control. The CHX presence abolished the DEX effect on ABCG2 expression (Fig. 1C), suggesting the involvement of *de novo* protein synthesis in the mechanism of ABCG2 regulation by DEX.

By QRT-PCR, two other PR ligands, 15 µM PROG and 5 µM RU486 were found to down-regulate ABCG2 expression levels in MCF7 cells after 72 h. The suppressive effect of DEX on ABCG2 expression could not be reversed by co-treatment with 5 µM RU486 antagonist (Table 1).

Our results also indicated that E2 by itself likely down-regulated ABCG2 expression at both transcript (Table 1) and protein levels (Fig. 2B). Interestingly, E2 displayed a partly-cumulative effect on the down-regulation of ABCG2 expression by DEX and RU486. (Table 1).

Furthermore, by immunoblotting, a 72-h exposure to either 1 nM E2, 5 µM DEX or 15 µM PROG induced an obvious decrease of ABCG2 protein expression in MCF7 cells (Fig. 2B). We validated our experimental conditions in stably-transfected positive HEK293-ABCG2 cells and negative HEK293-pcDNA3.1 controls (Fig. 2A) [13].

DEX and PROG effect on ABCG2 expression levels in PRA- and PRB-positive MDA-MB-231 cells (ABC28 cells)

By immunoblotting, we checked high PRA and PRB expression levels in ABC28 cells by comparison to MCF7 cells, while no expression was detected in MDA-MB-231 cells. A higher expression level for PRB than PRA was observed in MCF7 cells (Fig. 3A), while both expression levels were similar in ABC28 cells (PRA- and PRB-positive MDA-MB-231 cells) and no expression was observed in PRA- and PRB-negative CTC15 cells (Fig. 3B). By QRT-PCR analysis, PR expression was quantified in MCF7 cells while it was undetectable in MDA-MB-231. The well-known PR protein up-regulation by 1 nM E2 was also found in MCF7 cells (data not shown).

We studied the PROG and DEX effect in PR-negative MDA-MB-231 cells and MDA-MB-231-derived CTC15 cells either transfected or not with PRA and PRB expression vectors. 5 µM DEX and 15 µM PROG decreased by 2-fold ABCG2 mRNA expression (fold changes were respectively 0.52 ± 0.12 and 0.47 ± 0.05) in PR-negative MDA-MB-231 cells after 72 h. Theses findings were confirmed in PR-negative CTC15 cells (Fig. 3C). In contrast, ABCG2 expression levels were increased by PROG and DEX in PRA- and PRB-positive ABC28 cells by approximately 3.5 and 10-fold, respectively, in comparison to CTC15 cells (Fig. 3C).

Regulatory effects of PXR- and/or GR- activators on ABCG2 expression levels in MCF7 cells

Based on our observations, the ABCG2 mRNA levels were down-regulated by DEX and RU486 in PR-negative, PXR-, and GR-positive CTC15 cells (Fig. 3C). Since MCF7 cells express hPXR and GR [14] which is activated by many drugs including DEX (poor hPXR and GR activator) and RU486 (potent hPXR and GR activator) [15], we explored if PCN (weak hPXR and GR activator) and clotrimazole (powerful hPXR activator) regulate the ABCG2 expression. 10 µM PCN and 20 µM clotrimazole respectively strongly and weakly reduced ABCG2 transcripts after 72-h (Table 1).

DEX modulation of MCF7 cells sensivity to mitoxantrone, a well-known ABCG2 substrate

To determine whether the decrease of ABCG2 expression upon DEX treatment had functional consequences, the sensitivity of

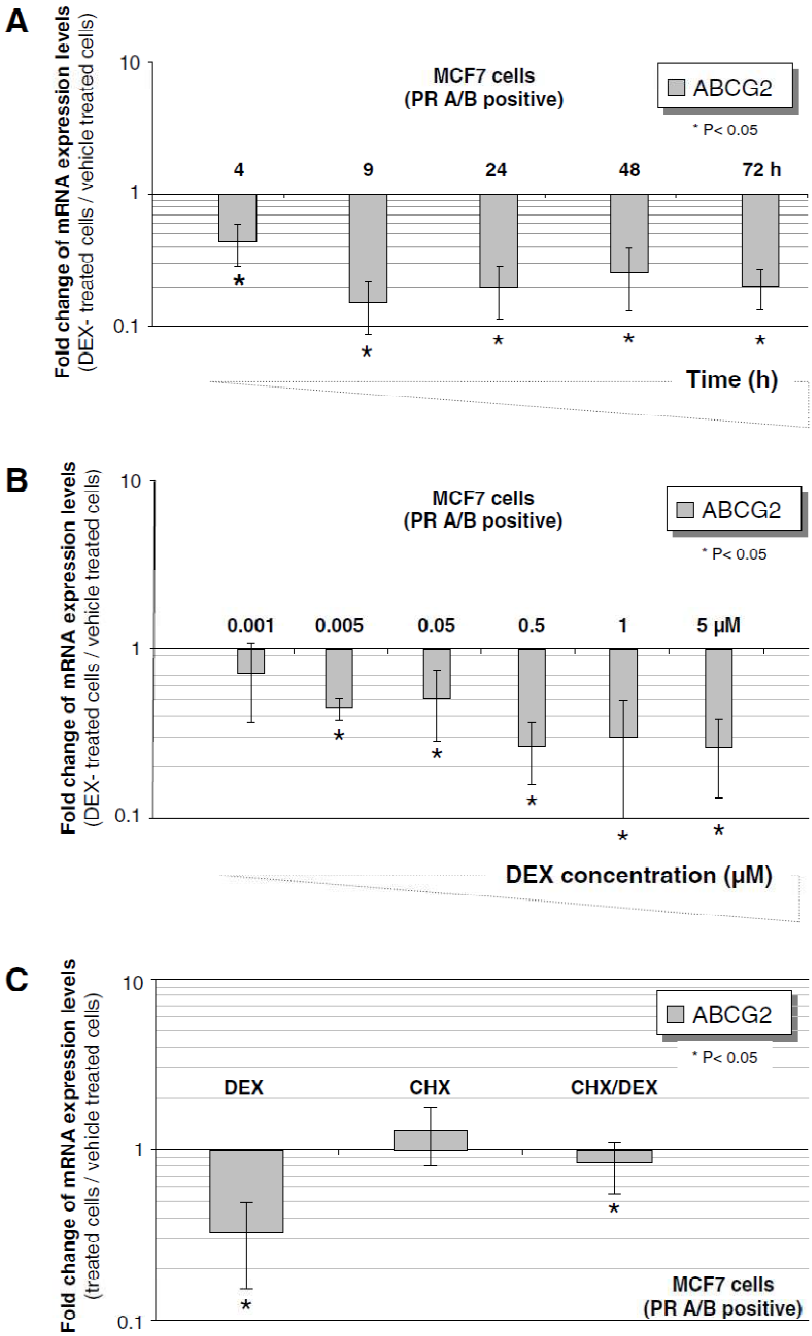

Fig. 1. Kinetics, dose dependence and cycloheximide alterations of DEX effects on the expression of ABCG2 mRNA in MCF7 cells. (A) Cells were exposed to 5 µM DEX for 4–72 h, and ABCG2 transcripts were measured by QRT-PCR at various time points. The fold changes are means ± SE. of at least four independent experiments. *y* is a logarithmic scale. $^{*}P < 0.05$; Student's *t* test. (B) Cells were exposed to various DEX concentrations, ranging from 0.001 to 25 µM, and ABCG2 transcripts were measured by QRT-PCR. The fold changes are means ± SE of at least four independent experiments. *y* is a logarithmic scale. $^{*}P < 0.05$; Student's *t* test. (C) Cells were exposed to either vehicle, 5 µM DEX, 30 µg/ml CHX, or co-treated with 5 µM DEX and 30 µg/ml CHX for 9 h. The fold changes are means ± SE of at least three independent experiments. *y* is a logarithmic scale. $^{*}P < 0.05$; Student's *t* test.

DEX-treated MCF7 cells to mitoxantrone (MIT) was compared to that of control cells. MCF7 cells were incubated for 24 h at 37 °C in DCC medium either containing or not 5 µM DEX. After DEX pre-incubation, 0.25 or 0.5 µM MIT was added, and cell death was evaluated after 72 h. Trypan blue assays of anticancer drug-challenged cells were performed as described in Materials and methods [12]. 0.25 µM MIT-induced approximately a 15%—increased cell death in DEX-treated cells than in untreated cells ($P < 0.05$) (Fig. 4), and a higher dose of MIT, 0.5 µM, seemed to be less affected by DEX sensitizing effect, but it still induced higher cell death than in DEX-primed cells ($P < 0.05$).

Discussion

By transcriptional or post-transcriptional mechanisms, physiological ligands of nuclear receptors are important determinants in the regulation of ABCG2 expression in cancer cells [2,3,8]. These variations may control substrates availability by either increasing

Table 1
The effect of various hormones, clotrimazole and PCN on the expression of ABCG2 in MCF7 cells

	Fold change of mRNA expression levels (treated cells/vehicle treated cells)			Fold of down-regulation	Student's test			
	n	Mean	±SD		Control	E2	DEX	RU486
Vehicle-treated cells	8	1.00	±0.05	1.00				
DEX (5 μM)	8	0.22	±0.09	−4.47	9.8E−11	7.0E−02 (NS)		
RU486 (5 μM)	8	0.46	±0.15	−3.21	3.3E−09		2.3E−01 (NS)	
DEX (5 μM)/RU486 (5 μM)	5	0.22	±0.11	−4.51	1.5E−10		2.3E−01 (NS)	
PROG (15 μM)	8	0.31	±0.27	−2.60	7.4E−06		2.3E−01 (NS)	
E2 (1 nM)	5	0.42	±0.14	−2.40	2.4E−09			
E2 (1 nM)/DEX (5 μM)	4	0.14	±0.05	−6.94	2.1E−11	1.2E−02	1.4E−01 (NS)	
E2 (1 nM)/RU486 (5 μM)	5	0.16	±0.06	−6.44	7.6E−11	1.8E−02		8.5E−02 (NS)
Clotrimazole (20 μM)	3	0.51	±0.27	−1.96	1.26E−02			
PCN (10 μM)	3	0.32	±0.06	−3.05	5.95E−07			

MCF7 cells were treated for 72 h with 5 μM DEX, 5 μM RU486, 15 μM PROG, 20 μM clotrimazole, 10 μM PCN, or 1 nM E2 in steroid-depleted medium. No effects of these molecules on cell viability were observed at all tested concentrations. ABCG2 transcripts were measured by QRT-PCR. Fold change of mRNA levels was quantified as described in Materials and methods. The QRT-PCR values indicated below are means ± SE. at least three independent experiments. $^{*}P < 0.05$; Student's *t* test.

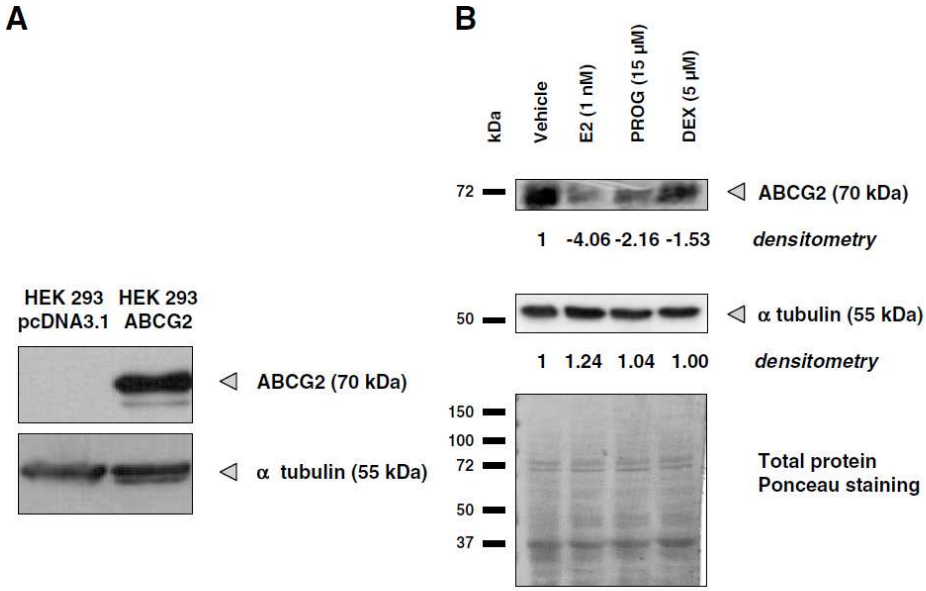

Fig. 2. Expression of ABCG2 protein in pcDNA3.1-transfected or ABCG2-transfected HEK293 cells (A) and effects of DEX-, E2-, RU486-, or PROG-treatment in MCF7 cells (B). (A) Crude membrane fractions (150 μg protein) were prepared from HEK293 cells transfected with either pcDNA3.1 vector or ABCG2-pcDNA3.1 vector. ABCG2 expression was quantified after incubation with ABCG2-monoclonal antibody. Equal protein loading was confirmed by alpha-tubulin immunoblotting of the PDVF membrane. (B) Crude membrane fractions (150 μg) were prepared from cells exposed to either vehicle, 5 μM DEX, 1 nM E2, or 15 μM PROG for 72 h. ABCG2 expression was quantified after incubation with ABCG2-monoclonal antibody. Densitometry was performed using the ImageJ® software. Equal protein loading was confirmed by Ponceau staining and by alpha-tubulin immunoblotting of the PDVF membrane.

or decreasing their elimination from cells. The aim of this work was to determine whether an anti-inflammatory treatment with the commonly-used synthetic steroid DEX may change the expression of ABCG2 transporter in breast cancer cells. We have shown for the first time that, in a time- and concentration-dependent manner, ABCG2 expression levels were down-regulated by DEX in ER-, PR-, GR-, and PXR-positive MCF7 breast cancer cells at both transcript and protein levels (Table 1). Furthermore, the DEX-induced regulation of ABCG2 was abolished by co-incubation with cycloheximide suggesting that this regulation required *de novo* protein synthesis.

Since DEX and PROG were able to down-regulate ABCG2 expression in ER- and PR-negative, GR- and PXR-positive MDA-MB-231-derived CTC15 cells and its parental counterpart MDA-MB-231 cells, we may suggest involvement of GR- and PXR-signaling pathway in ABCG2 regulation. Consequently, we tested the effects of various hPXR ligand (clotrimazole, PCN, and RU486) on ABCG2 regulation. Specific differences appeared in ligand specificity: hPXR strongly responded to clotrimazole while PCN and DEX were relatively weak hPXR activators [15]. Interestingly, PCN had similar effects on ABCG2 expression levels as DEX, in MCF7 cells, while clotrimazole weakly decreased ABCG2 expression. This suggested that PXR-signaling pathway activation might partly regulate ABCG2 expression levels in MCF7 cells. Nevertheless, it should be noted that, similarly to DEX and RU486, PCN is also a GR ligand and thus may activate GR-mediated regulatory effects [16]. The fact that PCN strongly decreased ABCG2 expression, this is supported by the finding that DEX regulation on ABCG2 may also be related to GR activation. Furthermore, DEX increased both retinoid X receptor-a and PXR mRNA expression, through GR-signaling pathway activation [17]. These observations reveal the existence of a functional cross-talk between GR and PXR, and may contribute to understand GR and PXR role in ABCG2 regulation by DEX in both MCF7 and MDA-MB-231 cells.

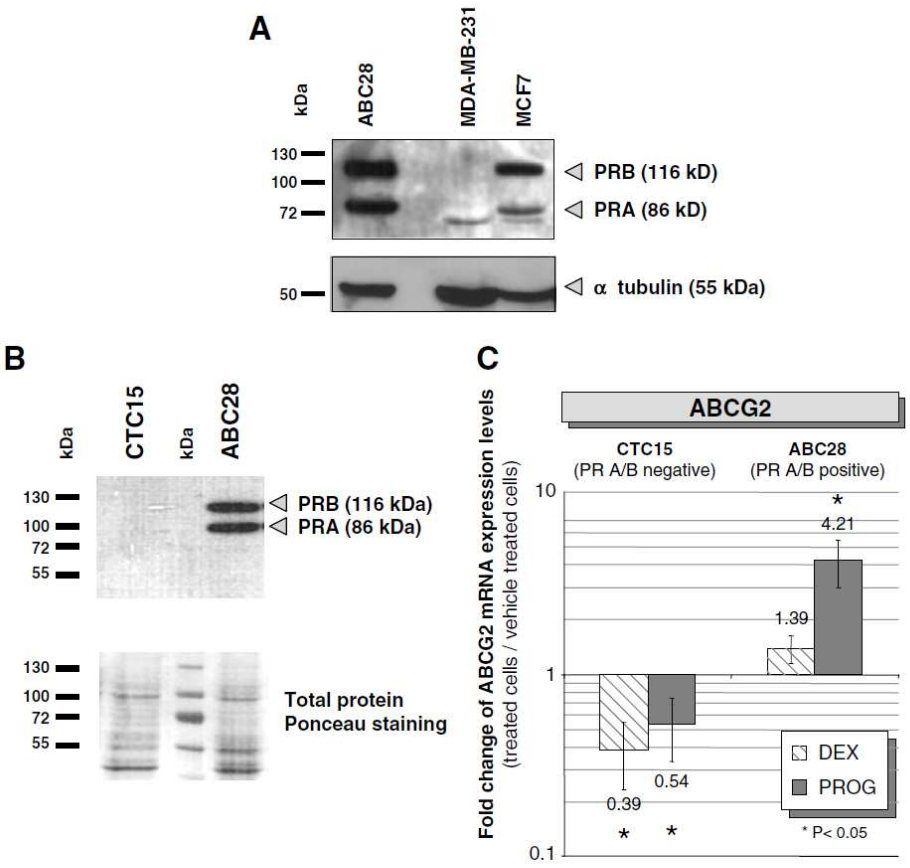

Fig. 3. Protein expression levels of PRA and PRB proteins in breast cancer cells (A) and PRA and PRB protein expression in ABC28 and CTC15 cells (B) and effects of DEX and PROG on ABCG2 mRNA levels (C). (A) Crude membrane fractions were prepared from MCF7 cells (150 μg), ABC28 cells (50 μg), and MDA-MB-231 cells (150 μg) cultured in DMEM medium. PRA and PRB expressions were quantified after incubation with Ab-8 (PRA/PRB)-monoclonal antibody. Protein loading was confirmed by alpha-tubulin immunoblotting labelling. (B) Crude membrane fractions were prepared from MDA-MB-231 cells transfected with either PSG5 (CTC15 cells) or PRA/PRB (ABC28 cells). PRA and PRB expressions were quantified after incubation with Ab-8 (PRA/PRB)-monoclonal antibody. It was reproduced in three independent experiments. Equal protein loading was confirmed by Ponceau staining of the PDVF membrane. (C) Cells were exposed to 5 μM DEX or 15 μM PROG for 72 h, and ABCG2 transcripts were measured by QRT-PCR. The fold changes are means ± SE of at least five independent experiments. *y* is a logarithmic scale. $^{*}P < 0.05$; Student's *t* test.

Nevertheless, PROG, DEX, and RU486 are known to interact with PR receptors [4]. We demonstrated that PROG and RU486 regulated ABCG2 expression levels in the same way as DEX in MCF7 cells. The well-known PR antagonist RU486 can also behave as a partial agonist for PR when selective co-regulators are recruited [18]. This may explain the similar regulatory effects produced by RU486, PROG and DEX on the regulation of ABCG2 expression *via* PRB in MCF7 cells which highly express PRB by comparison to PRA (Fig. 3A). In PRA- and PRB-positive ABC28 cells, DEX efficiently bound to the progesterone receptor (PR) [4] and was able to reverse the DEX-induced down-regulation observed in PR-negative CTC15 cells (Fig. 3C). These data further strengthen the idea that PR-mediated signaling is involved in DEX-treated breast cancer cell lines. The difference observed between MCF7 cells (ABCG2 down-regulation) and ABC28 cells (ABCG2 up-regulation) likely results from cellular context. Most of PROG pharmacological effects can be explained by three interactive mechanisms: (1) balance of the PRA/PRB ratio [6]: PRA and PRB expression levels are similar in ABC28 cells while PRA expression is several-fold lower than PRB in MCF7 cells (Fig. 3A), (2) balance in the co-regulatory transcriptional co-factors depending on cellular context, that could modulate the transcriptional PR activation (3), and differential PRA/PRB expression and gene activation *via* non-PRE interaction [19,20]. Recently, Wang et al. identified a functional PRE motif in ABCG2 promoter region [3]. Consequently, ABCG2 expression was strongly up-regulated by PROG and DEX through PR-pathway activation in PRA- and PRB-positive ABC28 cells (Fig. 3C).

Another major hormone of the mammary tissue, estradiol, is well-known to regulate growth, development and differentiation of protein levels in many reproductive tissues. Previously, Imai et al. reported that estrogens induced a post-transcriptional down-regulation of ABCG2 in MCF7 cells [8]. We indeed observed an important ABCG2 down-regulation at the protein level (Fig. 2B), but we demonstrated for the first time that E2 also modified ABCG2 expression at the transcript level in MCF7 cells (Table 1). Therefore, these data strongly suggest that E2 induced ABCG2 down-regulation both at transcriptional and post-transcriptional levels in MCF7 cells.

In MCF7 cells, our main findings are summarized in Fig. 4B. DEX could activate regulatory PR-, PXR-, and/or GR-signaling pathways to down-regulate ABCG2 levels. In parallel, E2 plays a critical role in ABCG2 down-regulation by three major ways: (1) E2 up-regulates PR protein level, and so likely DEX-potentiated down-regulation of ABCG2; (2) E2 activates estrogen-signaling pathway through ER, and likely leads to inhibit ABCG2 transcription; (3) E2 may also decrease ABCG2 protein level by a post-transcriptional pathway, as previously described by Imai et al. [8].

According to Pavek's study, DEX was not transported by ABCG2 and only weakly inhibited MIT efflux (approximately 10% inhibition at 50 μM, a 10-fold higher concentration than that used here) [21]. Since we observed that DEX exposure

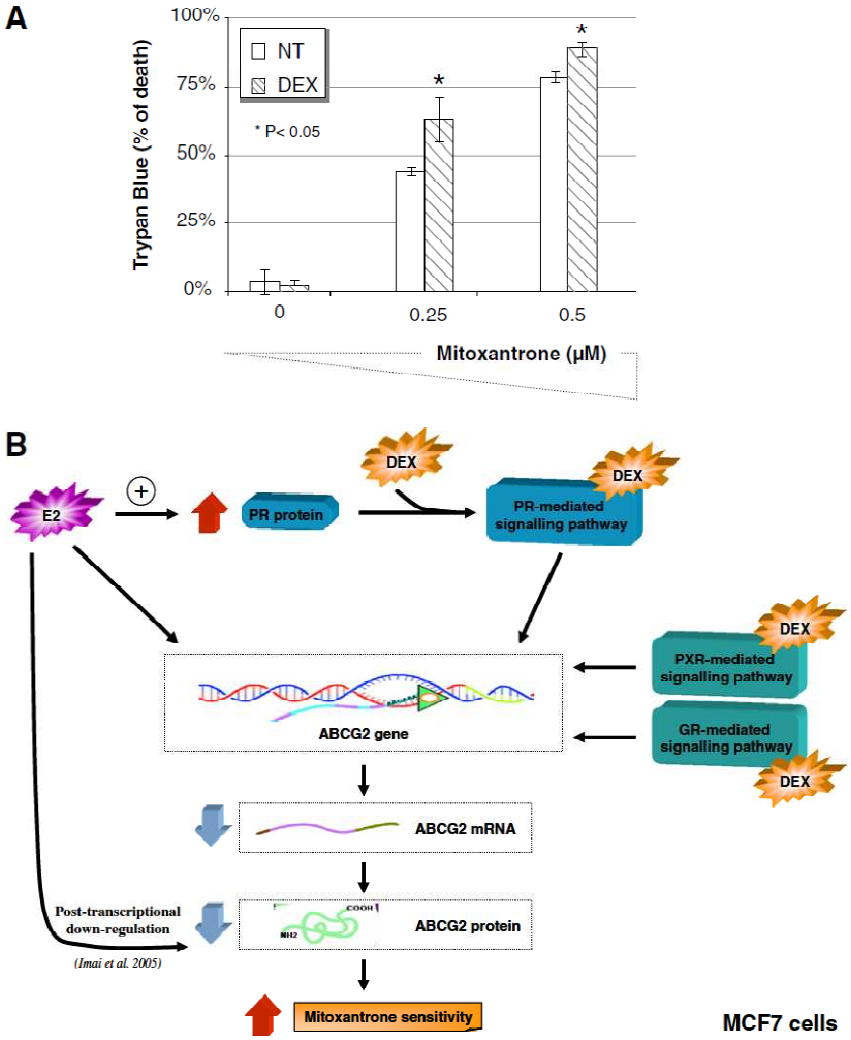

Fig. 4. Differential effects of DEX exposure on cell death induced by MIT (A) and proposed mechanisms of DEX regulation on ABCG2 expression in MCF7 cells (B). (A) MCF7 cells, either treated or not with 5 µM DEX for 24 h, were challenged with MIT (0.25 µM, 0.5 µM) for 72 h, and subjected to trypan blue assay. ABCG2 down-expression was associated with higher MIT-induced cell death. Cell viability was quantitated by trypan blue exclusion as described in Materials and methods. The results are representative of five independent experiments. $^{*}P < 0.05$; Student's *t* test. (B) According our observations, dexamethasone (DEX, orange shape) down-regulates ABCG2 protein level by binding to progesterone receptor (PR, blue octogon), Glucocorticoid Receptor or Pregnane X Receptor (GR or PXR, green octogons), and activates the corresponding regulatory signaling pathways. Estrogen (E2, pink shape) plays a role in ABCG2 down-regulation by up-regulating PR protein level and likely also by a transcriptional and post-transcriptional down-regulation. (For interpretation of the references to color in this figure legend, the reader is referred to the web version of this article.)

was able to enhance *in vitro* MIT toxicity in MCF7 cells (Fig. 4A), we may suggest that the latter was mainly related to the observed major decrease in ABCG2 expression. Finally, the DEX-induced decrease in ABCG2 expression in breast cancer cells might therefore enhance the MIT therapeutic efficiency. Consequently, by altering ABCG2 expression levels through PR-, GR-, and/or PXR-signaling pathways in PR-positive and negative breast tumors, a DEX therapy might significantly contribute to increase sensitivity to ABCG2 substrates.

Acknowledgments

We thank Drs. Pierre Chambon (IBMC, France) for helpful collaboration and Alexandre Pozza (IBCP, France) for technical assistance in ABCG2 immunoblotting.

References

[1] R.W. Robey, O. Polgar, J. Deeken, K.W. To, S.E. Bates, ABCG2: determining its relevance in clinical drug resistance, Cancer Metastasis Rev. 26 (2007) 39–57.
[2] P.L. Ee, S. Kamalakaran, D. Tonetti, X. He, D.D. Ross, W.T. Beck, Identification of a novel estrogen response element in the breast cancer resistance protein (ABCG2) gene, Cancer Res. 64 (2004) 1247–1251.
[3] H. Wang, E.W. Lee, L. Zhou, P.C. Leung, D.D. Ross, J.D. Unadkat, Q. Mao, Progesterone receptor (PR) isoforms PRA and PRB differentially regulate expression of the breast cancer resistance protein in human placental choriocarcinoma BeWo cells, Mol. Pharmacol. 73 (2008) 845–854.
[4] J.C. Leo, C. Guo, C.T. Woon, S.E. Aw, V.C. Lin, Glucocorticoid and mineralocorticoid cross-talk with progesterone receptor to induce focal adhesion and growth inhibition in breast cancer cells, Endocrinology 145 (2004) 1314–1321.
[5] P. Kastner, A. Krust, B. Turcotte, U. Stropp, L. Tora, H. Gronemeyer, P. Chambon, Two distinct estrogen-regulated promoters generate transcripts encoding the two functionally different human progesterone receptor forms A and B, EMBO J. 9 (1990) 1603–1614.
[6] J.D. Graham, C.L. Clarke, Expression and transcriptional activity of progesterone receptor A and progesterone receptor B in mammalian cells, Breast Cancer Res. 4 (2002) 187–190.
[7] W. Bhadhprasit, T. Sakuma, N. Hatakeyama, M. Fuwa, K. Kitajima, N. Nemoto, Involvement of glucocorticoid receptor and pregnane X receptor in the regulation of mouse CYP3A44 female-predominant expression by glucocorticoid hormone, Drug Metab. Dispos. 35 (2007) 1880–1885.
[8] Y. Imai, E. Ishikawa, S. Asada, Y. Sugimoto, Estrogen-mediated post transcriptional down-regulation of breast cancer resistance protein/ABCG2. Cancer Res. 65 (2005) 596–604.
[9] H. Wang, L. Zhou, A. Gupta, R.R. Vethanayagam, Y. Zhang, J.D. Unadkat, Q. Mao, Regulation of BCRP/ABCG2 expression by progesterone and 17(beta)-estradiol

in human placental BeWo cells, Am. J. Physiol. Endocrinol. Metab. 290 (2006) E798–E807 (First published December 13, 2005; doi:10.1152/ajpend0.00397.20050193-1849/06 $8.00).
[10] J.C. Leo, S.M. Wang, C.H. Guo, S.E. Aw, Y. Zhao, J.M. Li, K.M. Hui, V.C. Lin, Gene regulation profile reveals consistent anticancer properties of progesterone in hormone-independent breast cancer cells transfected with progesterone receptor, Int. J. Cancer 117 (2005) 561–568.
[11] M. Honorat, A. Mesnier, J. Vendrell, J. Guitton, I. Bieche, R. Lidereau, G.D. Kruh, C. Dumontet, P. Cohen, L. Payen, ABCC11 expression is regulated by estrogen in MCF7 cells, correlated with estrogen receptor {alpha} expression in postmenopausal breast tumors and overexpressed in tamoxifen-resistant breast cancer cells, Endocr. Relat. Cancer 15 (2008) 125–138.
[12] P. Graidist, A. Phongdara, K. Fujise, Antiapoptotic protein partners fortilin and MCL1 independently protect cells from 5-fluorouracil-induced cytotoxicity, J. Biol. Chem. 279 (2004) 40868–40875.
[13] A. Ahmed-Belkacem, A. Pozza, F. Munoz-Martinez, S.E. Bates, S. Castanys, F. Gamarro, A. Di Pietro, J.M. Perez-Victoria, Flavonoid structure-activity studies identify 6-prenylchrysin and tectochrysin as potent and specific inhibitors of breast cancer resistance protein ABCG2, Cancer Res. 65 (2005) 4852–4860.
[14] H. Dotzlaw, E. Leygue, P. Watson, L.C. Murphy, The human orphan receptor PXR messenger RNA is expressed in both normal and neoplastic breast tissue, Clin. Cancer Res. 5 (1999) 2103–2107.
[15] J.T. Moore, S.A. Kliewer, Use of the nuclear receptor PXR to predict drug interactions, Toxicology 153 (2000) 1–10.
[16] S. Tsurufuji, K. Sugio, F. Takemasa, The role of glucocorticoid receptor and gene expression in the anti-inflammatory action of dexamethasone, Nature 280 (1979) 408–410.
[17] J.M. Pascussi, L. Drocourt, J.M. Fabre, P. Maurel, M.J. Vilarem, Dexamethasone induces pregnane X receptor and retinoid X receptor-alpha expression in human hepatocytes: synergistic increase of CYP3A4 induction by pregnane X receptor activators, Mol. Pharmacol. 58 (2000) 361–372.
[18] M.E. Meyer, A. Pornon, J.W. Ji, M.T. Bocquel, P. Chambon, H. Gronemeyer, Agonistic and antagonistic activities of RU486 on the functions of the human progesterone receptor, EMBO J. 9 (1990) 3923–3932.
[19] X. Gao, Z. Nawaz, Progesterone receptors—animal models and cell signaling in breast cancer: role of steroid receptor coactivators and corepressors of progesterone receptors in breast cancer, Breast Cancer Res. 4 (2002) 182–186.
[20] D.M. Lonard, B.W. O'Malley, Expanding functional diversity of the coactivators, Trends Biochem. Sci. 30 (2005) 126–132.
[21] P. Pavek, G. Merino, E. Wagenaar, E. Bolscher, M. Novotna, J.W. Jonker, A.H. Schinkel, Human breast cancer resistance protein: interactions with steroid drugs, hormones the dietary carcinogen 2-amino-1-methyl-6-phenylimidazo(4,5-b)pyridine, and transport of cimetidine, J. Pharmacol. Exp. Ther. 312 (2005) 144–152.

V. CONCLUSIONS - PERSPECTIVES

L'expression d'ABCC11 est soumise à de nombreuses régulations impliquant différentes voies de signalisation dépendantes de récepteurs hormonaux comme ER ou PR. En effet, les œstrogènes régulent négativement l'expression d'ABCC11 alors que la PROG l'augmente. En plus, d'être régulée négativement par les œstrogènes et positivement par la progestérone, l'expression d'ABCC11 est modifiée par la fixation d'autres ligands de ces récepteurs. Ainsi, le tamoxifène (antagoniste d'ER) et la dexaméthasone (activateur de PR) induisent l'expression d'ABCC11. De manière intéressante, les cellules résistantes au tamoxifène (soumises à de faibles concentrations de tamoxifène pendant une longue durée) ont acquis un niveau élevé d'expression d'ABCC11. Bien que ces régulations semblent dépendantes de la présence d'ER ou PR, aucune donnée mécanistique n'est encore disponible. Afin d'élucider ces mécanismes, il faudrait identifier les sites régulateurs sur le promoteur d'ABCC11. La séquence de ce promoteur révèle la présence des sites potentiels ERE (*Estrogen Response Element*) et PRE (*Progesterone Response Element*) dont l'activité régulatrice pourrait être étudiée. Leur implication pourrait être confirmée si leur inactivation modifiait la réponse aux hormones. D'autres sites pourraient également être impliqués grâce à l'intervention de facteurs de transcription. Ces derniers pourraient être identifiés si leur présence était détectée sur le promoteur d'ABCC11 et si l'inactivation de leur site cible annihilait ou diminuait l'effet des hormones sur l'expression d'ABCC11.

Le TAM et la DEX peuvent être utilisés en association avec une chimiothérapie à base de substrats d'ABCC11. L'hormonothérapie à base de TAM est indiquée dans le traitement des cancers du sein ER+/PR+/- dont le niveau d'expression basale d'ABCC11 est déjà élevé. La DEX est administrée comme antiémétique pour soigner certains effets secondaires de la chimiothérapie. Malheureusement, en augmentant l'expression d'ABCC11, le TAM et la DEX influenceraient de manière négative la réponse aux traitements anticancéreux à base de substrats d'ABCC11. Cette situation souligne la valeur prédictive potentielle d'ABCC11.

De manière générale, le niveau d'expression d'ABCC11 est plus élevé dans le tissu cancéreux mammaire que dans le tissu normal. Ces tumeurs sur-expriment ABCC11 d'autant plus qu'elles expriment ER et/ou PR. Ce phénomène est aussi observé dans les tumeurs exprimant ERBB2 ou présentant un envahissement ganglionnaire. A l'inverse, plus le grade de la tumeur est élevé, moins ABCC11 est exprimée. Le niveau d'expression d'ABCC11 est aussi positivement corrélé à la récurrence, ce qui pourrait être la conséquence de la diminution de la sensibilité aux traitements.

En effet, dans le cadre de résistance à la chimiothérapie FEC (5-FU, épirubicine, cyclophosphamide), une surexpression d'ABCC11 a pu être observée. La plupart de ces données sont le résultat d'étude transcriptomique. Il serait complémentaire et informatif de valider ces observations en analysant l'expression protéique d'ABCC11 au sein de tumeurs du sein, et ce, en fonction du type de tumeur, de statuts pour les différents marqueurs et des traitements administrés. Il serait très intéressant d'étudier l'impact d'ABCC11 sur la réponse de tumeurs traitées par des substrats d'ABCC11 (5-FU, méthotrexate, aracytine …), ainsi que de comparer le niveau d'ABCC11 avant et après traitement par ces différentes molécules. De cette manière, la valeur prédictive d'ABCC11 pourrait être confirmée ou infirmée.

C. ETUDE STRUCTURE/ACTIVITE D'ABCC11

I. GENERATION D'UN MODÈLE *IN SILICO* D'ABCC11

1. La modélisation par homologie

Bien que de nombreuses études biochimiques aient été appliquées pour la caractérisation des transporteurs ABC, à ce jour, très peu d'entre eux ont été cristallisés. La plupart sont d'origine procaryote : 5 importateurs (BtuCD [91], ModBC-A [92], HI1470/1 [93], MalFG/K [94] et MetNI [95]) et 2 exportateurs (Sav1866 [96] et MsbA [97]). La protéine ABCB1 murine correspond au seul transporteur ABC de mammifère dont la structure a été décrite très récemment [98].

La cristallisation de ces protéines membranaires étant un processus difficile, la modélisation par homologie est devenue un outil important pour la caractérisation structurelle des transporteurs ABC humains. Applicable du fait de la forte conservation de la topologie au sein de la famille, cet outil a été largement utilisé pour localiser les sites fonctionnels tels que les sites de liaisons aux substrats, aux nucléotides ou aux inhibiteurs. La génération de tels modèles est également un support important pour la compréhension de certaines données biochimiques ainsi que pour guider les expérimentations.

La structure des importateurs étant différente de celles des exportateurs, la modélisation par homologie des transporteurs humains (tous exportateurs) se basent sur celle des exportateurs procaryotes. Différents modèles ont été créés et font l'objet de la revue qui suit.

→ Publication 7. « **ABC transporter structure prediction: Relevance of homology modeling studies** » par M. Honorat et coll.

Revue en révision dans Current Drug Metabolism

ABC TRANSPORTER STRUCTURE PREDICTION: RELEVANCE OF HOMOLOGY MODELING STUDIES

*Mylène Honorat[1,2], Pierre Falson[3], Raphael Terreux[3], Attilio Di Pietro[3], Charles Dumontet[1,2], and *Lea Payen[1,2,4]*

1 ISPB, Université Lyon1, 69008 Lyon, France
2 Inserm, U590, Centre Léon Bérard, FNCLCC, 69008, Lyon, France
3Equipe labellisée Ligue 2009, Institut de Biologie et Chimie des Protéines, UMR 5086 CNRS/Université Lyon 1, IFR128 BioSciences Gerland-Lyon Sud, 69367 Lyon Cedex 07, France
4 Hospices civils of Lyon, Biochemistry laboratory of Lyon Sud (CBS), France

*Corresponding author:
Dr. PAYEN Léa,
INSERM U590, 8 Avenue Rockefeller, 69008 Lyon, France
E-mail: Lea.payen-gay@univ-lyon1.fr
Tel.: +33478777236
Fax: +33478777088

ABSTRACT

Human ABC transporters are ubiquitous membrane proteins responsible for the efflux of multiple endogenous or exogenous compounds out of the cells. Face to their clinical interest, many biochemical studies have been carried out to characterize their transport functions. Currently, only mouse ABCB1 complete structure has been published at high-resolution, and could be compared to the bacterial ABC transporters Sav1866 and MsbA. As ABC transporters topology is highly conserved, homology modeling has been widely used for localizing functional sites such as drug-, nucleotide- and modulator-binding sites and for better understanding the biochemical data. The aim of our review was to make a current inventory on methods leading to homology modeling strategies that are strongly dependent on template alignments based on X-ray templates. This complete tool description should be useful to a wide population of biologists and biochemists who would judge important to display, in their own team, an *in silico* model of their target. They will find in this review the advantages and limits of such an approach, and the way to carry out their model. Supported by reliable models, since ABC transporters are often poly-specific, pharmaceutical companies will likely be able to predict whether a substrate compound would be taken in charge by one or more transporters. These data will likely predict the kinetic parameters of a new drug, and then have repercussion on its industrial development. Currently, homology strategy does not lead to selective model, and improvement of selectivity will be reached by development of more advance theoretical methods. To support the generation of specific models, additional crystal 3D templates obtained under different conformations as well as additional experimental biochemical data are needed. Finally, docking studies resulting from the generated models are discussed, and the relevance of these models is analyzed beside the available biochemical data.

Keywords

Human, ABC transporter, 3D-Structure, Homology, Modeling, Docking, Drug Disposition, Multidrug resistance

I. INTRODUCTION

With its 48 members, the human ABC (ATP-Binding Cassette) transporter family is one of the largest and most diverse protein groups found in all organisms, from bacteria to humans. These proteins are classified on the basis of their amino acid residue homology into seven sub-families, from ABCA to ABCG. Since they are often strongly expressed in normal barrier

tissues, like blood-brain barrier [1], liver [2] or intestine [3], these transporters are involved in essential physiological processes regulating the elimination of endogenous and exogenous molecules from cells. Some of them are apically expressed and are responsible for xenobiotic elimination from the liver, the kidney and the gastrointestinal tract, and have a protective role at the blood-brain barrier and the testes. Malignant cells exploit multidrug transporters, such as ABCB1, by increasing their expression and function levels. Indeed, some ABC members lead them to escape from the cytotoxic effects of chemotherapy. For example, in acute myeloid leukemia (AML), the patients expressing only one, or none, among ABCB1, ABCC3, and ABCG2 functional proteins had a better prognosis than those expressing two or three of them [4]. Furthermore, ABCB1 and ABCG2 have been found to constitute a predictive factor in patients treated with their substrates, respectively daunorubicin and mitoxantrone [5]. Similar findings were observed in other types of tumors including breast cancer or nasopharyngeal carcinoma [6-8].

In mammalian cells, they are responsible for the efflux of an astonishingly large array of endogenous and exogenous xenobiotics. These substrates are structurally and functionally unrelated, defining wide spectra of molecules. For example, they transport out of the cells organic anions, glutathione conjugates, nucleoside analogs or peptides [9]… Altogether, their high-expression levels associated to wide spectra lead to involvement in pharmacological kinetics of many drugs, and resistance to several anticancer agents [9]. ABC transporters are commonly involved in MultiDrug Resistance (MDR) phenotype. Consequently, inhibition of ABC-mediated drug efflux could restore the efficacy of chemotherapy in drug-resistant cancers. Modulation of ABCG2 or ABCC3, in addition to ABCB1, may be necessary in some patients in order to improve the outcome. Presently, three generations of ABCB1 inhibitors have been developed to enhance the effects of chemotherapeutic drugs on MDR cancer cells, both *in vitro* and *in vivo*. The third-generation inhibitors of ABCB1 inhibitors, including the anthranilamide derivative tariquidar (XR-9576) and the dibenzosuberane derivative zosuquidar (LY335979), are especially designed for high affinity modulation of transport and low pharmacokinetic interactions.

ABC transporters share similar structural topologies, with 2 MSDs (Membrane Spanning Domain) and 2 NBDs (Nucleotide-Binding Domains). The MSDs are composed by α-helix transmembrane segments (TMs) constituting the way by which substrates cross the membrane. ATP binding and hydrolysis, usually required for substrate transport activity, take place at the level of cytoplasmic NBDs. Different layouts are distinguished to form either full or half-transporters (figure 1). Full transporters contain at least two MSDs and two NBDs, while half-transporters are constituted by only one MSD and one NBD. Although some of ABCC members exhibit an additional N-terminal MSD, called MSD0, their full structures follow an MSD1-NBD1-MSD2-NBD2 arrangement (ABCA, ABCB and ABCC sub-families). Half-transporters are thought to form at least homodimers such as ABCG2 [10], or heterodimers such as ABCG5-ABCG8 [11], to carry out their transport function. They show either an MSD-NBD arrangement as for ABCB members, or an inverse NBD-MSD arrangement (ABCG) (figure 1). ABCE and ABCF sub-families contain NBDs that likely derive from ABC transporters, but neither the presence of MSDs nor any membrane transport functions have ever been described, suggesting a functional association of NBDs with partners that remain to be identified or a different mechanism where transport is not involved. In monomeric full transporter or dimeric half-transporters, the MSD tertiary structure leads to the formation of a transmembrane structure usually constituted of 12 TMs. At some steps of the catalytic cycle, the NBDs dimerize, face-to-face and head-to-tail, in a sandwich-like manner.

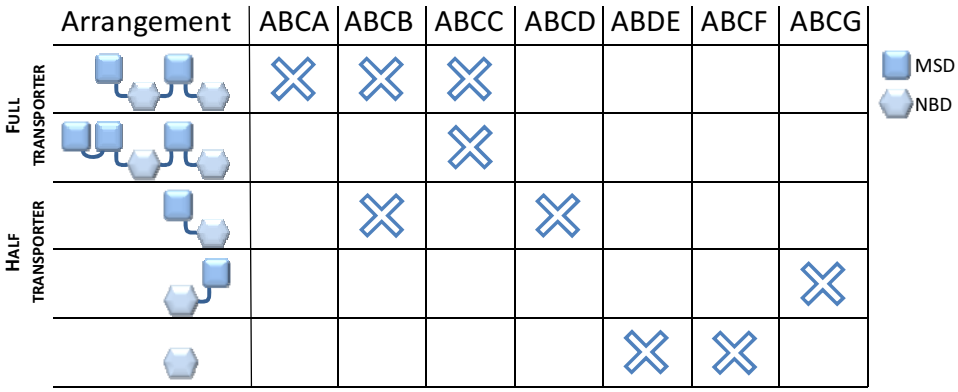

Figure 1: Human ABC transporter structure arrangements.

Because of their clinical interest, their activity and transport function have been widely characterized by various biochemical studies. The complete X-ray structures of only one mammalian and two prokaryotic ABC exporters have been determined: mouse ABCB1 [12], Sav1866 [13] and MsbA [14]. Five additional prokaryotic ABC importers have been crystallized, namely BtuCD [15], ModBC-A [16], HI1470/1 [17], MalFG/K [18] and MetNI [19]. Since ABC transporters topology is highly conserved, homology modeling has been widely used to localize functional binding sites such as towards drugs, nucleotides and modulators, and for better understanding the available biochemical data. Homology modeling is a useful tool to help interpretation of experimental biochemical data, and potentially to guide new experimental studies. Since the domain structural organization of importers is not shared by exporters, most of current 3-D homology models of human ABC transporters (which are all exporters) are based on bacterial exporter structures. These ABC 3-D models are necessary for the optimization of inhibitors, and the localization of substrate-binding sites. Finally, these findings lead to better understand the transport function of ABC transporters.

In this mini-review, we propose a brief overview on the common steps of ABC transporter catalytic cycle and high-resolution crystal 3D-structures of exporters. These basic findings will be useful to understand the following description of *in silico* models of some ABC transporters (ABCB1, ABCG2 and ABCC members) obtained by homology.

To help biologist and biochemists in generating their own models, we thought necessary to make the current inventory of methods leading to homology modeling strategies. These approaches are greatly used in various biochemistry laboratories to support hypotheses and, in some way, they have been partially validated using mutagenesis approaches of amino-residues involved in putative binding sites of substrates [20]. Consequently, the complete technical description of methods, procedures and softwares is useful to a wide population of biologists and biochemists that would judge important to display in their own team an *in silico* model of their target. They will also find both advantages and limits of such a tool.

In the drug discovery field, theses strategies are currently implemented for various metabolism proteins such as cytochrome P450. Recently, the FDA organization (Center for Drug Evaluation and Research (CDER)) decided to include data on the ability of new drugs to be transported. Consequently, they are largely involved in the improvement of these *in silico* models that need to be highly reliable and powerful to identify whether the molecules are substrates and/or modulators of transporters. Supported by reliable models, since ABC transporters are often poly-specific, industrial companies will likely be able to predict whether it would be taken in charge by one or more transporters. These data will likely predict the ADME parameters of the new drug and then have repercussion on its industrial development. Currently, homology strategy does not lead to selective model, and this improvement of

selectivity will be addressed by the development of more advanced theoretical methods. To support the generation of specific models, additional crystal 3D structures of templates obtained under different conformations and more experimental biochemical data are needed. Furthermore, docking studies resulting from the generated models are discussed, and the relevance of these models is analyzed towards the available biochemical data.

II. TRANSPORT ACTIVITY AND CATALYTIC CYCLE

Since the NBDs are highly conserved among ABC proteins, it is possible to assume a common translocation mechanism. Although high-resolution X-ray structures are available for isolated NBDs (as crystallized under several nucleotide-bound conditions [21] and even for complete transporters like BtuCD [15], Sav1866 [13], MsbA [14], ABCB1 [12] and the maltose transporter MalFG/K [18]), molecular details of conformational changes due to ATP binding and hydrolysis, as well as their transduction to MSDs, yet remains unclear.

II.1 General overview

Numerous mutagenesis studies have been carried out to characterize critical residues involved in ATP binding and hydrolysis functions. Several consensus sequences (Walker A, Walker B and ABC signature) and conserved single residues (within A-loop, Q-loop, D-loop and H-loop) have been identified [22] (figure 2). Within the NBD dimer, the catalytic site is composed by the Walker A motif of the *cis*-NBD and the ABC signature motif of the *trans*-NBD both sandwiching the γ-phosphate of ATP (*cis* for the same monomer, *trans* for the opposite monomer). The A-loop (containing an aromatic residue, usually a tyrosine) makes contact with the adenine ring of ATP and contributes to the nucleotide-binding affinity of NBD. The H-loop (histidine) directly interacts with the γ-phosphate of ATP, while the Q-loop interacts via a water molecule. The Q-loop is both in contact with the γ-phosphate of ATP and MSD, suggesting its central role in the conformational coupling between NBDs and MSDs. Residues in the D-loop from the *cis*-NBD make contact with residues in the *trans*-NBD, and therefore stabilize dimeric interactions.

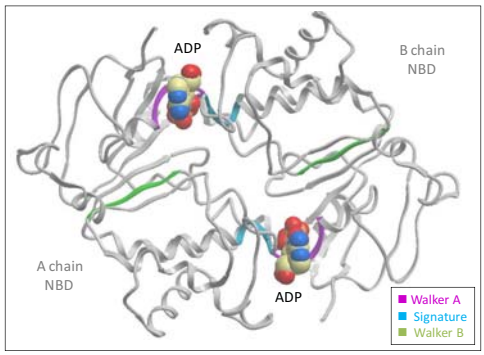

Figure 2: Overview of Sav1866 NBDs. Two ADP molecules are present at the NBD interface composed by one NBD from each monomer. Consensus sequences are shown in pink (Walker A), green (Walker B) and blue (Signature).

Several biochemical studies have described common bases of the catalytic cycle mechanism. Substrate first binds to a high-affinity state of the protein. Then, thanks to a conformational change inducing a transition to a low-affinity state, substrate is released in the extracellular space. Currently, two models of catalytic cycle are proposed [22]: (1) the "ATP switch model" considers that NBD dimerization induced by ATP binding is responsible for the transition to the low-affinity state; (2) the "occlusion-induced switch model" considers that the ATP-induced dimerization of the NBDs is followed by the tight binding/occlusion of a nucleotide to give the low-affinity state (figure 3). Considering the "ATP switch model", in

the resting state, one drug is bound at the inner membrane leaflet and the NBDs are distant. ATP binding closes the two NBDs and induces the high- to low-affinity transition (leading to drug release). Two ATP hydrolysis steps occur successively to form ADP and phosphate (Pi). The NBD dimer is consequently destabilized. Then, two phosphates and two ADP are released and the transporter undergoes a new catalytic turnover. According to the "occlusion-induced switch model", in the resting state, one drug is bound at the inner membrane leaflet and the NBDs are separated. ATP binding closes the two NBDs. The occlusion of one ATP induces the high-to-low affinity transition and decreases the affinity for the second ATP. The occluded ATP is hydrolyzed. One hypothesis supports that Pi is then released, ADP is exchanged for ATP and a new drug is bound, suggesting a stoechiometry of one ATP hydrolyzed per catalytic cycle. The other hypothesis considers that the second ATP is also occluded, hydrolyzed and released in the form of Pi and ADP to reset the transporter to its drug-binding competent mode.

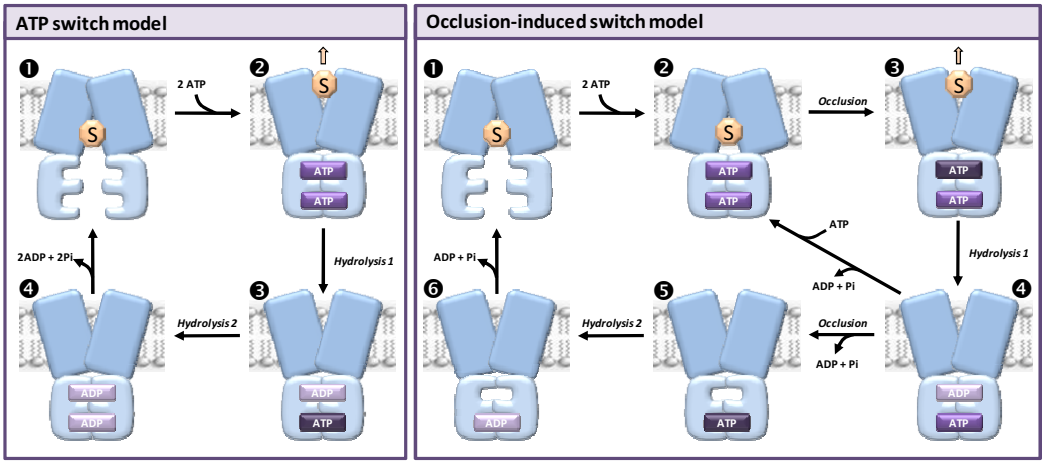

Figure 3. Schematic ABC transporter catalytic cycle. *Adapted from Seeger et al. 2009 [21]*

II.2 Insight into molecular mechanisms by molecular dynamic simulation

Molecular dynamic simulation has been used in the sub-millisecond/nanosecond range for describing the ATP binding to NBDs. In that context, Jones et al. carried out molecular dynamic simulations from the X-ray structure of dimeric MJ0796 E171Q mutant (PDB code 1L2T, 1.9 Å resolution) which provided insights into conformational states of the nucleotide-bound dimer [23]. Firstly, the 30 ns molecular dynamic simulations of both the apo (nucleotide free), ADP-bound, and ATP-bound states of the isolated monomer were carried out, based on the ATP-bound monomer from the MJ0796 dimer. This molecular dynamic study suggested that interaction of the conserved Gln90 residue with the catalytic magnesium ion (as previously reported for other P-loop-containing ATPases) mediates rotation of the helical sub-domain in response to nucleotide binding and hydrolysis [23]. The side chain of Gln90 could coordinate the active catalytic site [24], and it could act as a sensor of the β-phosphate of bound ATP [25]. More recently, Jones *et al.* carried out a new series of simulations and elastic network analyses to compare equilibrated pre- and post-hydrolysis conformations of the isolated ADP/ATP bound MJ0796 dimer [26]. These simulations revealed a large asymmetrical rotation located in the helical LSGGQ sub-domain of only one of monomers [26]. In the ADP/ATP-loaded dimer, the close contact of LSGGQ signature motif with the ATP γ-phosphate is partially lost because of conformational change characterized by intra-subunit relative rotation of the helical and catalytic domains in the ADP opening of the ADP-bound active site. These data allowed Jones et al. to suggest that this was sufficient for nucleotide exchange. They argued how these simulation findings supported a constant contact model for the function of the NBD dimer in contrast to the switch model

previously described, in which the NBDs are proposed to fully dissociate during the catalytic cycle [26]. Similarly, starting with the ATP-bound closed dimer, 50 ns molecular dynamic simulations of four possible combinations with ATP and ADP plus inorganic phosphate were carried out and revealed a possible dimer opening after ATP hydrolysis in the maltose transporter (MalK) NBD dimer [27]. The closed form is stable and can only be maintained in the presence of two bound ATPs. The opening of the interface of the NBD dimer occurs just after the hydrolysis of one ATP, rather than the ADP release from one or both binding sites. This opening is linked to the dissociation of LSGGQ motif from the bound nucleotide, which is induced by rearrangement of Pi and the bound Mg2+ ion in the active site after hydrolysis [27]. In 2010, Oliveira et al. identified specific regions (namely segments 11-19 and 93-124) involved in major conformational rearrangements induced by hydrolysis. They are localized in external area of the dimer [28]. Consequently, these simulations showed how the energy produced from hydrolysis is transduced from the binding pockets to the exterior of the protein. By alignment with the full-length transporter, they found that the 93-124 segment is in direct contact with the MSD, and likely participates in inter-domain communication. The conformational rearrangement of residues 38-43 likely leads to the release of inorganic phosphate produced upon hydrolysis [28]. In contrast to previous data [25, 26], these authors did not show relevant differences (positional deviation values) of conserved motifs (Walker A and B, ABC signature/LSGGQ sequence and D-loop) between the ATP-bound state and other states [28].

In conclusion, these molecular dynamic simulations are completely successful and highly adapted to estimate the movement of the NBDs during the catalytic cycle. They take advantage that the NBDs are highly conserved among ABC transporters, and algorithms of molecular simulation are currently sufficient to access to the entire duration of the catalytic cycle.

II.3 Differences in ABC transporters: characterizing specific aspects of their catalytic cycle mechanism

A number of variations of these common catalytic cycle schemes have been observed according to the considered transporter. Then to complete this section, we briefly describe specificities of ABCB1 and ABCC1 on respective catalytic cycle mechanism.

II.3.1 ABCB1 catalytic cycle

The two NBD sequences from ABCB1 are approximately 60% conserved. In addition, they both bind and hydrolyze ATP in an alternating fashion. Consequently, an alternating-site mechanism requires the hydrolysis of ATP one by one at the active site. The basis of alternative-site mechanism is supported by the hypothesis that all reaction intermediates are asymmetric, thus providing “memory” of the last active site which turned over [29-32]. An asymmetric state of catalytically-active native ABCB1 with two molecules of ATP analog, adenosine 5'-O-[3-thiotriphosphate] (ATP gamma S), has been reported by Sharom (2010) [33]. By fitting of the ATP gamma S-induced tryptophan residue quenching curves to a two-site equation, they revealed the presence of two binding sites for gamma S ATP, respectively with high affinity and low affinity, similar with that for native ATP [33]. Two molecules of ATP gamma S were bound to the protein. In agreement with biochemical data, the high-affinity binding state was found in the Glu552Ala/Glu1197Ala mutants, to be responsible for alteration of catalytic function [12, 34, 35]. Although gamma S ATP was slowly hydrolyzed by ABCB1 into ADP and thiophosphate, its rate was similar to that observed in the Glu552Ala/Glu1197Ala mutants, which form the occluded state in the presence of ATP [36]. Such a slow hydrolysis permits the accumulation of this intermediate state and its detection. Similarly, this short lived asymmetric intermediate state likely occurs during ATP hydrolysis,

then the occluded intermediate progresses very rapidly to the transition state [33]. They proposed that the tightly-bound ATP is hydrolyzed to ADP and Pi in the first site. The ADP affinity is decreased, resulting in the opening of dimer interface. Simultaneously, increasing its affinity for ATP, the second site is in tight-binding state and reduces the dimer interface of this site. Only after this step, Pi and ADP are released from the first site. This site can bind another ATP at low affinity to achieve another asymmetric occluded state [33]. Although, the substrate presence strongly increased the basal rate of ATP hydrolysis to access to an "accelerated" engagement of the NBDs to form the nucleotide sandwich dimer [37-39], this model proposes that at least one of the two NBD interfaces is always in the ATP high-affinity state. This suggests that NBD dimer does not dissociate during catalytic turnover and that the asymmetry of the structure is likely maintained continuously throughout the transport cycle.

Furthermore, based on biochemical studies and 3-D structures of mouse ABCB1, the MSD and NBD conformations are tightly linked. The high-to-low affinity transition of substrate binding site conformation is likely partially based on nucleotide binding [40]. Various mutagenesis studies identified critical amino-acid residues within TM12 and TM6 that alter the drug-resistance profile, and therefore are involved in the transport activity. Recently, Crowley's investigations highlighted TM12 involvement in coordinating drug-binding events with the process of nucleotide hydrolysis in ABCB1 [41]. Except for Ala980Cys mutation, they found that TM12 mutations strongly reduce ATPase activity, without altering the potency and degree of stimulation by various substrates (such as nicardipine and vinblastine). This suggests that TM12 helix is involved in basal ATP hydrolytic process [41]. Surprisingly, the crucial Leu976 and Phe978 residues in TM12 are close to the extracellular domains, and consequently far away from NBDs. This highlights cooperativity between MSDs and NBDs in the drug translocation process. In conclusion, TM6 and TM12 are important in the catalytic cycle of ABCB1, and participate to cooperative mechanisms [41, 42].

II.3.2 ABCC1 catalytic cycle

In contrast to ABCB1, the two NBDs of ABCC1 have considerably divergent sequences (only 27% identity), which results in a functional asymmetry [43]. Recently, in agreement with previous findings, isolated ABCC1 NBD1 displayed a weak ATPase activity, directly linked to its intrinsic ABCC1 property rather than to improper folding. Conformation residues in the catalytic site are different in presence of ATP and Mg2+, leading to an inactive conformation, while modeling NBD1-NBD2 dimer permits NBD2 to adopt an active conformation for ATP hydrolysis [44]. The ATP phosphate groups not only interact with the Walker A motif (α-phosphate with Ser686, β, γ-phosphates with Gly683, Lys684 and Ser685), but also tightly complex Mg2+. This ion is further coordinated by Ser685 and by the amide oxygen of the conserved Gln713 within the Q-loop. Mg2+ also interacts with Asp792, close to already described Asp793 [44] (figure 4). Residue Asp792 is suggested to contribute to the productive conformation of the catalytic complex [44].

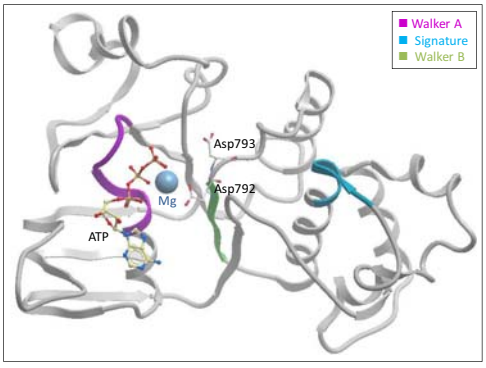

Figure 4. ABCC1 NBD1. The NBD on the N-terminal side of ABCC1 is represented with ATP and Mg2+ close to the side chains of Asp792 and Asp793. Walker A is shown in pink, Walker B in green and the ABC Signature in blue.

Usually, in NBD2, the residue localized immediately after the Walker B sequence is a glutamate. It is crucial for hydrolysis of the β-phosphodiester bond of ATP via its carboxylate side chain. However, this residue is an aspartate in NBD1 of ABCC proteins. This modification leads to particularities in binding and hydrolysis of the nucleotide at this NBD1. In fact, the NBDs are not interchangeable. Mutation of these two residues markedly affects the ability of the mutated NBD to bind, hydrolyze, and release nucleotides [45]. Although, an Asp793Glu mutation enhanced the conversion of ATP into ADP by NBD1, the mutation markedly decreased the ability to release ADP from NBD1. Consequently, the mutation decreased LTC4 transport activity, resulting in the inability to shift from a high- to low-affinity LTC4 binding state in the presence of ATP [45]. To complete this study, the Glu1455Asp mutation of NBD2 leads to an increase in ATP and ADP binding affinity. Glu1455Asp mutation locks the protein in a low-affinity substrate-binding state in the presence of ATP. Thus, the transition from a high-affinity substrate-binding state to a low-affinity substrate-releasing state may involve a conformational change that occurs after ATP binding to NBD2 and persists as long as the NBD is interacting with either ATP or ADP [45]. Additionally, the conversion of Trp653 to Tyr and/or Pro794 to Ala reverses the decrease in transport activity of the Asp793Glu mutant, by increasing ADP release from NBD1. Furthermore, this benefit was also obtained with the single mutation Pro794Ala with a 2-fold increase of LTC4 transport. Proline 794 is following the aspartate residue 793; an alanine is usually conserved at this 794 position in other NBDs of the ABC transporter family. Molecular dynamic simulation approaches showed that the Pro794Ala mutation strongly increases the flexibility of the region between the Walker B motif and the D-loop, and markedly increases the rate of Mg2+ and ADP release, suggesting that Pro794 contributes to the D-loop rigidity and to the stability of interactions between ADP and Lys684 and between Gln713 and Mg2+. In conclusion, it is suggested that ATP hydrolysis occurs at NBD1, albeit with low efficiency, and that ADP release from this site, at least in the Asp793Glu mutant protein, may be rate limiting in the transport cycle of ABCC1.

III. ABC TRANSPORTER CRYSTAL STRUCTURES

Because of their clinical interest, the activity and transport functions of ABC transporters have been extensively characterized by various biochemical studies. Only one mammalian ABC efflux protein and two prokaryotic ABC exporters have complete X-ray structures (mouse ABCB1, Sav1866 and MsbA). Since structure domain topology of the importers is not shared by the exporters, most of 3-D homology models of ABC exporters are currently based on these three structures.

Sav1866 is an ABC protein from the pathogen *Staphylococcus aureus* and is a homologue of human multidrug ABC transporters. It is a homodimeric ABC “half-transporter”, each monomer comprising covalently linked *N*-terminal MSD (amino-acid residues 1–320) and *C*-terminal NBD (residues 337–578). Recently, the 3-D crystal structure of Sav1866 was determined at 3.4 Å and 3.0 Å resolutions in a homodimeric complex with bound nucleotides, respectively AMP-PNP (an ATP-mimicking analog) and ADP, with the PDB codes 2ONJ and 2HYD. The structures displayed a remarkable feature of that protein in which both dimers are twisted and fit into each other, tightly interacting in ICLs (intracellular loops) and hinge regions [13]. Sav1866 X-ray structures were delivered under a dimer shape in outward-facing conformation where substrate cavity is exposed to the extracellular space [13, 46] (figure 5). In this conformation, bound substrates may be delivered into the aqueous extracellular space, depending on their hydrophobicity. ATP hydrolysis and ADP release are expected to bring the transporter back to an inward-facing conformation.

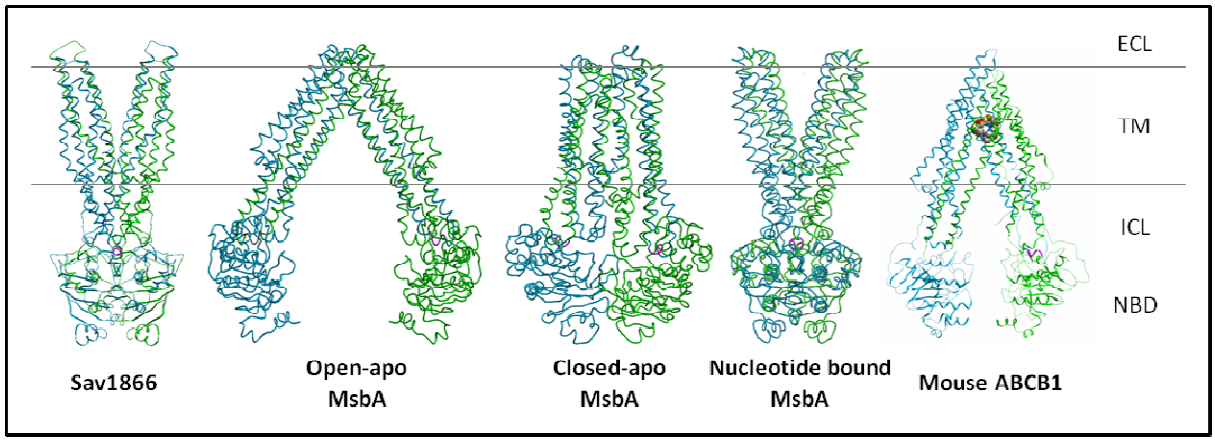

Figure 5: Sav1866, MsbA and ABCB1 X-ray structures. A monomer is colored in blue, and B monomer in green. Hinge sequences are shown in pink. OJZ cyclic peptide inhibitor of ABCB1 is shown in « ball » shape. ECL = Extracellular loops; TM = trans-membrane crossings; ICL = Intracellular loops; NBD = Nucleotide Binding Domain

MsbA is found in Gram-negative bacteria and transports lipid A and lipopolysaccharide (LPS) from the inward- to the outward-facing periplasmic leaflet of the membrane. MsbA is a half-transporter whose 3D structures have been obtained for the protein prepared from *Escherichia coli*, *Vibrio cholera* and *Salmonella typhimurium*, trapped in different conformations in the presence or absence of nucleotides [14]. Those structures display common features with that of Sav1866: MSD helices extend into the cytoplasm and interact with NBD, providing the link between the ATP catalytic site and the substrate transport pathway. In the nucleotide-bound state, the NBDs come together to form a canonical ATP dimer sandwich, significantly increasing the molecular interface within the protein. The two nucleotide-bound structures of *S. typhimurium* MsbA did not show significant differences between the AMPPNP and forward trapped ADP-vanadate state (outward or extracellular-facing V-shape) (figure 5). Conversely, the two free-nucleotide structures (apo structures) have two different inward (intracellular)-facing conformations. The nucleotide-bound conformation forms adopt an outward-facing V-shape between TM3/TM6 and TM1/TM2. Upon nucleotide binding, TM4/TM5/ICL2 move causing TM3/TM6 to split away from TM1/TM2, which results in an outward-facing conformation. Ward *et al.* [47] resolved a cryo-electron microscopy structures of MsbA reconstituted into a lipid bilayer in the presence of ADP-aluminum fluoride or AMPPNP. Although they suggested the presence of structural differences between the nucleotide transition states, they confirmed that an outward-facing conformation is observed in the presence of nucleotide [47]. Ward et al. built the open-apo MsbA model (*E. coli*) by using an MsbA-AMPPNP model as a starting point, manually positioning a monomer into the experimental electron-density map (figure 5). It may represent the functional inward-facing conformation. ICL2 crosses over and is still associated with the opposing monomer. This provides the only interaction existing between the two monomers. Thanks to experimental electron-density map calculated with the correct sign of the anomalous pairs, a closed-apo MsbA model was also generated by using the open-apo MsbA and MsbA-AMPPNP models as guides [14]. This structure, like the open-apo MsbA one, is nucleotide-free and represents another possible inward-facing conformation.

ABCB1 expression and high transport activity have frequently been associated with the decreased response to chemotherapy [48]. Because of clinical relevance, various strategies had been developed to inhibit its function, by using modulators. A first idea of the overall shape of the human protein was obtained at low resolution by electron microscopy [38, 49].

An efficient yeast expression system was successfully developed for the murine ABCB1 [50-52]. It allowed Chang's team to get an X-ray structure of a drug-binding competent state of the protein, at 3.8 Å resolution [12] (figure 5), constituting the most important step in the characterization of the mammalian ABC transporter structure. ABCB1 was crystallized in nucleotide-free (inward-facing) conformations defining an internal cavity of ~6,000 Å where the assumed drug-binding pocket is composed of hydrophobic and aromatic residues. This corresponds to a pre-transport state where substrate can bind but not reach the extracellular space, and NBDs are not dimerized but distant of 30 Å. Two additional ABCB1 co-crystal structures were obtained in the presence of the stereoisomers of cyclic peptide inhibitors (cyclic-tris-(R)-valineselenazole (QZ59-RRR) and cyclic-tris-(S)-valineselenazole (QZ59-SSS), which revealed that the protein can distinguish between these stereoisomers.

IV. HOMOLOGY MODELS BASED ON ABC PROTEIN CRYSTAL STRUCTURES

The ABC transporter family shows a high conservation in topology organization and amino-acid sequences. Taking advantage of this property, it is possible to successfully elaborate and use reliable homology models, to help in understanding the structural organization and localizing functional sites such as binding substrate-, nucleotide- and modulator-binding sites. These new insights can be mainly validated by biochemical data. In this section, we propose an overview on in silico models of some ABC transporters (ABCB1, ABCG2 and ABCC members).

IV.1 Homology modeling: a method to generate sequence homology-based structures

IV1.1 General procedure

Homology modeling starts with sequence alignment between the studied protein and selected crystallized protein template. For human ABC transporters, template proteins correspond to closest ABC exporters of which high-resolution X-ray structures are available. We can mention MsbA, Sav1866 and mouse ABCB1 that are listed in the protein data bank as the following PBD files:

- 3B5W: nucleotide-free MsbA from *Escherichia coli* (inward-facing conformation);
- 3B5X: nucleotide-free MsbA from *Vibrio cholerae* (inward facing-conformation);
- 3B5Z: ADP-bound MsbA from *Salmonella typhimurium* (outward facing-conformation);
- 3B60: AMP-PMP-bound MsbA from *Salmonella typhimurium* (outward facing-conformation);
- 2HYD: ADP-bound SAV1866 from *Staphylococcus aureus* (outward facing-conformation);
- 2ONJ: AMP-PMP-bound SAV1866 from *Staphylococcus aureus* (outward facing-conformation);
- 3G5U: mercury-bound ABCB1 from *Mus musculus* (inward facing-conformation);
- 3G60 and 3G61: OJZ (cyclic peptide) bound ABCB1 from *Mus musculus* (inward facing-conformation).

Sequence alignments between human ABC transporters and prokaryotic templates show that NBDs are highly conserved in comparison to MSDs (table 1). This was strongly supported by the fact that NBDs are involved in a general process of ATP catalysis, while MSDs are involved in the transport of variable substrates. Nevertheless, we must keep in mind the fact that, since ABC transporters are poly-specific by transporting structurally and functionally unrelated molecules, the expression default of one transporter can often be compensated by another one. For example, the human Dubin-Johnson syndrome is associated with nonsense mutations in the ABCC2 gene resulting in truncation and degradation of the protein. To date, this syndrome is considered to be benign and does not have a clear influence on the health or lifespan of affected individuals. This ABCC2 function is partially carried out by ABCC3 and

other transporters. Consequently, the specificity of transport is relative and directly linked to the tissue expression level and/or cellular localization.

By analyzing these sequence alignments, we noticed that ABCB1 MSDs are closer to prokaryotic MSDs than those of human ABCC1, ABCC4, ABCC5 and ABCG2. This observation leads to the conclusion that sequence alignments are not dependent on the species, as similar homology was reported in human sub-families compared to species. As a result, prokaryotic exporters can be considered as appropriated X-ray templates for mammalian exporters.

A		ABCB1		ABCC1		ABCC4		ABCC5		ABCG2	Sav1866	vcMsbA	stMsbA	ecMsbA
		MSD1	MSD2	MSD1	MSD2	MSD1	MSD2	MSD1	MSD2					
ABCB1	MSD1	100												
	MSD2	28	100											
ABCC1	MSD1	8	10	100										
	MSD2	11	9	11	100									
ABCC4	MSD1	12	15	26	9	100								
	MSD2	6	7	9	31	15	100							
ABCC5	MSD1	10	9	27	13	22	10	100						
	MSD2	12	13	8	29	10	32	9	100					
ABCG2		5	3	9	9	7	7	6	6	100				
Sav1866		13	16	13	13	11	13	8	9	6	100			
vcMsbA		16	13	1	12	8	14	9	11	10	19	100		
stMsbA		18	16	8	10	7	16	8	16	9	16	65	100	
ecMsbA		17	16	8	10	7	15	8	15	9	16	65	97	100

B		ABCB1		ABCC1		ABCC4		ABCC5		ABCG2	Sav1866	vcMsbA	stMsbA	ecMsbA
		NBD1	NBD2	NBD1	NBD2	NBD1	NBD2	NBD1	NBD2					
ABCB1	NBD1	100												
	NBD2	56	100											
ABCC1	NBD1	21	24	100										
	NBD2	27	27	22	100									
ABCC4	NBD1	30	28	28	27	100								
	NBD2	24	28	19	53	23	100							
ABCC5	NBD1	28	25	40	29	41	24	100						
	NBD2	27	29	19	50	23	50	25	100					
ABCG2		17	20	13	15	22	14	18	12	100				
Sav1866		44	43	27	31	28	28	31	29	20	100			
vcMsbA		41	41	27	30	28	29	32	31	14	46	100		
stMsbA		48	43	27	31	28	28	33	30	14	49	70	100	
ecMsbA		47	43	27	33	27	28	32	30	13	48	71	94	100

Table 1: Alignment scores between MSD (A) or NBD (B). Score were obtained using ClustalW sequence alignment tool.

ClustalW [53] and T-COFFEE software are classically used to perform automatic amino-acid alignment according to hydrophobicity, charge and lipohilic properties of the protein sequence. Nevertheless, homology results often have to be manually adjusted to align transmembrane crossings (TMs) of each protein. Those TMs can be predicted according to amino-acid residue composition by various secondary-structure prediction algorithms such as DAS (Dense Alignment Surface) Transmembrane Prediction server [54], Tmpred program, HMMTOP [55], PredictProtein server [56] or ESPRIPT program [57]. TM segments are essentially composed of lipohilic residues and are often organized in α-helix structure. Then the final alignment file is processed by modeling programs like Sybyl molecular modeling suite (Tripos, a Certara™ Company), MODELLER [58], ICM (Molsoft) or SWISS-MODEL [59]. To optimize the position of residue side chains, the generated models have to be minimized. Several energy minimization steps follow, to refine and correct amino acid side

chain positions in the model and generate the most stable and confident *in silico* 3D-structure. They can be performed using the GROMACS molecular dynamic package [60] or Sybyl molecular modeling suite. Finally, a verification phase can be assessed thanks to Procheck (ref) Prosaii [61], Proq [62] or Whatcheck [63].

IV.1.2 Modeling of human ABCB1, ABCC1, ABCC4, ABCC5 and ABCG2

ABCB1 is a full transporter following an MSD1-NBD1-MSD2-NBD2 arrangement, with a total of 12 membrane crossings. Mouse ABCB1 (mdr3) X-ray structure is the only one currently available. Although mdr3 is the closest mouse ABCB1 protein to human ABCB1 (87% of sequence identity), the two proteins are not exactly the same. Mouse mdr1 and mdr3 also show a similar percentage of sequence identity (84%) that nevertheless leads to significant differences in drug resistance phenotype [64]. This suggests that little primary sequence divergence is responsible for different drug transport. Homology models are thus still needed to elucidate human ABCB1 transport function, and to localize putative binding sites.

Various ABCB1 models have been built using prokaryote templates such as Sav1866 or MsbA, two half-transporters which can be aligned to each MSD-NBD half of ABCB1. Consequently, the generated *in silico* models of full-length ABCB1 are composed of separated MSD1-NBD1 and MSD2-NBD2 halves, and are then incomplete since they do not include the NBD1-MSD2 linker. Three models have been built using the Sav1866 crystal template (with outward-facing conformation) (table 2) by Becker *et al.* [65], Ravna *et al.* [66] and Stockner *et al.* [67]. As distances between helices 6 and 12 were much larger in the outward-facing model than suggested by cross-link experiments, some parts of MSD of the third model [67] were defined as mobile units and were symmetrically bend towards each other while NBDs were not moved. Similarly, human ABCB1 modeling, based on MsbA template, were performed by Becker *et al.* [65] and Ravna *et al.* [68] (table 2). In the second work, the amino-acid alignment of ABCB1 TM6 used for MsbA homology modeling was chosen to be in most accordance between cross-linking data and X-ray mouse ABCB1 structure. Thus TM6 orientations differ in both models. In parallel, Mares-Samano *et al.* [69] modeled the NBD moiety of ABCB1 to identify steroid binding sites (table 2). Since NBDs are highly conserved amongst the ABC family, numerous homology models were produced with several ABC transporter NBD crystal structures from *Escherichia coli* haemolysin B, *Lactococcus lactis* ABC transporter, *Plasmodium yoelii* MDR Protein 2, Tap1 ATPase domain and Tap1 C-Terminal domain. Finally, Pajeva *et al.* [70] built the first ABCB1 model based on the close mouse ABCB1.

		Alignment	TM prediction	Modelling	Refinement	Validation
MSD + NBD	**ABCB1**					
	Template	**Sav1866**				
	Becker et al. 2009	ClustalW		Modeller 9v1		Procheck
	Ravna et al. 2007	T-coffee	PredictProtein	ICM software	RefineModel macro of ICM	Savs Metaserver
	Stockner et al. 2009	ClustalW		Modeller 9v2	According cross linking data	
	Template	**MsbA**				
	Becker et al. 2009	ClustalW		Modeller 9v1		Procheck
	Ravna et al. 2009	T-coffee	PredictProtein	ICM software	RefineModel macro of ICM, According cross linking data	Savs Metaserver
	Template	**mABCB1**				
	Pajeva et al. 2009	MOE		MOE	MOE	MOE
NBD only	**Template**	***Escherichia coli* haemolysin B, *Lactococcus lactis* ABC transporter, *Plasmodium yoelii* MDR Protein 2, Tap1 ATPase domain and Tap1 C-Terminal domain**				
	Mares-Samano et al. 2009	ClustalW	Espript	Modeller 9v1		Ramachandran plots
MSD + NBD	**ABCC1**					
	Template	**ecMsbA**	*retracted structure*			
	Campbell et al. 2004					
	Template	**ABCB1 model**	*based on vcMsbA retracted structure*			
	Campbell et al. 2004					
	Template	**Sav1866**				
	De Gorter et al. 2008	ClustalW	DAS, Tmpred and HMMTOP	Modeller	GROMACS 3.0 molecular dynamic package	Procheck and What-if
MSD + NBD	**ABCC4**					
	Template	**Sav1866**				
	Ravna et al. 2008	T-coffee	PredictProtein	ICM software	RefineModel macro of ICM	Savs Metaserver
	Template	**ecMsbA**				
	Ravna et al. 2009	T-coffee	PredictProtein	ICM software	RefineModel macro of ICM	Savs Metaserver
MSD + NBD	**ABCC5**					
	Template	**Sav1866**				
	Ravna et al. 2008	T-coffee	PredictProtein	ICM software	RefineModel macro of ICM	Savs Metaserver
	Template	**ecMsbA**				
	Ravna et al.	T-coffee	PredictProtein	ICM software	RefineModel macro of ICM	Savs Metaserver
MSD only NBD only	**ABCG2**					
	Template	**ecMsbA**	*retracted structure*			
	Li et al. 2007					
	Template	**Sav1866**				
	Hazai et al. 2008					
	Template	**ecMalK**				
	Li et al. 2007			SWISS-MODEL		
	Hazai et al. 2008	ClustalW	DAS	Modeller 6	GROMACS molecular dynamic package	Procheck
	Mares-Samano et al. 2009	ClustalW	Espript	Modeller 9v1		Ramachandran plots

Table 2: Detailed methodologies employed for ABC transporter homology modeling.

As a member of the C-class, ABCC1 is a full transporter with an additional N-terminal domain (MSD0) which contains five transmembrane crossings. It displays an atypical MSD0-MSD1-NBD1-MSD2-NBD2 arrangement where MSD1 begins with the sixth TM. Up to now, only little is known about the structure and function of this supplementary domain. Recently, a 16-Å resolution was obtained for the nucleotide-free full-length ABCC1 protein by electron cryomicroscopy of 2D crystals, suggesting that MSD0 makes contacts on one side of 2 halves (MSD0 would interact with TM helices 14, 15 and 16 in MSD2 and 7 in MSD1) [71]. No template from X-ray crystal structure was available for either MSD0 or the linker between MSD0 and MSD1. Consequently by homology method, a partial ABCC1 3D *in silico* model (including only MSD1-NBD1 and MSD2-NBD2 halves) was generated, based on both MsbA and Sav1866 half-transporter templates (table 2). As based on the retracted MsbA structures, the two first ABCC1 *in silico* models generated by Campbell et al. [20] were not reliable, and therefore useless. Later, to validate their biochemical data, they generated a new *in silico* model based on Sav1866 template [72].

Similarly to ABCB1, ABCC4 displays an MSD1-NBD1-MSD2-NBD2 topology that can be modeled in two MSD-NBD halves. Two *in silico* ABCC4 models have been generated using either Sav1866 (outward-facing) [73] or *E. coli* MsbA (inward-facing) templates [68] (table 2).

ABCC5 is a full transporter sharing the same arrangement as ABCB1 and ABCC4. ABCC5 in silico models have been generated from Sav1866 and *E. coli* MsbA [66, 74] (table 2).

Since ABCG2 is a half-transporter following a NBD-MSD arrangement and different from those of the ABC crystallized transporters, ABCG2 models were built in two halves with separated NDB and MSD peptides (table 2) [69, 75, 76]. ABCG2 NBD was automatically modeled using *E. coli* MalK NBD as a template while MSD was built over the retracted ecMsbA and the Sav1866 templates.

IV.2 How in silico models may help for structure characterization

IV.2.1 ABCB1 modeling: substrate and ATP-binding site description

Based on Sav1866 template, the first ABCB1 *in silico* model was generated in nucleotide-bound catalytic state (outward facing) [65]. In the resulting structure, distances between residues correlated with cross-linking data. Many residues (Tyr401, Lys433, Asp555, Glu556, Ty1044, Lys1076, Asp1200 and Glu1201), identified as functionally important for ATP hydrolysis, were indeed located close to bound ATP. To identify functionally involved amino-acid residues, docking was performed for positioning known substrates (verapamil, rhodamine B, colchicine and vinblastine) into potential binding sites. Most of the positions were located in the outer membrane leaflet in the TM. Among putative positions, some were involving amino acid residues experimentally described to be inside the binding site. According to binding sites and ligand size, no pair of the ligand could bind at the same time.

Another Sav1866-based model of ABCB1 has been described [66]. The electrostatic potential surface (EPS) in the substrate translocation pathway and the positive/negative ratio of charged amino acids were in agreement with the transport of cationic amphiphilic and lipophilic substrates by ABCB1. Indeed, the EPS of the ABCB1 substrate translocation chamber was neutral with negative and weakly positive areas. The positive/negative ratio of charged amino-acids was lower in ABCB1 MSD than in ABCC5, which is known to transport organic anions. According to previous cross-linking studies, some residues were described to be structurally close to each other. Previous site-directed mutagenesis studies indicated that residues Ile306 (TM5), Ile340 (TM6) and Phe343 (TM6) were localized inside the potential binding site. Leu65 (TM1) was found to be involved in the putative translocation pathway.

The third model built with Sav1866 [67] was in accordance with both cysteine cross-linking data and the overall electron microscopy density map. As distances between helices 6 and 12 were much larger in this outward facing model than suggested by cross-linking results, some parts of MSD were moved to satisfy experimental data. This model suggested a possible transition between the outward facing conformation and the modified one. This would not compromise the structural integrity of MSD. Furthermore, experimental evidence suggested that substrate binding could induce translational and/or rotational movements of central helices 6 and 12.

Similarly, two ABCB1 models in two different catalytic states were produced according to MsbA crystal structures (in either presence or absence of nucleotides) [65]. Distances between residues correlated with cross-linking data. As observed with the Sav1866-based model, several residues (Tyr401, Lys433, Asp555, Glu556, Ty1044, Lys1076, Asp1200 and Glu1201) known to be involved in ATP hydrolysis, were indeed located close to ATP. Docking of verapamil, rhodamine B, colchicine and vinblastine showed that most positions were located in the outer membrane leaflet in the TM. Among putative positions, some were involving amino acid residues experimentally described to be within the binding site. The second MsbA-based model of ABCB1 was constructed by Ravna *et al.* [68].

Ravna (2009) generated three different ABCB1 models, based on different amino residue alignments obtained either after TM2 adjustments or after TM2/TM6 adjustments from previously published alignments [14,69]. In the model with TM2 adjustments, amino acids

(Val133/Gly939 and Cys127/Ala935) were oriented towards each other in accordance with both cross-linking data and the X-ray crystal structure of the *Mus musculus* ABCB1. In contrast, in model using TM2/TM6 adjustments, critical amino acids (Ile340 and Phe343) pointed away from the putative substrate binding site. In contrast and more realistically, in ABCB1 model based on TM6 Ravna's T-COFFEE alignment, these amino acid positions were in accordance both with cross-linking data and the X-ray crystal structure of the Mus musculus ABCB1. This work highlighted that the TM localization is essential to the reliability of the 3D *in silico* model.

Furthermore, the electrostatic potential surface in the substrate translocation pathway and the positive/negative ratio of charged amino-acids were in accordance with the transport of cationic amphiphilic and lipophilic substrates by ABCB1. Indeed, the electrostatic potential surface of the ABCB1 substrate translocation chamber was neutral with negative and weakly-positive areas [68]. According to previous cross-linking studies, some residues were described to be close, and both models confirmed those biochemical data. For other residues, distances between alpha carbons are longer in the MsbA-based model but in accordance with the mouse ABCB1 X-ray structure. This could be explained by the inward conformation of MsbA and mouse ABCB1 that was not used for cross-linking experiments. According to previous site-directed mutagenesis studies, residues Ile306 (TM5), Ile340 (TM6) and Phe343 (TM6) were localized in the putative drug binding site of both models [68]. Leu65 (TM1) was only found in the putative translocation pathway in the previously described Sav1866-based model, while Phe728 (TM7) and Val982 (TM12) were identified in this MsbA-based model of ABCB1. Those differences could come from conformational changes occurring between the inward-facing and the outward-facing states, respectively observed in the MsbA and Sav1866 structures. However, Ile306, Ile340, Phe343, Phe728 and Val982, which were identified in the MsbA-based model, were also observed in the putative binding site of mouse ABCB1 X-ray structure. This suggests that MsbA could be a useful template for human ABCB1 modeling and that, even though the V-shape is wider for MsbA, it reflects the inward facing conformation of mouse ABCB1.

Mares-Samano *et al.* generated the NBD moiety of ABCB1 to identify steroid-binding sites [69]. Docking led to the identification of a binding cavity for ATP formed by Tyr1044, the P-loop and His1232. Many amino acid residues were found to be able to interact with steroids.

Finally, one ABCB1 model was built from mouse ABCB1 structure [70], and used to compare the inward- and the outward-facing conformations. In the inward-facing model, TM4 and TM10 are accessible while, in the outward-facing model, they are not anymore, suggesting TM4 and TM10 involvements in conformation changes. Same residues of TM6 and TM12 seemed to be facing the drug-binding cavity in both models. Analysis of amino acid position and identified involvement in drug binding led the authors to conclude that the drug remains bound to the same residues during the conformation transition. As observed in mouse X-ray structure, QZ59 cyclic inhibitor binding involved different residues in the human ABCB1 model. Furthermore, docking results confirmed the possibility for binding of the same molecule in two different locations.

IV.2.2 ABCC1 modeling: Identification of residues involved in transport activity

Based on retracted MsbA structures, two first in silico models of ABCC1 were generated by Campbell et al. [20]. One was based on E. coli MsbA and the other one on an ABCB1 model, itself based on *V. cholerae* MsbA. The models were in agreement with the open-apo conformation (wide open) of E. coli MsbA compared to the closed-apo conformation of *V. cholerae* MsbA (used as a template for ABCB1). Three aromatic residues (Trp553, Trp1198 and Trp1246), previously demonstrated to be functionally important for ABCC1 activity,

were found to line the putative substrate translocation site. According to this model, an additional residue, Phe594, appeared to form aromatic interactions with those residues. Site-directed mutagenesis experiments confirmed the involvement of Phe594 in ABCC1 transport activity. Unfortunately, even though those models have correctly predicted functional importance of one amino acid, they were based on the retracted MsbA structure. A new *in silico* model based on Sav1866 template was then generated [72], and validated the position of Phe594 and Trp1246 in the putative substrate translocation pathway while this was not the case for Trp553 and Trp1198. The authors suggested that this model only represents one conformation in the transport cycle (outward-facing) and that the inward-facing conformation could reveal the access to other sets of amino acid residues. This may however not prevent using the homology model to guide and interpret biochemical data.

IV.2.3 ABCC4 modeling: Checklist of residues potentially located in the substrate translocation site

Two *in silico* ABCC4 models have been generated using either Sav1866 (outward-facing) or MsbA (inward-facing) templates. The first ABCC4 homology model was constructed with Sav1866 [73]. Amino acid residues located along the substrate translocation site were identified as good candidates for single-point mutation analysis. The same methodology was applied to create an ABCC4 model with *E. coli* MsbA [68]. The putative substrate-releasing pocket seems to contain the same amino acid residues, suggesting their contribution to both high- and low-affinity binding sites.

IV.2.4 ABCC5 modeling: Prediction of potential cGMP binding pocket

ABCC5 *in silico* models have been generated from Sav1866 and *E. coli* MsbA. The electrostatic potential surface in the substrate-translocation pathway and the positive/negative ratio of charged amino acids were in accordance with the transport of organic anions by ABCC5. Indeed, The EPS of ABCC5 substrate-translocation chamber was positive. Docking sessions were carried out, and two putative cGMP binding pockets were predicted: one involving TM1, 2, 11 and 12 and the other involving TM 3, 5, 7 and 8. A total of 42 amino acid residues were reported as putative cGMP binding residues (21 inside pocket 1, and 25 inside pocket 2) and represent targets for site-directed mutagenesis experiments. As Sav1866 is in outward-facing conformation, the authors agreed that it is probably in low-affinity state and that two or more binding sites remain to be confirmed in the substrate recognition conformation. This model would not represent the suitable template for high-affinity binding site modeling. Another model was thus performed with *E. coli* MsbA giving an inward-facing conformation [68]. According to the authors, the same residues were found in the putative substrate-binding sites.

IV.2.5 ABCG2 modeling: Models illustrating the previously-described functional importance of residues

The first ABCG2 model was built in two fractions, by separating the NBD and MSD domains [75]. The final model was in agreement with site-directed mutagenesis data, despite the retracted structure of MsbA was used for MSD building. In NBD, mutations within the Walker A motif (Thr82Ala, Lys86Met/Ile) leading to loss of transport activity showed specific changes. For example, Thr82Ala could affect dimer assembly by eliminating the interaction with Arg193 in the vicinal ABC signature motif. Lys86Met/Ile could result in the loss of interaction with the tri-phosphate group of ATP. The model failed to explain a role of the two trans-membrane GXXXG motifs supposed to be engaged in dimeric interaction. Mutation of Gly553 inside the TM5 of the model led to amino acid side chain clash and dimer disruption, explaining the endoplasmic-reticulum localization of G553 mutant of ABCG2. Arg482 mutation is known to affect the ABCG2 specificity. The mutation on the ABCG2

model enlarged the central TM cavity, and disrupted the positively-charged region formed by Arg482, Lys652, Ly452 and Lys543.

In another ABCG2 model [76], the NBDs were similar to those earlier described [75], and showed the two ATP molecules located at the surface of closed NBD. In the MSD part, residues Arg482, Leu554 and Asn557, previously described to influence substrate specificity, pointed towards the interior of the cavity. Docking of ABCG2 substrates (daunomycin, doxorubicin, mitoxantrone, Hoechst 33342, prazosin, rhodamine and phorphyrin) were carried out. Rhodamine and daunomycin showed distinct binding sites while daunomycin, doxorubicin and Hoechst 33342 were docked at the same location. Finally, phorphyrin was placed in the same binding site as prazosin. Ligands were caught between residues Leu554, Leu555 and Asn557 according to experiments that previously described an effect of Leu554 and Asn557 on drug transport.

The NBD domain of ABCG2 was also modeled alone in order to identify steroid-binding sites [69]. Docking led to the identification of a binding cavity for steroids formed by Phe52, His243 and the P-loop. Many amino-acid residues were found to potentially interact with steroids.

V.3 Future evolution

To improve the confidence of the models, further efforts have to be carried out on the characterization of additional crystallized structures of original ABC transporters with atypical topology (such as ABCG2, a half-transporter with inverse topology versus ABCB1, Sav1866 and MsbA). In addition, new structures co-crystallized with substrates will be necessary to better define the binding sites. Furthermore, these additional data will be integrated to molecular dynamic simulations to describe the entire movement of the pump body. To date, static models are relevant and fully satisfying for the biochemical approach about the identification of essential amino-acid residues involved in drug transport function. They also took advantage of the conserved topology among ABC transporters. However, molecular dynamic simulations are restrained for limited movements and periods of time. A next step is to stimulate wider movements of the entire pump and for a longer duration. To achieve that, new algorithms/tools have to be developed / improved: (1) for increasing the duration of simulations to the millisecond range; (2) for integrating thermodynamic properties including entropy and free energy. Indeed, to date methods used for carrying out molecular dynamics generate conformations close to the initial structure which is generally rather stable since obtained from crystals. These improvements would allow simulating wider movements, such as those of domains, and thus getting an overview of the entire substrate-efflux cycle.

LIST OF ABBREVIATIONS

ABC (ATP-Binding Cassette); ECL (Extracellular Loop); EPS (Electrostatic Potential Surface); ICL (Intracellular Loop); LPS (Lipopolysaccharide); MDR (MultiDrug Resistance); MRP (MultiDrug Resistance Protein); MSD (Membrane Spanning Domain); NBD (Nucleotide-Binding Domain); PDB (Protein Data Bank); Pi (Phosphate); TM (transmembrane segment).

ACKNOWLEDGMENTS

This work was supported by INSERM (UMR 590) and Université Lyon 1, and grants from Association pour la Recherche sur le Cancer (ARC 4007) and from the Ligue Nationale contre le Cancer (Equipe labellisée Ligue 2009). M.H. is recipient of doctoral fellowships from the Ligue Nationale contre le Cancer.

REFERENCES

[1] Scherrmann, J.M. Expression and function of multidrug resistance transporters at the blood-brain barriers. Expert Opin Drug Metab Toxicol, 2005, 1, 233-46.

[2] Klaassen, C.D.; Aleksunes, L.M. Xenobiotic, bile acid, and cholesterol transporters: function and regulation. Pharmacol Rev, 62, 1-96.

[3] Oostendorp, R.L.; Beijnen, J.H.; Schellens, J.H. The biological and clinical role of drug transporters at the intestinal barrier. Cancer Treat Rev, 2009, 35, 137-47.

[4] Benderra, Z.; Faussat, A.M.; Sayada, L.; Perrot, J.Y.; Tang, R.; Chaoui, D.; Morjani, H.; Marzac, C.; Marie, J.P.; Legrand, O. MRP3, BCRP, and P-glycoprotein activities are prognostic factors in adult acute myeloid leukemia. Clin Cancer Res, 2005, 11, 7764-72.

[5] Benderra, Z.; Faussat, A.M.; Sayada, L.; Perrot, J.Y.; Chaoui, D.; Marie, J.P.; Legrand, O. Breast cancer resistance protein and P-glycoprotein in 149 adult acute myeloid leukemias. Clin Cancer Res, 2004, 10, 7896-902.

[6] Honorat, M.; Guitton, J.; Dumontet, C.; Payen, L. Expression level and hormonal regulation of ABC transporters in breast cancer. Current cancer therapy review, 2010, in press.

[7] Larbcharoensub, N.; Leopairat, J.; Sirachainan, E.; Narkwong, L.; Bhongmakapat, T.; Rasmeepaisarn, K.; Janvilisri, T. Association between multidrug resistance-associated protein 1 and poor prognosis in patients with nasopharyngeal carcinoma treated with radiotherapy and concurrent chemotherapy. Hum Pathol, 2008, 39, 837-45.

[8] Noguchi, K.; Katayama, K.; Mitsuhashi, J.; Sugimoto, Y. Functions of the breast cancer resistance protein (BCRP/ABCG2) in chemotherapy. Adv Drug Deliv Rev, 2009, 61, 26-33.

[9] Dean, M.; Rzhetsky, A.; Allikmets, R. The human ATP-binding cassette (ABC) transporter superfamily. Genome Res, 2001, 11, 1156-66.

[10] Bhatia, A.; Schafer, H.J.; Hrycyna, C.A. Oligomerization of the human ABC transporter ABCG2: evaluation of the native protein and chimeric dimers. Biochemistry, 2005, 44, 10893-904.

[11] Graf, G.A.; Li, W.P.; Gerard, R.D.; Gelissen, I.; White, A.; Cohen, J.C.; Hobbs, H.H. Coexpression of ATP-binding cassette proteins ABCG5 and ABCG8 permits their transport to the apical surface. J Clin Invest, 2002, 110, 659-69.

[12] Aller, S.G.; Yu, J.; Ward, A.; Weng, Y.; Chittaboina, S.; Zhuo, R.; Harrell, P.M.; Trinh, Y.T.; Zhang, Q.; Urbatsch, I.L.; Chang, G. Structure of P-glycoprotein reveals a molecular basis for poly-specific drug binding. Science, 2009, 323, 1718-22.

[13] Dawson, R.J.; Locher, K.P. Structure of a bacterial multidrug ABC transporter. Nature, 2006, 443, 180-5.

[14] Ward, A.; Reyes, C.L.; Yu, J.; Roth, C.B.; Chang, G. Flexibility in the ABC transporter MsbA: Alternating access with a twist. Proc Natl Acad Sci U S A, 2007, 104, 19005-10.

[15] Locher, K.P.; Lee, A.T.; Rees, D.C. The E. coli BtuCD structure: a framework for ABC transporter architecture and mechanism. Science, 2002, 296, 1091-8.

[16] Gerber, S.; Comellas-Bigler, M.; Goetz, B.A.; Locher, K.P. Structural basis of trans-inhibition in a molybdate/tungstate ABC transporter. Science, 2008, 321, 246-50.

[17] Pinkett, H.W.; Lee, A.T.; Lum, P.; Locher, K.P.; Rees, D.C. An inward-facing conformation of a putative metal-chelate-type ABC transporter. Science, 2007, 315, 373-7.

[18] Oldham, M.L.; Khare, D.; Quiocho, F.A.; Davidson, A.L.; Chen, J. Crystal structure of a catalytic intermediate of the maltose transporter. Nature, 2007, 450, 515-21.

[19] Kadaba, N.S.; Kaiser, J.T.; Johnson, E.; Lee, A.; Rees, D.C. The high-affinity E. coli methionine ABC transporter: structure and allosteric regulation. Science, 2008, 321, 250-3.

[20] Campbell, J.D.; Koike, K.; Moreau, C.; Sansom, M.S.; Deeley, R.G.; Cole, S.P. Molecular modeling correctly predicts the functional importance of Phe594 in transmembrane helix 11 of the multidrug resistance protein, MRP1 (ABCC1). J Biol Chem, 2004, 279, 463-8.

[21] Kerr, I.D. Structure and association of ATP-binding cassette transporter nucleotide-binding domains. Biochim Biophys Acta, 2002, 1561, 47-64.

[22] Seeger, M.A.; van Veen, H.W. Molecular basis of multidrug transport by ABC transporters. Biochim Biophys Acta, 2009, 1794, 725-37.

[23] Jones, P.M.; George, A.M. Nucleotide-dependent allostery within the ABC transporter ATP-binding cassette: a computational study of the MJ0796 dimer. J Biol Chem, 2007, 282, 22793-803.

[24] Smith, C.A.; Rayment, I. X-ray structure of the magnesium(II).ADP.vanadate complex of the Dictyostelium discoideum myosin motor domain to 1.9 A resolution. Biochemistry, 1996, 35, 5404-17.

[25] Smith, P.C.; Karpowich, N.; Millen, L.; Moody, J.E.; Rosen, J.; Thomas, P.J.; Hunt, J.F. ATP binding to the motor domain from an ABC transporter drives formation of a nucleotide sandwich dimer. Mol Cell, 2002, 10, 139-49.

[26] Jones, P.M.; George, A.M. Opening of the ADP-bound active site in the ABC transporter ATPase dimer: evidence for a constant contact, alternating sites model for the catalytic cycle. Proteins, 2009, 75, 387-96.

[27] Wen, P.C.; Tajkhorshid, E. Dimer opening of the nucleotide binding domains of ABC transporters after ATP hydrolysis. Biophys J, 2008, 95, 5100-10.

[28] Oliveira, A.S.; Baptista, A.M.; Soares, C.M. Insights into the molecular mechanism of an ABC transporter: conformational changes in the NBD dimer of MJ0796. J Phys Chem B, 114, 5486-96.

[29] Callaghan, R.; Ford, R.C.; Kerr, I.D. The translocation mechanism of P-glycoprotein. FEBS Lett, 2006, 580, 1056-63.

[30] Sauna, Z.E.; Kim, I.W.; Nandigama, K.; Kopp, S.; Chiba, P.; Ambudkar, S.V. Catalytic cycle of ATP hydrolysis by P-glycoprotein: evidence for formation of the E.S reaction intermediate with ATP-gamma-S, a nonhydrolyzable analogue of ATP. Biochemistry, 2007, 46, 13787-99.

[31] Senior, A.E.; al-Shawi, M.K.; Urbatsch, I.L. The catalytic cycle of P-glycoprotein. FEBS Lett, 1995, 377, 285-9.

[32] Senior, A.E. Catalytic mechanism of P-glycoprotein. Acta Physiol Scand Suppl, 1998, 643, 213-8.

[33] Siarheyeva, A.; Liu, R.; Sharom, F.J. Characterization of an asymmetric occluded state of P-glycoprotein with two bound nucleotides: implications for catalysis. J Biol Chem, 285, 7575-86.

[34] Tombline, G.; Senior, A.E. The occluded nucleotide conformation of p-glycoprotein. J Bioenerg Biomembr, 2005, 37, 497-500.

[35] Sauna, Z.E.; Muller, M.; Peng, X.H.; Ambudkar, S.V. Importance of the conserved Walker B glutamate residues, 556 and 1201, for the completion of the catalytic cycle of ATP hydrolysis by human P-glycoprotein (ABCB1). Biochemistry, 2002, 41, 13989-4000.

[36] Tombline, G.; Bartholomew, L.A.; Urbatsch, I.L.; Senior, A.E. Combined mutation of catalytic glutamate residues in the two nucleotide binding domains of P-glycoprotein generates a conformation that binds ATP and ADP tightly. J Biol Chem, 2004, 279, 31212-20.

[37] Rosenberg, M.F.; Velarde, G.; Ford, R.C.; Martin, C.; Berridge, G.; Kerr, I.D.; Callaghan, R.; Schmidlin, A.; Wooding, C.; Linton, K.J.; Higgins, C.F. Repacking of the transmembrane domains of P-glycoprotein during the transport ATPase cycle. Embo J, 2001, 20, 5615-25.

[38] Rosenberg, M.F.; Kamis, A.B.; Callaghan, R.; Higgins, C.F.; Ford, R.C. Three-dimensional structures of the mammalian multidrug resistance P-glycoprotein demonstrate major conformational changes in the transmembrane domains upon nucleotide binding. J Biol Chem, 2003, 278, 8294-9.

[39] Rothnie, A.; Storm, J.; Campbell, J.; Linton, K.J.; Kerr, I.D.; Callaghan, R. The topography of transmembrane segment six is altered during the catalytic cycle of P-glycoprotein. J Biol Chem, 2004, 279, 34913-21.

[40] Martin, C.; Higgins, C.F.; Callaghan, R. The vinblastine binding site adopts high- and low-affinity conformations during a transport cycle of P-glycoprotein. Biochemistry, 2001, 40, 15733-42.

[41] Crowley, E.; O'Mara, M.L.; Reynolds, C.; Tieleman, D.P.; Storm, J.; Kerr, I.D.; Callaghan, R. Transmembrane helix 12 modulates progression of the ATP catalytic cycle in ABCB1. Biochemistry, 2009, 48, 6249-58.

[42] Callaghan, R.; Crowley, E.; Potter, S.; Kerr, I.D. P-glycoprotein: so many ways to turn it on. J Clin Pharmacol, 2008, 48, 365-78.

[43] Ramaen, O.; Sizun, C.; Pamlard, O.; Jacquet, E.; Lallemand, J.Y. Attempts to characterize the NBD heterodimer of MRP1: transient complex formation involves Gly771 of the ABC signature sequence but does not enhance the intrinsic ATPase activity. Biochem J, 2005, 391, 481-90.

[44] Ramaen, O.; Leulliot, N.; Sizun, C.; Ulryck, N.; Pamlard, O.; Lallemand, J.Y.; Tilbeurgh, H.; Jacquet, E. Structure of the human multidrug resistance protein 1 nucleotide binding domain 1 bound to Mg2+/ATP reveals a non-productive catalytic site. J Mol Biol, 2006, 359, 940-9.

[45] Payen, L.F.; Gao, M.; Westlake, C.J.; Cole, S.P.; Deeley, R.G. Role of carboxylate residues adjacent to the conserved core Walker B motifs in the catalytic cycle of multidrug resistance protein 1 (ABCC1). J Biol Chem, 2003, 278, 38537-47.

[46] Dawson, R.J.; Locher, K.P. Structure of the multidrug ABC transporter Sav1866 from Staphylococcus aureus in complex with AMP-PNP. FEBS Lett, 2007, 581, 935-8.

[47] Ward, A.; Mulligan, S.; Carragher, B.; Chang, G.; Milligan, R.A. Nucleotide dependent packing differences in helical crystals of the ABC transporter MsbA. J Struct Biol, 2009, 165, 169-75.

[48] Li, Y.; Yuan, H.; Yang, K.; Xu, W.; Tang, W.; Li, X. The structure and functions of P-glycoprotein. Curr Med Chem, 17, 786-800.

[49] Lee, J.Y.; Urbatsch, I.L.; Senior, A.E.; Wilkens, S. Nucleotide-induced structural changes in P-glycoprotein observed by electron microscopy. J Biol Chem, 2008, 283, 5769-79.

[50] Urbatsch, I.L.; Beaudet, L.; Carrier, I.; Gros, P. Mutations in either nucleotide-binding site of P-glycoprotein (Mdr3) prevent vanadate trapping of nucleotide at both sites. Biochemistry, 1998, 37, 4592-602.

[51] Lerner-Marmarosh, N.; Gimi, K.; Urbatsch, I.L.; Gros, P.; Senior, A.E. Large scale purification of detergent-soluble P-glycoprotein from Pichia pastoris cells and characterization of nucleotide binding properties of wild-type, Walker A, and Walker B mutant proteins. J Biol Chem, 1999, 274, 34711-8.

[52] Urbatsch, I.L.; Wilke-Mounts, S.; Gimi, K.; Senior, A.E. Purification and characterization of N-glycosylation mutant mouse and human P-glycoproteins expressed in Pichia pastoris cells. Arch Biochem Biophys, 2001, 388, 171-7.

[53] Thompson, J.D.; Higgins, D.G.; Gibson, T.J. CLUSTAL W: improving the sensitivity of progressive multiple sequence alignment through sequence weighting, position-specific gap penalties and weight matrix choice. Nucleic Acids Res, 1994, 22, 4673-80.

[54] Cserzo, M.; Wallin, E.; Simon, I.; von Heijne, G.; Elofsson, A. Prediction of transmembrane alpha-helices in prokaryotic membrane proteins: the dense alignment surface method. Protein Eng, 1997, 10, 673-6.

[55] Tusnady, G.E.; Simon, I. The HMMTOP transmembrane topology prediction server. Bioinformatics, 2001, 17, 849-50.

[56] Rost, B.; Yachdav, G.; Liu, J. The PredictProtein server. Nucleic Acids Res, 2004, 32, W321-6.

[57] Gouet, P.; Courcelle, E.; Stuart, D.I.; Metoz, F. ESPript: analysis of multiple sequence alignments in PostScript. Bioinformatics, 1999, 15, 305-8.

[58] Sali, A.; Blundell, T.L. Comparative protein modelling by satisfaction of spatial restraints. J Mol Biol, 1993, 234, 779-815.

[59] Arnold, K.; Bordoli, L.; Kopp, J.; Schwede, T. The SWISS-MODEL workspace: a web-based environment for protein structure homology modelling. Bioinformatics, 2006, 22, 195-201.

[60] Van Der Spoel, D.; Lindahl, E.; Hess, B.; Groenhof, G.; Mark, A.E.; Berendsen, H.J. GROMACS: fast, flexible, and free. J Comput Chem, 2005, 26, 1701-18.

[61] Sippl, M.J. Recognition of errors in three-dimensional structures of proteins. Proteins, 1993, 17, 355-62.

[62] Wallner, B.; Elofsson, A. Can correct protein models be identified? Protein Sci, 2003, 12, 1073-86.

[63] Hooft, R.W.; Vriend, G.; Sander, C.; Abola, E.E. Errors in protein structures. Nature, 1996, 381, 272.

[64] Devault, A.; Gros, P. Two members of the mouse mdr gene family confer multidrug resistance with overlapping but distinct drug specificities. Mol Cell Biol, 1990, 10, 1652-63.

[65] Becker, J.P.; Depret, G.; Van Bambeke, F.; Tulkens, P.M.; Prevost, M. Molecular models of human P-glycoprotein in two different catalytic states. BMC Struct Biol, 2009, 9, 3.

[66] Ravna, A.W.; Sylte, I.; Sager, G. Molecular model of the outward facing state of the human P-glycoprotein (ABCB1), and comparison to a model of the human MRP5 (ABCC5). Theor Biol Med Model, 2007, 4, 33.

[67] Stockner, T.; de Vries, S.J.; Bonvin, A.M.; Ecker, G.F.; Chiba, P. Data-driven homology modelling of P-glycoprotein in the ATP-bound state indicates flexibility of the transmembrane domains. Febs J, 2009, 276, 964-72.

[68] Ravna, A.W.; Sylte, I.; Sager, G. Binding site of ABC transporter homology models confirmed by ABCB1 crystal structure. Theor Biol Med Model, 2009, 6, 20.

[69] Mares-Samano, S.; Badhan, R.; Penny, J. Identification of putative steroid-binding sites in human ABCB1 and ABCG2. Eur J Med Chem, 2009, 44, 3601-11.

[70] Pajeva, I.K.; Globisch, C.; Wiese, M. Comparison of the inward- and outward-open homology models and ligand binding of human P-glycoprotein. Febs J, 2009, 276, 7016-26.

[71] Rosenberg, M.F.; Mao, Q.; Holzenburg, A.; Ford, R.C.; Deeley, R.G.; Cole, S.P. The structure of the multidrug resistance protein 1 (MRP1/ABCC1). crystallization and single-particle analysis. J Biol Chem, 2001, 276, 16076-82.

[72] DeGorter, M.K.; Conseil, G.; Deeley, R.G.; Campbell, R.L.; Cole, S.P. Molecular modeling of the human multidrug resistance protein 1 (MRP1/ABCC1). Biochem Biophys Res Commun, 2008, 365, 29-34.

[73] Ravna, A.W.; Sager, G. Molecular model of the outward facing state of the human multidrug resistance protein 4 (MRP4/ABCC4). Bioorg Med Chem Lett, 2008, 18, 3481-3.

[74] Ravna, A.W.; Sylte, I.; Sager, G. A molecular model of a putative substrate releasing conformation of multidrug resistance protein 5 (MRP5). Eur J Med Chem, 2008, 43, 2557-67.

[75] Li, Y.F.; Polgar, O.; Okada, M.; Esser, L.; Bates, S.E.; Xia, D. Towards understanding the mechanism of action of the multidrug resistance-linked half-ABC transporter ABCG2: a molecular modeling study. J Mol Graph Model, 2007, 25, 837-51.

[76] Hazai, E.; Bikadi, Z. Homology modeling of breast cancer resistance protein (ABCG2). J Struct Biol, 2008, 162, 63-74.

2. Génération du modèle *in silico* d'ABCC11

ABCC11 présente une structure composée selon l'arrangement : MSD1-NBD1-MSD2-NBD2. Nous avons généré deux modèles en nous basant sur l'homologie de séquence avec les protéines Sav1866 (conformation ouverte vers l'extracellulaire) et ABCB1 murine (conformation ouverte vers l'intracellulaire). Nous avons ainsi obtenu deux modèles illustrant deux états catalytiques différents.

Nous avons identifié plusieurs sites potentiels de liaison aux substrats 5FdUMP et GMPc. Ces sites font intervenir différents acides aminés dont la glycine 180 identifiée comme essentielle dans le transport du GMPc.

→ Publication 8. « **Generation of two homology models of ABCC11 respectively based on inward facing and outward facing states and localization of putative substrate binding sites for endogenous cGMP and anticancer 5FdUMP metabolite** » par M. Honorat et coll.

Article manuscrit

GENERATION OF TWO INWARD FACING AND OUTWARD FACING HOMOLOGY MODELS OF ABCC11 AND LOCALIZATION OF PUTATIVE SUBSTRATE BINDING SITES FOR ENDOGENOUS CGMP AND THE ANTICANCER 5FDUMP METABOLITE

*M. Honorat [2], R. Terreux[1,3], P. Falson[3], A. Di Pietro[3], C. Dumontet[2] and *L. Payen[1,2,4]*

1 Institut des Sciences Biologiques et Pharmaceutiques ISPB, Université Lyon1, 69008 Lyon, France ;
2 Inserm, U590, Centre Léon Bérard, FNCLCC, 69373, Lyon, France ;
3 Equipe labellisée Ligue 2009, Institut de Biologie et Chimie des Protéines, UMR 5086 CNRS/Université Lyon 1, IFR128 BioSciences Gerland-Lyon Sud, 69367 Lyon Cedex 07, France ;
4 Hospices civils of Lyon, Biochemistry laboratory of Lyon Sud (CBS), France

*Corresponding author:

Dr. PAYEN Léa pharmD. PhD.,
INSERM U590, 8 Avenue Rockefeller, 69008 Lyon, France;
E-mail: Lea.payen-gay@univ-lyon1.fr;
Tel.: +33478777236;
Fax: +33478777088

Keywords: ABCC11, homology models, 3 D-models, docking, 5FdUMP, cGMP

ABSTRACT

ABCC11/MRP8 (Multidrug Resistance protein 8) belongs to the ABCC transporter family. It is apically expressed in physiological barriers such as testis, liver, brain, and in normal and cancerous breast tissues. It secretes a number of endogenous (cAMP, cGMP, leukotriene C4…) and exogenous (active metabolite of 5-FluoroUracil (5FdUMP), methotrexate and aracytine) molecules. This last property could lead to MDR (multidrug resistance) phenotype by decreasing the intracellular retention of anticancer agents. Furthermore, ABCC11 is highly expressed in both estrogen receptor (ER)-positive breast tumors and progesterone receptor (PR)-positive breast tumors in postmenopausal patients. Since the ABCC11 structure was not available yet, we generated two independent ABCC11 models by homology modeling. Based on the X-ray structures of mouse mdr3 (homologous to human ABCB1) and Sav1866, we generated two respective models, in inward- or outward-facing conformations. Carrying out docking analyses, we described two common putative binding pockets for two ABCC11 substrates: cGMP and 5FdUMP. Interestingly, these two structurally-related substrates were able to bind to both pockets whatever the conformation (either cytoplasmically- or extracellularly-facing). These findings allowed the characterization of several amino-acid residues whose function might be critical in ABCC11 transport activity. These analyses constitute a useful tool for future biochemical analyses.

INTRODUCTION

With 48 members, the human ABC (ATP-Binding Cassette) transporter family constitutes one of the largest protein groups [1]. Some of them are especially and highly expressed at the apical cell side at the barriers, including blood-brain barrier [2], liver [3] or intestine [4]. By regulating the secretion of endogenous and exogenous molecules from cells, they are essential in the detoxification and protection mechanisms of the entire body and in drug disposition processes (ADME: Absorption, Distribution, Metabolism and Elimination).

ABCC11/MRP8 (Multidrug Resistance protein 8) belongs to sub-family C, which is composed of 12 members, (ABCC1/MRP1 being the firstly described one). The ABCC11 gene is mapped to the human chromosome 16q12 [5] and codes for a 4.5-kb transcript with a main open reading frame of 1382 amino acids [6]. The ABCC11 protein is expressed in normal breast and testis, and at low levels in liver, brain, and placenta [6-8]. Interestingly, in

axons from CNS (central nervous system) or peripheral nervous system, ABCC11 is apically expressed [8]. Its expression on physiological barriers combined to its apical cellular localization suggested its involvement in body detoxification. An inactivating polymorphism of ABCC11 (SNP Gly180Arg) was indeed correlated to earwax, sweat and colostrum secretion defaults [9-11]. This indicates that ABCC11 would be especially involved in ear protection and body detoxification, as well as in lactation process.

As described for its homologues, ABCC4 and ABCC5, this protein secretes endogenous substrates (including cAMP, cGMP, leukotriene C4, estrone 3-sulfate, E217βG (estradiol 17-β-D-glucuronide)) or glycocholateand taurocholate bile acids [8, 12, 13]), as well as exogenous-derived molecules such as dinitrophenyl S-glutathione, DHEAS (dehydroepiandrosterone 3-sulfate), the active metabolite of 5FU / 5-FluoroUracil (5FdUMP/5'-fluoro-2'-deoxyuridine monophosphate), methotrexate or aracytine [8, 12-17].

The high expression level of ABCC11 observed in breast tumors was associated to an alteration of the clinical response to paclitaxel, 5-fluorouracil, epirubicin and cyclophosphamide neo-adjuvant chemotherapy [18]. Similarly, its high expression levels have been associated with a low probability of overall survival in acute myeloid leukemia (AML) [17]. Furthermore, we observed that ABCC11 is over-expressed in ER (estrogen receptor)-positive cell lines resistant to tamoxifène [15] and in ERBB2 overexpressing breast cancers [19]. Like for other ABC transporters [19], ABCC11 expression is associated with ER and PR (progesterone receptor) status in breast tumors of postmenopausal patients [15, 20]. In conclusion, ABCC11 may be responsible for MDR (Multidrug Resistance) phenotype leading to cell resistance to a broad range of anticancer agents.

For a better understanding of ABCC11 transport activity, it is useful to study its structure. In alignment analysis of amino acid sequences, we and other observed that ABCC11 displays an ABC transporter topology similar to P-gp/ABCB1. It is predicted to contain two MSD (Membrane-Spanning Domain) and two NBD (Nucleotide-Binding Domain) in a classical MSD1-NBD1-MSD2-NBD2 topology with intracellular N- and C-termini. Each MSD is constituted by six transmembrane segments (TM). Since this protein has not been crystallized yet and since confident algorithm tools have been developed to generate homology models based on reference templates, we generated two in silico models in the present study. This has been revealed to be highly helpful for characterizing essential amino acid residues involved in transport function. These in silico models are based on the X-ray structure of eukaryotic (ABCB1) and prokaryotic (Sav1866) ABC transporters. Mouse ABCB1 X-ray structure, which shares 87% amino acid residue sequence homology with the human protein, was obtained in a drug-binding competent state of the protein, at 3.8 Å resolution [21]. ABCB1 was crystallized in nucleotide-free (inward-facing) conformation defining an internal cavity of ~6 Å where the NBDs are distant from 30 Å. In this structure, the assumed drug-binding pocket is exposed to the intracellular space, allowing drug binding before dimerisation of NBDs in the presence of ATP. This corresponds to a pre-transport state. In contrast, the Sav1866 crystal structure had been carried out in the presence of various nucleotides. This bacterial transporter from the pathogen Staphylococcus aureus is a homologue of human ABC transporters. It is a homodimeric ABC "half-transporter", each monomer comprising a N-terminal MSD and a C-terminal NBD. Recently, the 3-D crystal structure of Sav1866 was determined at respectively 3.4 Å and 3.0 Å resolutions [22, 23]. X-ray structures were delivered under a homodimer complex with nucleotides, and showed an outward-facing conformation [22, 23]. In this conformation, the substrate cavity is exposed to extracellular space and bound substrates can be delivered. ATP hydrolysis and ADP release are expected to bring the transporter back to an inward-facing conformation.

Using these generated models, we described putative binding sites of two ABCC11 substrates (5FdUMP and cGMP) by docking assays. Two binding sites were described in the transmembrane region: one on the extracellular side and the other on the intracellular side. These data led to the identification of several amino-acid residues possibly involved in cGMP or 5FdUMP transport activity.

MATERIAL AND METHODS

Prediction of ABCC11 transmembrane domain

Data were compiled from TM predictions of 6 independent software analyses: HMMTOP [24], SOSUI [25], TMHMM server, TMPRED, TOPRED [26] and PredictProtein [27]. The score represents the number of predictions for each amino residue to be located in plasma membrane (table 1). Considering the scale from 1 to 6, residues with score superior or equal to 4 were considered belonging to the TM. Nevertheless, although the score of TM12 was only predicted by 3 algorithms, comparison with other ABCC topologies led us to validate this TM12 position.

MSD1		MSD2	
TM1		TM7	
AA 162-188	R L I F D A L L G I V F V I A S V L G P I L L I P K I L	AA 803-828	Y M V S C I I F F F V V L I V F L T I F S F W W L S
Score	1 1 3 3 3 4 6 6 6 6 6 6 6 6 6 6 6 6 5 5 5 5 5 5 5 3 2 1	Score	2 4 5 5 6 6 6 6 6 6 6 6 6 6 6 6 6 6 5 5 5 5 4 2 2 1
TM2		TM8	
AA 195-226	Q L G N V V H G V G L C F A L F L S E C V K S L S F S S S W I I	AA 859-885	L S F Y Q L V Y G L N A L L L I C V G V C S S G I F T
Score	1 2 2 2 2 4 4 5 6 6 6 6 6 6 6 6 6 6 6 6 6 5 5 5 3 3 2 2 1 1 1 1	Score	1 1 1 3 3 4 6 6 6 6 6 6 6 6 6 6 6 6 6 6 6 6 6 4 2
TM3		TM9	
AA 270-307	Y L F E G V C Y G P L V L I T C A S L V I C S I S S Y F I I G Y T A F I A L	AA 937-968	F S E Q F L V L S L M V I A V L L I V S V L S P Y I L L M G A I
Score	1 2 2 2 2 2 2 2 3 3 3 3 3 3 4 4 4 4 4 4 4 4 4 3 2 2 2 2 2 1 1 1 1 1 1 1 1 1	Score	1 1 1 1 2 2 2 3 3 3 3 3 3 3 4 4 4 4 4 4 4 4 3 2 2 2 2 2 2 2 2 2
TM4		TM10	
AA 296-322	Y F I I G Y T A F I A I L C Y L L V F P L A V F M T R	AA 960-987	P Y I L L M G A I I M V I C F I Y Y M M F K K A I G V F
Score	1 2 2 2 3 4 4 4 4 4 4 4 4 4 4 4 4 4 4 4 4 3 3 2 2 1	Score	2 2 4 4 4 4 6 6 6 6 6 6 6 6 6 6 4 4 4 3 3 1 1 1 1 1 1 1
TM5		TM11	
AA 378-405	K C G L V Q S L T S I T L F I I P T V A T A V W V L I H	AA 1048-1076	L R L E I M T N L V T L A V A L F V A F G I S S T P Y S F
Score	1 2 3 4 4 4 4 5 5 6 6 6 6 6 6 6 6 6 6 6 6 6 6 5 5 4 1	Score	1 1 1 2 5 5 5 5 6 6 6 6 6 6 6 6 6 6 6 6 6 5 4 3 3 2 2 1 1
TM6		TM12	
AA 410-441	L K L T A S M A F S M L A S L N L L R L S V F F V P I A V K G K	AA 1072-1099	T P Y S F K V M A V N I V L Q L A S S F Q A T A R I G L
Score	1 1 2 2 2 2 3 5 6 6 6 6 6 6 6 6 6 6 6 6 6 6 5 5 4 4 3 3 3 3 2 2 1	Score	1 1 1 2 2 2 3 3 3 3 3 3 3 3 3 3 3 3 3 3 3 3 3 2 1 1 1 1
Score legend	1 2 3 4 5 6		

Table 1. Predictions of amino acid residue located inside the membrane. Transmembrane segments (TM) are numbered from 1 to 12. The position of the first and the last amino acid residues is indicated in the first column. The second line reports the prediction score by independent softwares: HMMTOP, SOSUI, TMHMM server, TMPRED, TOPRED and PredictProtein.

Selection of templates

PDB files generated from crystal structures were downloaded from the SWISS-MODEL template library. The mouse ABCB1 model is the most related structure to human ABCC11, and constitutes the first and single mammalian ABC transporter to be crystallized. It is available in a nucleotide-free conformation (PDB code 3G5U) that displays an inward-facing conformation, namely open toward the cytoplasm. One prokaryotic ABC transporter was also used as a template for modeling: Sav1866 from Staphylococcus aureus. Sav1866 is available as an ADP-bound structure (PDB code 2HYD) and shows an outward-facing conformation (open toward the extracellular space).

Sequence alignment

Primary sequences of human ABCC11 (Q96J66), mouse ABCB1 (P21447), S. aureus Sav1866 (Q99T13) were downloaded from the Swiss-prot database. Multiple sequence alignment of amino acid sequences was carried out using ClustalW 2.0 [28]. Taking in account TM predictions automatically carried out by softwares, sequence alignment was manually refined and validated (supplemental figure 1) to align ABCC11 TM with reference templates (ABCB1 and Sav1966).

Model building

Since Sav1866 is a half-transporter (only one MSD and one NBD) and since mABCB1 template was published in two-separated peptides (MSD1-NBD1 and MSD2-NBD2 domains without the flexible linker from residue 627 to 683), ABCC11 model was generated in two halves: MSD1-NBD1 and MSD2-NBD2 halves. Sequence alignments were submitted to SWISS-MODEL logarithm [29] to generate tri-dimensional models of ABCC11. Few modifications of sequence alignment were added by modeling (included in multiple sequence alignment shown in supplemental figure 1). One model was constructed upon mABCB1 structure bound with mercury (PDB code 3G5U). The other model was built upon Sav1866 structure in an ADP-bound conformation (PDB code 2HYD). In order to refine each model, several minimization steps were carried out with the Sybyl-X 1.1 software. Minimization refines and corrects amino acid side chain positions in the model. This allows to generate the most stable and confident 3D in silico structure. Powell method was used with AMBER force field and a dielectric constant of 80. ABCC11 models were generated in two halves: MSD1-NBD1 and MSD2-NBD2.

Ligand docking

Docking was performed with the Sybyl-X 1.1 software to localize putative binding site for substrates. According to amino-acid environment and substrate molecule structure, docking runs placed the studied substrate in the more reliable position. Independent docking runs were carried out for each ligand (cGMP and 5FdUMP). A volume including almost all the entire MSD fraction of ABCC11 was defined in order to identify binding sites either in the transmembrane part or at the membrane leaflet (extracellular or intracellular side). Two main binding pockets were described in each model, for each ligand. In order to refine substrate position, docking runs were performed again by only selecting the amino acid residues constituting those pockets.

RESULTS

ABCC11 modeling under two different conformational states.

Two complementary models of ABCC11 were generated either in free or nucleotide-bound state (figure 1). The first one was the ligand-free model based on mouse ABCB1 template. It adopted an inward-facing conformation corresponding to the high-affinity state for the substrate. The second one is the nucleotide-bound model based on Sav1866 template. It showed an outward-facing conformation. The ADP binding has likely closed the NBD dimer into a low-affinity state for substrate binding. In both models, MSD helices extended from membrane to cytoplasm. MSD domains presented two ICLs (intracellular loops). The first one was in contact with the cis-NBD (i.e. ICL1 of MSD1 with NBD1, and ICL1 of MSD2 with NBD2) while the second one made contact with the trans-NBD (i.e. ICL2 of MSD1 with NBD2, and ICL2 of MSD2 with NBD1) by specific sequences called hinges (figure 1). ICL provided the major contact between the MSDs and the NBDs. Since templates did not represent the entire protein, three ABCC11 segments were not modeled in each model. These three amino-residue sequences are: (i) the cytoplasmic N-terminal part (from Met1 to Ser142 for ABCB1-based model, and from Met1 to Glu147 for Sav1866-based model), (ii) the linker between NBD1 and MSD2 (from Lys732 to Glu781 for ABCB1-based model, and from Lys735 to Ser787 for Sav1866-based model) and (iii) the cytoplasmic C-terminal sequence (from Ala1377 to Arg1382 for ABCB1-based model, and from Thr1378 to Arg1382 for Sav1866-based model).

In the nucleotide-free model based on mABCB1 template, ABCC11 had a V-shape open forward the cytoplasm (figure 1). This inward-facing conformation showed distant NBDs and transmembrane helices bundled next to the extracellular side of membrane. In contrast, the conformation is logically reversed within the nucleotide-bound ABCC11 model based on the Sav1866 template (figure 1), ABCC11 NBDs are close to each other and MSDs adopted a V-shape open forward the extracellular space. This outward-facing conformation presented the TM helices bundled next to the NBDs, closing access from the cytoplasmic side of transmembrane domains. The NBDs were associated inside a dimer in which nucleotides are sandwiched.

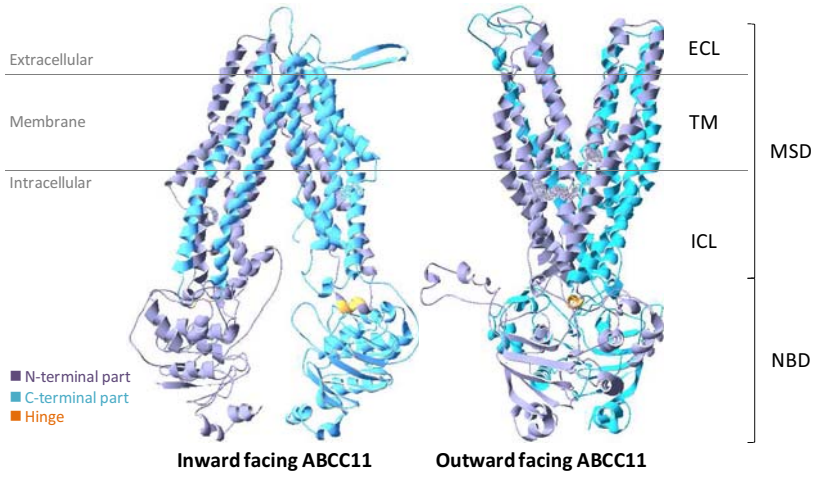

Figure 1: ABCC11 homology models. Inward-facing (ABCB1-based model) and outward-facing (Sav1866-based model) conformations are represented with the N-terminal part in purple and the C-terminal part in blue. Hinge sequences are represented in orange to show the interaction region between the cis-MSD and the trans-NBD. ECL(Extracellular Loop), TM (Transmembrane segment), ICL (Intracellular Loop), MSD (Membrane-spanning domain), NBD (Nucleotide-binding domain).

We then represented our models according to lipophilic potential of each amino acid residue. ABCC11 displayed a typical lipophilic region in the TM region (in red on figure 2A). We noticed that ECLs, ICLs and NBDs contained hydrophilic residues compatible with a cytoplasmic localization (in green and blue on figure 2A). Regarding the electrostatic potential profile that corresponds to residue side-chain charges, the ECLs and NBDs were negatively charged (in blue on figure 2B). ICL showed positively charged regions, especially at the membrane leaflet (in orange and red on figure 2B)

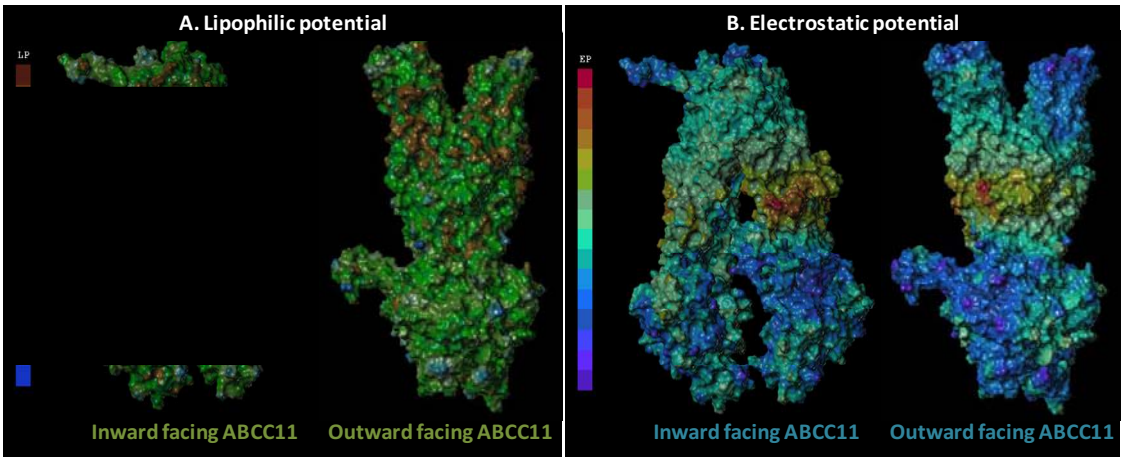

Figure 2: ABCC11 lipophilic (A) and electrostatic (B) potentials.

In the nucleotide-bound model (ABCC11 based on Sav1866), the NBDs formed a dimer in which the ADP molecules were at the interface and interacted with ABC consensus sequences (Walker A, Walker B and ABC signature) (figure 3). An additional domain by comparison to Sav1866 has been observed in the NBD1 sequence of ABCC11; it is composed by amino acid residues from Ile490 to Ser523 (IVNGALELERNGHASEGMTRPRDALGPEEEGNS). This sequence could not be correctly modeled by Swiss model software in the absence of template. This present sequence, may have important functions, it includes several charged amino-residues such as glutamate and arginine, and aromatic residues such as tryptophan.

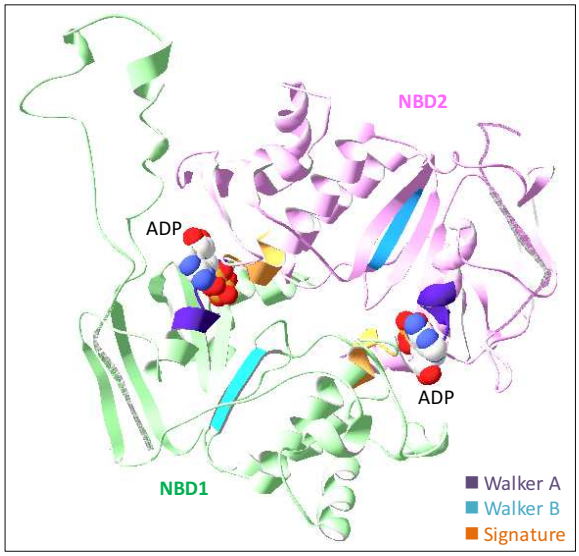

Figure 3: ABCC11 NBD overview. The ADP molecules are represented in ball-shape sandwiched between the NBDs of ABCC11. Consensus sequences are represented: Walker A in purple, Walker B in blue and ABC signature in orange.

Ligand-binding sites.

Docking analyzes of ABCC11 is a powerful tool for identifying amino acid residues that could be essential within the substrate- or modulator-binding sites. We carried out docking runs on cGMP and 5FdUMP. Cyclic GMP is a physiological ABCC11 endogenous substrate and 5FdUMP, the anticancer active metabolite of 5FU, is transported by ABCC11. Since 5FdUMP displays a mono-phosphate nucleoside structure, it was considered as a nucleoside-related molecule close to cGMP. Ligands were docked into a volume including almost all the entire MSD sequences (MSD1 and MSD2) of ABCC11. This allowed the characterization of binding sites at both intracellular and extracellular positions of plasma membrane. The TMs displayed positively-charged areas, especially in the substrate translocation chamber (in light green and light yellow on figure 2B).

We firstly carried out docking runs on the high-affinity ABCC11 model based on the mouse ABCB1 template. Interestingly, cGMP and 5FdUMP docked into similar binding sites. We selected the most reliable binding sites for both substrates. This selection was based on the high docking score and manual analysis of realistic amino acid environment. Both sites were located into TM regions: one was close to the intracellular side, and the other one was located close to the extracellular side. Amino acid residues within a 5 Å perimeter from the substrate were listed (table 2). The first site included residues belonging to TM5, 7, 8, 9 and 12. The second site included residues belonging to TM1, 6, 11 and 12. To confirm the putative sites and to increase the confidence of our analysis, we assessed similar docking runs to the ABCC11 model based on Sav1866. Interestingly, both previously described binding pockets were found in this outward-facing model.

Binding pocket 1 (intracellular side)								Binding pocket 2 (extracellular side)							
Inward facing model				Outward facing model				Inward facing model				Outward facing model			
	cGMP	5FdUMP			cGMP	5FdUMP			cGMP	5FdUMP			cGMP	5FdUMP	
ICL1.2		Leu381								Ser177	*			Ala176	*C
TM5	Leu385	Leu385		TM5	Ser387	Ser387	*			Val178	§		Ser177	Ser177	*
	Ile388	Ile388				Ile388		TM1	Pro181	Pro181	*C			Val178	
	Ile392		§		Phe391	Phe391	*			Ile182		TM1		Leu179	*
	Thr395		§			Thr395	* §		Ile184	Ile184			Gly180	Gly180	*C
TM7	Ile808	Ile808	*	TM6		Phe432	* §c		Ile185	Ile185			Pro181	Pro181	*C
	Phe811	Phe811				Phe433		ECL1.1	Ile188	Ile188			Ile184		
	Leu815		*C §	Link	Ile436	Ile436	*		Glu193			TM2	Phe210	Phe210	
TM8	Val876	Val876		MSD1-	Lys439				Glu194					Thr1054	
	Gly877	Gly877			Phe811	Phe811			Asn198	Asn198			Val1057	Val1057	
	Ser880	Ser880		TM7		Phe812	*	TM6	Leu421	Leu421			Thr1058	Thr1058	* §
	Ser881	Ser881				Val813				Ala422		TM11	Leu1059	Leu1059	
	Phe884	Phe884				Val814				Asn425	*C §		Ala1060	Ala1060	
ICL2.1		Thr885				Leu815	* §		Trp826	Trp826			Val1061	Val1061	
		Thr888				Leu872		ECL2.1	Trp830	Trp830			Ala1062	Ala1062	
		Asp931				Leu873			Leu831				Gln1086		§
		Gln932				Ile874			Ala1062	Ala1062			Leu1087		§
TM9	Pro935	Pro935				Val876		TM11	Leu1063				Ala1088		
		Ile936		TM8	Gly877	Gly877			Val1065	Val1065			Ser1089		
	Ser938	Ser938				Val878			Ala1066			TM12	Ser1090		§
	Glu939	Glu939			Ser880	Ser880			Val1078				Phe1091		
	Leu942	Leu942	§		Ser881	Ser881			Met1079	Met1079			Thr1094	Thr1094	§
	Val943				Phe884				Ala1080	Ala1080			Ala1095	Ala1095	*
	Leu946				Thr885			TM12	Val1081					Ile1097	§
TM12	Thr1094		§		Thr888				Asn1082	Asn1082		Link		Gly1098	§
	Ala1095		*		Arg889				Ile1083	Ile1083		MSD2-		Leu1099	
	Ile1097		§	ICL2.1	Glu928				Gln1086	Gln1086	§	NBD2		Thr1101	§
Link	Gly1098		§		Asp931									Glu1102	
MSD2-	Thr1101		§		Gln932										
NBD2	Glu1102	Glu1102													
		Ala1103		TM9	Pro935										
					Ile936										

* residue described in the putative binding pocket of ABCC5 (Ravna et al.)

*C residue described in the putative binding pocket of ABCC5 and conserved in ABCC11 (Ravna et al.)

§ residue described in the binding pocket of ABCB1 (Aller et al.)

§c residue described in the binding pocket of ABCB1 and conserved in ABCC11 (Aller et al.)

Table 2: Amino acid residue in a 5 Å perimeter around ligand.

The intracellular-side binding pocket 1 was composed by several residues, some of them showing specific and direct interaction with ligand (figure 4). In the inward-facing ABCC11, cGMP guanine group made a hydrogen bond with Ser880, and phosphate was located close to Ile392, Leu815 and Thr1094. In the outward-facing model, phosphate of cGMP both interacted with Ser387 and Ser880 by hydrogen bonds. The pentose group was interacting with Lys439 while the guanine group made two hydrogen bonds with Asp931 and one with Thr888. In the inward-facing ABCC11, 5FdUMP phosphate made one hydrogen bond with Ser880, and was close to Ile808, Phe811 and Leu942 side-chains. The hydroxyl of 5FdUMP pentose showed one hydrogen bond with Glu1102. In the outward-facing model, only the hydroxyl group of 5FdUMP pentose made a hydrogen bond with ABCC11, in this case with Gly877. The phosphate was located next to Phe811, Val814, Leu873 and Val876.

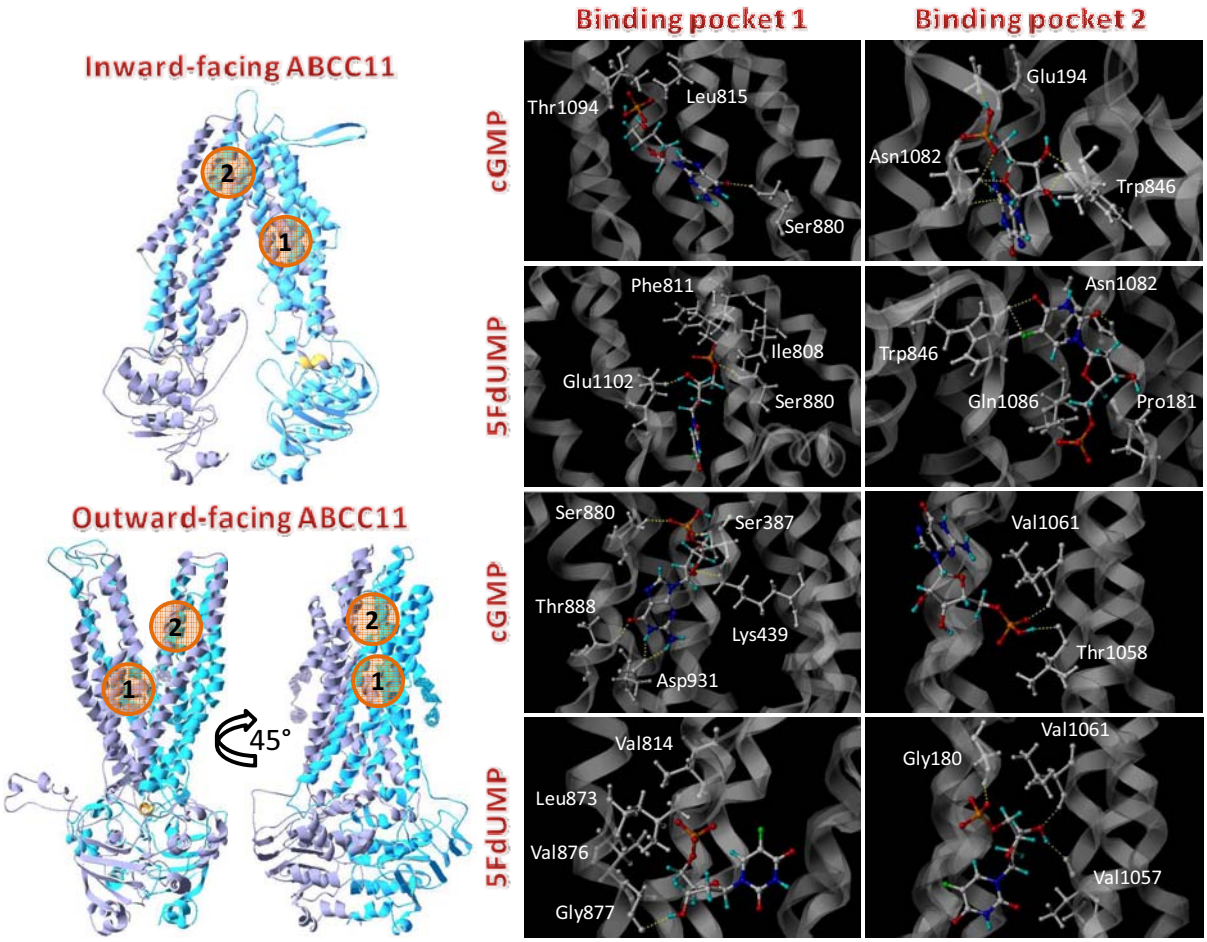

Figure 4: cGMP and 5FdUMP binding in the two putative binding pockets. On the left panel, binding pockets are localized with their number on the inward- or the outward-facing model of ABCC11. The outward-facing model is also shown after a 45° rotation to illustrate that the two binding pockets of the inward-facing model correspond to those found in the outward-facing model. On the right panel, each substrate is represented in the best scoring position with some of the residues around (in grey) and the putative hydrogen bonds (in yellow).

In the extracellular-side binding pocket 2 (figure 4) of the inward-facing conformation, phosphate of cGMP interacted with Glu194 by hydrogen bonds. Asn1082 was potentially highly relevant since it had four hydrogen bonds respectively with the guanine, the pentose and the phosphate groups of cGMP. Trp826 showed hydrogen bonds with both hydroxyl groups of the cGMP pentose. 5FdUMP pyrimidine group had two hydrogen bonds with Trp826 and one with Asn1082. 5FdUMP phosphate group was located next to Val178, Pro181 and Gln1086. In the outward-facing conformation, only two hydrogen bonds were observed between cGMP phosphate and Thr1058 and Val1061.5FdUMP phosphate displayed a hydrogen bond with Gly180. Additionally, Val1057 and Val1061 were connected by hydrogen bonds to the hydroxyl group of 5FdUMP pentose.

The same methodology was applied for the docking analysis of MK571, an ABCC11 inhibitor. MK571 bound efficiently with high scores to those two putative binding sites (figure 5). To confirm the putative sites and increase the confidence of our analyses, we finally carried out docking runs with 5FdUMP structurally related molecules (5FU and 5FdURD) that are not transported by ABCC11. In our two in silico models of ABCC11, these molecules were indeed not able to bind to the identified putative sites.

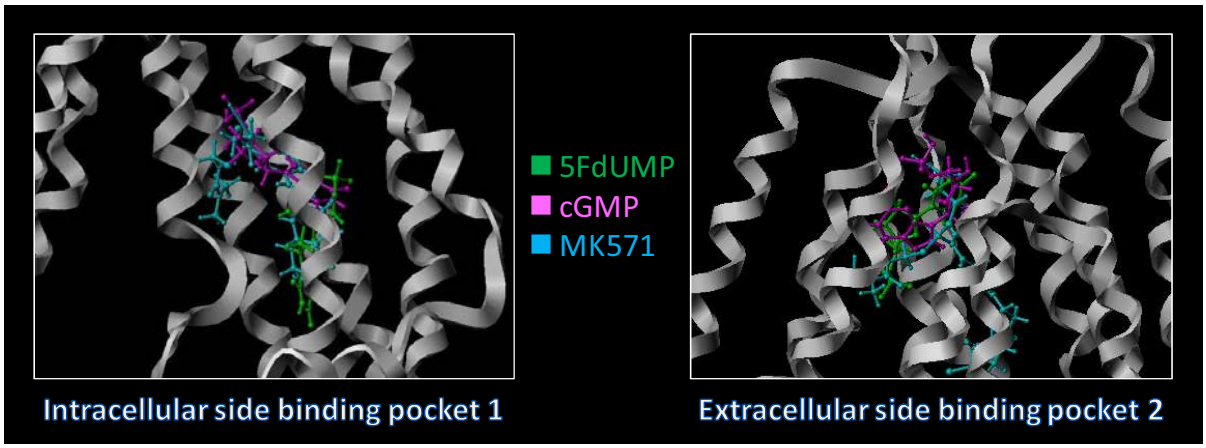

Figure 5: MK571 binding in the ABCC11 inward-facing model. MK571 (blue), 5FdUMP (green) and cGMP (pink) are shown in the intracellular- and the extracellular-side binding pockets.

DISCUSSION

Relying on recent crystal structures of ABC transporters, we successfully generated, by homology, two ABCC11 models under two different conformational states: (a) a ligand-free conformation based on mouse ABCB1 X-ray structure and (b) a nucleotide-bound conformation based on Sav1866 X-ray structure. Studying these two models in two distant steps of the catalytic cycle gives important knowledge about ABCC11 structure in highly-different conformations. Furthermore, it largely informs about putative regions which are submitted to important conformational changes and helps to understand the consequences that could be expected upon substrate binding.

Since the entire ABCB1 crystal model is not available yet and the Sav1866 transporter is a half-transporter, we were unable to model three ABCC11 domains: the cytoplasmic N-terminal part, the link between MSD1 and NBD2 and the cytoplasmic C-terminal part. According to amino acid sequence alignment (data not shown), the NBD1-MSD2 linker is highly variable in the ABCC sub-family. However, the N-terminal sequence of ABCC11 could correspond to the loop 0 (L0) of ABCC1 (linking ABCC1 MSD0 to MSD1) which have been described to be essential for ABCC1 function [30]. ABCC1 L0 indeed includes residue 208 to 270 corresponding to ABCC11 residues 1 to 49. The closest ABCC members to ABCC11 are ABCC4 and ABCC5. According to their sequence alignment, the ABCC11 sequence from residues 1 to 49 is not conserved in those members; ABCC4 does not present such a sequence and ABCC5 shows a partial conservation.

Since, ABCC11 has been localized at the apical side of nervous cells [8], we looked at a specific signature within the cytosolic C-terminus of ABCC11. Based on a similar finding in ABCC transporters, a PDZ-interacting domain responsible for the apical localization has been described at the C-terminal side of both ABCC7 [31] and ABCC2 [32] transporters. However, according to sequence alignment, ABCC11 C-terminus does not correspond to neither the ABCC7 TLR sequence nor the ABCC2 TKF sequence. Furthermore, similarly to ABCC8/SUR1 membrane targeting signal (Leu1566 and Phe1574) [33], we observed a putative membrane-targeting signal in ABCC11 at Leu1364 and Phe1372 positions. In contrast, the equivalent residues (Leu1260 and Phe1268) in ABCB1 were not involved in membrane targeting but in the proper protein folding [34]. In conclusion, this sequence function needs to be further studied by biochemical studies.

In both ABCC11 models, MSD helices extended from membrane to cytoplasm forming two ICLs in each MSD. The first one was in contact with the cis-NBD, while the second made contact with the trans-NBD (figure 1) by its “hinge” sequence. According to amino acid alignment (supplemental figure 1), hinge sequences are not conserved. And, by contrast to mABCB1 that shows similar hinge sequences (RTVI in MSD1 and RTVV in MSD2), ABCC11 does not display any conserved hinge sequences with KLIK in MSD1 and SSIH in MSD2. This contact between MSD and NBD is supposed to transfer conformational changes occurring from NBD to MSD. This arrangement has also been observed for another ABCC transporter, ABCC7 (CFTR), where Phe508 mediates a tertiary interaction between the NBD1 surface and the ICL2 from MSD2 [35]. The mutation of Phe508 is indeed responsible of most of the cases of cystic fibrosis, underlying the importance of this residue in ABCC7. In addition, the deletion of the equivalent residue in ABCB1 (Tyr490) disrupted packing of TM4, 5 and 12 by affecting interaction between NBD and ICL [36].

The nucleotide-free ABCC11 shows an inward-facing conformation wide open toward the cytoplasm and lacking NBD/NBD interaction. This conformation allows the entry of nucleotides and substrates to their respective binding site. Transport cycle is initiated by substrate binding within the MSDs [37]. At this resting state, the NBDs are separated and ATP binding closes the two NBDs [38]. This state corresponds to the nucleotide-bound ABCC11 model showing an outward-facing with close NBD and MSD open toward the extracellular space. The nucleotide-binding pocket is tightly closed, and substrates might not bind to the transporter from membrane leaflet or cytoplasm. This conformation illustrates the low-affinity state where the substrate is released into the extracellular space, and ATP hydrolysis and/or ADP release are required to go back to the high-affinity state for substrate.

Since some amino acid residues have to be membrane embedded and surrounded by lipids, ABCC11 presented a typical lipophilic region (figure 2A).The ECL, ICL and NBD were more hydrophilic, reliable with their location into the extra- or intra-cellular space. Regarding the electrostatic potential profile (figure 2B), ECLs and NBDs were negatively charged. The ICLs showed an interesting positively-charged region, especially at the membrane leaflet. This is explained by the presence of several lysine and arginine residues. Some of these residues are totally conserved among ABCC/MRP-related proteins (table 3): Arg338, Lys353 and Arg369. Similarly, at other locations (Arg233, Arg235, Lys245, Arg340, Lys350, Arg905, Arg918, Lys988, Arg989 and Arg1044), the positive charge is well conserved among ABCC members (arginine or lysine are generally observed at this position). The presence of those positive charges, just under the intracellular membrane side is likely involved in the drug transport process. Supported by ABCC1 findings, Lys396 [39] and Arg433 [40] of the ICL1 localized in MSD1, Arg1138, Lys1141, Arg1142 and Arg1197 of ICL2 belonging to MSD2 [41, 42] have been described to be functionally important. Although ABCC1 Arg433 and Arg1138 are not conserved in ABCC11, Lys396, Lys1141, Arg1142 and Arg1197 of ABCC1 respectively correspond to Arg235, Lys988, Arg989 and Arg1044 of ABCC11. Since they are involved in transport activity for organic anions, LTC4 and GSH, residues 988, 989 and 1044 could be involved in ABCC11 transport of these substrates. Furthermore, ABCC11 Lys989 corresponds to functional ABCC6 Arg1114 [43] and ABCC2 Arg1150 [44]. Positively-charged residues seem to preferentially locate near the negatively-charged heads of phospholipids. Then, they are rather located at the cytoplasmic side than the extracellular one, in accordance with the inside positive polarity of membrane. Arginine and lysine residues may influence the right inclusion of the protein into the membrane and enhance its stability [41]. ABCC11 TM region appeared more neutral and the substrate-translocation site was generally positive, consistent with the ability of ABCC11 to transport anions. A similar observation was made for an ABCC5 homology model whose substrate translocation chamber

was generally positive [45]. By contrast, the ABCB1 substrate translocation chamber was neutral with negative spots, consistent with transport of cationic amphiphilic and lipophilic substrates [45].

	MSD1																	
	ICL1					ICL2												
ABCC11	Arg229	Arg233	Arg235	Lys245	Lys250	Lys326	Arg338	Arg340	Lys350	Lys353	Lys359	Lys363	Arg369	Arg370	Lys371	Arg373	Lys374	Lys378
ABCC1		☑	☒	☑			☑	☒	☑	☑			☑				☑	☑
ABCC2	☒	☒	☑	☑			☑	☒	☑	☑			☑	☒	☑		☑	
ABCC3		☒	☑	☑			☑	☒	☑	☑		☑	☑					
ABCC4		☑	☑	☑			☑	☑	☒	☑	☑		☑	☒	☑			☒
ABCC5	☑	☑	☑	☑	☑		☑		☑	☑	☑		☑			☑	☒	☑
ABCC6		☑	☑	☑			☑	☑	☑	☑			☑					
ABCC10	☒		☒	☑			☑	☒	☒	☑			☑		☒			
ABCC12	☑	☑	☑	☒	☑		☑		☒	☑	☑		☑	☑	☒	☑	☑	☑
mABCB1	☑	☒	☑						☑		☑					☒	☒	☑

	MSD2															
	ICL1					ICL2										
ABCC11	Lys886	Arg889	Lys890	Lys898	Lys902	Arg905	Arg918	Lys981	Lys982	Lys988	Arg989	Arg995	Lys1017	Lys1026	Arg1027	Arg1044
ABCC1						☑				☑	☑	☑				☑
ABCC2						☑	☑			☒	☑	☑				☑
ABCC3						☑	☑			☑	☑	☑	☒			☑
ABCC4				☑		☒	☑			☑	☑	☑				☑
ABCC5	☑		☒		☒	☑	☑			☑	☑		☑			☑
ABCC6			☒	☒		☑				☒	☑					☑
ABCC10				☒	☒		☑	☒		☒	☑				☑	
ABCC12	☑				☑	☒	☑			☑	☒	☑	☑			☑
mABCB1	☑					☑			☑					☒		

☑ conserved residue; ☒ similar residue (lysine for arginine and vice-versa)

Table 3: Conservation of positively-charged amino acids in ICL of ABCC11.

Description of putative cGMP and 5FdUMP binding pockets.

To localize putative substrate and/or modulator sites, we carried out docking studies. This led to identification of putative important amino acid residues. For example, in an in silico ABCC1 model, four residues (Trp553, Trp1198, Trp1246 and Phe594) appeared to form an aromatic ring that lined the putative substrate translocation site. Trp553, Trp1198, Trp1246 were already known to be functionally important, and site-directed mutagenesis experiments confirmed the involvement of Phe594 in ABCC1 transport activity [46].

Using our ABCC11 models, docking experiments revealed two putative binding pockets for cGMP and 5FdUMP. Ectopic expression of ABCC11 has indeed been described to reduce basal intracellular levels of cGMP and 5FdUMP [12, 16]. The first binding pocket in ABCC11 was located next to the intracellular side of the transmembrane region. It involved TM5, 7, 8, 9 and 12 (table 2). In the inward-facing conformation of ABCC11, cGMP interacted with Ser880, while in the outward-facing model, it was Ser387, Lys439, Ser880, Thr888 andAsp931. In the inward-facing ABCC11, 5FdUMP was in interaction with Ser880 and Glu1102. In the outward-facing model, 5FdUMP made only one hydrogen bond with Gly877. The second ABCC11 binding pocket was close to extracellular space and formed by TM1, 6, 11 and 12. In the inward-facing ABCC11, cGMP could interact with Glu194, Asn1082 and Trp826 while, in the outward-facing conformation, only two hydrogen bonds were observed between cGMP and Thr1058 and Val1061, suggesting a less strong interaction. 5FdUMP could interact with Trp826, Asn1082, in the inward-facing model while, in the outward-facing model, Gly180, Val1057 and Val1061 were more involved for interactions.

Because of their spatial position and their putative interaction with ligand, many of those amino acid residues could be important for ligand binding. Some residues can indeed be responsible for substrate affinity toward ABCC11 by directly interacting with substrate. Others can be involved in any ABCC11 local conformation, and be critical for the substrate-binding pocket shape. Among residues previously cited, Trp826 (ECL), Ser880 (TM8), Val1061 (TM11) and Asn1082 (TM12) are of particular interest since they are involved in

hydrogen bonds with both ligands. Some of the residues constituting those pockets corresponded to residues described for ABCC5 (table 2), the phylogenetically closest ABCC of ABCC11 [47]. Indeed, Ravna et al also described 2 putative binding pockets for cGMP (common substrate between ABCC5 and ABCC11). The first binding pocket of ABCC11 involving TM5, 7, 8, 9 and 12 would correspond to one of the two binding pockets indentified in ABCC5 (also involving TM5, 7 and 8). The second ABCC11 binding pocket is formed by TM1, 6, 11 and 12, similarly to the second binding pocket described in ABCC5 [47]. Corresponding to ABCC11 Gly180 (TM1) and Ser387 (TM5), respective ABCC5 Gly196 and Val403 have indeed been described to be in ABCC5 cGMP putative binding pocket [47]. In addition, ABCC11 Thr1058 (TM11) corresponding residue in ABCC5 (Ile1107) has also been located in a binding pocket, as well as its equivalent in mABCB1 binding site (Tyr949). Ile1107 of ABCC5 would indeed interact with cGMP [47] while Tyr949 of mABCB1 and its equivalent in human ABCB1 were located in the QZ59-binding cavity [21, 48]. Some other residues (Ala176, Ser177, Leu179, Pro181, Phe391, Thr395, Asn425, Phe432, Ile436, Ile808, Phe812, Leu815 and Ala1095) have been identified in both ABCC11 and ABCC5 binding pockets. Some are even conserved between the two cGMP transporters (Ala176, Pro181, Leu815, Asn425), suggesting their putative function in drug process.

As listed in table 2, several ABCC11 residues identified around bound ligand have their equivalent in the QZ59-binding pocket of mABCB1. This is the case for Val 178 (TM1), Ile392 (TM5), Thr395 (TM5), Asn425 (TM6), Leu815 (TM7), Leu942 (TM9), Thr1058 (TM11), Gln1086 (TM12), Leu1087 (TM12), Ser1090 (TM12), Thr1094 (TM12), Ala1095 (TM12), Ile1097, Gly1098, Thr1101 and Phe432 (TM6) that are conserved in both mABCB1 and ABCC11. In addition, Ser1090 corresponds both to ABCC1 Tyr1243 [49] and ABCB1 Val982 [50]described as important for the transport function. It also has to be observed that there are equivalents to residues Thr395, Phe432, Asn425and Leu815 located in both ABCB1 and ABCC5 binding pocket.

In parallel, numerous residues were located in both ABCC11 binding pockets 1 and 2: Thr1094, Ala1095, Ile1097, Gly1098, Thr1101 and Glu1102. Thr1094, Ala1095, Ile1097, Gly1098, Thr1101 were indeed found in ABCC5 and/or mABCB1 binding cavity. Finally, some residues found in the drug-binding pockets have an equivalent in other ABC transporter that has been described as essential for transport function: Ile198 (ABCC1 Lys347[39]), Pro935 (ABCB1 Gly830 [51]), Ile1083 (ABCC1 Tyr1236 [49], ABCB1 Leu975 [50]), Arg1050 (ABCC2 Arg1210 [52]), Ala1088 (ABCC1 Thr1241 [49]) and Arg1096 (ABCC2 Arg1257 [52]). Site-directed mutagenesis experiments should confirm the functional involvement of those residues.

Several aromatic residues were found in ABCC11 binding pockets. Some of them (Phe432 andPhe812) are not conserved among ABCCs, while others are highly (Phe210 in ABCC1, ABCC2, ABCC3, ABCC6 and ABCC12, Trp826 and Trp830 in ABCC1, ABCC2, ABCC3, ABCC4, ABCC5, ABCC6 and ABCC12) or moderately (Phe391 in ABCC4, Phe433 in ABCC4 and ABCC6, Phe811 in ABCC1, ABCC6 and ABCC12, Phe884 in ABCC5, ABCC10 and ABCC12 and Phe1091 in ABCC4 and ABCC5) conserved. Although nothing has been currently described for their analogues in ABCC members, Phe1091 corresponds to Phe983 of ABCB1 that was involved in the inhibition of drug transport by flupentixol [53]. However, some aromatic residues have been described to be critical in ABCC1 transport activity [46, 54, 55]. Although Trp1045 is not predicted in putative site, it is conserved in all ABCC members. In ABCC1, Trp1198 was supposed to be involved in the tertiary structure of the protein [54],and could act in a similar manner in ABCC11.

Gly180 was found inside the binding pocket, located next to the extracellular side of ABCC11 transmembrane region. Conserved in ABCC5, Gly180 is prone to G602A SNP (single nucleotide polymorphism) inducing the Gly180Arg mutation. It was correlated to earwax type since people carrying AA phenotype have dry earwax while AG and GG phenotypes correspond to wet earwax [9]. Since some components are common to earwax and colostrum or sweat, the SNP has also been correlated to colostrum and sweat secretion defaults [10, 11]. In addition, ABCC11-180Arg lost its transport capacity for cGMP [9]. This is consistent with its location in our model where Gly180 could directly interact with ligand. In the inward-facing model, Gly180 side-chain points toward phospholipids, while it points toward the cGMP in the outward-facing model. Thus, it seems that Gly180 could be in contact with ligand only in the nucleotide-bound state where substrate is ready to be released. Our prediction does not show any hydrogen bond between the Gly180 side-chain and cGMP. In the case of G602A SNP, Gly is mutated into Arg. Gly is a neutral residue with a little side-chain while Arg side chain is longer and positively charged. To explain the default of transport of ABCC11-Arg180, we can suggest that the Arg side-chain alters local ABCC11 conformation and thus cGMP interaction with the inward-facing state. In the outward-facing state, this positive charge could also promote interactions with cGMP and avoid the release of cGMP into extracellular space. Toyoda et al described a default of N-glycosylation that would induce protein degradation [56]. In conclusion, Arg180 is likely modifying the proper folding of ABCC11 rather than being directly involved in substrate binding.

The observation of two potential binding pockets strongly suggests that the ligands can bind to two different sites. Indeed, the QZ59-SSS cyclic peptide inhibitor showed two different binding sites in mouse ABCB1 crystal structure [21]. Docking runs have shown that MK571 (inhibitor of many ABCCs, including ABCC11) also could bind to both sites. This is in agreement with the fact that, it is known as a competitive inhibitor of ABCC1-mediated LTC4 transport [57]. This suggests that MK571 binding to one site would not permit ligand transport. At the moment, no data allow us to know if ligands bind simultaneously to both sites, randomly to each site, or preferentially to one or the other site. Another hypothesis would be that the ligand would first bind to the intracellular side of transmembrane region, and then transit to extracellular side (subsequent to conformational changes). This hypothesis could not be excluded until intermediary step conformations are available. Molecular dynamic experiments with the inward-facing model containing substrate could inform us about possible substrate transport inside the transporter.

CONCLUSION

Thanks to homology modeling, we have provided two ABCC11 models at different catalytic states. In both models, we have identified two putative binding pockets for substrate, and pointed several amino acid residues that could interact with bound substrate.

LIST OF ABBREVIATIONS

5FdUMP (5'-Fluoro-2'-Deoxyuridine Monophosphate); 5FU (5-FluoroUracil); ABC (ATP-Binding Cassette); AML(Acute Myeloid Leukemia);DHEAS (Dehydroepiandrosterone 3-Sulfate); E217βG (Estradiol 17-β-D Glucuronide); ECL (Extracellular Loop); EPS (Electrostatic Potential Surface); ER (Estrogen Receptor);FEC (5-fluorouracil, epirubicin and cyclophosphamide); ICL (Intracellular Loop); MDR (MultiDrug Resistance); MRP (MultiDrug Resistance Protein); MSD (Membrane Spanning Domain); NBD (Nucleotide-Binding Domain); PDB (Protein Data Bank); PR (Progesterone Receptor); TM (transmembrane segment).

AKNOWLEDGEMENTS

This work was supported by INSERM (UMR 590) and Université Lyon 1, and grants from Association pour la Recherche sur le Cancer (ARC 4007) and from Ligue Nationale contre le Cancer (Equipe labellisée Ligue 2009). M.H. is recipient of doctoral fellowships from the Ligue Nationale contre le Cancer.

REFERENCES

[1] Dean, M., A. Rzhetsky, and R. Allikmets The human ATP-binding cassette (ABC) transporter superfamily. Genome Res, 2001, 11, 1156-66.

[2] Scherrmann, J.M. Expression and function of multidrug resistance transporters at the blood-brain barriers. Expert Opin Drug Metab Toxicol, 2005, 1, 233-46.

[3] Klaassen, C.D. and L.M. Aleksunes Xenobiotic, bile acid, and cholesterol transporters: function and regulation. Pharmacol Rev, 62, 1-96.

[4] Oostendorp, R.L., J.H. Beijnen, and J.H. Schellens The biological and clinical role of drug transporters at the intestinal barrier. Cancer Treat Rev, 2009, 35, 137-47.

[5] Tammur, J., C. Prades, I. Arnould, A. Rzhetsky, A. Hutchinson, M. Adachi, J.D. Schuetz, K.J. Swoboda, L.J. Ptacek, M. Rosier, M. Dean, and R. Allikmets Two new genes from the human ATP-binding cassette transporter superfamily, ABCC11 and ABCC12, tandemly duplicated on chromosome 16q12. Gene, 2001, 273, 89-96.

[6] Bera, T.K., S. Lee, G. Salvatore, B. Lee, and I. Pastan MRP8, a new member of ABC transporter superfamily, identified by EST database mining and gene prediction program, is highly expressed in breast cancer. Mol Med, 2001, 7, 509-16.

[7] Bieche, I., I. Girault, E. Urbain, S. Tozlu, and R. Lidereau Relationship between intratumoral expression of genes coding for xenobiotic-metabolizing enzymes and benefit from adjuvant tamoxifen in estrogen receptor alpha-positive postmenopausal breast carcinoma. Breast Cancer Res, 2004, 6, R252-63.

[8] Bortfeld, M., M. Rius, J. Konig, C. Herold-Mende, A.T. Nies, and D. Keppler Human multidrug resistance protein 8 (MRP8/ABCC11), an apical efflux pump for steroid sulfates, is an axonal protein of the CNS and peripheral nervous system. Neuroscience, 2006, 137, 1247-57.

[9] Yoshiura, K., A. Kinoshita, T. Ishida, A. Ninokata, T. Ishikawa, T. Kaname, M. Bannai, K. Tokunaga, S. Sonoda, R. Komaki, M. Ihara, V.A. Saenko, G.K. Alipov, I. Sekine, K. Komatsu, H. Takahashi, M. Nakashima, N. Sosonkina, C.K. Mapendano, M. Ghadami, M. Nomura, D.S. Liang, N. Miwa, D.K. Kim, A. Garidkhuu, N. Natsume, T. Ohta, H. Tomita, A. Kaneko, M. Kikuchi, G. Russomando, K. Hirayama, M. Ishibashi, A. Takahashi, N. Saitou, J.C. Murray, S. Saito, Y. Nakamura, and N. Niikawa A SNP in the ABCC11 gene is the determinant of human earwax type. Nat Genet, 2006, 38, 324-30.

[10] Miura, K., K. Yoshiura, S. Miura, T. Shimada, K. Yamasaki, A. Yoshida, D. Nakayama, Y. Shibata, N. Niikawa, and H. Masuzaki A strong association between human earwax-type and apocrine colostrum secretion from the mammary gland. Hum Genet, 2007, 121, 631-3.

[11] Martin, A., M. Saathoff, F. Kuhn, H. Max, L. Terstegen, and A. Natsch A Functional ABCC11 Allele Is Essential in the Biochemical Formation of Human Axillary Odor. J Invest Dermatol, 2009,

[12] Guo, Y., E. Kotova, Z.S. Chen, K. Lee, E. Hopper-Borge, M.G. Belinsky, and G.D. Kruh MRP8, ATP-binding cassette C11 (ABCC11), is a cyclic nucleotide efflux pump and a resistance factor for fluoropyrimidines 2',3'-dideoxycytidine and 9'-(2'-phosphonylmethoxyethyl)adenine. J Biol Chem, 2003, 278, 29509-14.

[13] Chen, Z.S., Y. Guo, M.G. Belinsky, E. Kotova, and G.D. Kruh Transport of bile acids, sulfated steroids, estradiol 17-beta-D-glucuronide, and leukotriene C4 by human multidrug resistance protein 8 (ABCC11). Mol Pharmacol, 2005, 67, 545-57.

[14] Kruh, G.D., Y. Guo, E. Hopper-Borge, M.G. Belinsky, and Z.S. Chen ABCC10, ABCC11, and ABCC12. Pflugers Arch, 2007, 453, 675-84.

[15] Honorat, M., A. Mesnier, J. Vendrell, J. Guitton, I. Bieche, R. Lidereau, G.D. Kruh, C. Dumontet, P. Cohen, and L. Payen ABCC11 expression is regulated by estrogen in MCF7 cells, correlated with estrogen receptor alpha expression in postmenopausal breast tumors and overexpressed in tamoxifen-resistant breast cancer cells. Endocr Relat Cancer, 2008, 15, 125-38.

[16] Oguri, T., Y. Bessho, H. Achiwa, H. Ozasa, K. Maeno, H. Maeda, S. Sato, and R. Ueda MRP8/ABCC11 directly confers resistance to 5-fluorouracil. Mol Cancer Ther, 2007, 6, 122-7.

[17] Guo, Y., K. Kock, C.A. Ritter, Z.S. Chen, M. Grube, G. Jedlitschky, T. Illmer, M. Ayres, J.F. Beck, W. Siegmund, G. Ehninger, V. Gandhi, H.K. Kroemer, G.D. Kruh, and M. Schaich Expression of ABCC-type nucleotide exporters in blasts of adult acute myeloid leukemia: relation to long-term survival. Clin Cancer Res, 2009, 15, 1762-9.

[18] Park, S., C. Shimizu, T. Shimoyama, M. Takeda, M. Ando, T. Kohno, N. Katsumata, Y.K. Kang, K. Nishio, and Y. Fujiwara Gene expression profiling of ATP-binding cassette (ABC) transporters as a

predictor of the pathologic response to neoadjuvant chemotherapy in breast cancer patients. Breast Cancer Res Treat, 2006, 99, 9-17.

[19] Honorat, M., J. Guitton, C. Dumontet, and L. Payen Expression level and hormonal regulation of ABC transporters in breast cancer. Current cancer therapy review, 2010, in press.

[20] Honorat, M., A. Mesnier, J. Vendrell, A.D. Pietro, V. Lin, C. Dumontet, P. Cohen, and L. Payen ABCC11 (Multidrug Resistance Protein 8) expression is regulated by dexamethasone in breast cancer cells and is associated to progesterone receptor status in breast tumors. 2010, manuscript.

[21] Aller, S.G., J. Yu, A. Ward, Y. Weng, S. Chittaboina, R. Zhuo, P.M. Harrell, Y.T. Trinh, Q. Zhang, I.L. Urbatsch, and G. Chang Structure of P-glycoprotein reveals a molecular basis for poly-specific drug binding. Science, 2009, 323, 1718-22.

[22] Dawson, R.J. and K.P. Locher Structure of a bacterial multidrug ABC transporter. Nature, 2006, 443, 180-5.

[23] Dawson, R.J. and K.P. Locher Structure of the multidrug ABC transporter Sav1866 from Staphylococcus aureus in complex with AMP-PNP. FEBS Lett, 2007, 581, 935-8.

[24] Tusnady, G.E. and I. Simon The HMMTOP transmembrane topology prediction server. Bioinformatics, 2001, 17, 849-50.

[25] Hirokawa, T., S. Boon-Chieng, and S. Mitaku SOSUI: classification and secondary structure prediction system for membrane proteins. Bioinformatics, 1998, 14, 378-9.

[26] von Heijne, G. Membrane protein structure prediction. Hydrophobicity analysis and the positive-inside rule. J Mol Biol, 1992, 225, 487-94.

[27] Rost, B., G. Yachdav, and J. Liu The PredictProtein server. Nucleic Acids Res, 2004, 32, W321-6.

[28] Thompson, J.D., D.G. Higgins, and T.J. Gibson CLUSTAL W: improving the sensitivity of progressive multiple sequence alignment through sequence weighting, position-specific gap penalties and weight matrix choice. Nucleic Acids Res, 1994, 22, 4673-80.

[29] Arnold, K., L. Bordoli, J. Kopp, and T. Schwede The SWISS-MODEL workspace: a web-based environment for protein structure homology modelling. Bioinformatics, 2006, 22, 195-201.

[30] Westlake, C.J., Y.M. Qian, M. Gao, M. Vasa, S.P. Cole, and R.G. Deeley Identification of the structural and functional boundaries of the multidrug resistance protein 1 cytoplasmic loop 3. Biochemistry, 2003, 42, 14099-113.

[31] Moyer, B.D., J. Denton, K.H. Karlson, D. Reynolds, S. Wang, J.E. Mickle, M. Milewski, G.R. Cutting, W.B. Guggino, M. Li, and B.A. Stanton A PDZ-interacting domain in CFTR is an apical membrane polarization signal. J Clin Invest, 1999, 104, 1353-61.

[32] Harris, M.J., M. Kuwano, M. Webb, and P.G. Board Identification of the apical membrane-targeting signal of the multidrug resistance-associated protein 2 (MRP2/MOAT). J Biol Chem, 2001, 276, 20876-81.

[33] Sharma, N., A. Crane, J.P.t. Clement, G. Gonzalez, A.P. Babenko, J. Bryan, and L. Aguilar-Bryan The C terminus of SUR1 is required for trafficking of KATP channels. J Biol Chem, 1999, 274, 20628-32.

[34] Loo, T.W., M.C. Bartlett, and D.M. Clarke The dileucine motif at the COOH terminus of human multidrug resistance P-glycoprotein is important for folding but not activity. J Biol Chem, 2005, 280, 2522-8.

[35] Serohijos, A.W., T. Hegedus, A.A. Aleksandrov, L. He, L. Cui, N.V. Dokholyan, and J.R. Riordan Phenylalanine-508 mediates a cytoplasmic-membrane domain contact in the CFTR 3D structure crucial to assembly and channel function. Proc Natl Acad Sci U S A, 2008, 105, 3256-61.

[36] Loo, T.W., M.C. Bartlett, and D.M. Clarke Introduction of the most common cystic fibrosis mutation (Delta F508) into human P-glycoprotein disrupts packing of the transmembrane segments. J Biol Chem, 2002, 277, 27585-8.

[37] Honorat, M., P. Falson, C. Dumontet, A.D. Pietro, R. Terreux, and L. Payen ABC transporter structure prediction: Relevance of homology modeling studies. Current Drug Metabolism, 2010, accepted,

[38] Deeley, R.G., C. Westlake, and S.P. Cole Transmembrane transport of endo- and xenobiotics by mammalian ATP-binding cassette multidrug resistance proteins. Physiol Rev, 2006, 86, 849-99.

[39] Haimeur, A., G. Conseil, R.G. Deeley, and S.P. Cole Mutations of charged amino acids in or near the transmembrane helices of the second membrane spanning domain differentially affect the substrate specificity and transport activity of the multidrug resistance protein MRP1 (ABCC1). Mol Pharmacol, 2004, 65, 1375-85.

[40] Conrad, S., H.M. Kauffmann, K. Ito, E.M. Leslie, R.G. Deeley, D. Schrenk, and S.P. Cole A naturally occurring mutation in MRP1 results in a selective decrease in organic anion transport and in increased doxorubicin resistance. Pharmacogenetics, 2002, 12, 321-30.

[41] Conseil, G., R.G. Deeley, and S.P. Cole Functional importance of three basic residues clustered at the cytosolic interface of transmembrane helix 15 in the multidrug and organic anion transporter MRP1 (ABCC1). J Biol Chem, 2006, 281, 43-50.

[42] Situ, D., A. Haimeur, G. Conseil, K.E. Sparks, D. Zhang, R.G. Deeley, and S.P. Cole Mutational analysis of ionizable residues proximal to the cytoplasmic interface of membrane spanning domain 3 of the multidrug resistance protein, MRP1 (ABCC1): glutamate 1204 is important for both the expression and catalytic activity of the transporter. J Biol Chem, 2004, 279, 38871-80.

[43] Le Saux, O., Z. Urban, C. Tschuch, K. Csiszar, B. Bacchelli, D. Quaglino, I. Pasquali-Ronchetti, F.M. Pope, A. Richards, S. Terry, L. Bercovitch, A. de Paepe, and C.D. Boyd Mutations in a gene encoding an ABC transporter cause pseudoxanthoma elasticum. Nat Genet, 2000, 25, 223-7.

[44] Mor-Cohen, R., A. Zivelin, N. Rosenberg, M. Shani, S. Muallem, and U. Seligsohn Identification and functional analysis of two novel mutations in the multidrug resistance protein 2 gene in Israeli patients with Dubin-Johnson syndrome. J Biol Chem, 2001, 276, 36923-30.

[45] Ravna, A.W., I. Sylte, and G. Sager Molecular model of the outward facing state of the human P-glycoprotein (ABCB1), and comparison to a model of the human MRP5 (ABCC5). Theor Biol Med Model, 2007, 4, 33.

[46] Campbell, J.D., K. Koike, C. Moreau, M.S. Sansom, R.G. Deeley, and S.P. Cole Molecular modeling correctly predicts the functional importance of Phe594 in transmembrane helix 11 of the multidrug resistance protein, MRP1 (ABCC1). J Biol Chem, 2004, 279, 463-8.

[47] Ravna, A.W., I. Sylte, and G. Sager A molecular model of a putative substrate releasing conformation of multidrug resistance protein 5 (MRP5). Eur J Med Chem, 2008, 43, 2557-67.

[48] Pajeva, I.K., C. Globisch, and M. Wiese Comparison of the inward- and outward-open homology models and ligand binding of human P-glycoprotein. Febs J, 2009, 276, 7016-26.

[49] Zhang, D.W., S.P. Cole, and R.G. Deeley Determinants of the substrate specificity of multidrug resistance protein 1: role of amino acid residues with hydrogen bonding potential in predicted transmembrane helix 17. J Biol Chem, 2002, 277, 20934-41.

[50] Loo, T.W. and D.M. Clarke Defining the drug-binding site in the human multidrug resistance P-glycoprotein using a methanethiosulfonate analog of verapamil, MTS-verapamil. J Biol Chem, 2001, 276, 14972-9.

[51] Loo, T.W. and D.M. Clarke Functional consequences of glycine mutations in the predicted cytoplasmic loops of P-glycoprotein. J Biol Chem, 1994, 269, 7243-8.

[52] Ryu, S., T. Kawabe, S. Nada, and A. Yamaguchi Identification of basic residues involved in drug export function of human multidrug resistance-associated protein 2. J Biol Chem, 2000, 275, 39617-24.

[53] Dey, S., P. Hafkemeyer, I. Pastan, and M.M. Gottesman A single amino acid residue contributes to distinct mechanisms of inhibition of the human multidrug transporter by stereoisomers of the dopamine receptor antagonist flupentixol. Biochemistry, 1999, 38, 6630-9.

[54] Koike, K., C.J. Oleschuk, A. Haimeur, S.L. Olsen, R.G. Deeley, and S.P. Cole Multiple membrane-associated tryptophan residues contribute to the transport activity and substrate specificity of the human multidrug resistance protein, MRP1. J Biol Chem, 2002, 277, 49495-503.

[55] Ito, K., S.L. Olsen, W. Qiu, R.G. Deeley, and S.P. Cole Mutation of a single conserved tryptophan in multidrug resistance protein 1 (MRP1/ABCC1) results in loss of drug resistance and selective loss of organic anion transport. J Biol Chem, 2001, 276, 15616-24.

[56] Toyoda, Y., A. Sakurai, Y. Mitani, M. Nakashima, K. Yoshiura, H. Nakagawa, Y. Sakai, I. Ota, A. Lezhava, Y. Hayashizaki, N. Niikawa, and T. Ishikawa Earwax, osmidrosis, and breast cancer: why does one SNP (538G>A) in the human ABC transporter ABCC11 gene determine earwax type? Faseb J, 2009, 23, 2001-13.

[57] Leier, I., G. Jedlitschky, U. Buchholz, S.P. Cole, R.G. Deeley, and D. Keppler The MRP gene encodes an ATP-dependent export pump for leukotriene C4 and structurally related conjugates. J Biol Chem, 1994, 269, 27807-10.

SUPPLEMENTAL FIGURES

Supplemental figure 1.

ABCC11 and mABCB1 sequence alignment

Primary sequences of human ABCC11 (Q96J66) and mouse ABCB1 (P21447) were obtained from the Swiss-prot database (http://www.uniprot.org/). Multiple sequence alignment of these proteins was performed using ClustalW 2.0 (http://www.ebi.ac.uk/Tools/clustalw2/index.html). Sequence alignment was manually refined in order to align trans-membrane segments of each protein and according ABCC11 trans-membrane domain predictions.

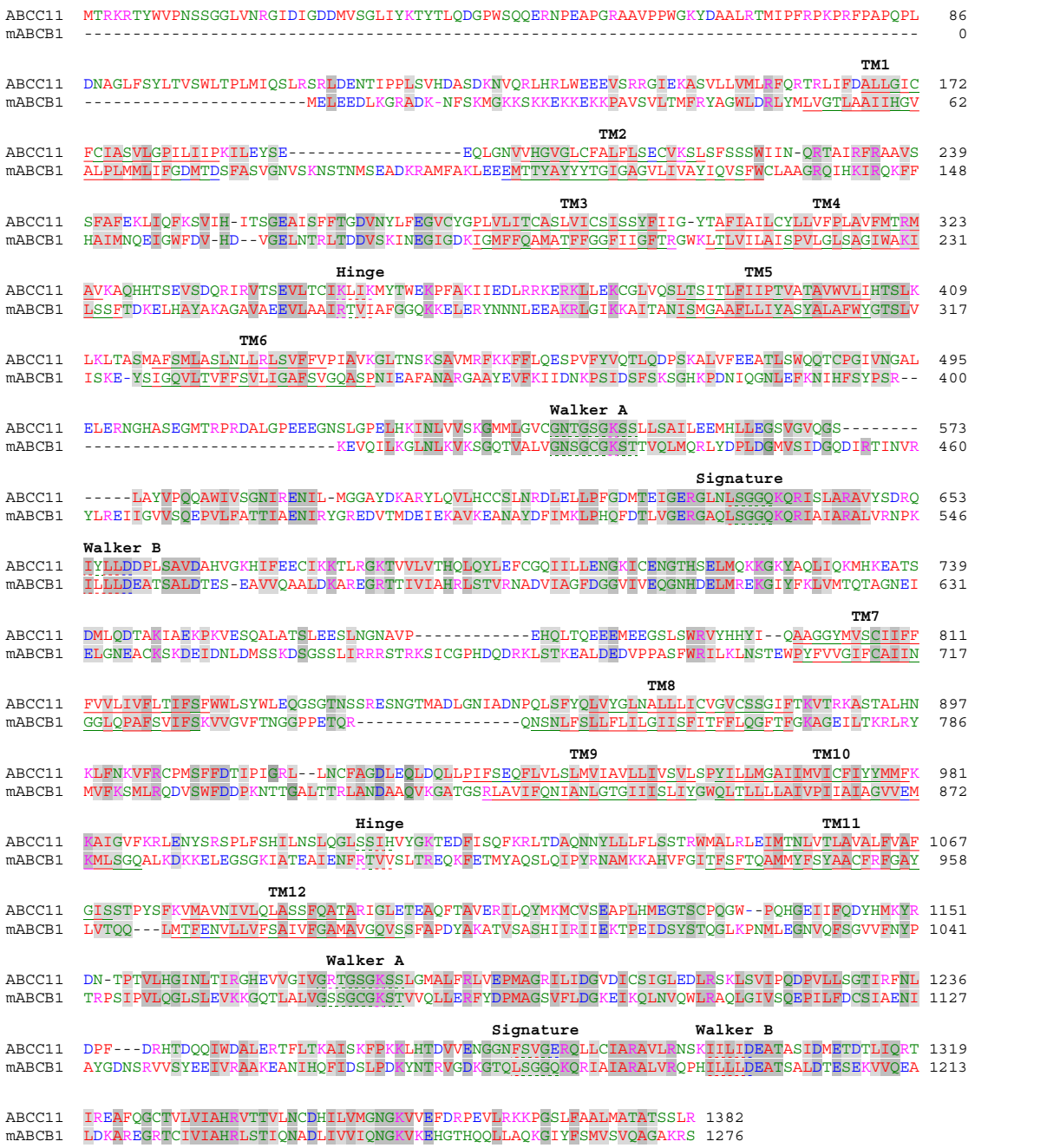

ABCC11 and Sav1866 sequence alignment

Primary sequences of human ABCC11 (Q96J66) and S. aureus SAV1866 (Q99T13) were obtained from the Swiss-prot database (http://www.uniprot.org/). Multiple sequence alignment of these proteins was performed using ClustalW 2.0 (http://www.ebi.ac.uk/Tools/clustalw2/index.html). Sequence alignment was manually refined in order to align trans-membrane segments of each protein and according ABCC11 trans-membrane domain predictions.

Amino acid residue
Small + hydrophobic + Y
Acid / Basic
Hydroxyl + Amine + Basic + Q
Identical/Similar

Sequence
Transmembrane segment
Consensus sequence

```
ABCC11  MTRKRTYWVPNSSGGLVNRGIDIGDDMVSGLIYKTYTLQDGPWSQQERNPEAPGRAAVPPWGKYDAALRTMIPFRPKPRFPAPQPL   86
SAV1866 ----------------------------------------------------------------------------------     0

                                                                                          TM1
ABCC11  DNAGLFSYLTVSWLTPLMIQSLR-SRLDENTIPPLSVHDASDKNVQRLHRLWEEEVSRRGIEKASVLLVMLRFQRTRLIFDALLGI  171
SAV1866 ------------------------------------------------------------MIKRYLQFVKPYKYRIFATIIVGI   24

                                                  TM2
ABCC11  CFCIASVLGPILIIPKILEYSEE-------QLGNVVHGVGLCFALFLSECVKSLSFSSSWIINQRTAIRFRAAVSSFAFEKLIQFK  250
SAV1866 IKFGIPMLIPLLIKYATDGVINNHALTTDEKVHHLTIAIGIALFIFVIVRPPIEFIRQYLAQWTSNKILYDIRKKLYNHLQALSAR  110

                                                TM3                                TM4
ABCC11  SVIHITSGEAISFFTGDVNYLFEGVCYGPLVLITCASLVICSISSYFIIG-YTAFIAILCYLLVFPLAVFMTRMAVKAQHHTSEVS  335
SAV1866 FYANNQVGQVISRVINDVEQTKDFILTGLMNIWLDCITIIIALSIMFFLDVKLTLAALFIFPFYILTVYVFFGRLRKLTRERSQAL  196

                                  Hinge                                    TM5
ABCC11  DQRIRVTSEVLTCIKLIKMYTWEKPFAKIIEDLRRKERKLLEKCGLVQSLTSITLFIIPTVATAVWVLI--HTSLKLKLTASMAFS  419
SAV1866 AEVQGFLHERVQGISVVKSFAIEDNEAKNFDKKNTNFLTRALKHTRWNAYSFAAINTVTDIGPIIVIGVGAYLAISGSITVGTLAA  282

                TM6
ABCC11  MLASLNLLRLSVFFVPIAVKGLTNSKSAVMRFKKFFLQESPVFYVQTLQDPSKALVFEEATLSWQQTCPGIVNGALELERNGHASE  505
SAV1866 FVGYLELLFGPLRRLVASFTTLTQSFASMDRVFQLIDEDYDIKNGVGAQPIEIKQGRIDIDHVSFQYNDN----------------  352

                                        Walker A
ABCC11  GMTRPRDALGPEEEGNSLGPELHKINLVVSKGMMLGVCGNTGSGKSSLLSAILEEMHLLEGSVGVQGS-------------LAYVP  578
SAV1866 ----------------EAPILKDINLSIEKGETVAFVGMSGGGKSTLINLIPRFYDVTSGQILIDGHNIKDFLTGSLRNQIGLVQ  421

                                                                  Signature          Walker B
ABCC11  QQAWIVSGNIRENILMGG-AYDKARYLQVLHCCSLNRDLELLPFGDMTEIGERGLNLSGGQKQRISLARAVYSDRQIYLLDDPLSA  663
SAV1866 QDNILFSDTVKENILLGRPTATDEEVVEAAKMANAHDFIMNLPQGYDTEVGERGVKLSGGQKQRLSIARIFLNNPPILILDEATSA  507

ABCC11  VDAHVGKHIFEECIKKTLRGKTVVLVTHQLQYLEFCGQIILLENGKICENGTHSELMQKKGKYAQLIQKMHKEATSDMLQDTAKIA  749
SAV1866 LDLES-ESIIQEALDVLSKDRTTLIVAHRLSTITHADKIVVIENGHIVETGTHRELIAKQGAYEHLYSIQNL--------------  578

                                                                  TM7
ABCC11  EKPKVESQALATSLEESLNGNAVPEHQLTQEEEMEEGSLSWKVYHHYI--QAAGGYMVSCIIFFFVVLIVFLTIFSFWWLSYWLEQ  833
SAV1866 ---------------------------------------MIKRYLQFVKPYKYRIFATIIVGIIKFGIPMLIPLLIKYAIDGVINNH   48

                                                TM8
ABCC11  GSGTNSSRESNGTMADLGNIADNPQLSFYQLVYGLNALLLICVGVCSSGIFTKVTRKASTALHNKLFNKVFRCPMSFFDTIPIGRL  919
SAV1866 ALTTDEK--------------VHHLTIAIGIALFIFVIVRPPIEFIRQYLAQWTSNKILYDIRKKLYNHLQALSARFYANNQVGQV  120

                                    TM9                                TM10
ABCC11  LNCFAGDLEQLDQLLPIFSEQFLVLSLMVIAVLLIVSVLSPYILLMGAIIMVICFIYYMMFKKAIGVFKRLENYSRSPLFSHILNS 1005
SAV1866 ISRVINDVEQTKDFILTGLMNIWLDCITIIIALSIMFFLDVKLTLAALFIFPFYILTVYVFFGRLRKLTRERSQALAEVQGFLHER  206

                Hinge                                                  TM11                TM12
ABCC11  LQGLSSIHVYGKTEDFISQFKRLTDAQNNYLLLFLSSTRWMALRLEIMTNLVTLAVALFVAFGISSTPYSFKVMAVNIVLQLASSF 1091
SAV1866 VQGISVVKSFAI---EDNEAKNFDKKNTNFLTRALKHTRWNAYSFAAINTVTDIGPIIVIGVGAYL-AISGSITVGTLAAFVGYLE  288

ABCC11  QATARIGLETEAQFTAVERILQYMKMCVSEAPLHMEGTSCPQGWPQHGE--IIFQDYHMKYRDNTPTVLHGINLTIRGHEVVGIVG 1175
SAV1866 LLFGPLRRLVASFTTLTQSFASMDRVFQLIDEDYDIKNGVGAQPIEIKQGRIDIDHVSFQYNDNEAPILKDINLSIEKGETVAFVG  374

        Walker A
ABCC11  RTGSGKSSLGMALFRLVEPMAGRILIDGVDICSIGLEDLRSKLSVIPQDPVLLSGTIRFNLDPFD-RHTDQQIWDALERTFLTKAI 1260
SAV1866 MSGGGKSTLINLIPRFYDVTSGQILIDGHNIKDFLTGSLRNQIGLVQQDNILFSDTVKENILLGRPTATDEEVVEAAKMANAHDFI  460

                        Signature              Walker B
ABCC11  SKFPKKLHTDVVENGGNFSVGERQLLCIARAVLRNSKIILIDEATASIDMETDTLIQRTIREAFQGCTVLVIAHRVTTVLNCDHIL 1346
SAV1866 MNLPQGYDTEVGERGVKLSGGQKQRLSIARIFLNNPPILILDEATSALDLESESIIQEALDVLSKDRTTLIVAHRLSTITHADKIV  546

ABCC11  VMGNGKVVEFDRPEVLRKKPGSLFAALMATATSSLR 1382
SAV1866 VIENGHIVETGTHRELIAKQGAYEHLYSIQNL----  578
```

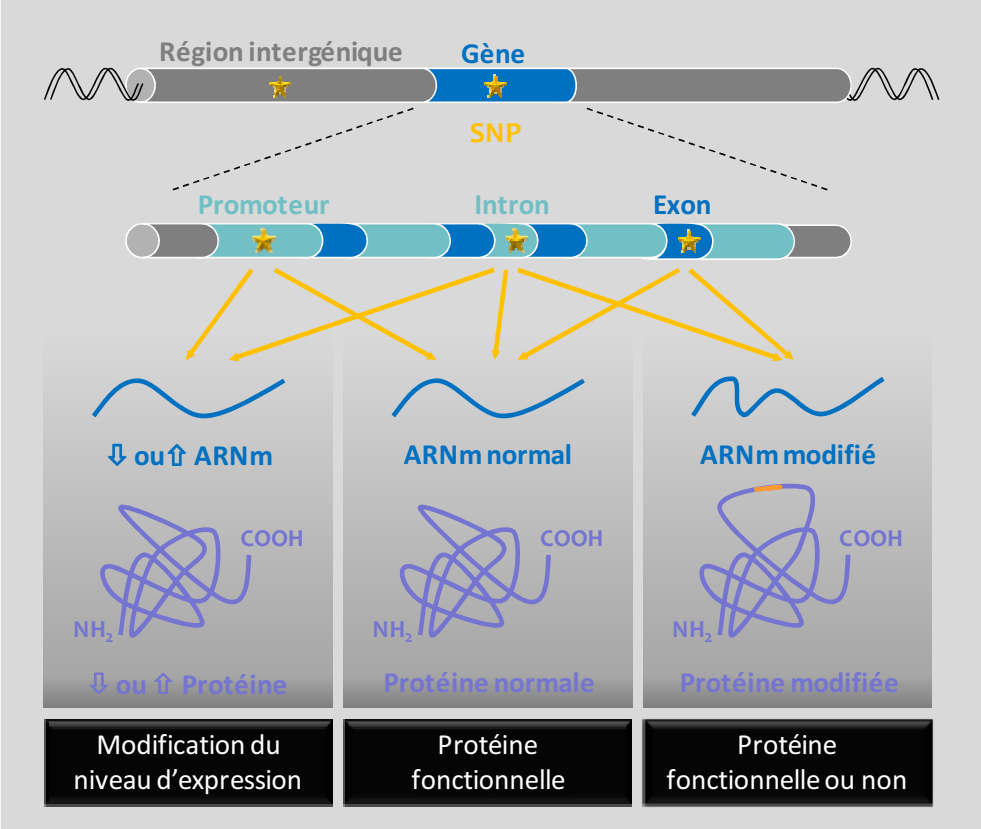

Figure 10. Illustration de l'impact des SNP sur la région génique.

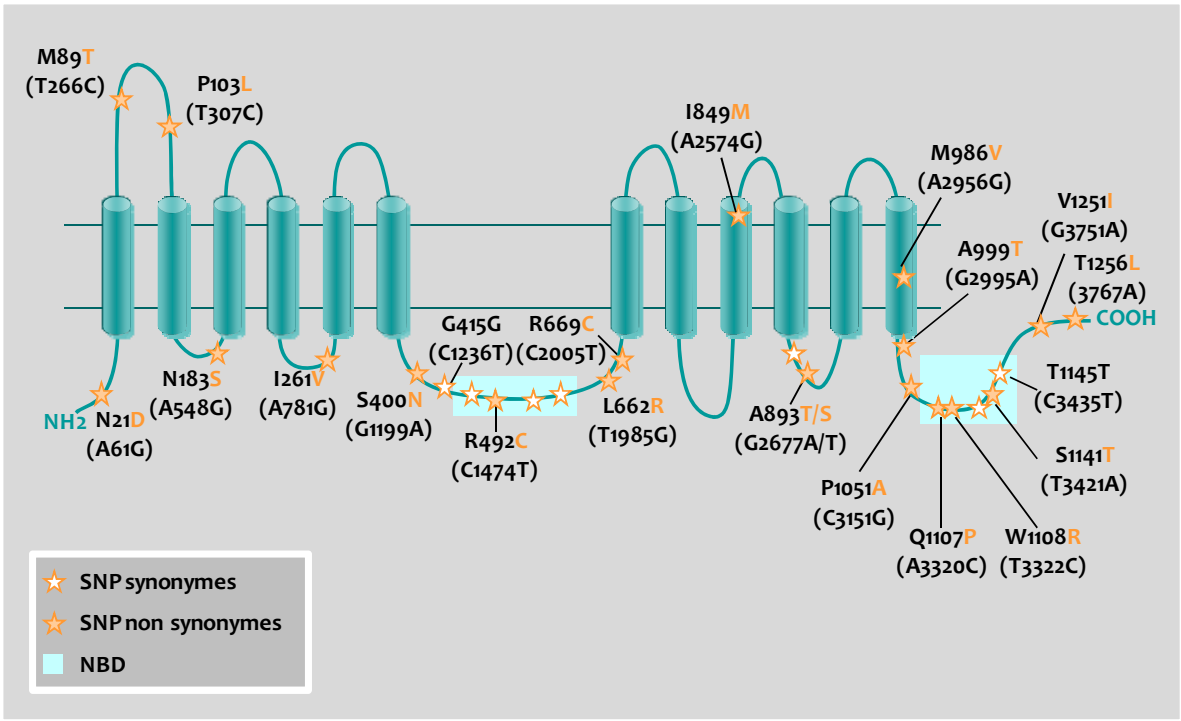

Figure 11. SNP sur ABCB1.
Les SNP sont reportés sur le schéma de la structure potentielle d'ABCB1. *Figure inspirée de Maeda et al. 2008 [99].*

II. IMPACT DES SNP SUR L'EXPRESSION ET L'ACTIVITE D'ABCC11

1. Les SNP au sein des transporteurs ABC humains

1.1 Définition général d'un SNP

Des variabilités génétiques d'origine naturelle sont observées dans la population générale. Cette variabilité est appelée polymorphisme. Les SNP (*Single Nucleotide Polymorphism*) correspondent à la substitution d'un nucléotide, localisés à n'importe quel endroit dans le gène (exons, promoteur, introns…). Dans tous les cas, la substitution peut ou non avoir des conséquences fonctionnelles (**Figure 10**). Une localisation sur une région promotrice (par exemple, motif d'interaction avec les récepteurs nucléaires comme ERE) ou sur un intron (par exemple, signal d'épissage de l'ARN messager) peut altérer le niveau d'expression de la protéine. Au niveau de la partie codante du gène, sont distingués les SNP synonymes (sans modification de l'acide aminé codé) et non synonymes (modification de l'acide aminé). La modification d'un acide aminé peut être à l'origine d'un changement de conformation, d'une modification de la stabilité ou d'une localisation anormale de la protéine, altérant ou non la fonction de la protéine.

Ces variabilités génétiques touchent également les transporteurs ABC. Les plus décrites concernent les transporteurs humains ABCB1, ABCG2 et ABCC1.

1.2 SNP sur ABCB1

Un grand nombre de SNP ont été décrits dans le gène *ABCB1* dont plus de 60 se situent dans la région codante. Dans cette dernière sont retrouvés des SNP synonymes et non synonymes mais pas de SNP non sens (induisant la formation d'un codon stop). Les polymorphismes les plus décrits correspondent aux polymorphismes synonymes C1236T et C3435T et au polymorphisme G2677A/T non synonymes (A896T/S) (**Figure 11**).

1.2.1. SNP C3435T

Le SNP C3435T, un SNP synonyme, code l'isoleucine 1145 localisée dans le second NBD d'ABCB1. Sa fréquence varie beaucoup selon les ethnies ; il est retrouvé, par exemple, chez 62 % des américains d'origine européennes contre 13 % des américains d'origine africaine [100].

a. Impact sur l'expression d'ABCB1

De nombreuses données contradictoires furent reportées sur le niveau d'expression de la protéine ABCB1-C3435T. Le SNP C3435T, a d'abord été associé à une diminution [101] puis à une augmentation [102] de l'expression d'ABCB1 dans le duodénum où cette expression a finalement été décrite comme normale [103].

Pathologie	Population	Risque	Référence
Tumeur épithéliale rénale	212 caucasiens	⇧	Siegsmund et al. 2002
Cancer du sein	104 iraniens	⇔	Taheri et al.
Cancer du sein	183 iraniens	⇔	Tatari et al. 2009
Cancer du sein	107 turques	⇧	Turgut et al. 2007
Cancer du sein	96 patients	⇧	Goerges et al. 2009
Cancer du sein	334 caucasiens	⇧	Cizmarikova et al.
Cancer du colon	372 patients	⇧[a]	Kurzawski et al. 2005
Cancer colorectal	255 iraniens	⇧	Khedri et al.
Cancer colorectal	1124 caucasiens	⇩	Andersen et al. 2009
Cancer du poumon	182 espagnols	⇔	Gervasini et al. 2006
Glioblastome	362 ♂ caucasiens	⇧[b]	Miller et al. 2005
Leucémie lymphoblastique aigue	288 caucasiens	⇧[c]	Jamroziak et al. 2004
Leucémie lymphoblastique aigue	218 mexicains	⇔[c]	Leal-Ugarte et al. 2008
Colite ulcérative	149 caucasiens	⇧	Schwab et al. 2003
Maladie de Crohn	126 caucasiens	⇔	Schwab et al. 2003
Maladie de Parkinson	95 caucasiens	⇔	Furuno et al. 2002
Maladie de Parkinson	107 caucasiens	⇔	Drozdzik et al. 2003
Maladie de Parkinson	59 caucasiens	⇧[d]	Drozdzik et al. 2003
Infection par le VIH	137 caucasiens	⇔	Ifergan et al. 2002
Infection par le VIH	411 patients	⇔[e]	Bleiber et al. 2004

a chez les patients d'un âge<50 ans; b pas de corrélation chez les femmes; c pathologie pédiatrique; d risque de développement après exposition aux pesticides; e progression avant le traitement

Tableau 3. Influence du SNP C3435T sur le développement de certaines pathologies.

La même controverse est retrouvée dans les cellules NK (*natural killer*) CD56+ où a été décrit une diminution [104] ou une absence de modification de l'expression d'ABCB1-C3435T [105]. Pour finir, aucune modification du niveau d'expression n'a été démontrée dans des lymphocytes CD8+, CD4+ et CD19+ [105] ou dans des cellules de leucémies aigues lymphoïdes [106] ou myéloïdes [107]. Une analyse globale des multiples résultats observés jusqu'alors a finalement conclu que le polymorphisme C3435T n'altérait pas le niveau d'expression d'ABCB1 à la surface cellulaire mais pourrait induire une modification subtile de la conformation de la protéine [108].

b. Impact sur l'activité de transport

Bien qu'une étude ait rapporté un efflux moins efficace de la rhodamine dans des leucocytes CD56+ [104], il semblerait qu'ABCB1 C3435T n'influence pas l'efflux de cette molécule aussi bien dans les leucocytes CD56+ ou CD4+ [109] que dans les cellules CD34+ de moelle osseuse [110], les cellules de leucémies aigues myéloïdes [107] ou les cellules Hela [111].

Dans plusieurs types cellulaires, cette activité de transport normale a également été observée pour le paclitaxel, le vérapamil, la daunorubicine, la vinblastine, la calcéine-AM, la digoxine et la cyclophosphorine A [111, 112]. Au niveau du placenta, le polymorphisme n'a pas non plus montré d'influence sur le transport de saquinavir [113].

c. SNP C3435T et pathologies

Plusieurs études se sont intéressées à l'influence du polymorphisme C3435T sur la prévalence de certaines pathologies. En effet, les individus porteurs de l'allèle T seraient plus susceptibles à développer des tumeurs épithéliales rénales [114] ou des colites ulcératives [115] (tableau **3**). Pour certaines pathologies telles que le cancer du sein [116-120] ou le cancer du colon [121-123], les associations peuvent être contradictoires et ne permettent pas de conclure sur l'influence du SNP C3435T (**Tableau 3**). Aucune influence du polymorphisme C3435T n'a été établit sur la prévalence au cancer du poumon [124], à la maladie de Crohn [115], à la maladie de Parkinson [125, 126] (à l'exception des cas d'exposition aux pesticides [125]) et au SIDA [127, 128] (**Tableau 3**). Même si la prévalence pour les leucémies reste à confirmer [129, 130], le polymorphisme C3435T a été associé à une meilleure survie dans le cas de leucémies myéloïdes aigues [131] et de leucémies lymphoïdes aigues chez l'enfant [129]. Il n'aurait pas d'influence sur la survie des patients atteints de leucémie lymphoïdes aigues [106]. De manière surprenante, dans le cas de myélome plasmocytaire, l'hétérozygotie (CT) serait un facteur de bon pronostic [132].

Normale	Diminuée	Augmentée	Controversée
Cilostazol	Clopridogel	Phénytoïne	Digoxine
Cyclosporine		Lansoprazole	Efavirenz
Dicloxacilline		Fluvoxamine	Nelfinavir
Docétaxel			Féxofénadine
Lopéramide			Tacrolimus
Nortriptyline			
Paroxetine			
Talinolol			

Tableau 4. Influence du SNP C3435T sur la concentration plasmatique ou la disponibilité orale de certains médicaments.

d. Impact sur la pharmacocinétique des médicaments

L'impact du SNP C3435T sur la pharmacocinétique des médicaments a été défini pour différentes molécules, substrats décrits ou potentiels d'ABCB1 (**Tableau 4**). De nombreuses controverses ont été publiées sur l'exposition à la digoxine, à la fexofénadine ou au tacrolimus entre autres. Le SNP fut par exemple corrélé à une augmentation [101, 133-135], à une diminution [136] ou à une absence de différence [137] du taux plasmatique en digoxine. Il fut également associé à une diminution [100] ou une absence de modification [138] de la concentration plasmatique en fexofénadine. Et enfin, la concentration plasmatique en tacrolimus serait diminuée pour les individus CC (homozygotes de l'allèle naturelle) [139-141] même si une étude montre qu'il n'y a pas de modification [142] et qu'aucune association n'a été faite avec la neuro-toxicité induite par le tacrolimus [143]. L'exposition a certains antiviraux (nelfinavir et éfavirenz) utilisés contre le VIH fait aussi l'objet de controverses [144] [145]. Toutes ces observations mériteraient l'investissement dans des méta-analyses comme celle décrite pour la cyclosporine A. En effet, les données contradictoires concernant la cyclosporine A [146-149] furent compilées dans une récente méta-analyse incluant 1036 individus et concluant que le polymorphisme C3435T n'influençait pas significativement les paramètres pharmacocinétiques de la cyclosporine A bien que les individus CC montrent une diminution de l'exposition à cette molécule par rapport aux individus CT et TT [150].

En parallèle, pour d'autres médicaments, les données publiées sont plus claires. Les individus TT (portant les deux allèles polymorphes) montrent une diminution de la concentration plasmatique en clopridrogel dont l'absorption intestinale pourrait être altérée [151]. Chez ces mêmes individus (TT), la concentration plasmatique mesurée serait significativement plus élevée que chez les autres individus après administration de médicaments tels que la phénytoïne [152] ou le lansoprazole [153]. Pour finir, le polymorphisme n'a pour l'instant pas montré d'influence sur la pharmacocinétique du talinolol [103], de la nortriptyline [154], du lopéramide [155], de la dicloxacilline [156], du docétaxel [157], du cilostazol [158], de la nimodipine [159], de la cloxacilline [160] et de la paroxetine [161].

Pathologie	Population	Réponse	Traitement	Référence
Cancer du sein	68 patients	⇧	chimiothérapie néo-adjuvante[a]	Kafka et al. 2003
Cancer du sein	96 patients	⇔	chimiothérapie néo-adjuvante[b]	Goerges et al. 2009
Cancer du sein	41 patients	⇔	chimiothérapie néo-adjuvante[c]	Rodrigues et al. 2008
Cancer du sein	334 caucasiens	⇩	chimiothérapie néo-adjuvante[d]	Cizmarikova et al.
Myélome multiple	92 patients	⇧	bortezomib	Buda et al. 2009
Epilepsie	315 patients	⇧	antiépileptiques	Siddiqui et al. 2003
Infection par le VIH	80 caucasiens	⇧	antiviraux (éfavirenz et nelfinavir)	Fellay et al. 2002
Infection par le VIH	149 caucasiens	⇔	antiviraux	Nasi et al. 2003
Infection par le VIH	461 patients	⇧[e]	antiviraux	Brumme et al. 2003
Infection par le VIH	48 patients	⇔	antiviraux	Hass et al. 2003
Infection par le VIH	367 patients	⇔	antiviraux (éfavirenz et nelfinavir)	Hass et al. 2005
Infection par le VIH	72 patients	⇔	antiviraux	Winzer et al. 2005

a anthracyclines et/ou taxanes; b 5-fluorouracil/épirubicine/cyclophosphamide; c 5-fluorouracil/doxorubicine/cyclophosphamide; d épirubucine ou doxorubicine e augmente la durée du maintien du taux de virus <500 copies/mL

Tableau 5. Influence du SNP C3435T sur la réponse aux traitements.

e. SNP C3435T et réponses au traitement

Du fait de l'influence du polymorphisme sur la pharmacocinétique de certains médicaments, il apparaît logique que le SNP C3435T influence aussi la réponse à certains traitements pharmacologiques (**Tableau 5**) ainsi que les effets indésirables liés à ces traitements. Dans le cadre de traitements du cancer du sein, la réponse à la chimiothérapie néo-adjuvante à base d'anthracyclines et/ou de taxanes serait améliorée pour les individus portant l'allèle 3435T [162]. Mais cet avantage n'est pas observé lorsque cette chimiothérapie combine le 5-fluorouracil, la doxorubicine et le cyclophosphamide [119]. Il semblerait que les individus porteurs du SNP C3435T répondent également mieux aux traitements antiépileptiques [163]. La réponse aux traitements antiviraux contre le SIDA fait encore l'objet de controverse car elles seraient améliorée ou non modifiée suivant les études [144, 145, 164-167]. Pour l'un de ces antiviraux, une protection a été décrite : la névirapine cause moins de dommages hépatiques chez les individus porteurs de l'allèle 3435T [168]. Cette protection n'existe cependant pas contre la neuro-toxicité induite par d'autres médicaments comme l'éfavirenz [169] ou le tacrolimus [143]. A l'inverse, les effets secondaires peuvent être plus grands chez les individus TT ; c'est le cas pour l'hypotension induite par la nortriptyline [154] et les diarrhées causées par la chimiothérapie combinant l'irinotécan et le cisplatine [170].

1.2.2. Impact du SNP G2677T/A (A893S/T)

Le SNP G2677T/A correspond à l'alanine 893 qui peut être mutée en sérine (G2667T) ou en thréonine (G2677A). La fréquence de la mutation A893S étant plus élevée, les données concernant cette mutation sont plus nombreuses que celles concernant la protéine A893T.

a. Impact sur l'expression d'ABCB1

Le niveau d'expression de la protéine ABCB1 Ser/Thr893 a été rapporté comme semblable à celui de la protéine naturelle dans des cellules HEK-293-T [171], des cellules du duodénum [103] et des cellules de leucémie myéloïdes aigues [107] même si une expression plus faible (mais non significative) a pu être observée au niveau placentaire [172]. Seule une étude a rapporté un niveau d'expression plus faible au niveau de tissus rénaux normaux de patients homozygotes TT [114].

b. Impact sur la fonction d'ABCB1

L'activité de transport de la protéine ABCB1-A893T serait augmentée pour la calcéine-AM [171]. Pourtant, la protéine ABCB1-A893S, elle, présenterait une activité de transport normal de la calcéine-AM ainsi que du vérapamil, de la vinblastine, de la rhodamine 123, de la daunorubicine, de la cyclosporine A et du saquinavir [105, 107, 109, 111-113, 171, 173, 174]. Pour d'autres substrats, les observations sont moins claires. L'efflux de la digoxine, par exemple, est normal dans des cellules LLC-PK1 [112] voire augmentée dans des NIH-3T3 [100]. L'efficacité de transport du paclitaxel pourrait être diminuée dans des cellules HEK-293-T [171] ou normale [111].

Concernant le profil de chimiorésistance, il est semblable à celui d'ABCB1wt pour la daunorubicine, la valinomycine, l'actinomycine D, la colchicine, l'adryamicine et la vinblastine voir légèrement modifié (plus de résistance) pour la doxorubicine [175, 176].

c. Impact sur la pharmacocinétique et l'action des médicaments

La présence du polymorphisme n'a pas d'influence sur la pharmacocinétique du talinolol [103], de la nimodipine [159], de la cloxacilline [160] ou de la paroxetine [161]. Tout comme le SNP C3435T, le SNP G2677T fut à la fois corrélé à une diminution [100] et à un niveau normal [138] de la concentration plasmatique en fexofénadine. Bien qu'une étude n'est rapportée aucun effet du SNP sur la pharmacocinétique du tacrolimus [142], deux autres études décrivirent que les individus GG montraient une diminution de la concentration plasmatique en tacrolimus [140, 141]. Pourtant, aucune association n'a été faite entre le polymorphisme et la neurotoxicité induite par le tacrolimus [143]. De manière paradoxal, ce polymorphisme est associé avec la neurotoxicité induite par la cyclosporine A [143] alors que son transport ne semble pas modifié. Aucune corrélation n'a été trouvée entre l'expression du SNP et la réponse aux anti-VIH [165]. Il a pourtant été observé que les patients GA montrent une meilleure augmentation du nombre de cellules CD4+ que les patients GG ou GT après 6 mois de thérapie antivirale (lamivudine, stavudine et éfavirenz) [177]. A l'inverse, il existerait une association avec la réponse à la paroxetine (antidépresseur) [178].

1.2.3. SNP C1236T

Le SNP synonyme C1236T concerne la glycine 412. La protéine ABCB1 portant le SNP C1236T montre une expression normale dans des cellules de leucémie myéloïdes aigues [107] et une activité de transport normal de la rhodamine 123, du paclitaxel, du vérapamil, de la daunorubicine, de la vinblastine, de la calcéine-AM et de la rhodamine [107, 111].

Le SNP C1236T n'aurait, d'une part, pas d'influence sur la pharmacocinétique du cilostazol [158]. Ce SNP a été associé à la neurotoxicité induite par le traitement au tacrolimus [143] mais les individus CC ne montrent qu'une tendance non significative à une plus faible concentration plasmatique en tacrolimus [141, 142]. D'autre part, il a été associé à une augmentation de l'exposition à l'irinotécan et à son métabolite, le SN-38 (homozygote TT) [179]. Il modifierait aussi l'absorption orale de la cloxacilline et sa pharmacocinétique puisque les individus TT montrent une plus forte concentration sérique de cloxacilline sans modification de la clairance rénale [160]. Le SNP C1236T a également été associé à la neurotoxicité induite par cyclosporine A [143]. Pour finir, il a été observé que les individus porteurs des génotypes CT et TT sont protégés contre la progression du statut séropositif à la déclaration en SIDA [180].

1.2.4. Association des SNP G2677T/A et C3435T

Le polymorphisme G2677T/A s'avère associé au polymorphisme C3435T [172, 181]. La présence des deux SNP n'aurait pas d'influence sur l'expression en ARNm ABCB1 ; en effet le niveau est semblable entre les individus GG-CC et TT-TT [182]. Le transport de la rhodamine 123 [182], du vérapamil, de la digoxine, de la vinblastine et de la cyclosporine A est normal [112]. L'haplotype G2677T/C3435T n'influence pas non plus les paramètres pharmacocinétiques de la cyclosporine [182], du cilostazol [158] et de la fexofénadine [183] bien que les individus TT montrent une concentration plasmatique supérieure aux individus GC (mais non significative). Par contre, une différence est observée en présence d'itraconazole (un inhibiteur d'ABCB1) ; les individus TT montrent alors une augmentation de la concentration plasmatique en fexofenadine [183] potentiellement due à l'inhibition d'ABCB1 au niveau intestinale. Aucune corrélation n'a été établie entre l'association des deux SNP et la réponse virale ou immunologique au traitement anti-VIH [167].

1.2.5. Association des SNP C1236T/G2677T/A et C3435T

L'étude de la fréquence des différents SNP sur ABCB1 a permit de mettre en évidence une forte association entre le SNP C3435T et d'autres SNP d'ABCB1. Ces associations définirent des haplotypes dont les plus fréquents combinent les polymorphismes C3435T, G2677T/A et C1236T [100, 174, 184, 185]. La fréquence des allèles diffèrent en fonction des ethnies [108]. Les individus d'origine africaine portent plutôt l'allèle naturel (CGC). Les individus caucasiens montrent une fréquence équivalente pour les haplotypes CGC ou TTT (variant). A l'inverse, les populations d'origine asiatique et indienne présentent l'haplotype TTT de manière dominante. Plutôt que de considérer le polymorphisme C3435T seul, de nombreuses études furent entreprises en considérant l'haplotype TTT.

L'haplotype C1236T/G2677T/C3435T n'influencerait pas l'expression de la protéine ABCB1. Mais les protéines ABCB1 TTT (3 polymorphismes) ont montré une sensibilité au vérapamil (inhibiteur) différente de la protéine naturelle bien que cette sensibilité soit normale pour la rapamycine (autre inhibiteur). L'analyse de la sensibilité à la trypsine du variant TTT suggère une modification de la structure tertiaire protéique, potentiellement due à une altération du profil de glycosylation de la protéine [111].

L'haplotype C1236T/G2677T/C3435T n'influencerait pas le transport de la calcéine-AM, du paclitaxel, de la vinblastine, de la daunorubicine, de la rhodamine 123 et du vérapamil [111, 171]. Par contre, son activité d'efflux de la digoxine serait augmentée (*in vitro*) [100]. L'haplotype TTT ne serait pas sans conséquence sur l'exposition à certains médicaments puisqu'il a été associé à une réduction de la clairance rénale de l'irinotecan [186] et à une augmentation de l'exposition à la cyclosporine A [187]. De plus, les individus TTT auraient besoin d'une dose plus élevée en tacrolimus pour atteindre la même concentration plasmatique que les individus CGC [141]. Ils montreraient également une diminution de la disponibilité orale de la fexofenadine [100] ou du clopidrogel [151] par rapport aux individus TGT. Pour finir, cet haplotype a été associée à une réponse altérée au traitement de la dépression par paroxetine [178].

1.2.6. Autres SNP sur ABCB1

De nombreux autres SNP ont été décrits sur ABCB1. Certains ne montrent pas d'effet ni sur l'expression, ni sur l'activité de transport de la protéine ABCB1. C'est le cas du SNP A61G (protéine ABCB1-N21D) qui est exprimée normalement [103, 171] et transporte correctement le vérapamil, la calcéine-AM et le paclitaxel [171, 173]. La présence de ce polymorphisme n'a pas non plus d'influence sur la pharmacocinétique du talinolol [103] ou de la paroxetine [161]. De même, les SNP T307C et G2995A sont sans effet ; les protéines correspondantes transportent correctement le vérapamil et la calcéine-AM [173].

Dans certains cas, le niveau d'expression d'ABCB1 n'est pas modifié par le polymorphisme et son activité de transport est modifiée de manière substrat spécifique. Ainsi, le variant M89T est plus résistant à la daunorubicine, à la doxorubicine et à la valinomycine mais pas à l'actinomycine D [175]. Les cellules exprimant ABCB1-G185V sont respectivement plus, autant et moins résistantes à la colchicine, à l'adryamicine et à la vinblastine que celles exprimant ABCB1 naturelle [176]. La protéine ABCB1-S400N, dont le niveau d'expression et la localisation membranaire est normale [103, 171, 188], transporte correctement le vérapamil, la calcéine-AM et le paclitaxel [171, 173], confère une résistance normale à la doxorubicine et n'a pas d'influence sur la pharmacocinétique du talinolol [103]. Par contre, le transport de la rhodamine 123 est diminué [188] et la résistance à la vinblastine et à la vincristine est augmentée [188]. Le variant L662R (SNP T1985G) quant à lui montre une expression et un profil de résistance à la daunorubicine et à l'actinomycine D normaux mais une résistance accrue pour la doxorubicine et la valinomycine [175].

Autre exemple : la protéine ABCB1-R669C dont l'expression est normale [171] montre une activité de transport de la calcéine-AM et du paclitaxel semblable à celle de la protéine naturelle [171] mais une chimiorésistance accrue à la daunorubicine, à la doxorubicine, à la valinomycine et à l'actinomycine [175]. Le polymorphisme C3151G (protéine P1051A) n'induit pas de modification ni de l'expression d'ABCB1 ni de la résistance à la daunorubicine, à la doxorubicine et à l'actinomycine D mais une augmentation de la résistance à la valinomycine [175]. Bien qu'exprimée à un niveau semblable à ABCB1wt, la protéine ABCB1-W1108R n'engendre pas autant de résistance à la daunorubicine, à la doxorubicine et la valinomycine que la protéine naturelle et le niveau de résistance à l'actinomycine D reste normal [175]. Le SNP T3421A code la protéine ABCB1-S1141T exprimée normalement [171] [175] et transportant correctement la calcéine-AM et le paclitaxel [171].

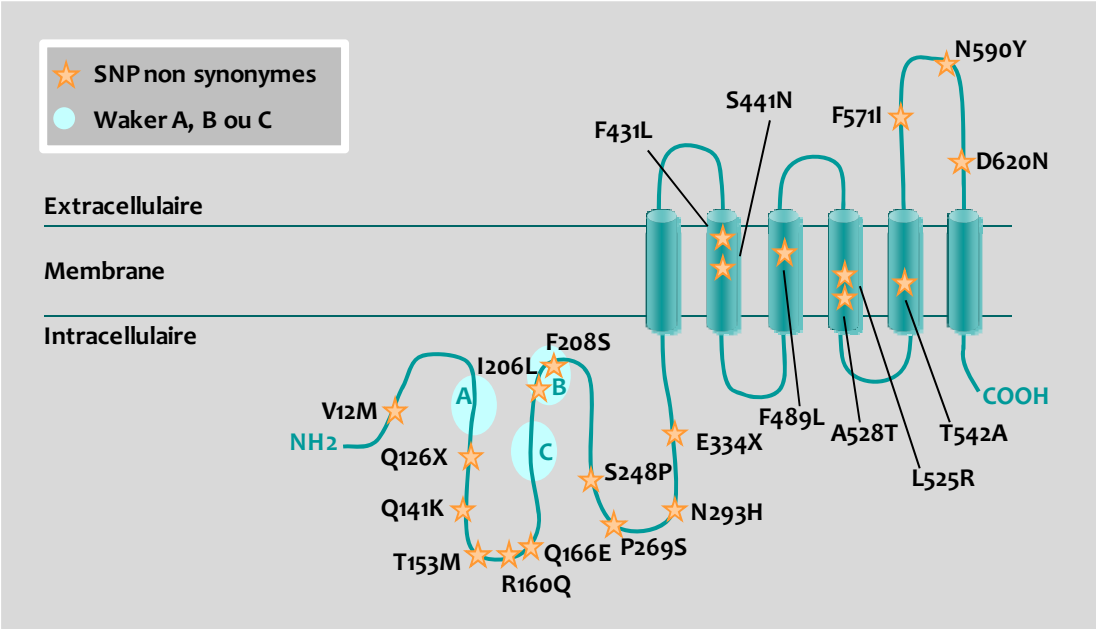

Figure 12. SNP non synonymes sur ABCG2.
Les SNP non synonymes sont reportés sur le schéma de la structure potentielle d'ABCG2. X symbolise la formation d'un codon stop. *Figure inspirée de Tamura et al. 2006 [189].*

	V12M	Q126X	Q141K	T153M	Q166E	I206L	F208S	S248P	P269S	E334X	F431L	S441N	F489L	F571I	N590Y	D620N
Fréquence (%)	2-90	0-1,7	0-35,5	3,3	N.D.	10	N.D.	N.D.	N.D.	N.D.	0,8	0,5	0,5-0,8	0,5	0-1	0,5
Expression																
Protéine	✓	⇩	⇩	✓	✓	✓	⇩	✓	✓	⇩	✓	⇩	✓	✓	✓	✓
Localisation membranaire	✓	N.D.	✓	N.D.	N.D.	N.D.	×	✓	N.D.	N.D.	✓	×	✓	N.D.	N.D.	N.D.
Transport																
Méthotrexate	✓	×	✓	✓	✓	⇩	×	×	⇩	×	×	×	⇩	✓	⇩	✓
Porphyrine	✓	×	✓	✓	✓	⇩	×	×	N.D.	×	✓	×	⇩	✓	✓	✓
Chimiorésistance																
SN-38	✓	N.D.	⇩	N.D.	N.D.	N.D.	×	×	N.D.	N.D.	⇩	×	⇩	N.D.	N.D.	✓
Mitoxantrone	✓	N.D.	⇩	N.D.	N.D.	N.D.	×	×	N.D.	N.D.	⇩	×	⇩	N.D.	N.D.	✓
Topotécan	✓	N.D.	⇩	N.D.	N.D.	N.D.	N.D.	N.D.	N.D.	N.D.	N.D.	N.D.	N.D.	N.D.	N.D.	✓
Diflomotécan	✓	N.D.	⇩	N.D.	N.D.	N.D.	N.D.	N.D.	N.D.	N.D.	N.D.	N.D.	N.D.	N.D.	N.D.	✓

Tableau 6. Conséquences des SNP synonymes sur l'expression et l'activité d'ABCG2.
Fréquence décrite dans Tamura et al. 2006 [189]. Les SNP A160Q, N293H, L525R, A528T et T542A ne sont pas représentés car aucune donnée n'est actuellement disponible. ✓ = semblable à ABCG2wt ; ⇩ = diminué par rapport à ABCG2wt ; × = perdu par rapport à ABCG2wt ; N.D. = non déterminé

Son profil de chimiorésistance à la daunorubicine et à l'actinomycine D est normal [175] alors que la résistance à la doxorubicine et à la valinomycine est augmentée par rapport à ABCB1 naturelle [175]. Enfin, la protéine ABCB1-V1251I montre une augmentation de l'activité de transport de la calcéine-AM [171] sans modification du niveau d'expression.

Certains polymorphismes situés au niveau des introns ont pu être corrélés à un phénotype de résistance aux médicaments contre l'épilepsie [190]. Un autre polymorphisme intronique, le SNP T-129C, a été corrélé à une expression plus faible d'ABCB1 placentaire [172] mais ne modifie ni la fonction d'efflux de rhodamine 123 [110], ni la concentration plasmatique en tacrolimus [141]. Il serait tout de même corrélé à une meilleur augmentation du nombre de cellules CD4+ chez des patients CC après 6 mois de thérapie antivirale (lamivudine, stavudine et éfavirenz) [177].

1.3 SNP sur ABCG2

De nombreux SNP ont été identifiés et décrits sur le gène *ABCG2*. Certains SNP situés au niveau de la région promotrice induiraient une modification du niveau en ARNm ABCG2. Le SNP C-15994T (rs7699188), par exemple, a été corrélé à une augmentation du niveau d'expression en ARNm ABCG2 qui pourrait faire suite à la formation d'un nouveau site de fixation aux facteurs de transcription [191]. D'autres polymorphismes (A–15846C et C–30477G/rs2127861) montrent une augmentation du niveau d'expression en ARNm sans identification de nouveaux sites de fixations aux facteurs de transcription [191]. A l'inverse, le SNP C-15622T a été corrélé à une diminution de l'expression en ARNm [191].

L'apparition de site de fixation aux facteurs de transcription peut aussi être observée au niveau des introns. En effet, le SNP C16702T (rs2046134), corrélé à une augmentation de l'expression en ARNm, induirait la formation d'un nouveau site [191]. D'autres SNP montrent une association avec le niveau d'expression en ARNm ABCG2 : le SNP T12283TC (augmentation) et le SNP G1143A ou rs2622604 (diminution) [191]. Ce dernier a aussi été corrélé à l'apparition d'insuffisance médullaire (leucopénie, neutropénie, anémie) dans le cadre de traitements à base d'irinotécan (substrat d'ABCG2) [192]. Les SNP rs17731538 (intron 2) et rs13120400 (intron 9) ont été associés à la réponse au méthotrexate dans le cadre du traitement du psoriasis [193].

Les polymorphismes les plus étudiés sont les SNP non synonymes, dont les SNP G527A (V12M) et C914A (Q141K), qui modifient un acide aminé et sont susceptibles d'avoir d'importantes conséquences sur la structure et la fonction d'ABCG2 (**Figure 12**, **Tableau 6**).

1.3.1. SNP G527A (V12M)

Des données contradictoires ont été rapportées concernant l'effet du SNP G527A. En effet, certains travaux rapportèrent qu'il n'etait pas associé à une modification de l'expression, de la localisation cellulaire ou de l'activité d'ABCG2 [194, 195], alors que Mizuarai et al. observa une modification de la localisation cellulaire de la protéine ABCG2-V12M (augmentation de la présence en intracellulaire au lieu de sa migration au niveau de la membrane plasmatique). La mutation V12M se situe dans une région terminale qui n'a pas été reconnue comme une séquence signal de la localisation mais soulève la question de l'importance de cette région dans l'efficacité d'acheminement à la membrane. La mutation est également associée à une perte de résistance à la mitoxantrone et au topotécan [196]. Par ailleurs, une étude portant sur le transport du Hoechst 33342 n'a pas été en mesure d'éclaircir l'impact de ce polymorphisme sur l'activité de transport des cellules porteuses de ce SNP. En effet, celle-ci fut à la fois diminuée dans des cellules Sf9 exprimant ABCG2-V12M et inchangée dans des cellules HEK 293/ABCG2-V12M [197]. Néanmoins, les cellules exprimant la protéine ABCG2-V12M (transfectants stables HEK-293 ou FlpIn 293) seraient résistantes à plusieurs substrats d'ABCG2 : le SN-38, la mitoxantrone, le topotécan et le diflomotécan [195, 197] et présenteraient une activité ATPase comparable à celle des cellules exprimant la protéine naturelle [197].

1.3.2. SNP C914A (Q141K)

Le polymorphisme C914A (Q141K) fut sans conteste le SNP le plus étudié. Au niveau des patients, de nombreuses observations et corrélations ont été faites. Bien que les cellules intestinales de porteurs de ce SNP présentent une expression normale d'ABCG2 (ARNm et protéine) [198], ils montrent une augmentation du taux plasmatique de diflomotécan [199], de topotécan [200], de gefinitib [201], d'atorvastatine et de rosuvastatine [202]. Les porteurs de l'allèle A montre également une clairance diminuée pour l'erlotinib (substrat d'ABCG2 [201]) [203]. Par contre, le SNP C914A n'aurait pas de conséquences sur la pharmacocinétique de l'irinotecan [204].

Dans les lignées cellulaires transfectées, ABCG2-Q141K est exprimée à un niveau inférieure à ABCG2 naturelle [189, 194, 195, 205]. Rapportée au niveau de protéine exprimée, l'activité de transport de cette protéine n'est pas modifiée pour certains substrats : E1S (estrone-3-sulfate), DHEAS (dehydroepiandrosterone sulfate), MTX (méthotrexate) et PAH (acide *p*-aminohippurique) [205].

Pourtant, les cellules exprimant ABCG2-Q141K montrent une diminution d'efflux de certains substrats (mitoxantrone [197], topotécan [194] et urate [206]) et d'activité ATPase [197]. Cela suggère que cet acide aminé serait impliqué dans le transport des certains substrats mais pas d'autres (présence de plusieurs sites de fixation pour les substrats). Concernant la résistance aux médicaments, les cellules exprimant le variant Q141K sont plus sensibles au SN-38, à la mitoxantrone, au topotecan et au diflomotécan que des cellules exprimant la protéine naturelle [194-197].

1.3.3. Autres SNP sur ABCG2

Certains polymorphismes (T153M, Q166E, F571I et D620N) semblent ne pas avoir de conséquences ni sur l'expression ni sur l'activité de la protéine ABCG2. A l'inverse, certains SNP paraissent complètement délétères. En effet, les protéines ABCG2-Q126X et ABCG2-E334X sont incomplètes (formation d'un codon stop précoce) et ne transportent ni le MTX ni la porphyrine [189]

Certains variants montrent une expression similaire à celle d'ABCG2wt pourtant leur activité est modifiée. C'est le cas des protéines portant les polymorphismes I206L, S248P, P269S, F431L, F489L et N590Y qui montrent une diminution plus ou moins importante de l'activité de transport du MTX, de la porphyrine et/ou de l'E1S [189, 195, 207]. De plus, les cellules exprimant ABCG2-F248P, ABCG2 F431L ou ABCG2-F489L ne sont plus autant résistantes ni au SN-38 ni à la mitoxantrone [189, 195].

D'autres polymorphismes engendrent à la fois une diminution de l'expression et une perte d'activité. Le variant F208S par exemple est très faiblement exprimé [189, 195] car il serait dégradé par le protéasome [208]. La présence du variant F208S ne semble pourtant pas modifier la pharmacocinétique de l'irinotécan [179]. Les cellules exprimant ABCG2-F208S ne sont cependant pas résistantes au SN-38 et à la mitoxantrone [195]. Le SNP S441N, quant à lui, diminue le niveau d'expression protéique et modifie la localisation cellulaire de la protéine ABCG2 ; le variant est observée en intracellulaire et non membranaire [195, 205]. Son activité de transport est perdue pour le MTX et la porphyrine [189]. Les cellules exprimant ce variant ont perdu leur phénotype de résistance au SN-38 et à la mitoxantrone [189, 195].

SNP	Substitution		SNP	Substitution	
	ARNm	Protéine		ARNm	Protéine
rs177339	C202G	A9A	rs4148356	G2343A	R723Q
rs41395947	G303C	C43S	rs28364004	G2740T	L855L
rs41494447	C393T	T73I	rs45517537	G2756A	A861T
rs61731711	C424T	I83I	rs16967004	C2830T	G885G
rs8187844	C450T	S92P	rs61731704	G2905A	L910L
rs61731710	A487G	P104P	rs45531136	A2983G	K936K
§		T117M	rs45607431	T3133C	H986H
rs8187848	G864A	R230Q	rs35529209	G3140A	A989T
rs8187849	C881T	L236L	rs35934123	G3142A	A989A
rs45560437	G991A	P272P	rs13337489	G3315C	C1047S
rs246221	T1000A	V275V	rs41410450	G3348A	R1058Q
rs45562336	T1039C	S288S	rs28364000	C3355T	P1060P
rs76776400	A1082G	K303E	rs74985930	G3560A	V1129I
rs8187851	C1222T	L349L	rs28706727	G3611A	V1146I
rs8187852	G1232A	V353M	rs4148377	G3625A	P1150P
rs35587	T1237C	N354N	rs28363996	C3775T	A1200A
rs8187853	G1243A	T356T	rs9933640	C3955T	A1206A
rs77428024	A1410G	N412S	rs45533037	C4060T	F1295F
rs60782127	G1474T	R433S	rs2230671	G4177A	S1334S
rs78513702	T1590G	V472G	rs28364006	A4184G	T1337A
rs72547522	A1752C	D526A	rs8057331	C4377T	T1401M
rs35605	T1859C	L562L	rs34526519	C4393T	A1406A
rs8187858	C1879T	Y568Y	rs34327330	C4408T	F1411F
£	G1898A	R633Q	rs36115566	G4519A	T1448T
rs8187859	C2086T	D637D	rs35148086	C4627T	I1484I
rs8187863	C2176T	S667S	§		S1512L
rs2301666	C2182T	P669P	rs35980404	C4756T	D1527D
rs45511401	G2187T	G671V			

§ SNP identifié par Perdu et al. 2000

£ SNP identifié par Le Saux et al. 2000

Tableau 7. SNP retrouvés sur la partie codante du gène ABCC1.
Les lignes grises foncées correspondent aux SNP non synonymes. *Source NCBI dbSNP database.*

1.4 SNP sur ABCC1

Un très grand nombre de SNP ont été répertoriés au niveau du gène ABCC1 dont la plupart se situe au niveau des introns mais certains sont aussi retrouvés au niveau des extrémités 3' et 5'. Les polymorphismes les plus étudiés restent cependant ceux situés au niveau de la partie codante d'ABCC1 (**Tableau 7**, **Figure 13**). Parmi eux, plusieurs ont été décrits sans influence (SNP S92F, T117M, R230Q, R633Q, G671V, C1047S et S1512L) [209, 210].

Certains SNP montrent une expression normale mais une activité de transport altérée pour certains substrats. La protéine R433S est normalement localisée sur la membrane, transporte correctement l'E217βG (17beta-oestradiol-17beta-D-glucuronide) et procure une résistance au VP-16 et la vincristine [211]. Pourtant, son transport du LTC4 (leucotriène C4) et de l'estrone sulfate est altéré et, à l'inverse, elle engendre une résistance accrue à la doxorubicine [211]. Le SNP A989T montre une expression et un transport du LTC4 et du MTX normaux mais une diminution du transport de l'E217βG [210].

D'autres SNP montrent des résultats parfois sujets à la controverse. La protéine ABCC1-T73I, par exemple, est localisée normalement, transporte correctement le LTC4, l'E217βG et le méthotrexate [210] et montre un profil de résistance normal pour la daunorubicine, la doxorubicine, la vinblastine et la vincristine [212]. Pourtant, une diminution de résistance est observée pour le méthotrexate, l'étoposide et la vincristine qui varie selon le type cellulaire utilisé pour l'étude [212]. Les variations observées en fonction du type cellulaire et le paradoxe existant entre un transport normal du MTX et une résistance diminuée indiquent que des analyses complémentaires doivent être effectuées pour conclure sur l'effet du SNP T73I. Le SNP R723Q ne modifie pas non plus la localisation membranaire, ni le transport du LTC4, de l'E217βG et du MTX [210]. Par contre, une diminution de la résistance à la daunorubicine, à la doxorubicine, à l'étoposide, à la vinblastine et à la vincristine est observée [212]. La résistance au MTX est sujet à controverse puisqu'elle est diminuée ou non selon le type cellulaire [212] bien que son transport ait été décrit comme normal [210]. Le SNP R1058Q n'influence pas non plus la localisation de la protéine ABCC1 qui transporte normalement le LTC4, l'E217βG et le MTX [210, 212]. La résistance à la vincristine n'est pas modifiée alors qu'elle est diminuée pour l'étoposide, la daunorubicine et la doxorubicine. Par contre la résistance au MTX et à la vinblastine varient selon le type cellulaire [212].

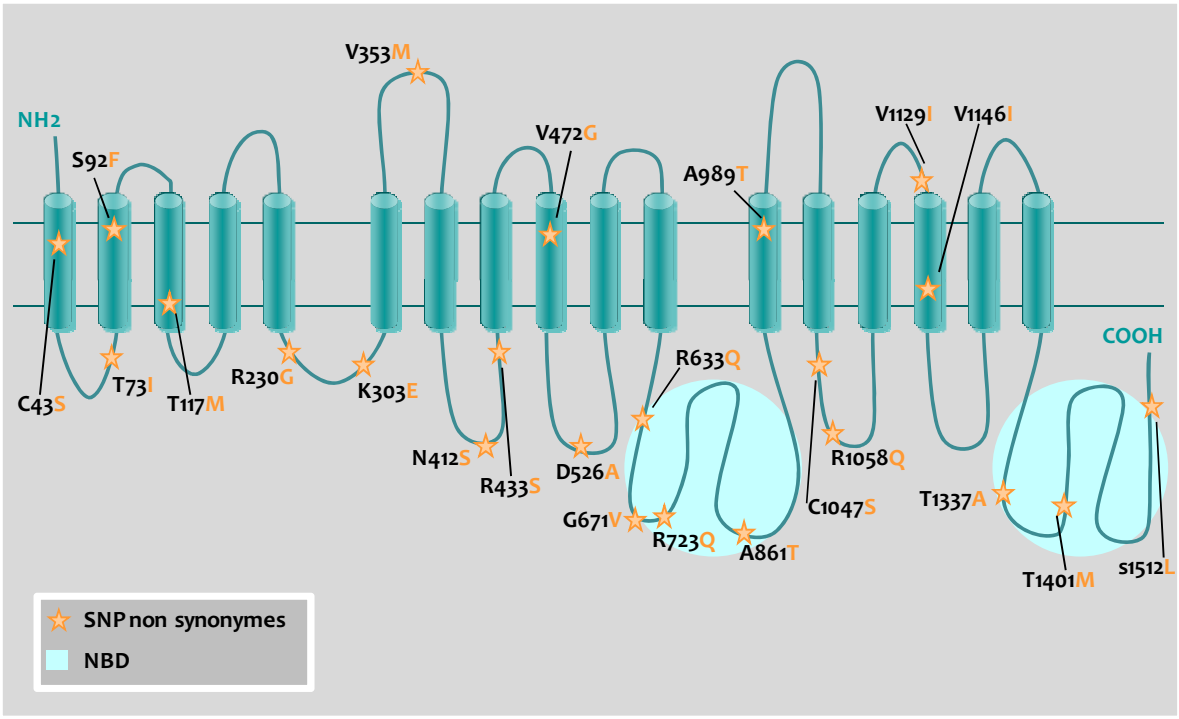

Figure 13. SNP non synonymes sur ABCC1.
Les SNP sont reportés sur le schéma de la structure potentielle d'ABCC1. Figure inspirée de Letourneau et al. 2005.

Le SNP C43S est le plus sujet à la controverse d'une part pour son impact sur la localisation d'ABCC1 et d'autre part sur le transport de certains substrats. En effet, sa localisation membranaire a été à la fois décrite intacte ou altérée [212, 213]. De plus, une diminution de sensibilité à la trypsine a été observée et suggérerait une modification de sa conformation qui empêcherait l'accès au site de clivage de la trypsine [213]. Le transport du GSH (gluthation), de l'E217βG et du LTC4 est normal ainsi que la résistance à la daunorubicine, à l'étoposide et à la vinblastine [212]. A l'inverse, la résistance à l'arsénite est diminuée [213]. Pour finir, le profil de résistance à la vincristine et à la doxorubicine reste à confirmer car la résistance a été décrite normale mais aussi altérée [212, 213].

Très peu de données existent concernant d'autres paramètres que l'expression ou l'activité de transport. Les SNP rs35592 (intron 9) et rs2238476 (intron 23) ont montré une association avec l'efficacité du MTX dans le traitement du psoriasis tout comme le SNP T1337A qui a été associé à une plus grande efficacité du MTX dans ce contexte [193]. Les SNP introniques rs11075291, rs1967120, rs3784862, rs246240, rs3784864, and rs2238476 ont quant à eux été associés à une augmentation de la toxicité du MTX dans le traitement du psoriasis [193]. De manière surprenante, le SNP G671V, décrit sans impact sur l'expression ou l'activité d'ABCC1, a été associé au développement d'une cardio-toxicité induite par un traitement du lymphome non-hodgkinien à base d'anthracyclines (arythmie) [214]. Les SNP rs4148382 and rs212093 dans la région 3' du gène *ABCC1* modifieraient l'activité pulmonaire puisqu'ils ont été respectivement associés à un volume expiratoire forcé plus élevé et plus faible [215]. Et le SNP rs35621 (intron 14) a été associé avec un volume expiratoire forcé excessif [215].

SNP	Substitution		SNP	Substitution	
	ARNm	Protéine		ARNm	Protéine
rs16945988	G 120A	R19H	rs16945946	C 1721T	L553L
rs17822931	G 602A	G180R	rs41282045	C 1952T	R630W
rs16945974	A 748G	Q228Q	rs16945930	G 2006A	V648I
rs61739612	C 900A	P279H	rs61745566	G 2119C	T685T
	C 900G	P279R		G 2119T	
rs11860868	A 1009G	P315P	rs16945928	G 2123A	V687I
rs11863236	C 1014A	A317E	rs16945926	A 2268G	K735R
rs8047091	A 1186G	K374K	rs11866251	C 2500T	F812F
rs73540894	G 1261A	A399A	rs12443685	G 2722A	K886K
rs58759389	G 1306A	A414A	rs55713504	C 2877G	S938X
rs59815620	G 1535A	V491I	rs41280943	A 2972G	M970V
rs61742020	A 1649T	K529X	rs59029650	G 3048A	R995Q
	A 1649C	K529Q	rs61739606	A 3893T	N1277Y
rs17822471	C 1701T	T546M	rs16945916	A 4095G	H1344R

Tableau 8. SNP retrouvés sur la partie codante du gène ABCC11.
Les lignes grises foncées correspondent aux SNP non synonymes. X indique la formation d'un codon STOP qui met fin à la traduction. *Source NCBI dbSNP database.*

2. Influence des SNP sur l'expression et l'activité d'ABCC11

2.1 SNP sur ABCC11

A ce jour, plus de 300 SNP (307) ont été identifiés dans la région où se situe le gène ABCC11. Ces polymorphismes sont localisés dans les régions 5', 3', les introns ou les exons. La région codante compte 28 SNP dont 18 non synonymes, répertoriés dans le **Tableau 8**.

Le premier SNP fut décrit en 2006 et correspond à la substitution G602A. Elle induit la mutation de la glycine 180 en arginine. Ce SNP a été corrélé au type de cérumen sécrété dans l'oreille [216]. En effet, il existe deux types de sécrétion : le cérumen mouillé (brun-jaunâtre et humide) et le cérumen sec (absence de sécrétion). Les individus portant au moins un allèle sauvage (GG ou GA) présentent un phénotype mouillé alors que les individus homozygotes pour le SNP (AA) présentent un phénotype sec. Des cellules LLC-PK1 ont été transfectées pour exprimer la protéine naturelle (glycine 180) ou mutée (arginine 180). La protéine mutée est exprimée trois fois plus abondamment que la protéine naturelle mais perd sa capacité à transporter le GMPc. Au niveau des glandes cérumineuses, ABCC11 est exprimée sur les granules et les vacuoles intracellulaires, ainsi que sur la membrane apicale des cellules sécrétrices. La protéine mutée perd la localisation granulaire et vacuolaire [217]. De plus, elle n'est pas N-glycosylée et est, de ce fait, reconnue comme une protéine anormale qui est alors ubiquitinée et dégradée.

Des composants communs entrent dans la composition du cérumen, du colostrum et de la sueur [218]. Une étude a établit la corrélation entre le type de cérumen et la sécrétion de colostrum [219]. Le colostrum correspond au lait, riche en protéine, sécrété en fin de grossesse et en début d'allaitement. La fréquence de femmes ne sécrétant pas de colostrum est significativement supérieure chez les femmes présentant un phénotype sec (homozygotes pour le SNP). De plus, le volume de colostrum sécrété par ces dernières est significativement plus faible que chez les femmes ayant un phénotype mouillé. Une seconde étude démontra qu'ABCC11 est aussi exprimée dans les glandes sudoripares et que les individus porteurs du polymorphisme G602A sécrètent une sueur axillaire très pauvre en composants odorants [220]. Les sécrétions en acides aminés conjugués et en stéroïdes responsables de l'odeur sont respectivement abolies et significativement diminuées.

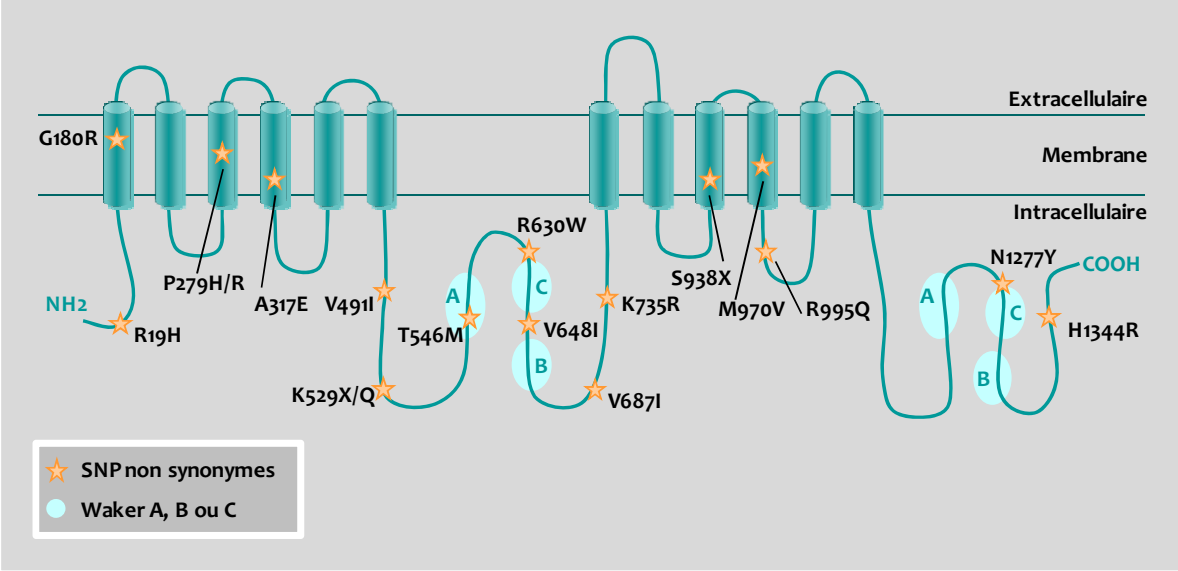

Figure 14. SNP sur ABCC11.
Les SNP sont reportés sur le schéma de la structure potentielle d'ABCC11. X symbolise la formation d'un codon stop.

	Acide aminé conservé chez les ABCC							
	1	2	3	4	5	6	10	12
R19H								
G180R	☑				☑		☑	☑
P279H/R								☑
A317E								
V491I								
K529X/Q								
T546M								
R630W				☑	☑			☑
V648I	☑		☑	☑		☑	☑	☑
V687I			☑					☑
K735R							☑	☑
S938X								
M970V								
R995Q	☑	☑	☑	☑				☑
N1277Y	☑	☑	☑	☑	☑			☑
H1344R								☑

Tableau 9. Conservation des acides aminés concernés par le polymorphisme.
Les acides aminés d'ABCC11 sujets au SNP non synonymes sont représentés dans ce tableau. La conservation de chaque acide aminé au sein de la sous-famille des ABCC (MRP) a été obtenue par l'alignement des séquences protéiques sous ClustalW2 et est symbolisée par le symbole ☑. Chaque membre est symbolisé par son numéro (1 = ABCC1, 2 = ABCC2 etc...)

ABCC11 pourrait donc être impliquée dans le processus de sécrétion du cérumen, du colostrum et de la sueur. Le polymorphisme G602A serait responsable d'un défaut d'activité d'ABCC11 et aurait de multiples conséquences physiologiques. Ses répercussions pourraient être importantes dans le cadre d'une chimiothérapie à base de substrats d'ABCC11. En effet, si le polymorphisme peut être à l'origine d'une modification de l'activité, il peut modifier la quantité de médicaments anticancéreux à laquelle sont exposées les cellules cancéreuses.

L'impact potentiel des SNP non synonymes sur ABCC11 peut être supposé selon plusieurs critères :

1) la localisation de la mutation. Les polymorphismes G180R, P279H/R, A317E, S938X, M970V sont localisés dans les MSD (**Figure 14**) et peuvent avoir des conséquences sur l'interaction avec le substrat et donc modifier le spectre de substrats de la protéine. Les mutations T546M, R630W, V648I, V687I, N1277Y et H1344R se situent dans un NBD (**Figure 14**) et peuvent altérer la fixation et l'hydrolyse de l'ATP, ainsi que l'interaction avec certains substrats tels que les stéroïdes. Au niveau des boucles intracellulaires entre les traversées membranaires, se trouve la substitution R995Q qui peut bouleverser des régions charnières nécessaires pour les changements de conformation intervenant dans le transport.

2) la conservation de l'acide aminé muté. Certains acides aminés concernés par le polymorphisme comme la glycine 180, l'arginine 630, la valine 648, l'arginine 995 et l'asparagine 1277 sont très conservés au sein de la sous-famille des ABCC (alignement par ClustalW2) (**Tableau 9**). En effet, l'acide aminé est retrouvé chez 3 voire 6 autres membres de la sous-famille. D'autres acides aminés sont seulement retrouvés chez 1 ou 2 ABCC tel que la phénylalanine 279, la valine 687, la lysine 735 et l'histidine 1344. A l'inverse, l'arginine 19, l'alanine 317, la valine 491, la leucine 529, la thréonine 546, la sérine 938 et la méthionine 970 sont uniquement retrouvés chez ABCC11 (**Tableau 9**). La thréonine 546 n'est pas conservée mais traduit une originalité parmi les ABCC. En effet, tous les autres membres présentent une valine à cette position, suggérant que la thréonine apporte peut-être une singularité à ABCC11. De plus elle se situe dans une région consensus (walker A) extrêmement conservée.

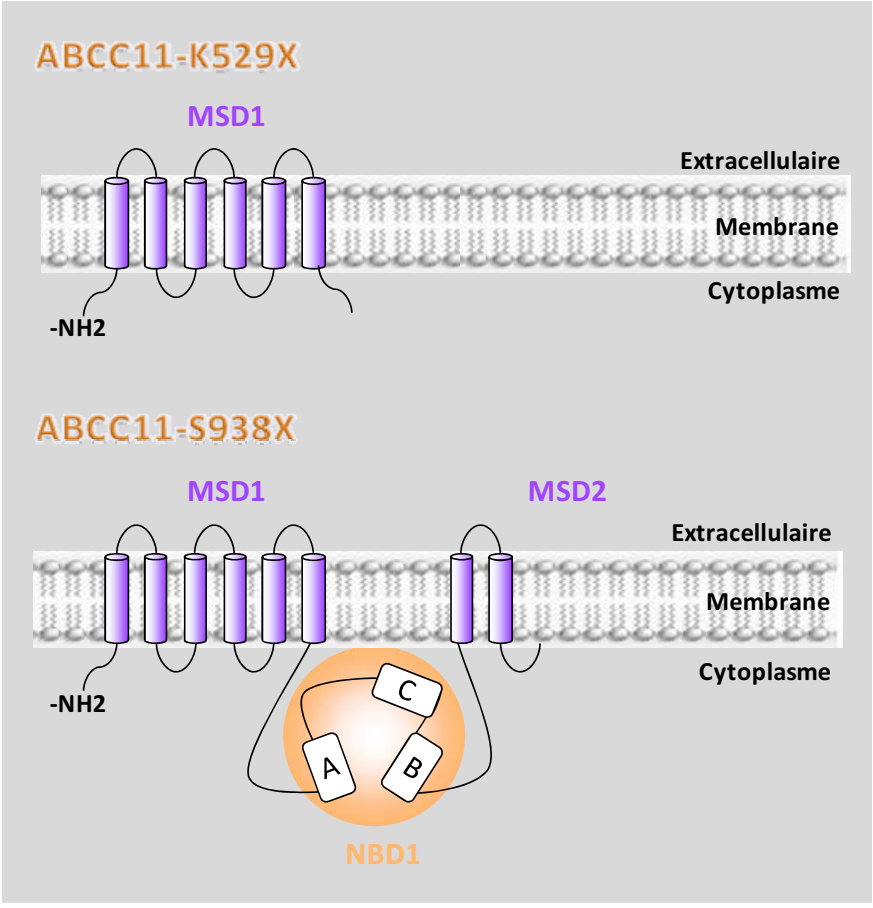

Figure 15. Représentation schématique de l'impact des protéines ABCC11-K529X et ABCC11-S938X.

3) la différence entre l'acide aminé d'origine et l'acide aminé polymorphe. L'apparition d'un codon stop est sans conteste la modification qui suggère le plus facilement une altération. Les mutations K529X, S938X induiraient la formation de protéines tronquées, respectivement composées du MSD1 ou du MSD1, du NBD1 et de 2 TM du MSD2 (**Figure 15**). La modification des charges peut altérer les interactions avec le substrat ou les interactions au sein de la protéine. Citons par exemple, l'alanine 317 (non chargée) qui devient un glutamate (chargé). Pour finir, l'apparition d'un acide aminé avec une structure différente peut également modifier la conformation de la protéine et donc ses interactions avec les substrats. La mutation R630W induit par exemple l'apparition d'un tryptophane structurellement plus imposant que l'arginine et ne comportant pas de charge positive.

Afin, d'une part, d'identifier l'impact des SNP non synonymes, et d'autres part, de caractériser les acides aminés importants dans la structure d'ABCC11, nous avons décidé d'analyser l'expression et l'activité de protéines ABCC11 polymorphes.

2.2 Matériels et Méthodes

2.2.1. Génération des lignées cellulaires

a. Clonage de l'ADNc ABCC11 dans le plasmide pcDNA3 et le plasmide pcDNA5/FRT

L'ADNc d'ABCC11 a précédemment été obtenu à partir de tissu mammaire. Pour cela, les ARNm de cellules mammaires normales provenant de plusieurs individus ont été rétro-transcrit en ADNc. L'ADNc d'ABCC11 a ensuite été amplifié par PCR puis inclu dans le plasmide pGem®-T easy. Afin de transférer l'ADNc d'ABCC11 dans le plasmide pcDNA3, ce dernier est extrait du plasmide pGem®-T easy à l'aide d'enzymes de restriction (BamHI et NotI) puis inséré dans pcDNA3 (préalablement coupé avec les mêmes enzymes de restriction).

Pour cela, le plasmide pcDNA3 vide et le plasmide pGem®-T easy ABCC11 sont digérés en parallèle par 10 UI de BamHI (fermentas) et de NotI (fermentas) dans le tampon tango 1X (fermentas) pendant 1 h à 37°C. Les produits de digestion sont séparés sur gel d'agarose 1 % contenant du Bromure d'Ethidium (BET) (migration 100 V, 1 h, tampon TAE 1X). En effet, les fragments d'ADN (chargés négativement) migrent vers l'anode (chargée positivement). La vitesse de migration dépend de la taille du fragment et permet de séparer les fragments selon leur longueur. Le BET intercalé dans les fragments d'ADN est fluorescent sous les UV et rend l'ADN visible sous forme de bandes fluorescentes. Les bandes correspondant à l'ADNc d'ABCC11 et à pcDNA3 ouvert sont prélevées.

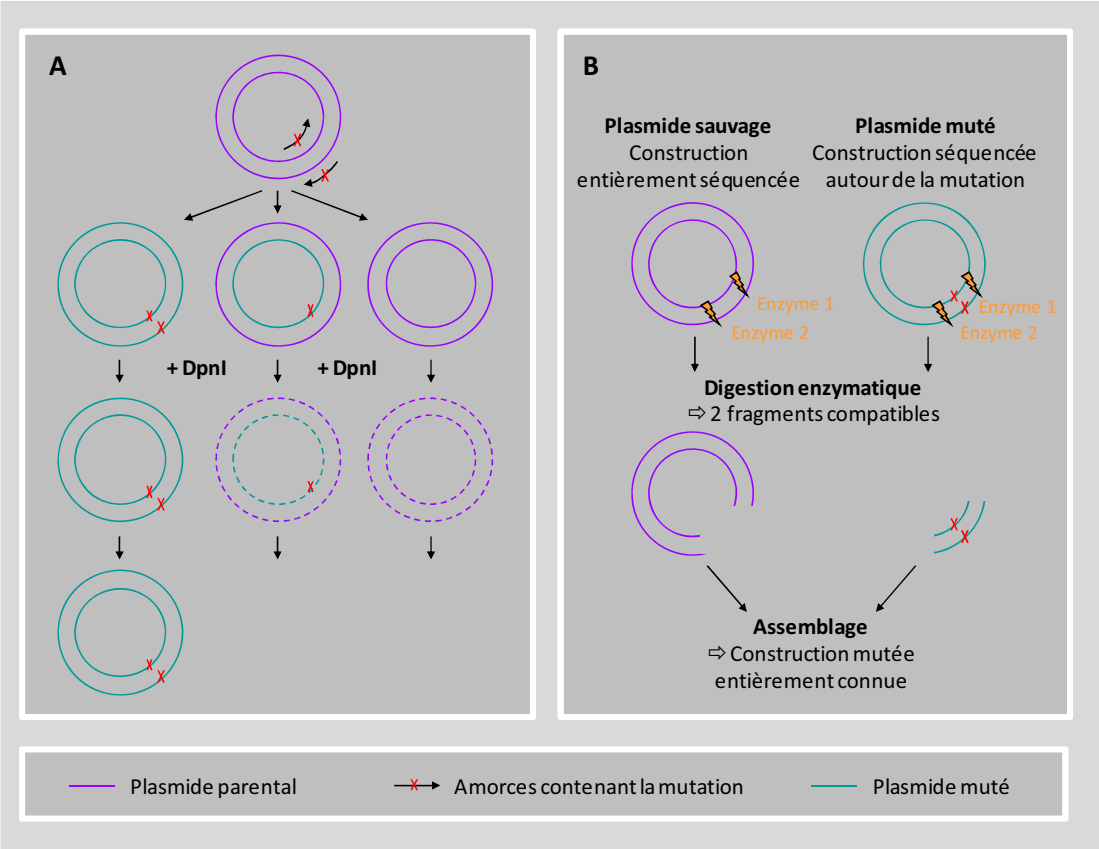

Figure 16. Principe de la mutagenèse dirigée et du sous-clonage.
A) Mutagenèse dirigée. Après la réaction PCR en présence des amorces contenant la mutation, un mélange de plasmides est obtenu: des plasmides sauvages (méthylés), des plasmides mutés (non méthylés) et des plasmides mi-sauvage/mi-mutés (hémi-méthylés). DpnI dégrade les plasmides méthylés ou hémi-méthylés, ne laissant que des plasmides mutés. **B) Sous-clonage.** La région du plasmide contenant la mutation est découpée puis introduite dans le plasmide sauvage pour former une construction entièrement correcte.

Les fragments d'ADN sont purifiés sur bille (kit GeneClean®) selon les instructions du fournisseur (Q-BIOgene) et repris dans un 10 µL d'eau. L'ADNc et le plasmide pcDNA3 sont ensuite liés par l'ADN ligase T4 (Roche) qui agit pendant 15 minutes à température ambiante. 1 µL du produit de ligation est utilisé pour transformer 50 µL de bactéries compétentes DH5α (Invitrogen™). La transformation est réalisée par choc thermique : les bactéries sont mises en présence du plasmide pendant 30 minutes à 4 °C, puis successivement incubées 1 minute à 37 °C et 1 minute à 4 °C. Le choc thermique déstabilise la membrane plasmique et permet l'entrée du plasmide dans la bactérie. Les bactéries transformées sont étalées sur boite de Pétri (LB Agar + Ampicilline 100 µg/mL) et incubées 1 nuit à 37 °C. Les bactéries obtenues sous forme de colonie sont résistantes à l'ampicilline et possèdent donc le plasmide pcDNA3 contenant le gène de résistance à l'ampicilline. Plusieurs colonies sont individuellement amplifiées par une incubation d'une nuit à 37 °C dans du milieu LB. Les plasmides contenus par chaque clone bactérien (1 colonie = 1 clone) sont extraits à l'aide du kit miniprep (Macherey-Nagel). Le profil de digestion enzymatique (BamHI et NotI) est contrôlé pour s'assurer de l'obtention d'un plasmide contenant l'ADNc ABCC11 et non d'un plasmide vide (plasmide refermé sur lui-même après ligation). Une fois un plasmide correct identifié, il est séquencé (via GenomExpress).

De la même manière que pour transférer l'ADNc ABCC11 de pGem®-T easy à pcDNA3, nous avons transféré l'ADNc ABCC11 de pcDNA3 à pcDNA5/FRT.

b. Mutagenèse dirigée de l'ADNc ABCC11

- **Principe**

La mutagenèse dirigée est réalisée à l'aide d'une réaction PCR qui fait intervenir deux amorces complémentaires contenant la mutation désirée. Les plasmides parentaux sont ensuite éliminés par une enzyme de restriction (DpnI) qui digère spécifiquement les brins d'ADN méthylés (ou hémi-méthylés) (**Figure 16A**). En effet, le plasmide parental a été amplifié dans des bactéries compétentes qui méthylent l'ADN qu'elles synthétisent. A l'inverse, les plasmides amplifiés par PCR (comportant la mutation) sont synthétisés *in vitro* et ne sont pas méthylés. Après amplification dans des bactéries compétentes (DH5α), les plasmides sont discriminés selon leur profil de digestion. En effet, l'amorce utilisée pendant la PCR apporte, en plus de la mutation désirée, une mutation silencieuse ajoutant ou éliminant un site de restriction enzymatique. Une fois le plasmide sélectionné, la région entourant la mutation est séquencée puis sous-clonée (**Figure 16B**). La polymérase utilisée au cours de la PCR ne présente pas une haute fidélité et peut faire des erreurs donc amener d'autres mutations.

SNP	Mutation	Amorce	Profil de restriction	
			Enzyme	Modification
G120A	Arg19His	5' GGTGGCCTCGTGAATCATGGCATCGATATAGGC 3'	ClaI	+
G602A	Gly180Arg	5' ATTGCCAGTGTACTCAGGCCAATATTGATTATA 3'	Eco88I	-
C1014A	Ala317Glu	5' CTGGTTTTCCCACTCGAGGTATTCATGACAAGA 3'	XhoI	+
G1535A	Val491Ile	5' ACCTGTCCCGGCATCATCAATGGGGCACTGGAG 3'	SmaI	-
C1701T	Thr546Met	5' GGGGTCTGCGGCAACATGGGGAGTGGGAAGAGC 3'	SapI	+
C1952T	Arg630Trp	5' ACAGAGATTGGAGAGTGGGGCCTCAACCTCTCT 3'	BsrBI	-
G2006A	Val648Ile	5' AGCCTGGCCCGCGCCATCTATTCCGATCGTCAG 3'	PvuI	+
G2123A	Val687Ile	5' AGGGGGAAGACGGTCATCCTGGTGACCCACCAG 3'	PshAI	-
A2268G	Lys735Arg	5' ATCCAGAAGATGCATAGGGAAGCCACTTCGGAC 3'	Mph1103I	+
C2877G	Ser938Stop	5' CTCTTGCCCATCTTTTGAGAGCAATTCCTGGTC 3'	AlwNI	-
A2972G	Met970Val	5' ATGGGCGCCATAATCGTGGTTATTTGCTTCATT 3'	NarI	+
G3048A	Arg995Glu	5' CTGGAGAACTATAGCCAGTCTCCTTTATTCTCC 3'	Eco31I	-
A4095G	His1344Arg	5' GTGCTGAACTGTGACCGCATTCTGGTTATGGGC 3'	Mva1269I	+

Tableau 10. Amorces utilisées pour la mutagénèse dirigée.
Les nucléotides modifiés apparaissent en gras et en rouge. Le site de restriction ajouté ou supprimé est souligné pour chaque amorce.

Segment	Cycles	Température	Temps
1	1	94°C	10 min
2	10	94°C	10 sec
		55°C	30 sec
		68°C	8 min
3	25	94°C	15 sec
		55°C	30 sec
		68°C	8 min + 20 sec / cycle
4	1	68°C	7 min

Tableau 11. Programme PCR de la mutagénèse dirigée.

Afin d'éliminer le risque d'avoir une mutation dans le reste du plasmide, la région qui contient la mutation est découpée. Elle est ensuite intégrée à la place de la séquence correspondante sauvage, dans un plasmide dont la séquence entière est correcte. Ce plasmide a en effet été entièrement séquencé et n'a pas été soumis à la PCR.

- **Mode Opératoire**

Génération de la mutation

La mutation est introduite au cours d'une PCR réalisée avec le kit Expand Long Template PCR System (Roche). Le mélange réactionnel est composé de 350 µM de dNTP (A, T, G et C), 300 nM de chaque amorce (**Tableau 10**), 30 ng de plasmide (pcDNA5/FRT ABCC11wt), 3.75 U d'enzymes (Taq polymérase et Tgo polymérase) dans le tampon 1X (Expand Long Template Buffer 1, 17.5 mM $MgCl_2$). Le mélange réactionnel est ensuite soumis au programme PCR décrit dans le **Tableau 11**.

Elimination des brins parentaux : Digestion DpnI

Après une étape de purification sur bille (GeneClean® II kit) selon les instructions du fournisseur (Q-biogene), le produit de la PCR est soumis à 1 heure de digestion à 37 °C par 10 U de DpnI en tampon tango 1X (Fermentas).

Amplification et séparation des plasmides

Le produit de digestion par DpnI est utilisé pour transformer des bactéries compétentes (DH5α). Les plasmides (1 µL) et les bactéries (50 µL) sont mis en présence pendant 30 minutes à 4 °C. Ainsi les plasmides adhèrent à la surface des membranes bactériennes qui sont ensuite perméabilisées par un choc thermique: 1 minute à 37 °C puis 1 minute à 4 °C. Les bactéries sont ensuite transférées dans 500 µL de milieu de culture (LB 20 g/L) et incubées pendant 1 h à 37 °C sous agitation (temps nécessaire à l'expression du gène de résistance à l'ampicilline codé par le plasmide). La totalité des bactéries est ensuite étalée sur une gélose LB/Amp (LB Agar 32 g/L et Ampicilline 100 µg/mL) finalement incubée à 37 °C sur la nuit. Les colonies résistantes à l'ampicilline contiennent chacune un plasmide différent (1 colonie provenant de la prolifération d'une bactérie transformée).

SNP	Enzyme 1	Enzyme 2	Tampon
G120A	KpnI	BbvCI	NEBuffer 2
G602A	BbvCI	Bsp1407I	NEBuffer 4
C1014A	AgeI	Bsp1407I	Tango 1X
G1535A	SmaI	PmaCI	Tango 1X
C1701T	SmaI	PmaCI	Tango 1X
C1952T	SmaI	PmaCI	Tango 1X
G2006A	SmaI	PmaCI	Tango 1X
G2123A	Bsp1407I	BstEII	Tango 2X
A2268G	BstEII	ClaI	Tango 1X
C2877G	BstEII	ClaI	Tango 1X
A2972G	BstEII	ClaI	Tango 1X
G3048A	BstEII	ClaI	Tango 1X
A4095G	NotI	ClaI	Orange

Tableau 12. Enzymes de restriction utilisées pour le sous-clonage.

Discrimination des plasmides mutés et sauvages

Les plasmides sont extraits des colonies bactériennes à l'aide du kit « NucleoSpin® Plasmid » selon les instructions du fournisseur (Macherey Nagel). Selon l'enzyme dont le site de restriction a été ajouté/supprimé par la mutagenèse dirigée, les plasmides sont soumis à 1 h de digestion enzymatique. Les produits de la digestion sont mis en présence de bleu de charge (Bleu de bromophenol 0.06 %, Sucrose 10 %). Les différents fragments obtenus sont ensuite séparés par électrophorèse en gel d'agarose 1 % (130 V, 45 minutes). Le gel d'agarose utilisé contient également du BET qui s'intercale dans l'ADN et qui rend les fragments visibles sur plaque UV. Les plasmides contenant la mutation désirée (profil de digestion différent du plasmide sauvage) sont identifiés. La région entourant la mutation est alors séquencée (GenomExpress, Grenoble).

Sous-clonage de la mutation

Une fois que la région entourant la mutation a été séquencée et validée, elle est découpée du plasmide par deux enzymes de restriction (**Tableau 12**) lors d'une digestion d'1 h (3 µg de plasmide, 10 U de chaque enzyme en tampon approprié 1X). En parallèle, le plasmide sauvage (contenant ABCC11wt) est découpé de la même manière. Les produits de la digestion sont mis en présence de bleu de charge (Bleu de bromophenol 0.06 %, Sucrose 10 %). Les deux fragments issus de la digestion sont séparés par électrophorèse en gel d'agarose 1 % (130 V, 45 minutes) dans du tampon TAE 1X (Tris 40 mM, EDTA 1 mM, pH 8). Deux bandes sont prélevées par découpage du gel après migration : 1) la bande correspondant au petit fragment contenant la mutation (A) et 2) la bande correspondant au reste du plasmide sauvage (B). Les fragments sont extraits du gel à l'aide du kit « GeneClean® II » selon les instructions du fournisseur.

Le fragment B (reste du plasmide) est soumis à une étape de déphosphorylation ; la totalité de l'ADN est digéré pendant 1 h à 37 °C par 2 U de phosphatase alcaline en tampon 1 X (dephosphorylation buffer, Roche). Cette étape évite que le reste du plasmide se referme sur lui même. Le tampon de la réaction de déphosphorylation étant incompatible avec celui de la ligation, le fragment B est ensuite purifié (kit « GeneClean® II »).

A l'aide du kit « Rapid DNA Ligation » (Roche), les deux fragments sont finalement reliés pour former à nouveau un plasmide. La quantité de fragment B utilisée est généralement de 300 ng et le rapport molaire de B/A est de 2/1 (2 fragments A pour 1 fragment B). La quantité de fragment A est calculée selon la formule suivante :

$$\text{quantité de A} = \frac{\text{quantité de B} \times \text{taille de A}}{\text{taille de B}} \times \text{rapport } \frac{B}{A}$$

Les fragments A et B sont mis en présence de 5 U de T4 DNA ligase dans les tampons « T4 DNA ligation buffer » et « DNA ligation buffer » ramenés à 1X. La réaction de ligation s'effectue pendant 15 minutes à température ambiante. Le produit de ligation est utilisé pour transformer des bactéries DH5α. Les plasmides obtenus sont amplifiés et extraits avec le kit « NucleoSpin® Plasmid ». Les plasmides contenant la mutation désirée sont discriminés par leur profil de digestion et séquencés autour de la séquence sous-clonée pour vérification.

c. Génération des lignées MCF7 pcDNA3 +/- ABCC11 et HEK pcDNA3 +/- ABCC11

Les cellules MCF7 sont des cellules issues d'un carcinome mammaire humain. Les cellules HEK 293 correspondent quant à elles à des cellules de rein humain embryonnaire. Ces lignées cellulaires sont cultivées dans des conditions classiques : milieu DMEM (Dulbecco's Modified Eagle Medium) contenant 4,5 g/L de D-Glucose, supplémenté avec 10 % sérum de veau fétal (SVF), 1 % L-Glutamine (200 mM), et 1 % d'antibiotiques (pénicilline 2 UI/mL, streptomycine 200 µg/mL).

La transfection permet l'entrée d'un plasmide dans une cellule eucaryote afin qu'elle exprime l'ADNc. Nous avons utilisé l'agent de transfection ExGEN 500 (BD Biosciences). Ce produit est composé d'un polymère cationique à base de polyéthylènimine linéaire. Des complexes chargés positivement se forment entre le polymère et l'ADN. Après interaction avec les membranes cellulaires, une endocytose du complexe permet l'entrée de l'ADN qui sera ensuite libéré dans le cytoplasme, acheminé vers le noyau et protégé de la dégradation par l'agent ExGEN 500.

Des cellules MCF7 ou HEK 293 sont ensemencées dans une boite de Pétri. Lorsque la confluence atteint les 70 %, la transfection est réalisée avec 5 µg de plasmide pcDNA3 vide ou pcDNA3 ABCC11 et l'agent de transfection ExGEN 500, selon les recommandations du fournisseur. 24 h après la transfection, les cellules sont mises en présence de l'agent de sélection Généticine 0.5 mg/mL (PAA) dont la résistance est codée par le pcDNA3. Ainsi seules les cellules contenant le plasmide survivront et seront donc sélectionnées.

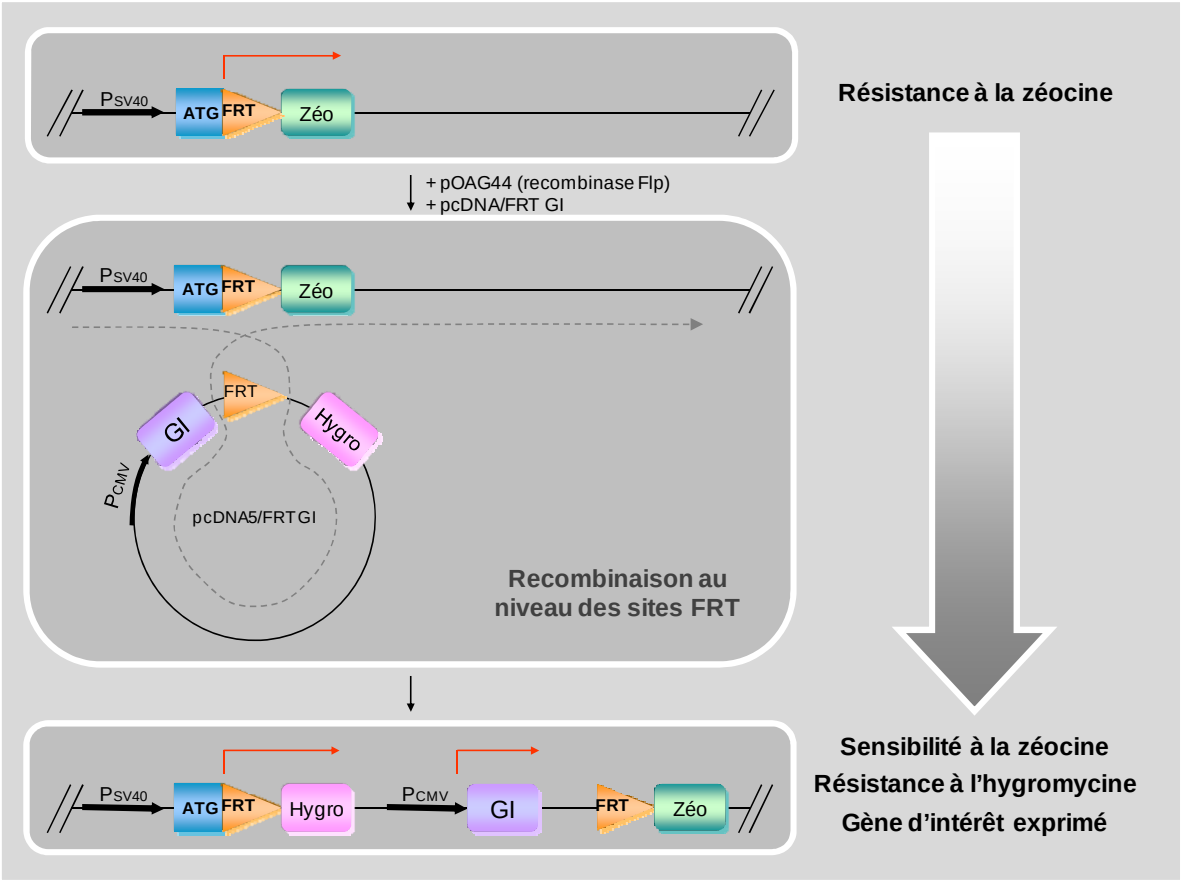

Figure 17. Système FlpIn/FRT.
La cellule exprime normalement un gène de résistance à la zéocine (Zeo) sous le contrôle du promoteur de SV40 (PSV40). La recombinase Flp exprimée par le plasmide pOAG44 permet d'insérer le gène de résistance à l'hygromycine (Hygro) derrière l'ATG qui lui manquait. Le gène d'intérêt (GI) est inséré à la suite sous le contrôle du promoteur de cytomégalovirus (PCMV). La cellule devient alors sensible à la zéocine (gène dépourvue d'ATG) et résistante à l'hygromycine. Elle exprime également le gène d'intérêt.

d. Génération des lignées FlpIn pcDNA5 +/- ABCC11

▪ **Système FlpIn**

Afin d'établir des transfectants exprimant stablement la protéine ABCC11 naturelle ou mutée, nous avons utilisé le système FlpIn (Dr. A. Di Pietro - IBCP Lyon) composé de 3 éléments clés :

▪ la lignée cellulaire FlpIn 293 dérivée des cellules de rein embryonnaire HEK 293. Elle présente un génome modifié par l'ajout d'un gène de résistance à la zéocine précédé par une séquence FRT (Flp recombinase target).

▪ le plasmide pOAG44 codant de manière transitoire la recombinase Flp.

▪ le plasmide pcDNA5/FRT comprenant un gène de résistance à l'hygromycine B précédé d'une séquence FRT mais dépourvu d'ATG. Ce plasmide peut également contenir un gène d'intérêt à la suite du gène de résistance.

Une double transfection permet d'introduire les deux plasmides pOAG44 et pcDNA5/FRT au sein des cellules Flp In 293. La recombinase codée par pOAG44 reconnaît les sites FRT contenus dans le génome cellulaire et dans le plasmide pcDNA5/FRT. Elle induit une recombinaison (**Figure 17**) permettant l'insertion du gène de résistance à l'hygromycine et du gène d'intérêt. Le gène de résistance à l'hygromycine est exprimé grâce à la présence en aval d'une séquence ATG. Le gène de résistance à la zéocine n'est plus à la suite de l'ATG et n'est donc plus exprimé. Le gène d'intérêt est exprimé sous le contrôle du promoteur CMV (cytomégalovirus) qui le précède. De cette manière, les cellules transfectées de manière stable (avec une intégration dans le génome) sont devenues sensibles à la zéocine et résistantes à l'hygromycine B. Le gène d'intérêt est intégré en un seul exemplaire et dans un endroit précis du génome. La population de cellules transfectées obtenue se compose donc de clones identiques ce qui rend inutile la sélection ultérieure de clone cellulaire.

▪ **Transfection des cellules FlpIn 293**

1 000 000 de cellules FlpIn 293 sont ensemencés dans chaque puits d'une plaque 6 puits. Après 24 h d'incubation à 37 °C sous 5 % de CO_2, 4 µg de pOAG44 et 444 ng de pcDNA5/FRT +/- ABCC11 sont mis en présence des cellules et la transfection est réalisée à l'aide de Lipofectamine™ 2000 (invitrogen™) selon les recommandations du fournisseur. Les cellules sont ensuite incubées à 37°C sous 5% de CO_2 pendant 24 heures. Les cellules sont ensuite trypsinées et transférées dans un flasque T75. Après 24 h, l'agent de sélection (hygromycine B 200 µg/mL) est ajouté dans le milieu de culture.

2.2.2. Analyse de l'expression

a. Expression en ARNm (RT-PCR-Q)

Les ARNm totaux des cellules sont extraits puis rétro-transcrit en ADNc. Une PCR (*Polymerase Chain Reaction*) quantitative spécifique d'un gène d'intérêt permet de quantifier la quantité d'ADNc de ce gène, proportionnelle à la quantité d'ARNm présente au départ.

▪ **Extraction des ARNm totaux**

Les cellules à analyser sont lysées dans 1 mL de TRIzol®. 200 µL de chloroforme sont ajoutés. Après centrifugation (15 minutes à 15 000 g 4°C), les ARN sont récupérés avec la phase supérieure. Cette phase est mélangée volume à volume (environ 500 µL) avec de l'isopropanol qui précipite les ARN. Après centrifugation (15 minutes à 15 000 g 4°C), les ARN forment un culot qui est lavé 3 fois par 500 µL d'éthanol 70°. Pour ce faire, le surnageant est éliminé et le culot est repris dans 500 µL d'éthanol 70°. Une centrifugation (5 minutes à 15 000 g 4°C) permet de retrouver le culot et d'éliminer l'éthanol. Après les 3 lavages, le culot est séché 5 minutes à 72 °C puis solubilisé dans 20 µL d'eau DEPC (Diethyl Pyrocarbonate, inhibiteur de nucléase). La concentration en ARNm est quantifiée au NanoDrop (Thermo Scientific).

▪ **Rétro-transcription des ARNm en ADNc (RT)**

1 µg d'ARNm est incubé dans un mélange réactionnel contenant 30 ng/µL d'amorces aléatoires (Random Primers), 0.5 mM de dNTP, 10 mM de DTT (dithiothreitol) et 10 U/µL de M-MLV-RT (*Moloney Murine Leukemia Virus Reverse Transcriptase*) dans du tampon 1X (First Strand Buffer). La rétro-transcription des ARNm en ADNc est effectuée pendant 1 h à 37 °C. Les ADNc obtenus sont finalement dilués au 1/15ème pour éviter les interférences entre le tampon de RT et celui de la PCR qui suit.

▪ **PCR quantitative (PCR-Q)**

Standardisation – PCR 18S

Une PCR quantitative est réalisée pour mesurer la quantité d'ADNc correspondant aux ARN ribosomaux 18S. Le taux d'ARN 18S (et donc d'ADNc) est équivalent au sein d'une même lignée et sert de référence. En effet, les résultats obtenus pour la PCR quantitative du gène d'intérêt sont rapportés à ceux obtenus pour la PCR 18S.

La PCR est une réaction en chaîne de polymérisation qui permet d'amplifier une séquence d'ADN donnée. Pour cela, deux amorces sont choisies de manière à encadrer la séquence à amplifier. A la fin de chaque cycle, la séquence entourée par les deux amorces est amplifiée de manière exponentielle.

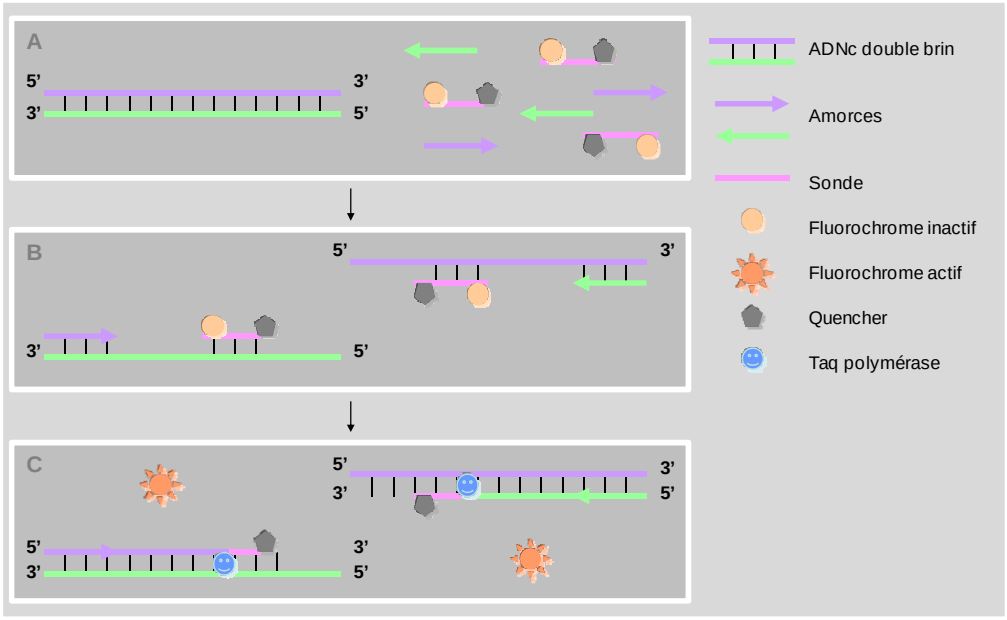

Figure 18. Illustration de la PCR quantitative (type 18S).
A) L'ADN double brin est mis en présence des amorces complémentaires et des sondes. B) Les amorces et les sondes se fixent à leur séquence complémentaire. Le fluorochrome fixé à la sonde en 5' est inactivé par la présence du quencher en 3'. C) Pendant l'élongation, la Taq polymérase se retrouve au niveau de l'amorce et la dégrade en 5'. Le fluorochrome se retrouve libre et à distance du quencher, il devient alors fluorescent. Plus la quantité d'ADN au départ est importante, plus la polymérase synthétise d'ADN et dégrade la sonde et plus la fluorescence émise est élevée.

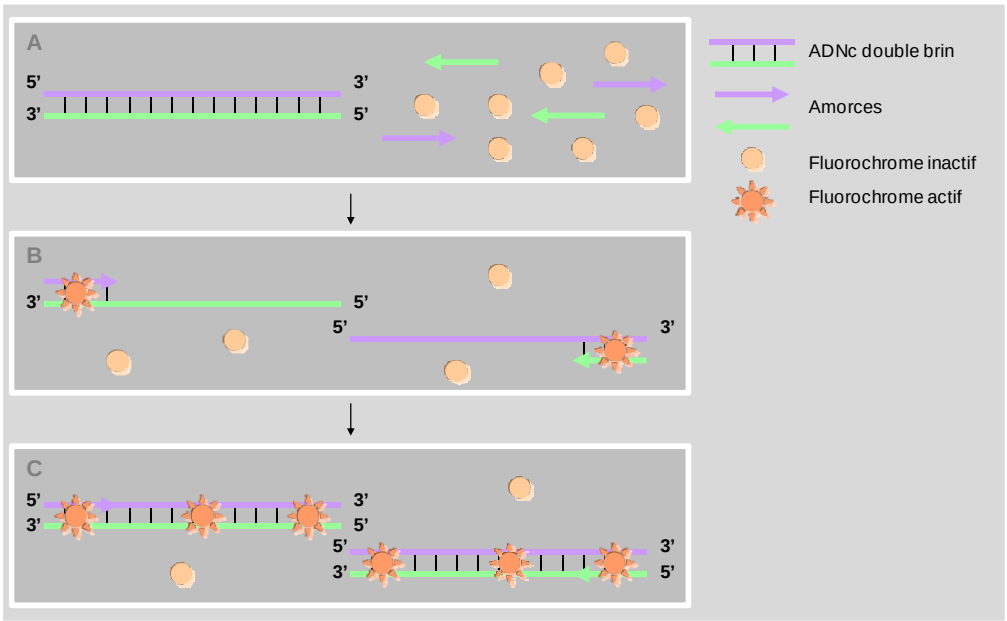

Figure 19. Illustration de la PCR quantitative (SYBR Green).
A) L'ADN double brin est mis en présence des amorces complémentaires et du fluorochrome inactif (type SYBR Green). B) Les amorces se fixent à leur séquences complémentaires. Le fluorochrome s'intègre pendant l'appariement et devient fluorescent. C) Pendant l'élongation, d'autres fluorochromes s'introduisent dans l'ADN double brin et augmente la fluorescence émise.

Dans le cas de la PCR quantitative des ADNc 18S, la polymérase utilisée est la Taq polymérase. Elle présente une activité 5'-exonucléasique. Les ADNc sont mis en présence d'amorces spécifiques et de sondes qui vont se fixer à leur séquence complémentaire. La sonde présente, à l'extrémité 5', un fluorochrome émetteur (reporter) qui est inhibé par un second fluorochrome suppresseur (quencher) placé à l'extrémité 3'. Lors de l'étape d'élongation, la Taq polymérase synthétise l'ADN à partir de l'amorce. Lorsqu'elle arrive au niveau de la sonde fixée, elle dégrade son extrémité 5' et libère le fluorochrome émetteur. Ceci entraîne une émission fluorescente proportionnelle à la quantité d'ADN synthétisé donc à la quantité d'ADN au départ (**Figure 18**). Les résultats sont exprimés en Ct (*crossing threshold*) correspondant au cycle où le signal fluorescent dépasse celui du bruit de fond.

Mode opératoire

La PCR est réalisée sur 1.67 µL d'ADNc dilué au 1/15ème dans le mélange réactionnel suivant : 1.5 mM de Mg^{2+}, 0.2 mM de dNTP, les amorces et les sondes (Applied biosystems, Warrington UK) et la Taq polymerase dans du tampon 1X (10X PCR Rxn buffer). La réaction de PCR s'effectue suivant 35 cycles de 2 étapes : 95 °C pendant 15 secondes puis 60 °C pendant 1 minute.

PCR du gène d'intérêt

Principe

La PCR quantitative fait intervenir un agent liant l'ADN double brin naissant: le SYBR safe. Ce fluorochrome fluoresce lorsqu'il se complexe à l'ADN. Durant la PCR, et plus particulièrement pendant l'étape d'élongation, une augmentation de la fluorescence proportionnelle à la quantité d'ADN double brin synthétisé est observée (**Figure 19**). Lorsque la PCR est suivie en temps réel, l'augmentation du signal de fluorescence est observée pendant l'étape d'élongation puis l'émission décroît complètement avec l'étape suivante de dénaturation de l'ADN. Par conséquent, la fluorescence est mesurée à la fin de chaque étape d'élongation pour chacun des cycles.

A la fin de l'amplification, le point de fusion des produits de PCR (amplicon) est déterminé. Pour cela, la température est augmentée de manière régulière. A la température de fusion, les deux brins d'ADN se séparent et la fluorescence décroit rapidement. Cette température dépend de la composition en nucléotide et de la longueur de l'amplicon. Pour une même paire d'amorces, tous les amplicons ont la même température de fusion. Le cas contraire indique qu'il y a eu formation de dimères d'amorces, mésappariement ou contamination (ADN génomique).

Gène d'intérêt	Amorces			Programme
ABCC5	5'	AGGGGCAAGAAAGAGAAGGTGAGG	3'	50 cycles (95 °C - 15 s; 63 °C - 7 s et 72 °C - 15 s)
	5'	GAGGGGGTCGTCCAGGATGTAGAT	3'	
ABCC11	5'	GTCTGGGTTCTCATCCACACATCC	3'	50 cycles (95 °C - 15 s; 63 °C - 7 s et 72 °C - 15 s)
	5'	CCAGAGCTTTGCTGGGGTCTTGTA	3'	
ABCG2	5'	TGCAACATGTACTGGCGAAGA	3'	50 cycles (95 °C - 15 s; 62 °C - 15 s et 72 °C - 15 s)
	5'	TCTTCCACAAGCCCCAGG	3'	
TK1	5'	GGGGCAGATCCAGGTGATTC	3'	50 cycles (95 °C - 15 s; 58 °C - 8 s et 72 °C - 10 s)
	5'	GCATACTTGATCACAGGCACTT	3'	
TK2	5'	TTACCTTCGGACCAATCCTG	3'	50 cycles (95 °C - 0 s; 60 °C - 10 s et 72 °C - 12 s)
	5'	TGCTTCCGATTCTCTGGAGT	3'	

Tableau 13. Séquences des amorces et programmes utilisés pour la PCR quantitative.

Par exemple, les dimères d'amorces étant plus petits que les amplicons, la température de fusion détectée sera inférieure à celle attendue. Tout résultat de quantification ne sera donc validé que si la température de fusion est correcte.

Mode opératoire

La PCR est réalisée sur 1.67 µL d'ADNc dilué au 1/15ème dans le mélange réactionnel suivant : 2 mM de $MgCl_2$ et 0.25 mM d'amorces (**Tableau 13**) dans le tampon 1X (LightCycler® FastStart Reaction Mix SYBR Green). La réaction de PCR commence par une étape 10 minutes à 95°C puis s'effectue selon un programme dépendant du gène d'intérêt (**Tableau 13**). Elle est suivie par une étape permettant d'obtenir le point de fusion (0 sec à 95 °C, 15 sec à 65 °C et 0 sec à 95 °C).

b. Expression protéique par Western blot

- **Principe**

Les protéines sont extraites des cellules, séparées selon leur poids moléculaire par électrophorèse puis transférées sur membrane de nitrocellulose. La membrane est incubée avec un anticorps primaire (anti-protéine d'intérêt) puis avec un anticorps secondaire (anti-anticorps primaire) couplé à la peroxydase. Pour finir, la membrane est imprégnée par le substrat de la peroxydase (ECL pour *Enhanced ChemoLuminescence*). Ce dernier est dégradé en un produit chimio-luminescent qui va imprégner un film photo-radiographique. La protéine d'intérêt apparaît sur le film sous la forme d'une bande au niveau de son poids moléculaire (mesuré grâce à un marqueur de taille). L'intensité de la bande est proportionnelle à la quantité de protéine présente dans l'échantillon. L'homogénéité des dépôts de chaque échantillon est visualisée grâce à une coloration des protéines totales au rouge ponceau.

- **Mode Opératoire**

Extraction des protéines

Environ 15 millions de cellules sont lysées par une incubation d'une heure dans 50 µL tampon de lyse (Tris 50 mM, $MgCl_2$ 10 mM, SDS 0.25 %, PMSF 75 µg/mL, TPCK 10 µg/mL, Inhibiteur de protéase (Roche), nucléase benzonase® 1 U/µL, orthovanadate de sodium 1 mM). Après centrifugation (10 minutes à 15 000 g à 4°C), les débris cellulaires sont éliminés sous forme de culot. Le surnageant correspond aux protéines totales.

Les protéines sont dosées selon la méthode de Bradford. Une gamme étalon est réalisée avec 5 points (0, 250, 500, 750 et 1000 µg/mL de BSA). 10 µL de chaque point de gamme et de chaque échantillon sont déposés en triplicate dans 300 µL de Bleu de Coomassie. Le bleu de Commassie de couleur marron réagit avec les protéines et devient bleu.

ANTICORPS PRIMAIRES				
Protéine d'intérêt	**Fournisseur**	**Concentration**	**Dilution**	**Origine**
ABCC11	Santa Cruz	200 µg/mL	100	IgG de lapin
Tubuline alpha	Sigma	1 mg/mL	2000	IgG de souris
ANTICORPS SECONDAIRES				
Protéine d'intérêt	**Fournisseur**		**Dilution**	**Origine**
IgG de souris	Sigma	-	8000	IgG de lapin
IgG de lapin	Sigma	-	3000	IgG de chèvre

Tableau 14. Condition d'utilisation des anticorps en western blot.

L'intensité de la coloration bleu est proportionnelle à la quantité de protéines et peut être mesurée à 595 nm à l'aide du lecteur de plaque Multiscan Ex (Thermo Scientific).

Electrophorèse

Pour chaque échantillon, le volume équivalent à 100 µg de protéines totales est dilué volume à volume avec du tampon Triton X-100 0.5 % contenant 2 U/µL de nucléase benzonase®. Cette étape casse la structure tertiaire des protéines et dégrade l'ADN qui rend l'échantillon visqueux. Chaque échantillon est repris dans du tampon Laemmli 1X (Tris 0.06 M, SDS 2 % ; 2-mercaptoéthanol 5 %, Glycérol 10 %, Bleu de Bromophénol 0.1 %) qui charge les protéines de manière négative. Ainsi chargées, les protéines soumises à champ électrique seront attirées par l'anode.

Plus les protéines sont petites, plus elles passeront facilement à travers les mailles du gel d'acrylamide. Les échantillons sont donc placés en haut d'un gel d'acrylamide 8 % (côté cathode). Puis les protéines sont séparées selon leur poids moléculaire par migration électrophorétique (1 h, 130 V) dans du tampon TGS 1X (Tris 25 mM, Glycine 186 mM, SDS 0.1 %). En parallèle, un marqueur de poids moléculaire (Dual color prestained precision plus protein, Bio-rad) est soumis à la même migration. Il permettra d'avoir une échelle de taille sur le gel sous la forme de bandes colorées.

Transfert

Les protéines du gel sont transférées sur une membrane de PVDF (polyfluorure de vinylidène) de manipulation plus simple que le gel fragile. Pour cela, le gel est mis au contact d'une membrane de PVDF et soumis à un courant électrique de 20 V pendant 5 minutes (*iBlot™ Dry Blotting System* – Invitrogen™). Le gel est placé du côté de la cathode et la membrane du côté de l'anode. Les protéines chargées négativement quittent le gel pour aller se poser sur la membrane.

Révélation

Afin d'assurer la spécificité de la révélation en saturant les sites de fixation potentiels non utilisés de la membrane, cette dernière est incubée sous agitation pendant 1 h dans une solution de TBS-Tween 20 (0.05%) + 5% de lait. La membrane est ensuite incubée avec l'anticorps primaire (dirigé contre la protéine d'intérêt). Les conditions d'utilisation de cet anticorps sont détaillées en **Tableau 14**. Après 3 lavages de 10 minutes en TBS-Tween 20 (0.05%) + 5% de lait (sous agitation), la membrane est incubée avec l'anticorps secondaire (dirigé contre l'anticorps primaire) pendant 1 heure sous agitation.

Après 3 lavages de 10 minutes en TBS-Tween 20 (0.05%), la membrane est recouverte par 1 mL d'ECL (Solution A et B mélangées volume à volume). En chambre noire, la membrane est mise en contact avec un film auto-radiographique. La peroxydase de l'anticorps secondaire dégrade l'ECL en un produit chimio-luminescent qui imprègne le film. La protéine d'intérêt apparaît sous la forme d'une bande noire (au niveau de son poids moléculaire) dont l'intensité est proportionnelle à la quantité de protéine et peut être quantifié avec le logiciel ImageJ®.

Coloration des protéines au Rouge Ponceau

Afin de colorer la totalité des protéines, la membrane est incubée pendant 5 minutes en présence de colorant Rouge Ponceau puis lavées pendant 5 minutes en en TBS-Tween 20 (0.05%). La membrane est ensuite séchée à l'air libre.

c. Expression protéique par marquage immuno-fluorescent

- **Principe**

Les cellules en culture sont fixées puis perméabilisées pour être mises en présence d'un anticorps primaire (dirigé contre la protéine d'intérêt) puis d'un anticorps secondaire fluorescent (dirigé contre l'anticorps primaire) et enfin de DAPI qui imprègne les noyaux cellulaires. Le marquage fluorescent du noyau et des protéines d'intérêt est ensuite observé par microscopie confocale à fluorescence.

- **Mode opératoire**

300 000 cellules sont ensemencées sur une lame de verre traitée (Labteck) comportant 4 puits différenciés. Après 24 h d'incubation à 37 °C et sous 5 % de CO_2, le milieu de culture est éliminé, les cellules sont rincées au PBS 1X et incubées 10 minutes en présence de méthanol 100 % (étape de fixation sur le support). Après 3 lavages de 5 minutes au PBS 1X, les cellules sont perméabilisées au PBS Triton 0.1 % pendant 20 minutes. De nouveau après 3 lavages de 5 minutes au PBS 1X, les sites antigéniques aspécifiques sont bloqués par une incubation de 30 minutes en présence de PBS 1X, SVF 1%, BSA 0.1%. Puis 150 µL d'anticorps anti ABCC11 de Santa-Cruz (IgG de lapin, 2 µg/mL) sont mis en présence des cellules pendant une nuit à 4 °C. Après 3 lavages de 5 minutes au PBS 1X, les cellules sont incubées pendant 1h30, à l'abri de la lumière, avec 100 µL d'anticorps secondaire fluorescent anti-IgG de lapin de DAKO (IgG de porc). Les noyaux sont ensuite marqués par incubation de 10 minutes en présence de 200 µL de DAPI 1 µg/mL. Après 3 lavages de 5 minutes au PBS 1X, la partie supérieure délimitant les puits sur la lame est éliminée. Une fois la lame sèche (après 15 minutes à température ambiante), une lamelle est disposée sur les cellules avec une goutte de milieu de montage aqueux, faramount (Dakocytomation).

2.2.3. Analyse de la Chimiorésistance par test de cytotoxicité au MTT

Le test de cytotoxicité au MTT permet de mesurer la concentration en médicament inhibant 50 % de la prolifération cellulaire (CI50). Après traitement, les cellules sont incubées en présence de MTT (bromure de 3-(4,5-dimethylthiazol-2-yl)-2,5-diphenyl tetrazolium)) puis sont solubilisées dans de l'isopropanol/HCl. Le MTT de couleur jaune est réduit par la succinate déshydrogénase mitochondriale des cellules vivantes en formazan de couleur bleu-violacée. L'intensité de la coloration est donc proportionnelle au nombre de cellules vivantes. La différence d'absorbance à 490 et 560 nm est mesurée pour calculer la CI50.

Les cellules sont ensemencées à hauteur de 6000 cellules par puits en plaque 96 puits. Après 24 h d'incubation à 37°C sous 5 % de CO_2, les cellules sont traitées en triplicate par des dilutions croissantes en médicaments (dilution en cascade). Après 72 h de traitement, les cellules sont mises en présence 5 mg/mL de MTT pendant 2 h. Le milieu de culture contenant le MTT est ensuite aspiré puis remplacé par 100 µL d'Isopropanol 90 % / HCl 1 %. Après 15 minutes d'attente à température ambiante, l'absorbance est mesurée à 490 nm (bruit de fond) et à 560 nm (absorbance du MTT réduit) à l'aide du lecteur de plaque Multiscan Ex (Thermo Scientific). La différence entre les deux absorbances est calculée pour chaque puits. La moyenne est réalisée pour chaque traitement et rapportée à la moyenne obtenue pour les cellules non traitées (témoin 100 % de viabilité).

2.2.4. Analyse de l'activité de transport du 5FdUMP par HPLC-MS/MS

Les cellules sont mises en présence du 5FdURD (5-Fluoro-2'-Deoxyuridine) pour une période d'accumulation où le 5FdURD rentre dans la cellule et se métabolise en 5FdUMP (5-FluoroDésoxy-Uracile MonoPhosphate, substrat d'ABCC11). Après lavage, les cellules sont soumises ou non à une période d'efflux (sortie du 5FdUMP via ABCC11) en présence ou non d'inhibiteur d'ABCC11 (MK571). Les surnageants d'efflux sont récupérés pour dosage du 5FdUMP extracellulaire par HPLC MS/MS. Après lavage, les cellules sont reprises dans du méthanol pour le dosage du 5FdUMP intracellulaire. La concentration en 5FdUMP est ensuite rapportée à la quantité de protéine totale. En analysant les quantités de 5FdUMP intra- et extracellulaires de lignées cellulaires exprimant différents variants d'ABCC11, il est possible de savoir si la protéine est plus ou moins fonctionnelle au niveau du transport du 5FdUMP.

500 000 cellules par puits sont ensemencées dans une plaque 6 puits et incubées 24 h à 37 °C et sous 5 % de CO_2. Après élimination du milieu de culture, les cellules sont soumises à une étape d'accumulation du 5FdURD par une incubation de 15 minutes avec du 5FdURD 100 µM (en milieu de culture). Un contrôle est réalisé avec une incubation dans du milieu de culture vide. Le milieu de traitement est ensuite éliminé et les cellules sont rincées 3 fois par 2 mL de PBS à 4°C. Les cellules peuvent ensuite être soumises ou non à une étape d'efflux. Pour cela, elles sont de nouveau incubées pendant 15 minutes avec du milieu de culture supplémenté ou non par 15 µM de MK571 (inhibiteur). Le milieu d'efflux ou surnageant est récupéré pour dosage du 5FdUMP extracellulaire par HPLC-MS/MS (Pr. Guitton, CBS Lyon Sud). Les cellules sont finalement rincées 3 fois au PBS à 4°C. Pour toutes les conditions (accumulation seule, accumulation + efflux normal, accumulation + efflux en présence de MK571), les cellules sont grattées dans 1 mL de PBS à 4°C sur de la glace (maintien d'une température froide pour arrêter le transport du 5FdUMP). 100 µL de la suspension cellulaire est réservée pour un dosage protéique. Le reste de la suspension cellulaire est centrifugée 5 minutes à 1500 g à 4°C. Les culots de cellules sont finalement repris dans 100 µL de méthanol et serviront au dosage du 5FdUMP extracellulaire par HPLC-MS/MS (Pr. Guitton, U820).

Le dosage des protéines est réalisée en mélangeant 20 µL de suspension cellulaire, 50 µL de NaOH 1N (lyse des cellules) et 1 mL de Bleu de Coomassie. Chaque échantillon est ensuite répartie en triplicate dans une plaque de 96 puits, en parallèle d'une gamme étalon (0, 250, 500, 750 et 1000 µg/mL de BSA) réalisée sur le même schéma (20 µL du point de gamme, 50 µL de NaOH 1N et 1 mL de Bleu de Coomassie). Le bleu de Commassie de couleur marron réagit avec les protéines et devient bleu. L'intensité de la coloration bleu est proportionnelle à la quantité de protéines et peut être mesurée à 595 nm à l'aide du lecteur de plaque Multiscan Ex (Thermo Scientific).

Lignée cellulaire	ARNm ABCC11		
	R2	R3	R4
HEK pcDNA3	1	1	1
HEK ABCC11 wt	1870	59,25	30,27
HEK ABCC11*602	83,2	11,5	7,17

Tableau 15. Quantification du niveau en ARNm ABCC11 à différents passages.
Les ARNm ont été extraits de cellules à différents repiquages (intervalle entre repiquage ≈ 3 jours). A partir de ces ARNm ont été effectuées des RT-PCR-Q spécifiques pour le gène ABCC11. Les résultats concernant ABCC11 ont été rapportés aux résultats obtenus pour un gène de référence codant pour la sous-unité ribosomale 18S.

Lignée cellulaire	n	ABCC11
Flp5	4	1
Flp ABCC11wt	4	2835
Flp ABCC11*1014	2	366,81
Flp ABCC11*1701	2	1135
Flp ABCC11*1952	3	1430
Flp ABCC11*2006	2	1910
Flp ABCC11*2123	2	988

Tableau 16. Quantification des ARNm ABCC11 dans les transfectants Flp In 293.
Les ARNm ont été extraits des cellules puis soumis à une RT-PCR-Q spécifique pour le gène ABCC11. Les résultats concernant ABCC11 ont été rapportés aux résultats obtenus pour un gène de référence codant pour la sous-unité ribosomale 18S.

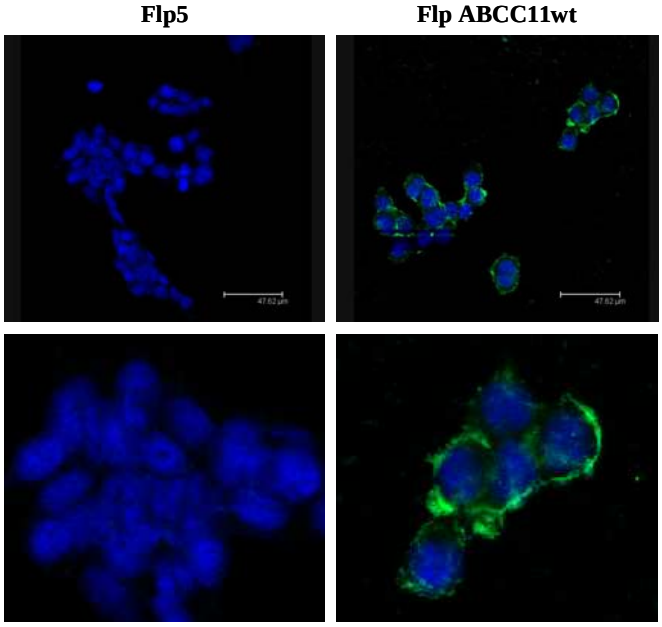

Figure 20. Marquage immuno-fluorescent de la protéine ABCC11.
Les cellules en culture ont été fixées puis marquées par un anticorps immuno-fluorescent dirigé contre la protéine ABCC11 (fluorescence verte). L'ADN des noyaux cellulaires a été coloré au DAPI (fluorescence bleue).

2.3 Résultats

2.3.1. Génération de transfectants stables

Par mutagenèse dirigée, nous avons reproduit la plupart des SNP non synonymes : G120A, G602A, C1014A, G1535A, C1701T, C1952T, G2006A, G2123A, A2268G, C2877G, G3048A, A4095G. Dans un premier temps, nous avons transfecté des cellules MCF7 (carcinome mammaire) dans lesquelles nous n'avons pas obtenu de surexpression d'ABCC11 naturelle. Puis, nous avons généré des transfectants à partir de cellules HEK 293 T. Les transfectants HEK ABCC11wt (transfectant pcDNA3 ABCC11wt) et HEK ABCC11*602 (transfectant pcDNA3 ABCC11*602, portant la mutation G602A) ont montré une surexpression en ARNm ABCC11 par rapport au HEK pcDNA3 (transfectées avec le vecteur vide) (**Tableau 15**). Mais cette surexpression s'est avérée instable au cours du temps et a été perdue après un très faible nombre de repiquage cellulaire.

Finalement, nous avons opté pour la lignée Flp In 293. Les transfectants obtenus ont été appelés :

- Flp 5 (Flp In 293 transfectées par le vecteur vide pcDNA5/FRT) ;
- Flp ABCC11wt (Flp In 293 transfectées par pcDNA5/FRT ABCC11 de type sauvage) ;
- Flp ABCC11*1014, Flp ABCC11*1701, Flp ABCC11*1952, Flp ABCC11*2006 et Flp ABCC11*2123 (respectivement pour les Flp In 293 transfectées par pcDNA5/FRT ABCC11 mutée en 1014, en 1701, en 1952, en 2006 ou en 2123).

2.3.2. Caractérisation des transfectants Flp In 293 (1)

a. Comparaison des niveaux d'ARNm ABCC11

Par RT-PRC-Q, nous avons pu observer une forte surexpression en ARNm ABCC11, aussi bien dans les Flp ABCC11wt que dans les Flp ABCC11 mutée (**Tableau 16**).

b. Analyse de l'expression protéique d'ABCC11

Nous avons analysé l'expression d'ABCC11 par un marquage immuno-fluorescent. Nous avons pu observer une surexpression de la protéine ABCC11 naturelle dans la lignée Flp ABCC11wt par rapport à la lignée Flp5 (**Figure 20**). Cette protéine montre une tendance à se localiser à la membrane cellulaire sans exclure une présence au niveau du cytoplasme. Aucune donnée n'est disponible sur l'expression protéique des ABCC11 mutées.

Lignée cellulaire	5FdURD	MTX
	FR	FR
Flp5	1,0 ± 0	1,0 ± 0
Flp ABCC11wt	2,2 ± 0,5	1,3 ± 0,2
Flp ABCC11*1014	1,3 ± 1,0	0,6 ± 0,1
Flp ABCC11*1701	0,8 ± 0,5	0,8 ± 0,3
Flp ABCC11*1952	1,0 ± 0,3	0,6 ± 0,2
Flp ABCC11*2006	1,2 ± 0,5	0,5 ± 0,2
Flp ABCC11*2123	2,6 ± 0,7	0,6 ± 0,5

Tableau 17. Chimiorésistance des transfectants Flp In 293.
La moyenne des facteurs de résistance est indiquée plus ou moins l'écart-type (N = 5). MTX = méthotrexate

N 1	5FdUMP (ng/mg de protéines)							
	Surnageants				Cellules			
Lignée	U	U + E	U + E/MK	Inhibition	U	U + E	U + E/MK	Inhibition
Flp5	189	43	52	21%	852	698	900	29%
Flp ABCC11wt	883 ⇧	127 ⇧	73	-43%	3446 ⇧	7505 ⇧	5921	-21%
Flp ABCC11*1014	105 ⇩	100 ⇧	83	-17%	2153 ⇧	809 ⇧	1002	24%
Flp ABCC11*1701	25 ⇩	24 ⇩	31	29%	76 ⇩	88 ⇩	92	5%
Flp ABCC11*1952	56 ⇩	11 ⇩	13	18%	115 ⇩	32 ⇩	108	238%
Flp ABCC11*2006	42 ⇩	29 ⇔	0	-100%	1836 ⇧	837 ⇧	522	-38%
Flp ABCC11*2123	173 ⇔	33 ⇔	26	-21%	1940 ⇧	642 ⇔	711	11%

N 2	5FdUMP (ng/mg de protéines)							
	Surnageants				Cellules			
Lignée	U	U + E	U + E/MK	Inhibition	U	U + E	U + E/MK	Inhibition
Flp5	1148	97	126	30%	3142	2399	2593	8%
Flp ABCC11wt	2337 ⇧	246 ⇧	184	-25%	4634 ⇧	6183 ⇧	3773	-39%
Flp ABCC11*1014	428 ⇩	56 ⇩	76	36%	2476 ⇩	1770 ⇩	2305	30%
Flp ABCC11*1701	234 ⇩	33 ⇩	16	-52%	200 ⇩	211 ⇩	196	-7%
Flp ABCC11*1952	201 ⇩	63 ⇩	19	-70%	306 ⇩	104 ⇩	112	8%
Flp ABCC11*2006	669 ⇩	63 ⇩	54	-14%	3945 ⇧	2880 ⇧	1899	-34%
Flp ABCC11*2123	851 ⇩	7 ⇩	47	571%	2560 ⇩	302 ⇩	1728	472%

Tableau 18. Analyse du transport du 5FdUMP par HPLC MS/MS.
Les cellules sont incubées dans du milieu de culture en présence de 5FdURD, qui entre dans les cellules pour être métabolisé en 5FdUMP (période U pour *uptake*). Ce dernier étant substrat d'ABCC11, il sera efflué des cellules pendant une seconde phase d'incubation dans du milieu contenant ou non un inhibiteur d'ABCC11, le MK571 (période U+E pour *uptake +efflux* et U+E/MK pour *uptake +efflux en présence de MK571*). La concentration de 5FdUMP contenu dans le milieu d'efflux (surnageant) et dans les cellules est quantifiée par HPLC MS/MS puis rapportée à la concentration en protéine totale de l'échantillon (reflétant le nombre de cellules). Deux expériences sont représentées (N1 et N2). Les variations de concentration en 5FdUMP entre chaque lignée et la lignée Flp5 (contrôle n'exprimant pas ABCC11) sont illustrées par les symboles ⇩ (diminution) ⇔ (pas de modification) ⇧ (augmentation). L'inhibition de l'efflux induite par la présence de MK571 est indiquée en rouge (augmentation de l'efflux du 5FdUMP) ou en bleue (diminution).

c. Analyse de la chimiorésistance

Les niveaux de résistance à différents anticancéreux ont été analysés par test de cytotoxicité au MTT (**Tableau 17**). D'après les facteurs de résistance (FR) obtenus, ABCC11 confère une résistance au 5FdURD (FR = 2.2) mais pas au méthotrexate (FR = 1.3). Les lignées cellulaires exprimant la protéine mutée en 1014, 1701, 1952 et 2006 montrent un niveau de résistance au 5FdURD équivalent à la lignée cellulaire Flp5. La lignée cellulaire Flp ABCC11*2123 semble présenter le même profil de résistance que la lignée cellulaire exprimant la protéine naturelle. Concernant le méthotrexate, les lignées cellulaires exprimant une protéine mutée ont un facteur de résistance semblable à celui des Flp ABCC11wt.

d. Transport du 5FdUMP

- **Analyse de l'efflux du 5FdUMP**

L'activité d'efflux du 5FdUMP a été analysée dans les différentes lignées cellulaires. Pour cela, les cellules ont été, dans une première phase, incubées dans du milieu de culture en présence de 5FdURD, qui entre dans les cellules pour être métabolisé en 5FdUMP. Ce dernier étant substrat d'ABCC11, il est efflué des cellules pendant la seconde phase d'incubation dans du milieu contenant ou non un inhibiteur d'ABCC11, le MK571. Le 5FdUMP est ensuite quantifié dans le milieu d'efflux (surnageants) et les cellules. La concentration en 5FdUMP est rapportée à la concentration en protéine totale, proportionnelle au nombre de cellules dans l'échantillon.

Les résultats préliminaires (n=2) (**Tableau 18**) indiquent qu'après la période d'incubation avec le 5FdURD (période U pour *uptake*), la quantité de 5FdUMP intracellulaire varie de manière importante entre chaque lignée cellulaire. En effet, la lignée Flp ABCC11wt et la lignée Flp ABCC11*2006 montrent une quantité plus importante de 5FdUMP intracellulaire que les Flp5. A l'inverse, les lignées Flp ABCC11*1701 et 1952 montrent une diminution de cette quantité. Pour finir, les lignées Flp ABCC11*1014 et 2123 montrent soit une augmentation, soit une diminution en fonction de l'expérience analysée (résultats non reproductibles). Après la période d'efflux (U+E pour *uptake* + *efflux*), les cellules Flp5 montrent une diminution logique de la quantité de 5FdUMP intracellulaire, en partie inhibée par la présence de MK571 (inhibition de l'efflux de 29 et 8 %). De manière surprenante, les Flp ABCC11wt et Flp ABCC11*2006 montrent une augmentation de la quantité de 5FdUMP dans la cellule après la période d'efflux. De plus, cette quantité diminue sous l'effet du MK571.

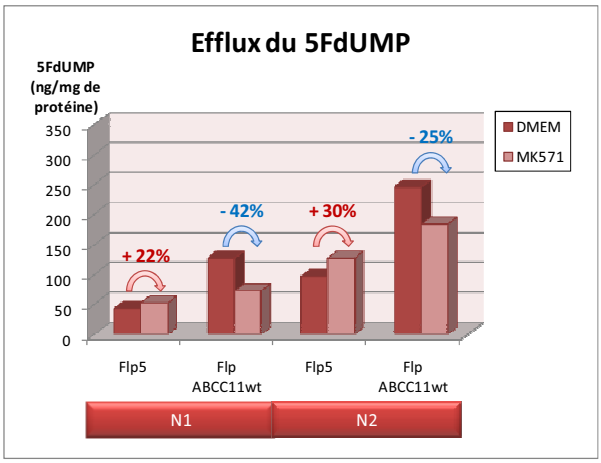

Figure 21. Efflux du 5FdUMP dans les lignées Flp5 et Flp ABCC11wt.
Les cellules sont mises en présence de 5FdURD qui entre dans les cellules où il est métabolisé en 5FdUMP. Puis les cellules sont placées dans du milieu contenant du MK571 (MK571) ou non (DMEM), un inhibiteur d'ABCC11. Le 5FdUMP retrouvé dans le surnageant est dosé par HPLC MS/MS et rapporté à la concentration en protéine totale. N1 et N2 représente 2 expériences différentes.

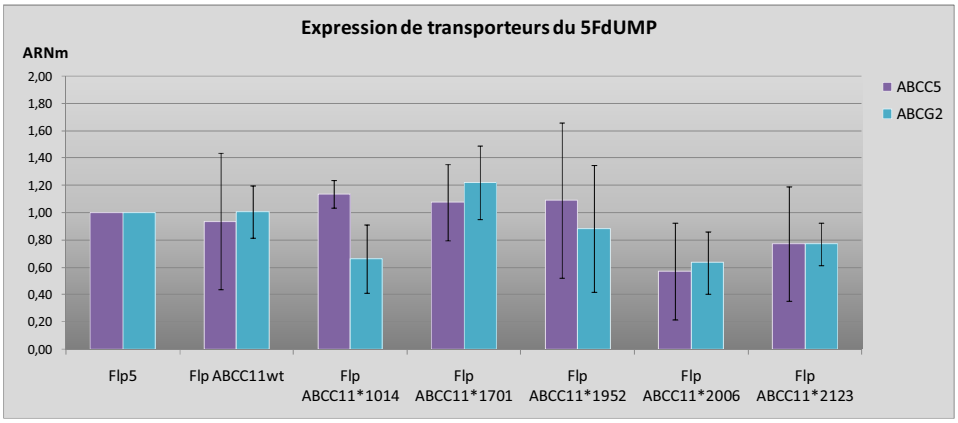

Figure 22. Quantification du niveau d'expression d'autres transporteurs du 5FdUMP.
Les niveaux d'expression en ARNm d'ABCC5 et d'ABCG2 ont été quantifiés par RT-PCR-Q (n=3 au minimum).

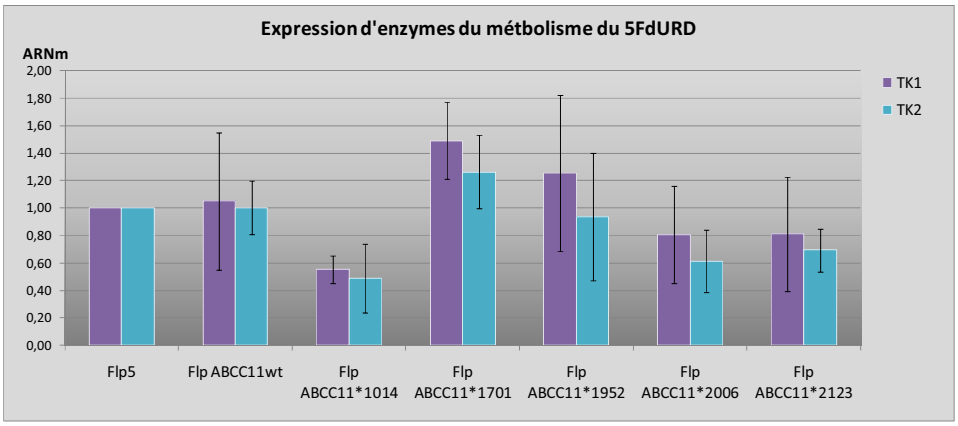

Figure 23. Quantification du niveau d'expression de certaines enzymes du métabolisme du 5FdURD.
Les niveaux d'expression en ARNm de la TK1 et de la TK2 (*Thymidine Kinase 1 et 2*) ont été quantifiés par RT-PCR-Q (n=3 au minimum).

Ce phénomène n'est pas observé pour les autres lignées cellulaires qui montrent une diminution de la quantité de 5FdUMP intracellulaire après la période d'efflux. Le MK571 semble inhiber une partie de l'efflux du 5FdUMP pour les lignées Flp ABCC11*1014, 1952 et 2123. L'effet du MK571 n'est pas reproductible sur la lignée Flp ABCC11*1701.

Le 5FdUMP est bien retrouvé dans le milieu d'efflux. Dans toutes les conditions, la quantité de 5FdUMP est plus élevée dans le surnageant des Flp ABCC11wt que dans celui des Flp5. De plus, les cellules Flp ABCC11wt semblent sensibles à la présence de MK571 dans le milieu d'efflux. En effet, lorsque l'efflux est réalisé en présence de MK571, la quantité de 5FdUMP retrouvé dans le surnageant est diminuée par rapport à celle observée en absence de MK571 (**Figure 21**). Pour les autres lignées, les résultats ne sont pas reproductibles et difficilement analysables.

▪ **Analyse du niveau d'expression des autres transporteurs ABC**

D'autres transporteurs ABC sont responsables d'une résistance accrue au 5-FU (précurseurs du 5FdUMP) tels qu'ABCC5 [221] et ABCG2 [222]. Il a été démontré que le 5FdUMP est transporté par ABCC5 mais rien n'a encore été décrit pour ABCG2 qui pourrait potentiellement le transporter aussi. Afin de vérifier leur niveau d'expression basale et de voir si la surexpression d'ABCC11 modifie ce niveau, nous avons quantifié l'expression d'ABCC5 et d'ABCG2 par RT-PCR-Q (**Figure 22**). Il n'y a pas de différence significative de l'expression de ces trois transporteurs entre toutes les lignées cellulaires.

▪ **Analyse du niveau d'expression des acteurs du métabolisme du 5FdURD**

La quantité de 5FdUMP variant significativement entre les lignées cellulaires, nous avons analysé l'expression en ARNm de certaines enzymes impliquées dans le métabolisme du 5FdURD en 5FdUMP. Pour cela, nous avons quantifié le niveau d'expression en ARNm de la TK1 et de la TK2 (*Thymidine Kinase 1 et 2*) par RT-PCR-Q (**Figure 23**). Aucune différence significative n'a été observée entre les lignées cellulaires.

Afin de confirmer ces résultats en partie préliminaires et de compléter l'étude, nous avons réalisé de nouveaux tests sur des cellules décongelées (repiquage précoce). Bien que la surexpression en ARNm ABCC11 ait été confirmée sur ces lignées décongelées, les profils de résistance au 5FdURD ne sont pas retrouvés.

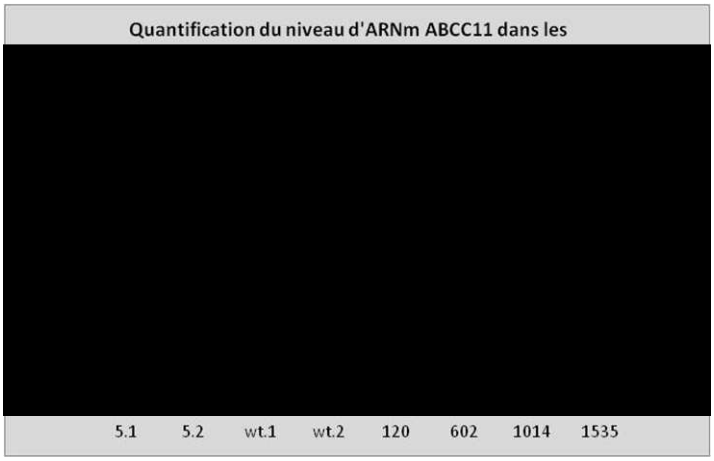

Figure 24. Expression en ARNm ABCC11 au sein des transfectants Flp In 293.
Les ARNm ont été extraits des cellules puis soumis à une RT-PCR-Q spécifique pour le gène ABCC11. Les résultats concernant ABCC11 ont été rapportés aux résultats obtenus pour un gène de référence codant pour la sous-unité ribosomale 18S. R2, R3, R4 et R5 représentent des repiquages successifs (intervalle ≈ 3 jours), R2 ayant lieu approximativement 15 jours après la transfection.

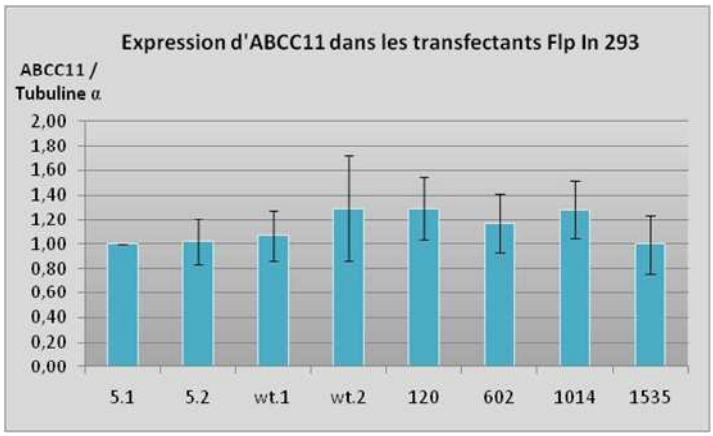

Figure 25. Expression de la protéine ABCC11 au sein des transfectants Flp In 293.
Les niveaux d'expression d'ABCC11 et de la tubuline α ont été mesurés par western blot puis quantifié avec le logiciel Image J®. Les résultats présentés sont les rapports d'expression ABCC11/tubuline. N= 4.

Lignée cellulaire	Facteurs de résistance					
	5FdURD	AraC	Fluda	Gemci	Dauno	Perme
Flp5.1	1,0 ± 0,0	1,0 ± 0,0	1,0 ± 0,0	1,0 ± 0,0	1,0 ± 0,0	1,0 ± 0,0
Flp5.2	1,2 ± 0,7	1,1 ± 0,1	1,0 ± 0,2	1,1 ± 0,3	1,0 ± 0,2	0,9 ± 0,1
Flp ABCC11wt.1	1,1 ± 0,3	1,2 ± 0,3	0,8 ± 0,1	1,1 ± 0,3	0,9 ± 0,0	1,3 ± 0,4
Flp ABCC11wt.2	1,6 ± 0,8	1,8 ± 0,8	1,2 ± 0,1	3,0 ± 2,0	1,1 ± 0,1	0,9 ± 0,1
Flp ABCC11*120	1,2 ± 0,3	1,0 ± 0,2	0,9 ± 0,1	1,1 ± 0,2	1,0 ± 0,1	1,1 ± 0,1
Flp ABCC11*602	0,4 ± 0,1	1,1 ± 0,5	0,9 ± 0,1	1,0 ± 0,3	0,8 ± 0,1	0,9 ± 0,1
Flp ABCC11*1014	1,5 ± 0,8	1,2 ± 0,3	0,9 ± 0,0	1,1 ± 0,4	0,9 ± 0,1	0,8 ± 0,2
Flp ABCC11*1535	2,0 ± 1,2	0,9 ± 0,5	1,2 ± 0,2	1,6 ± 0,6	1,0 ± 0,1	1,0 ± 0,1

Tableau 19. Chimiorésistance des transfectants Flp In 293.
Les CI50 ont été évaluées pour chaque médicament par test MTT. Les facteurs de résistance ont été calculés en rapportant les résultats à la CI50 de la lignée cellulaire Flp5.1. N=4. AraC = aracytine; Fluda = fludarabine; Gemci = gemcitabine; Dauno = daunorubicine; Perme = permetrexed.

2.3.3. Caractérisation des transfectants Flp In 293 (2)

Un nouveau panel de transfectants Flp In 293 a été généré. Il est constitué de lignées cellulaires transfectées avec le vecteur vide (2 transfectants, Flp5.1 et Flp5.2), le vecteur codant pour la protéine naturelle (2 transfectants, Flp ABCC11wt.1 et Flp ABCC11wt.2) ou un des vecteurs codant pour une protéine mutée au niveau du MSD1 (Flp ABCC11*120, Flp ABCC11*602, Flp ABCC11*1014 et Flp ABCC11*1535).

a. Comparaison des niveaux d'ARNm ABCC11

Le niveau en ARNm ABCC11 a été quantifié par RT-PCR-Q dans les transfectants Flp In 293. Sur la **Figure 24**, il est possible de voir l'évolution de la quantité en ARNm ABCC11 en fonction du nombre de repiquage réalisé depuis la transfection. Le niveau en ARNm ABCC11 est très élevé lors du deuxième repiquage (R2, environ 15 jours après la transfection) dans les cellules transfectées avec un vecteur codant ABCC11 naturelle ou mutée (Flp ABCC11wt.1, Flp ABCC11wt.2, Flp ABCC11*120, Flp ABCC11*602, Flp ABCC11*1014 et Flp ABCC11*1535) par rapport aux lignées Flp5.1 et Flp5.2. Dès le troisième repiquage, ce niveau diminue mais reste au moins 1000 fois supérieur au niveau observé chez les Flp5.1 et les Flp5.2.

b. Expression de la protéine ABCC11

Le niveau d'expression en protéine ABCC11 a été analysé par western blot. D'après les résultats présentés en **Figure 25**, il n'y a pas de différence significative entre les différents transfectants ; les niveaux d'expression semblent équivalents dans toutes les lignées cellulaires. Aucune surexpression d'ABCC11 n'est donc été observée au niveau protéique.

c. Analyse de la chimiorésistance

Des tests MTT ont été réalisés pour déterminer les CI50 des transfectants Flp In 293 pour le 5FdURD, l'aracytine (AraC), la fludarabine (Fluda), la gemcitabine (Gemci), la daunorubicine (Dauno) et le permetrexed (Perme). Afin de raisonner en facteur de résistance, chaque CI50 a été rapportée sur celle de la lignée cellulaire Flp5.1. D'après les résultats (**Tableau 19**), la résistance au 5FdURD n'est pas retrouvée et aucune lignée ne semble montrer une résistance quelconque aux médicaments testés.

2.4 Discussion

2.4.1. Analyse des transfectants HEK 293 T

Afin d'étudier l'influence du polymorphisme SNP sur la protéine ABCC11, nous avons commencé par générer des transfectants cellulaires stables surexprimant ABCC11 sauvage ou mutée dans des cellules HEK 293 T (HEK ABCC11wt et HEK ABCC11*602). La surexpression a été observée au niveau ARNm pour des repiquages précoces mais rapidement perdue avec le temps (**Tableau 15**). Bien que la quantification des ARNm ait été réalisée plusieurs jours après la transfection, il se peut que les ARNm observés de manière précoce proviennent de la transcription du plasmide non intégré dans les cellules. De ce fait, au fur et à mesure des repiquages, le plasmide aurait été perdu en parallèle de l'expression d'ABCC11. Ceci signifie que la pression de sélection exercée par la généticine n'aurait pas été suffisante pour sélectionner les cellules ayant intégré le plasmide dans leur génome.

2.4.2. Analyse des transfectants Flp In 293

Nous avons alors décidé d'utiliser une autre lignée cellulaire : les Flp In 293. Ces cellules sont dérivées des HEK 293 et ont été génétiquement modifiées pour intégrer le gène d'intérêt dans un site précis de leur génome. Ce phénomène est permis par la présence d'un site de recombinaison FRT placé dans un seul endroit du génome. Le gène d'intérêt est porté sur un plasmide pcDNA5/FRT comportant aussi un site de recombinaison FRT. La co-transfection du plasmide pcDNA5/FRT/gène d'intérêt et d'un plasmide codant pour la recombinase Flp permet l'insertion du gène d'intérêt au niveau du site FRT génomique. Cette technologie nous a permit d'établir plusieurs lignées cellulaires exprimant ou non une protéine sauvage ou mutée : Flp5 (vecteur vide), Flp ABCC11wt, Flp ABCC11*1014, Flp ABCC11*1701, Flp ABCC11*1952, Flp ABCC11*2006 et Flp ABCC11*2123.

Une surexpression d'ABCC11 a été observée au niveau ARNm (dans les lignées exprimant ABCC11wt et mutée) (**Tableau 16**) et protéique (dans la lignée Flp ABCC11wt) (**Figure 20**). D'après l'analyse du profil de chimiorésistance (**Tableau 17**), la protéine ABCC11 sauvage engendrerait une résistance au 5FdURD (FR=2.2) mais pas au MTX (FR=1.3). L'analyse du profil de résistance des lignées exprimant une protéine mutée nous indique que seule la lignée Flp ABCC11*2123 présente un profil de résistance équivalent à la lignée Flp ABCC11wt. Toutes les autres lignées ont perdu leur capacité à résister au 5FdURD suggérant que les SNP situés en 1014, 1701, 1952 et 2006 soient responsables d'une diminution de l'activité d'ABCC11.

L'activité d'efflux du 5FdUMP a été analysée dans les différentes lignées cellulaires. Les résultats préliminaires (n=2) (**Tableau 18**) indiquent qu'après la période d'incubation avec le 5FdURD, le 5FdUrd est bien métabolisé en 5FdUMP dans toutes les cellules mais que la quantité de 5FdUMP varie de manière importante entre chaque lignée cellulaire. En effet, certaines lignées montrent plus (Flp ABCC11wt et Flp ABCC11*2006) ou moins (Flp ABCC11*1701 et 1952) de 5FdUMP intracellulaire que les Flp5. Les lignées Flp ABCC11*1014 et 2123 montrent des résultats non reproductibles entre les deux expériences préliminaires. ABCC11 transportant le 5FdUMP [223], il serait logique d'observer une diminution de ce taux intracellulaire dans les Flp ABCC11wt. Pourtant, ce n'est pas le cas, et ce de manière reproductible. Aucune modification du niveau d'expression en ARNm d'ABCC5 et d'ABCG2 n'a été observée au sein des transfectants (**Figure 22**). La modification de l'expression de ces deux transporteurs aurait pu en effet expliquer les variations de 5FdUMP intracellulaire, ABCC5 transportant le 5FdUMP [221] et ABCG2 étant un transporteur potentielle du 5FdUMP (responsable d'une résistance accrue au 5-FU, précurseur du 5FdUMP) [222]. De plus, la modification du taux intracellulaire de 5FdUMP ne peut pas non plus être expliquée par une modification de l'expression d'une des enzymes du métabolisme du 5FdURD testées (TK1 et TK2) (**Figure 23**). Ces résultats indiquent que la modification de l'expression d'ABCC11 induit une modification du taux intracellulaire de 5FdUMP d'une façon encore indéterminée.

Après la période d'efflux, les cellules Flp5 montrent une diminution logique de la quantité de 5FdUMP intracellulaire, en partie inhibée par la présence de MK571 (inhibition de l'efflux de 29 et 8 %). Le MK571 inhibant ABCC11, il serait logique d'observer une augmentation du taux intracellulaire de 5FdUMP sous l'effet du MK571, dans les cellules Flp ABCC11wt. Cependant et de manière surprenante, elles montrent une augmentation de la quantité de 5FdUMP intracellulaire après l'efflux qui diminue sous l'effet du MK571. En parallèle, dans toutes les conditions, la quantité de 5FdUMP est plus élevée dans le surnageant des Flp ABCC11wt que dans celui des Flp5. Pourtant, d'après l'analyse des surnageants, les cellules Flp ABCC11wt semblent bien sensibles à la présence de MK571 dans le milieu d'efflux (**Figure 21**) puisqu'il diminue la quantité de 5FdUMP extracellulaire. La simple surexpression d'ABCC11 explique difficilement ces paradoxes.

Il est à noter que l'augmentation du métabolite actif en intracellulaire n'empêche pourtant pas les Flp ABCC11wt d'être résistantes au 5FdURD et ce d'autant plus si le niveau de 5FdUMP intracellulaire est réellement augmentée par rapport au Flp5. Il se pourrait qu'ABCC11 soit impliquée dans le transport de molécules intervenant dans des processus plus complexes (modification indirecte du métabolisme du 5FdUMP ou transport du 5FdUMP dans des vacuoles empêchant l'accès à la cible cellulaire). Pour les autres lignées cellulaires, les résultats de l'analyse du transport du 5FdUMP sont aussi difficilement interprétables car tout comme pour les Flp ABCC11wt, l'analyse des surnageants manque de cohérence avec l'analyse des cellules auquel s'ajoute un manque de reproductibilité. Il est difficilement possible de relier les profils de résistance au 5FdURD à ceux du transport du 5FdUMP.

Ces résultats n'ont malheureusement pas pu être plus exploités sur les cellules décongelées. Bien que les cellules aient été congelées à un repiquage précoce et que l'expression en ARNm ABCC11 ait été observée, la résistance au 5FdURD n'a pas été retrouvée dans les lignées montrant une résistance au préalable. Devant cette situation, il n'était pas judicieux d'entreprendre de nouvelles analyses et nous avons décidé d'établir de nouveaux transfectants. Malheureusement, la seconde génération de transfectants FlpIn n'a montré de surexpression d'ABCC11 qu'au niveau ARNm et non au niveau protéique (**Figure 24** et **Figure 25**). En absence de surexpression d'ABCC11, les cellules n'ont logiquement pas montré de différence dans le profil de résistance à divers anticancéreux (**Tableau 19**).

2.4.3. Conclusion

Bien que le projet d'analyser l'impact des SNP sur ABCC11 soit très intéressant, nous n'avons à ce jour pas de résultats reproductibles et donc interprétables sur l'effet des polymorphismes génétiques que nous avons réussi à générer *in vitro*. Il faudrait trouver de nouveaux outils cellulaires afin de pouvoir exprimer de manière stable les différents variants d'ABCC11.

III. CONCLUSIONS - PERSPECTIVES

Grâce à la modélisation par homologie, nous avons généré deux structures *in silico* dans deux conformations différentes soit ouverte vers l'extracellulaire ou ouverte vers l'intracellulaire. Ces deux modèles illustrent deux états catalytiques différents et permettent de voir quels sont les acides amines potentiellement critiques dans l'architecture de la protéine, dans les mouvements nécessaires au transport, ainsi que dans la liaison avec certains substrats. Nous avons d'ailleurs identifié plusieurs sites potentiels de liaison au 5FdUMP et au GMPc et confirmé l'importance de la glycine 180 précédemment identifiée comme essentielle dans le transport du GMPc.

Bien que nous ne puissions pas profondément interpréter les résultats concernant l'impact des SNP sur ABCC11, il apparaît important de chercher de nouveaux outils et de nouvelles techniques pour analyser l'activité d'ABCC11. De plus, l'association des analyses biochimiques et bioinformatiques serait un travail pertinent. Il serait en effet intéressant d'allier les effets fonctionnels d'une mutation à son impact sur la structure *in silico* de la protéine ou sur l'interaction simulée avec les substrats.

D. ETUDE L'IMPACT DU MBLI-87 SUR LA RESISTANCE A L'IRINOTECAN INDUITE PAR ABCG2 (COLLABORATION)

Il existe actuellement plusieurs molécules (GF120918, imatinib et gefitinib [224]) capable d'inhiber l'activité d'ABCG2 (BCRP). Ces modulateurs permettent d'accroître la cytotoxicité des anticancéreux substrats d'ABCG2 *in vitro* mais se révèlent non spécifiques (inhibition de plusieurs transporteurs) ou toxiques *in vivo*. C'est pourquoi l'identification d'un composé actif *in vivo* qui ne modifie pas les paramètres pharmacocinétiques des médicaments anticancéreux et dénué d'effet toxique aux doses efficaces reste un objectif important.

Nous nous sommes intéressés, en étroite collaboration avec plusieurs équipes de recherche (UMR 5086 et UMR 5063), à un modulateur non compétitif récemment identifié *in vitro* : le MBLI-87. Il est aussi efficace que le GF120918 *in vitro* et est spécifique d'ABCG2. Nous avons étudié son efficacité chez la souris SCID (*Severe Combined Immunodeficiency*). Pour cela, nous avons analysé l'efficacité d'un traitement à l'irinotécan (dont le métabolite actif SN-38 est transporté par ABCG2) sur la croissance de tumeurs surexprimant ou non ABCG2 (**Figure 26**). L'irinotécan empêche complètement le développement de tumeurs contrôles composées de cellules HEK pcDNA3 (vecteur vide) mais ne fait que retarder le développement des tumeurs surexprimant ABCG2. L'association du MBLI-87 avec le traitement anticancéreux augmente significativement l'efficacité de l'irinotécan sur la croissance des tumeurs ABCG2 positive. De plus, les doses de MBLI-87 utilisées sont bien en dessous des doses tolérées. Ces données suggèrent que le MBLI-87 serait un excellent candidat pour prévenir l'efflux des médicaments par ABCG2, sans altérer les concentrations plasmatiques en anticancéreux. Il constituerait également un bon moyen d'améliorer l'imprégnation des tissus par les médicaments substrats d'ABCG2 et potentiellement de combattre la résistance aux anticancéreux.

→ Publication 9. « **The acridone derivative MBLI-87 sensitizes breast cancer resistance protein-expressing xenografts to irinotecan** » par O. Arnaud, A. Boumendjel, A. Gèze, M. Honorat, E.L. Matera, J. Guitton, W. D. Stein, S.E. Bates, P. Falson, C. Dumontet, A. Di Pietro et L. Payen.

Article accepté dans European Journal Of Cancer

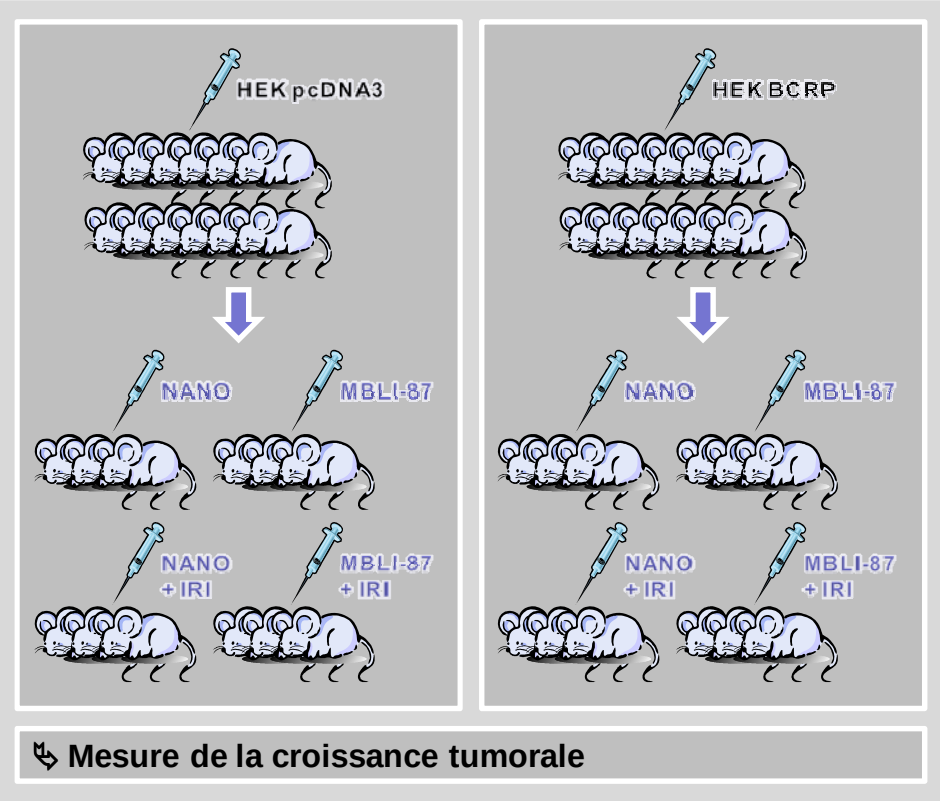

Figure 26. Analyse de l'effet modulateur du MBLI-87 sur la croissance des tumeurs établies chez la souris.
Après injection sous-cutanée des cellules HEK pcDNA3 (contrôle) ou HEK BCRP, les souris sont divisées en 4 groupes de traitement : nanoparticules seules (NANO, vecteur du MBLI-87), MBLI-87 seul (MBLI-87), nanoparticules et irinotécan (NANO + IRI) et MBLI-87 et irinotécan (MBLI-87 + IRI). La taille des tumeurs est ensuite mesurée 3 fois par semaine pour établir une courbe de croissance.

Une optimisation de ce test-préclinique est actuellement en cours, en « humanisant » le schéma thérapeutique, et en modélisant les résultats en vue d'une meilleure extrapolation des données à l'homme. Pour cela, nous devrons tout d'abord définir les paramètres pharmacocinétiques des différentes molécules en traitant des souris SCID. Le sang des souris sera prélevé après différentes durées de traitement pour déterminer la concentration plasmatique des molécules par HPLC MS/MS (Pr. J. Guitton, CBS Lyon Sud). Toutes les données seront traitées et modélisées (Pr. M. Tod, EA3738, Lyon Sud) afin d'établir le modèle de croissance tumorale chez les souris non traitées, le modèle de la cinétique de l'effet anti-tumoral du CPT-11, et enfin le modèle de la cinétique de l'effet reversant du MBLI-87. Ces différents modèles permettront de caractériser de manière quantitative l'action des différentes molécules à travers un petit nombre de paramètres caractéristiques, dépendant soit des molécules, soit de l'espèce. Ces modèles permettront d'explorer, par simulation, l'effet de différents schémas posologiques non étudiés. Par des techniques appropriées, ils peuvent également servir à simuler les expériences chez l'homme, afin de les optimiser et de réduire le nombre d'expériences nécessaires. Ainsi, nous pourrons optimiser notre modèle de xénogreffes (conditions expérimentales, doses administrées et schémas thérapeutiques), afin de rendre les observations plus facilement extrapolables à l'homme et pouvoir sélectionner de bons modulateurs en vue d'un développement pharmaceutique.

THE ACRIDONE DERIVATIVE MBLI-87 SENSITIZES BREAST CANCER RESISTANCE PROTEIN-EXPRESSING XENOGRAFTS TO IRINOTECAN

O. Arnaud[4], A. Boumendjel[3], A. Gèze[3], M. Honorat[1,2], E.L. Matera[2], J. Guitton[1,6], W. D. Stein[5], S.E. Bates[5], P. Falson[4], C. Dumontet[1,2], A. Di Pietro[4], L. Payen[1,2].

1. ISPB, Université Lyon1, 69008 Lyon;
2. Inserm, U590, Centre Léon Bérard, FNCLCC, 69008 France;
3. Département de Pharmacochimie Moléculaire UMR 5063 CNRS/ Université de Grenoble, 38041 Grenoble cedex 9, France;
4. Equipe labellisée Ligue 2009, Institut de Biologie et Chimie des Protéines, UMR 5086 CNRS/Université Lyon 1, IFR128 BioSciences Gerland-Lyon Sud, 69367 Lyon Cedex 07, France ;
5. Medical Oncology Branch, Center for Cancer Research, National Institutes of Health, Bethesda, MD 20892, USA.
6. Hospices Civils de Lyon, Centre Hospitalier Lyon-Sud, Laboratoire de Ciblage Thérapeutique en Cancérologie, 69495 Pierre-Bénite, France ;

Correspondence and reprint requests

Dr. PAYEN Léa, INSERM U590, 8, Avenue Rockefeller, 69008 Lyon, France; E-mail: Lea.payen@recherche.univ-lyon1.fr; Tel.: +33478777236; Fax: +33478777088

FINANCIAL SUPPORTS

This work was supported by INSERM (UMR 590) and Université Lyon 1, and grants from Association pour la Recherche sur le Cancer (ARC 4007), Ligue Nationale contre le Cancer (Equipe labellisée Ligue 2009) and LST (Lyon Science Transfert). M.H. and O. A. are respectively recipient of doctoral fellowships from the Ligue Nationale contre le Cancer and the Ministère de l'Enseignement Supérieur et de la Recherche.

ABSTRACT

The breast cancer resistance protein ABCG2 confers cellular resistance to irinotecan (CPT-11) and its active metabolite SN-38. We utilized ABCG2-expressing xenografts as a model to evaluate the ability of a non-toxic ABCG2 inhibitor to increase intracellular drug accumulation. We assessed the activity of irinotecan in vivo in SCID mice: irinotecan completely inhibited the development of control pcDNA3.1 xenografts, while only delaying the growth of ABCG2-expressing xenografts. Addition of MBLI-87, an acridone derivative inhibitor, significantly increased the irinotecan effect against the growth of ABCG2-expressing xenografts. In vitro, MBLI-87 was as potent as GF120918 against ABCG2-mediated irinotecan efflux, and additionally was specific for ABCG2. A significant sensitization to irinotecan was achieved despite the fact that doses remained well below a maximum tolerated dose (due to the rather limited solubility of MBLI-87). This suggested that MBLI-87 is an excellent candidate to prevent drug efflux by ABCG2, without altering plasmatic concentrations of irinotecan and SN-38 after IP (intra-peritoneal) injections. This could constitute a useful strategy to improve drug pharmacology, to facilitate drug penetration into normal tissue compartments protected by ABCG2, and potentially to reverse drug resistance in cancer cells.

Keywords

ABC transporter, ABCG2, Irinotecan, MultiDrug Resistance, Reversion

INTRODUCTION

Multidrug efflux pumps from the ATP-binding cassette (ABC) family are thought to play important roles in drug absorption and distribution, normal tissue protection, and potentially anticancer drug-resistance. Although efforts to reverse drug resistance using ABCB1/P-glycoprotein (Pgp) inhibitors essentially failed in the past, it is not known whether this was because the target was not as prevalent as previously thought, or due to either inadequate inhibition, or concurrent expression of other transporters able to compensate for the inhibition of Pgp. The question of whether inhibitors of other ABC transporters could be exploited clinically has rarely been addressed. Since a number of the targeted anticancer agents have been found to be substrates or modulators of multidrug efflux pumps, it has become important to define their possible role in multidrug resistance. Furthermore, inhibition of the multidrug efflux pumps has potential utility beyond reversal of resistance, such as to improve the delivery of substrate drugs to the central nervous system (CNS) (1-3). For example, it was recently reported that CNS penetration of lapatinib in animal models is limited by both Pgp and ABCG2 (4). Our strategy is to use reversal of drug resistance in xenografts as a proof of concept that an improved drug delivery and accumulation, through inhibition of efflux pumps, can indeed be achieved in vivo. HEK293 human embryonic kidney cells were previously shown to be able to grow as xenografts in SCID mice (4). This offered the possibility of a defined model system in which transfected ABCG2 would be the only difference from control xenografts, and that levels would not be too high, in contrast to other model systems in which drug selection had been utilized to achieve ABCG2 upregulation. This would lay the groundwork for re-testing the hypothesis that ABC transporters contribute to drug resistance and that their inhibition could prove useful in patients, for targeting ABC transporters that prevent drug accumulation in the CNS, or for improving and normalizing oral drug bioavailability.

Breast cancer resistance protein ABCG2 is an important ABC half-transporter that effluxes a wide range of substrates, including natural compounds such as porphyrins, and anticancer drugs such as mitoxantrone, irinotecan (CPT-11) (5) and SN-38, its pharmacologically-active metabolite, then overlapping the substrate spectra of ABCB1 and ABCC1 (6). Few potent inhibitors have been described, including GF120918, Ko143 as a derivative of fumitremorgin C (a highly toxic tremorgenic mycotoxin isolated from Aspergillus fumigatus), imatinib and gefitinib (GEFI, ZD1839, Iressa) (7). The latter compound is an efficient tyrosine-kinase inhibitor developed for inhibiting the epidermal growth factor receptor (EGFR) and used in lung cancer clinical trials (8, 9). Controversial data have been reported about its transport by ABCG2 (9, 10). This is apparently due to the fact that gefitinib is a substrate at low concentrations whereas inhibitory properties are observed in vivo at higher concentrations (11, 12). Nevertheless, high and maximum tolerated doses of gefitinib (over 75 mg/kg) are routinely used to demonstrate its ability to reverse the SN-38-dependent resistant phenotype (10, 12, 13). The requirement for such high gefitinib doses would obviously constitute serious limitations for ABCG2 modulation in clinical setting. New ABCG2 inhibitors have been recently designed and optimized among flavonoids, based on flavone (14) and acridone (15) derivatives. One acridone, MBLI-87, also called acridone 4b, was found to be as potent in vitro as GF120918 against ABCG2-mediated mitoxantrone efflux (15), with the advantage of not inhibiting ABCB1 and ABCC1 (16). To further characterize MBLI-87 effects against ABCG2 transport activity, we evaluated its in vitro inhibition of irinotecan efflux and its in vivo modulatory effect on ABCG2-related drug resistance in xenografts.

MATERIAL AND METHODS

Cell cultures.

The two HEK293 cell models used, transfected with either wild-type ABCG2 or empty pcDNA3.1 vector (17), were cultured as described (14).

Animal studies.

SCID mice (Charles River Laboratories) were handled in accordance with the Guide for the Care and Use of Laboratory Animals, and all procedures followed protocols approved by the Animal Facility veterinarian board. Eight week-old female mice were subcutaneously inoculated with either pcDNA3.1- or ABCG2-HEK293 cells (8.2 x 106 in 100 µL PBS/inoculation). Since pcDNA3.1- and ABCG2-xenografts differently responded to irinotecan therapy, each mouse was implanted on the left and right flanks with the same tumor cell type. Volume was determined, in mm3, by measuring tumor length (l) and width (w), and using the formula: volume = (4*3.14((l+w)/2)3)/3. Time zero was the day of cell inoculation.

Drug Formulation and Administration.

MBLI-87, which was not soluble in either water or saline vehicles, was formulated in enzymatically-modified cyclodextrin-based colloidal suspension. An organic phase containing acetone (30 mL), (γCD-C10 at 2 mg/ml) (18, 19), benzyl benzoate (600 µl), a lipophilic surfactant Montane® 80 (8 mg/ml) and the drug (9 mg) was added into 60 ml of glucose (3.6 % w/w) supplemented with the hydrophilic surfactant Montanox® 80 (4 mg/ml) under magnetic stirring (500 rpm) at 25°C. After organic solvent elimination, the suspension volume was adjusted to reach isotonicity. The nanoparticle size, measured by quasi-elastic light scattering, was around 185-195 nm (PI 0.05)(20). The filtrated (0.45 µm) suspension of MBLI-87-loaded nanoparticles (later called MBLI-87), at 0.16 mg/ml, was I.P. (intra-peritoneal) administered as a 2.4-mg/kg dose for 5 days/week on two consecutive weeks followed by a 15-day rest period. Unloaded colloidal suspension (without MBLI-87) was called NANO (MBLI-87 vehicle).

Irinotecan, kindly provided by Dr. Hamedi-Sangsari (MAP-France company), was I.P. administrated at 30 mg/kg (0.1 ml water), 3 days/week on 2 consecutive weeks followed by a 15-day rest period.

Tumor-bearing SCID mice were randomized into eight groups before receiving drugs, the day after cell implantation. The two-week period of drug administration plus its 15-day rest constituted one therapy cycle; mice thus received 2 cycles over 8 weeks.

Western Blot Analysis.

Xenografts were resuspended in a hypotonic buffer (5 mM EDTA, 10 mM Tris/HCl pH8, 10 mM KCl, protease inhibitor cocktail) in an ice-cold dounce homogenizer for 1 h before homogenization on ice for 30 times. After centrifugation (15 min, 1000 g), supernatants were collected, and protein content quantified using Bicinchonic Acid assay. 10 µg proteins were separated by 10% SDS-polyacrylamide gel electrophoresis. PVDF membranes were probed with the anti-ABCG2 monoclonal antibody BXP-21 (Tebu-bio), and a polyclonal alpha-tubulin antibody (Sigma). ABCG2 was detected using the Enhanced Chemiluminescence Plus detection kit (Amersham Pharmacia Biotech), and densitometry performed using the quantityOne® software.

In vitro cellular quantification of irinotecan.

Cells were first plated at 750 000 cells/well in 6-well plates. They were loaded with 2 µM irinotecan in the DMEM medium (without FBS) for 60 min at 37 °C in the absence or presence of either 5 µM GF 120418, 5 µM MBLI-87 or 10 µM fumitremorgin C. During the uptake period, irinotecan could be metabolised into SN-38. After two washings with ice-cold PBS (to inhibit active efflux capabilities), cells were collected in 1 mL of ice-cold PBS, submitted to centrifugation (5 min at 1500 g) and lysed into 500 µL of pure methanol. Finally, intracellular irinotecan accumulation was quantified in a cell aliquot by HPLC MS/MS. The mixture was then submitted to vortex (30 s) and to centrifugation (5 min at 13 000 g). Calibration curves and quality control for irinotecan were prepared in 500 µL of methanol. Camptothecin, used as an internal standard, was added at 200 ng/mL. The organic layer was removed and evaporated to dryness under a stream of nitrogen. The residues were resuspended in 200 µL of mobile phase and 10 µL were injected into HPLC device. The mass spectrometry analysis was performed in positive-ion mode with electrospray source, and irinotecan and camptothecin were quantitated in selected reaction-monitoring mode. Specific transitions for SN-38, APC and SN-38G were also monitored in order to assess potential metabolism from irinotecan into the cells. Results (expressed in ng irinotecan/mg prot.) were normalized to cellular protein content (Bradford assay).

Pharmacokinetic analysis.

Irinotecan disposition was evaluated in tumor-free SCID mice after a single MBLI-87 (3.45 mg/kg) and/or irinotecan (20 mg/kg) intra-peritoneally administered dose (injection route used in in vivo protocol). 0.5, 1, 3, 6, or 24 h after injection, approximately 1 mL of blood was collected with heparinized syringes (5 animals per time point). Plasma fractions were extracted from each blood sample by centrifugation (5 min, 5 000 g).Solid phase extraction (SPE) was performed to extract irinotecan and SN-38 from mouse plasma samples. Briefly, the samples (50 µl) were spiked with 20 µl of camptothecin (internal standard at 1 µg/ml) and 300 µl of formic acid at 2% were added. According to the time of the kinetics, plasma samples were diluted in a free-drug blank plasma before extraction. Then, the mixture was transferred to SPE HLB Oasis cartridge (Waters, USA). The cartridges were washed and then, the analytes were eluted with methanol. The solvent was evaporated to dryness under nitrogen and the residue was reconstituted with 100 µl of mobile phase and 10 µl was injected into the HPLC tandem mass spectrometry apparatus. The mass spectrometry analysis was performed in the same conditions than those described previously for in vitro experiments. (see previous "In vitro cellular quantification of irinotecan" section). Results are expressed in ng Irinotecan/ml plasma.

Statistical analysis.

Irinotecan accumulation histograms (Figure 1) were constructed with Excel, and expressed as mean as ±SD. The statistical analyses (unilateral t-test) were performed with Excel. Growth curves were constructed with Excel as a plot of tumor volume ± SE against time. In figures 3A and B, statistical evaluation was carried out with the non-parametric Mann Whitney test. In Figure 3C and Table 1, growth curves were constructed with SigmaPlot® (Systat Software, San Jose, CA), by analyzing data as a plot of tumor volume ± SE against time, and the statistical analyses (paired t-test) were performed with Sigmastat® (Systat Software).

RESULTS AND DISCUSSION

To compare the in vitro effects of MBLI-87 on irinotecan accumulation in both pcDNA3.1-HEK293 cells (control) and ABCG2-expressing HEK293 cells, cell lines were incubated for 60 min with 2 µM irinotecan in the absence or presence of either 5 µM MBLI-87, 5 µM

GF120918 or 10 µM fumitremorgin C (Figure 1). Then, cellular accumulation of irinotecan was quantified by HPLC MS/MS. This clearly demonstrated that irinotecan was less accumulated, by approximately 1.7-fold, in ABCG2-expressing HEK293 cells than in control cells. In ABCG2-HEK293 cells, irinotecan accumulation was increased by co-exposure to any ABCG2 modulator (10 µM fumitremorgin C, 5 µM GF120918 or 5 µM MBLI-87), while these modulators had no effect in the control cells (Figure 1). This demonstrated that MBLI-87 is indeed a potent inhibitor of ABCG2, increasing irinotecan cellular accumulation.

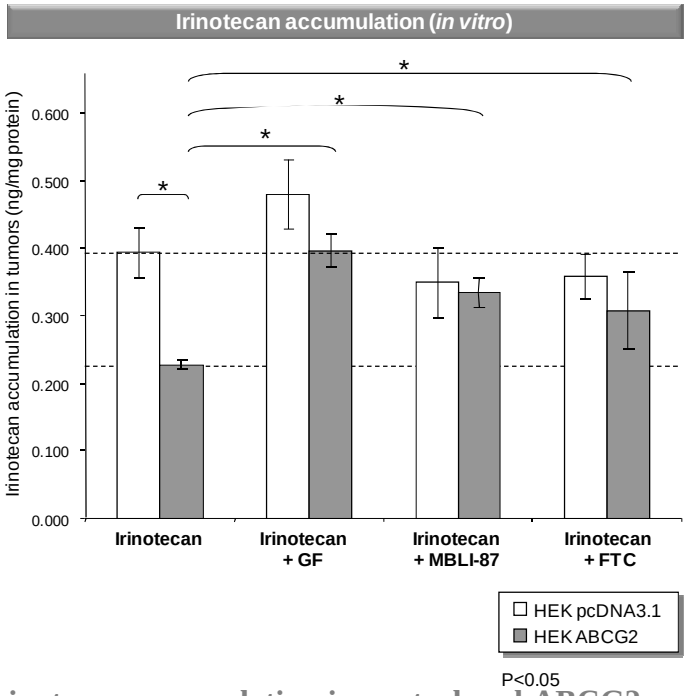

Figure 1. In vitro irinotecan accumulation in control and ABCG2-expressing cells. Cells were loaded with 2 µM irinotecan in DMEM medium (without FBS) for 60 min at 37 °C in the absence or presence of either 5 µM GF120418, 5 µM MBLI-87 or 10 µM fumitremorgin C. Intracellular irinotecan accumulation was quantified by HPLC MS/MS. Results were expressed as ng irinotecan/mg protein.

We have used pcDNA3.1 and ABCG2 stable transfectants in HEK293 cells as a cellular tool (17) to characterize both in vitro and in vivo effects of ABCG2 modulators. In contrast to drug-selected ABCG2 cancer cells, these models allow access to a true negative control (here the empty pcDNA3.1 transfected cell line) in order to validate the specificity, and to exactly evaluate the net effect of our modulatory molecule on the ABCG2 target. We previously established both the tumorigenicity of HEK293 cells (21), the concentration range of irinotecan and MBLI-87, the non-toxic doses of drug combinations and the schedule of their administration to SCID mice over the 8-week protocol. We characterized the maximum tolerated doses of irinotecan (30 mg/kg for 3 days/week) in combination with either control NANO (300 µL for 5 days/week) or MBLI-87 (2.4 mg/kg in 300 µL NANO for 5 days/week). Higher doses were not used as they resulted in loss of weight and modifications in behaviour, both defined as reference elements by the Animal Facility veterinarian board to in vivo quantify the toxicity of the molecules. No difference in toxicity was observed according the treatments.

MBLI-87 could not be solubilised in either oil, saline or water vehicles. Since the chronic administration schedule of 50 µL pure DMSO is not recommended by our ethical committee, we used a specific and complex formulation in nanoparticles (NANO) to allow its administration to mice. Consequently, for evaluating the net MBLI-87 effect on the growth of

ABCG2-expressing xenografts, we carried out control conditions with the nanoparticles alone (NANO). When the tumor volume approximately reached 1800 mm3, mice were sacrificed and ABCG2 expression levels were quantified by western blotting. As expected, the ABCG2 protein was only detected in ABCG2 xenografts (Figure 2A). Since control (pcDNA3.1) tumors did not grow during the first 60 days, we did not check any irinotecan effect on ABCG2 expression. Interestingly, the irinotecan treatment, whether combined with MBLI-87 or under control conditions (NANO), resulted in higher ABCG2 expression in xenografts (Figure 2, A and B), whereas MBLI-87 alone had no effect (Figure 2B). This strongly suggested that the anticancer agent irinotecan selected ABCG2-expressing cells having high efflux capability, which then could limit irinotecan chemotherapeutic activity or disposition.

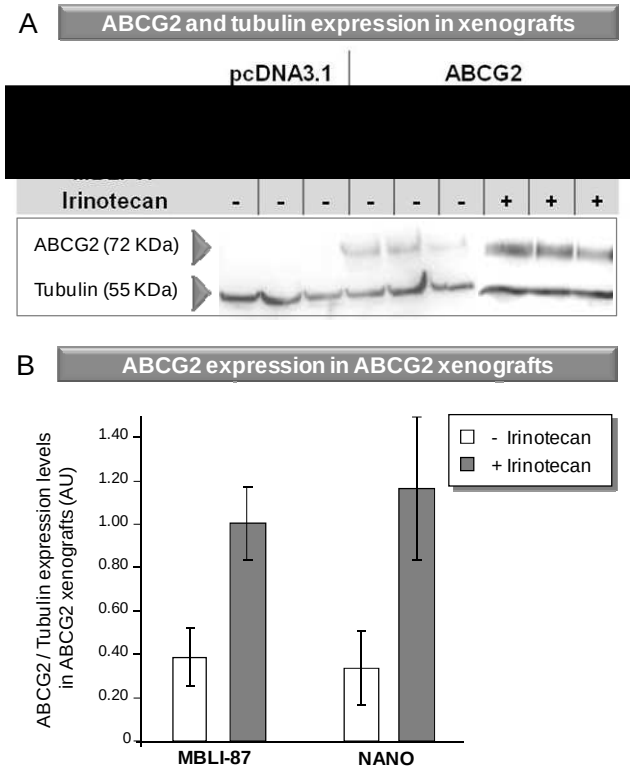

Figure 2. A) ABCG2 expression in xenografts. As soon as the tumor volume reached 1800 mm3, approximately, mice were sacrificed, and crude membrane fractions were prepared from (T31 to T110) individual xenografts. By immunoblotting, ABCG2 expression was quantified with the anti-ABCG2 BXP21 antibody, as described in Material and Methods. B) Effects of treatment with irinotecan and/or MBLI-87 on ABCG2 expression levels. ABCG2 expression was quantified as in A, and normalized to the alpha-tubulin content (ABCG2 expression levels /tubulin expression levels). Protein level ratios were expressed as arbitrary units (AU). The values are means ± S.E.

We next evaluated MBLI-87 circumvention of in vivo drug resistance by submitting mice to two chemotherapy cycles, administering irinotecan (30 mg/kg for 3 days/week) in combination with either control NANO (300 µL for 5 days/week) or MBLI-87 (2.4 mg/kg in 300 µL NANO for 5 days/week), the day after cell implantation. The first drug therapy period (from DAY1 to DAY15) avoided physical variability of irinotecan distribution in xenografts (since tumors were small and not completely established in 3-D tissue). This first chemotherapy period likely potentiated drug effects on the implanted cells, through a direct action on cells. In contrast, the second drug therapy period (from DAY 30 to DAY 45) was performed when xenograft volumes were in the mean range of 100 mm3, an established tumor size. Although some concentration variability was observed, both SN-38 and irinotecan were

detected in xenografts, by LC-MS/MS, 24 h after irinotecan administration. Control xenografts, treated with NANO, grew and reached a maximal volume at DAY 28, whereas they did not grow at all during the 8-week period following irinotecan therapy (Figure 3A). NANO-irinotecan and MBLI-87-Irinotecan therapies completely prevented the growth of control xenografts during the first 8 weeks (Figure 3A). In contrast, irinotecan only delayed the growth of ABCG2-expressing xenografts by approximately 10 days (Figure 3C, versus Figure 3B). MBLI-87 alone did not significantly modify the growth of either pcDNA3.1- or ABCG2- xenografts when compared to control NANO (Figure 3A and Figure 3B).

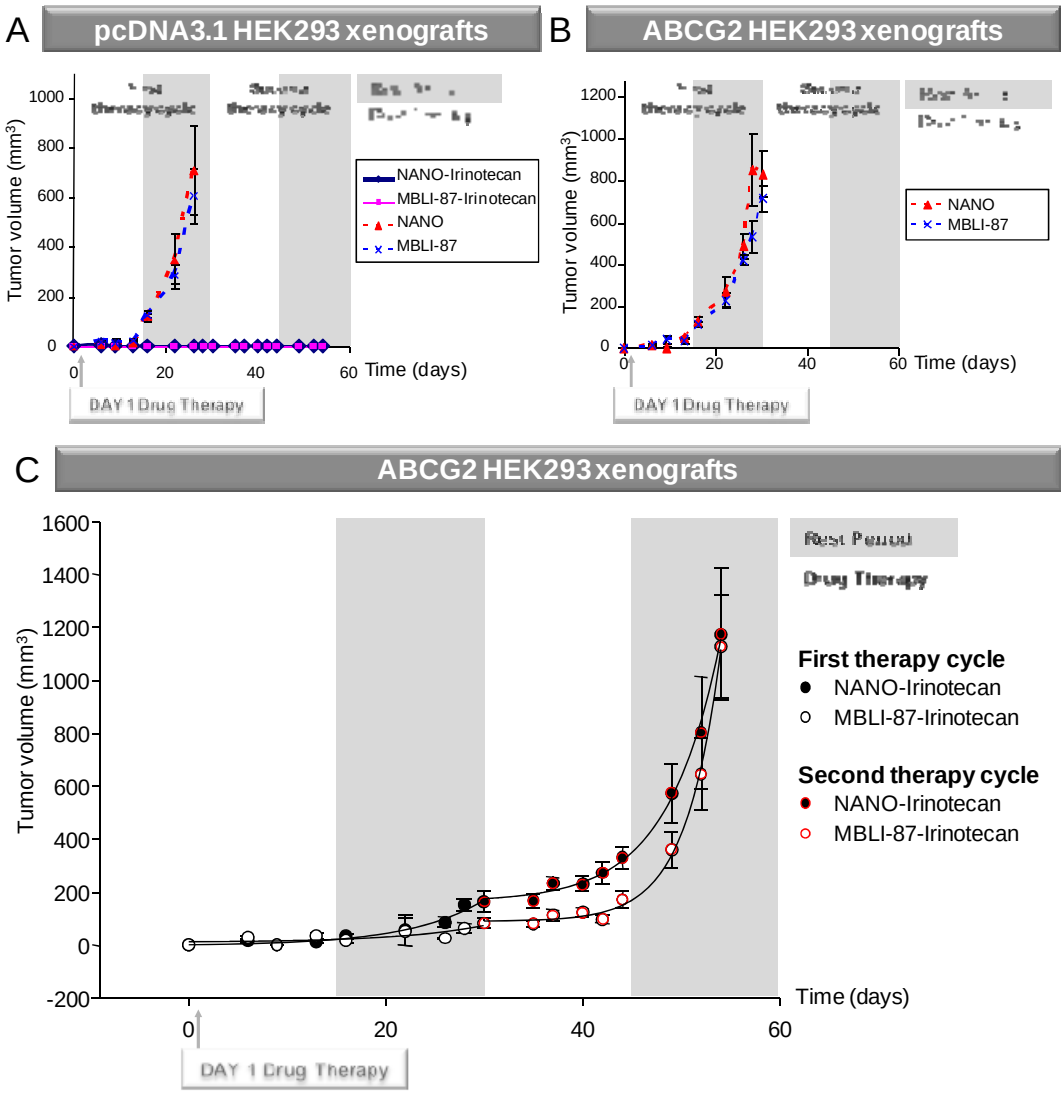

Figure 3. Activity of MBLI-87, NANO and irinotecan, either alone or in combination, against control (A) and ABCG2-expressing (B and C) xenografts. Doses and schedules are detailed in Material and Methods. **A and B.** The data at each time period were averaged. The tumor volume values were plotted against time. Differences with P-values < 0.05 were considered as statistically significant between two sets of xenograft volume (N=6/group). **C.** Mice were treated with either NANO or MBLI-87 in combination with irinotecan. The data were sets of tumor measurements (in sixes) at four time periods: first therapy period, first rest period, second therapy period and second rest period, for two parallel therapy conditions: MBLI-87-Irinotecan (N=5) and NANO-irinotecan (N=6). The data at each time period were averaged and Standard Errors computed. A plot was made of tumor volume ± SE against time.

During the second chemotherapy cycle (DAY16-to-DAY54 period), we observed an inhibition by MBLI-87 of ABCG2-dependent resistance to irinotecan (Figure 3C): ABCG2 tumor growth was delayed by co-administration of MBLI-87 and irinotecan, in comparison to NANO and irinotecan during the first rest period and the second therapy period. The data points of the overall MBLI-87 series were significantly below (Paired t-test, $p<0.001$) those of the NANO series. This was especially true over the times 35-to-54 days. The points of the Figure 3C were better fitted (F test, at $p<0.01$) for both test and control series, as two separate time courses (rather than a single one) following the augmented (three-parameter) exponential growth equation: $y = y0 + a*\exp(b*t)$, where y0 +1 was the computed size at t =0, a is 1.71828 times the increment in size at time equal to1/b, while b is the growth rate (Table 1). Although there was no statistically-supported difference ($p=0.115$) for the whole 0-to-30 days period, a significant difference was indeed observed over the first rest period (16-to-30 days), $p=0.039$ (Table 1). Fig. 3C, although not statistically significant, looked as if the growth rate during the second therapy period (DAY 30-45) was slower for irinotecan-MBLI-87 than for irinotecan-NANO. In which case, the accelerated rate after therapy was discontinued and was faster for irinotecan-MBLI-87. It started from a lower point and got to the same at the end. After statistical analysis, the entire growth period comprising the second drug therapy and rest combined (DAY 30-54) did have enough points and gave a satisfactory p value ($p<0.001$) for the difference in the growth rates b (irinotecan-NANO) – b (irinotecan-MBLI-87) =0.1857 – 0.2836= -0,0979 ; t = -4,251 with 16 degrees of freedom (P = <0,001), and 95 percent confidence interval for difference of means: -0,147 to -0,0491(the power of performed test with alpha = 0,050: 0,981). The growth rate in the irinotecan-MBLI-87 case was 50% higher and this was supported at $p<0.001$(Table 1). Actually, a credible explanation is that the xenograft speeds up its growth when treatment with irinotecan-MBLI-87 was discontinued. Indeed, it is probably the best explanation of why the two curves grew closer together. A similar phenomenon was observed for tumor growth in humans upon cessation of treatment with bevacizumab (Avastin) (22), also suggesting a tumor growth acceleration after drug removal. It is quite interesting for us to find evidence for an apparently similar phenomenon in an animal model. Consequently, this model may be close to the human schedule (22). However, expecting to have a “permanent” benefit after therapy stops is probably premature.

TABLE 1. Parameters of MBLI-87-irinotecan and NANO- irinotecan exponential growth equations.

The points of the Figure 3C were better fitted (F test, at $p<0.01$) for both test and control series, as two separate time courses (rather than a single one) following the augmented (three parameter) exponential growth equation: $y = y0 + a*\exp(b*t)$, where y0 +1 is the computed size at t =0, a is 1.71828 times the increment in size at time equal to1/b, while b is the growth rate.

	COEFFICIENT	STD. ERROR		P VALUE
NANO-CPT-11 (0 to 30 days)				
	Rsqr=0.9702	**f=-0.6424+3.2693*exp(0.1322*x)**		
y0	-0.6424	10.2939	ns	0.9523
a	3.2693	2.9354	ns	0.308
b	0.1322	0.0294	*	0.0041
MBLI-87-CPT-11 (0 to 30 days)				
	Rsqr=0.7293	**f=9.7198+2.0402*exp(0.1162*x)**		
y0	9.7198	16.1066	ns	0.5683
a	2.0402	6.0361	ns	0.7469
b	0.1162	0.0954	ns	0.2691
NANO-CPT-11 (30 to 54 days)				
	Rsqr=0.9954	**f=163.1692+0.0437*exp(0.1857*x)**		
y0	163.1692	19.6266	**	0.0002
a	0.0437	0.0361	ns	0.2709
b	0.1857	0.0152	***	<0.0001
MBLI-87-CPT-11 (30 to 54 days)				
	Rsqr=0.9969	**f=91.6966+0.0002*exp(0.2836*x)**		
y0	91.6966	11.4804	**	0.0002
a	0.0002	0.0002	ns	0.3233
b	0.2836	0.0173	***	<0.0001

With the aim of identifying a specific, non-toxic inhibitor of ABCG2, we tested MBLI-87, an ABCG2-specific inhibitor not interacting with ABCB1. MBLI-87 could not be experimentally assayed at a maximum tolerable dose, due to limited solubility, and was not toxic for mice, the usable dose being here limited by the maximal volume that could be injected (300 µL). Furthermore, since ABCG2 is physiologically expressed in tissue (liver, BHE and intestine), we evaluated the influence of MBLI-87 on SN38 and irinotecan in plasma in pharmacokinetic experiments. Irinotecan disposition was evaluated in tumor-free mice after a single MBLI-87 (3.45 mg/kg) and/or irinotecan (20 mg/kg) intra-peritoneally injected dose, close to the intravenous route used in human. Under our conditions, irinotecan concentrations followed two-phase decays (Figure 4A). Irinotecan concentrations were maximal at 30 min, decreased strongly after 3h exposure and remained detectable after 24h. We also quantified SN-38, the active metabolite of irinotecan, in plasma. Interestingly, with a slight delay likely due to metabolism kinetics, the maximal concentration of SN38 was reached at a 3-h time exposure and decreased strongly but remained still detectable at 24h after injection (Figure 4B). The median per time point were similar for the different conditions. Consequently, MBLI-87 had no effect on SN38 and irinotecan concentrations and then on their associated toxicity. Such a lack of interference of MBLI-87 towards irinotecan and SN38 plasmatic disposition encourage further studies.

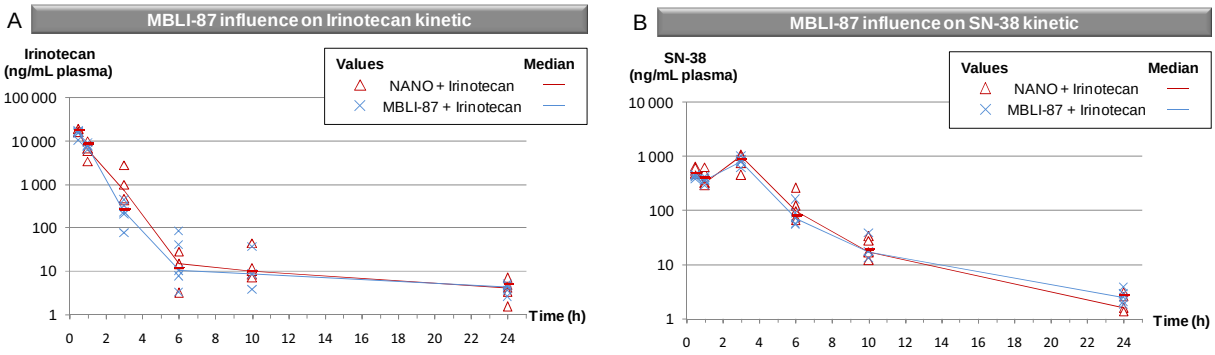

Figure 4. Representative plots of irinotecan (A) and SN-38 (B) plasma concentrations as a function of time. Mice were treated by I.P. injection of irinotecan in combination with MBLI-87 or NANO (5 mice per condition). HPLC MS/MS determined irinotecan and SN-38 plasma concentrations (ng/mL plasma) are represented as plots as a function of time. Irinotecan (A) or SN-38 (B) plasma concentration of each mice is shown in the absence (red triangles / NANO + irinotecan) or in presence of MBLI-87 (blue crosses / MBLI-87 + irinotecan). Medians are either represented by a red (NANO + irinotecan) or a blue line (MBLI-87 + irinotecan).

Optimization of both injectable MBLI-87 preparation and in vivo therapeutic protocol, will be useful to finally achieve complete ABCG2 inhibition. If MBLI-87 is indeed confirmed as a potent non-toxic inhibitor towards other drugs and in other model systems, it will constitute a good candidate for further developments aimed at improving bioavailability of substrate drugs, CNS penetration, accumulation of targeted agents in stem cells, and possibly to overcome multidrug resistance in cancer.

REFERENCES

1. Shukla S, Zaher H, Hartz A, Bauer B, Ware JA, Ambudkar SV. Curcumin inhibits the activity of ABCG2/BCRP1, a multidrug resistance-linked ABC drug transporter in mice. Pharm Res 2009;26(2):480-7.
2. Deeken JF, Figg WD, Bates SE, Sparreboom A. Toward individualized treatment: prediction of anticancer drug disposition and toxicity with pharmacogenetics. Anticancer Drugs 2007;18(2):111-26.
3. Loscher W, Potschka H. Blood-brain barrier active efflux transporters: ATP-binding cassette gene family. NeuroRx 2005;2(1):86-98.

4. Polli JW, Olson KL, Chism JP, John-Williams LS, Yeager RL, Woodard SM, et al. An unexpected synergist role of P-glycoprotein and breast cancer resistance protein on the central nervous system penetration of the tyrosine kinase inhibitor lapatinib (N-{3-chloro-4-[(3-fluorobenzyl)oxy]phenyl}-6-[5-({[2-(methylsulfonyl)ethy l]amino}methyl)-2-furyl]-4-quinazolinamine; GW572016). Drug Metab Dispos 2009;37(2):439-42.
5. Smith NF, Figg WD, Sparreboom A. Pharmacogenetics of irinotecan metabolism and transport: an update. Toxicol In Vitro 2006;20(2):163-75.
6. Chu XY, Suzuki H, Ueda K, Kato Y, Akiyama S, Sugiyama Y. Active efflux of CPT-11 and its metabolites in human KB-derived cell lines. J Pharmacol Exp Ther 1999;288(2):735-41.
7. Nicolle E, Boumendjel A, Macalou S, Genoux E, Ahmed-Belkacem A, Carrupt PA, et al. QSAR analysis and molecular modeling of ABCG2-specific inhibitors. Adv Drug Deliv Rev 2009;61(1):34-46.
8. Hida T, Ogawa S, Park JC, Park JY, Shimizu J, Horio Y, et al. Gefitinib for the treatment of non-small-cell lung cancer. Expert Rev Anticancer Ther 2009;9(1):17-35.
9. Lemos C, Jansen G, Peters GJ. Drug transporters: recent advances concerning BCRP and tyrosine kinase inhibitors. Br J Cancer 2008;98(5):857-62.
10. Stewart CF, Leggas M, Schuetz JD, Panetta JC, Cheshire PJ, Peterson J, et al. Gefitinib enhances the antitumor activity and oral bioavailability of irinotecan in mice. Cancer Res 2004;64(20):7491-9.
11. Elkind NB, Szentpetery Z, Apati A, Ozvegy-Laczka C, Varady G, Ujhelly O, et al. Multidrug transporter ABCG2 prevents tumor cell death induced by the epidermal growth factor receptor inhibitor Iressa (ZD1839, Gefitinib). Cancer Res 2005;65(5):1770-7.
12. Leggas M, Panetta JC, Zhuang Y, Schuetz JD, Johnston B, Bai F, et al. Gefitinib modulates the function of multiple ATP-binding cassette transporters in vivo. Cancer Res 2006;66(9):4802-7.
13. Yanase K, Tsukahara S, Asada S, Ishikawa E, Imai Y, Sugimoto Y. Gefitinib reverses breast cancer resistance protein-mediated drug resistance. Mol Cancer Ther 2004;3(9):1119-25.
14. Ahmed-Belkacem A, Pozza A, Munoz-Martinez F, Bates SE, Castanys S, Gamarro F, et al. Flavonoid structure-activity studies identify 6-prenylchrysin and tectochrysin as potent and specific inhibitors of breast cancer resistance protein ABCG2. Cancer Res 2005;65(11):4852-60.
15. Boumendjel A, Macalou S, Ahmed-Belkacem A, Blanc M, Di Pietro A. Acridone derivatives: design, synthesis, and inhibition of breast cancer resistance protein ABCG2. Bioorg Med Chem 2007;15(8):2892-7.
16. Macalou S, Pozza A, Terreux R, Magnard S, Boumendjel A, Pietro AD. Acridone-based inhibitors suggest adjacent ABCG2-specific inhibitory site and catalytic transport site. submitted.
17. Robey RW, Honjo Y, Morisaki K, Nadjem TA, Runge S, Risbood M, et al. Mutations at amino-acid 482 in the ABCG2 gene affect substrate and antagonist specificity. Br J Cancer 2003;89(10):1971-8.
18. Choisnard L, Geze A, Putaux JL, Wong YS, Wouessidjewe D. Nanoparticles of beta-cyclodextrin esters obtained by self-assembling of biotransesterified beta-cyclodextrins. Biomacromolecules 2006;7(2):515-20.
19. Gèze A. LC, J.-L. Putaux, D. Wouessidjewe. Colloidal systems made of biotransesterified alpha, beta and gamma cyclodextrins grafted with C10 alkyl chains. Materials Science and Engineering C 29 2009:458-462.
20. Choisnard L, Geze A, Yameogo BG, Putaux JL, Wouessidjewe D. Miscellaneous nanoaggregates made of beta-CD esters synthesised by an enzymatic pathway. Int J Pharm 2007;344(1-2):26-32.
21. Zhang Y, Bressler JP, Neal J, Lal B, Bhang HE, Laterra J, et al. ABCG2/BCRP expression modulates D-Luciferin based bioluminescence imaging. Cancer Res 2007;67(19):9389-97.
22. Stein WD, Yang J, Bates SE, Fojo T. Bevacizumab reduces the growth rate constants of renal carcinomas: a novel algorithm suggests early discontinuation of bevacizumab resulted in a lack of survival advantage. Oncologist 2008;13(10):1055-62.

E. CONCLUSION GENERALE

Les mécanismes de chimiorésistance font actuellement l'objet de nombreuses études et les transporteurs ABC représentent une thématique qui s'inscrit dans la lutte contre le cancer.

La protéine ABCC11 a été impliquée dans la résistance des cancers du sein traités par des combinaisons thérapeutiques incluant certains de ses substrats. Bien que ces derniers n'aient pas tous encore été identifiés, nous savons que le 5FdUMP (métabolite du 5FU) ou l'aracytine font partie des anticancéreux dont l'efficacité sera partiellement dépendante de l'activité d'ABCC11. Le niveau d'expression en ARNm d'ABCC11 est variable selon l'origine tissulaire et la physiopathologie. Dans un processus tumoral, la nature, le type, le stade, l'expression de marqueurs (récepteurs hormonaux par exemple) et les thérapeutiques (tamoxifène, dexaméthasone) peuvent influer sur le niveau d'expression d'ABCC11. Il apparaît donc que l'efficacité d'une thérapie à base de substrats d'ABCC11 dépend de nombreux paramètres et implique une personnalisation du traitement.

Afin de valider cette valeur prédictive d'ABCC11, différentes études cliniques pourraient être mises en place. Il serait en effet intéressant de confirmer l'implication d'ABCC11 sur la réponse aux traitements et les rechutes observées en clinique. Pour cela, une méta-analyse transcriptomique et/ou protéomique prospective devra être mise en place, sur un grand panel de tumeurs du sein, traitées par des chimiothérapies incluant des substrats d'ABCC11, avant et après rechute. L'évolution du profil d'expression d'ABCC11 pourrait être évaluée à la fois sur des sous groupes ayant un niveau endogène élevé d'ABCC11 ou au contraire ne l'exprimant pas. Sachant que la chimiorésistance est multifactorielle et résultante de multiples mécanismes, il faudra raisonner par voies fonctionnelles (voies de signalisation, cycle cellulaire, apoptose) et évaluer l'implication d'autres acteurs (autres transporteurs ABC, modification du niveau d'expression de la cible ou d'un acteur du métabolisme de l'anticancéreux,). Ces informations permettront de s'affranchir du biais lié à ces autres paramètres. Pour réaliser cette approche, des outils de biologie moléculaire et d'analyse à grande échelle sur des micro-biospsies (puces à ADN, puces à tissu / « *tissue microarray* », séquençage à haut débit) ainsi que des compétences bioinformatiques seront nécessaires et complémentaires.

Ces études pourraient aussi être adaptées, de manière intéressante, dans le cadre des traitements adjuvants à la chimiothérapie. Le niveau d'expression d'ABCC11 pourrait être évalué avant et après traitement au tamoxifène (hormonothérapie) ou à la dexaméthasone (thérapie anti-inflammatoire ou anti-émétique). Les tumeurs concernées par ces études pourront être traitées (1) soit par des chimiothérapies sans substrat d'ABCC11 qui n'influeront pas l'expression d'ABCC11 (confirmation de l'effet directe des molécules adjuvantes sur ABCC11) ; (2) soit par des chimiothérapies comportant au moins un substrat d'ABCC11 et dont l'issue (rechute, survie) pourra être corrélée au niveau d'expression d'ABCC11 (confirmation de l'effet indirecte des molécules adjuvantes sur la réponse à la chimiothérapie). Ces groupes permettraient également de confirmer l'induction de l'expression d'ABCC11 via des voies de régulation pouvant impliquer ER, PXR, GR et/ou PR et l'influence de cette surexpression sur la réponse au traitement.

La perspective d'adapter le traitement à chaque individu reste un objectif important, et n'est encore que très limitée en pratique courante (herceptine, tamoxifène). Après l'analyse de toutes ces données, ABCC11 pourra peut être intégrée comme un nouveau facteur et participer à l'amélioration de la prise en charge du cancer du sein.

D'autre part, de nombreux efforts sont également mis en œuvre pour identifier des modulateurs de l'activité des transporteurs ABC. En plus de présenter un potentiel thérapeutique supplémentaire face à la résistance aux médicaments anticancéreux, ils peuvent permettre une meilleure pénétration dans les tissus à traiter comme à travers certaine protection telle que la barrière hémato-encéphalique (exprimant ABCB1/Pgp ou ABCG2/BCRP par exemple).

Il est donc important de coupler la caractérisation moléculaire de l'interaction de la protéine avec ses inhibiteurs et d'évaluer la toxicité et l'efficacité de ces derniers, chez l'animal dans le cadre d'étude pré-cliniques. En effet, plus la cible est caractérisée (fonctionnement et structure), plus la prédiction bioinformatique est performante pour prédire la structure des modulateurs. De nombreux outils biochimiques et bioinformatiques (illustrés par la modélisation *in silico* d'ABCC11) ont, à ce jour, été mis au point et démontrent de plus en plus leur capacité et leur indispensabilité dans le monde de la recherche. Dans le cadre de la validation de ces hypothèses, la génération de lignées sur-exprimant ABCC11 reste un objectif important qui, en particulier, permettra de sélectionner *in vitro* des modulateurs de l'activité d'ABCC11.

De nombreuses chimiothèques sont actuellement disponibles. Elles pourraient servir à l'identification de molécules actives (tête de séries) pouvant être optimisées grâce à la conception de séries structurales réalisées par nos collaborateurs chimistes. L'utilisation des outils bioinformatiques apparaîtra à ce moment là comme un élément clé pour améliorer l'efficacité des ces modulateurs. Pour cela, les meilleurs modulateurs pourront être placés dans la structure *in silico* d'ABCC11, permettre d'identifier le(s) site(s) de liaison et amener à la génération de structure plus affines et spécifiques d'ABCC11. De ce fait, de nouvelles structures pourront être mises à jour et testées *in vitro*. L'absence d'effet toxique des meilleurs modulateurs pourra ensuite être analysée *in vivo* sur des animaux de laboratoire tels que les souris. Une fois que l'influence de ces modulateurs sur les paramètres pharmacocinétiques des anticancéreux sera connue, ils pourront être testés en combinaison avec ces anticancéreux, dans le cadre de traitement de xénogreffes cancéreuses chez la souris. Le but ultime sera d'identifier un ou plusieurs modulateurs améliorant l'efficacité des thérapies anticancéreuses tout en limitant les effets secondaires.

Pour conclure, le travail que nous avons effectué sur ABCC11 s'inscrit parfaitement dans la démarche d'améliorer la prise en charge des patients atteints par le cancer et présente encore de nombreuses perspectives de découverte.

F. BIBLIOGRAPHIE

[1] Tavassoéli, F.A.; Devilee, P., *Tumours of the Breast and Female Genital Organs*. Pathology and Genetics. Vol. IARC WHO Classification of Tumours, No 4. 2003.

[2] Weigelt, B.; Peterse, J.L.; van 't Veer, L.J. Breast cancer metastasis: markers and models. *Nat Rev Cancer*, **2005**, 5, 591-602.

[3] Stacker, S.A.; Achen, M.G.; Jussila, L.; Baldwin, M.E.; Alitalo, K. Lymphangiogenesis and cancer metastasis. *Nat Rev Cancer*, **2002**, 2, 573-83.

[4] McGuire, W.L. Prognostic factors for recurrence and survival in human breast cancer. *Breast Cancer Res Treat*, **1987**, 10, 5-9.

[5] Coleman, R.E.; Rubens, R.D. The clinical course of bone metastases from breast cancer. *Br J Cancer*, **1987**, 55, 61-6.

[6] Esteva, F.J.; Valero, V.; Pusztai, L.; Boehnke-Michaud, L.; Buzdar, A.U.; Hortobagyi, G.N. Chemotherapy of metastatic breast cancer: what to expect in 2001 and beyond. *Oncologist*, **2001**, 6, 133-46.

[7] Harrison, K.M.; Muss, H.B.; Ball, M.R.; McWhorter, M.; Case, D. Spinal cord compression in breast cancer. *Cancer*, **1985**, 55, 2839-44.

[8] LoRusso, P. Analysis of skeletal-related events in breast cancer and response to therapy. *Semin Oncol*, **2001**, 28, 22-7.

[9] Gosden, J.R.; Middleton, P.G.; Rout, D. Localization of the human oestrogen receptor gene to chromosome 6q24----q27 by in situ hybridization. *Cytogenet Cell Genet*, **1986**, 43, 218-20.

[10] Ponglikitmongkol, M.; Green, S.; Chambon, P. Genomic organization of the human oestrogen receptor gene. *Embo J*, **1988**, 7, 3385-8.

[11] Enmark, E.; Pelto-Huikko, M.; Grandien, K.; Lagercrantz, S.; Lagercrantz, J.; Fried, G.; Nordenskjold, M.; Gustafsson, J.A. Human estrogen receptor beta-gene structure, chromosomal localization, and expression pattern. *J Clin Endocrinol Metab*, **1997**, 82, 4258-65.

[12] Jensen E.V., J.H.I. Basic guides to the mechanism of estrogen action. *Recent Prog Horm Res*, **1962**, 18, 387-414.

[13] Walter, P.; Green, S.; Greene, G.; Krust, A.; Bornert, J.M.; Jeltsch, J.M.; Staub, A.; Jensen, E.; Scrace, G.; Waterfield, M.; et al. Cloning of the human estrogen receptor cDNA. *Proc Natl Acad Sci U S A*, **1985**, 82, 7889-93.

[14] Kuiper, G.G.; Enmark, E.; Pelto-Huikko, M.; Nilsson, S.; Gustafsson, J.A. Cloning of a novel receptor expressed in rat prostate and ovary. *Proc Natl Acad Sci U S A*, **1996**, 93, 5925-30.

[15] Weihua, Z.; Andersson, S.; Cheng, G.; Simpson, E.R.; Warner, M.; Gustafsson, J.A. Update on estrogen signaling. *FEBS Lett*, **2003**, 546, 17-24.

[16] Nilsson, S.; Makela, S.; Treuter, E.; Tujague, M.; Thomsen, J.; Andersson, G.; Enmark, E.; Pettersson, K.; Warner, M.; Gustafsson, J.A. Mechanisms of estrogen action. *Physiol Rev*, **2001**, 81, 1535-65.

[17] Faus, H.; Haendler, B. Post-translational modifications of steroid receptors. *Biomed Pharmacother*, **2006**, 60, 520-8.

[18] Sentis, S.; Le Romancer, M.; Bianchin, C.; Rostan, M.C.; Corbo, L. Sumoylation of the estrogen receptor alpha hinge region regulates its transcriptional activity. *Mol Endocrinol*, **2005**, 19, 2671-84.

[19] Maeda, M. The conserved residues of the ligand-binding domains of steroid receptors are located in the core of the molecules. *J Mol Graph Model*, **2001**, 19, 543-51, 601-6.

[20] Matthews, J.; Gustafsson, J.A. Estrogen signaling: a subtle balance between ER alpha and ER beta. *Mol Interv*, **2003**, 3, 281-92.

[21] Paruthiyil, S.; Parmar, H.; Kerekatte, V.; Cunha, G.R.; Firestone, G.L.; Leitman, D.C. Estrogen receptor beta inhibits human breast cancer cell proliferation and tumor formation by causing a G2 cell cycle arrest. *Cancer Res*, **2004**, 64, 423-8.

[22] Strom, A.; Hartman, J.; Foster, J.S.; Kietz, S.; Wimalasena, J.; Gustafsson, J.A. Estrogen receptor beta inhibits 17beta-estradiol-stimulated proliferation of the breast cancer cell line T47D. *Proc Natl Acad Sci U S A*, **2004**, 101, 1566-71.

[23] Weigel, N.L.; Zhang, Y. Ligand-independent activation of steroid hormone receptors. *J Mol Med*, **1998**, 76, 469-79.

[24] Wrenn, C.K.; Katzenellenbogen, B.S. Structure-function analysis of the hormone binding domain of the human estrogen receptor by region-specific mutagenesis and phenotypic screening in yeast. *J Biol Chem*, **1993**, 268, 24089-98.

[25] Merot, Y.; Metivier, R.; Penot, G.; Manu, D.; Saligaut, C.; Gannon, F.; Pakdel, F.; Kah, O.; Flouriot, G. The relative contribution exerted by AF-1 and AF-2 transactivation functions in estrogen receptor alpha transcriptional activity depends upon the differentiation stage of the cell. *J Biol Chem*, **2004**, 279, 26184-91.

[26] Lorenzo, J. A new hypothesis for how sex steroid hormones regulate bone mass. *J Clin Invest*, **2003**, 111, 1641-3.

[27] Chambliss, K.L.; Yuhanna, I.S.; Anderson, R.G.; Mendelsohn, M.E.; Shaul, P.W. ERbeta has nongenomic action in caveolae. *Mol Endocrinol*, **2002**, 16, 938-46.

[28] Razandi, M.; Pedram, A.; Merchenthaler, I.; Greene, G.L.; Levin, E.R. Plasma membrane estrogen receptors exist and functions as dimers. *Mol Endocrinol*, **2004**, 18, 2854-65.

[29] Baulieu, E.E.; Binart, N.; Cadepond, F.; Catelli, M.G.; Chambraud, B.; Garnier, J.; Gasc, J.M.; Groyer-Schweizer, G.; Oblin, M.E.; Radanyi, C.; et al. Receptor-associated nuclear proteins and steroid/antisteroid action. *Ann N Y Acad Sci*, **1990**, 595, 300-15.

[30] Kumar, V.; Chambon, P. The estrogen receptor binds tightly to its responsive element as a ligand-induced homodimer. *Cell*, **1988**, 55, 145-56.

[31] McKenna, N.J.; O'Malley, B.W. Nuclear receptors, coregulators, ligands, and selective receptor modulators: making sense of the patchwork quilt. *Ann N Y Acad Sci*, **2001**, 949, 3-5.

[32] Bunone, G.; Briand, P.A.; Miksicek, R.J.; Picard, D. Activation of the unliganded estrogen receptor by EGF involves the MAP kinase pathway and direct phosphorylation. *Embo J*, **1996**, 15, 2174-83.

[33] Kato, S.; Endoh, H.; Masuhiro, Y.; Kitamoto, T.; Uchiyama, S.; Sasaki, H.; Masushige, S.; Gotoh, Y.; Nishida, E.; Kawashima, H.; Metzger, D.; Chambon, P. Activation of the estrogen receptor through phosphorylation by mitogen-activated protein kinase. *Science*, **1995**, 270, 1491-4.

[34] Korach, K.S. Insights from the study of animals lacking functional estrogen receptor. *Science*, **1994**, 266, 1524-7.

[35] Lubahn, D.B.; Moyer, J.S.; Golding, T.S.; Couse, J.F.; Korach, K.S.; Smithies, O. Alteration of reproductive function but not prenatal sexual development after insertional disruption of the mouse estrogen receptor gene. *Proc Natl Acad Sci U S A*, **1993**, 90, 11162-6.

[36] Eddy, E.M.; Washburn, T.F.; Bunch, D.O.; Goulding, E.H.; Gladen, B.C.; Lubahn, D.B.; Korach, K.S. Targeted disruption of the estrogen receptor gene in male mice causes alteration of spermatogenesis and infertility. *Endocrinology*, **1996**, 137, 4796-805.

[37] Ogawa, S.; Taylor, J.A.; Lubahn, D.B.; Korach, K.S.; Pfaff, D.W. Reversal of sex roles in genetic female mice by disruption of estrogen receptor gene. *Neuroendocrinology*, **1996**, 64, 467-70.

[38] Ogawa, S.; Lubahn, D.B.; Korach, K.S.; Pfaff, D.W. Behavioral effects of estrogen receptor gene disruption in male mice. *Proc Natl Acad Sci U S A*, **1997**, 94, 1476-81.

[39] Thomas, T.; Gallo, M.A.; Thomas, T.J. Estrogen receptors as targets for drug development for breast cancer, osteoporosis and cardiovascular diseases. *Curr Cancer Drug Targets*, **2004**, 4, 483-99.

[40] Pearce, S.T.; Jordan, V.C. The biological role of estrogen receptors alpha and beta in cancer. *Crit Rev Oncol Hematol*, **2004**, 50, 3-22.

[41] Winneker, R.C.; Fensome, A.; Zhang, P.; Yudt, M.R.; McComas, C.C.; Unwalla, R.J. A new generation of progesterone receptor modulators. *Steroids*, **2008**, 73, 689-701.

[42] Lydon, J.P.; DeMayo, F.J.; Funk, C.R.; Mani, S.K.; Hughes, A.R.; Montgomery, C.A., Jr.; Shyamala, G.; Conneely, O.M.; O'Malley, B.W. Mice lacking progesterone receptor exhibit pleiotropic reproductive abnormalities. *Genes Dev*, **1995**, 9, 2266-78.

[43] Kastner, P.; Krust, A.; Turcotte, B.; Stropp, U.; Tora, L.; Gronemeyer, H.; Chambon, P. Two distinct estrogen-regulated promoters generate transcripts encoding the two functionally different human progesterone receptor forms A and B. *Embo J*, **1990**, 9, 1603-14.

[44] Mangelsdorf, D.J.; Thummel, C.; Beato, M.; Herrlich, P.; Schutz, G.; Umesono, K.; Blumberg, B.; Kastner, P.; Mark, M.; Chambon, P.; Evans, R.M. The nuclear receptor superfamily: the second decade. *Cell*, **1995**, 83, 835-9.

[45] Gao, X.; Nawaz, Z. Progesterone receptors - animal models and cell signaling in breast cancer: Role of steroid receptor coactivators and corepressors of progesterone receptors in breast cancer. *Breast Cancer Res*, **2002**, 4, 182-6.

[46] Giangrande, P.H.; Pollio, G.; McDonnell, D.P. Mapping and characterization of the functional domains responsible for the differential activity of the A and B isoforms of the human progesterone receptor. *J Biol Chem*, **1997**, 272, 32889-900.

[47] Richer, J.K.; Jacobsen, B.M.; Manning, N.G.; Abel, M.G.; Wolf, D.M.; Horwitz, K.B. Differential gene regulation by the two progesterone receptor isoforms in human breast cancer cells. *J Biol Chem*, **2002**, 277, 5209-18.

[48] Felts, S.J.; Karnitz, L.M.; Toft, D.O. Functioning of the Hsp90 machine in chaperoning checkpoint kinase I (Chk1) and the progesterone receptor (PR). *Cell Stress Chaperones*, **2007**, 12, 353-63.

[49] Lange, C.A. Integration of progesterone receptor action with rapid signaling events in breast cancer models. *J Steroid Biochem Mol Biol*, **2008**, 108, 203-12.

[50] McKenna, N.J.; Lanz, R.B.; O'Malley, B.W. Nuclear receptor coregulators: cellular and molecular biology. *Endocr Rev*, **1999**, 20, 321-44.

[51] Conneely, O.M.; Lydon, J.P.; De Mayo, F.; O'Malley, B.W. Reproductive functions of the progesterone receptor. *J Soc Gynecol Investig*, **2000**, 7, S25-32.

[52] Conneely, O.M.; Lydon, J.P. Progesterone receptors in reproduction: functional impact of the A and B isoforms. *Steroids*, **2000**, 65, 571-7.

[53] Shyamala, G.; Yang, X.; Silberstein, G.; Barcellos-Hoff, M.H.; Dale, E. Transgenic mice carrying an imbalance in the native ratio of A to B forms of progesterone receptor exhibit developmental abnormalities in mammary glands. *Proc Natl Acad Sci U S A*, **1998**, 95, 696-701.

[54] Shyamala, G.; Yang, X.; Cardiff, R.D.; Dale, E. Impact of progesterone receptor on cell-fate decisions during mammary gland development. *Proc Natl Acad Sci U S A*, **2000**, 97, 3044-9.

[55] Graham, J.D.; Yeates, C.; Balleine, R.L.; Harvey, S.S.; Milliken, J.S.; Bilous, A.M.; Clarke, C.L. Progesterone receptor A and B protein expression in human breast cancer. *J Steroid Biochem Mol Biol*, **1996**, 56, 93-8.

[56] Brettes J-P., M.C., Gairard B., Bellocq J-P., *Transfert des bases fondamentales à la clinique: une pathologie exemplaire, le cancer du sein*, in *Cancer du sein*, Masson, Editor. 2007. p. 50-70.

[57] Slamon, D.J.; Clark, G.M.; Wong, S.G.; Levin, W.J.; Ullrich, A.; McGuire, W.L. Human breast cancer: correlation of relapse and survival with amplification of the HER-2/neu oncogene. *Science*, **1987**, 235, 177-82.

[58] Slamon, D.J.; Godolphin, W.; Jones, L.A.; Holt, J.A.; Wong, S.G.; Keith, D.E.; Levin, W.J.; Stuart, S.G.; Udove, J.; Ullrich, A.; et al. Studies of the HER-2/neu proto-oncogene in human breast and ovarian cancer. *Science*, **1989**, 244, 707-12.

[59] Seshadri, R.; Firgaira, F.A.; Horsfall, D.J.; McCaul, K.; Setlur, V.; Kitchen, P. Clinical significance of HER-2/neu oncogene amplification in primary breast cancer. The South Australian Breast Cancer Study Group. *J Clin Oncol*, **1993**, 11, 1936-42.

[60] Press, M.F.; Pike, M.C.; Chazin, V.R.; Hung, G.; Udove, J.A.; Markowicz, M.; Danyluk, J.; Godolphin, W.; Sliwkowski, M.; Akita, R.; et al. Her-2/neu expression in node-negative breast cancer: direct tissue quantitation by computerized image analysis and association of overexpression with increased risk of recurrent disease. *Cancer Res*, **1993**, 53, 4960-70.

[61] Ravdin, P.M.; Chamness, G.C. The c-erbB-2 proto-oncogene as a prognostic and predictive marker in breast cancer: a paradigm for the development of other macromolecular markers--a review. *Gene*, **1995**, 159, 19-27.

[62] Hudziak, R.M.; Schlessinger, J.; Ullrich, A. Increased expression of the putative growth factor receptor p185HER2 causes transformation and tumorigenesis of NIH 3T3 cells. *Proc Natl Acad Sci U S A*, **1987**, 84, 7159-63.

[63] Chazin, V.R.; Kaleko, M.; Miller, A.D.; Slamon, D.J. Transformation mediated by the human HER-2 gene independent of the epidermal growth factor receptor. *Oncogene*, **1992**, 7, 1859-66.

[64] Guy, C.T.; Webster, M.A.; Schaller, M.; Parsons, T.J.; Cardiff, R.D.; Muller, W.J. Expression of the neu protooncogene in the mammary epithelium of transgenic mice induces metastatic disease. *Proc Natl Acad Sci U S A*, **1992**, 89, 10578-82.

[65] Pietras, R.J.; Arboleda, J.; Reese, D.M.; Wongvipat, N.; Pegram, M.D.; Ramos, L.; Gorman, C.M.; Parker, M.G.; Sliwkowski, M.X.; Slamon, D.J. HER-2 tyrosine kinase pathway targets estrogen receptor and promotes hormone-independent growth in human breast cancer cells. *Oncogene*, **1995**, 10, 2435-46.

[66] Hudziak, R.M.; Lewis, G.D.; Winget, M.; Fendly, B.M.; Shepard, H.M.; Ullrich, A. p185HER2 monoclonal antibody has antiproliferative effects in vitro and sensitizes human breast tumor cells to tumor necrosis factor. *Mol Cell Biol*, **1989**, 9, 1165-72.

[67] Shepard, H.M.; Lewis, G.D.; Sarup, J.C.; Fendly, B.M.; Maneval, D.; Mordenti, J.; Figari, I.; Kotts, C.E.; Palladino, M.A., Jr.; Ullrich, A.; et al. Monoclonal antibody therapy of human cancer: taking the HER2 protooncogene to the clinic. *J Clin Immunol*, **1991**, 11, 117-27.

[68] Carter, P.; Presta, L.; Gorman, C.M.; Ridgway, J.B.; Henner, D.; Wong, W.L.; Rowland, A.M.; Kotts, C.; Carver, M.E.; Shepard, H.M. Humanization of an anti-p185HER2 antibody for human cancer therapy. *Proc Natl Acad Sci U S A*, **1992**, 89, 4285-9.

[69] Pietras, R.J.; Pegram, M.D.; Finn, R.S.; Maneval, D.A.; Slamon, D.J. Remission of human breast cancer xenografts on therapy with humanized monoclonal antibody to HER-2 receptor and DNA-reactive drugs. *Oncogene*, **1998**, 17, 2235-49.

[70] Greenberg, P.A.; Hortobagyi, G.N.; Smith, T.L.; Ziegler, L.D.; Frye, D.K.; Buzdar, A.U. Long-term follow-up of patients with complete remission following combination chemotherapy for metastatic breast cancer. *J Clin Oncol*, **1996**, 14, 2197-205.

[71] Pietras, R.J.; Fendly, B.M.; Chazin, V.R.; Pegram, M.D.; Howell, S.B.; Slamon, D.J. Antibody to HER-2/neu receptor blocks DNA repair after cisplatin in human breast and ovarian cancer cells. *Oncogene*, **1994**, 9, 1829-38.

[72] Pegram, M.; Hsu, S.; Lewis, G.; Pietras, R.; Beryt, M.; Sliwkowski, M.; Coombs, D.; Baly, D.; Kabbinavar, F.; Slamon, D. Inhibitory effects of combinations of HER-2/neu antibody and chemotherapeutic agents used for treatment of human breast cancers. *Oncogene*, **1999**, 18, 2241-51.

[73] Pietras, R.J.; Poen, J.C.; Gallardo, D.; Wongvipat, P.N.; Lee, H.J.; Slamon, D.J. Monoclonal antibody to HER-2/neureceptor modulates repair of radiation-induced DNA damage and enhances radiosensitivity of human breast cancer cells overexpressing this oncogene. *Cancer Res*, **1999**, 59, 1347-55.

[74] Baselga, J.; Norton, L.; Albanell, J.; Kim, Y.M.; Mendelsohn, J. Recombinant humanized anti-HER2 antibody (Herceptin) enhances the antitumor activity of paclitaxel and doxorubicin against HER2/neu overexpressing human breast cancer xenografts. *Cancer Res*, **1998**, 58, 2825-31.

[75] Baselga, J.; Tripathy, D.; Mendelsohn, J.; Baughman, S.; Benz, C.C.; Dantis, L.; Sklarin, N.T.; Seidman, A.D.; Hudis, C.A.; Moore, J.; Rosen, P.P.; Twaddell, T.; Henderson, I.C.; Norton, L. Phase II study of weekly intravenous trastuzumab (Herceptin) in patients with HER2/neu-overexpressing metastatic breast cancer. *Semin Oncol*, **1999**, 26, 78-83.

[76] Cobleigh, M.A.; Vogel, C.L.; Tripathy, D.; Robert, N.J.; Scholl, S.; Fehrenbacher, L.; Wolter, J.M.; Paton, V.; Shak, S.; Lieberman, G.; Slamon, D.J. Multinational study of the efficacy and safety of humanized anti-HER2 monoclonal antibody in women who have HER2-overexpressing metastatic breast cancer that has progressed after chemotherapy for metastatic disease. *J Clin Oncol*, **1999**, 17, 2639-48.

[77] Pegram, M.D.; Lipton, A.; Hayes, D.F.; Weber, B.L.; Baselga, J.M.; Tripathy, D.; Baly, D.; Baughman, S.A.; Twaddell, T.; Glaspy, J.A.; Slamon, D.J. Phase II study of receptor-enhanced chemosensitivity using recombinant humanized anti-p185HER2/neu monoclonal antibody plus cisplatin in patients with HER2/neu-overexpressing metastatic breast cancer refractory to chemotherapy treatment. *J Clin Oncol*, **1998**, 16, 2659-71.

[78] Slamon, D.J.; Leyland-Jones, B.; Shak, S.; Fuchs, H.; Paton, V.; Bajamonde, A.; Fleming, T.; Eiermann, W.; Wolter, J.; Pegram, M.; Baselga, J.; Norton, L. Use of chemotherapy plus a monoclonal antibody against HER2 for metastatic breast cancer that overexpresses HER2. *N Engl J Med*, **2001**, 344, 783-92.

[79] Zhao, R.; Goldman, I.D. Resistance to antifolates. *Oncogene*, **2003**, 22, 7431-57.

[80] Humeniuk, R.; Menon, L.G.; Mishra, P.J.; Gorlick, R.; Sowers, R.; Rode, W.; Pizzorno, G.; Cheng, Y.C.; Kemeny, N.; Bertino, J.R.; Banerjee, D. Decreased levels of UMP kinase as a mechanism of fluoropyrimidine resistance. *Mol Cancer Ther*, **2009**,

[81] Fotoohi, K.; Jansen, G.; Assaraf, Y.G.; Rothem, L.; Stark, M.; Kathmann, I.; Gregorczyk, J.; Peters, G.J.; Albertioni, F. Disparate mechanisms of antifolate resistance provoked by methotrexate and its metabolite 7-hydroxymethotrexate in leukemia cells: implications for efficacy of methotrexate therapy. *Blood*, **2004**, 104, 4194-201.

[82] Banerjee, D.; Ercikan-Abali, E.; Waltham, M.; Schnieders, B.; Hochhauser, D.; Li, W.W.; Fan, J.; Gorlick, R.; Goker, E.; Bertino, J.R. Molecular mechanisms of resistance to antifolates, a review. *Acta Biochim Pol*, **1995**, 42, 457-64.

[83] Ferry, K.V.; Hamilton, T.C.; Johnson, S.W. Increased nucleotide excision repair in cisplatin-resistant ovarian cancer cells: role of ERCC1-XPF. *Biochem Pharmacol*, **2000**, 60, 1305-13.

[84] Szakacs, G.; Paterson, J.K.; Ludwig, J.A.; Booth-Genthe, C.; Gottesman, M.M. Targeting multidrug resistance in cancer. *Nat Rev Drug Discov*, **2006**, 5, 219-34.

[85] Scherrmann, J.M. Expression and function of multidrug resistance transporters at the blood-brain barriers. *Expert Opin Drug Metab Toxicol*, **2005**, 1, 233-46.

[86] Klaassen, C.D.; Aleksunes, L.M. Xenobiotic, bile acid, and cholesterol transporters: function and regulation. *Pharmacol Rev*, 62, 1-96.

[87] Oostendorp, R.L.; Beijnen, J.H.; Schellens, J.H. The biological and clinical role of drug transporters at the intestinal barrier. *Cancer Treat Rev*, **2009**, 35, 137-47.

[88] Dean, M.; Rzhetsky, A.; Allikmets, R. The human ATP-binding cassette (ABC) transporter superfamily. *Genome Res*, **2001**, 11, 1156-66.

[89] Benderra, Z.; Faussat, A.M.; Sayada, L.; Perrot, J.Y.; Chaoui, D.; Marie, J.P.; Legrand, O. Breast cancer resistance protein and P-glycoprotein in 149 adult acute myeloid leukemias. *Clin Cancer Res*, **2004**, 10, 7896-902.

[90] Noguchi, K.; Katayama, K.; Mitsuhashi, J.; Sugimoto, Y. Functions of the breast cancer resistance protein (BCRP/ABCG2) in chemotherapy. *Adv Drug Deliv Rev*, **2009**, 61, 26-33.

[91] Locher, K.P.; Lee, A.T.; Rees, D.C. The E. coli BtuCD structure: a framework for ABC transporter architecture and mechanism. *Science*, **2002**, 296, 1091-8.

[92] Gerber, S.; Comellas-Bigler, M.; Goetz, B.A.; Locher, K.P. Structural basis of trans-inhibition in a molybdate/tungstate ABC transporter. *Science*, **2008**, 321, 246-50.

[93] Pinkett, H.W.; Lee, A.T.; Lum, P.; Locher, K.P.; Rees, D.C. An inward-facing conformation of a putative metal-chelate-type ABC transporter. *Science*, **2007**, 315, 373-7.

[94] Oldham, M.L.; Khare, D.; Quiocho, F.A.; Davidson, A.L.; Chen, J. Crystal structure of a catalytic intermediate of the maltose transporter. *Nature*, **2007**, 450, 515-21.

[95] Kadaba, N.S.; Kaiser, J.T.; Johnson, E.; Lee, A.; Rees, D.C. The high-affinity E. coli methionine ABC transporter: structure and allosteric regulation. *Science*, **2008**, 321, 250-3.

[96] Dawson, R.J.; Locher, K.P. Structure of a bacterial multidrug ABC transporter. *Nature*, **2006**, 443, 180-5.

[97] Ward, A.; Reyes, C.L.; Yu, J.; Roth, C.B.; Chang, G. Flexibility in the ABC transporter MsbA: Alternating access with a twist. *Proc Natl Acad Sci U S A*, **2007**, 104, 19005-10.

[98] Aller, S.G.; Yu, J.; Ward, A.; Weng, Y.; Chittaboina, S.; Zhuo, R.; Harrell, P.M.; Trinh, Y.T.; Zhang, Q.; Urbatsch, I.L.; Chang, G. Structure of P-glycoprotein reveals a molecular basis for poly-specific drug binding. *Science*, **2009**, 323, 1718-22.

[99] Maeda, K.; Sugiyama, Y. Impact of genetic polymorphisms of transporters on the pharmacokinetic, pharmacodynamic and toxicological properties of anionic drugs. *Drug Metab Pharmacokinet*, **2008**, 23, 223-35.

[100] Kim, R.B.; Leake, B.F.; Choo, E.F.; Dresser, G.K.; Kubba, S.V.; Schwarz, U.I.; Taylor, A.; Xie, H.G.; McKinsey, J.; Zhou, S.; Lan, L.B.; Schuetz, J.D.; Schuetz, E.G.; Wilkinson, G.R. Identification of functionally variant MDR1 alleles among European Americans and African Americans. *Clin Pharmacol Ther*, **2001**, 70, 189-99.

[101] Hoffmeyer, S.; Burk, O.; von Richter, O.; Arnold, H.P.; Brockmoller, J.; Johne, A.; Cascorbi, I.; Gerloff, T.; Roots, I.; Eichelbaum, M.; Brinkmann, U. Functional polymorphisms of the human multidrug-resistance gene: multiple sequence variations and correlation of one allele with P-glycoprotein expression and activity in vivo. *Proc Natl Acad Sci U S A*, **2000**, 97, 3473-8.

[102] Nakamura, T.; Sakaeda, T.; Horinouchi, M.; Tamura, T.; Aoyama, N.; Shirakawa, T.; Matsuo, M.; Kasuga, M.; Okumura, K. Effect of the mutation (C3435T) at exon 26 of the MDR1 gene on expression level of MDR1 messenger ribonucleic acid in duodenal enterocytes of healthy Japanese subjects. *Clin Pharmacol Ther*, **2002**, 71, 297-303.

[103] Siegmund, W.; Ludwig, K.; Giessmann, T.; Dazert, P.; Schroeder, E.; Sperker, B.; Warzok, R.; Kroemer, H.K.; Cascorbi, I. The effects of the human MDR1 genotype on the expression of duodenal P-glycoprotein and disposition of the probe drug talinolol. *Clin Pharmacol Ther*, **2002**, 72, 572-83.

[104] Hitzl, M.; Drescher, S.; van der Kuip, H.; Schaffeler, E.; Fischer, J.; Schwab, M.; Eichelbaum, M.; Fromm, M.F. The C3435T mutation in the human MDR1 gene is associated with altered efflux of the P-glycoprotein substrate rhodamine 123 from CD56+ natural killer cells. *Pharmacogenetics*, **2001**, 11, 293-8.

[105] Oselin, K.; Nowakowski-Gashaw, I.; Mrozikiewicz, P.M.; Wolbergs, D.; Pahkla, R.; Roots, I. Quantitative determination of MDR1 mRNA expression in peripheral blood lymphocytes: a possible role of genetic polymorphisms in the MDR1 gene. *Eur J Clin Invest*, **2003**, 33, 261-7.

[106] Efferth, T.; Sauerbrey, A.; Steinbach, D.; Gebhart, E.; Drexler, H.G.; Miyachi, H.; Chitambar, C.R.; Becker, C.M.; Zintl, F.; Humeny, A. Analysis of single nucleotide polymorphism C3435T of the multidrug resistance gene MDR1 in acute lymphoblastic leukemia. *Int J Oncol*, **2003**, 23, 509-17.

[107] van der Holt, B.; Van den Heuvel-Eibrink, M.M.; Van Schaik, R.H.; van der Heiden, I.P.; Wiemer, E.A.; Vossebeld, P.J.; Lowenberg, B.; Sonneveld, P. ABCB1 gene polymorphisms are not associated with treatment outcome in elderly acute myeloid leukemia patients. *Clin Pharmacol Ther*, **2006**, 80, 427-39.

[108] Fung, K.L.; Gottesman, M.M. A synonymous polymorphism in a common MDR1 (ABCB1) haplotype shapes protein function. *Biochim Biophys Acta*, **2009**, 1794, 860-71.

[109] Oselin, K.; Gerloff, T.; Mrozikiewicz, P.M.; Pahkla, R.; Roots, I. MDR1 polymorphisms G2677T in exon 21 and C3435T in exon 26 fail to affect rhodamine 123 efflux in peripheral blood lymphocytes. *Fundam Clin Pharmacol*, **2003**, 17, 463-9.

[110] Calado, R.T.; Falcao, R.P.; Garcia, A.B.; Gabellini, S.M.; Zago, M.A.; Franco, R.F. Influence of functional MDR1 gene polymorphisms on P-glycoprotein activity in CD34+ hematopoietic stem cells. *Haematologica*, **2002**, 87, 564-8.

[111] Kimchi-Sarfaty, C.; Oh, J.M.; Kim, I.W.; Sauna, Z.E.; Calcagno, A.M.; Ambudkar, S.V.; Gottesman, M.M. A "silent" polymorphism in the MDR1 gene changes substrate specificity. *Science*, **2007**, 315, 525-8.

[112] Morita, N.; Yasumori, T.; Nakayama, K. Human MDR1 polymorphism: G2677T/A and C3435T have no effect on MDR1 transport activities. *Biochem Pharmacol*, **2003**, 65, 1843-52.

[113] Molsa, M.; Heikkinen, T.; Hakkola, J.; Hakala, K.; Wallerman, O.; Wadelius, M.; Wadelius, C.; Laine, K. Functional role of P-glycoprotein in the human blood-placental barrier. *Clin Pharmacol Ther*, **2005**, 78, 123-31.

[114] Siegsmund, M.; Brinkmann, U.; Schaffeler, E.; Weirich, G.; Schwab, M.; Eichelbaum, M.; Fritz, P.; Burk, O.; Decker, J.; Alken, P.; Rothenpieler, U.; Kerb, R.; Hoffmeyer, S.; Brauch, H. Association of the P-glycoprotein transporter MDR1(C3435T) polymorphism with the susceptibility to renal epithelial tumors. *J Am Soc Nephrol*, **2002**, 13, 1847-54.

[115] Schwab, M.; Schaeffeler, E.; Marx, C.; Fromm, M.F.; Kaskas, B.; Metzler, J.; Stange, E.; Herfarth, H.; Schoelmerich, J.; Gregor, M.; Walker, S.; Cascorbi, I.; Roots, I.; Brinkmann, U.; Zanger, U.M.; Eichelbaum, M. Association between the C3435T MDR1 gene polymorphism and susceptibility for ulcerative colitis. *Gastroenterology*, **2003**, 124, 26-33.

[116] Taheri, M.; Mahjoubi, F.; Omranipour, R. Effect of MDR1 polymorphism on multidrug resistance expression in breast cancer patients. *Genet Mol Res*, 9, 34-40.

[117] Tatari, F.; Salek, R.; Mosaffa, F.; Khedri, A.; Behravan, J. Association of C3435T single-nucleotide polymorphism of MDR1 gene with breast cancer in an Iranian population. *DNA Cell Biol*, **2009**, 28, 259-63.

[118] Cizmarikova, M.; Wagnerova, M.; Schonova, L.; Habalova, V.; Kohut, A.; Linkova, A.; Sarissky, M.; Mojzis, J.; Mirossay, L.; Mirossay, A. MDR1 (C3435T) polymorphism: relation to the risk of breast cancer and therapeutic outcome. *Pharmacogenomics J*, 10, 62-9.

[119] George, J.; Dharanipragada, K.; Krishnamachari, S.; Chandrasekaran, A.; Sam, S.S.; Sunder, E. A single-nucleotide polymorphism in the MDR1 gene as a predictor of response to neoadjuvant chemotherapy in breast cancer. *Clin Breast Cancer*, **2009**, 9, 161-5.

[120] Turgut, S.; Yaren, A.; Kursunluoglu, R.; Turgut, G. MDR1 C3435T polymorphism in patients with breast cancer. *Arch Med Res*, **2007**, 38, 539-44.

[121] Andersen, V.; Ostergaard, M.; Christensen, J.; Overvad, K.; Tjonneland, A.; Vogel, U. Polymorphisms in the xenobiotic transporter Multidrug Resistance 1 (MDR1) and interaction with meat intake in relation to risk of colorectal cancer in a Danish prospective case-cohort study. *BMC Cancer*, **2009**, 9, 407.

[122] Khedri, A.; Nejat-Shokouhi, A.; Salek, R.; Esmaeili, H.; Mokhtarifar, A.; Entezari Heravi, R.; Tatari, F.; Behravan, J.; Miladpour, B.; Omidvar Tehrani, S. Association of the colorectal cancer and MDR1 gene polymorphism in an Iranian population. *Mol Biol Rep*,

[123] Kurzawski, M.; Drozdzik, M.; Suchy, J.; Kurzawski, G.; Bialecka, M.; Gornik, W.; Lubinski, J. Polymorphism in the P-glycoprotein drug transporter MDR1 gene in colon cancer patients. *Eur J Clin Pharmacol*, **2005**, 61, 389-94.

[124] Gervasini, G.; Carrillo, J.A.; Garcia, M.; San Jose, C.; Cabanillas, A.; Benitez, J. Adenosine triphosphate-binding cassette B1 (ABCB1) (multidrug resistance 1) G2677T/A gene polymorphism is associated with high risk of lung cancer. *Cancer*, **2006**, 107, 2850-7.

[125] Drozdzik, M.; Bialecka, M.; Mysliwiec, K.; Honczarenko, K.; Stankiewicz, J.; Sych, Z. Polymorphism in the P-glycoprotein drug transporter MDR1 gene: a possible link between environmental and genetic factors in Parkinson's disease. *Pharmacogenetics*, **2003**, 13, 259-63.

[126] Furuno, T.; Landi, M.T.; Ceroni, M.; Caporaso, N.; Bernucci, I.; Nappi, G.; Martignoni, E.; Schaeffeler, E.; Eichelbaum, M.; Schwab, M.; Zanger, U.M. Expression polymorphism of the blood-brain barrier component P-glycoprotein (MDR1) in relation to Parkinson's disease. *Pharmacogenetics*, **2002**, 12, 529-34.

[127] Bleiber, G.; May, M.; Suarez, C.; Martinez, R.; Marzolini, C.; Egger, M.; Telenti, A. MDR1 genetic polymorphism does not modify either cell permissiveness to HIV-1 or disease progression before treatment. *J Infect Dis*, **2004**, 189, 583-6.

[128] Ifergan, I.; Bernard, N.F.; Bruneau, J.; Alary, M.; Tsoukas, C.M.; Roger, M. Allele frequency of three functionally active polymorphisms of the MDR-1 gene in high-risk HIV-negative and HIV-positive Caucasians. *Aids*, **2002**, 16, 2340-2.

[129] Jamroziak, K.; Mlynarski, W.; Balcerczak, E.; Mistygacz, M.; Trelinska, J.; Mirowski, M.; Bodalski, J.; Robak, T. Functional C3435T polymorphism of MDR1 gene: an impact on genetic susceptibility and clinical outcome of childhood acute lymphoblastic leukemia. *Eur J Haematol*, **2004**, 72, 314-21.

[130] Leal-Ugarte, E.; Gutierrez-Angulo, M.; Macias-Gomez, N.M.; Peralta-Leal, V.; Duran-Gonzalez, J.; De La Luz Ayala-Madrigal, M.; Partida-Perez, M.; Barros-Nunez, P.; Ruiz-Diaz, D.; Moreno-Ortiz, J.M.; Peregrina-Sandoval, J.; Meza-Espinoza, J.P. MDR1 C3435T polymorphism in Mexican children with acute lymphoblastic leukemia and in healthy individuals. *Hum Biol*, **2008**, 80, 449-55.

[131] Illmer, T.; Schuler, U.S.; Thiede, C.; Schwarz, U.I.; Kim, R.B.; Gotthard, S.; Freund, D.; Schakel, U.; Ehninger, G.; Schaich, M. MDR1 gene polymorphisms affect therapy outcome in acute myeloid leukemia patients. *Cancer Res*, **2002**, 62, 4955-62.

[132] Drain, S.; Catherwood, M.A.; Orr, N.; Galligan, L.; Rea, I.M.; Hodkinson, C.; Drake, M.B.; Kettle, P.J.; Morris, T.C.; Alexander, H.D. ABCB1 (MDR1) rs1045642 is associated with increased overall survival in plasma cell myeloma. *Leuk Lymphoma*, **2009**, 50, 566-70.

[133] Johne, A.; Kopke, K.; Gerloff, T.; Mai, I.; Rietbrock, S.; Meisel, C.; Hoffmeyer, S.; Kerb, R.; Fromm, M.F.; Brinkmann, U.; Eichelbaum, M.; Brockmoller, J.; Cascorbi, I.; Roots, I. Modulation of steady-state kinetics of digoxin by haplotypes of the P-glycoprotein MDR1 gene. *Clin Pharmacol Ther*, **2002**, 72, 584-94.

[134] Kurata, Y.; Ieiri, I.; Kimura, M.; Morita, T.; Irie, S.; Urae, A.; Ohdo, S.; Ohtani, H.; Sawada, Y.; Higuchi, S.; Otsubo, K. Role of human MDR1 gene polymorphism in bioavailability and interaction of digoxin, a substrate of P-glycoprotein. *Clin Pharmacol Ther*, **2002**, 72, 209-19.

[135] Verstuyft, C.; Schwab, M.; Schaeffeler, E.; Kerb, R.; Brinkmann, U.; Jaillon, P.; Funck-Brentano, C.; Becquemont, L. Digoxin pharmacokinetics and MDR1 genetic polymorphisms. *Eur J Clin Pharmacol*, **2003**, 58, 809-12.

[136] Sakaeda, T.; Nakamura, T.; Horinouchi, M.; Kakumoto, M.; Ohmoto, N.; Sakai, T.; Morita, Y.; Tamura, T.; Aoyama, N.; Hirai, M.; Kasuga, M.; Okumura, K. MDR1 genotype-related pharmacokinetics of digoxin after single oral administration in healthy Japanese subjects. *Pharm Res*, **2001**, 18, 1400-4.

[137] Gerloff, T.; Schaefer, M.; Johne, A.; Oselin, K.; Meisel, C.; Cascorbi, I.; Roots, I. MDR1 genotypes do not influence the absorption of a single oral dose of 1 mg digoxin in healthy white males. *Br J Clin Pharmacol*, **2002**, 54, 610-6.

[138] Drescher, S.; Schaeffeler, E.; Hitzl, M.; Hofmann, U.; Schwab, M.; Brinkmann, U.; Eichelbaum, M.; Fromm, M.F. MDR1 gene polymorphisms and disposition of the P-glycoprotein substrate fexofenadine. *Br J Clin Pharmacol*, **2002**, 53, 526-34.

[139] Macphee, I.A.; Fredericks, S.; Tai, T.; Syrris, P.; Carter, N.D.; Johnston, A.; Goldberg, L.; Holt, D.W. Tacrolimus pharmacogenetics: polymorphisms associated with expression of cytochrome p4503A5 and P-glycoprotein correlate with dose requirement. *Transplantation*, **2002**, 74, 1486-9.

[140] Zheng, H.; Webber, S.; Zeevi, A.; Schuetz, E.; Zhang, J.; Bowman, P.; Boyle, G.; Law, Y.; Miller, S.; Lamba, J.; Burckart, G.J. Tacrolimus dosing in pediatric heart transplant patients is related to CYP3A5 and MDR1 gene polymorphisms. *Am J Transplant*, **2003**, 3, 477-83.

[141] Anglicheau, D.; Verstuyft, C.; Laurent-Puig, P.; Becquemont, L.; Schlageter, M.H.; Cassinat, B.; Beaune, P.; Legendre, C.; Thervet, E. Association of the multidrug resistance-1 gene single-nucleotide polymorphisms with the tacrolimus dose requirements in renal transplant recipients. *J Am Soc Nephrol*, **2003**, 14, 1889-96.

[142] Goto, M.; Masuda, S.; Saito, H.; Uemoto, S.; Kiuchi, T.; Tanaka, K.; Inui, K. C3435T polymorphism in the MDR1 gene affects the enterocyte expression level of CYP3A4 rather than Pgp in recipients of living-donor liver transplantation. *Pharmacogenetics*, **2002**, 12, 451-7.

[143] Yanagimachi, M.; Naruto, T.; Tanoshima, R.; Kato, H.; Yokosuka, T.; Kajiwara, R.; Fujii, H.; Tanaka, F.; Goto, H.; Yagihashi, T.; Kosaki, K.; Yokota, S. Influence of CYP3A5 and ABCB1 gene polymorphisms on calcineurin inhibitor-related neurotoxicity after hematopoietic stem cell transplantation. *Clin Transplant*, **2009**,

[144] Fellay, J.; Marzolini, C.; Meaden, E.R.; Back, D.J.; Buclin, T.; Chave, J.P.; Decosterd, L.A.; Furrer, H.; Opravil, M.; Pantaleo, G.; Retelska, D.; Ruiz, L.; Schinkel, A.H.; Vernazza, P.; Eap, C.B.; Telenti, A. Response to antiretroviral treatment in HIV-1-infected individuals with allelic variants of the multidrug resistance transporter 1: a pharmacogenetics study. *Lancet*, **2002**, 359, 30-6.

[145] Haas, D.W.; Smeaton, L.M.; Shafer, R.W.; Robbins, G.K.; Morse, G.D.; Labbe, L.; Wilkinson, G.R.; Clifford, D.B.; D'Aquila, R.T.; De Gruttola, V.; Pollard, R.B.; Merigan, T.C.; Hirsch, M.S.; George, A.L., Jr.; Donahue, J.P.; Kim, R.B. Pharmacogenetics of long-term responses to antiretroviral regimens containing Efavirenz and/or Nelfinavir: an Adult Aids Clinical Trials Group Study. *J Infect Dis*, **2005**, 192, 1931-42.

[146] von Ahsen, N.; Richter, M.; Grupp, C.; Ringe, B.; Oellerich, M.; Armstrong, V.W. No influence of the MDR-1 C3435T polymorphism or a CYP3A4 promoter polymorphism (CYP3A4-V allele) on dose-adjusted cyclosporin A trough concentrations or rejection incidence in stable renal transplant recipients. *Clin Chem*, **2001**, 47, 1048-52.

[147] Min, D.I.; Ellingrod, V.L. C3435T mutation in exon 26 of the human MDR1 gene and cyclosporine pharmacokinetics in healthy subjects. *Ther Drug Monit*, **2002**, 24, 400-4.

[148] Balram, C.; Sharma, A.; Sivathasan, C.; Lee, E.J. Frequency of C3435T single nucleotide MDR1 genetic polymorphism in an Asian population: phenotypic-genotypic correlates. *Br J Clin Pharmacol*, **2003**, 56, 78-83.

[149] Yates, C.R.; Zhang, W.; Song, P.; Li, S.; Gaber, A.O.; Kotb, M.; Honaker, M.R.; Alloway, R.R.; Meibohm, B. The effect of CYP3A5 and MDR1 polymorphic expression on cyclosporine oral disposition in renal transplant patients. *J Clin Pharmacol*, **2003**, 43, 555-64.

[150] Jiang, Z.P.; Wang, Y.R.; Xu, P.; Liu, R.R.; Zhao, X.L.; Chen, F.P. Meta-analysis of the effect of MDR1 C3435T polymorphism on cyclosporine pharmacokinetics. *Basic Clin Pharmacol Toxicol*, **2008**, 103, 433-44.

[151] Taubert, D.; von Beckerath, N.; Grimberg, G.; Lazar, A.; Jung, N.; Goeser, T.; Kastrati, A.; Schomig, A.; Schomig, E. Impact of P-glycoprotein on clopidogrel absorption. *Clin Pharmacol Ther*, **2006**, 80, 486-501.

[152] Kerb, R.; Aynacioglu, A.S.; Brockmoller, J.; Schlagenhaufer, R.; Bauer, S.; Szekeres, T.; Hamwi, A.; Fritzer-Szekeres, M.; Baumgartner, C.; Ongen, H.Z.; Guzelbey, P.; Roots, I.; Brinkmann, U. The predictive value of MDR1, CYP2C9, and CYP2C19 polymorphisms for phenytoin plasma levels. *Pharmacogenomics J*, **2001**, 1, 204-10.

[153] Kodaira, C.; Sugimoto, M.; Nishino, M.; Yamade, M.; Shirai, N.; Uchida, S.; Ikuma, M.; Yamada, S.; Watanabe, H.; Hishida, A.; Furuta, T. Effect of MDR1 C3435T polymorphism on lansoprazole in healthy Japanese subjects. *Eur J Clin Pharmacol*, **2009**, 65, 593-600.

[154] Roberts, R.L.; Joyce, P.R.; Mulder, R.T.; Begg, E.J.; Kennedy, M.A. A common P-glycoprotein polymorphism is associated with nortriptyline-induced postural hypotension in patients treated for major depression. *Pharmacogenomics J*, **2002**, 2, 191-6.

[155] Pauli-Magnus, C.; Feiner, J.; Brett, C.; Lin, E.; Kroetz, D.L. No effect of MDR1 C3435T variant on loperamide disposition and central nervous system effects. *Clin Pharmacol Ther*, **2003**, 74, 487-98.

[156] Putnam, W.S.; Woo, J.M.; Huang, Y.; Benet, L.Z. Effect of the MDR1 C3435T variant and P-glycoprotein induction on dicloxacillin pharmacokinetics. *J Clin Pharmacol*, **2005**, 45, 411-21.

[157] Goh, B.C.; Lee, S.C.; Wang, L.Z.; Fan, L.; Guo, J.Y.; Lamba, J.; Schuetz, E.; Lim, R.; Lim, H.L.; Ong, A.B.; Lee, H.S. Explaining interindividual variability of docetaxel pharmacokinetics and pharmacodynamics in Asians through phenotyping and genotyping strategies. *J Clin Oncol*, **2002**, 20, 3683-90.

[158] Yoo, H.D.; Cho, H.Y.; Lee, Y.B. Population pharmacokinetic analysis of cilostazol in healthy subjects with genetic polymorphisms of CYP3A5, CYP2C19 and ABCB1. *Br J Clin Pharmacol*, 69, 27-37.

[159] Zhao, Y.; Zhai, D.; He, H.; Li, T.; Chen, X.; Ji, H. Effects of CYP3A5, MDR1 and CACNA1C polymorphisms on the oral disposition and response of nimodipine in a Chinese cohort. *Eur J Clin Pharmacol*, **2009**, 65, 579-84.

[160] Yin, O.Q.; Tomlinson, B.; Chow, M.S. Effect of multidrug resistance gene-1 (ABCB1) polymorphisms on the single-dose pharmacokinetics of cloxacillin in healthy adult Chinese men. *Clin Ther*, **2009**, 31, 999-1006.

[161] Gex-Fabry, M.; Eap, C.B.; Oneda, B.; Gervasoni, N.; Aubry, J.M.; Bondolfi, G.; Bertschy, G. CYP2D6 and ABCB1 genetic variability: influence on paroxetine plasma level and therapeutic response. *Ther Drug Monit*, **2008**, 30, 474-82.

[162] Kafka, A.; Sauer, G.; Jaeger, C.; Grundmann, R.; Kreienberg, R.; Zeillinger, R.; Deissler, H. Polymorphism C3435T of the MDR-1 gene predicts response to preoperative chemotherapy in locally advanced breast cancer. *Int J Oncol*, **2003**, 22, 1117-21.

[163] Siddiqui, A.; Kerb, R.; Weale, M.E.; Brinkmann, U.; Smith, A.; Goldstein, D.B.; Wood, N.W.; Sisodiya, S.M. Association of multidrug resistance in epilepsy with a polymorphism in the drug-transporter gene ABCB1. *N Engl J Med*, **2003**, 348, 1442-8.

[164] Brumme, Z.L.; Dong, W.W.; Chan, K.J.; Hogg, R.S.; Montaner, J.S.; O'Shaughnessy, M.V.; Harrigan, P.R. Influence of polymorphisms within the CX3CR1 and MDR-1 genes on initial antiretroviral therapy response. *Aids*, **2003**, 17, 201-8.

[165] Haas, D.W.; Wu, H.; Li, H.; Bosch, R.J.; Lederman, M.M.; Kuritzkes, D.; Landay, A.; Connick, E.; Benson, C.; Wilkinson, G.R.; Kessler, H.; Kim, R.B. MDR1 gene polymorphisms and phase 1 viral decay during HIV-1 infection: an adult AIDS Clinical Trials Group study. *J Acquir Immune Defic Syndr*, **2003**, 34, 295-8.

[166] Nasi, M.; Borghi, V.; Pinti, M.; Bellodi, C.; Lugli, E.; Maffei, S.; Troiano, L.; Richeldi, L.; Mussini, C.; Esposito, R.; Cossarizza, A. MDR1 C3435T genetic polymorphism does not influence the response to antiretroviral therapy in drug-naive HIV-positive patients. *Aids*, **2003**, 17, 1696-8.

[167] Winzer, R.; Langmann, P.; Zilly, M.; Tollmann, F.; Schubert, J.; Klinker, H.; Weissbrich, B. No influence of the P-glycoprotein polymorphisms MDR1 G2677T/A and C3435T on the virological and immunological response in treatment naive HIV-positive patients. *Ann Clin Microbiol Antimicrob*, **2005**, 4, 3.

[168] Ciccacci, C.; Borgiani, P.; Ceffa, S.; Sirianni, E.; Marazzi, M.C.; Altan, A.M.; Paturzo, G.; Bramanti, P.; Novelli, G.; Palombi, L. Nevirapine-induced hepatotoxicity and pharmacogenetics: a retrospective study in a population from Mozambique. *Pharmacogenomics*, 11, 23-31.

[169] Haas, D.W.; Ribaudo, H.J.; Kim, R.B.; Tierney, C.; Wilkinson, G.R.; Gulick, R.M.; Clifford, D.B.; Hulgan, T.; Marzolini, C.; Acosta, E.P. Pharmacogenetics of efavirenz and central nervous system side effects: an Adult AIDS Clinical Trials Group study. *Aids*, **2004**, 18, 2391-400.

[170] Lara, P.N., Jr.; Natale, R.; Crowley, J.; Lenz, H.J.; Redman, M.W.; Carleton, J.E.; Jett, J.; Langer, C.J.; Kuebler, J.P.; Dakhil, S.R.; Chansky, K.; Gandara, D.R. Phase III trial of irinotecan/cisplatin compared with etoposide/cisplatin in extensive-stage small-cell lung cancer: clinical and pharmacogenomic results from SWOG S0124. *J Clin Oncol*, **2009**, 27, 2530-5.

[171] Gow, J.M.; Hodges, L.M.; Chinn, L.W.; Kroetz, D.L. Substrate-dependent effects of human ABCB1 coding polymorphisms. *J Pharmacol Exp Ther*, **2008**, 325, 435-42.

[172] Tanabe, M.; Ieiri, I.; Nagata, N.; Inoue, K.; Ito, S.; Kanamori, Y.; Takahashi, M.; Kurata, Y.; Kigawa, J.; Higuchi, S.; Terakawa, N.; Otsubo, K. Expression of P-glycoprotein in human placenta: relation to genetic polymorphism of the multidrug resistance (MDR)-1 gene. *J Pharmacol Exp Ther*, **2001**, 297, 1137-43.

[173] Kimchi-Sarfaty, C.; Gribar, J.J.; Gottesman, M.M. Functional characterization of coding polymorphisms in the human MDR1 gene using a vaccinia virus expression system. *Mol Pharmacol*, **2002**, 62, 1-6.

[174] Kroetz, D.L.; Pauli-Magnus, C.; Hodges, L.M.; Huang, C.C.; Kawamoto, M.; Johns, S.J.; Stryke, D.; Ferrin, T.E.; DeYoung, J.; Taylor, T.; Carlson, E.J.; Herskowitz, I.; Giacomini, K.M.; Clark, A.G. Sequence diversity and haplotype structure in the human ABCB1 (MDR1, multidrug resistance transporter) gene. *Pharmacogenetics*, **2003**, 13, 481-94.

[175] Jeong, H.; Herskowitz, I.; Kroetz, D.L.; Rine, J. Function-altering SNPs in the human multidrug transporter gene ABCB1 identified using a Saccharomyces-based assay. *PLoS Genet*, **2007**, 3, e39.

[176] Kioka, N.; Tsubota, J.; Kakehi, Y.; Komano, T.; Gottesman, M.M.; Pastan, I.; Ueda, K. P-glycoprotein gene (MDR1) cDNA from human adrenal: normal P-glycoprotein carries Gly185 with an altered pattern of multidrug resistance. *Biochem Biophys Res Commun*, **1989**, 162, 224-31.

[177] Parathyras, J.; Gebhardt, S.; Hillermann-Rebello, R.; Grobbelaar, N.; Venter, M.; Warnich, L. A pharmacogenetic study of CD4 recovery in response to HIV antiretroviral therapy in two South African population groups. *J Hum Genet*, **2009**, 54, 261-5.

[178] Kato, M.; Fukuda, T.; Serretti, A.; Wakeno, M.; Okugawa, G.; Ikenaga, Y.; Hosoi, Y.; Takekita, Y.; Mandelli, L.; Azuma, J.; Kinoshita, T. ABCB1 (MDR1) gene polymorphisms are associated with the clinical response to paroxetine in patients with major depressive disorder. *Prog Neuropsychopharmacol Biol Psychiatry*, **2008**, 32, 398-404.

[179] Mathijssen, R.H.; Marsh, S.; Karlsson, M.O.; Xie, R.; Baker, S.D.; Verweij, J.; Sparreboom, A.; McLeod, H.L. Irinotecan pathway genotype analysis to predict pharmacokinetics. *Clin Cancer Res*, **2003**, 9, 3246-53.

[180] Bellusci, C.P.; Rocco, C.A.; Aulicino, P.C.; Mecikovsky, D.; Bologna, R.; Sen, L.; Mangano, A. MDR1 3435T and 1236T alleles delay disease progression to pediatric AIDS but have no effect on HIV-1 vertical transmission. *Aids*, 24, 833-40.

[181] Lee, S.S.; Kim, S.Y.; Kim, W.Y.; Thi-Le, H.; Yoon, Y.R.; Yea, S.S.; Shin, J.G. MDR1 genetic polymorphisms and comparison of MDR1 haplotype profiles in Korean and Vietnamese populations. *Ther Drug Monit*, **2005**, 27, 531-5.

[182] Ansermot, N.; Rebsamen, M.; Chabert, J.; Fathi, M.; Gex-Fabry, M.; Daali, Y.; Besson, M.; Rossier, M.; Rudaz, S.; Hochstrasser, D.; Dayer, P.; Desmeules, J. Influence of ABCB1 gene polymorphisms and P-glycoprotein activity on cyclosporine pharmacokinetics in peripheral blood mononuclear cells in healthy volunteers. *Drug Metab Lett*, **2008**, 2, 76-82.

[183] Shon, J.H.; Yoon, Y.R.; Hong, W.S.; Nguyen, P.M.; Lee, S.S.; Choi, Y.G.; Cha, I.J.; Shin, J.G. Effect of itraconazole on the pharmacokinetics and pharmacodynamics of fexofenadine in relation to the MDR1 genetic polymorphism. *Clin Pharmacol Ther*, **2005**, 78, 191-201.

[184] Tang, K.; Ngoi, S.M.; Gwee, P.C.; Chua, J.M.; Lee, E.J.; Chong, S.S.; Lee, C.G. Distinct haplotype profiles and strong linkage disequilibrium at the MDR1 multidrug transporter gene locus in three ethnic Asian populations. *Pharmacogenetics*, **2002**, 12, 437-50.

[185] Saito, K.; Miyake, S.; Moriya, H.; Yamazaki, M.; Itoh, F.; Imai, K.; Kurosawa, N.; Owada, E.; Miyamoto, A. Detection of the four sequence variations of MDR1 gene using TaqMan MGB probe based real-time PCR and haplotype analysis in healthy Japanese subjects. *Clin Biochem*, **2003**, 36, 511-8.

[186] Sai, K.; Kaniwa, N.; Itoda, M.; Saito, Y.; Hasegawa, R.; Komamura, K.; Ueno, K.; Kamakura, S.; Kitakaze, M.; Shirao, K.; Minami, H.; Ohtsu, A.; Yoshida, T.; Saijo, N.; Kitamura, Y.; Kamatani, N.; Ozawa, S.; Sawada, J. Haplotype analysis of ABCB1/MDR1 blocks in a Japanese population reveals genotype-dependent renal clearance of irinotecan. *Pharmacogenetics*, **2003**, 13, 741-57.

[187] Chowbay, B.; Cumaraswamy, S.; Cheung, Y.B.; Zhou, Q.; Lee, E.J. Genetic polymorphisms in MDR1 and CYP3A4 genes in Asians and the influence of MDR1 haplotypes on cyclosporin disposition in heart transplant recipients. *Pharmacogenetics*, **2003**, 13, 89-95.

[188] Woodahl, E.L.; Yang, Z.; Bui, T.; Shen, D.D.; Ho, R.J. Multidrug resistance gene G1199A polymorphism alters efflux transport activity of P-glycoprotein. *J Pharmacol Exp Ther*, **2004**, 310, 1199-207.

[189] Tamura, A.; Watanabe, M.; Saito, H.; Nakagawa, H.; Kamachi, T.; Okura, I.; Ishikawa, T. Functional validation of the genetic polymorphisms of human ATP-binding cassette (ABC) transporter ABCG2: identification of alleles that are defective in porphyrin transport. *Mol Pharmacol*, **2006**, 70, 287-96.

[190] Soranzo, N.; Cavalleri, G.L.; Weale, M.E.; Wood, N.W.; Depondt, C.; Marguerie, R.; Sisodiya, S.M.; Goldstein, D.B. Identifying candidate causal variants responsible for altered activity of the ABCB1 multidrug resistance gene. *Genome Res*, **2004**, 14, 1333-44.

[191] Poonkuzhali, B.; Lamba, J.; Strom, S.; Sparreboom, A.; Thummel, K.; Watkins, P.; Schuetz, E. Association of breast cancer resistance protein/ABCG2 phenotypes and novel promoter and intron 1 single nucleotide polymorphisms. *Drug Metab Dispos*, **2008**, 36, 780-95.

[192] Cha, P.C.; Mushiroda, T.; Zembutsu, H.; Harada, H.; Shinoda, N.; Kawamoto, S.; Shimoyama, R.; Nishidate, T.; Furuhata, T.; Sasaki, K.; Hirata, K.; Nakamura, Y. Single nucleotide polymorphism in ABCG2 is associated with irinotecan-induced severe myelosuppression. *J Hum Genet*, **2009**, 54, 572-80.

[193] Warren, R.B.; Smith, R.L.; Campalani, E.; Eyre, S.; Smith, C.H.; Barker, J.N.; Worthington, J.; Griffiths, C.E. Genetic variation in efflux transporters influences outcome to methotrexate therapy in patients with psoriasis. *J Invest Dermatol*, **2008**, 128, 1925-9.

[194] Imai, Y.; Nakane, M.; Kage, K.; Tsukahara, S.; Ishikawa, E.; Tsuruo, T.; Miki, Y.; Sugimoto, Y. C421A polymorphism in the human breast cancer resistance protein gene is associated with low expression of Q141K protein and low-level drug resistance. *Mol Cancer Ther*, **2002**, 1, 611-6.

[195] Tamura, A.; Wakabayashi, K.; Onishi, Y.; Takeda, M.; Ikegami, Y.; Sawada, S.; Tsuji, M.; Matsuda, Y.; Ishikawa, T. Re-evaluation and functional classification of non-synonymous single nucleotide polymorphisms of the human ATP-binding cassette transporter ABCG2. *Cancer Sci*, **2007**, 98, 231-9.

[196] Mizuarai, S.; Aozasa, N.; Kotani, H. Single nucleotide polymorphisms result in impaired membrane localization and reduced atpase activity in multidrug transporter ABCG2. *Int J Cancer*, **2004**, 109, 238-46.

[197] Morisaki, K.; Robey, R.W.; Ozvegy-Laczka, C.; Honjo, Y.; Polgar, O.; Steadman, K.; Sarkadi, B.; Bates, S.E. Single nucleotide polymorphisms modify the transporter activity of ABCG2. *Cancer Chemother Pharmacol*, **2005**, 56, 161-72.

[198] Zamber, C.P.; Lamba, J.K.; Yasuda, K.; Farnum, J.; Thummel, K.; Schuetz, J.D.; Schuetz, E.G. Natural allelic variants of breast cancer resistance protein (BCRP) and their relationship to BCRP expression in human intestine. *Pharmacogenetics*, **2003**, 13, 19-28.

[199] Sparreboom, A.; Gelderblom, H.; Marsh, S.; Ahluwalia, R.; Obach, R.; Principe, P.; Twelves, C.; Verweij, J.; McLeod, H.L. Diflomotecan pharmacokinetics in relation to ABCG2 421C>A genotype. *Clin Pharmacol Ther*, **2004**, 76, 38-44.

[200] Sparreboom, A.; Loos, W.J.; Burger, H.; Sissung, T.M.; Verweij, J.; Figg, W.D.; Nooter, K.; Gelderblom, H. Effect of ABCG2 genotype on the oral bioavailability of topotecan. *Cancer Biol Ther*, **2005**, 4, 650-8.

[201] Li, J.; Cusatis, G.; Brahmer, J.; Sparreboom, A.; Robey, R.W.; Bates, S.E.; Hidalgo, M.; Baker, S.D. Association of variant ABCG2 and the pharmacokinetics of epidermal growth factor receptor tyrosine kinase inhibitors in cancer patients. *Cancer Biol Ther*, **2007**, 6, 432-8.

[202] Keskitalo, J.E.; Zolk, O.; Fromm, M.F.; Kurkinen, K.J.; Neuvonen, P.J.; Niemi, M. ABCG2 polymorphism markedly affects the pharmacokinetics of atorvastatin and rosuvastatin. *Clin Pharmacol Ther*, **2009**, 86, 197-203.

[203] Thomas, F.; Rochaix, P.; White-Koning, M.; Hennebelle, I.; Sarini, J.; Benlyazid, A.; Malard, L.; Lefebvre, J.L.; Chatelut, E.; Delord, J.P. Population pharmacokinetics of erlotinib and its pharmacokinetic/pharmacodynamic relationships in head and neck squamous cell carcinoma. *Eur J Cancer*, **2009**, 45, 2316-23.

[204] de Jong, F.A.; Marsh, S.; Mathijssen, R.H.; King, C.; Verweij, J.; Sparreboom, A.; McLeod, H.L. ABCG2 pharmacogenetics: ethnic differences in allele frequency and assessment of influence on irinotecan disposition. *Clin Cancer Res*, **2004**, 10, 5889-94.

[205] Kondo, C.; Suzuki, H.; Itoda, M.; Ozawa, S.; Sawada, J.; Kobayashi, D.; Ieiri, I.; Mine, K.; Ohtsubo, K.; Sugiyama, Y. Functional analysis of SNPs variants of BCRP/ABCG2. *Pharm Res*, **2004**, 21, 1895-903.

[206] Woodward, O.M.; Kottgen, A.; Coresh, J.; Boerwinkle, E.; Guggino, W.B.; Kottgen, M. Identification of a urate transporter, ABCG2, with a common functional polymorphism causing gout. *Proc Natl Acad Sci U S A*, **2009**, 106, 10338-42.

[207] Lee, S.S.; Jeong, H.E.; Yi, J.M.; Jung, H.J.; Jang, J.E.; Kim, E.Y.; Lee, S.J.; Shin, J.G. Identification and functional assessment of BCRP polymorphisms in a Korean population. *Drug Metab Dispos*, **2007**, 35, 623-32.

[208] Nakagawa, H.; Tamura, A.; Wakabayashi, K.; Hoshijima, K.; Komada, M.; Yoshida, T.; Kometani, S.; Matsubara, T.; Mikuriya, K.; Ishikawa, T. Ubiquitin-mediated proteasomal degradation of non-synonymous SNP variants of human ABC transporter ABCG2. *Biochem J*, **2008**, 411, 623-31.

[209] Conrad, S.; Kauffmann, H.M.; Ito, K.; Deeley, R.G.; Cole, S.P.; Schrenk, D. Identification of human multidrug resistance protein 1 (MRP1) mutations and characterization of a G671V substitution. *J Hum Genet*, **2001**, 46, 656-63.

[210] Letourneau, I.J.; Deeley, R.G.; Cole, S.P. Functional characterization of non-synonymous single nucleotide polymorphisms in the gene encoding human multidrug resistance protein 1 (MRP1/ABCC1). *Pharmacogenet Genomics*, **2005**, 15, 647-57.

[211] Conrad, S.; Kauffmann, H.M.; Ito, K.; Leslie, E.M.; Deeley, R.G.; Schrenk, D.; Cole, S.P. A naturally occurring mutation in MRP1 results in a selective decrease in organic anion transport and in increased doxorubicin resistance. *Pharmacogenetics*, **2002**, 12, 321-30.

[212] Yin, J.Y.; Huang, Q.; Yang, Y.; Zhang, J.T.; Zhong, M.Z.; Zhou, H.H.; Liu, Z.Q. Characterization and analyses of multidrug resistance-associated protein 1 (MRP1/ABCC1) polymorphisms in Chinese population. *Pharmacogenet Genomics*, **2009**, 19, 206-16.

[213] Leslie, E.M.; Letourneau, I.J.; Deeley, R.G.; Cole, S.P. Functional and structural consequences of cysteine substitutions in the NH2 proximal region of the human multidrug resistance protein 1 (MRP1/ABCC1). *Biochemistry*, **2003**, 42, 5214-24.

[214] Wojnowski, L.; Kulle, B.; Schirmer, M.; Schluter, G.; Schmidt, A.; Rosenberger, A.; Vonhof, S.; Bickeboller, H.; Toliat, M.R.; Suk, E.K.; Tzvetkov, M.; Kruger, A.; Seifert, S.; Kloess, M.; Hahn, H.; Loeffler, M.; Nurnberg, P.; Pfreundschuh, M.; Trumper, L.; Brockmoller, J.; Hasenfuss, G. NAD(P)H oxidase and multidrug resistance protein genetic polymorphisms are associated with doxorubicin-induced cardiotoxicity. *Circulation*, **2005**, 112, 3754-62.

[215] Siedlinski, M.; Boezen, H.M.; Boer, J.M.; Smit, H.A.; Postma, D.S. ABCC1 polymorphisms contribute to level and decline of lung function in two population-based cohorts. *Pharmacogenet Genomics*, **2009**, 19, 675-84.

[216] Yoshiura, K.; Kinoshita, A.; Ishida, T.; Ninokata, A.; Ishikawa, T.; Kaname, T.; Bannai, M.; Tokunaga, K.; Sonoda, S.; Komaki, R.; Ihara, M.; Saenko, V.A.; Alipov, G.K.; Sekine, I.; Komatsu, K.; Takahashi, H.; Nakashima, M.; Sosonkina, N.; Mapendano, C.K.; Ghadami, M.; Nomura, M.; Liang, D.S.; Miwa, N.; Kim, D.K.; Garidkhuu, A.; Natsume, N.; Ohta, T.; Tomita, H.; Kaneko, A.; Kikuchi, M.; Russomando, G.; Hirayama, K.; Ishibashi, M.; Takahashi, A.; Saitou, N.; Murray, J.C.; Saito, S.; Nakamura, Y.; Niikawa, N. A SNP in the ABCC11 gene is the determinant of human earwax type. *Nat Genet*, **2006**, 38, 324-30.

[217] Toyoda, Y.; Sakurai, A.; Mitani, Y.; Nakashima, M.; Yoshiura, K.; Nakagawa, H.; Sakai, Y.; Ota, I.; Lezhava, A.; Hayashizaki, Y.; Niikawa, N.; Ishikawa, T. Earwax, osmidrosis, and breast cancer: why does one SNP (538G>A) in the human ABC transporter ABCC11 gene determine earwax type? *Faseb J*, **2009**, 23, 2001-13.

[218] Jirka, M. An alpha(2)-globulin component present in sweat, saliva, tears, human milk, colostrum and cerumen. *FEBS Lett*, **1968**, 1, 77-80.

[219] Miura, K.; Yoshiura, K.; Miura, S.; Shimada, T.; Yamasaki, K.; Yoshida, A.; Nakayama, D.; Shibata, Y.; Niikawa, N.; Masuzaki, H. A strong association between human earwax-type and apocrine colostrum secretion from the mammary gland. *Hum Genet*, **2007**, 121, 631-3.

[220] Martin, A.; Saathoff, M.; Kuhn, F.; Max, H.; Terstegen, L.; Natsch, A. A Functional ABCC11 Allele Is Essential in the Biochemical Formation of Human Axillary Odor. *J Invest Dermatol*, **2009**,

[221] Pratt, S.; Shepard, R.L.; Kandasamy, R.A.; Johnston, P.A.; Perry, W., 3rd; Dantzig, A.H. The multidrug resistance protein 5 (ABCC5) confers resistance to 5-fluorouracil and transports its monophosphorylated metabolites. *Mol Cancer Ther*, **2005**, 4, 855-63.

[222] Yuan, J.H.; Cheng, J.Q.; Jiang, L.Y.; Ji, W.D.; Guo, L.F.; Liu, J.J.; Xu, X.Y.; He, J.S.; Wang, X.M.; Zhuang, Z.X. Breast cancer resistance protein expression and 5-fluorouracil resistance. *Biomed Environ Sci*, **2008**, 21, 290-5.

[223] Guo, Y.; Kotova, E.; Chen, Z.S.; Lee, K.; Hopper-Borge, E.; Belinsky, M.G.; Kruh, G.D. MRP8, ATP-binding cassette C11 (ABCC11), is a cyclic nucleotide efflux pump and a resistance factor for fluoropyrimidines 2',3'-dideoxycytidine and 9'-(2'-phosphonylmethoxyethyl)adenine. *J Biol Chem*, **2003**, 278, 29509-14.

[224] Nicolle, E.; Boumendjel, A.; Macalou, S.; Genoux, E.; Ahmed-Belkacem, A.; Carrupt, P.A.; Di Pietro, A. QSAR analysis and molecular modeling of ABCG2-specific inhibitors. *Adv Drug Deliv Rev*, **2009**, 61, 34-46.